

A New Model of Amyotrophic Lateral Sclerosis
in *Drosophila melanogaster*:
Precise Genetic Engineering, Characterization
and Genetic Suppression

Aslı Şahin

B.S., Boğaziçi University, 2009

M.A., Brown University, 2012

A Dissertation Submitted in Partial Fulfillment of the Requirements for the Degree of
Doctor of Philosophy
in The Division of Biology and Medicine, The Department of Molecular Biology, Cell
Biology, and Biochemistry
at Brown University

Providence, Rhode Island
May 2016

© Copyright 2016 by Aslı Şahin

This dissertation by Aslı Şahin is accepted in its present form
by the Department of Molecular Biology, Cell Biology, and Biochemistry
as satisfying the dissertation requirement for the degree of Doctor of Philosophy.

Date _____

Robert A. Reenan, Ph.D., Advisor

Recommended to the Graduate Council

Date _____

Justin Fallon, Ph.D., Reader and Chairman

Date _____

Anne Hart, Ph.D., Reader

Date _____

Kristi Wharton, Ph.D., Reader

Date _____

Nancy Bonini, Ph.D., Outside Reader

Approved by the Graduate Council

Date _____

Peter Weber, Ph.D., Dean of the Graduate School

staining and apoptosis assays, new generation sequencing techniques including RNA sequencing, EMS mutagenesis, biochemical assays such as SOD1 activity assay.

Rotation Advisor: Dr. Kimberly Mowry February 2010 – March 2010

I investigated the role of lsm proteins in vegetal mRNA localization in *Xenopus* eggs. Some of the techniques I was exposed to in this laboratory are in vitro transcription reaction to radio-label and dye-label mRNAs, Western blotting, RT-PCR, immunolabelling of oocytes through injection, confocal microscopy.

Rotation Advisor: Dr. Gary Wessel November 2009 – February 2010

I examined Vasa protein and mRNA localization in the posterior enterocoel (PE) region in order to understand germ line determinants of sea star species *A. miniata* and *A. forbesii*. Some of the techniques I was exposed to in this laboratory are immunolabelling 3'UTRs of various transcripts, working with an organism whose genome is not fully sequenced, 3' and 5' RACE based sequencing, whole mount in situ hybridization, cloning, and confocal microscopy.

Bogazici University
Department of Molecular Biology and Genetics

Istanbul, Turkey
June 2008-July 2009

Advisor: Dr. Nazli Basak

Worked in the Suna and Inan Kirac Foundation Neurodegeneration Research Laboratory as an undergraduate project student. Investigated the mRNA expression changes upon silencing Alsin gene by siRNA transfection in various vertebrate cell culture models. Gained skills in vertebrate cell culture such as basic passaging, co-culturing, freezing, differentiation, siRNA transfection of various cell lines (N2a, U87M6 and C2C12, NSC34 cell lines) and qRT-PCR, designing siRNAs via in vitro transcription.

University of North Carolina at Chapel Hill
Department of Biochemistry and Biophysics

Chapel Hill, NC
January 2008 – May 2008

Advisor: Dr. Aziz Sancar

I completed a senior thesis project to investigate Excision Repair Mechanisms on Diflorotoluene base. Some of the techniques I exposed to in this laboratory are excision assay on sequencing gel and working with radioactive labeled bases.

Bogazici University
Department of Psychology

Istanbul, Turkey
September 2007-January 2008

Advisor: Dr. Resit Canbeyli

I volunteered for husbandry care of mice and rats. I performed behavioral tests such as Forced Swimming Tests in studies of depression. I also learned perfusion and brain slicing of rats and mice.

University Hospital Hamburg-Eppendorf
Institute for Cell Biochemistry and Neurobiology

Hamburg, Germany
July 2007- September 2007

Advisor: Dr. Stefan Kindler

I gained experience in cloning, Sanger Sequencing Reaction and big dye reaction while designing dendritic mRNA labeling for the Kindler laboratory to use in their studies on Fragile X Syndrome.

Zubeyde Hanim Dogumevi (Hospital), Genetic Laboratory

Bursa, Turkey

Advisor: Dr. Taner Durak

January 2006- February 2006

I shadowed Dr. Taner Durak while he was seeing patients in the hospital environment. I performed various chromosome analyses and karyotyping on my own blood.

Teaching
Experience

Brown University

-Mentor for various undergraduate students at Reenan Laboratory.
(Names are available upon request)

-Completed "Teaching in American classroom course" which is ultimately designed for teaching foreign graduate students to ease them with American education system.

-Recipient of three Sheridan Center Teaching Certificate Programs

-Genetics Laboratory - *Teaching Assistant*

Spring Semester 2010

I ran weekly genetics laboratory session for Genetics 101 students. Assisted in the design and implementation of experiments and course curriculum. Graded all lab reports and assignments.

-Howard Hughes Medical Institution (HHMI) Summer Research Program

One of the Lecturers of the Orientation Class and Teaching Assistant for

Disease Hunters for 9 week program

Summer Semester 2010-2014

I taught the basic laboratory and bioinformatics skills to 32 undergraduates participating HHMI summer program in the first week of the program every year from 2010 to 2014. During the following 9 weeks, I made 8-10 of these students – disease hunters- to perform experiments within my thesis project at the Reenan Laboratory. At the end they gave elevator talks and poster presentations.

Publications

Savva YA, Jepson JE, Sahin A, Sugden AU, Dorsky JS, Alpert L, Lawrence C, Reenan RA. Auto-regulatory RNA editing fine-tunes mRNA re-coding and complex behaviour in *Drosophila*. *Nat Commun*. 2012 Apr 24;3:790. (Contribution: checked the alteration of RNA editing along with Savva YA, observed for the first time altered climbing behavior in mutant *Drosophila* lines, and performed behavioral analyses along with Jepson JE.)

Jepson JE, Savva YA, Yokose C, Sugden AU, Sahin A, Reenan RA. Engineered alterations in RNA editing modulate complex behavior in *Drosophila*: regulatory diversity of adenosine deaminase acting on RNA (ADAR) targets. *J Biol Chem*. 2011 Mar 11;286(10):8325-37. (Contribution: performed behavioral analyses along with Jepson JE.)

Presentations
and Posters

Sahin A, Reenan RA. Genetically accurate ALS models with SOD1 mutations in *Drosophila melanogaster*.

- Oral presentation at German-Turkish Workshop on Molecular Neurosciences 2012
- Oral presentation at Brown University annual MCB retreat as selected student speaker 2013

- Oral presentation at Karadeniz Technical University Biology Student Association of Turkey 2014 in Trabzon, Turkey as an invited speaker.

- Poster presentation at EMBO 2012 conference in Nice, France.

- Poster presentation at Neurofly 2012 conference in Padua, Italy.

Podcast and Radio Program Guest in a Turkish Science Podcast: Bilim Kazani

DEDICATION

✕ I dedicate my PhD thesis to my aunt Ayten Er ✕

Who was rejected from a Botany PhD Program at Ege University, Izmir in 1999 after completing her M.S. degree.

✕

She was told that the program would not accept any PhD students that year, because all the applicants were female.

She was told that fieldwork was not for females.

✕✕

Currently, she is a very ambitious primary school teacher in a very disadvantaged neighborhood, where majority of her students have not seen “the Mediterranean” despite living one hour away from it. She takes her students to the beach at least once in their 5-year-long primary school time.

✕✕✕

You are such an inspiration to me.

I want to be for Arda what you are to me! Imagine how much I admire you!

ACKNOWLEDGMENTS

I would like to thank all of the people who have helped make my graduate school experience full of personal and professional growth. The cover page has my name, but without your personal and professional help, none of this would be possible.

First, I would like to thank my advisor Dr. Robert Reenan for making me excited enough to go to the opposite direction that I envisioned myself for. By end of my undergraduate studies, I was sure of two things in my life: (i) I did not want to work on ALS and (ii) even if I did something neurodegeneration related, I did not want to do anything related to SOD1 gene specifically. My amazement with RNA editing and his curiosity over my graduate school application made us meet in Suna-Inan Kirac ALS conference in Istanbul and build the foundation for this thesis project. Dr. Reenan has been a very unusual mentor and I have learned so much working with him. I really think that his infinite excitement and beyond smart and crazy ideas expanded my scientific skills and knowledge tremendously. I'm ready for the next scientific challenge, cheers to you!

I would also like to thank both past and present members of the Reenan Lab, who have both been wonderful friends and colleagues. Working on the RNA editing project with Dr. James Jepson, Dr. Yiannis Savva and Dr. Arthur Sugden was the most productive and fun times of my research life. Dr. Cindi Staber was always a great help even though she left shortly after I joined the lab. I only wish we could have spend more time together in the Reenan Lab. Comments of Dr. Leila Rieder and Dr. Selena Gell on my preliminary examination as well as my scientific presentation skills were the basis of essential scientific skills that I have acquired today. I am grateful to have such wonderful mentors and scientific siblings. Of those Dr. Yiannis Savva and Dr. Leila Rieder were at Brown University with me from my first day to this day. Dr. Leila Rieder was a great friend who helped me overcome all my personal and cultural problems. She read parts of my thesis even though my big thesis submission day overlapped with her big wedding day. Dr. Yiannis Savva and Dr. Leila Rieder always knew what I was going through and I vented frustrations and successes primarily to them. I would like to especially

acknowledge Dr. Yiannis Savva who became a second mentor to me in the last year of my graduate school life. He patiently helped me edit my thesis draft from beginning to end. I'm looking forward to do more projects with him in the future.

I could not have accomplished this much for this thesis project if I did not have help from Brown University HHMI summer undergraduate researchers (a.k.a. Disease Hunters). Thanks to Dr. Michael McKeown who made me a teaching assistant for the HHMI summer course. Every summer for the last 5 summers that I was at Brown University, I had 8 new undergraduate students who did not have any research experience before. Of these students, every year one very talented student joined Reenan Lab to work with me. Their names would take the whole page so I will only mention three of these students will be never forgotten. Abby Kerson was my first undergraduate student with who I experienced being a mentor for the first time and made all the mentorship mistakes. Emily Jang was such a talented student and a joy to work with. I experienced letting a very much-needed student go to follow her research dreams in another lab for her own good. Lastly, Kirsten Bredvik who made this project continue when my hands were tied while writing this thesis. She is (and probably will be) the only person whom read this thesis from the beginning to the end in its most raw form. Even though English language has too many adjectives that I am always amazed with, I don't think any of them covers my gratuities towards these students.

Next I would like to thank my committee members Dr. Justin Fallon, Dr. Anne Hart, Dr. Kristi Wharton, and Dr. Michael McKeown. They challenged me as any thesis committee would do. However, in my case, these great role models also became ALS researchers, who happen to know the field at least as much as I did. I hope I did not let you down during this thesis project. I value time more than anything in the world and I will never ever forget the time you spent to come up with solutions to my thesis and my personal problems. Dr. Kristi Wharton was also a second mentor and a collaborator with her students Aaron Held and Paxton Major. I appreciate all your contributions. I would like to also acknowledge my outside reader Nancy Bonini. I have always thought that the prospect of her presence at my big thesis day was too good to be true. I want to thank her

for making time to read my thesis.

I also need to acknowledge several of people who have most contributed to my development outside of the lab. Firstly, I would like to thank my T-house crew who has made living in Providence a pleasure. Dr. Altar Sorkac and soon-to-be Dr. Mustafa Talay were some of my best friends and study buddies in college. Their presence by my side throughout my graduate student life has never made me feel alone. In addition to them, Dr. Ali Bilgin Arslan, Dr. James Niemeyer and soon-to-be Dr. Jackie Hynes will be always remembered as I constantly treasure my time at the T-house. Next, I would like to thank everyone with whom I had amazing conversations at the Graduate Student Bar and all my friends living all over the world to whom I constantly whine in lengthy e-mails especially Leven Bas, Ruya Koskun, Selen Karaca, Ozgun Ozer, Can Kivanc, Utku Oren, Meren (who will either become a legendary professor by the time my thesis become public if he eats, drinks water and sleeps or become a part of his precious microbes. Either way I am proud to acknowledge him as a collaborator), Susanna Angelino (to help me to accept myself as the way I am), Atilgan Yilmaz (because of whom I picked the Reenan Lab), Zak Swartz. I'm proud and grateful to meet these people in my graduate student life. Bunch of thanks for providing outlets for my down times and a needed distraction from the life of a graduate student.

I also acknowledge my blog readers. They may claim that my blog was a part of their decision in studying "Bio-something" as I call it, however I really don't think they would dig through the internet to find my blog out of the many negative sources about studying biology, if they did not have it in them. Please do not blame me when you are suffering while writing your own PhD theses.

At Brown University, I met wonderful colleagues. I am sure in the future I will proudly yell "yes, we went to Brown University together" about many of them. I only hope they will remember me as well. I also want to thank ALS Association for funding my preliminary results and Suna Inan Kırac Foundation for supporting my first three years of graduate studies. Who would have thought a scientist unconditionally funded (I

did not have to work on ALS) by an ALS patient would identify possible ALS suppressors. I would like to acknowledge karma for that.

Finally, I would like to thank my beloved family: A. Şahins, for their unwavering support and belief in my abilities. My parents never questioned why I chose this path even if they don't understand it. They let me pursue my dreams and content themselves with skype calls. My mum Aysel, coming home from work in her suit and cooking delicious meals in 30 minutes, never stops multi-tasking, was my role model when it came to spending my time efficiently. I don't think running 10 experiments at once without making any mistakes would be possible if I haven't learned from her early on. My father Asım, pronounced as awe-some, as awesome he is, never made me worry about anything and became an example when it comes to slowing down and enjoying life. My brother, my person, Arda, left teenagerhood, became my best friend during the time of my graduate studies summarized in thesis. His first tattoo summarizes everything I tried to tell here about my family, imagine how stellar he is. I'm proud of him so much that I cannot imagine how he will turn out when he gets white hair.

I cannot express the gratitude I feel towards everyone who has helped me reach this point.

I thank you all.

I thank my flies, as well!

TABLE OF CONTENTS

Title Page.....	i
Copyright Page.....	ii
Signature Page.....	iii
Curriculum Vitae.....	iv
Dedication.....	vii
Acknowledgments.....	viii
Table of Contents.....	xii
List of Tables.....	xiv
List of Figures.....	xv

CHAPTER I: Introduction

Amyotrophic Lateral Sclerosis Caused by Mutations in Superoxide Dismutase 1.....	1
Amyotrophic Lateral Sclerosis.....	1
Mutant Copper-Zinc Superoxide Dismutase 1 (SOD1)-Induced ALS.....	4
Etiology of Copper-Zinc Superoxide Dismutase 1 (SOD1) Gene in ALS.....	4
Copper-Zinc Superoxide Dismutase 1 Protein Function.....	5
SOD1 Protein Loss of Function as a Possible Cause of ALS.....	8
SOD1 Gain of Toxic Function as Possible Cause of ALS.....	12
SOD1-Mediated ALS Pathology in the Light of Overall ALS Pathology.....	14
Protein Inclusions.....	15
Oxidative Stress and Mitochondrial Dysfunction.....	17
Motor Neuron Death.....	18
Excitotoxicity.....	19
Misfolded SOD1-Specific Protein/Transcriptome Signatures.....	20
Current SOD1-Mediated ALS Model Systems.....	22
Transgenic SOD1 Rodent Models with Intact Endogenous SOD1.....	23
Transgenic SOD1 Animal Models in Null SOD1 Background.....	28
Transgenic SOD1 Models in Other Model Organisms.....	28
Non-Transgenic SOD1 Animal Models.....	30
ALS Models with Mutant SOD1 Patient-Derived Induced Pluripotent Stem Cells.....	34
A Novel <i>Drosophila</i> ALS Model.....	38
Precise Genetic Engineering Through Ends-out Homologous Recombination.....	38
Genetic Screens in the Model Organism <i>Drosophila melanogaster</i>	40
Ethyl Methanesulfonate (EMS) as a Chemical Mutagenesis Agent.....	42
Genetic Interventions to Modify SOD1 Phenotype in Rodent Models.....	44
Open Questions and Current Motivations For This Study.....	48
References.....	50
Figures.....	69
Tables.....	72

CHAPTER 2:

Generation and Characterization of a Knock-in Model for Amyotrophic Lateral Sclerosis in <i>Drosophila</i>	82
Abstract.....	83
Introduction.....	84
Materials and Methods.....	90

Results.....	102
Discussion and Future Directions.....	118
References.....	124
Figures.....	131
Tables.....	148
CHAPTER 3:	
Transcriptional Profiling of ALS-linked SOD1 Mutations in <i>Drosophila</i>	152
Abstract.....	153
Introduction.....	153
Materials and Methods.....	156
Results.....	159
Discussion and Future Directions.....	165
References.....	168
Figures.....	172
Tables.....	179
CHAPTER 4:	
Chemical Mutagenesis Screen for Mutations Suppressing <i>dSod1^{G85R}</i> Lethality: Identifying New Avenues to Therapy Through Forward Genetics.....	181
Abstract.....	182
Introduction.....	182
Materials and Methods.....	185
Results.....	187
Discussion and Future Directions.....	195
References.....	198
Figures.....	201
Tables.....	204
CHAPTER 5: Discussion.....	205
Gaps In The Current Knowledge Within The Amyotrophic Lateral Sclerosis Field.....	206
Superoxide Dismutase 1: First ALS-associated Gene.....	206
Mimicking Human Disease Alleles in SOD1 Generates Unique Phenotypes for A Genetic Screen in <i>Drosophila</i>	211
Riluzole Treatment is not as Effective in <i>Drosophila</i> as in Human Patients.....	214
The Dosage of Sod1 Protein Plays a Critical Role in ALS Pathogenesis.....	215
An Allele Previously Characterized as Deficient <i>dSod1^{-/-}</i> is not Null.....	216
Other ALS causing genes and SOD1: where does SOD1 stand in ALS pathogenesis?.....	217
Concluding Remarks.....	219
References.....	223
APPENDIX I:	
Loss of Heterochromatic Gene Silencing in <i>Drosophila</i> ALS Model with <i>dSOD1^{G85R}</i> Mutation.....	223
APPENDIX II:	
Specific RNA Editing is not Affected in <i>dSOD1^{G85R}</i> <i>Drosophila</i> ALS Model.....	233

APPENDIX III:
 Engineered Alterations in RNA Editing Modulate Complex Behavior in *Drosophila*:
 Regulatory diversity of Adenosine Deaminase Acting on RNA (ADAR) Targets.....249

APPENDIX IV:
 Auto-Regulatory RNA Editing Fine-Tunes mRNA Re-Coding and Complex Behaviour
 in *Drosophila*..... 296

LIST OF TABLES

1.1	ALS-causing mutant genes mapped in familial ALS patients and ALS-associated genes, their known protein functions and their possible contribution to ALS.	72
1.2	The possible commonalities of SOD1-mediated ALS with other ALS-associated genes	78
1.3	Examples of known genetic suppressors of SOD1-mediated ALS <i>in vivo</i>	81
2.1	The SOD1 point mutations investigated in this study	148
2.2	Riluzole and Melatonin are not effective therapies for <i>dSod1</i> ^{G85R/G85R} flies	149
2.3	Genetic stocks used in this study	150
2.4	Primer sequences used in this study	151
3.1	Gene Ontology (GO) analysis of transcription changes in <i>dSod1</i> ^{H71Y/H71Y} adults	179
4.1	Candidate suppressors that are identified from the forward genetic screen	204
B.1	Measurement of A-to-I editing percentage in male <i>Drosophila</i> thorax	243
B.2	Measurement of A-to-I editing percentage in female <i>Drosophila</i> thorax	245
B.3	Measurement of A-to-I editing percentage in male <i>Drosophila</i> head	246
B.4	Measurement of A-to-I editing percentage in female <i>Drosophila</i> head	247

LIST OF FIGURES

1.1	Distribution of fALS-causing mutant genes.	69
1.2	Comparison of human SOD1 (hSOD1) and <i>Drosophila</i> SOD1 (<i>dSod1</i>)	70
1.3	Ends-out homologous recombination	71
2.1	Targeted point mutations introduced to the endogenous locus via homologous recombination	131
2.2	Targeted mutations lower organismal fitness and cause eclosion defects	132
2.3	Lifespan of flies expressing targeted mutations	133
2.4	Eclosed <i>dSod1</i> ^{H71Y/H71Y} flies are sensitive to oxidative stress	134
2.5	<i>dSod1</i> mutant larvae display crawling defect in a dosage dependent manner	135
2.6	<i>dSod1</i> mutant adults display climbing defect	136
2.7	<i>dSod1</i> ^{H71Y} wandering 3 rd instar larvae have minor neuromuscular junction structural changes	137
2.8	<i>dSod1</i> mutant adults experience muscle atrophy and progressive denervation	138
2.9	<i>dSod1</i> ^{G85R/G85R} mutant legs exhibit more severe denervation in the distal legs	139
2..10	<i>dSod1</i> ^{G85R} and <i>dSod1</i> ^{H71Y} wandering 3 rd instar larvae have minor neuromuscular junction defects	140
2.11	Absence of gliosis, apoptosis and motor neuron cell body loss in <i>dSod1</i> mutants	141
2.12	Superoxide dismutase activity is diminished in homozygous <i>dSod1</i> ^{G85R} and <i>dSod1</i> ^{H71Y} mutants	142
2.13	Protein expression of mutant SOD1 alleles is altered in <i>Drosophila</i> adults	143

2.14	Lack of dSod1 in the insoluble protein fraction	144
2.15	<i>dSod1^{G85R}</i> allele causes survival defects through gain of toxic function	145
2.16	Wild type dSod1 expression suppresses eclosion and locomotion defect	146
2.17	Protein expression of mutant <i>dSod1</i> alleles is not altered by the presence of extra wild type dSod1	147
3.1	Transcriptional analysis of <i>dSod1^{H71Y/H71Y}</i> compared to <i>dSod1^{WTLoxP/WTLoxP}</i>	172
3.2	Altered pathways in <i>dSod1^{H71Y/H71Y}</i>	173
3.3	Map205 expression changes in <i>dSod1</i> mutants and <i>dTDP-43</i> mutants	175
3.4	Intron skipping in the Appl transcript	176
3.5	Up-regulated Splicing in the Cpo transcript	177
3.6	3'UTR extension defects in Ptp10D transcript	178
4.1	Forward genetic screen design to identify suppressors for <i>dSod1^{G85R/G85R}</i> lethality	201
4.2	Genetic mapping of the lethality of EMS 81 and EMS 102	202
4.3	Molecular mapping of the lethality of EMS 81 and EMS 102	203
A.1	Abnormal chromatin structure in <i>dSOD1^{G85R/G85R}</i> adult brains	230
A.2	HP1 mRNA expression is altered in other <i>dSOD1</i> alleles	231
A.3	Heterochromatic gene silencing of PEV reporter (<i>Hok^{mw}</i>) is reduced in <i>Drosophila</i> ALS model carrying heterozygous <i>dSOD1^{G85R}</i> mutation	232
B.1	dAdar protein levels have not changed in response to the presence of <i>dSOD1^{G85R}</i> allele	242
B.2	dAdar mRNA expression is altered in other <i>dSOD1</i> alleles	243
C.1	Visualization of dADAR expression using ends-out homologous recombination	277

C.2	Molecular reporter of RNA editing reveals neuron-specific patterns of dADAR activity	278
C.3	Varied impacts on mRNA re-coding following reduction of dADAR expression	279
C.4	Dynamic control of dADAR expression underlies developmental patterns of editing at low efficiency sites	280
C.5	Global reduction in dADAR activity leads to altered patterns of locomotor activity	281
C.6	RNA editing is required for appropriate male courtship	282
C.7	Knockdown of dADAR in fruitless-expressing neurons alters the male courtship song	283
C.8	Model for neuron to neuron variation in editing levels within the <i>Drosophila</i> nervous system	284
D.1	<i>dAdar</i> auto-editing selectively modulates mRNA re-coding	319
D.2	Inhibiting or hard-wiring <i>dAdar</i> auto-regulation results in widespread alterations in RNA editing of target adenosines	320
D.3	Hard-wiring of <i>dAdar</i> auto-editing modifies the quantitative pattern of RNA editing	321
D.4	Spatial regulation of dADAR auto-editing	322
D.5	dADAR auto-editing in <i>Drosophilid</i> species of the <i>D. melanogaster</i> subgroup	323
D.6	Auto-editing modifies the sub-nuclear localization of dADAR	324
D.7	Dysregulation of <i>dAdar</i> auto-editing alters complex behaviours	325
D.8	Environmental modulation of dADAR auto-editing	326

CHAPTER 1

Amyotrophic Lateral Sclerosis (ALS) Caused by Mutations in Superoxide Dismutase 1 (SOD1)

AMYOTROPHIC LATERAL SCLEROSIS

Amyotrophic Lateral Sclerosis (ALS) is a fatal, incurable neurodegenerative disease in which upper and lower motor neurons progressively “die back” from the neuromuscular junction and muscles begin to weaken due to denervation (Dadon-Nachum, Melamed, & Offen, 2011). Even though ALS is considered to be an orphan disease, it is the most common adult-onset motor neuron disorder with annual 2 per 100,000 incidence and 5 per 100,000 prevalence rates (O’Toole *et al.*, 2008). ALS Association estimates 30,000 ALS patients in the United States alone, and 5,000 new cases appear every year globally (McGuire & Nelson, 2006). Men are at a slightly higher risk than women (1.3:1 ratio) (McGuire & Nelson, 2006). By the time the disease’s first signs of limb weakness, muscle cramps, weight loss, and asymmetric paralysis appear, 80% of the motor neurons are already dead (Mitsumoto, 2001).

Not only is the diagnosis of ALS devastating, but the treatment options for ALS patients are very bleak — there is only one FDA-approved drug for ALS: Riluzole, a palliative glutamate-release inhibitor (Bensimon, Lacomblez, & Meininger, 1994). Riluzole only extends the life expectancy of a patient on average 2-3 months (Lacomblez *et al.*, 1996; Miller *et al.*, 1996). Depending on the location of motor neuron degeneration, symptoms and disease progression vary between ALS patients. The death of upper motor neurons in the motor cortex of the brain leads to spasticity and hyperexcitability of reflexes, whereas the death of lower motor neurons in the brain stem and the spinal cord leads to weakening of the muscles controlling voluntary movement (Pasinelli & Brown, 2006). In the later stages of the disease, three to five years after disease onset, the diaphragm is also denervated and the only option for a patient is to live

with long-term mechanical ventilation assistance (Pasinelli & Brown, 2006). Cognition in most ALS patients is largely intact during disease progression. However, in some cases frontotemporal dementia (FTD) accompanies ALS. FTD exhibits itself as behavioral and emotional changes accompanied by language impairment, in contrast to the type of dementia with memory loss as seen in Alzheimer's disease patients (Swinnen & Robberecht, 2014; Ng, Rademakers, & Miller, 2015). In a complex disease such as ALS, especially in the past where next generation sequencing was not available, patients with familial disease history (fALS) provided many clues that can help pinpoint the relevant genes that cause the disease. However, only 10% of ALS patients have a family history (Leblond *et al.*, 2014) (Figure 1.1). Today, mostly through exome/genome sequencing, mutations in 61 genes (plus 2 loci with unknown genes, and many susceptibility genes have been identified through genome wide association studies (GWAS)) in ALS patients versus matched controls (Abel *et al.*, 2012; Peters, Ghasemi, & Brown, 2015). Full names and the known functions of these genes can be found at Table 1.1. However, the mutations responsible for ALS in almost a quarter of fALS patients remain unidentified. Despite the heterogeneity of familial forms of ALS, the clinical features and pathology of sporadic forms of ALS (sALS) are very similar to the presentation of fALS, suggesting a common mechanism for neurodegeneration. According to the current literature on pathological analysis of autopsied motor neurons of sALS, fALS, or ALS-FTD patients with diverse genetic causes, ALS pathogenesis can be summarized in general terms by: (I) cytoplasmic misfolded and ubiquitinated protein inclusions on histochemical analysis and dysfunction of protein quality control machinery, (II) altered RNA metabolism with a direct or indirect effect of RNA-binding

proteins, (III) motor neuron death with possible induction by non-neuronal cells (e.g. astroglia and microglia), and (IV) neuronal cytoskeletal architecture dysfunction (Peters *et al.*, 2015). These altered cellular mechanisms mentioned above will be further covered in more detail later in this chapter.

MUTANT COPPER-ZINC SUPEROXIDE DISMUTASE 1 (SOD1)-INDUCED ALS

Etiology of Copper-Zinc Superoxide Dismutase 1 (SOD1) Gene in ALS

In 1993, Copper-Zinc Superoxide Dismutase 1 (SOD1) was the first gene identified to be mutated in ALS in 1993 through linkage analysis (Rosen *et al.*, 1993). Then, a span of 8 years passed before another fALS-causing gene was discovered (Yang *et al.*, 2001). Approximately, 20% of familial ALS (fALS) and 3% of sporadic (sALS) cases result from mutations in the SOD1 gene (Figure 1.1) (Saccon *et al.*, 2013). Despite its small size, more than 150 different mutations within the 153 amino acid SOD1 protein have been reported in ALS patients (Figure 1.2A) (Chiti & Dobson, 2006). In fact, some amino acids such as G93 have been identified as mutated to six other amino acids indicating that numerous changes at the same location can cause ALS (Bunton-Stasyshyn *et al.*, 2014). Mutations scattered throughout the SOD1 gene have been shown to modify protein stability, enzymatic activity, and metal-binding properties, while others maintain wild type SOD1-like properties (Valentine, Doucette, & Zittin Potter, 2005). However, all of these mutations result in essentially the same outcome: adult-onset, dominantly

inherited, rapidly progressive ALS¹. Intriguingly, cytoplasmic SOD1 inclusions have been reported in some sporadic ALS (sALS) post-mortem spinal cord tissues and in an ALS patient with a mutation in another ALS-associated gene senataxin despite the lack of a SOD1 mutation (Gruzman *et al.*, 2007; Forsberg *et al.*, 2010; Bosco *et al.*, 2010). All of these observations strengthen the hypothesis of a common mechanism of neurodegeneration and emphasize the role of SOD1 in the general pathogenesis of ALS. Uncovering how specific mutations in SOD1 ultimately lead to the dysfunction and death of motor neurons may shed light on how ALS develops and progresses in patients with the sporadic or familial disease and will help in the quest for therapeutic strategies.

Copper-Zinc Superoxide Dismutase 1 Protein Function

SOD1 is ubiquitously expressed and highly conserved across species from spinach to humans according to the primary and tertiary protein structure (Bertini, Manganl, & Viezzoli, 1998). Despite its small size of 16kD, it constitutes 1% of the total soluble cytoplasmic protein population in neuronal cells (Pardo *et al.*, 1995). The most well characterized and well-studied function of SOD1 is superoxide scavenging. As a cytoplasmic antioxidant enzyme, SOD1 forms homodimers to convert the toxic byproduct of oxidative phosphorylation, superoxide radical (O_2^-), into oxygen (O_2) and hydrogen peroxide (H_2O_2) (McCord & Fridovich, 1969). The H_2O_2 product is then rendered harmless by the enzyme peroxidase in the cytoplasm (Valentine *et al.*, 2005).

¹ There are rare exceptions to dominantly inherited SOD1 mutations: D90A mutation in Scandinavian populations (Andersen *et al.*, 1995), reported single cases of L126S, L117V and G27delGGACCA (a 6bp deletion in exon 2) present itself as homozygote and recessive (Takehisa *et al.*, 2001; Zinman *et al.*, 2009; Synofzik *et al.*, 2012). Juvenile ALS cases are also exceptions to fast progression of ALS.

SOD1 protein has relatively simple tertiary structure. Each SOD1 subunit binds to one copper (Cu^{2+}) and one zinc (Zn^{2+}) ion (Figure 1.2C). Each subunit contains five beta sheets connected to each other with six short loops, two of which encase the metal (Cu^{2+} and Zn^{2+}) binding region. An intrasubunit sulphide bond between cysteines 57 and 146 further stabilizes the structure of the monomer. A small portion of the protein – 17 amino acids out of 153 amino acids per monomer – is involved in the formation of the dimer interface, which is stabilized by numerous hydrogen bonds and hydrophobic contacts (Figure 1.2A) (Valentine *et al.*, 2005).

There are two other Superoxide Dismutase genes in mammals: SOD2 and SOD3 (Fukai & Ushio-Fukai, 2011), but the cellular localization of these enzymes is non-cytoplasmic. SOD2 employs a manganese (Mn) metal cofactor and localizes to the mitochondrial matrix. SOD3 uses iron (Fe) metal as a cofactor and localizes to the extracellular matrix (Zelko, Mariani, & Folz, 2002). SOD1 is the only cytoplasmic SOD-family enzyme. Given the antioxidant enzymatic function, mutations in the SOD1 protein can cause a decrease in cytoplasmic superoxide dismutase activity by altering its protein stability or metal binding properties in ALS patients. Moreover, the mutant enzyme may catalyze additional toxic reactions and cause an increase in the production of free radicals. Additionally, since the SOD1 protein utilizes Cu^{2+} and Zn^{2+} ions, in the case of a mutation, liberated free Cu^{2+} and Zn^{2+} ions could cause Cu/Zn mediated neurotoxicity (Valentine *et al.*, 2005). In this mechanistic interpretation, SOD1 helps establish Cu^{2+} and Zn^{2+} homeostasis in the cytoplasm by buffering these ions (Elliott, 2001).

It has been proposed that the SOD1 protein has additional roles other than superoxide scavenging, especially given the fact that SOD1 protein localizes not only to

the cytoplasm where it serves its canonical function, but also to the nucleus, lysosomes and intermembrane space of mitochondria (Valentine *et al.*, 2005). In fact, in the yeast *Saccharomyces cerevisiae*, reconstituting only 2% of the total SOD1 protein amount restores its protective antioxidant enzymatic activity (Corson *et al.*, 1998), calling into question the necessity for a large cytoplasmic abundance of SOD1 protein to scavenge oxygen radicals, and suggesting the possibility of alternative, not-yet-fully-investigated roles for SOD1.

An example of such an unexpected role is the recent report that cytoplasmic wild type SOD1 is relocated to the nucleus within 20 minutes of intrinsic or extrinsic oxidative stress induction in human cell lines. In the same study, chromatin immunoprecipitation (ChIP) analyses revealed that SOD1 acts as a transcription factor in the nucleus by binding to the promoter regions of various genes that are associated with oxidative stress (Tsang *et al.*, 2014).

Other interactions of SOD1 protein have revealed interesting associations. Mutant SOD1, but not wild type SOD1, is found to bind to neurofilament light chain (*NFL*) mRNA in patient-derived induced pluripotent stem cells (Chen *et al.*, 2014). Additionally, mutant SOD1 can bind to vascular endothelial growth factor (*VEGF*) mRNA in a complex with ribonucleoproteins TIA-1-related (TIAR) and human antigen R (HuR) in the cytoplasm and negatively affect their stability (Lu *et al.*, 2007, 2009). It is apparent from these recent results that there are new areas of exploration involving non-canonical functions for wild type and mutant SOD1.

SOD1 Protein Loss of Function as a Possible Cause of ALS

Given that mutations throughout the entirety of the human SOD1 (hSOD1) gene can cause ALS, it is likely that there is a central effect shared by all mutant SOD1 alleles leading to a common pathway of motor neuron degeneration. Loss of SOD1 function was the first hypothesis for the common ALS mechanism. Due to experimental difficulties it is not possible to measure dismutase activity from post-mortem motor neurons specifically. However, numerous groups reported dismutase activity ranging 25%-100% (with average of 58%±17) from red blood or nervous system cells of patients carrying 48 different mutant SOD1 proteins (Saccon *et al.*, 2013). Tissue choice seems to be unrelated to dismutase activity levels, since similar activity levels, ~50% reduction, are reported from SOD1^{A4V/+} patient frontal cortex and red blood cells (Rosen *et al.*, 1994).

Lack of a uniform reduction in the dismutase activity from patient samples weakened the SOD1 loss of function hypothesis of ALS. It is important to note here that these groups measured “overall” dismutase activity within a given tissue amount rather than measuring per unit of SOD1 protein (Saccon *et al.*, 2013). Thus, the total amount of SOD1, including SOD1 protein half-life, correct folding of the protein, Cu²⁺ and Zn²⁺ loading of the protein, other post-translational modifications, and stability of mutant protein are not considered. In order to address stability of the mutant protein, especially in SOD1 mutant samples with lower “overall” dismutase activity, four groups measured the “intrinsic” SOD1 activity instead, where they normalized the dismutase activity to the SOD1 protein amount and detected a range of dismutase activity from 0% to 150% compared to wild type controls (Borchelt *et al.*, 1994; Zu *et al.*, 1997; Chia *et al.*, 2010; Marin *et al.*, 2012).

The “intrinsic” SOD1 activity results raise the discussion of whether the mutant SOD1 proteins are capable of enzymatic activity as opposed to a hypothesis that the mutant SOD1 is not accessible to perform its function. Overall, it is clear that regardless of the measurement method –“intrinsic” or “overall”– some mutant forms of SOD1 retain almost full enzymatic ability, even in homozygous patients. For instance, homozygous SOD1^{D90A/ D90A} patients maintain 93% of dismutase ability (Andersen *et al.*, 1995). Moreover, overexpression of the mutant SOD1 alleles on the SOD1 null background, in yeast and cell culture, suggests no direct correlation between SOD1 dismutase activity and clinical phenotype severity (Borchelt *et al.*, 1994; Ratovitski *et al.*, 1999).

The generation of model organisms lacking SOD1 protein further weakened the SOD1 loss of function hypothesis. Five different groups published SOD1 null mouse lines by targeted deletion of various segments, exons, or the entire genomic sequence of the SOD1 gene (Reaume *et al.*, 1996; Huang *et al.*, 1997; Ho *et al.*, 1998; Matzuk *et al.*, 1998; Yoshida *et al.*, 2000). The experimental results using these five mouse lines are strikingly similar. Mice lacking SOD1 did not necessarily exhibit motor neuron death nor ubiquitinated protein inclusions in the cytoplasm, but they were sensitive to motor neuron injuries (Reaume *et al.*, 1996) and paraquat-induced neurodegeneration (Ho *et al.*, 1998). Furthermore, SOD1 null mice had accelerated age-related muscle denervation, weight and muscle mass loss, as well as various non-neuronal problems such as reduced fertility (Ho *et al.*, 1998; Matzuk *et al.*, 1998) and heart defects (Yoshida *et al.*, 2000).

Invertebrate systems provide a rapid and powerful tool for assessing genetic affects of mutation, and *Drosophila* has proven itself as a highly relevant system to model human disease (Bilen & Bonini, 2005; Rajan & Perrimon, 2013; Debattisti & Scorrano, 2013; Konsolaki, 2013; Casci & Pandey, 2015). *Drosophila* has three superoxide genes as in humans: cytoplasmic *dSod1*, mitochondrial *dSod2* and extracellular matrix localized *dSod3*. All of *Drosophila* superoxide genes are highly similar to their human counterparts in terms of both sequence homology and enzymatic function. Similar to the mice studies, *Drosophila* lacking *dSod1* have a shortened life span (Staveley, Hilliker, & Phillips, 1991; Missirlis *et al.*, 2003) that can be extended by specific overexpression of hSOD1^{wt} in motor neurons with a D42 driver using the Gal4 binary expression system (Parkes, Elia, *et al.*, 1998). Unfortunately, *Drosophila* literature on the *dSod1* null mutation is not as clear as in mice. Two original SOD1 deficiency alleles were generated through gamma-ray radiation: *X-16* and *X-39* (Staveley *et al.*, 1991). The *X-16* allele contains an 11bp deletion in the beginning of the first exon causing a frame shift after the 7th amino acid within the *dSod1* peptide (Phillips *et al.*, 1995). The *X-39* allele is reported to have a 395bp deletion² spanning the 96bp of the promoter region and the entirety of exon 1 (Phillips *et al.*, 1995). When initially made in 1991 until 2003, homozygosity for *X-39* and *X-16* alleles resulted in semilethality at the pupal stage (Staveley *et al.*, 1991) and a reduced average life span of 7-10 days for the eclosed adults (Parkes, Elia, *et al.*, 1998; Missirlis *et al.*, 2003). Although the eclosion rates of these two alleles were different, they both give an eclosion defect (Staveley *et*

² As a part of characterization of *dSod1* mutants in the 2nd chapter, this deletion is found to be 397 base pairs instead of 395 base pairs.

al., 1991; Phillips *et al.*, 1995). This difference may very likely stem from additional background mutations, caused through the gamma-ray induction of mutations in the parental lines. The evidence for background mutations is even more apparent today as these alleles are homozygous lethal at the 1st instar larval stage (Please see chapter 2).

Mockett and colleagues overcame homozygous background mutation concern in 2003 by generating a deficiency line combining these two alleles into the trans-heterozygote: *dSod1*^{X-39/X-16}. *dSod1*^{X-39/X-16} flies exhibit a survival of 7-10 days, decreased fertility as well as decreased eclosion rate (Mockett *et al.*, 2003). Unfortunately, in the literature many publications analyze dSod1 “null” phenotype in *Drosophila* using the n108³ line by referring it as dSod1^{-/-} or dSod1 knock-out. The n108 allele is generated by ethyl methanesulfonate (EMS) mutagenesis that has simply one amino acid change of G49S instead of a full deficiency at the locus. *dSod1*^{G49S} presents as null in gel-based SOD1 activity assays explaining the “null” description of the allele ((Phillips *et al.*, 1989). However, SOD1 monomers cannot necessarily maintain their dimer structure in the gel-based assays as well as they do *in vivo* in the cytoplasm. This uncertainty demonstrates a limitation in measuring dismutase activity with gel-based systems. For instance, the hSOD1^{G85R} allele shows no activity on gel-based assays while it rescues SOD1 activity-dependent yeast lethality (Ratovitski *et al.*, 1999). Thus, until a targeted deletion of *dSod1* locus is made by precise genetic engineering techniques such as homologous recombination or new generation genome engineering techniques such as CRISPR or TALENs, *dSod1*^{X-39/X-16} suffices for *Drosophila* dSod1 deficiency

³ n1 is another name for the n108 allele.

experiments, as opposed to the *n108* allele with detectable SOD1 protein production as shown in Chapter 2⁴ (Figure 2.13).

In *Caenorhabditis elegans*, as in *Drosophila*, two deletion alleles were generated by mutagenesis instead of targeting: tm783 and tm776. In parallel to other model organisms, both of these alleles result in a shortened life span as homozygotes (Yanase *et al.*, 2009). Background mutations on the original chromosomes resulting from the mutagenesis protocol do not seem to cause any issues in *C. elegans*, probably due to the ability to freeze the original stocks. Freezing inhibits accumulation of new mutations in every generation. In summary, while loss of SOD1 function causes increased susceptibility to neurodegeneration, it does not recapitulate all the symptoms of human ALS in model organisms.

SOD1 Gain of Toxic Function as Possible Cause of ALS

The second hypothesis for a common mechanism associated with SOD1-mediated ALS is the idea that a dominantly inherited gain of toxic function of SOD1 mutant protein could lead to neurodegeneration. High molecular-weight SOD1 isoforms have been observed in tissues from ALS patients (Shibata *et al.*, 1996; Brown, 1998), SOD1-induced transgenic model organisms including mice (Kato, 2008), *Drosophila* (Watson *et al.*, 2008) and *Caenorhabditis elegans* (Wang, Farr, Hall, *et al.*, 2009), as well as in patient-derived induced pluripotent cells (Muqit & Feany, 2002). These observations have led many investigators to the conclusion that SOD1-associated fALS is an aberrant protein conformation disorder, similar to Alzheimer's disease, Parkinson's disease,

⁴ The n108 allele is referred to as dSod1^{G51S} in chapter 2. The G49S mutation in the n108 line corresponds to G51S, according to the human SOD1 numbering.

Huntington's disease, and other neurodegenerative diseases in which protein aggregates are present. In fact, these SOD1-positive proteinaceous aggregates may have prion-like properties as in mad cow disease (Bovine spongiform encephalopathy) and Creutzfeldt-Jakob disease. SOD1-positive proteinaceous aggregates have been demonstrated to lead to the spread of ALS from one motor neuron to another upon death of diseased motor neurons (Münch, O'Brien, & Bertolotti, 2011), secretion from astrocytes to motor neurons (Basso *et al.*, 2013), or transmission from one mouse ALS mouse model to another upon injection (Ayers *et al.*, 2014). Prion-like transmission of wild type and mutant SOD1 protein between cells is reviewed in (Grad & Cashman, 2014)).

The SOD1 inclusions in ALS patients and in ALS *in vivo* and *in vitro* models contain ubiquitinated SOD1 and neurofilament proteins, chaperones such as Hsc70, and other known components of the protein degradation pathways (Wang, Farr, Zeiss, *et al.*, 2009). Thus, one of the newly-supported hypotheses for how mutant SOD1 leads to ALS is the initiation of the unfolded protein response (UPR) pathway. UPR can protect the cell by up-regulating chaperone synthesis or trigger the apoptosis pathway if the misfolded protein sensor signal is prolonged (Atkin *et al.*, 2006, 2008). However, transgenic animal models have demonstrated that the presence of mutant SOD1 is not necessarily sufficient to cause ALS (Turner & Talbot, 2008). For instance, a transgenic mouse line containing 18 hSOD1^{G93A} transgene copies developed locomotor deficits and paralysis due to gain of toxic function of mutant hSOD1. Conversely, a line mentioned in the same study containing 2-4 hSOD1^{G93A} transgene copies did not show disease symptoms (Gurney *et al.*, 1994).

All of these observations suggest that neither the loss of SOD1 function, nor the gain of mutant SOD1 function is the lone cause of SOD1-mediated toxicity.

SOD1-MEDIATED ALS PATHOLOGY IN THE LIGHT OF OVERALL ALS PATHOLOGY

The pathogenic processes underlying ALS are multifactorial and, at present, it is not fully understood which disease alterations are casual and which are secondary responses. A central question in the field is whether mutations in the diverse causative genes merge on a shared molecular pathway leading to specifically motor neuron death and degeneration. Table 1.1 lists all the causative genes found in fALS patients. At first glance, these genes seem functionally very different from each other. However, when the cellular mechanisms pathologically altered due to these mutations are investigated in detail, and their relationship with mutant SOD1 protein is taken into account (Table 1.2 summarizes the relationship of all the genes implicated in ALS with SOD1), a complex interplay between multiple pathogenic processes appears: (i) protein inclusions and/or dysfunction in the protein quality control machinery, (ii) oxidative stress and mitochondrial dysfunction, (iii) motor neuron death dependent or independent from astrocyte-mediated toxicity, (iv) excitotoxicity, (v) mislocalization of key proteins especially those important in RNA metabolism and their abnormal protein interactions with mutant SOD1 resulting in altered protein expression or transcriptomic changes. This section aims to highlight possible links between known genetic causes of ALS, relating predominantly to mutant SOD1 literature (Table 1.2).

Protein Inclusions

The first signature pathology in SOD1 patients is misfolded and accumulated SOD1 species with phosphorylated neurofilament inclusions (Ince *et al.*, 1998). After identification of other ALS-causing genes such as TARDBP, FUS, C9orf72 and pathological protein aggregates of these mutant proteins, it became clear that ubiquitinated protein inclusions are a cardinal feature of ALS, whether as primary consequences of mutations in the affected proteins such as TARDBP, FUS, SOD1 or as secondary phenomena induced by the underlying disease process as in sALS patients. It is widely believed in the field that the protein content of pathogenic inclusions resulting from SOD1 mutations and the other ALS related mutant proteins are exclusive from each other (Peters *et al.*, 2015), even though studies showing the commonalities between SOD1 versus other ALS associated protein inclusions exists. In fact, SOD1 inclusions are reported in other fALS patients with C9orf72, OPTN, SQSTM1, SigR1, DCTN1, SETX, PRPH mutations and in sALS patients (Larivière *et al.*, 2003; Zhang *et al.*, 2007; Gruzman *et al.*, 2007; Ström *et al.*, 2008; Deng, Bigio, *et al.*, 2011; Keller *et al.*, 2012; Prause *et al.*, 2013), emphasizing the possibility of a common ALS pathway. (Table 1.2)

The report of SOD1 positive proteinaceous inclusions in fALS patients with C9orf72 mutations is especially important because currently pathogenic GGGGCC (G₄C₂) repeat expansions in the C9orf72 locus are the most common cause of ALS (Figure 1.1 and Table 1.1) (Keller *et al.*, 2012). The function of the wild type C9orf72 (chromosome 9 open reading frame 72) is unknown. In 2011, three independent teams discovered hundreds to thousands copies of G₄C₂ expansion in C9orf72 locus in ALS patients, whereas healthy population usually has <33 repeats (DeJesus-Hernandez *et*

al., 2011; Renton *et al.*, 2011; Gijselinck *et al.*, 2012). Most of the G₄C₂ expansion cases are heterozygous for the expanded hexanucleotide allele, however homozygous cases are also present (Fratta *et al.*, 2013; Cooper-Knock *et al.*, 2013). Even though repeat sizes vary between samples from the cerebellum, frontal cortex, and blood; the expansion size in the cerebellum correlates with the disease severity (van Blitterswijk *et al.*, 2013).

Other commonly aggregated proteins in ALS, TDP-43 and FUS share cellular pathology with SOD1 in terms of protein inclusions. Even though TDP-43 inclusions are reported in TDP-43 mutant patients and FUS inclusions are reported in FUS mutant patients with lack of SOD1 aggregation, antibodies specifically detecting for misfolded SOD1 determined that SOD1 is still a key factor in TDP-43 and FUS ALS patients (Pokrishevsky *et al.*, 2012). TDP-43 inclusions are also reported in SOD1 patients (Okamoto *et al.*, 2011), indicating TDP-43 and SOD1 inclusions are not completely exclusive from one another.

The signature of TDP-43 and FUS-mediated ALS, mislocalization of these mutant proteins from nucleus to the cytoplasm is reported in SOD1 mutant ALS patients as well as transgenic SOD1 rodent models (Shan, Vocadlo, & Krieger, 2009; Casas *et al.*, 2013; Miyazaki *et al.*, 2013; Deitch *et al.*, 2014; Sabatelli *et al.*, 2015; Cai *et al.*, 2015). Furthermore, it has been suggested that cytoplasmic TDP-43 directly interacts with mutant SOD1 to promote aggresome formation (Higashi *et al.*, 2010; Somalinga *et al.*, 2012; Xia *et al.*, 2014).

As an expected response to balance the cytoplasmic protein inclusions, ER stress and UPR pathways are activated in ALS pathogenesis (Matus *et al.*, 2013). Implication

of various major players of these pathways, UBQLN2 (Ubiquilin 2), VCP (Valosin containing protein), SQSTM1 (Sequestosome-1 or p62), CHMP2B (Chromatin-modifying protein 2b), VAPB (Vesicle-associated membrane protein-associated protein B), and SigR1 (Sigma non-opioid intracellular receptor 1), stressed the role of protein inclusions in ALS (Shaw, 2010; Deng, Chen, *et al.*, 2011; Teyssou *et al.*, 2013). Furthermore, two of these ALS-causing genes VCP and SQSTM1 have been implied to directly interact with mutant SOD1.

VCP, which is an AAA⁺-ATPase responsible for ubiquitin dependent extraction of substrates for degradation, is proposed to have a role in ubiquitination of misfolded SOD1. VCP colocalizes with Dornfin, which is an E3 ubiquitin ligase shown to interact with mutated SOD1 (Niwa *et al.*, 2002; Ishigaki *et al.*, 2004). Consistent with this, overexpression of Dornfin increases the life span of transgenic G93A mice up to 30 days (Sone *et al.*, 2010). Similarly, mutant SQSTM1 causes early onset and faster progression of ALS by co-aggregating with SOD1 (Gal *et al.*, 2007, 2009; Zhang *et al.*, 2011; Yang & Fan, 2014) (Table 1.2).

Oxidative Stress and Mitochondrial Dysfunction

Mitochondria have a central role in intracellular energy production. Dysfunction of mitochondria, or any kind of imbalance between the generation and removal of reactive oxygen species (ROS) leads to oxidative stress. Even though the consensus in the field is that SOD1 gains a toxic function when mutated in ALS, the loss of the oxidative stress scavenger role has not been ruled out completely, as discussed earlier in this chapter. In most of the ALS animal models, oxidative stress exacerbates the motor

neuron death (Alexander *et al.*, 2004; McGoldrick *et al.*, 2013). In addition to not alleviating cellular stress, mutant SOD1 aggregates in vacuoles in the mitochondrial intermembrane space, leading to organelle dysfunction selectively in the motor neurons (Liu *et al.*, 2004; Vande Velde *et al.*, 2008; Deng, Chen, *et al.*, 2011). There is growing evidence that oxidative stress generation and mitochondrial dysfunction are not specific for SOD1-mediated motor neuron degeneration. In sALS and fALS cases with mutations in TDP-43, PARK7 (Parkinson Protein 7), CHCHD10 (coiled-coil-helix-coiled-coil-helix domain containing 10, a mitochondrial gene with an unknown function implicated in ALS), OMA1 (Overlapping With The M-AAA Protease 1 Homolog, a mitochondrial zinc metallopeptidase), mitochondrial dysfunction and oxidative stress are signatures, leading to oxidized cellular DNA, lipids, and proteins (Bao *et al.*, 2003; Milani *et al.*, 2013; D'Amico *et al.*, 2013; Wang *et al.*, 2013; Magrané *et al.*, 2014) (Table 1.2).

Motor Neuron Death

There is not yet a consensus on whether motor neurons die in ALS through apoptosis, necrosis, or a combination of both (Re *et al.*, 2014; Sanhueza *et al.*, 2015). However, one of the common pathways activated by many ALS-causing genes is apparent from Table 1.2: the nuclear factor- κ B (NF- κ B) pathway, which plays an ancient and key role in innate immunity. The central role of NF- κ B family of transcription factors is to regulate the expression of a wide array of genes involved in various physiological processes, including inflammation and apoptosis. The only interactome study for ALS to date recently investigated transcriptome changes that occur in non-cell autonomous ALS pathogenesis, and it demonstrated the importance of NF- κ B as a master regulator of ALS

(Ikiz *et al.*, 2015). As the name suggests, an interactome study aims to explain the transcriptome changes using the minimum possible number of activated transcription factors. This specific interactome study links all the >600 motor neuron transcriptome changes that occur *in vitro*, upon treatment of motor neurons with SOD1 mutant astrocyte containing medium. As a result, the study underlines the importance of NF- κ B pathway by identifying NF- κ B and 7 other transcription factors as master regulators of ALS, and by inhibiting motor neuron death through induction of chemicals that block NF- κ B activity (Ikiz *et al.*, 2015). Complementing the critical role of NF- κ B in SOD1-mediated ALS, other ALS-implicated genes PLEKHG5 (Pleckstrin homology domain containing family G), TBK1 (TANK-binding kinase 1), OPTN, and SQSTM1 are directly involved in the NF- κ B pathway (Maystadt *et al.*, 2007; Zhu *et al.*, 2007; Nagabhushana, Bansal, & Swarup, 2011; Sako *et al.*, 2012; Akizuki *et al.*, 2013; Abe & Barber, 2014).

Another common mechanism of motor neuron death apparent from Table 1.2 is that astrocytes expressing mutant ALS-causing genes are toxic to motor neurons *in vivo* and *in vitro* (Ilieva, Polymenidou, & Cleveland, 2009; Re *et al.*, 2014). Astrocyte-mediated toxicity is demonstrated from sALS, C9orf72, TDP-43, and DAO patients, as well as SOD1 patients (Haidet-Phillips *et al.*, 2011; Paul & de Belleruche, 2014; Rojas *et al.*, 2014; Meyer *et al.*, 2014) (Table 1.2).

Excitotoxicity

Excitotoxicity, glutamate accumulation in the synapse in the context of ALS, was one of the widely studied aspects of ALS pathogenesis due to apparent glutamate pathology in postmortem tissue analysis from patients with or without SOD1 mutations

or in transgenic animal models with SOD1 mutations (Shaw & Ince, 1997). In fact, the only FDA approved drug for ALS treatment, Riluzole, helps glutamate uptake at the synapse (Miller, Mitchell, & Moore, 2012). However, it is still not clear whether gross glutamate pathology and hyperexcitability of the motor neurons are primary causes or secondary effects of ALS. (Glutamate mediated hyperexcitability is widely discussed in the introduction part of Appendix I.) Weinger and colleagues showed that the excitability of motor neurons is not specific to SOD1 patients. Motor neurons derived from patient iPSCs with C9orf72 and FUS mutations were also hyperexcitable (Wainger *et al.*, 2014).

Misfolded SOD1-specific protein/transcriptome signatures

As new generation sequencing techniques and genome-wide microarray techniques become widely available, it is becoming more and more clear that seemingly unrelated ALS-causing genes bear a common transcriptomic/proteinomic profiles when compared with each other. For instance, two independent groups revealed that C9orf72 and SOD1 patient iPSC derived motor neurons exhibit common aberrant transcriptomes (Donnelly *et al.*, 2013; Kiskinis *et al.*, 2014). A common transcriptomic signature is especially important because for more than a decade, SOD1 was the only known cause of ALS. Other than SOD1, the main genes associated with ALS, namely TDP-43, FUS and C9orf72 expansion repeats, are all related to RNA metabolism by their protein function or by the nature of the repeats. However, how or if SOD1 contributes to RNA pathology was unknown.

Recent studies have aimed at assigning roles for SOD1 other than superoxide scavenging, especially in its mutated forms. One study proposed that mutant SOD1

interacts with cytoplasmic, mislocalized TDP-43 to regulate the stability of neurofilament (NFL) mRNA (Strong *et al.*, 2007; Volkening *et al.*, 2009). In addition, splicing defects are reported in SOD1 transgenic animal models such as neurotoxic splice variant of Peripherin, another ALS-causing gene. This phenotype is predominant in the hSOD1^{G37R} transgenic mouse model (Robertson *et al.*, 2003). Another striking phenomenon that is clear from recent studies is that the expression or protein levels of many ALS-associated genes are altered in SOD1 *in vivo* or *in vitro* systems. For instance, nuclear FUS protein levels are severely reduced in G93A transgenic mice, which is characteristic of FUS mutant systems (Miyazaki *et al.*, 2013).

Expression of wild type forms of various ALS-associated genes increases the life span of SOD1 transgenic mouse models. One example is overexpression of wild type Angiogenin in hSOD1^{G93A} transgenic mice, which results in increased life span and prolonged motor neuron survival (Kieran *et al.*, 2008). On the other hand, loss of wild type forms of some ALS genes, such as Alsin exacerbates motor neuron dysfunction in the hSOD1^{H46R} transgenic mouse model (Hadano *et al.*, 2010). Finally, many ALS-causing genes, such as Chromogranin B, have been demonstrated to interact with only mutant or misfolded SOD1, but not the wild type version (Urushitani *et al.*, 2006).

Table 1.2 summarizes the studies exploring relationships between mutant SOD1 and other ALS causing genes. In addition to these striking mutant SOD1 protein interactions, expected partners of wild type SOD1 were also associated with ALS. PARK7, a copper chaperone acting on SOD1 (Giroto *et al.*, 2014), or TRPM7 (Transient receptor potential cation channel, subfamily M, member 7), a divalent cation

channel that exports Cu^{+2} and Zn^{+2} cations, is required for proper SOD1 folding (Inoue, Branigan, & Xiong, 2010).

CURRENT SOD1-MEDIATED ALS MODEL SYSTEMS

Targeted gene mutagenesis has been used to analyze the phenotypes resulting from specific gene mutations in various genetic models. This has enabled researchers to properly model human diseases in the other organisms. However, because of the high cost, labor intensiveness, and time requirements, targeted mutagenesis has not been widely used to introduce human disease-causing point mutations into the orthologous genes of rodents. Instead, transgenic animals are frequently engineered. In ALS studies, many of these models rely on an exogenously overexpressed mutant protein in a background of the endogenous wild type enzyme. There are few endogenously mutated alleles available in mice, *Drosophila* and dogs, which will be further discussed later in this chapter. Endogenously mutated alleles are critical in our understanding of SOD1 mediated ALS as they mimic the genetic architecture and expression of the human disease as closely as possible.

In current ALS research, transgenic models are usually being studied to understand ALS pathology. Currently, 15 different SOD1 mutations have been used by more than 30 different groups to generate transgenic ALS models in mice, rats, swine *Drosophila melanogaster*, *Caenorhadditis elegans*, zebrafish and *Xenopus laevis* (Trotti *et al.*, 1999; Kato, 2008; Joyce *et al.*, 2011; Chieppa *et al.*, 2014). These groups expressed a mutant transgene containing either hSOD1, mouse SOD1 (mSOD1), rat SOD1 (rSOD1), or zebrafish SOD1 under SOD1-, neuron-, muscle- or astrocyte-specific

promoters (Turner & Talbot, 2008; Joyce *et al.*, 2011). Without a doubt, these transgenic rodent animal models expressing mutant SOD1 under cell type-specific promoters have been important in understanding the non-cell autonomous nature of glial cells and muscle in ALS. The non-cell autonomous basis of ALS is intensively reviewed by Cleveland and colleagues in Ilieva *et al.*, 2009.

Transgenic SOD1 Rodent Models with Intact Endogenous SOD1

Currently, at least 21 mice and 3 rat models of ALS with SOD1 mutations are available (Kato, 2008). Even though these transgenic SOD1 models have variable ages of disease onset and rates of disease progression, they recapitulate many features of ALS, including axonal and mitochondrial dysfunction, progressive neuronal dysfunction, gliosis and motor neuron loss. Considering the fact that different mutations and animal line backgrounds have been used in these transgenic studies, differential onset age and progression is an expected result. However the fact that the ALS phenotype of these animals depends on the transgene expression level is alarming. In all current models, when total (wild type and/or mutant) SOD1 copy number is increased, the disease symptoms become more severe (Alexander *et al.*, 2004; Wang, Farr, Hall, *et al.*, 2009). Thus, whether the ALS-like phenotypes of these models stem from overexpression of the mutant allele or from aspects of the SOD1 mutation itself is not known.

The transgenic G1⁵ mouse line overexpressing hSOD1^{G93A} under the hSOD1 promoter, in addition to the endogenous mSOD1^{wt/wt}, are the most well studied ALS

⁵ The original published name of this line is G1. Later, the G1 line is mentioned as G1H (with ~25 transgene copies) and G1L (with ~18 transgene copies) (Kato, 2008). The

animal model for dissecting the molecular mechanisms of SOD1-mediated ALS. This transgenic line also has been widely used for extensive drug trials. Even though the G93A mutation has little effect on SOD1 enzymatic activity, G93A transgenic mice containing 18-25 hSOD1 transgene copies develop locomotor deficits and paralysis at ~90 days of age and die at ~135 days due to gain of toxic function of mutant hSOD1. However, neither G93A transgenic mice created in the same study with fewer hSOD1^{G93A} transgene copies (2-4), nor hSOD1^{A4V} transgenic mice carrying 3-5 transgene copies developed ALS symptoms (Gurney *et al.*, 1994). Later, low G93A transgene copy mice were naturally generated due to intra-locus recombination events during meiosis. Strikingly, as the transgenic gene copy number is decreased, the disease of onset is delayed and the disease progression slowed (Alexander *et al.*, 2004). Subsequently, another group has extensively analyzed one of the low copy transgenic line SOD1^{G93Adl} (~8 copies of the transgene) and recapitulated all the previously shown ALS-like phenotype in high copy G93A mice, suggesting that this line should be used in the drug trials instead of the high copy one (Acevedo-Arozena *et al.*, 2011).

G85R transgenic mice recapitulated the ALS phenotype similarly to high-copy-number-G93A mice, supposedly with a relatively low amount of mutant protein overexpression. Neuronal and glial SOD1-positive inclusions were first described in the G85R transgenic mice model, in addition to decreased excitatory amino acid transporter 2 (EAAT2), which was targeted by most of the initial drug trials (Bruijn *et al.*, 1997). Bruijn and colleagues reported hSOD1^{G85R} protein levels equivalent to endogenous mSOD1^{wt} based on soluble protein availability on denaturing polyacrylamide gel (SDS-

GIH line is the one that is almost exclusively used in drug trials (McGoldrick *et al.*, 2013).

PAGE) experiments. However, this certainly does not indicate a low copy number of transgene present in G85R transgenic mice model, since the half-life of G85R protein is reported to be relatively low compared to the wild type (Borchelt *et al.*, 1994), and most of the cytoplasmic G85R protein cannot be extracted by regular denaturing buffers since it resides within insoluble complexes (Wang, Farr, Zeiss, *et al.*, 2009). In fact, in a hSOD1^{G85R-YFP} mutant mouse line generated by another group, mice developed ALS only if they were homozygous for the transgene carrying chromosome, each having multiple insertions of 210-300 hSOD1^{G85R-YFP} transgene copies and 592 hSOD1^{wt-YFP} transgene copies (Wang, Farr, Zeiss, *et al.*, 2009).

The same group performed RNA sequencing experiments on laser-dissected motor neuron cell bodies of pre-symptomatic G85R transgenic mice (Bandyopadhyay *et al.*, 2013). In ALS, dendrites are affected initially, rather than the cell bodies. However, there is not currently available a method to isolate motor neuron dendrites. The group specifically concentrated on mRNA processing in order to link SOD1-mediated ALS with other ALS-causing genes functioning in RNA metabolism. Even though they mentioned a small number of transcript changes, and a lack of major disturbances in mRNA processing, they showed two examples of 3'-UTR elongation: Gak and Limk1 mRNAs, both of which do not have a well-characterized neuronal function. The group also compared splicing defects of the G85R transcriptome with previously published results for a knock-down mouse model of another ALS-causing gene, the RNA metabolism gene TDP-43 (Polymenidou *et al.*, 2011), and they reported 8/287 shared abnormal splicing events. In this case, however, the investigators were only testing a cell

autonomous motor neuron model of cell death, and no information was available from other cell types.

Although some of these models recapitulated ALS disease phenotypes, non-matching protein production and variable transgene number raised questions related to the wild type control line used in these studies. In all of the transgenic rodent models, the line used as the control expresses relatively low amounts of wild type hSOD1 and even if the total SOD1 protein amount is equal, there is a huge gap between the inserted transgene number and amounts of protein produced. For instance, in the original G93A mouse model, the characterized line G1 (which is the line that is used almost exclusively in ALS drug screening studies) has almost the same amount of SOD1 protein as the wild type line based on detection by immunoblotting. However, the mutant line has 18 copies of transgene whereas the wild type line has 7 (Gurney *et al.*, 1994). Thus, the comparative analysis of copy number and expression level of control and mutant lines and the wild type lines is not straightforward.

These inconclusive modeling strategies became even more confusing when two groups crossed the hSOD1^{G93A}, hSOD1^{G85R} and hSOD1^{A4V} mice lines with a control line that overexpresses wild type hSOD1 (hSOD1^{wt}). The disease onset of trans-heterozygote hSOD1^{G85R} and hSOD1^{G93A} mice became earlier upon crossing to hSOD1^{wt}, while hSOD1^{A4V} crossed to hSOD1^{wt} mice developed ALS-like symptoms for the first time (Jaarsma *et al.*, 2000; Deng *et al.*, 2006), unlike mice with hSOD1^{A4V} alone (Gurney *et al.*, 1994). Moreover, the same group and another group recapitulated some ALS symptoms such as mitochondrial dysfunction, axon degeneration, and premature motor neuron death and SOD1 aggregation by simply overexpressing hSOD1^{wt} in mice

(Graffmo et al., 2013; Jaarsma et al., 2000). One hypothesis for hSOD1^{wt} overexpression being cytotoxic is that the copper chaperone for SOD (CCS), required for the copper (Cu²⁺) metal binding of the SOD1 monomer, could not compensate for the increased protein amount (Jonsson *et al.*, 2006). Without Cu²⁺ binding, SOD1 cannot fold properly despite lacking mutations and expose sites that are not normally exposed (Son & Elliott, 2014). One example for such exposure is that Derlin-1 and SOD1 interaction. Derlin-1 (Degradation in endoplasmic reticulum protein 1) is an ER membrane protein that can trigger ER-associated degradation (ERAD) pathway. In the correct folded form of SOD1, Derlin-1 binding site is not exposed to the cytoplasm. When misfolded, SOD1 binds to the C-terminal cytoplasmic domain of Derlin-1 and triggers ER stress, which might eventually result in autophagy in the motor neuron (Mori *et al.*, 2011). In addition, the incomplete Cu²⁺-charging of the SOD1 variants also suggests that there is a reduced availability of Cu²⁺ ions in the cytoplasm which might cause adverse effects (Bertinato, Iskandar, & L'Abbé, 2003). Another effect of abundant SOD1 protein in the cytoplasm is overloading of the mitochondrial intermembrane space with SOD1, which is associated with vacuolization and other morphological changes in the mitochondria (Bergemalm *et al.*, 2006) and a phenotype that is seen in hSOD1^{wt} overexpressed mouse line (Jaarsma et al., 2000). Complementarily, it has been shown that oxidative stress can prompt wild type SOD1 protein acquiring toxic properties. In H₂O₂-induced oxidative stress conditions, the oxidized wild type SOD1 can be conjugated with polyubiquitin and can interact with the Hsc70 chaperone as mutant SOD1 does (Ezzi, Urushitani, & Julien, 2007). These unpredicted results brought the focus of the field back to the role of oxidative stress in

gain of toxic SOD1 function because the endogenous wild type SOD1 gene is functional in transgenic models.

Transgenic SOD1 Animal Models in Null SOD1 Background

In order to explore the effect of the endogenous wild type SOD1 gene present in these transgenic models, Cleveland laboratory crossed their hSOD1^{G85R} transgenic line with 15 transgenic copies (expressing the same amount of SOD1 as wild type on immunoblotting) to a mouse line that is null for endogenous SOD1 (mSOD1^{-/-}). Elimination of two copies of the wild type SOD1 protein in the hSOD1^{G85R} overexpression line did not change the overall phenotype of shorter life span, motor neuron death and aggregation (Bruijn *et al.*, 1998). However, it has not further analyzed whether the lack of phenotype change in the transgenic mice in SOD1 null background is due to the extreme overexpression of the mutant protein. A SOD1 null background could potentially induce a mouse line that normally do not develop ALS-like symptoms such as transgenic hSOD1^{A4V} mice (Gurney *et al.*, 1994).

Transgenic SOD1 Models in Other Model Organisms

Unfortunately, ALS modeling in other model organisms has the same limitations as rodent models, since all depend on the overexpression of mutant SOD1 in the presence of the endogenous wild type gene. In *Drosophila*, the traditional Gal4-UAS system has been used extensively to generate transgenic fruit flies. This approach has been successfully employed to drive expression of a number of mutant proteins, including hSOD1, creating a number of *Drosophila* ALS disease models. In one *Drosophila* SOD1-

induced ALS model, hSOD1^{G85R} and hSOD1^{A4V} were driven under a neuron-specific promoter. Although the flies did not have motor neuron loss, they exhibited ALS-like symptoms such as climbing difficulties, defective neural electrophysiology, and ubiquitinated SOD1 aggregates and chaperone response in both motor neurons and glial cells (Watson *et al.*, 2008). In a second *Drosophila* SOD1-induced ALS model, ubiquitous overexpression of zinc-deficient hSOD1^{D83S} resulted in locomotor dysfunction, altered mitochondrial structure and reduced ATP (adenosine triphosphate) levels and sensitivity to paraquat and zinc toxicity (Bahadorani *et al.*, 2013). While tissue specific expression of hSOD1^{D83S} did not alter survival, neuronal and glial-but not muscular- expression resulted in locomotion defect.

Similar to the *Drosophila* models, pan-neuronal hSOD1^{G85R} overexpression in *C. elegans* did not lead to motor neuron death but resulted in locomotor defect, SOD1 aggregation, abnormal presynaptic release (based on chemical sensitivity assays: decelerated paralysis on aldicarb, wild type-like for levamisole) including reduced synaptic vesicles. In the same study, pan-neuronal hSOD1^{H46R} and hSOD1^{H48Q} overexpression resulted in a less severe form of the pan-neuronal hSOD1^{G85R} overexpression phenotype (Wang, Farr, Hall, *et al.*, 2009). Muscle specific hSOD1^{G85R}, hSOD1^{G93A} and hSOD1^{G127X} overexpression also resulted in locomotion defects and SOD1 aggregation in the muscle (Gidalevitz *et al.*, 2009). Ubiquitous expression of hSOD1^{A4V}, hSOD1^{G93A} and hSOD1^{G37R} caused *C. elegans* vulnerability to paraquat-induced oxidative stress and age dependent increase in accumulation of SOD1 aggregates (Oeda, 2001).

Zebrafish expressing zebrafish SOD1 protein containing the G93A mutation under the SOD1 promoter recapitulated the motor neuron loss seen in ALS patients. In addition, mutant zebrafish had motor defects, muscle atrophy and reduced survival rate (Ramesh *et al.*, 2010).

In summary, expression of SOD1 proteins can be utilized to provide toxic insult to neurons in a number of model systems, but it remains unresolved whether the nature of these toxic effects are recapitulating casual human disease mechanisms.

Non-Transgenic SOD1 Animal Models

One aspect of SOD1's enigmatic toxicity that transgenic modeling results demonstrate well is that SOD1 protein dosage plays a critical role in the development of ALS. A more accurate approach that can be used to compare different ALS mutations is to knock in SOD1 mutations where the mutant gene copy number is constant and consistent with wild type controls. Replacing the endogenous gene with the mutant gene ensures consistent and equivalent expression levels by subjecting the mutant gene to the same promoter, enhancer elements, chromatin state, and chromosomal location as the wild type copy. Targeted mutagenesis has not yet been utilized to model ALS in any model organism. The description of a natural mouse strain homozygous or heterozygous for the E77K mutation in the mouse SOD1 gene displayed no apparent phenotypic changes—potentially dissuading researchers from knocking in other SOD1 mutations into the endogenous mSOD1 locus (Luche *et al.*, 1997). However, non-transgenic SOD1 mutants have been isolated and studied as an outcome of random gene mutagenesis in

mice and *Drosophila*, as well as naturally occurring SOD1-mutant dogs with canine degenerative myelopathy that resembles human ALS.

Long before any attempts were made to model ALS in order to study it in the laboratory, dogs were known to develop an ALS like disease: canine degenerative myelopathy (DM). Dogs with DM develop late-onset (~8 years of age) asymmetric paralysis due to degenerative myelopathy. Post-mortem spinal cord analysis from DM dogs exhibited axonal lesions with astrogliosis. DM Dogs did not necessarily develop any motor neuron loss, probably because of early-stage euthanasia, hence early-stage post-mortem analysis. Later, homozygous SOD1 E40K and S18T mutations were linked to DM, making DM dogs potential organisms for ALS study (Awano *et al.*, 2009; Wininger *et al.*, 2011). Naturally mutated residues in dogs are very well conserved in humans and are reportedly mutated to other amino acids in ALS patients at position E40, however the exact missense mutation (E40K) has not been identified yet in humans. These pre-euthanasia animals have not been further studied thus far in the context of ALS. Nevertheless, post-mortem spinal cord tissue revealed SOD1-positive aggregates with gliosis (Awano *et al.*, 2009; Wininger *et al.*, 2011; Crisp *et al.*, 2013; Zeng *et al.*, 2014). It is important to note also that the SOD1 mutations identified in dogs retain full enzymatic capacity (Crisp *et al.*, 2013).

Recently, a group isolated an endogenous SOD1 mutant from a ENU-mediated mouse genetic screen (Joyce *et al.*, 2015): D83G, a mutation that has been found in patients (Millecamps *et al.*, 2010). Homozygous mSOD1^{D83G/D83G} mice retaining no “overall” dismutase activity and very little stable SOD1 protein (detected by SDS-PAGE) die early and display progressive motor and behavioral deficits and loss of muscle force

due to progressive degeneration of lower and upper motor neurons-unlike SOD1 null mice- supporting the gain of toxic function of mutant SOD1 (Joyce *et al.*, 2015). The presence of SOD1-positive proteinaceous inclusions has not been examined in this research.

Similar to the mutagenized mouse model, five lines expressing different dSod1 point mutations have been isolated in *Drosophila*: n108 (dSod1^{G49S}), n145 (exact mutation has not been determined, stock not available), n58 (dSod1^{G83D}), n64 (dSod1^{G42E}), n83 (dSod1^{H69Y}, stock not available⁶) (Campbell, Hilliker, & Phillips, 1986; Phillips *et al.*, 1995). Even though *Drosophila* have a robust neuromuscular system, none of these lines has been characterized in light of ALS pathogenesis. Their “overall” dismutase activity is measured as null in homozygotes and 10-14% in heterozygotes on a gel-based system (Phillips *et al.*, 1995). The n64 allele has been shown to confer shortened life span (<5 days) when it is trans-heterozygous with the n108 allele: dSod1^{G42E /G49S} (O’Keefe *et al.*, 2011). Other than this study, no one has further characterized any of these alleles except the n108 allele: dSod1^{G49S}.

dSod1^{G49S/G49S} flies exhibit a shortened life span (1-3 weeks depending on diet) (Parkes, Kirby, *et al.*, 1998; Rogina & Helfand, 2000; X. Sun *et al.*, 2012), exhibit neurodegeneration in the retina (Phillips *et al.*, 1995), extreme sensitivity to paraquat (Parkes, Kirby, *et al.*, 1998; Kirby *et al.*, 2008) and some other oxidative stress agents such as buthionine sulfoximine, ionizing radiation and hyperoxia (Parkes, Kirby, *et al.*, 1998), vulnerability to DNA damage (Mishra *et al.*, 2014), and decreased eclosion rates (Staveley *et al.*, 1991; Parkes, Kirby, *et al.*, 1998). In addition, homozygous males

⁶ This mutation is the same as the H71Y mutation described in the chapter 2. In Chapter 2, the human SOD1 amino acid numbering system has been kept.

are sterile and females have reduced fertility (Parkes, Kirby, *et al.*, 1998). The survival, fertility and oxidative stress sensitivity defects can be ameliorated by transgenic hSOD1^{wt} expression (Parkes, Kirby, *et al.*, 1998). In addition, ubiquitous expression of bovine SOD1, though claimed expression is only 30% of endogenous dSod1 protein amount based on native-polyacrylamide gel, restores male fertility and oxidative stress sensitivity to normal wild type levels. However, adult survival is only restored to 30% of normal levels, which further strengthens the SOD1 toxic gain of function hypothesis in *Drosophila* (Reveillaud *et al.*, 1994).

Drosophila is a very widely used model organism for testing various chemicals and drugs. The dSod1^{G49S/G49S} line has been also used for longevity studies. A low-calorie diet (X. Sun *et al.*, 2012), a supplemental antioxidant single-celled microalga *Hematococcus pluvialis* (Huangfu *et al.*, 2013) and cranberry anthocyanin extract (Wang *et al.*, 2015) have significantly increased the life span of dSod1^{G49S/G49S} flies.

Furthermore, two groups have combined the dSod1^{G49S} allele with other disease models. Glial expression of dSod1^{G49S} exacerbates an astrocyte-based Alexander disease model in *Drosophila* (L. Wang, Colodner, & Feany, 2011). In humans, Alexander disease is caused by dominant mutations in the gene encoding glial fibrillary acidic protein (GFAP) and is characterized by seizures, demyelination, neurodegeneration, and abnormal aggregation of mutant GFAP in astrocytes. As opposed to Alexander disease, dSod1^{G49S} extends life span of β -amyloid peptide (A β) neuronal expression-based Alzheimer's Disease (Rival *et al.*, 2009). Rival and colleagues proposed that the oxidative stress stemming from the dSod1^{G49S} allele drives A β -plaques to form bigger aggregates as opposed to smaller, soluble toxic aggregates of the A β -plaques.

There is no doubt that these models advanced our understanding of SOD1-mediated ALS, and they fully recapitulated the human ALS phenotype with one major exception: humans develop the disease when they are heterozygous for the mutation, whereas all of these animals seem to require homozygosity for the SOD1 mutation in order to develop disease symptoms. Heterozygous animals seemed healthy in all of the aforementioned non-transgenic disease models, except in 27% of reported cases of canines developing DM as heterozygotes (Zeng *et al.*, 2014). Heterozygous mutant dogs did not display SOD1 accumulation as homozygous mutant dogs did (Nakamae *et al.*, 2015). Given the importance of mutant SOD1 protein dosage in accelerating the ALS-like phenotype in transgenic SOD1-mediated ALS models (Acevedo-Arozena *et al.*, 2011), it is possible that heterozygotes may develop symptoms later in life beyond their life span.

ALS Models with Mutant SOD1 Patient-Derived Induced Pluripotent Stem Cells

Although research on ALS patients is limited to post-mortem tissue and sequencing analyses, reprogramming of somatic cells into induced pluripotent stem cells (iPSCs) provides an opportunity to produce previously inaccessible cell types for disease-related studies. It was not clear whether iPSCs could be generated directly from elderly patient fibroblasts until the laboratory of Kevin Eggan differentiated motor neurons from an 82-year-old ALS patient (Dimos *et al.*, 2008). Since then, iPSCs have been created from fALS patients carrying SOD1, TDP-43, C9orf72, VCP, FUS, FIG4, ANG or VAPB mutations as well as from patients with sALS (Richard & Maragakis, 2014; Li *et al.*, 2015). These iPSCs technically can be differentiated into any ALS-relevant cell

types including motor neurons, astrocytes, and muscle cells among others and can be cultured together in the same dish or alone (Reviewed in (Richard & Maragakis, 2014)).

To advance our knowledge of non-cell autonomous ALS, co-culturing studies have been done with regular neuron and muscle cell lines or neuron and astrocyte cell lines but not with iPSC-derived cell types yet. In fact, to date, mature muscle cells have not been derived from iPSCs. Myogenic progenitors, which can be generated from iPSCs, are too immature to display the full spectrum of characteristics necessary to model a late-onset disease ALS. However, astrocytes, another important cell type in ALS pathogenesis, can be successfully differentiated from patient-derived iPSCs (Serio *et al.*, 2013; Li *et al.*, 2015).

Human embryonic stem cell-derived motor neurons are sensitive to the toxic effect of glial cells overexpressing hSOD1^{G93A} (Di Giorgio *et al.*, 2008) and hSOD1^{G37R} (Marchetto *et al.*, 2008). Unexpectedly, astrocytes derived from TDP-43 patients were not toxic to wild type motor neurons *in vitro* (Serio *et al.*, 2013). Whether this observation was specific to mutations in TDP-43 or specific to the patient genetic background remains to be explored. Astrocytes have been derived from SOD1 mutant patients as well, but have not been investigated in the context of ALS yet (Li *et al.*, 2015). Thus, for the purpose of this introduction, I will summarize the studies done with motor neurons derived from iPSCs from patients with SOD1 mutations.

In 2014, three different groups have independently generated iPSCs from individuals with SOD1 mutations to investigate early pathological events in ALS motor neurons. Chen *et al.*, 2014, with SOD1^{A4V/+} and SOD1^{D90A/+} patient fibroblasts, and Kiskinis *et al.*, 2014, with SOD1^{D90A/+} patient fibroblasts, developed a well-controlled

induced pluripotent motor neuron culture by using isogenic controls through TALEN-mediated genetic correction of the SOD1 mutation. Both groups generated electrophysiologically active motor neuron cultures and recapitulated the progressive nature of the decrease in cell viability observed in humans. Although mutant SOD1 aggregation is thought to be a key molecular event driving neurodegeneration, in these two studies soluble SOD1 protein was extremely low as well as the levels of mutant SOD1 aggregation. This is consistent with the idea that soluble oligomeric forms of mutant SOD1 are indeed the pathogenic species in the early ALS pathology.

Insoluble SOD1 protein detection may also depend on the efficacy of proteostasis mechanism. In Kiskinis *et al.*, 2014, the insoluble SOD1 species were detected only after inhibiting the proteasome. In Chen *et al.*, 2014, SOD1 aggregates were not detectable via immunochemistry. However, very small aggregates were spotted by an extremely sensitive method: immunogold-staining followed by electron microscopy analysis. Chen and colleagues observed that SOD1^{A4V/+} and SOD1^{D90A/+}-mutant motor neurons, but not other types of neurons, have reduced soma size and altered dendritic structure, which was linked to exhibited neurofilament aggregation preceding apoptosis. They have also assigned a new role for mutant SOD1 in neurofilament mRNA stability (Chen *et al.*, 2014). According to this model, misfolded SOD1 binds to the 3' UTR of the neurofilament light chain (*NFL*) mRNA leading to its inaccessibility for other neurofilament subunits. Altered availability of neurofilament subunits then triggers dendrite degeneration followed by apoptosis. Kiskinis and colleagues, on the other hand, characterized transcriptome changes via RNA sequencing from SOD1^{A4V/+}-mutant motor neurons and showed that these motor neurons, but not other types of cells derived from

the same patient, expressed markers of increased oxidative stress, unfolded protein response and endoplasmic reticulum stress, altered cytoskeleton structure and subcellular transportation, as well as increased mitochondria function (Kiskinis *et al.*, 2014). Additionally, they showed that a subset of these transcriptional changes were also present in motor neurons derived from the iPSCs from ALS patients with pathogenic G₄C₂ repeat expansions in the C9orf72 locus. The transcriptome similarity between SOD1^{A4V/+} and C9orf72 repeat expansion patients suggests that these distinct disease-causing mutations act through a common molecular pathway to cause motor neuron degeneration.

In 2013, another group performed a similar comparison. Donnelly and colleagues analyzed transcriptional changes in iPSCs from patients with C9orf72 repeat expansions via microarray analysis (Donnelly *et al.*, 2013). As a comparison, they used motor neurons derived from patients carrying SOD1^{D90A/+} and suggested a common ALS toxicity of SOD1 and C9orf72 repeat expansions. However, they did not characterize SOD1^{D90A/+} motor neurons in detail. Kiskinis and colleagues compared their own SOD1^{A4V/+} RNA sequencing results with Donnelly and colleagues' SOD1^{D90A/+} microarray transcriptome changes. A quarter (357 out of 1489) of the transcript changes were the same (Kiskinis *et al.*, 2014), indicating that even though these different mutations share common pathways leading to ALS toxicity, observed differences in expression may stem from the methodology of choice to analyze transcriptome changes as well as the differential toxicity of SOD1 mutants and patient genome background. The third group chose to study ALS from patient derived iPSCs. Wainger and colleagues demonstrated that membrane hyperexcitability, which is a characteristic feature of ALS, is consistent between the motor neurons derived from patients with SOD1^{A4V/+},

SOD1^{D90V/+}, SOD1^{G85S/+}, C9orf72, and FUS mutations as opposed to motor neurons derived from healthy individuals or in isogenic controls in the SOD1 case (Wainger *et al.*, 2014).

Even though iPSC models are *in vitro* models, they have the unique advantage of a human genetic background. However, patient derived-iPSCs still represent a new method facing a number of technical challenges. It is debatable whether reprogramming is complete in these models in terms of gene expression and DNA methylation. Moreover, the effect of viral induction of the reprogramming cocktails might have a problematic outcome in the disease-modeling step. In addition, this method largely simplifies involvement of other cell types and forces the choice of studying cell-autonomous versus cell-non-autonomous mechanism. As this new technology advances, there is no question that iPSCs will be an excellent complement to *in vivo* animal models and a potentially useful tool for *in vitro* drug screenings and personalized medicine.

A NOVEL *DROSOPHILA* ALS MODEL

Precise Genetic Engineering Through Ends-out Homologous Recombination

Generating a *Drosophila* ALS SOD1 model by homologous recombination (HR) would provide a facile system to address the phenotypic consequences of SOD1 ALS-causing mutations, as well as analyzing levels of SOD1 protein, superoxide dismutase activity and misfolding of SOD1 toxic gain of function mutations contributing to ALS. In addition to the general advantages of a small, quick, and well-established model organism, *Drosophila* is a reasonable organism to specifically knock in ALS-causing

SOD1 point mutations for several reasons. First, SOD1 is a small, well-conserved protein in terms of sequence, structure and function between organisms (Bertini *et al.*, 1998). hSOD1 and *dSod1* differ only at 49/153 residues, and 22 of these different residues have similar side chain chemistry. (Figure 1.2A) Second, overexpression of mutant hSOD1 in *Drosophila* has already recapitulated various ALS- relevant phenotypes (Watson *et al.*, 2008). Third, ends-out homologous recombination, which is identical in concept to the gene replacement techniques used routinely in rodents, is much faster and cheaper in *Drosophila* (Staber *et al.*, 2011).

HR relies on DNA sequence homology and recombination to substitute an engineered mutation into the endogenous allele (Rong & Golic, 2000) (Figure 1.3). The main requirement for HR is an *in vivo* linear template, with enough sequence homology to the endogenous gene to allow exchange between introduced DNA and the corresponding chromosomal locus. Upon a double stranded break, the endogenous DNA repair machinery can utilize this linear template to repair the broken strand. Since the template strand will include a novel mutation in it, the end product will be a precisely mutated form of the endogenous gene. In *Drosophila*, targeted gene mutagenesis requires an extra step, the generation of temporary transgenic animal, because *Drosophila* germ cells have not been cultured yet (Staber *et al.*, 2011). Although HR is a still not a widely used technique in *Drosophila*, many laboratories including ours have used this method to engineer various genes. HR has not widely been used to specifically model human disease in *Drosophila* other than epilepsy (L. Sun *et al.*, 2012; Schutte *et al.*, 2014), but with the advances in CRISPR/Cas9 technology, this is expected to change.

Genetic Screens in the Model Organism *Drosophila melanogaster*

Drosophila, with its conserved nervous system genes and 100,000 neurons, each synapsing about 1000 times, provides a simple but elegant model organism to study human neurodegenerative diseases (Wade, 2010). In addition, the availability of genetic tools that have accumulated since Thomas Hunt Morgan established fruit flies as a genetic model that allows scientists to investigate any complex biological question with various methods, make *Drosophila* an invaluable model organism. *Drosophila* has a very compact genome with ~125 million base pairs of DNA, which corresponds to ~5% of the size of a human genome (Wolf & Rockman, 2011). *Drosophila* is predicted to have ~15,000 genes (Adams *et al.*, 2000). Out of 287 known human disease genes, 197 of them have a homolog in *Drosophila* (St Johnston, 2002).

Certainly there are many advantages of using flies to study complex pathways, diseases, and altered cellular mechanisms in the cell, but maybe one of the strongest advantages of using flies as a model organism is the power to mutagenize a large number of progeny quickly with a 2 week generation time and without ethical concerns. Since the beginning of *Drosophila* research, especially in the pre-genome sequencing era, scientists took advantage of the ability to carry out large-scale genetic screens to identify new genes. Drosophilists mutagenize flies and identify phenotypes based on the numerous external features on the exoskeleton such as bristles, wing veins, and compound eyes. One of the most famous genetic screens in *Drosophila* identified important embryonic development genes and resulted in Edward B. Lewis, Christiane Nüsslein-Volhard and Eric F. Wieschaus receiving a Nobel prize in 1995 (Lewis, 1978; Nüsslein-Volhard & Wieschaus, 1980). Shortly after their discovery, human homologs of these genes were

discovered that contribute in a similar fashion to human embryogenesis. In fact, human genes are often identified after their *Drosophila* homologs are discovered as an outcome of genetic screens.

In the post-genome sequencing era, the focus of genetic screens shifted from identifying new genes to finding modifiers of known genes: either suppressors or enhancers. Today, there are numerous methods of *de novo* induction of DNA changes in *Drosophila* and various ways of screening them. Drosophilists have to design their genetic screens carefully, based on the questions to be answered. Traditional methods such as chemical mutagenesis and irradiation screening might be the fastest and most unbiased way of introducing genetic mutations. However, laborious mapping of mutations and the possibility of background mutations limit the effectiveness of these traditional methods.

On the other hand, newer methods such as deficiency kits or insertion mutagenesis utilizing transposable elements (TE) shorten mapping time tremendously but lose the unbiased power of mutagenesis. For instance, the most common current form of TE mutagenesis screen is the P-element insertion screen. This method is very effective at inducing mutations, which brings the added benefit of molecularly tagging the locus by insertion. As a drawback, P-elements generally target in a very biased way to insert near promoter regions but not inside the coding portion of genes, and thus, mutations generated through P-elements are generally not as disruptive as chemical mutations, an gain-of-function alleles are unlikely (Hummel & Klämbt, 2008). The Piggyback TE inserts in a more unbiased fashion based on a general TTAA sequence specificity, but in this case the TE is more prone to inducing a loss-of-function mutation (Bellen *et*

al., 2011). In contrast, traditional methods based on chemical mutagenesis are capable of introducing gain-of-function mutations as well as loss-of-function mutations.

Ethyl Methanesulfonate (EMS) as a Chemical Mutagenesis Agent

Ethyl methanesulfonate (EMS) is the most commonly used chemical mutagen in *Drosophila* because it is easy to administer and causes the highest frequency of mutations with the lowest possible bias and toxicity. EMS is an alkylating agent that mainly induces single base changes in the genome, which may alter gene function by causing missense or nonsense mutations or altering splice sites (Bökel, 2008). Upon induction, EMS usually adds an alkyl group to Guanine. Alkylated Guanine (O⁶-alkyl-G) acts like Adenine and base pairs with Thymine. Thus the majority (75% to 100%) of the EMS induced mutations are GC to AT transitions (Pastink *et al.*, 1991).

In general, with EMS mutagenesis, the mutation frequency of a gene depends on the size of the gene and is directly proportional to the G content. One can argue that the preference for Guanines by EMS is the only bias of this mutagenesis method. Nevertheless, EMS can cause other types of mutations such as transversions, frameshifts and deletions at much lower frequencies. For instance, the formation of O⁴-ethyl-T by EMS may cause this agent to produce TA to GC transitions. Previous EMS mutagenesis screens convincingly demonstrate the ability of EMS as a potent mutagen (Pastink *et al.*, 1991; Arrizabalaga & Lehmann, 1999; Bentley *et al.*, 2000). In 1999, a genetic screen with 35mM EMS identified 68 *nanos* mutants on the 1661-bp *nanos* transgene that lacks ability to be translationally repressed by *bicoid*, leading to female sterility. In the screen, Arrizabalaga and colleagues selected for sterile females that resulted in the loss of

function of *nanos* (Arrizabalaga & Lehmann, 1999). Among 186,000 chromosomes screened and 68 mutants were isolated: 60 of the mutations were in exons and 8 of them were in introns. 58 of the exonic mutations were single base pair mutations leading to new stop codons, splice sites and missense mutations: 50 GC→AT transitions (expected mutation), 6 AT→TA transversions, and 2 TA→GC transversions were observed. 27 of these mutations created termination codons. In addition to the single base pair changes, a 3bp in-frame deletion and 13bp insertion were recovered. This example demonstrates that EMS is a very effective mutagen. A commonly used EMS concentration of 25mM introduces ~1 mutation every 150-300kb (St Johnston, 2002).

A disadvantage of EMS in the past has been that it was very difficult and laborious to map point mutations to a specific gene. This problem has been partially solved by balancer chromosomes, classic meiotic recombination chromosomes with various markers (mapping chromosomes), single nucleotide polymorphism (SNP) maps, deficiency and duplication kits such as the Pacman BAC system, as well as the availability of Sanger and Next-generation sequencing methods (Martin, Dobi, & St Johnston, 2001; Berger *et al.*, 2001). In 2009, Blumenstiel and colleagues demonstrated that whole genome sequencing has drastically increased the speed of EMS-induced mutation mapping by a single sequencing run from a third-instar larvae. They sequenced 79% of the *Drosophila* genome with at least 8-fold coverage (Blumenstiel *et al.*, 2009).

GENETIC INTERVENTIONS TO MODIFY SOD1 PHENOTYPE IN RODENT MODELS

Mutations in the first ALS-associated gene SOD1 was the most common cause of ALS for 18 years (Rosen *et al.*, 1993), until the discovery of C9orf72 G₄C₂ repeat expansions in 2011 (DeJesus-Hernandez *et al.*, 2011; Renton *et al.*, 2011; Gijssels *et al.*, 2012). Thus, the majority of therapeutic studies have aimed to alleviate ALS pathogenesis in SOD1 mutant rodent models. As mentioned earlier in this chapter, an endogenously mutant mouse line has been generated relatively recently in 2015 (Joyce *et al.*, 2015). Consequently, this mouse line has not been utilized in any drug trials or genetic suppression studies yet; transgenic mouse lines have been used instead. Numerous chemicals aiming to restore the altered cellular pathways discussed earlier in this chapter such as mitochondrial dysfunction, motor neuron death, glutamate excitotoxicity and protein misfolding have been administered to transgenic rodent models and these studies were reviewed previously (McGoldrick *et al.*, 2013). Moreover, suppressor proteins have been proposed to alleviate some of the ALS-like phenotypes and/or result in a moderate amount of life span extension of rodent ALS models that upon ablation or genetic overexpression/delivery via injection. Some of the known genetic suppressors of SOD1 mutant rodent alleles are listed at Table 1.3.

One group of suppressors effective for transgenic SOD1 mice are general neuronal survival factors such as Insulin like Growth Factor (IGF-1), Glial Derived Neurotrophic Factor (GDNF), and Vascular Endothelial Growth Factor (VEGF) (Kaspar, 2003; Azzouz *et al.*, 2004). These factors are usually administered to the mouse spinal cord or muscles via viral delivery or direct injection and they confer moderate life span extension and/or suppression of ALS pathogenesis phenotypes, listed

in Table 1.3. However, it is currently not clear whether their suppression effects are directly related to the disease pathogenesis or are palliative and improve general neuronal health.

Activators of misfolded protein response proteins such as HSP-70, Dorfin, Derlin-1 and Angiogenin have direct targets in known ALS pathogenesis. In fact, Dorfin and Derlin-1 exclusively bind to misfolded mutant SOD1 (Niwa *et al.*, 2002; Sone *et al.*, 2010; Mori *et al.*, 2011). Overexpression of Dorfin, which is an E3 ubiquitin ligase that specifically ubiquitinates mutant SOD1 to promote its degradation (Niwa *et al.*, 2002), leads to life span extension (~30 days) of the transgenic G1 hSOD1^{G93A} mouse line (Sone *et al.*, 2010). Derlin-1 overexpression, on the other hand, activates the ERAD pathway through binding exclusively to the mutant SOD1 and results in decreased motor neuron death in the transgenic G1 hSOD1^{G93A} mouse line (Mori *et al.*, 2011). In agreement with this result, overexpression of another ER stress regulator protein and another ALS-associated protein, Angiogenin, extends life span of the transgenic G1 hSOD1^{G93A} mouse line for ~10days (Kieran *et al.*, 2008).

It is apparent from previously published transcriptome analysis studies performed on ALS patient tissues as well as transgenic mouse lines that expression of various proteins are altered or mislocalized during ALS pathogenesis (Jiang *et al.*, 2005; Wang *et al.*, 2006; Offen *et al.*, 2009; Shan *et al.*, 2009; Kiskinis *et al.*, 2014). As expected, restoring some of these expression changes improves some of the phenotypes exhibited by the transgenic ALS mice. For example, in ALS, the nuclear Survival of Motor Neuron (SMN) protein is reduced significantly (Achsel *et al.*, 2013). Restoring the nuclear SMN protein in ALS transgenic mice, through transgenesis, improves locomotion deficits and

leads to decreased motor neuron death and gliosis, but does not extend the life span (Turner *et al.*, 2014). Conversely, β -amyloid (A β) peptides are highly elevated in ALS patients as well as in ALS transgenic mice (Koistinen *et al.*, 2006). Therefore, depletion of Amyloid Beta Precursor Protein (APP) levels aids to restore locomotion deficits and motor neuron survival in G1 hSOD1^{G93A} mice without extending life span (Bryson *et al.*, 2012). Similar effects have been observed in other ALS-associated cellular pathway components. For example, glutamate excitotoxicity is a signature of ALS pathogenic tissue as discussed earlier in this chapter and in Appendix I. Overexpression of glutamate receptor Excitatory Amino-Acid Transporter 2 (EAAT2) relieves glutamate accumulation in synapses, and as a result improves locomotion and motor neuron survival of G1 hSOD1^{G93A} mice, but does not prolong survival (Guo *et al.*, 2003).

Proteins that modify the ALS-like phenotypes in rodents may be gene products whose human counterparts are potentially involved in the etiology of ALS, SOD1-mediated neurodegeneration, and therefore may be potential targets for drug interventions. As seen in the genetic suppressor examples above and Table 1.3, these therapeutic studies almost exclusively used the G1 hSOD1^{G93A} mouse line that is discussed in detail earlier this chapter, so this mouse line is considered to be the standard model for therapeutic studies for the pathogenesis of ALS. To date, there have been hundreds of publications describing therapeutic agents that extend the life span of this mouse line in moderate amounts, however none of them besides Riluzole has shown corresponding clinical efficacy. Riluzole is the only FDA approved chemical used for ALS patients and is capable of extending life span for 2 months (Miller *et al.*, 2012). It was first described to extend the life span of the G1 hSOD1^{G93A} mouse for 60 days

(Gurney *et al.*, 1996, 1998). Later, ALS Therapy Development Institute (ALS-TDI) revealed that the same dosage of Riluzole did not expand the life span of the same G1 hSOD1^{G93A} mouse line even for a week (Scott *et al.*, 2008). In fact, they re-studied the known therapeutic agents that were previously reported to extend the life span of the G1 hSOD1^{G93A} mouse line and discovered that one third of them resulted in an insignificant life span extension (Scott *et al.*, 2008). Consequently, in 2008 ALS-TDI published a standard guideline regarding therapeutic experiments that utilize the G1 hSOD1^{G93A} mouse line as the experimental subject. Despite these guidelines, 90% of the promising therapeutic agents with the capacity to improve life span or postpone disease onset of transgenic rodent models failed before passing all the tests required for drug trials in actual ALS patients. In rare cases, some chemicals passed all the necessary requirements for a human trial. However, they were eventually shown to have no significant effect on ALS patients (Perrin, 2014).

The main reason for this failure is currently attributed to poorly conducted studies, according to ALS-TDI (Perrin, 2014). However, the overexpression nature of the ALS model organisms and in some cases overexpression of the genetic suppressor tested offer additional potential explanations for the high failure rate of these therapeutic studies. In 2008, another non-profit ALS company Prize4Life launched an ALS Treatment Prize with the ultimate goal of 25% life span extension for G1 hSOD1^{G93A} mouse line. Unfortunately, according to Prize4Life official prize website, despite hundreds of groups competing for this prize, to date no compound tested has demonstrated the ability to prolong lifespan even by 10%. It remains to be explored whether the failure of the compound and the genetic suppression were due to the

disability of the compound itself and whether the extensive overexpression of the mutant allele set an unachievable obstacle. As the endogenously mutant mouse line and other more accurate ALS models, where the disease phenotype is independent from the overexpression level of the allele, are used for future ALS therapeutic studies, the answers of these discrepancies will become clearer.

OPEN QUESTIONS AND CURRENT MOTIVATIONS FOR THIS STUDY

In spite of decades of effort, the casual nature of the sequence of events prominent in ALS pathogenesis remains elusive. In the last decade, increased efforts to pinpoint relevant genes in fALS have revealed many pieces of the ALS puzzle (Table 1.1). Nevertheless, the most obvious question is still: How does mutant SOD1 protein, the first discovered ALS-causing gene, result in motor neuron-specific degeneration? Based on the complex and often conflicting current literature, SOD1-mediated ALS is not a simple gain of toxic function or loss of function disease, because neither the addition of exogenous copy of mutant protein nor the loss of endogenous enzymatic activity necessarily causes full ALS symptoms. The evolving consensus in the field is that the role of oxidative stress is not independent from SOD1 gain of toxic function, because oxidative stress may also induce wild type SOD1 protein to misfold and form toxic aggregates. The only way to test this hypothesis is carefully and accurately comparing effects of same mutant and wild type SOD1 amount *in vivo* in a system where this can also be correlated with organismal phenotype. A non-transgenic animal model allowing such accurate comparison was not utilized to understand ALS pathology until 2015 (Joyce *et al.*, 2015).

Drosophila provides an ideal genetic system, including an elaborate nervous system that allows precise *in vivo* engineering of human disease-causing mutations to model neurodegenerative diseases and provides the unique ability to perform large-scale genetic screens to identify genetic suppressors that alleviate disease states. In this thesis work, in order to evaluate the role of SOD1 pathway in ALS pathogenesis, I have introduced four human disease-causing point mutations (G37R, H48R, G85R and H71Y) into the endogenous *dSod1* locus via ends-out homologous recombination in *Drosophila*. The following chapters of this thesis work augment our understanding of the mechanisms of SOD1 protein and how these processes contribute to ALS pathology. First, I have studied *dSod1* mutant flies for altered cellular mechanisms in ALS (Chapter 2). Next, I have taken an unbiased approach to understand the ALS disease state in *Drosophila* by performing a detailed expression profile from *dSod1* mutants using deep sequencing technologies (Chapter 3). Lastly, I have performed a large-scale genetic screen aiming to identify suppressors to reverse lethality resulting from severe ALS mutations in *Drosophila* (Chapter 4). This thesis work demonstrates a major step forward in our understanding of the molecular mechanisms and suppressors of mutant SOD1 when a precisely controlled system is studied.

REFERENCES

- ABE, T. & BARBER, G.N. (2014) Cytosolic-DNA-Mediated, STING-Dependent Proinflammatory Gene Induction Necessitates Canonical NF- κ B Activation through TBK1. *Journal of Virology* **88**, 5328–5341.
- ABEL, O., POWELL, J.F., ANDERSEN, P.M. & AL-CHALABI, A. (2012) ALSod: A user-friendly online bioinformatics tool for amyotrophic lateral sclerosis genetics. *Human mutation* **33**, 1345–1351.
- ACEVEDO-AROZENA, A., KALMAR, B., ESSA, S., RICKETTS, T., JOYCE, P., KENT, R., ROWE, C., PARKER, A., GRAY, A., HAFEZPARAST, M., THORPE, J.R., GREENSMITH, L. & FISHER, E.M.C. (2011) A comprehensive assessment of the SOD1G93A low-copy transgenic mouse, which models human amyotrophic lateral sclerosis. *Disease models & mechanisms* **4**, 686–700.
- ACHSEL, T., BARABINO, S., COZZOLINO, M. & CARRI, M.T. (2013) The intriguing case of motor neuron disease: ALS and SMA come closer. *Biochemical Society transactions* **41**, 1593–1597.
- ADAMS, M.D., CELNIKER, S.E., HOLT, R.A., EVANS, C.A., GOCAYNE, J.D., AMANATIDES, P.G., ET AL. (2000) The genome sequence of *Drosophila melanogaster*. *Science (New York, N.Y.)* **287**, 2185–2195.
- AKIZUKI, M., YAMASHITA, H., UEMURA, K., MARUYAMA, H., KAWAKAMI, H., ITO, H. & TAKAHASHI, R. (2013) Optineurin suppression causes neuronal cell death via NF- κ B pathway. *Journal of neurochemistry* **126**, 699–704.
- ALEXANDER, G.M., ERWIN, K.L., BYERS, N., DEITCH, J.S., AUGELLI, B.J., BLANKENHORN, E.P. & HEIMAN-PATTERSON, T.D. (2004) Effect of transgene copy number on survival in the G93A SOD1 transgenic mouse model of ALS. *Brain research. Molecular brain research* **130**, 7–15.
- ANDERSEN, P.M., NILSSON, P., ALA-HURULA, V., KERÄNEN, M.L., TARVAINEN, I., HALTIA, T., NILSSON, L., BINZER, M., FORSGREN, L. & MARKLUND, S.L. (1995) Amyotrophic lateral sclerosis associated with homozygosity for an Asp90Ala mutation in CuZn-superoxide dismutase. *Nature genetics* **10**, 61–66.
- ARRIZABALAGA, G. & LEHMANN, R. (1999) A Selective Screen Reveals Discrete Functional Domains in *Drosophila* Nanos. *Genetics* **153**, 1825–1838.
- ATKIN, J.D., FARG, M.A., TURNER, B.J., TOMAS, D., LYSAGHT, J.A., NUNAN, J., REMBACH, A., NAGLEY, P., BEART, P.M., CHEEMA, S.S. & HORNE, M.K. (2006) Induction of the unfolded protein response in familial amyotrophic lateral sclerosis and association of protein-disulfide isomerase with superoxide dismutase 1. *The Journal of biological chemistry* **281**, 30152–30165.
- ATKIN, J.D., FARG, M.A., WALKER, A.K., MCLEAN, C., TOMAS, D. & HORNE, M.K. (2008) Endoplasmic reticulum stress and induction of the unfolded protein response in human sporadic amyotrophic lateral sclerosis. *Neurobiology of disease* **30**, 400–407.
- AWANO, T., JOHNSON, G.S., WADE, C.M., KATZ, M.L., JOHNSON, G.C., TAYLOR, J.F., PERLOSKI, M., BIAGI, T., BARANOWSKA, I., LONG, S., MARCH, P.A., OLBY, N.J., SHELTON, G.D., KHAN, S., O'BRIEN, D.P., LINDBLAD-TOH, K. & COATES, J.R. (2009) Genome-wide association analysis reveals a SOD1 mutation in canine degenerative myelopathy that resembles amyotrophic lateral sclerosis. *Proceedings of the National Academy of Sciences of the United States of America* **106**, 2794–2799.

- AYERS, J.I., FROMHOLT, S., KOCH, M., DEBOSIER, A., MCMAHON, B., XU, G. & BORCHELT, D.R. (2014) Experimental transmissibility of mutant SOD1 motor neuron disease. *Acta neuropathologica* **128**, 791–803.
- AZZOUZ, M., RALPH, G.S., STORKEBAUM, E., WALMSLEY, L.E., MITROPHANOUS, K.A., KINGSMAN, S.M., CARMELIET, P. & MAZARAKIS, N.D. (2004) VEGF delivery with retrogradely transported lentivector prolongs survival in a mouse ALS model. *Nature* **429**, 413–417.
- BAHADORANI, S., MUKAI, S.T., RABIE, J., BECKMAN, J.S., PHILLIPS, J.P. & HILLIKER, A.J. (2013) Expression of zinc-deficient human superoxide dismutase in *Drosophila* neurons produces a locomotor defect linked to mitochondrial dysfunction. *Neurobiology of aging* **34**, 2322–2330.
- BANDYOPADHYAY, U., COTNEY, J., NAGY, M., OH, S., LENG, J., MAHAJAN, M., MANE, S., FENTON, W.A., NOONAN, J.P. & HORWICH, A.L. (2013) RNA-Seq profiling of spinal cord motor neurons from a presymptomatic SOD1 ALS mouse. *PloS one* **8**, e53575.
- BANDYOPADHYAY, U., NAGY, M., FENTON, W.A. & HORWICH, A.L. (2014) Absence of lipofuscin in motor neurons of SOD1-linked ALS mice. *Proceedings of the National Academy of Sciences of the United States of America* **111**, 11055–11060.
- BAO, Y.-C., TSURUGA, H., HIRAI, M., YASUDA, K., YOKOI, N., KITAMURA, T. & KUMAGAI, H. (2003) Identification of a human cDNA sequence which encodes a novel membrane-associated protein containing a zinc metalloprotease motif. *DNA research : an international journal for rapid publication of reports on genes and genomes* **10**, 123–128.
- BASSO, M., POZZI, S., TORTAROLO, M., FIORDALISO, F., BISIGHINI, C., PASETTO, L., SPALTRO, G., LIDONNICI, D., GENSANO, F., BATTAGLIA, E., BENDOTTI, C. & BONETTO, V. (2013) Mutant copper-zinc superoxide dismutase (SOD1) induces protein secretion pathway alterations and exosome release in astrocytes: implications for disease spreading and motor neuron pathology in amyotrophic lateral sclerosis. *The Journal of biological chemistry* **288**, 15699–15711.
- BELLEN, H.J., LEVIS, R.W., HE, Y., CARLSON, J.W., EVANS-HOLM, M., BAE, E., KIM, J., METAXAKIS, A., SAVAKIS, C., SCHULZE, K.L., HOSKINS, R.A. & SPRADLING, A.C. (2011) The *Drosophila* gene disruption project: progress using transposons with distinctive site specificities. *Genetics* **188**, 731–743.
- BENSIMON, G., LACOMBLEZ, L. & MEININGER, V. (1994) A controlled trial of riluzole in amyotrophic lateral sclerosis. ALS/Riluzole Study Group. *The New England journal of medicine* **330**, 585–591.
- BENTLEY, A., MACLENNAN, B., CALVO, J. & DEAROLF, C.R. (2000) Targeted Recovery of Mutations in *Drosophila*. *Genetics* **156**, 1169–1173.
- BERGEMALM, D., JONSSON, P.A., GRAFFMO, K.S., ANDERSEN, P.M., BRÄNNSTRÖM, T., REHNMARK, A. & MARKLUND, S.L. (2006) Overloading of stable and exclusion of unstable human superoxide dismutase-1 variants in mitochondria of murine amyotrophic lateral sclerosis models. *The Journal of neuroscience : the official journal of the Society for Neuroscience* **26**, 4147–4154.
- BERGER, J., SUZUKI, T., SENTI, K.A., STUBBS, J., SCHAFFNER, G. & DICKSON, B.J. (2001) Genetic mapping with SNP markers in *Drosophila*. *Nature genetics* **29**, 475–481.
- BERTINATO, J., ISKANDAR, M. & L'ABBÉ, M.R. (2003) Copper deficiency induces the upregulation of the copper chaperone for Cu/Zn superoxide dismutase in weanling male rats. *The Journal of nutrition* **133**, 28–31.

- BERTINI, I., MANGANL, S. & VIEZZOLI, M.S. (1998) Structure and Properties of Copper-Zinc Superoxide Dismutases. *Advances in Inorganic Chemistry* **45**, 127–250. Elsevier.
- BILEN, J. & BONINI, N.M. (2005) Drosophila as a model for human neurodegenerative disease. *Annual review of genetics* **39**, 153–171.
- VAN BLITTERSWIJK, M., DEJESUS-HERNANDEZ, M., NIEMANTSVERDRIET, E., MURRAY, M.E., HECKMAN, M.G., DIEHL, N.N., ET AL. (2013) Association between repeat sizes and clinical and pathological characteristics in carriers of C9ORF72 repeat expansions (Xpansize-72): a cross-sectional cohort study. *The Lancet. Neurology* **12**, 978–988.
- BLUMENSTIEL, J.P., NOLL, A.C., GRIFFITHS, J. A, PERERA, A.G., WALTON, K.N., GILLILAND, W.D., HAWLEY, R.S. & STAEHLING-HAMPTON, K. (2009) Identification of EMS-induced mutations in *Drosophila melanogaster* by whole-genome sequencing. *Genetics* **182**, 25–32.
- BÖKEL, C. (2008) EMS screens : from mutagenesis to screening and mapping. *Methods in molecular biology (Clifton, N.J.)* **420**, 119–138.
- BORCHELT, D.R., LEE, M.K., SLUNT, H.S., GUARNIERI, M., XU, Z.S., WONG, P.C., BROWN, R.H., PRICE, D.L., SISODIA, S.S. & CLEVELAND, D.W. (1994) Superoxide dismutase 1 with mutations linked to familial amyotrophic lateral sclerosis possesses significant activity. *Proceedings of the National Academy of Sciences of the United States of America* **91**, 8292–8296.
- BOSCO, D.A., MORFINI, G., KARABACAK, N.M., SONG, Y., GROS-LOUIS, F., PASINELLI, P., GOOLSBY, H., FONTAINE, B.A., LEMAY, N., MCKENNA-YASEK, D., FROSCH, M.P., AGAR, J.N., JULIEN, J.-P., BRADY, S.T. & BROWN, R.H. (2010) Wild-type and mutant SOD1 share an aberrant conformation and a common pathogenic pathway in ALS. *Nature neuroscience* **13**, 1396–1403.
- BROWN, R.H. (1998) SOD1 aggregates in ALS: cause, correlate or consequence? *Nature medicine* **4**, 1362–1364.
- BRUIJN, L.I., BECHER, M.W., LEE, M.K., ANDERSON, K.L., JENKINS, N. A, COPELAND, N.G., SISODIA, S.S., ROTHSTEIN, J.D., BORCHELT, D.R., PRICE, D.L. & CLEVELAND, D.W. (1997) ALS-linked SOD1 mutant G85R mediates damage to astrocytes and promotes rapidly progressive disease with SOD1-containing inclusions. *Neuron* **18**, 327–338.
- BRUIJN, L.I., HOUSEWEART, M.K., KATO, S., ANDERSON, K.L., ANDERSON, S.D., OHAMA, E., REAUME, A.G., SCOTT, R.W. & CLEVELAND, D.W. (1998) Aggregation and motor neuron toxicity of an ALS-linked SOD1 mutant independent from wild-type SOD1. *Science (New York, N.Y.)* **281**, 1851–1854.
- BRYSON, J.B., HOBBS, C., PARSONS, M.J., BOSCH, K.D., PANDRAUD, A., WALSH, F.S., DOHERTY, P. & GREENSMITH, L. (2012) Amyloid precursor protein (APP) contributes to pathology in the SOD1(G93A) mouse model of amyotrophic lateral sclerosis. *Human molecular genetics* **21**, 3871–3882.
- BUNTON-STASYSHYN, R.K.A., SACCON, R.A., FRATTA, P. & FISHER, E.M.C. (2014) SOD1 Function and Its Implications for Amyotrophic Lateral Sclerosis Pathology: New and Renascent Themes. *The Neuroscientist : a review journal bringing neurobiology, neurology and psychiatry*.
- CAI, M., LEE, K.-W., CHOI, S.-M. & YANG, E.J. (2015) TDP-43 modification in the hSOD1(G93A) amyotrophic lateral sclerosis mouse model. *Neurological research* **37**, 253–262.

- CAMPBELL, S.D., HILLIKER, A.J. & PHILLIPS, J.P. (1986) Cytogenetic analysis of the cSOD microregion in *Drosophila melanogaster*. *Genetics* **112**, 205–215.
- CARDONA, A.E., PIORO, E.P., SASSE, M.E., KOSTENKO, V., CARDONA, S.M., DIJKSTRA, I.M., HUANG, D., KIDD, G., DOMBROWSKI, S., DUTTA, R., LEE, J.-C., COOK, D.N., JUNG, S., LIRA, S.A., LITTMAN, D.R. & RANSOHOFF, R.M. (2006) Control of microglial neurotoxicity by the fractalkine receptor. *Nature neuroscience* **9**, 917–924. Nature Publishing Group.
- CASAS, C., HERRANDO-GRABULOSA, M., MANZANO, R., MANCUSO, R., OSTA, R. & NAVARRO, X. (2013) Early presymptomatic cholinergic dysfunction in a murine model of amyotrophic lateral sclerosis. *Brain and behavior* **3**, 145–158.
- CASCI, I. & PANDEY, U.B. (2015) A fruitful endeavor: modeling ALS in the fruit fly. *Brain research* **1607**, 47–74.
- CHEN, H., QIAN, K., DU, Z., CAO, J., PETERSEN, A., LIU, H., BLACKBOURN, L.W., HUANG, C.-L., ERRIGO, A., YIN, Y., LU, J., AYALA, M. & ZHANG, S.-C. (2014) Modeling ALS with iPSCs reveals that mutant SOD1 misregulates neurofilament balance in motor neurons. *Cell stem cell* **14**, 796–809.
- CHIA, R., TATTUM, M.H., JONES, S., COLLINGE, J., FISHER, E.M.C. & JACKSON, G.S. (2010) Superoxide dismutase 1 and tgSOD1 mouse spinal cord seed fibrils, suggesting a propagative cell death mechanism in amyotrophic lateral sclerosis. *PloS one* **5**, e10627.
- CHIEPPA, M.N., PEROTA, A., CORONA, C., GRINDATTO, A., LAGUTINA, I., VALLINO COSTASSA, E., LAZZARI, G., COLLEONI, S., DUCHI, R., LUCCHINI, F., CARAMELLI, M., BENDOTTI, C., GALLI, C. & CASALONE, C. (2014) Modeling amyotrophic lateral sclerosis in hSOD1 transgenic swine. *Neuro-degenerative diseases* **13**, 246–254.
- CHITI, F. & DOBSON, C.M. (2006) Protein misfolding, functional amyloid, and human disease. *Annual review of biochemistry* **75**, 333–366.
- COOPER-KNOCK, J., HIGGINBOTTOM, A., CONNOR-ROBSON, N., BAYATTI, N., BURY, J.J., KIRBY, J., NINKINA, N., BUCHMAN, V.L. & SHAW, P.J. (2013) C9ORF72 transcription in a frontotemporal dementia case with two expanded alleles. *Neurology* **81**, 1719–1721.
- CORSON, L.B., STRAIN, J.J., CULOTTA, V.C. & CLEVELAND, D.W. (1998) Chaperone-facilitated copper binding is a property common to several classes of familial amyotrophic lateral sclerosis-linked superoxide dismutase mutants. *Proceedings of the National Academy of Sciences of the United States of America* **95**, 6361–6366.
- CRISP, M.J., BECKETT, J., COATES, J.R. & MILLER, T.M. (2013) Canine degenerative myelopathy: biochemical characterization of superoxide dismutase 1 in the first naturally occurring non-human amyotrophic lateral sclerosis model. *Experimental neurology* **248**, 1–9.
- D'AMICO, E., FACTOR-LITVAK, P., SANTELLA, R.M. & MITSUMOTO, H. (2013) Clinical perspective on oxidative stress in sporadic amyotrophic lateral sclerosis. *Free radical biology & medicine* **65**, 509–527.
- DADON-NACHUM, M., MELAMED, E. & OFFEN, D. (2011) The 'dying-back' phenomenon of motor neurons in ALS. *Journal of molecular neuroscience : MN* **43**, 470–477.
- DEBATTISTI, V. & SCORRANO, L. (2013) *D. melanogaster*, mitochondria and neurodegeneration: small model organism, big discoveries. *Molecular and cellular neurosciences* **55**, 77–86.

- DEITCH, J.S., ALEXANDER, G.M., BENSINGER, A., YANG, S., JIANG, J.T. & HEIMAN-PATTERSON, T.D. (2014) Phenotype of transgenic mice carrying a very low copy number of the mutant human G93A superoxide dismutase-1 gene associated with amyotrophic lateral sclerosis. *PloS one* **9**, e99879.
- DEIVASIGAMANI, S., VERMA, H.K., UEDA, R., RATNAPARKHI, A. & RATNAPARKHI, G.S. (2014) A genetic screen identifies Tor as an interactor of VAPB in a *Drosophila* model of amyotrophic lateral sclerosis. *Biology open* **3**, 1127–1138.
- DEJESUS-HERNANDEZ, M., MACKENZIE, I.R., BOEVE, B.F., BOXER, A.L., BAKER, M., RUTHERFORD, N.J., ET AL. (2011) Expanded GGGGCC hexanucleotide repeat in noncoding region of C9ORF72 causes chromosome 9p-linked FTD and ALS. *Neuron* **72**, 245–256.
- DENG, H.-X., BIGIO, E.H., ZHAI, H., FECTO, F., AJROUD, K., SHI, Y., YAN, J., MISHRA, M., AJROUD-DRISS, S., HELLER, S., SUFIT, R., SIDDIQUE, N., MUGNAINI, E. & SIDDIQUE, T. (2011) Differential involvement of optineurin in amyotrophic lateral sclerosis with or without SOD1 mutations. *Archives of neurology* **68**, 1057–1061.
- DENG, H.-X., CHEN, W., HONG, S.-T., BOYCOTT, K.M., GORRIE, G.H., SIDDIQUE, N., ET AL. (2011) Mutations in UBQLN2 cause dominant X-linked juvenile and adult-onset ALS and ALS/dementia. *Nature* **477**, 211–215.
- DENG, H.-X., SHI, Y., FURUKAWA, Y., ZHAI, H., FU, R., LIU, E., GORRIE, G.H., KHAN, M.S., HUNG, W.-Y., BIGIO, E.H., LUKAS, T., DAL CANTO, M.C., O'HALLORAN, T. V & SIDDIQUE, T. (2006) Conversion to the amyotrophic lateral sclerosis phenotype is associated with intermolecular linked insoluble aggregates of SOD1 in mitochondria. *Proceedings of the National Academy of Sciences of the United States of America* **103**, 7142–7147.
- DIMOS, J.T., RODOLFA, K.T., NIAKAN, K.K., WEISENTHAL, L.M., MITSUMOTO, H., CHUNG, W., CROFT, G.F., SAPHIER, G., LEIBEL, R., GOLAND, R., WICHTERLE, H., HENDERSON, C.E. & EGGAN, K. (2008) Induced pluripotent stem cells generated from patients with ALS can be differentiated into motor neurons. *Science (New York, N.Y.)* **321**, 1218–1221.
- DONNELLY, C.J., ZHANG, P.-W., PHAM, J.T., HAEUSLER, A.R., HEUSLER, A.R., MISTRY, N.A., ET AL. (2013) RNA toxicity from the ALS/FTD C9ORF72 expansion is mitigated by antisense intervention. *Neuron* **80**, 415–428. Elsevier.
- ELLIOTT, J.L. (2001) Zinc and copper in the pathogenesis of amyotrophic lateral sclerosis. *Progress in neuro-psychopharmacology & biological psychiatry* **25**, 1169–1185.
- EZZI, S.A., URUSHITANI, M. & JULIEN, J.-P. (2007) Wild-type superoxide dismutase acquires binding and toxic properties of ALS-linked mutant forms through oxidation. *Journal of neurochemistry* **102**, 170–178.
- FORSBERG, K., JONSSON, P.A., ANDERSEN, P.M., BERGEMALM, D., GRAFFMO, K.S., HULTDIN, M., JACOBSSON, J., ROSQUIST, R., MARKLUND, S.L. & BRÄNNSTRÖM, T. (2010) Novel antibodies reveal inclusions containing non-native SOD1 in sporadic ALS patients. *PloS one* **5**, e11552.
- FRATTA, P., POULTER, M., LASHLEY, T., ROHRER, J.D., POLKE, J.M., BECK, J., ET AL. (2013) Homozygosity for the C9orf72 GGGGCC repeat expansion in frontotemporal dementia. *Acta neuropathologica* **126**, 401–409.

- FUKADA, Y., YASUI, K., KITAYAMA, M., DOI, K., NAKANO, T., WATANABE, Y. & NAKASHIMA, K. (2007) Gene expression analysis of the murine model of amyotrophic lateral sclerosis: studies of the Leu126delTT mutation in SOD1. *Brain research* **1160**, 1–10.
- FUKAI, T. & USHIO-FUKAI, M. (2011) Superoxide dismutases: role in redox signaling, vascular function, and diseases. *Antioxidants & redox signaling* **15**, 1583–1606.
- GAL, J., STRÖM, A.-L., KILTY, R., ZHANG, F. & ZHU, H. (2007) p62 accumulates and enhances aggregate formation in model systems of familial amyotrophic lateral sclerosis. *The Journal of biological chemistry* **282**, 11068–11077.
- GAL, J., STRÖM, A.-L., KWINTER, D.M., KILTY, R., ZHANG, J., SHI, P., FU, W., WOOTEN, M.W. & ZHU, H. (2009) Sequestosome 1/p62 links familial ALS mutant SOD1 to LC3 via an ubiquitin-independent mechanism. *Journal of neurochemistry* **111**, 1062–1073.
- GIDALEVITZ, T., KRUPINSKI, T., GARCIA, S. & MORIMOTO, R.I. (2009) Destabilizing protein polymorphisms in the genetic background direct phenotypic expression of mutant SOD1 toxicity. *PLoS genetics* **5**, e1000399.
- GIFONDORWA, D.J., ROBINSON, M.B., HAYES, C.D., TAYLOR, A.R., PREVETTE, D.M., OPPENHEIM, R.W., CARESS, J. & MILLIGAN, C.E. (2007) Exogenous delivery of heat shock protein 70 increases lifespan in a mouse model of amyotrophic lateral sclerosis. *The Journal of neuroscience : the official journal of the Society for Neuroscience* **27**, 13173–13180.
- GIJSELINCK, I., VAN LANGENHOVE, T., VAN DER ZEE, J., SLEEGERS, K., PHILTJENS, S., KLEINBERGER, G., ET AL. (2012) A C9orf72 promoter repeat expansion in a Flanders-Belgian cohort with disorders of the frontotemporal lobar degeneration-amyotrophic lateral sclerosis spectrum: a gene identification study. *The Lancet. Neurology* **11**, 54–65.
- DI GIORGIO, F.P., BOULTING, G.L., BOBROWICZ, S. & EGGAN, K.C. (2008) Human embryonic stem cell-derived motor neurons are sensitive to the toxic effect of glial cells carrying an ALS-causing mutation. *Cell stem cell* **3**, 637–648. Elsevier.
- GIROTTO, S., CENDRON, L., BISAGLIA, M., TESSARI, I., MAMMI, S., ZANOTTI, G. & BUBACCO, L. (2014) DJ-1 is a copper chaperone acting on SOD1 activation. *The Journal of biological chemistry* **289**, 10887–10899.
- GRAD, L.I. & CASHMAN, N.R. (2014) Prion-like activity of Cu/Zn superoxide dismutase: Implications for amyotrophic lateral sclerosis. *Prion* **8**, 1–9.
- GRUZMAN, A., WOOD, W.L., ALPERT, E., PRASAD, M.D., MILLER, R.G., ROTHSTEIN, J.D., BOWSER, R., HAMILTON, R., WOOD, T.D., CLEVELAND, D.W., LINGAPPA, V.R. & LIU, J. (2007) Common molecular signature in SOD1 for both sporadic and familial amyotrophic lateral sclerosis. *Proceedings of the National Academy of Sciences of the United States of America* **104**, 12524–12529.
- GUO, H., LAI, L., BUTCHBACH, M.E.R., STOCKINGER, M.P., SHAN, X., BISHOP, G.A. & LIN, C.G. (2003) Increased expression of the glial glutamate transporter EAAT2 modulates excitotoxicity and delays the onset but not the outcome of ALS in mice. *Human molecular genetics* **12**, 2519–2532.
- GURNEY, M.E., CUTTING, F.B., ZHAI, P., DOBLE, A., TAYLOR, C.P., ANDRUS, P.K. & HALL, E.D. (1996) Benefit of vitamin E, riluzole, and gabapentin in a transgenic model of familial amyotrophic lateral sclerosis. *Annals of neurology* **39**, 147–157.

- GURNEY, M.E., FLECK, T.J., HIMES, C.S. & HALL, E.D. (1998) Riluzole preserves motor function in a transgenic model of familial amyotrophic lateral sclerosis. *Neurology* **50**, 62–66.
- GURNEY, M.E., PU, H., CHIU, A Y., DAL CANTO, M.C., POLCHOW, C.Y., ALEXANDER, D.D., CALIENDO, J., HENTATI, A, KWON, Y.W. & DENG, H.X. (1994) Motor neuron degeneration in mice that express a human Cu,Zn superoxide dismutase mutation. *Science (New York, N.Y.)* **264**, 1772–1775.
- HADANO, S., OTOMO, A., KUNITA, R., SUZUKI-UTSUNOMIYA, K., AKATSUKA, A., KOIKE, M., AOKI, M., UCHIYAMA, Y., ITOYAMA, Y. & IKEDA, J.-E. (2010) Loss of ALS2/Alsin exacerbates motor dysfunction in a SOD1-expressing mouse ALS model by disturbing endolysosomal trafficking. *PLoS one* **5**, e9805.
- HAIDET-PHILLIPS, A.M., HESTER, M.E., MIRANDA, C.J., MEYER, K., BRAUN, L., FRAKES, A., SONG, S., LIKHTE, S., MURTHA, M.J., FOUST, K.D., RAO, M., EAGLE, A., KAMMESHEIDT, A., CHRISTENSEN, A., MENDELL, J.R., BURGHEES, A.H.M. & KASPAR, B.K. (2011) Astrocytes from familial and sporadic ALS patients are toxic to motor neurons. *Nature biotechnology* **29**, 824–828. Nature Publishing Group, a division of Macmillan Publishers Limited. All Rights Reserved.
- HIGASHI, S., TSUCHIYA, Y., ARAKI, T., WADA, K. & KABUTA, T. (2010) TDP-43 physically interacts with amyotrophic lateral sclerosis-linked mutant CuZn superoxide dismutase. *Neurochemistry international* **57**, 906–913.
- HO, Y.S., GARGANO, M., CAO, J., BRONSON, R.T., HEIMLER, I. & HUTZ, R.J. (1998) Reduced fertility in female mice lacking copper-zinc superoxide dismutase. *The Journal of biological chemistry* **273**, 7765–7769.
- HUANG, T.T., YASUNAMI, M., CARLSON, E.J., GILLESPIE, A.M., REAUME, A.G., HOFFMAN, E.K., CHAN, P.H., SCOTT, R.W. & EPSTEIN, C.J. (1997) Superoxide-mediated cytotoxicity in superoxide dismutase-deficient fetal fibroblasts. *Archives of biochemistry and biophysics* **344**, 424–432.
- HUANGFU, J., LIU, J., SUN, Z., WANG, M., JIANG, Y., CHEN, Z.-Y. & CHEN, F. (2013) Antiaging effects of astaxanthin-rich alga *Haematococcus pluvialis* on fruit flies under oxidative stress. *Journal of agricultural and food chemistry* **61**, 7800–7804. American Chemical Society.
- HUMMEL, T. & KLÄMBT, C. (2008) P-element mutagenesis. *Methods in molecular biology (Clifton, N.J.)* **420**, 97–117.
- IKIZ, B., ALVAREZ, M.J., RÉ, D.B., LE VERCHE, V., POLITI, K., LOTTI, F., PHANI, S., PRADHAN, R., YU, C., CROFT, G.F., JACQUIER, A., HENDERSON, C.E., CALIFANO, A. & PRZEDBORSKI, S. (2015) The Regulatory Machinery of Neurodegeneration in In Vitro Models of Amyotrophic Lateral Sclerosis. *Cell reports*.
- ILIEVA, H., POLYMENIDOU, M. & CLEVELAND, D.W. (2009) Non-cell autonomous toxicity in neurodegenerative disorders: ALS and beyond. *The Journal of cell biology* **187**, 761–772.
- INCE, P.G., TOMKINS, J., SLADE, J.Y., THATCHER, N.M. & SHAW, P.J. (1998) Amyotrophic lateral sclerosis associated with genetic abnormalities in the gene encoding Cu/Zn superoxide dismutase: molecular pathology of five new cases, and comparison with previous reports and 73 sporadic cases of ALS. *Journal of neuropathology and experimental neurology* **57**, 895–904.
- INOUE, K., BRANIGAN, D. & XIONG, Z.-G. (2010) Zinc-induced neurotoxicity mediated by transient receptor potential melastatin 7 channels. *The Journal of biological chemistry* **285**, 7430–7439.

- ISHIGAKI, S., HISHIKAWA, N., NIWA, J., IEMURA, S., NATSUME, T., HORI, S., KAKIZUKA, A., TANAKA, K. & SOBUE, G. (2004) Physical and functional interaction between Dornin and Valosin-containing protein that are colocalized in ubiquitylated inclusions in neurodegenerative disorders. *The Journal of biological chemistry* **279**, 51376–51385.
- JAARSMA, D., HAASDIJK, E.D., GRASHORN, J. A., HAWKINS, R., VAN DUIJN, W., VERSPAGET, H.W., LONDON, J. & HOLSTEGE, J.C. (2000) Human Cu/Zn superoxide dismutase (SOD1) overexpression in mice causes mitochondrial vacuolization, axonal degeneration, and premature motoneuron death and accelerates motoneuron disease in mice expressing a familial amyotrophic lateral sclerosis mutant SO. *Neurobiology of disease* **7**, 623–643.
- JIANG, Y.-M., YAMAMOTO, M., KOBAYASHI, Y., YOSHIHARA, T., LIANG, Y., TERAOKA, S., TAKEUCHI, H., ISHIGAKI, S., KATSUNO, M., ADACHI, H., NIWA, J., TANAKA, F., DOYU, M., YOSHIDA, M., HASHIZUME, Y. & SOBUE, G. (2005) Gene expression profile of spinal motor neurons in sporadic amyotrophic lateral sclerosis. *Annals of neurology* **57**, 236–251.
- JONSSON, P.A., GRAFFMO, K.S., ANDERSEN, P.M., BRÄNNSTRÖM, T., LINDBERG, M., OLIVEBERG, M. & MARKLUND, S.L. (2006) Disulphide-reduced superoxide dismutase-1 in CNS of transgenic amyotrophic lateral sclerosis models. *Brain : a journal of neurology* **129**, 451–464.
- JOYCE, P.I., FRATTA, P., FISHER, E.M.C. & ACEVEDO-AROZENA, A. (2011) SOD1 and TDP-43 animal models of amyotrophic lateral sclerosis: recent advances in understanding disease toward the development of clinical treatments. *Mammalian genome : official journal of the International Mammalian Genome Society* **22**, 420–448.
- JOYCE, P.I., MCGOLDRICK, P., SACCON, R.A., WEBER, W., FRATTA, P., WEST, S.J., ET AL. (2015) A novel SOD1-ALS mutation separates central and peripheral effects of mutant SOD1 toxicity. *Human molecular genetics* **24**, 1883–1897.
- KANEKURA, K., HASHIMOTO, Y., NIKURA, T., AISO, S., MATSUOKA, M. & NISHIMOTO, I. (2004) Alsin, the product of ALS2 gene, suppresses SOD1 mutant neurotoxicity through RhoGEF domain by interacting with SOD1 mutants. *The Journal of biological chemistry* **279**, 19247–19256.
- KASPAR, B.K. (2003) Retrograde Viral Delivery of IGF-1 Prolongs Survival in a Mouse ALS Model. *Science* **301**, 839–842.
- KATO, S. (2008) Amyotrophic lateral sclerosis models and human neuropathology: similarities and differences. *Acta neuropathologica* **115**, 97–114.
- KELLER, B.A., VOLKENING, K., DRÖPPELMANN, C.A., ANG, L.C., RADEMAKERS, R. & STRONG, M.J. (2012) Co-aggregation of RNA binding proteins in ALS spinal motor neurons: evidence of a common pathogenic mechanism. *Acta neuropathologica* **124**, 733–747.
- KIERAN, D., SEBASTIA, J., GREENWAY, M.J., KING, M.A., CONNAUGHTON, D., CONCANNON, C.G., FENNER, B., HARDIMAN, O. & PREHN, J.H.M. (2008) Control of motoneuron survival by angiogenin. *The Journal of neuroscience : the official journal of the Society for Neuroscience* **28**, 14056–14061.
- KIRBY, K., JENSEN, L.T., BINNINGTON, J., HILLIKER, A.J., ULLOA, J., CULOTTA, V.C. & PHILLIPS, J.P. (2008) Instability of superoxide dismutase 1 of *Drosophila* in mutants deficient for its cognate copper chaperone. *The Journal of biological chemistry* **283**, 35393–35401.

- KISKINIS, E., SANDOE, J., WILLIAMS, L.A., BOULTING, G.L., MOCCIA, R., WAINGER, B.J., ET AL. (2014) Pathways disrupted in human ALS motor neurons identified through genetic correction of mutant SOD1. *Cell stem cell* **14**, 781–795.
- KNIPPENBERG, S., SIPOS, J., THAU-HABERMANN, N., KÖRNER, S., RATH, K.J., DENGLER, R. & PETRI, S. (2013) Altered expression of DJ-1 and PINK1 in sporadic ALS and in the SOD1(G93A) ALS mouse model. *Journal of neuropathology and experimental neurology* **72**, 1052–1061.
- KOISTINEN, H., PRINJHA, R., SODEN, P., HARPER, A., BANNER, S.J., PRADAT, P.-F., LOEFFLER, J.-P. & DINGWALL, C. (2006) Elevated levels of amyloid precursor protein in muscle of patients with amyotrophic lateral sclerosis and a mouse model of the disease. *Muscle & nerve* **34**, 444–450.
- KONSOLAKI, M. (2013) Fruitful research: drug target discovery for neurodegenerative diseases in *Drosophila*. *Expert opinion on drug discovery* **8**, 1503–1513.
- KUŹMA-KOZAKIEWICZ, M., CHUDY, A., KAŹMIERCZAK, B., DZIEWULSKA, D., USAREK, E. & BARAŃCZYK-KUŹMA, A. (2013) Dynactin Deficiency in the CNS of Humans with Sporadic ALS and Mice with Genetically Determined Motor Neuron Degeneration. *Neurochemical research*.
- LACOMBLEZ, L., BENSIMON, G., LEIGH, P.N., GUILLET, P. & MEININGER, V. (1996) Dose-ranging study of riluzole in amyotrophic lateral sclerosis. Amyotrophic Lateral Sclerosis/Riluzole Study Group II. *Lancet* **347**, 1425–1431.
- LARIVIÈRE, R.C., BEAULIEU, J.-M., NGUYEN, M.D. & JULIEN, J.-P. (2003) Peripherin is not a contributing factor to motor neuron disease in a mouse model of amyotrophic lateral sclerosis caused by mutant superoxide dismutase. *Neurobiology of disease* **13**, 158–166.
- LEBLOND, C.S., KANEH, H.M., DION, P. A & ROULEAU, G. A (2014) Dissection of genetic factors associated with amyotrophic lateral sclerosis. *Experimental Neurology*.
- LEWIS, E.B. (1978) A gene complex controlling segmentation in *Drosophila*. *Nature* **276**, 565–570.
- LI, Q., SPENCER, N.Y., PANTAZIS, N.J. & ENGELHARDT, J.F. (2011) Alsin and SOD1(G93A) proteins regulate endosomal reactive oxygen species production by glial cells and proinflammatory pathways responsible for neurotoxicity. *The Journal of biological chemistry* **286**, 40151–40162.
- LI, Y., BALASUBRAMANIAN, U., COHEN, D., ZHANG, P.-W., MOSMILLER, E., SATTLER, R., MARAGAKIS, N.J. & ROTHSTEIN, J.D. (2015) A comprehensive library of familial human amyotrophic lateral sclerosis induced pluripotent stem cells. *PloS one* **10**, e0118266. Public Library of Science.
- LIU, J., LILLO, C., JONSSON, P.A., VANDE VELDE, C., WARD, C.M., MILLER, T.M., SUBRAMANIAM, J.R., ROTHSTEIN, J.D., MARKLUND, S., ANDERSEN, P.M., BRÄNNSTRÖM, T., GREDEL, O., WONG, P.C., WILLIAMS, D.S. & CLEVELAND, D.W. (2004) Toxicity of familial ALS-linked SOD1 mutants from selective recruitment to spinal mitochondria. *Neuron* **43**, 5–17.
- LU, L., WANG, S., ZHENG, L., LI, X., SUSWAM, E.A., ZHANG, X., WHEELER, C.G., NABORS, L.B., FILIPPOVA, N. & KING, P.H. (2009) Amyotrophic lateral sclerosis-linked mutant SOD1 sequesters Hu antigen R (HuR) and TIA-1-related protein (TIAR): implications for impaired post-transcriptional regulation of vascular endothelial growth factor. *The Journal of biological chemistry* **284**, 33989–33998.
- LU, L., ZHENG, L., VIERA, L., SUSWAM, E., LI, Y., LI, X., ESTÉVEZ, A.G. & KING, P.H. (2007) Mutant Cu/Zn-superoxide dismutase associated with amyotrophic lateral sclerosis destabilizes vascular

- endothelial growth factor mRNA and downregulates its expression. *The Journal of neuroscience : the official journal of the Society for Neuroscience* **27**, 7929–7938.
- LUCHE, R.M., MAIWALD, R., CARLSON, E.J. & EPSTEIN, C.J. (1997) Novel mutations in an otherwise strictly conserved domain of CuZn superoxide dismutase. *Molecular and cellular biochemistry* **168**, 191–194.
- LUIGETTI, M., LATTANTE, S., ZOLLINO, M., CONTE, A., MARANGI, G., DEL GRANDE, A. & SABATELLI, M. (2011) SOD1 G93D sporadic amyotrophic lateral sclerosis (SALS) patient with rapid progression and concomitant novel ANG variant. *Neurobiology of aging* **32**, 1924.e15–e18.
- MAGRANÉ, J., CORTEZ, C., GAN, W.-B. & MANFREDI, G. (2014) Abnormal mitochondrial transport and morphology are common pathological denominators in SOD1 and TDP43 ALS mouse models. *Human molecular genetics* **23**, 1413–1424.
- MANCUSO, R., OLIVÁN, S., RANDO, A., CASAS, C., OSTA, R. & NAVARRO, X. (2012) Sigma-1R agonist improves motor function and motoneuron survival in ALS mice. *Neurotherapeutics : the journal of the American Society for Experimental NeuroTherapeutics* **9**, 814–826.
- MARCHETTO, M.C.N., MUOTRI, A.R., MU, Y., SMITH, A.M., CEZAR, G.G. & GAGE, F.H. (2008) Non-cell-autonomous effect of human SOD1 G37R astrocytes on motor neurons derived from human embryonic stem cells. *Cell stem cell* **3**, 649–657. Elsevier.
- MARIN, E.P., DERAKHSHAN, B., LAM, T.T., DAVALOS, A. & SESSA, W.C. (2012) Endothelial cell palmitoylproteomic identifies novel lipid-modified targets and potential substrates for protein acyl transferases. *Circulation research* **110**, 1336–1344.
- MARTIN, S.G., DOBI, K.C. & ST JOHNSTON, D. (2001) A rapid method to map mutations in Drosophila. *Genome biology* **2**, RESEARCH0036.
- MATUS, S., VALENZUELA, V., MEDINAS, D.B. & HETZ, C. (2013) ER Dysfunction and Protein Folding Stress in ALS. *International journal of cell biology* **2013**, 674751.
- MATZUK, M.M., DIONNE, L., GUO, Q., KUMAR, T.R. & LBOVITZ, R.M. (1998) Ovarian function in superoxide dismutase 1 and 2 knockout mice. *Endocrinology* **139**, 4008–4011.
- MAYSTADT, I., REZSÓHAZY, R., BARKATS, M., DUQUE, S., VANNUFFEL, P., REMACLE, S., LAMBERT, B., NAJIMI, M., SOKAL, E., MUNNICH, A., VIOLLET, L. & VERELLEN-DUMOULIN, C. (2007) The nuclear factor kappaB-activator gene PLEKHG5 is mutated in a form of autosomal recessive lower motor neuron disease with childhood onset. *American journal of human genetics* **81**, 67–76.
- MCCORD, J.M. & FRIDOVICH, I. (1969) Superoxide dismutase. An enzymic function for erythrocyte hemocuprein. *The Journal of biological chemistry* **244**, 6049–6055.
- MCGOLDRICK, P., JOYCE, P.I., FISHER, E.M.C. & GREENSMITH, L. (2013) Rodent models of amyotrophic lateral sclerosis. *Biochimica et biophysica acta* **1832**, 1421–1436.
- MCGUIRE, V. & NELSON, L.M. (2006) Epidemiology of ALS. In *Amyotrophic Lateral Sclerosis* (ed G.P. MITSUMOTO H, PRZEDBORSKI S), pp. 17–41, 1st edition. Taylor and Francis, New York.
- MEYER, K., FERRAIUOLO, L., MIRANDA, C.J., LIKHTE, S., MCELROY, S., RENUSCH, S., DITSWORTH, D., LAGIER-TOURENNE, C., SMITH, R.A., RAVITS, J., BURGHESE, A.H., SHAW, P.J., CLEVELAND, D.W., KOLB, S.J. & KASPAR, B.K. (2014) Direct conversion of patient fibroblasts demonstrates non-cell

- autonomous toxicity of astrocytes to motor neurons in familial and sporadic ALS. *Proceedings of the National Academy of Sciences of the United States of America* **111**, 829–832.
- MILANI, P., AMBROSI, G., GAMMOH, O., BLANDINI, F. & CEREDA, C. (2013) SOD1 and DJ-1 converge at Nrf2 pathway: a clue for antioxidant therapeutic potential in neurodegeneration. *Oxidative medicine and cellular longevity* **2013**, 836760.
- MILLECAMPS, S., SALACHAS, F., CAZENEUVE, C., GORDON, P., BRICKA, B., CAMUZAT, A., ET AL. (2010) SOD1, ANG, VAPB, TARDBP, and FUS mutations in familial amyotrophic lateral sclerosis: genotype-phenotype correlations. *Journal of medical genetics* **47**, 554–560.
- MILLER, R.G., BOUCHARD, J.P., DUQUETTE, P., EISEN, A., GELINAS, D., HARATI, Y., MUNSAT, T.L., POWE, L., ROTHSTEIN, J., SALZMAN, P. & SUFIT, R.L. (1996) Clinical trials of riluzole in patients with ALS. ALS/Riluzole Study Group-II. *Neurology* **47**, S86–S90; discussion S90–S92.
- MILLER, R.G., MITCHELL, J.D. & MOORE, D.H. (2012) Riluzole for amyotrophic lateral sclerosis (ALS)/motor neuron disease (MND). *The Cochrane database of systematic reviews* **3**, CD001447.
- MISHRA, M., SHARMA, A., SHUKLA, A.K., KUMAR, R., DWIVEDI, U.N. & KAR CHOWDHURI, D. (2014) Genotoxicity of dichlorvos in strains of *Drosophila melanogaster* defective in DNA repair. *Mutation research. Genetic toxicology and environmental mutagenesis* **766**, 35–41.
- MISSIRLIS, F., HU, J., KIRBY, K., HILLIKER, A.J., ROUAULT, T.A. & PHILLIPS, J.P. (2003) Compartment-specific protection of iron-sulfur proteins by superoxide dismutase. *The Journal of biological chemistry* **278**, 47365–47369.
- MITSUMOTO, H. (2001) The Clinical features and prognosis in ALS. In *Amyotrophic Lateral Sclerosis: A Guide for Patients and Families* (eds H. MITSUMOTO & MUNSAT THEODORE L.), p. 27, 2nd edition. Demos, New York.
- MIAZAKI, K., YAMASHITA, T., MORIMOTO, N., SATO, K., MIMOTO, T., KURATA, T., IKEDA, Y. & ABE, K. (2013) Early and selective reduction of NOP56 (Asidan) and RNA processing proteins in the motor neuron of ALS model mice. *Neurological research* **35**, 744–754.
- MOCKETT, R.J., RADYUK, S.N., BENES, J.J., ORR, W.C. & SOHAL, R.S. (2003) Phenotypic effects of familial amyotrophic lateral sclerosis mutant Sod alleles in transgenic *Drosophila*. *Proceedings of the National Academy of Sciences of the United States of America* **100**, 301–306.
- MORI, A., YAMASHITA, S., UCHINO, K., SUGA, T., IKEDA, T., TAKAMATSU, K., ISHIZAKI, M., KOIDE, T., KIMURA, E., MITA, S., MAEDA, Y., HIRANO, T. & UCHINO, M. (2011) Derlin-1 overexpression ameliorates mutant SOD1-induced endoplasmic reticulum stress by reducing mutant SOD1 accumulation. *Neurochemistry international* **58**, 344–353.
- MÜNCH, C., O'BRIEN, J. & BERTOLOTTI, A. (2011) Prion-like propagation of mutant superoxide dismutase-1 misfolding in neuronal cells. *Proceedings of the National Academy of Sciences of the United States of America* **108**, 3548–3553.
- MUQIT, M.M.K. & FEANY, M.B. (2002) Modelling neurodegenerative diseases in *Drosophila*: a fruitful approach? *Nature reviews. Neuroscience* **3**, 237–243.
- NAGABHUSHANA, A., BANSAL, M. & SWARUP, G. (2011) Optineurin is required for CYLD-dependent inhibition of TNF α -induced NF- κ B activation. *PLoS one* **6**, e17477.

- NAKAMAE, S., KOBATAKE, Y., SUZUKI, R., TSUKUI, T., KATO, S., YAMATO, O., SAKAI, H., URUSHITANI, M., MAEDA, S. & KAMISHINA, H. (2015) Accumulation and aggregate formation of mutant superoxide dismutase 1 in canine degenerative myelopathy. *Neuroscience*.
- NAKAMURA, K., KIMPLE, A.J., SIDEROVSKI, D.P. & JOHNSON, G.L. (2010) PB1 domain interaction of p62/sequestosome 1 and MEKK3 regulates NF-kappaB activation. *The Journal of biological chemistry* **285**, 2077–2089.
- NARDO, G., IENACO, R., FUSI, N., HEATH, P.R., MARINO, M., TROLESE, M.C., FERRAIUOLO, L., LAWRENCE, N., SHAW, P.J. & BENDOTTI, C. (2013) Transcriptomic indices of fast and slow disease progression in two mouse models of amyotrophic lateral sclerosis. *Brain : a journal of neurology* **136**, 3305–3332.
- NG, A.S.L., RADEMAKERS, R. & MILLER, B.L. (2015) Frontotemporal dementia: a bridge between dementia and neuromuscular disease. *Annals of the New York Academy of Sciences* **1338**, 71–93.
- NIWA, J.-I., ISHIGAKI, S., HISHIKAWA, N., YAMAMOTO, M., DOYU, M., MURATA, S., TANAKA, K., TANIGUCHI, N. & SOBUE, G. (2002) Dornin ubiquitylates mutant SOD1 and prevents mutant SOD1-mediated neurotoxicity. *The Journal of biological chemistry* **277**, 36793–36798.
- NÜSSLEIN-VOLHARD, C. & WIESCHAUS, E. (1980) Mutations affecting segment number and polarity in *Drosophila*. *Nature* **287**, 795–801.
- O'KEEFE, L. V., COLELLA, A., DAYAN, S., CHEN, Q., CHOO, A., JACOB, R., PRICE, G., VENTER, D. & RICHARDS, R.I. (2011) *Drosophila* orthologue of WWOX, the chromosomal fragile site FRA16D tumour suppressor gene, functions in aerobic metabolism and regulates reactive oxygen species. *Human molecular genetics* **20**, 497–509.
- O'TOOLE, O., TRAYNOR, B.J., BRENNAN, P., SHEEHAN, C., FROST, E., CORR, B. & HARDIMAN, O. (2008) Epidemiology and clinical features of amyotrophic lateral sclerosis in Ireland between 1995 and 2004. *Journal of neurology, neurosurgery, and psychiatry* **79**, 30–32.
- OEDA, T. (2001) Oxidative stress causes abnormal accumulation of familial amyotrophic lateral sclerosis-related mutant SOD1 in transgenic *Caenorhabditis elegans*. *Human Molecular Genetics* **10**, 2013–2023.
- OFFEN, D., BARHUM, Y., MELAMED, E., EMBACHER, N., SCHINDLER, C. & RANSMAYR, G. (2009) Spinal cord mRNA profile in patients with ALS: comparison with transgenic mice expressing the human SOD-1 mutant. *Journal of molecular neuroscience : MN* **38**, 85–93.
- OKAMOTO, Y., IHARA, M., URUSHITANI, M., YAMASHITA, H., KONDO, T., TANIGAKI, A., OONO, M., KAWAMATA, J., IKEMOTO, A., KAWAMOTO, Y., TAKAHASHI, R. & ITO, H. (2011) An autopsy case of SOD1-related ALS with TDP-43 positive inclusions. *Neurology* **77**, 1993–1995.
- PARDO, C.A., XU, Z., BORCHELT, D.R., PRICE, D.L., SISODIA, S.S. & CLEVELAND, D.W. (1995) Superoxide dismutase is an abundant component in cell bodies, dendrites, and axons of motor neurons and in a subset of other neurons. *Proceedings of the National Academy of Sciences of the United States of America* **92**, 954–958.
- PARKES, T.L., ELIA, A.J., DICKINSON, D., HILLIKER, A.J., PHILLIPS, J.P. & BOULIANNE, G.L. (1998) Extension of *Drosophila* lifespan by overexpression of human SOD1 in motorneurons. *Nature genetics* **19**, 171–174.

- PARKES, T.L., KIRBY, K., PHILLIPS, J.P. & HILLIKER, A.J. (1998) Transgenic analysis of the cSOD-null phenotypic syndrome in *Drosophila*. *Genome / National Research Council Canada = Génome / Conseil national de recherches Canada* **41**, 642–651.
- PASINELLI, P. & BROWN, R.H. (2006) Molecular biology of amyotrophic lateral sclerosis: insights from genetics. *Nature reviews. Neuroscience* **7**, 710–723.
- PASTINK, A., HEEMSKERK, E., NIVARD, M.J., VAN VLIET, C.J. & VOGEL, E.W. (1991) Mutational specificity of ethyl methanesulfonate in excision-repair-proficient and -deficient strains of *Drosophila melanogaster*. *Molecular & general genetics : MGG* **229**, 213–218.
- PAUL, P. & DE BELLEROCHE, J. (2014) The role of D-serine and glycine as co-agonists of NMDA receptors in motor neuron degeneration and amyotrophic lateral sclerosis (ALS). *Frontiers in synaptic neuroscience* **6**, 10.
- PERRIN, S. (2014) Preclinical research: Make mouse studies work. *Nature* **507**, 423–425.
- PETERS, O.M., GHASEMI, M. & BROWN, R.H. (2015) Emerging mechanisms of molecular pathology in ALS. *The Journal of clinical investigation* **125**, 1767–1779.
- PHILLIPS, J.P., CAMPBELL, S.D., MICHAUD, D., CHARBONNEAU, M. & HILLIKER, A.J. (1989) Null mutation of copper/zinc superoxide dismutase in *Drosophila* confers hypersensitivity to paraquat and reduced longevity. *Proceedings of the National Academy of Sciences of the United States of America* **86**, 2761–2765.
- PHILLIPS, J.P., TAINER, J.A., GETZOFF, E.D., BOULIANNE, G.L., KIRBY, K. & HILLIKER, A.J. (1995) Subunit-destabilizing mutations in *Drosophila* copper/zinc superoxide dismutase: neuropathology and a model of dimer dysequilibrium. *Proceedings of the National Academy of Sciences of the United States of America* **92**, 8574–8578.
- POKRISHEVSKY, E., GRAD, L.I., YOUSEFI, M., WANG, J., MACKENZIE, I.R. & CASHMAN, N.R. (2012) Aberrant localization of FUS and TDP43 is associated with misfolding of SOD1 in amyotrophic lateral sclerosis. *PloS one* **7**, e35050.
- POLYMENIDOU, M., LAGIER-TOURENNE, C., HUTT, K.R., HUELGA, S.C., MORAN, J., LIANG, T.Y., LING, S.-C., SUN, E., WANCEWICZ, E., MAZUR, C., KORDASIEWICZ, H., SEDAGHAT, Y., DONOHUE, J.P., SHIUE, L., BENNETT, C.F., YEO, G.W. & CLEVELAND, D.W. (2011) Long pre-mRNA depletion and RNA missplicing contribute to neuronal vulnerability from loss of TDP-43. *Nature neuroscience* **14**, 459–468.
- PRAUSE, J., GOSWAMI, A., KATONA, I., ROOS, A., SCHNIZLER, M., BUSHUVEN, E., DREIER, A., BUCHKREMER, S., JOHANN, S., BEYER, C., DESCHAUER, M., TROOST, D. & WEIS, J. (2013) Altered localization, abnormal modification and loss of function of Sigma receptor-1 in amyotrophic lateral sclerosis. *Human molecular genetics* **22**, 1581–1600.
- RAJAN, A. & PERRIMON, N. (2013) Of flies and men: insights on organismal metabolism from fruit flies. *BMC biology* **11**, 38.
- RAMESH, T., LYON, A.N., PINEDA, R.H., WANG, C., JANSSEN, P.M.L., CANAN, B.D., BURGHEES, A.H.M. & BEATTIE, C.E. (2010) A genetic model of amyotrophic lateral sclerosis in zebrafish displays phenotypic hallmarks of motoneuron disease. *Disease models & mechanisms* **3**, 652–662.

- RATOVITSKI, T., CORSON, L.B., STRAIN, J., WONG, P., CLEVELAND, D.W., CULOTTA, V.C. & BORCHELT, D.R. (1999) Variation in the biochemical/biophysical properties of mutant superoxide dismutase 1 enzymes and the rate of disease progression in familial amyotrophic lateral sclerosis kindreds. *Human molecular genetics* **8**, 1451–1460.
- RE, D.B., LE VERCHE, V., YU, C., AMOROSO, M.W., POLITI, K.A., PHANI, S., IKIZ, B., HOFFMANN, L., KOOLEN, M., NAGATA, T., PAPADIMITRIOU, D., NAGY, P., MITSUMOTO, H., KARIYA, S., WICHTERLE, H., HENDERSON, C.E. & PRZEDBORSKI, S. (2014) Necroptosis drives motor neuron death in models of both sporadic and familial ALS. *Neuron* **81**, 1001–1008. Elsevier.
- REA, S.L., WALSH, J.P., WARD, L., YIP, K., WARD, B.K., KENT, G.N., STEER, J.H., XU, J. & RATAJCZAK, T. (2006) A novel mutation (K378X) in the sequestosome 1 gene associated with increased NF-kappaB signaling and Paget's disease of bone with a severe phenotype. *Journal of bone and mineral research : the official journal of the American Society for Bone and Mineral Research* **21**, 1136–1145.
- REAUME, A.G., ELLIOTT, J.L., HOFFMAN, E.K., KOWALL, N.W., FERRANTE, R.J., SIWEK, D.F., WILCOX, H.M., FLOOD, D.G., BEAL, M.F., BROWN, R.H., SCOTT, R.W. & SNIDER, W.D. (1996) Motor neurons in Cu/Zn superoxide dismutase-deficient mice develop normally but exhibit enhanced cell death after axonal injury. *Nature genetics* **13**, 43–47.
- RENTON, A.E., MAJOUNIE, E., WAITE, A., SIMÓN-SÁNCHEZ, J., ROLLINSON, S., GIBBS, J.R., ET AL. (2011) A hexanucleotide repeat expansion in C9ORF72 is the cause of chromosome 9p21-linked ALS-FTD. *Neuron* **72**, 257–268.
- REVEILLAUD, I., PHILLIPS, J., DUYF, B., HILLIKER, A., KONGPACHITH, A. & FLEMING, J.E. (1994) Phenotypic rescue by a bovine transgene in a Cu/Zn superoxide dismutase-null mutant of *Drosophila melanogaster*. *Molecular and cellular biology* **14**, 1302–1307.
- RICHARD, J.-P. & MARAGAKIS, N.J. (2014) Induced pluripotent stem cells from ALS patients for disease modeling. *Brain Research* **1607**, 15–25.
- RIVAL, T., PAGE, R.M., CHANDRARATNA, D.S., SENDALL, T.J., RYDER, E., LIU, B., LEWIS, H., ROSAHL, T., HIDER, R., CAMARGO, L.M., SHEARMAN, M.S., CROWTHER, D.C. & LOMAS, D.A. (2009) Fenton chemistry and oxidative stress mediate the toxicity of the beta-amyloid peptide in a *Drosophila* model of Alzheimer's disease. *The European journal of neuroscience* **29**, 1335–1347.
- ROBERTSON, J., DOROUDCHI, M.M., NGUYEN, M.D., DURHAM, H.D., STRONG, M.J., SHAW, G., JULIEN, J.-P. & MUSHYNSKI, W.E. (2003) A neurotoxic peripherin splice variant in a mouse model of ALS. *The Journal of cell biology* **160**, 939–949.
- ROGINA, B. & HELFAND, S.L. (2000) Cu, Zn superoxide dismutase deficiency accelerates the time course of an age-related marker in *Drosophila melanogaster*. *Biogerontology* **1**, 163–169.
- ROJAS, F., CORTES, N., ABARZUA, S., DYRDA, A. & VAN ZUNDERT, B. (2014) Astrocytes expressing mutant SOD1 and TDP43 trigger motoneuron death that is mediated via sodium channels and nitroxidative stress. *Frontiers in cellular neuroscience* **8**, 24.
- RONG, Y.S. & GOLIC, K.G. (2000) Gene targeting by homologous recombination in *Drosophila*. *Science (New York, N.Y.)* **288**, 2013–2018.
- ROSEN, D.R., BOWLING, A.C., PATTERSON, D., USDIN, T.B., SAPP, P., MEZEY, E., MCKENNA-YASEK, D., O'REGAN, J., RAHMANI, Z. & FERRANTE, R.J. (1994) A frequent ala 4 to val superoxide dismutase-1

- mutation is associated with a rapidly progressive familial amyotrophic lateral sclerosis. *Human molecular genetics* **3**, 981–987.
- ROSEN, D.R., SIDDIQUE, T., PATTERSON, D., FIGLEWICZ, D.A., SAPP, P., HENTATI, A., DONALDSON, D., GOTO, J., O'REGAN, J.P. & DENG, H.X. (1993) Mutations in Cu/Zn superoxide dismutase gene are associated with familial amyotrophic lateral sclerosis. *Nature* **362**, 59–62.
- SABATELLI, M., ZOLLINO, M., CONTE, A., DEL GRANDE, A., MARANGI, G., LUCCHINI, M., MIRABELLA, M., ROMANO, A., PIACENTINI, R., BISOGNI, G., LATTANTE, S., LUIGETTI, M., ROSSINI, P.M. & MONCADA, A. (2015) Primary fibroblasts cultures reveal TDP-43 abnormalities in amyotrophic lateral sclerosis patients with and without SOD1 mutations. *Neurobiology of aging* **36**, 2005.e5–e2005.e13.
- SACCON, R.A., BUNTON-STASYSHYN, R.K.A., FISHER, E.M.C. & FRATTA, P. (2013) Is SOD1 loss of function involved in amyotrophic lateral sclerosis? *Brain : a journal of neurology* **136**, 2342–2358.
- SAKO, W., ITO, H., YOSHIDA, M., KOIZUMI, H., KAMADA, M., FUJITA, K., HASHIZUME, Y., IZUMI, Y. & KAJI, R. (2012) Nuclear factor κ B expression in patients with sporadic amyotrophic lateral sclerosis and hereditary amyotrophic lateral sclerosis with optineurin mutations. *Clinical neuropathology* **31**, 418–423.
- SANHUEZA, M., CHAI, A., SMITH, C., MCCRAY, B.A., SIMPSON, T.I., TAYLOR, J.P. & PENNETTA, G. (2015) Network Analyses Reveal Novel Aspects of ALS Pathogenesis. *PLoS genetics* **11**, e1005107. Public Library of Science.
- SASABE, J., MIYOSHI, Y., SUZUKI, M., MITA, M., KONNO, R., MATSUOKA, M., HAMASE, K. & AISO, S. (2012) D-amino acid oxidase controls motoneuron degeneration through D-serine. *Proceedings of the National Academy of Sciences of the United States of America* **109**, 627–632.
- SCHUTTE, R.J., SCHUTTE, S.S., ALGARA, J., BARRAGAN, E. V, GILLIGAN, J., STABER, C., SAVVA, Y.A., SMITH, M.A., REENAN, R. & O'DOWD, D.K. (2014) Knock-in model of Dravet syndrome reveals a constitutive and conditional reduction in sodium current. *Journal of neurophysiology* **112**, 903–912.
- SCOTT, S., KRANZ, J.E., COLE, J., LINCUM, J.M., THOMPSON, K., KELLY, N., BOSTROM, A., THEODOSS, J., AL-NAKHALA, B.M., VIEIRA, F.G., RAMASUBBU, J. & HEYWOOD, J.A. (2008) Design, power, and interpretation of studies in the standard murine model of ALS. *Amyotrophic lateral sclerosis : official publication of the World Federation of Neurology Research Group on Motor Neuron Diseases* **9**, 4–15.
- SERIO, A., BILICAN, B., BARMADA, S.J., ANDO, D.M., ZHAO, C., SILLER, R., BURR, K., HAGHI, G., STORY, D., NISHIMURA, A.L., CARRASCO, M.A., PHATNANI, H.P., SHUM, C., WILMUT, I., MANIATIS, T., SHAW, C.E., FINKBEINER, S. & CHANDRAN, S. (2013) Astrocyte pathology and the absence of non-cell autonomy in an induced pluripotent stem cell model of TDP-43 proteinopathy. *Proceedings of the National Academy of Sciences of the United States of America* **110**, 4697–4702.
- SHAN, X., VOCADLO, D. & KRIEGER, C. (2009) Mislocalization of TDP-43 in the G93A mutant SOD1 transgenic mouse model of ALS. *Neuroscience Letters* **458**, 70–74.
- SHAW, C.E. (2010) Capturing VCP: another molecular piece in the ALS jigsaw puzzle. *Neuron* **68**, 812–814.
- SHAW, P.J. & INCE, P.G. (1997) Glutamate, excitotoxicity and amyotrophic lateral sclerosis. *Journal of neurology* **244 Suppl**, S3–S14.

- SHIBATA, N., HIRANO, A., KOBAYASHI, M., SIDDIQUE, T., DENG, H.X., HUNG, W.Y., KATO, T. & ASAYAMA, K. (1996) Intense superoxide dismutase-1 immunoreactivity in intracytoplasmic hyaline inclusions of familial amyotrophic lateral sclerosis with posterior column involvement. *Journal of neuropathology and experimental neurology* **55**, 481–490.
- SOMALINGA, B.R., DAY, C.E., WEI, S., ROTH, M.G. & THOMAS, P.J. (2012) TDP-43 identified from a genome wide RNAi screen for SOD1 regulators. *PloS one* **7**, e35818.
- SON, M. & ELLIOTT, J.L. (2014) Mitochondrial defects in transgenic mice expressing Cu,Zn Superoxide Dismutase mutations, the role of Copper Chaperone for SOD1. *Journal of the Neurological Sciences*.
- SONE, J., NIWA, J., KAWAI, K., ISHIGAKI, S., YAMADA, S., ADACHI, H., KATSUNO, M., TANAKA, F., DOYU, M. & SOBUE, G. (2010) Dorfin ameliorates phenotypes in a transgenic mouse model of amyotrophic lateral sclerosis. *Journal of neuroscience research* **88**, 123–135.
- ST JOHNSTON, D. (2002) The art and design of genetic screens: *Drosophila melanogaster*. *Nature reviews. Genetics* **3**, 176–188.
- STABER, C.J., GELL, S., JEPSON, J.E.C. & REENAN, R.A. (2011) Perturbing A-to-I RNA editing using genetics and homologous recombination. *Methods in molecular biology (Clifton, N.J.)* **718**, 41–73.
- STAVELEY, B.E., HILLIKER, A.J. & PHILLIPS, J.P. (1991) Genetic organization of the cSOD microregion of *Drosophila melanogaster*. *Genome / National Research Council Canada = G enome / Conseil national de recherches Canada* **34**, 279–282.
- STR M, A.-L., SHI, P., ZHANG, F., GAL, J., KILTY, R., HAYWARD, L.J. & ZHU, H. (2008) Interaction of amyotrophic lateral sclerosis (ALS)-related mutant copper-zinc superoxide dismutase with the dynein-dynactin complex contributes to inclusion formation. *The Journal of biological chemistry* **283**, 22795–22805.
- STRONG, M.J., VOLKENING, K., HAMMOND, R., YANG, W., STRONG, W., LEYSTRA-LANTZ, C. & SHOESMITH, C. (2007) TDP43 is a human low molecular weight neurofilament (hNFL) mRNA-binding protein. *Molecular and cellular neurosciences* **35**, 320–327.
- SUN, L., GILLIGAN, J., STABER, C., SCHUTTE, R.J., NGUYEN, V., O'DOWD, D.K. & REENAN, R. (2012) A knock-in model of human epilepsy in *Drosophila* reveals a novel cellular mechanism associated with heat-induced seizure. *The Journal of neuroscience : the official journal of the Society for Neuroscience* **32**, 14145–14155.
- SUN, X., KOMATSU, T., LIM, J., LASLO, M., YOLITZ, J., WANG, C., POIRIER, L., ALBERICO, T. & ZOU, S. (2012) Nutrient-dependent requirement for SOD1 in lifespan extension by protein restriction in *Drosophila melanogaster*. *Aging cell* **11**, 783–793.
- SWINNEN, B. & ROBBERECHT, W. (2014) The phenotypic variability of amyotrophic lateral sclerosis. *Nature reviews. Neurology* **10**, 661–670.
- SYNOFZIK, M., RONCHI, D., KESKIN, I., BASAK, A.N., WILHELM, C., GOBBI, C., BIRVE, A., BISKUP, S., ZECCA, C., FERN NDEZ-SANTIAGO, R., KAUGESAAR, T., SCH LS, L., MARKLUND, S.L. & ANDERSEN, P.M. (2012) Mutant superoxide dismutase-1 indistinguishable from wild-type causes ALS. *Human molecular genetics* **21**, 3568–3574.
- TAKEHISA, Y., UJIKE, H., ISHIZU, H., TERADA, S., HARAGUCHI, T., TANAKA, Y., NISHINAKA, T., NOBUKUNI, K., IHARA, Y., NAMBA, R., YASUDA, T., NISHIBORI, M., HAYABARA, T. & KURODA, S. (2001) Familial

- amyotrophic lateral sclerosis with a novel Leu126Ser mutation in the copper/zinc superoxide dismutase gene showing mild clinical features and lewy body-like hyaline inclusions. *Archives of neurology* **58**, 736–740.
- TEULING, E., AHMED, S., HAASDIJK, E., DEMMERS, J., STEINMETZ, M.O., AKHMANOVA, A., JAARSMA, D. & HOOGENRAAD, C.C. (2007) Motor neuron disease-associated mutant vesicle-associated membrane protein-associated protein (VAP) B recruits wild-type VAPs into endoplasmic reticulum-derived tubular aggregates. *The Journal of neuroscience : the official journal of the Society for Neuroscience* **27**, 9801–9815.
- TEYSSOU, E., TAKEDA, T., LEBON, V., BOILLÉE, S., DOUKOURÉ, B., BATAILLON, G., SAZDOVITCH, V., CAZENEUVE, C., MEININGER, V., LEGUERN, E., SALACHAS, F., SEILHEAN, D. & MILLECAMPS, S. (2013) Mutations in SQSTM1 encoding p62 in amyotrophic lateral sclerosis: genetics and neuropathology. *Acta neuropathologica* **125**, 511–522.
- TROTTI, D., ROLFS, A., DANBOLT, N.C., BROWN, R.H. & HEDIGER, M.A. (1999) SOD1 mutants linked to amyotrophic lateral sclerosis selectively inactivate a glial glutamate transporter. *Nature neuroscience* **2**, 427–433.
- TSANG, C.K., LIU, Y., THOMAS, J., ZHANG, Y. & ZHENG, X.F.S. (2014) Superoxide dismutase 1 acts as a nuclear transcription factor to regulate oxidative stress resistance. *Nature communications* **5**, 3446. Nature Publishing Group.
- TURNER, B.J., ALFAZEMA, N., SHEEAN, R.K., SLEIGH, J.N., DAVIES, K.E., HORNE, M.K. & TALBOT, K. (2014) Overexpression of survival motor neuron improves neuromuscular function and motor neuron survival in mutant SOD1 mice. *Neurobiology of aging* **35**, 906–915.
- TURNER, B.J. & TALBOT, K. (2008) Transgenics , toxicity and therapeutics in rodent models of mutant SOD1-mediated familial ALS. *Progress in Neurobiology* **85**, 94–134.
- URUSHITANI, M., SIK, A., SAKURAI, T., NUKINA, N., TAKAHASHI, R. & JULIEN, J.-P. (2006) Chromogranin-mediated secretion of mutant superoxide dismutase proteins linked to amyotrophic lateral sclerosis. *Nature neuroscience* **9**, 108–118. Nature Publishing Group.
- VALENTINE, J.S., DOUCETTE, P. A & ZITTIN POTTER, S. (2005) Copper-zinc superoxide dismutase and amyotrophic lateral sclerosis. *Annual review of biochemistry* **74**, 563–593.
- VANDE VELDE, C., MILLER, T.M., CASHMAN, N.R. & CLEVELAND, D.W. (2008) Selective association of misfolded ALS-linked mutant SOD1 with the cytoplasmic face of mitochondria. *Proceedings of the National Academy of Sciences of the United States of America* **105**, 4022–4027.
- VOLKENING, K., LEYSTRA-LANTZ, C., YANG, W., JAFFEE, H. & STRONG, M.J. (2009) Tar DNA binding protein of 43 kDa (TDP-43), 14-3-3 proteins and copper/zinc superoxide dismutase (SOD1) interact to modulate NFL mRNA stability. Implications for altered RNA processing in amyotrophic lateral sclerosis (ALS). *Brain research* **1305**, 168–182.
- WADE, N. (2010) Decoding the Human Brain, With Help From a Fly. *The New York Times*, D4.
- WAINGER, B.J., KISKINIS, E., MELLIN, C., WISKOW, O., HAN, S.S.W., SANDOE, J., PEREZ, N.P., WILLIAMS, L.A., LEE, S., BOULTING, G., BERRY, J.D., BROWN, R.H., CUDKOWICZ, M.E., BEAN, B.P., EGGAN, K. & WOOLF, C.J. (2014) Intrinsic membrane hyperexcitability of amyotrophic lateral sclerosis patient-derived motor neurons. *Cell reports* **7**, 1–11. Elsevier.

- WANG, J., FARR, G.W., HALL, D.H., LI, F., FURTAK, K., DREIER, L. & HORWICH, A.L. (2009) An ALS-linked mutant SOD1 produces a locomotor defect associated with aggregation and synaptic dysfunction when expressed in neurons of *Caenorhabditis elegans*. *PLoS genetics* **5**, e1000350. Public Library of Science.
- WANG, J., FARR, G.W., ZEISS, C.J., RODRIGUEZ-GIL, D.J., WILSON, J.H., FURTAK, K., RUTKOWSKI, D.T., KAUFMAN, R.J., RUSE, C.I., YATES, J.R., PERRIN, S., FEANY, M.B. & HORWICH, A.L. (2009) Progressive aggregation despite chaperone associations of a mutant SOD1-YFP in transgenic mice that develop ALS. *Proceedings of the National Academy of Sciences of the United States of America* **106**, 1392–1397.
- WANG, L., COLODNER, K.J. & FEANY, M.B. (2011) Protein misfolding and oxidative stress promote glial-mediated neurodegeneration in an Alexander disease model. *The Journal of neuroscience : the official journal of the Society for Neuroscience* **31**, 2868–2877.
- WANG, L., LI, Y.M., LEI, L., LIU, Y., WANG, X., MA, K.Y. & CHEN, Z.-Y. (2015) Cranberry anthocyanin extract prolongs lifespan of fruit flies. *Experimental gerontology* **69**, 189–195.
- WANG, W., LI, L., LIN, W.-L., DICKSON, D.W., PETRUCCELLI, L., ZHANG, T. & WANG, X. (2013) The ALS disease-associated mutant TDP-43 impairs mitochondrial dynamics and function in motor neurons. *Human molecular genetics* **22**, 4706–4719.
- WANG, X.-S., SIMMONS, Z., LIU, W., BOYER, P.J. & CONNOR, J.R. (2006) Differential expression of genes in amyotrophic lateral sclerosis revealed by profiling the post mortem cortex. *Amyotrophic lateral sclerosis : official publication of the World Federation of Neurology Research Group on Motor Neuron Diseases* **7**, 201–210.
- WANG, Z., LIU, J., CHEN, S., WANG, Y., CAO, L., ZHANG, Y., KANG, W., LI, H., GUI, Y., CHEN, S. & DING, J. (2011) DJ-1 modulates the expression of Cu/Zn-superoxide dismutase-1 through the Erk1/2-Elk1 pathway in neuroprotection. *Annals of neurology* **70**, 591–599.
- WATANABE, S., AGETA-ISHIHARA, N., NAGATSU, S., TAKAO, K., KOMINE, O., ENDO, F., MIYAKAWA, T., MISAWA, H., TAKAHASHI, R., KINOSHITA, M. & YAMANAKA, K. (2014) SIRT1 overexpression ameliorates a mouse model of SOD1-linked amyotrophic lateral sclerosis via HSF1/HSP70i chaperone system. *Molecular brain* **7**, 62.
- WATSON, M.R., LAGOW, R.D., XU, K., ZHANG, B. & BONINI, N.M. (2008) A drosophila model for amyotrophic lateral sclerosis reveals motor neuron damage by human SOD1. *The Journal of biological chemistry* **283**, 24972–24981.
- WININGER, F.A., ZENG, R., JOHNSON, G.S., KATZ, M.L., JOHNSON, G.C., BUSH, W.W., JARBOE, J.M. & COATES, J.R. (2011) Degenerative Myelopathy in a Bernese Mountain Dog with a Novel SOD1 Missense Mutation. *Journal of Veterinary Internal Medicine* **25**, 1166–1170.
- WOLF, M.J. & ROCKMAN, H.A. (2011) *Drosophila*, genetic screens, and cardiac function. *Circulation research* **109**, 794–806.
- XIA, Q., WANG, H., ZHANG, Y., YING, Z. & WANG, G. (2014) Loss of TDP-43 Inhibits Amyotrophic Lateral Sclerosis-Linked Mutant SOD1 Aggresome Formation in an HDAC6-Dependent Manner. *Journal of Alzheimer's disease : JAD*.
- XU, X., DENIC, A., JORDAN, L.R., WITTENBERG, N.J., WARRINGTON, A.E., WOOTLA, B., PAPKE, L.M., ZOECKLEIN, L.J., YOO, D., SHAVER, J., OH, S.-H., PEASE, L.R. & RODRIGUEZ, M. (2015) A natural

- human IgM that binds to gangliosides is therapeutic in murine models of amyotrophic lateral sclerosis. *Disease models & mechanisms*.
- YAMASHITA, S., MORI, A., KIMURA, E., MITA, S., MAEDA, Y., HIRANO, T. & UCHINO, M. (2010) DJ-1 forms complexes with mutant SOD1 and ameliorates its toxicity. *Journal of neurochemistry* **113**, 860–870.
- YANASE, S., ONODERA, A., TEDESCO, P., JOHNSON, T.E. & ISHII, N. (2009) SOD-1 deletions in *Caenorhabditis elegans* alter the localization of intracellular reactive oxygen species and show molecular compensation. *The journals of gerontology. Series A, Biological sciences and medical sciences* **64**, 530–539.
- YANG, Y. & FAN, D. (2014) [To screen for SQSTM1/p62 gene in Chinese patients with familial amyotrophic lateral sclerosis carrying superoxide dismutase 1 mutation]. *Zhonghua nei ke za zhi* **53**, 957–960.
- YANG, Y., HENTATI, A., DENG, H.X., DABBAGH, O., SASAKI, T., HIRANO, M., HUNG, W.Y., OUAHCHI, K., YAN, J., AZIM, A.C., COLE, N., GASCON, G., YAGMOUR, A., BEN-HAMIDA, M., PERICAK-VANCE, M., HENTATI, F. & SIDDIQUE, T. (2001) The gene encoding alsin, a protein with three guanine-nucleotide exchange factor domains, is mutated in a form of recessive amyotrophic lateral sclerosis. *Nature genetics* **29**, 160–165.
- YOSHIDA, T., MAULIK, N., ENGELMAN, R.M., HO, Y.S. & DAS, D.K. (2000) Targeted disruption of the mouse Sod I gene makes the hearts vulnerable to ischemic reperfusion injury. *Circulation research* **86**, 264–269.
- ZELKO, I.N., MARIANI, T.J. & FOLZ, R.J. (2002) Superoxide dismutase multigene family: a comparison of the CuZn-SOD (SOD1), Mn-SOD (SOD2), and EC-SOD (SOD3) gene structures, evolution, and expression. *Free Radical Biology and Medicine* **33**, 337–349.
- ZENG, R., COATES, J.R., JOHNSON, G.C., HANSEN, L., AWANO, T., KOLICHESKI, A., IVANSSON, E., PERLOSKI, M., LINDBLAD-TOH, K., O'BRIEN, D.P., GUO, J., KATZ, M.L. & JOHNSON, G.S. (2014) Breed distribution of SOD1 alleles previously associated with canine degenerative myelopathy. *Journal of Veterinary Internal Medicine* **28**, 515–521.
- ZHANG, F., STRÖM, A.-L., FUKADA, K., LEE, S., HAYWARD, L.J. & ZHU, H. (2007) Interaction between familial amyotrophic lateral sclerosis (ALS)-linked SOD1 mutants and the dynein complex. *The Journal of biological chemistry* **282**, 16691–16699.
- ZHANG, X., LI, L., CHEN, S., YANG, D., WANG, Y., ZHANG, X., WANG, Z. & LE, W. (2011) Rapamycin treatment augments motor neuron degeneration in SOD1(G93A) mouse model of amyotrophic lateral sclerosis. *Autophagy* **7**, 412–425.
- ZHAO, W. (2013) Negative regulation of TBK1-mediated antiviral immunity. *FEBS Letters* **587**, 542–548.
- ZHU, G., WU, C.-J., ZHAO, Y. & ASHWELL, J.D. (2007) Optineurin negatively regulates TNF α -induced NF- κ B activation by competing with NEMO for ubiquitinated RIP. *Current biology : CB* **17**, 1438–1443.
- ZINMAN, L., LIU, H.N., SATO, C., WAKUTANI, Y., MARVELLE, A.F., MORENO, D., MORRISON, K.E., MOHLKE, K.L., BILBAO, J., ROBERTSON, J. & ROGAEVA, E. (2009) A mechanism for low penetrance in an ALS family with a novel SOD1 deletion. *Neurology* **72**, 1153–1159.

ZU, J.S., DENG, H.X., LO, T.P., MITSUMOTO, H., AHMED, M.S., HUNG, W.Y., CAI, Z.J., TAINER, J.A. & SIDDIQUE, T. (1997) Exon 5 encoded domain is not required for the toxic function of mutant SOD1 but essential for the dismutase activity: identification and characterization of two new SOD1 mutations associated with familial amyotrophic lateral sclerosis. *Neurogenetics* **1**, 65–71.

FIGURES

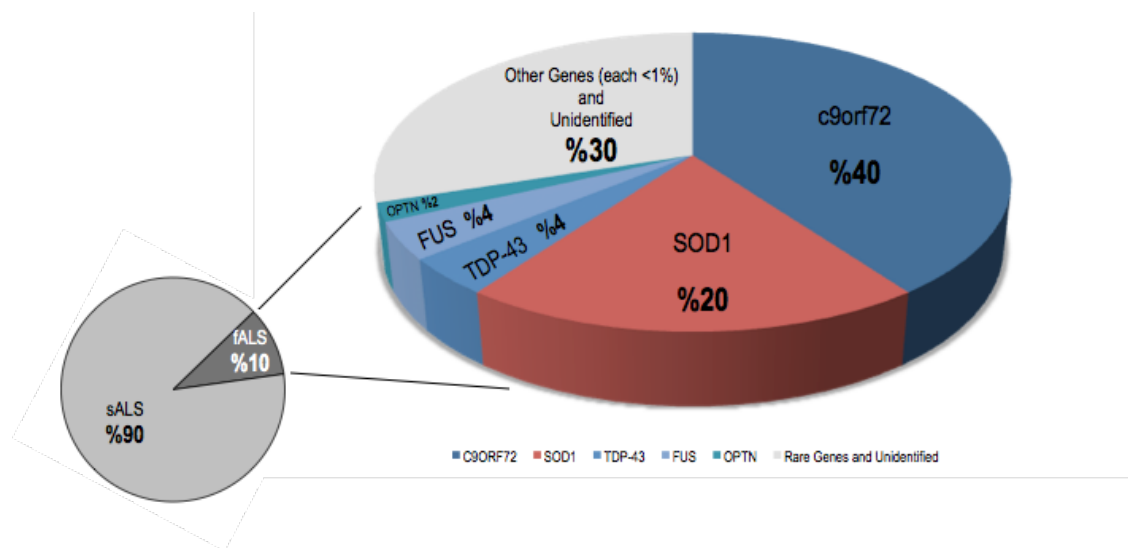


Figure 1.1. Distribution of fALS-causing mutant genes. All genes that explain equal or less than 1% of fALS cases are included in the other genes category. Full names and the details of the genes can be found in Table 1.1 and Table 1.2. The percentages in this figure is taken from a table from (Peters *et al.*, 2015).

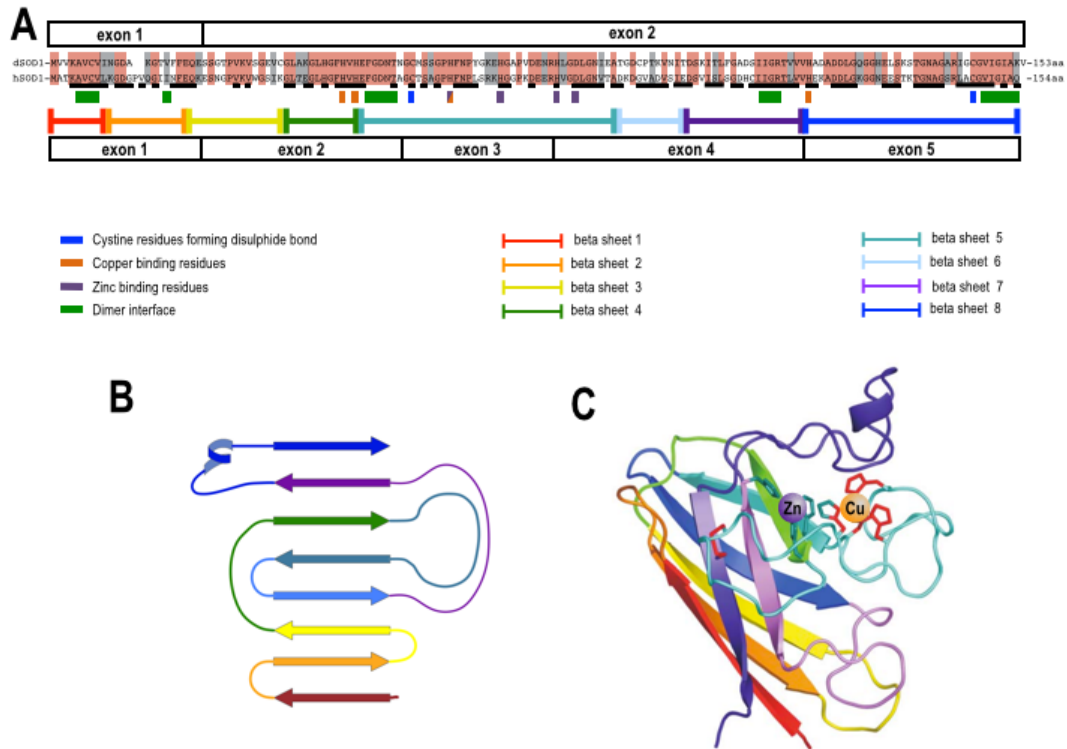


Figure 1.2. Comparison of human SOD1 (hSOD1) and *Drosophila* SOD1 (*dSod1*). **A)** Alignment of hSOD1 primary sequence with 5 exons and dSod1 primary sequence with 2 exons, domains involved in Cu, Zn metal binding, intramolecular disulfide bond formation, dimer interface, mutations linked to familial ALS and hSOD1 residues each contributing to one of 8 beta sheets in the tertiary structure of hSOD1. (Adapted from Abel et al., 2012 and Saccon et al., 2013). Key: Orange residues are conserved; grey are similarly charged domains between organisms; black bars are mutations mapped from hSOD1 patients. (Adapted from Watson et al., 2008). **B)** hSOD1 secondary structure (Figure from Valentine et al., 2005). **C)** Tertiary structure of copper- and zinc- bound hSOD1 monomer, which is composed of 5 antiparallel β -sheets and linkers. (Adapted from Valentine et al., 2005).

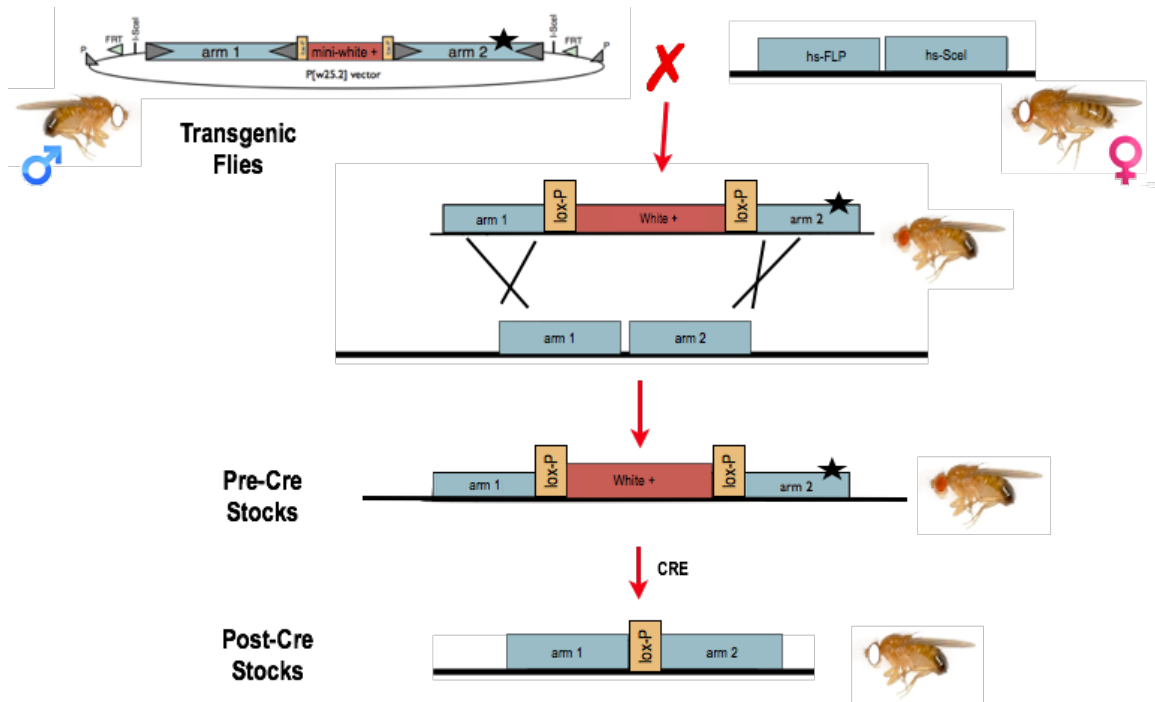


Figure 1.3. Ends-out homologous recombination. We used standard P element transposition techniques to generate transgenic *Drosophila* lines expressing the template allele. A *mini-white* gene (red) is used to track the template allele. Transgenic flies with the P[w25.2] vector are mated with white eyed-flies expressing FLP recombinase and I-SceI endonuclease under a heat shock promoter. FLP recombinase recognizes FRT sites and mobilizes the targeting construct circularly. Subsequent cutting by the I-SceI endonuclease generates the linear recombinogenic template which is recognized by the DNA repair machinery. If homologous recombination occurs, the targeted mutation will be introduced to the endogenous locus and *mini-white* is expressed. The *mini-white* gene is excised at the final step by Cre recombinase, leaving behind a single LoxP site targeted to intron 1.

TABLES

Table 1.1. ALS-causing mutant genes mapped in familial ALS patients and ALS-associated genes, their known protein functions and their possible contribution to ALS. The fraction fALS cases are acquired from (Peters *et al.*, 2015), the updated gene list is acquired from ALSod platform website (Abel *et al.*, 2012). FTD- Frontotemporal dementia, UPR- Unfolded Protein Response.

Gene (Encoded protein, if different)	Fraction fALS %	Drosophila ortholog	Full Name	Protein Function	Possible Function in ALS
C9orf72 or ALS-FTD1	40	none	Chromosome 9 open reading frame 72	-transcription regulation -pre-mRNA splicing regulation -membrane traffic via Rab GTPase family	-forms intra nuclear RNA foci -forms cytoplasmic RNA peptide aggregates -FTD
SOD1 or ALS1	20	dSod1	Superoxide dismutase 1	-major cytosolic antioxidant	-aggregates -oxidative stress related neuronal toxicity
TARDBP (TDP-43) or ALS10	5	TBPH	TAR DNA binding protein	-transcription regulation -pre-mRNA splicing regulation -miRNA biogenesis -RNA transport & stabilization	-aggregates -loss of nuclear function -FTD
FUS or ALS6	5	Caz and CG14718	Fusion in sarcoma	-transcription regulation -DNA/RNA metabolism (splicing, miRNA processing) -regulates protein synthesis at synapse	-aggregates -loss of nuclear function
OPTN (Optineurin) or ALS12	2-3	nemo	Optineurin	-Golgi maintenance/ membrane trafficking -autophagy/ apoptosis -transcription activation	-co-aggregates with TDP-43, FUS, SOD1 aggregates -activation of NF-κB apoptosis pathway
PFN1 (Profilin-1) or ALS18	1-2	Chickadee	Profilin-1	-Regulates ATP- mediated actin polymerization	-co-aggregation with TDP- 43
VCP (VCP or p97) or	1-2	Ter94	Valosin containing protein	-AAA+-ATPase -ubiquitin dependent extraction of	-increases TDP-43 aggregates -causes TDP-43 redistribution

Gene (Encoded protein, if different)	Fraction fALS %	Drosophila ortholog	Full Name	Protein Function	Possible Function in ALS
ALS14				substrates from multiprotein complexes for degradation	-less clearing of stress granules
ANG (Angiogenin) or ALS9	1-2	none	Angiogenin	-formation of new blood vessels -RNA processing -tRNA modification -RNase activity -assembly of stress granules -neurite outgrowth and pathfinding	-alters ubiquitination of SOD1 -less stress granules formation -starvation stress for motor neurons
ATXN2 (Ataxin-2) or ALS13	1-2	Atx2	Ataxin-2	-RNA processing -regulation of receptor tyrosine kinase -endocytosis	- interacts with TDP-43 -repeat expansion -abnormal localization
TUBA4A (Tubulin α 4A)	1	alphaTub8 5E	Tubulin α 4A	-major component of microtubules -neuronal cell skeleton	-destabilizes microtubule network
UBQLN2 (Ubiquilin 2) or ALS15	<1	GC14224	Ubiquilin 2	-protein degradation via UPR	-increases TDP-43, FUS, OPTN aggregates
TAF15	<1	caz and CG14718	TAF15 RNA polymerase II, TATA box-binding protein-associated factor	-transcription initiation -RNA polymerase II gene component	-aggregates in sALS -interacts with TDP-43 and FUS
EWSR1	<1	caz and CG14718	Ewing sarcoma breakpoint region 1	-transcriptional repressor	-aggregates in sALS -interacts with TDP-43 and FUS
hnRNPA1 or ALS20	<1	Hrb98DE	Heterogeneous nuclear ribonucleoprotein A1	-packing and transport of mRNA -miRNA biogenesis	-FTD -interacts with TDP-43 and FUS -self-assembly with prion-like domains
hnRNPA2B1 (hnRNPA2/B1)	<1	Hrb87F Hrb98DE Rb97D	Heterogeneous nuclear ribonucleoprotein A2/B1	-packing and transport of mRNA -miRNA biogenesis	-interacts with TDP-43 and FUS -self-assembly with prion-like domains
SETX (Senataxin) or ALS4	<1	CG7504	Senataxin	-DNA/RNA helicase activity -DNA/RNA metabolism	-less neuronal differentiation -less neurite growth
CREST	<1	CG10555	Synovial sarcoma	-Ca ²⁺ dependent	-interacts with FUS

Gene (Encoded protein, if different)	Fraction fALS %	Drosophila ortholog	Full Name	Protein Function	Possible Function in ALS
(SS18L1)			translocation gene on chromosome 18- like 1	transcriptional activator	-less neurite growth
MATR3 (Matrin 3) or ALS21	<1	none	Matrin 3	-RNA processing -stabilizing mRNAs -gene silencing -chromatin organization	-interacts with TDP-43 -aggregates in C9orf72 patients -mislocalization to the cytoplasm
SQSTM1 (p62 or sequestosome-1)	<1	Ref(2)P or p62	Sequestosome 1	-Autophagy -UPR degradation -immune response -regulator of NF-κB apoptosis pathway	-less mutant SOD1 autophagic degradation
CHMP2B or ALS17	<1	CHMP2B	Chromatin- modifying protein 2b	-vesicle formation around ubiquitin tagged proteins to form endosomes -trans-Golgi network -lysosome	-disrupts endosomal structure -aggregates of autophagosomes -aggregation of TDP-43, p62, ubiquitin inclusions
ALS2 (Alsin)	<1	CG7158	Alsin	-endosome fusion -neurite outgrowth	-less axonal growth -lysosome dependent clearance of p62
VAPB or ALS8	<1	Vap-33-1	Vesicle- associated membrane protein- associated protein B	-ER-golgi transport -secretion	-aggregation of TDP-43 -aberrant synaptic microtubule cytoskeleton
SIGMAR1 or SigR1 or ALS16	<1	none	Sigma non- opioid intracellular receptor 1	-lipid transport through ER -BDNF & EGF signaling	-apoptosis induced by ER stress -interacts with VAPB
DCTN1 (Dynactin 1) or p150 or Glued	<1	glued	Dynactin 1	-ER-to-golgi transport -movement of lysosomes/ endosomes -chromosome movement -nuclear positioning -axonogenesis	-aggregation of SOD1 -disrupted axonal transport -less stable tubulin -less synaptic vesicles in neurites
SPG11 or ALS5	<1	CG13531	Spastic paraplegia 11	-neuronal cell skeleton -axonal transport -synaptic vesicles	-neurofilament aggregates
NEFH	<1	none	Neurofilament heavy polypeptide	-maintaining a proper axon diameter	

Gene (Encoded protein, if different)	Fraction fALS %	Drosophila ortholog	Full Name	Protein Function	Possible Function in ALS
PRPH (Peripherin)	<1	none	Peripherin	-regulating neurite elongation during development -axonal regeneration after injury	-disrupted neurofilament network -co-aggregation with SOD1
ARHGEF28	≥2 families	CG10188	Rho guanine nucleotide exchange factor (GEF) 28	-RNA binding -protein binding -metal ion binding -guanine nucleotide exchange factor in pathways of integrins and growth factor receptors. -axonal branching, synapse formation and dendritic morphogenesis.	-more ubiquitinated inclusions -regulates NEFL expression and aggregation -apoptosis
BCL11B	≥2 families	CG9650	B-cell CLL/lymphoma 11B	-innate immunity -RNA polymerase II core promoter proximal region sequence-specific DNA binding	not determined
BCL6	≥1 family	Kruppel	B-cell CLL/lymphoma 6	-DNA binding -Sirt1-dependent epigenetic repression	not determined
CDH13 (cadherin 13)	≥8 families	neuronal cadherin	Cadherin 13	-calcium-dependent cell adhesion protein -negative regulator of neural cell growth	not determined
CDH22 (cadherin 22)	≥3 families	neuronal cadherin	Cadherin 22	-calcium-dependent cell adhesion protein	not determined
CHCHD10 or ALS-FTD2	≥5 families	CG5010 and CG31008 and CG3100	Coiled-coil- helix-coiled-coil- helix domain containing 10	-mitochondrial protein, function unknown	-FTD -mitochondrial dysfunction
CHGB (chromogranin B)	≥1 family	none	Chromogranin B (secretory granin 1)	-neuroendocrine secretory granule protein	- sequestered in the ER/transGolgi network
CNTN6	≥2 families	Contactin	Contactin 6	-Neural Adhesion Molecule	not determined
CRIM1	≥1 family	cross veinless 2	Cysteine rich motor neuron protein 1	-interact with growth factors implicated in motor neuron differentiation and survival	not determined
CRYM Mu-crystallin	≥1 family	CG4872	Mu-crystallin	- transcription corepressor activity -thyroid hormone binding	-altered expression in SOD1 mouse model
CX3CR1	≥2	AlstR	Chemokine (C-X3-C motif)	-cytokine receptor activity	-a shorter survival time and faster progression rate of the

Gene (Encoded protein, if different)	Fraction fALS %	Drosophila ortholog	Full Name	Protein Function	Possible Function in ALS
	families		receptor 1		disease's symptoms with the <i>CX3CRI</i> ^{V249I} genetic variant -deletion makes G93A SOD1 mice worse
DAO	≥2 families	CG11236	D-amino-acid oxidase	-act as a detoxifying agent which removes D-amino acids (mainly D-serine) accumulated during aging. -contributes to dopamine synthesis.	-motor neuron degeneration via D-serine accumulation
DIAPH3	≥6 families	diaphanous	Diaphanous- related formin 3	-binds to GTP-bound form of Rho and to profilin.	-possibly profilin related neurodegeneration
DOC2B	≥1 family	rabphilin -3A	Double C2-like domains, beta	-involved in calcium-triggered exocytosis	not determined
ERBB4 or ALS19	≥2 families	Egfr	V-erb-b2 avian erythroblastic leukemia viral oncogene homolog 4	-transmembrane receptor protein tyrosine kinase activity	-ErbB4 receptor protein is particularly enriched in glutamatergic synapses but not in ocular motor neuron synapses
FIG4 or ALS11	≥10 families	CG17840	FIG4 Homolog	-synthesis and turnover of phosphatidylinositol -biogenesis of endosome carrier vesicles	not determined
FEZF2	≥1 family	earmuff	FEZ Family Zinc Finger 2	-transcription repressor	not determined
GLE1	≥3 families	CG14749	GLE1 RNA export mediator	-innate immunity -required for the export of mRNAs containing poly(A) tails from the nucleus into the cytoplasm.	not determined
GRB14	≥1 family	pico	Growth factor receptor-bound protein 14	-adapter protein which modulates coupling of cell surface receptor kinases with specific signaling pathways. -binds to, and suppresses signals from, the activated insulin receptor (INSR).	not determined
LMNB1	≥1 family	LamC	Lamin B1	-components of the nuclear lamina	not determined
LUM	≥1 family	none	Lumican	-extracellular matrix structural constituent	not determined
NETO1	≥1 family	neto	Neuropilin (NRP) and tolloid (TLL)-	-development and/or maintenance of neuronal circuitry	not determined

Gene (Encoded protein, if different)	Fraction fALS %	Drosophila ortholog	Full Name	Protein Function	Possible Function in ALS
			like 1		
NIPA1	≥7 families	spichthyin	Non Imprinted In Prader- Willi/Angelman Syndrome 1	-magnesium and other divalent ion -transmembrane transporter activity	-polyalanine repeat expansions associated with ALS
OMA1	≥3 families	none	OMA1 zinc metallopeptidase	-quality control system in the inner membrane of mitochondria.	not determined
PARK7	≥1 family	DJ-1alpha	Parkinson protein 7	-peroxidase, protects cells against oxidative stress and cell death.	-forms complexes with mutant SOD1 and ameliorates its toxicity
PCP4	≥1 family	igloo	Purkinje cell protein 4	-calmodulin binding	not determined
PLEKHG5	≥1 family	CG42674	Pleckstrin homology domain containing, family G (with RhoGef domain) member 5	-Rho guanyl- nucleotide exchange factor activity - activation of NF- κB apoptosis pathway	- activation of NF-κB apoptosis pathway
RAMP3	≥2 families	none	Receptor (G protein-coupled) activity modifying protein 3	- angiogenesis - transports the calcitonin gene- related peptide type 1 receptor (CALCRL) and GPER1 to the plasma membrane.	not determined
RNASE2	≥1 family	none	Ribonuclease, RNase A family, 2	-nucleic acid binding - ribonuclease activity	not determined
SOX5	≥1 family	Sox102F	SRY (sex determining region Y)-box 5	-transcription activator	not determined
SYNE	≥2 families	Msp-300	Spectrin repeat containing, nuclear envelope 1	-DNA binding -nucleotide binding -actin binding -ATP binding	not determined
SYT9	≥3 families	Syt1	Synaptotagmin IX	-lamin binding -Ca(2+)-dependent exocytosis	not determined
TBK1	≥18 families	ik2	TANK-binding kinase 1	-nucleic acid binding -protein kinase activity -innate immunity	-phosphorylates OPTN
TRPM7	≥1 family	CG30079	Transient receptor potential cation channel,	-actin binding -protein	not determined

Gene (Encoded protein, if different)	Fraction fALS %	Drosophila ortholog	Full Name	Protein Function	Possible Function in ALS
			subfamily M, member 7	serine/threonine kinase activity	
ALS3	≥1 family		unknown	-locus at 2q33.2	not determined
ALS7	≥1 family		unknown	-locus at 20q13	not determined

Table 1.2- The possible commonalities of SOD1-mediated ALS with other ALS-associated genes. The updated gene list is acquired from ALSod platform website (Abel *et al.*, 2012). MN- Motor neurons, tg- transgenic, OE-overexpression, wt-wild type, ROS-Reactive oxygen species, TF- Transcription Factor.

Gene (Encoded protein, if different)	Full Name	Possible Commonalities with SOD1-Mediated ALS or Common Signature with SOD1-Mediated ALS	Reference
Unknown sALS	Sporadic ALS	- SOD1 inclusions	- (Gruzman <i>et al.</i> , 2007)
		- Astrocytes derived from patients toxic to MNs	- (Haidet-Phillips <i>et al.</i> , 2011)
		- Oxidative stress signature	- (D'Amico <i>et al.</i> , 2013)
C9orf72 or ALS-FTD1	Chromosome 9 open reading frame 72	- Co-aggregates with SOD1	- (Keller <i>et al.</i> , 2012)
		- Common transcriptome change	- (Kiskinis <i>et al.</i> , 2014) - (Donnelly <i>et al.</i> , 2013)
TARDBP (TDP-43) or ALS10	TAR DNA binding protein	- Astrocytes expressing mutant form toxic to MNs	- (Meyer <i>et al.</i> , 2014)
		-Hyperexcitability of MNs signature	- (Wainger <i>et al.</i> , 2014)
		- Reduction of TDP-43 in the nuclei with/without cytoplasmic mislocalization in patients with SOD1 mutations and SOD1 G93A tg mice	- (Sabatelli <i>et al.</i> , 2015) - (Miyazaki <i>et al.</i> , 2013)
		- Cytoplasmic translocation of TDP-43 in G93A tg mouse model	- (Deitch <i>et al.</i> , 2014) - (Shan <i>et al.</i> , 2009)
		- Expression of phosphorylated and truncated TDP-43 increased in G93A tg mouse model	- (Cai <i>et al.</i> , 2015)
		- Accumulation of nuclear TDP-43 presymptomatic stages of G93A tg mouse model	- (Casas <i>et al.</i> , 2013)
		- Loss of TDP-43 inhibits SOD1 aggregates formation	- (Xia <i>et al.</i> , 2014) - (Somalinga <i>et al.</i> , 2012)
		-Physically interacts with mutant SOD1, not wt, in cytoplasm	- (Higashi <i>et al.</i> , 2010)
		- SOD1 misfolding in the TDP-43 mutant patients	- (Pokrishevsky <i>et al.</i> , 2012)
		-TDP-43 inclusions in SOD1 patients	- (Okamoto <i>et al.</i> , 2011)
- Mutant TDP-43 impairs mitochondrial	- (Wang <i>et al.</i> , 2013)		

		dynamics and function in motor neurons in cell culture and in G93A tg mouse model	(Magrané <i>et al.</i> , 2014)
		- Astrocytes expressing mutant form toxic to MNs	- (Rojas <i>et al.</i> , 2014)
		- Stabilizes neurofilament (NFL) mRNA by interacting with SOD1	- (Strong <i>et al.</i> , 2007) - (Volkening <i>et al.</i> , 2009)
FUS or ALS6	Fusion in sarcoma	- Hyperexcitability of MNs signature	- (Wainger <i>et al.</i> , 2014)
		- SOD1 misfolding in the FUS mutant patients	- (Pokrishevsky <i>et al.</i> , 2012)
		- Motor neuron specific reduced nuclear FUS levels in G93A tg mice	- (Miyazaki <i>et al.</i> , 2013)
OPTN (Optineurin) or ALS12	Optineurin	- Co-aggregates with SOD1	- (Keller <i>et al.</i> , 2012) - (Deng, Bigio, <i>et al.</i> , 2011)
		- Activation of NF- κ B-mediated apoptosis pathway	- (Akizuki <i>et al.</i> , 2013) - (Zhu <i>et al.</i> , 2007) - (Nagabhushana <i>et al.</i> , 2011) - (Sako <i>et al.</i> , 2012)
VCP (VCP or p97) or ALS14	Valosin containing protein	- Alters ubiquitination of SOD1: VCP colocalizes with Dorfin, which is the E3 ubiquitin ligase for SOD1.	- (Niwa <i>et al.</i> , 2002) - (Ishigaki <i>et al.</i> , 2004)
		- Dorfin OE increased the life span of the G93A tg mouse for 30 days.	- (Sone <i>et al.</i> , 2010)
		- Enriched in the conditioned media of G93A SOD1 astrocytes.	- (Basso <i>et al.</i> , 2013)
ANG (Angiogenin) or ALS9	Angiogenin	- MNs from G93A and G93D mice reveals increased angiogenin levels	- (Nardo <i>et al.</i> , 2013) - (Luigetti <i>et al.</i> , 2011)
		- Angiogenin delivery increased lifespan and MN survival of G93A tg mice.	- (Kieran <i>et al.</i> , 2008)
TUBA4A (Tubulin α 4A)	Tubulin α 4A	- rHlgM12, by up-regulating α -tubulin levels increases survival in G86R and G93A tg mice	- (Xu <i>et al.</i> , 2015)
SQSTM1 (p62 or sequestosome-1)	Sequestosome 1	- Less mutant SOD1 autophagic degradation	- (Gal <i>et al.</i> , 2009)
		- Enhances SOD1 aggregate formation	- (Gal <i>et al.</i> , 2007)
		- Co-aggregates with SOD1	- (Gal <i>et al.</i> , 2007) - (Zhang <i>et al.</i> , 2011) - (Hadano <i>et al.</i> , 2010)
		- Protein amounts reduced in G85R and G93A SOD1 tg mice	- (Bandyopadhyay, Nagy, Fenton, & Horwich, 2014)
		- Mutant p62 cause earlier onset and faster disease progression in SOD1 ALS patients	- (Yang & Fan, 2014)
		- Activation of NF- κ B-mediated apoptosis pathway	- (Nakamura <i>et al.</i> , 2010) - (Rea <i>et al.</i> , 2006)
ALS2 (Alsin)	Alsin	- Loss of Alsin exacerbates motor dysfunction in H46R but not in G93A tg mice by disturbing endolysosomal trafficking	- (Hadano <i>et al.</i> , 2010)
		- Expression of alsin long transcript, but not alsin short transcript protects MNs from SOD1- mediated toxicity in cell culture	- (Kanekura <i>et al.</i> , 2004)
		- Expression of wt alsin attenuates SOD1G93A-mediated ROS production by glial cells in co-culture studies.	- (Li <i>et al.</i> , 2011)
VAPB or ALS8	Vesicle-associated membrane protein-associated protein B	- Knockdown of SOD1 suppressed the VAPB phenotype in a <i>Drosophila</i> genetic screen	- (Deivasigamani <i>et al.</i> , 2014)
		- VAPB protein levels are lowered in G93A tg mice in symptomatic stage but not in early stage	- (Teuling <i>et al.</i> , 2007)

SIGMAR1 or SigR1 or ALS16	Sigma non- opioid intracellular receptor 1	-SigR1 accumulations were observed in in G93A tg mice - Soluble SigR1 protein levels were decreased in G93A tg mice - Treatment with the S1R agonist PRE-084 improves locomotor function and MN survival in presymptomatic and early symptomatic G93A tg mice	- (Prause <i>et al.</i> , 2013) - (Prause <i>et al.</i> , 2013) - (Mancuso <i>et al.</i> , 2012)
DCTN1 (Dynactin 1) or p150 or Glued SETX (Senataxin) or ALS4	Dynactin 1	- SOD1 inclusions: interaction between mutant SOD1 and the dynein motor plays a critical role in the formation of large inclusions containing mutant SOD1 - Expression lowered in presymptomatic G93A tg mice	- (Zhang <i>et al.</i> , 2007) (Ström <i>et al.</i> , 2008) - (Kuźma-Kozakiewicz <i>et al.</i> , 2013)
PRPH (Peripherin)	Senataxin	-SOD1 inclusions	- (Gruzman <i>et al.</i> , 2007)
CHGB (chromogranin B)	Peripherin	- Co-aggregation with SOD1 - Neurotoxic peripherin splice variant in G37R tg mice	- (Larivière <i>et al.</i> , 2003) - (Robertson <i>et al.</i> , 2003)
CRYM Mu-crystallin	chromogranin B (secretogranin 1)	- Interact only with mutant forms SOD1 but not with wt SOD1	- (Urushitani <i>et al.</i> , 2006)
CX3CR1	Mu-crystallin	- Altered expression in Leu126delTT SOD1 mouse model	- (Fukada <i>et al.</i> , 2007)
DAO	chemokine (C-X3-C motif) receptor 1	- Deletion makes G93A SOD1 mice worse	- (Cardona <i>et al.</i> , 2006)
OMA1	D-amino-acid oxidase	- Astrocytes expressing mutant form toxic to MNs - Suppression in DAO activity (D-serine accumulation) was seen in G93A tg SOD1 mice model	- (Paul & de Belleruche, 2014) - (Sasabe <i>et al.</i> , 2012)
PARK7	OMA1 zinc metallopeptidase	- Both OMA1 and SOD1 utilizes zinc	- (Bao <i>et al.</i> , 2003)
PLEKHG5	Parkinson protein 7	- Oxidative stress signature: works as peroxidase, converge with SOD1 at Nrf2 a master TF of oxidative stress genes - Forms complexes with mutant SOD1 and ameliorates its toxicity - Copper chaperone acting on SOD1 - Altered expression in SOD1 G93A tg mice - Modulates the expression of SOD1	- (Milani <i>et al.</i> , 2013) - (Yamashita <i>et al.</i> , 2010) - (Giroto <i>et al.</i> , 2014) - (Knippenberg <i>et al.</i> , 2013) - (Z. Wang <i>et al.</i> , 2011)
TBK1	Pleckstrin homology domain containing, family G member 5	- Activation of NF-κB-mediated apoptosis pathway	- (Maystadt <i>et al.</i> , 2007)
TRPM7	TANK-binding kinase 1	- Activation of innate immunity - Divalent cation channel, mutant SOD1 cause cation (copper and zinc) toxicity	- (Abe & Barber, 2014) - (Zhao, 2013) - (Inoue <i>et al.</i> , 2010)

Table 1.3. Examples of known genetic suppressors of SOD1-mediated ALS *in vivo*. The hSOD1^{G93A} mouse line mentioned refers to the classical high copy G1 mouse unless otherwise specified (Gurney *et al.*, 1994). MN- Motor neurons, tg- transgenic, OE- overexpression, ND-not determined, KO-knock out.

Suppressor Gene	Mouse Mutant	Neuronal Effect	Life Span Extension
ALS-related genes			
Angiogenin OE	G93A	- Improved locomotion - Decreased MN death	10-12 days (Kieran <i>et al.</i> , 2008)
α-tubulin upregulation with rHIgM12	G86R and G93A	- Decreased MN death	8 days and 10 days (Xu <i>et al.</i> , 2015)
Neurotrophic factors			
IGF-1	G93A	- Smaller SOD1 aggregates - Decreased apoptosis - Decreased gliosis	40 days viral delivery to spinal cord and 22 days viral delivery to muscles (Kaspar, 2003)
GDNF	G93A	ND	10 days viral delivery to spinal cord and 7 days viral delivery to muscles (Kaspar, 2003)
VEGF	G93A	- Improved locomotion - Decreased MN death	30 days viral delivery to muscles (Azzouz <i>et al.</i> , 2004)
Other neuronal genes			
Derlin-1 OE	G93A	- Decreased MN death	ND (Mori <i>et al.</i> , 2011)
SMN1 OE	G93A	- Improved locomotion - Decreased MN death - Decreased gliosis	0 days (Turner <i>et al.</i> , 2014)
Dorfin OE	G93A	- Decreased SOD1 aggregates - Decreased MN death - No difference in gliosis	30 days (Sone <i>et al.</i> , 2010)
SIRT 1 OE	G93A low copy	- Smaller SOD1 aggregates	15 days (no effect on high copy G93A) (Watanabe <i>et al.</i> , 2014)
HSP 70 OE	G93A	- Improved locomotion - Decreased MN death - No difference in gliosis	<7 days injection 3 times a week to muscles (Gifondorwa <i>et al.</i> , 2007)
EAAT1 OE	G93A	- Improved locomotion	0 days (Guo <i>et al.</i> , 2003)
APP KO	G93A	- Improved locomotion - Decreased MN death	0 days (Bryson <i>et al.</i> , 2012)

CHAPTER 2

Generation and Characterization of a Knock-in Model for Amyotrophic Lateral Sclerosis in *Drosophila*

The homologous recombination for this chapter was designed with help from Dr. Robert Reenan and Dr. Cindi Staber. The cloning experiments for HR alleles were performed by Pinar Deniz and Mallory Kerner. Survival experiments (Figure 2.3, 2.4) and locomotion assays (Figure 2.5C, 2.6) was performed with help from Brown University Summer HHMI undergraduate scholars (2011-2014), Kirsten Bredvik, Abby Kerson, Emily Jang, Ceren Iskender and Gunes Birdal. Protein gels and Figure 2.15 and 16B,C were performed with help from Kirsten Bredvik. Figure 2.2D, 2.5A,B, electrophysiology experiments were performed by Aaron Held. NMJ analysis was performed by Aaron Held and Paxton Major. The leg denervation analysis (Figure 2.8B and 2.9) was done by Paxton Major. Experimental feedback was given by Dr. Robert Reenan and Dr. Kristi Wharton. Figure 2.7 and 2.10 were crafted by Aaron Held and the rest of the figures were crafted by myself.

ABSTRACT

Amyotrophic Lateral Sclerosis (ALS), the most common adult-onset motor neuron disease in the world, can be caused by mutations scattered along the full length of the Copper-Zinc Superoxide Dismutase 1 (SOD1) gene. Although ALS was characterized two decades ago as progressive muscle weakness due to extensive loss of motor neurons, the mechanisms underlying this incurable disease still remain elusive. More than 150 different point mutations have been found in the 153 amino acid encoding SOD1 gene of ALS patients. Despite substantial investigations in current SOD1-ALS animal models and post-mortem tissue analyses, the cellular mechanisms by which mutant SOD1 protein acquires toxic function are not well understood. One of the strongest hypotheses in the field suggests that aggregation due to misfolded SOD1 mediates cellular cytotoxicity. On the other hand, oxidative stress seems to play a critical role in ALS pathogenesis, since some transgenic models, especially those with low transgene copy number, do not develop disease symptoms unless they are challenged by reactive oxygen species. To address concerns about the dosage of mutant SOD1 in disease pathogenesis, we have genetically engineered four human ALS-causing SOD1 point mutations (G37R, H48R, H71Y and G85R) into the endogenous locus of *Drosophila* SOD1 (*dSod1*) via ends-out homologous recombination (HR); and analyzed the molecular, biochemical and behavioral alterations that arise from these mutations. Contrary to previous transgenic models, we have recapitulated ALS-like phenotypes in the fast ALS progression-causing SOD1 mutants without overexpressing the mutant protein. *Drosophila* carrying mutations causing fast disease progression in ALS patients (G85R and H71Y) exhibited neurodegeneration, locomotion deficit, and shortened life span whereas *Drosophila*

carrying mutations causing slow disease progression in ALS patients (G37R and H48R) were indistinguishable when compared to controls.

INTRODUCTION

Amyotrophic Lateral Sclerosis (ALS) is a lethal and aggressive disease in which upper and lower motor neurons progressively die back from the neuromuscular junction leading to death, which usually ensues within 3-5 years after diagnosis. ALS was characterized almost two centuries ago (Charcot & Joffry, 1869), and it is currently the most common adult onset motor neuron disease in the world. Despite its prevalence, the mechanism of disease pathogenesis leading to exclusive demise of motor neurons still remains a mystery, and currently there is no cure or an effective therapy. Over 50 genes have been linked to ALS thus far, suggesting an overwhelming genetic heterogeneity of the disease, rather than a common theme in neurodegeneration (Abel *et al.*, 2012; Sreedharan & Brown, 2013; Leblond *et al.*, 2014). Still, approximately 90% of ALS cases occur sporadically, with no causal genetic locus.

Superoxide Dismutase 1 (SOD1, also called Cu/Zn SOD1) was the initial gene linked to ALS in 1993 (Rosen *et al.*, 1993). Even though SOD1 only encodes a small protein of 153 amino acids (16kDa), it constitutes 1% of the cytoplasmic protein repertoire (Pardo *et al.*, 1995). In the cytoplasm, SOD1 forms dimers and removes superoxides, which are naturally occurring byproducts of oxidative phosphorylation. Even though superoxide scavenging is the main function of SOD1, recently other cytoplasmic and nuclear functions of SOD1 were revealed (Bunton-Stasyshyn *et al.*, 2014). Strong evidence indicates that in ALS, SOD1 mutations exhibit dominant

toxic gain of function properties at the protein level. Since its discovery, more than 150 SOD1 mutations have been identified in ALS patients. Most of these mutations are point mutations, which are dominantly inherited (Abel *et al.*, 2012; Saccon *et al.*, 2013). Some of these mutations confer early or late age of onset, fast or slow disease progression, and a number of them modify SOD1 in terms of protein stability, enzymatic activity, and metal-binding properties, while others maintain wild type SOD1-like properties (Valentine, Doucette, & Zittin Potter, 2005). Thus, SOD1 mutations range in heterogeneity in terms of their measured properties and their proposed mechanisms of action.

Currently, 3% of sporadic ALS (sALS) and 20-25% of familial ALS (fALS) are explained by SOD1 mutations (Peters, Ghasemi, & Brown, 2015). Intriguingly, cytoplasmic SOD1 inclusions have been reported in ALS patients regardless of SOD1 mutations (Gruzman *et al.*, 2007; Forsberg *et al.*, 2010; Bosco *et al.*, 2010), strengthening the hypothesis that there is a common mechanism for neurodegeneration in ALS and emphasizing a critical role for SOD1 regarding the general pathogenesis of the disease. Uncovering how mutations in SOD1 ultimately lead to the dysfunction and the ultimate death of motor neurons may shed light on how ALS develops and progresses in all patients with the sporadic or familial disease.

SOD1 is highly conserved across a broad spectrum of phyla, and it was the most prevalent cause of ALS until the recent discovery of C9orf72 repeat expansions in 2011 (DeJesus-Hernandez *et al.*, 2011; Renton *et al.*, 2011; Gijssels *et al.*, 2012). Thus, many disease model animals expressing a variety of SOD1 mutations are available. Consistent with the gain of toxic function hypothesis, neither *Drosophila* (Staveley,

Hilliker, & Phillips, 1991; Missirlis *et al.*, 2003), nor rodent models (Reaume *et al.*, 1996; Huang *et al.*, 1997; Ho *et al.*, 1998; Matzuk *et al.*, 1998; Yoshida *et al.*, 2000) lacking the SOD1 gene developed neurodegenerative phenotypes. In order to examine the gain of function of SOD1 mutants in mutant alleles, more than 15 transgenic animal models were generated thus far (Trotti *et al.*, 1999; Kato, 2008; Joyce *et al.*, 2011). The majority of transgenic animals recapitulated many characteristics of ALS, including progressive motor deficits, paralysis, motor neuron degeneration, and early lethality (McGoldrick *et al.*, 2013). However, ALS-like phenotypes in these animals are highly dependent on transgene expression levels. In all current models, when SOD1 copy number is increased, the ALS-like phenotypes become more severe (Alexander *et al.*, 2004; Wang, Farr, Hall, *et al.*, 2009). Conversely, alleles expressing a low transgene copy number do not develop ALS-like phenotypes (Gurney *et al.*, 1994). Conceivably, overexpression may give rise to phenotypes not directly relevant to the disorder. Thus, whether the ALS-like phenotypes of these models stem from overexpression of the mutant allele or from aspects of the SOD1 mutation itself is currently unknown. Another complication arising from transgenic models is that the control line used in these experiments expresses relatively low protein amounts of wild type SOD1 (hSOD1^{wt}). In some studies, the control and the mutant SOD1 protein expression levels are equal based on denaturing immunoblotting analyses, while there is a huge difference between the genomic inserted transgene copies. For instance, the original hSOD1^{G93A} mouse model, which is the line used almost exclusively in ALS drug screening studies, has almost the same amount of SOD1 protein as the wild type line based on detection by denaturing immunoblotting. However, the mutant line contains 18 copies of the transgene while the

wild type line has 7 (Gurney *et al.*, 1994). Thus, the comparative analysis of the mutant lines and the wild type lines based on denaturing immunoblotting results is not straightforward and possibly inaccurate. These inconclusive and outdated modeling strategies became even more confusing when two groups crossed the hSOD1^{G93A}, hSOD1^{G85R} and hSOD1^{A4V} mouse lines with a control line that overexpresses hSOD1^{wt}. The disease onset of trans-heterozygote hSOD1^{G85R} and hSOD1^{G93A} mice arise much earlier upon crossing them to hSOD1^{wt}, while hSOD1^{A4V} crossed to hSOD1^{wt} mice developed ALS-like phenotypes (Jaarsma *et al.*, 2000; Deng *et al.*, 2006) absent in mice with the hSOD1^{A4V} transgene alone (Gurney *et al.*, 1994). Moreover, many groups demonstrated that hSOD1^{wt} can acquire toxic properties upon stress challenges and overexpression of hSOD1^{wt} alone is able to recapitulate some ALS phenotypes such as mitochondrial dysfunction, axon degeneration, and premature motor neuron death accompanied with SOD1 protein aggregation by simply overexpressing hSOD1^{wt} in mice (Jaarsma *et al.*, 2000; Ezzi, Urushitani, & Julien, 2007; Graffmo *et al.*, 2013). (The hypotheses for how hSOD1^{wt} can become toxic are discussed in Chapter 1 in detail.)

Controversial transgenic modeling results demonstrate that SOD1 protein dosage plays a critical role in the development of ALS pathogenesis and there is a long-standing need for the generation of more accurate ALS models. Therefore, a more precise way to compare different ALS-causing mutations is to generate knock-in SOD1 mutant models where the gene copy number is constant and consistent with the appropriate wild type controls. The introduction of disease causing mutations within the endogenous locus ensures consistent and equivalent protein expression levels by subjecting the mutated version of the gene to the same promoter, enhancer elements, chromatin state, and

chromosomal location as the wild type copy. Precise targeted mutagenesis has not yet been utilized to genetically model ALS in any model organisms. However, non-transgenic SOD1 mutants have been isolated and studied as an outcome of random gene mutagenesis in mice (Joyce et al., 2015) as well as naturally occurring SOD1-mutant dogs with canine degenerative myelopathy (DM) that resembles human ALS (Awano et al., 2009; Crisp, Beckett, Coates, & Miller, 2013; Wininger et al., 2011; Zeng et al., 2014). In addition, a non-transgenic SOD1 allele (mentioned as *dSod1*^{G51S} in this study) has been isolated from an Ethyl methanesulfonate (EMS) screen in *Drosophila* (Campbell, Hilliker, & Phillips, 1986). However, this allele was not a cognate ALS patient mutation and was mis-characterized as “null” allele, and as a result was not investigated in ALS-like phenotypes (Campbell et al., 1986; Staveley et al., 1991; Phillips et al., 1995; Parkes et al., 1998; Kirby et al., 2008; O’Keefe et al., 2011; Mishra et al., 2014).

Recently, a group isolated an endogenous SOD1 mutant from a N-ethyl-N-nitrosourea (ENU)-mediated genetic screen (Joyce et al., 2015): D83G, a mutation that had previously been identified in ALS patients (Millecamps et al., 2010). Despite lack of SOD1-positive proteinaceous inclusions, homozygous mSOD1^{D83G/D83G} mice retain no detectable dismutase activity, very little stable SOD1 protein, and die prematurely (Joyce et al., 2015). Furthermore, these mice display progressive motor and behavioral deficits and loss of muscle force due to progressive degeneration of lower and upper motor neurons-unlike SOD1 null mice- providing strong evidence that supports the gain of toxic function for mutant SOD1 (Joyce et al., 2015). The endogenous SOD1 mutant mice demonstrated that ALS-like phenotypes are achievable in model organisms without the

necessity for transgenic overexpression of the mutant allele.

Invertebrate systems provide a rapid and powerful tool for assessing the genetic affects of disease-causing mutations, and *Drosophila* has proven itself as a highly relevant system to model various human diseases (Bilen & Bonini, 2005; Rajan & Perrimon, 2013; Debattisti & Scorrano, 2013; Konsolaki, 2013; Casci & Pandey, 2015). A *Drosophila* ALS model generated by homologous recombination is a fast and efficient model to analyze both decreased levels of superoxide dismutase activity and misfolded SOD1 toxic gain of function mutations contributing to ALS. In addition to the general advantages of a small, quick, and well-established model organism, *Drosophila* is a powerful and advantageous organism in which to specifically knock in ALS-causing SOD1 point mutations for several reasons. First, SOD1 is a small protein, well-conserved between organisms in terms of sequence, structure and function (Bertini, Manganl, & Viezzoli, 1998). hSOD1 and *dSod1* differ only at 49/153 residues, and 22 of these different residues posses a similar side chain chemistry (Figure 2.1). Second, overexpression of hSOD1 in *Drosophila* has already recapitulated a variety of ALS-like phenotypes such as locomotion deficit, gliosis, reduced synaptic transmission, SOD1 protein aggregation and mitochondrial defect (Watson *et al.*, 2008; Bahadorani *et al.*, 2013). Third, ends-out homologous recombination (HR), which is identical in concept to the gene replacement techniques used routinely in rodents, is much faster, cheaper and successfully applied method in *Drosophila* (Staber *et al.*, 2011) that is previously used to model epilepsy in flies (Sun *et al.*, 2012; Schutte *et al.*, 2014). In order to provide new insights into the mechanisms of SOD1-mediated ALS and investigate the effects of a SOD1 mutations at endogenous expression levels, we have

generated and characterized a novel model for familial ALS in *Drosophila* where endogenous dSod1 is precisely engineered to harbor G37R, H48R, H71Y and G85R point mutations. These mutations are identical to the ALS mutations leading to pathological changes in human familial ALS and they all result in different disease onset and progression in patients (Table 2.1). These studies provide the foundation for contributing new insights into the understanding of the cellular determinants leading to SOD1-mediated ALS and uncover ALS-related cellular responses in a dosage sensitive manner.

MATERIALS AND METHODS

***Drosophila* Strains**

Drosophila were raised at a constant 25°C, on standard cornmeal molasses food and under 12 h day/night cycles. *dSod1*^{X-39} and *dSod1*^{G51S} line (n1 or n108) were ordered from Bloomington Drosophila Stock Center (BDSC stock numbers 24492 and 24490, respectively). The names of the dSod1 mutations are kept based on the human SOD1 amino acid numbering system throughout this work. The *dSod1*^{X-16} line was a kind gift from Dr. William C. Orr from Wayne State University. The full list of *Drosophila* lines used in this study can be found in Table 2.3.

Homologous Recombination

We performed ends-out homologous recombination to create three independent lines of *dSod1*^{WTLoxP}, *dSod1*^{G37R}, *dSod1*^{H48R}, *dSod1*^{H71Y}, and *dSod1*^{G85R} using a similar methodology that is reported previously (Staber *et al.*, 2011). Briefly, we utilized the ends-out targeting vector p[w25.2] that contains the *mini white* marker (*white*⁺), a

selectable red eye color, flanked by *LoxP* sites for subsequent removal by Cre-recombinase (Figure 1.3). Homology arm 1, corresponding to exon1 of *dSod1*, and homology arm 2, corresponding to exon2 of *dSod1*, were cloned and sequenced in pTOPO (Life Technologies) and then shuttled into the multiple cloning sites of the vector to generate p[w25-dSod1], which was then introduced into the *Drosophila* genome by standard P-element transgenic methods (Genetic Services). Full targeting region coordinates were: Chr3L:11,103,794-11,108,715 (4922 nucleotides). All targeting was done in a w¹¹¹⁸ background, as previously described, and performed in a wild type Chromosome 3 background (Gell & Reenan, 2013). A full list of cloning, mutagenic, and sequencing primers can be found in Table 2.4. Targeting was performed to generate multiple independent targeting events that incorporate (G37R, H48R, H71Y and G85R) or exclude engineered mutations (*WTLoxP*). All targeted animals have a *LoxP* “scar” of 72 nucleotides.

After generating the transgenic flies, white or mosaic-eyed females were collected from heat-shocked vials and then crossed with *yw;ey-Flp,noc^{sco}/CyO* males and only red-eyed female progeny were selected for additional validation. Targeted alleles were validated by PCR amplification, using primers outside the region of targeting and primers specific to the *white*⁺ marker. Following recombination, the *white*⁺ minigene selection cassette was removed via genetic crosses, which introduced Cre-recombinase. All targeted alleles were sequenced to verify that no unintended mutations were introduced. It is important to note here that all of the targeted alleles contain a natural polymorphism at the site 1013 having a C instead of an A, which leads to N98K missense mutation in human amino acid numbering system (N96K in *Drosophila* dSod1 numbering system),

which is also referred as *dSod1^{fast}* allele in the literature (Phillips *et al.*, 1995). The *dSod1^{G51S}* allele that is generated through EMS mutagenesis does not contain this polymorphism, and it is *dSod1^{slow}* allele. *dSod1^{fast}* and *dSod1^{slow}* alleles do not result in a phenotypic change in *Drosophila* they are named after their differential mobility on a native polyacrylamide gel (Lee, Misra, & Ayala, 1981; Hudson *et al.*, 1994; Phillips *et al.*, 1995). All three knock-in lines from each line were backcrossed to *w¹¹¹⁸*, a white-eyed genetic background, for five generations. *Drosophila* stocks were kept as heterozygotes using 3rd chromosome balancers. Heterozygous *dSod1* alleles that used in the experiments were generated by crossing mutant lines to the wild type line *WTLoxP*.

Eclosion Assay

For the eclosion percentages described in Figure 2.2.C, we set up at least 12 vials of cohorts of 2-3 heterozygous males and virgin females at 25°C, on standard cornmeal molasses food and under 12 h day/night cycles. The parents were transferred to a new vial every day. The heterozygous *dSod1* alleles were balanced over a third chromosome balancer: *TM3,GFP,ser,w⁺* (BDSC stock number: 4534). When the progeny started eclosing, heterozygous progeny having red eyes due to the balancer were counted and homozygous progeny having white eyes due to lack of the balancer that eclosed or stuck in the pupal case were counted. The progeny carrying homozygous balancers died early in development due to a recessive lethal marker on the balancer chromosome. The progeny from each vial were counted until the number of homozygous mutants reached 200. Then, the eclosion percentages were calculated by (total number of eclosed homozygous adults)/(total number of homozygous pupal cases)*100. The results of 12

vials were averaged and one way-ANOVA analysis was performed, followed by Tukey HSD test.

To determine the eclosion percentages in Figure 2.2.D, 2 males and 3 female virgins were mated and then bred every day for a maximum of 3 weeks. Flies were raised under 12h day/night cycles at 25°C on a standard diet of cornmeal supplemented with yeast. Heterozygous *dSod1* alleles were balanced over *TM6C,Sb,Tb,e*. Two weeks after the initial lay, the number of dead Tb^+ pupae and empty Tb^+ pupal cases were counted, and percentage eclosion was calculated using the formula: $(Tb^+ \text{ empty}) / (Tb^+ \text{ empty} + Tb^+ \text{ dead})$. $N > 100$ for each genotype, and statistics were calculated using Fisher's exact test.

Survival Assay

For the survival assay, parental flies were raised at 25°C, on standard cornmeal molasses food and under 12 h day/night cycles. The parental flies were collected from population density controlled broods (2-3 males and females in each vial) in order to avoid any confounding effects due to over-crowding. The parents were allowed to mate and lay eggs for 2 days before being transferred to fresh food twice. Three trials of survival analysis were performed for each genotype. For the heterozygous genotypes, in order to eliminate maternal effects on the *dSod1* mutant allele, in trial 1 the mutant allele was passed from the mother and in trial 2 the mutant allele was passed from the father. The third trial was either identical to either the trial 1 cross or the trial 2 cross. The offspring from these parents were collected over a period of 24 hours and sorted by sex. 12 males and 12 females were kept in vials containing standard cornmeal molasses food. For each genotype multiple replicate vials were set up so the total sample size was 200-

300 for each sex. Flies were transferred onto fresh food three times a week by blinded undergraduate researchers. The number of deaths was recorded. The survival assay described in Figure 2.3 was performed at 18°C and the survival assay described in Figure 2.15 was performed at 25°C. Once all the flies were dead, log rank test was performed for statistical analysis.

Riluzole, Melatonin, H₂O₂ Feeding Assay

All chemicals were delivered to *Drosophila* in instant food (Nutri-Fly Instant, Genesee, 66-118). Instant food is prepared based on the manufacturer recipe. For each vial, 2 grams instant food was dissolved in 5mL milliQ water or the chemical solution. For each bottle 21 grams instant food was dissolved in 50mL milliQ water or the chemical solution.

2% concentration of hydrogen peroxide (H₂O₂) was diluted from 30% stock (Fisher Chemical H325-100) and delivered to 1-day-post eclosion *Drosophila* in vials. Each vial contained 50 males or 50 females. Three trials of H₂O₂ survival analysis were performed for each genotype and sex. As in survival analysis, for the heterozygous genotypes in order to eliminate the maternal effects on the *dSod1* mutant allele, in trial 1 the mutant allele is passed from the mother and in trial 2 the mutant allele is passed from the father. Trial three was identical either to the trial 1 cross or the trial 2 cross. The number of deaths was recorded every 8 hours by blinded undergraduate researchers. Once all the flies were dead, log rank test was performed for statistical analysis.

X mM Riluzole (Sigma Aldrich-1744-22-5) is dissolved into 2X mM emulsifier 2-hydroxypropyl- β cyclodextrin (Fisher-AC297560250) as described in (Rival *et*

al., 2004). 1,2,4 mM Riluzole and 1,2,4 mM Melatonin (Fisher-ICN10225401) (together or separately) were fed to 50 female and 30 male parental *dSod1^{G85R}/TM3,GFP,Ser,w⁺* flies in each bottle. The parental flies were discarded after day 5. Eclosed progeny was kept in regular molasses based food and their survival period is recorded. Since Melatonin is sensitive to daylight, in the experiments involved Melatonin, the bottles were kept in dark.

Larval Motility Assay (Manual Version)

Larval motility assay was performed as previously described in (Batlevi *et al.*, 2010). Larvae were selected during the wandering 3rd instar stage. They were washed in 1X PBS and placed on a 1% agarose plate made with 0.5% TBE (100mm by 15mm petri dish) and were allowed 1 minute to acclimate. The plate was placed on a 1mm by 1mm square grid and the larvae were allowed to crawl for 2 minutes. The total number of squares a larva crossed was counted by blinded undergraduate researchers. We considered a square to be crossed when the larvae's posterior end crossed a line and the total number of squares crossed was counted. Dunnett's test following one-way ANOVA was used to compare the experimental group to the wild type.

Larval Motility Assay (Computational Version)

In the computational larval motility assay, 5 larvae were allowed to crawl on 22cm diameter dish filled with 1% agarose in H₂O₂. The larvae were videotaped for 1.5 minutes and videos were analyzed using a Matlab program that calculates total distance traveled for each larva. >30 larvae were used per group. If two larvae collided, the data

was discarded in case it altered behavior. Experiments used either mid-3rd instar larvae or wandering 3rd instar larvae. Wandering 3rd instars were identified as fully-grown larva that had exited the food but not inverted their anterior spiracles. Mid-3rd instars were pulled from the food approximately 24 hours before wandering. Tukey HSD test was used to calculate significance.

Adult Climbing Assay (Negative Geotaxis Assays)

10 adult male or female flies at the appropriate age were placed into a vial without food and negative geotaxis assays were conducted in three trials with each group consisting of 20 vials for each sex and genotype. The flies were gently tapped to the bottom of a vial and allowed to climb for 5 minutes. The number of flies reaching above a 75% mark of the total cylinder length in 5 min was recorded and the average calculated. Dunnett's test following one-way ANOVA was used to compare the experimental group to the wild type.

Western Blotting

For all the denaturing gels that are shown in the figures, protein samples were homogenized in Leammli buffer (Biorad) and β -mercaptoethanol, and run out on a 4-20% gradient gel (Biorad Mini-Protean-TGX, 456-1093). For the mutant tissue that shows trace amounts of dSod1 protein on denaturing gels (dSod1^{G85R/G85R}, dSod1^{H71Y/H71Y}, dSod1^{G51S/G51S}), various protein extraction solutions were assayed, e.g. RIPA buffer in combination with proteinase inhibitor cocktails, but no significant improvements were observed. For adult tissue, the abdomen region was discarded and for larval tissue

intestines were removed. Unless otherwise specified, one adult fly or one larva was homogenized in 50µl sample buffer and 10µl sample was run on 100 Volts. Samples were transferred to nitrocellulose membrane for 1 hour at 4°C. For developmental time point western blots, the total protein amount was equalized between different samples via Coomassie Protein Assay with manufacturer instructions (Thermo Scientific, 1856209). Rabbit polyclonal anti-dSod1 antibody (a kind gift from Dr. William C. Orr from Wayne State University) was used at 1:3000, and anti-actin (Millipore) was used at 1:50000. Horseradish peroxidase (HRP)-conjugated goat anti-mouse secondary antibody (Abcam ab5930) was used at 1:5000 and HRP-conjugated goat anti-rabbit secondary antibody (Jackson Immuno 111-0350144) was used at 1:10,000. Immunoreactive bands were visualized by ECL chemiluminescence detection reagent (Genesee, Amersham ECL Reagent, 84-817). Non-saturated bands were quantified on ImageJ (National Institutes of Health) and expressed as a ratio in relation to the internal reference actin. At least three biological replicates were quantified.

For high salt buffer protein extraction experiments, the following buffers have been tried: (i) 750mM NaCl, 50mM Tris-HCl (pH 7.5), 10mM NaF, 5mM EDTA (ii) 750mM NaCl, 50mM Tris-HCl (pH 7.5), 5mM EDTA, proteinase inhibitor cocktail (Roche), 0,1% Triton-X (iii) 5% SDS, 50mM Tris-HCl (pH 7.5), 5mM EDTA, 175mM NaCl (iv) 5% SDS, 50mM Tris-HCl (pH 7.5), 5mM EDTA, 175mM NaCl, 8M urea (v) 750mM NaCl, 50mM Tris-HCl (pH 8.8), 10mM NaF, 5mM EDTA (vi) 750mM NaCl, 50mM Tris, 10mM NaF, 5mM EDTA (vi) Biorad Ready Prep Protein Extraction Kit (Soluble/Insoluble, 163-2083). The extraction conditions were similar to the methodology that was reported previously (Watson *et al.*, 2008). Briefly, 5 male adults

(abdomen discarded) were homogenized in 100µl high salt buffer. 30µl of the protein sample was removed and run as “total” protein sample. The rest of the protein sample was spun at 10,000g for 30 minutes in 4°C. 30µl of the protein sample was removed and run as “supernatant” protein sample. The pellet was re-suspended in 100µl of high salt buffer and spun at 10,000g for 30 minutes in 4°C twice. Finally, the pellet was re-suspended in 50µl high salt buffer and run as “pellet” sample.

Native PAGE

For non-denaturing gels, protein samples from 2 adult flies (abdomen discarded) were homogenized in 50µl Native Sample Buffer (Biorad, 161-0738) and run out on a 10% gradient gel (Biorad Mini-Protean-TGX, 456-1033) for 5-8 hours, on 100 volts at 4°C. The following protein standards were used: pre-stained IEF Standards (BioRad, 161-0310) and non-stained Novex NativeMARK Unstained Protein Standard (Fisher Scientific, LC0725). As a positive control, human (ENZO, 80-1642) or bovine (ENZO, ALX-202-022-UT50) SOD1 protein isolates were diluted in native sample buffer and 50 units were loaded to the well. The gel was blotted with 1:3000 dSod1 antibody and the transfer conditions were the same as described in the previous western blotting section.

SOD Activity Assay

For SOD activity assay, conditions were similar to those in the preceding native gel methods with one exception: 5 adult flies (abdomen discarded) or 5 larvae were homogenized in 50µl native sample buffer. Briefly, after running the gel for 5-8 hours, the gel was washed 3 times in distilled water. The gel was incubated 15 minutes in 10mg Nitroblue Tetrazolium (NBT, Sigma N5514-10TAB) and 4mg riboflavin (Fisher BP167-

50) solution. Then, the gel was incubated 15 minutes in TEMED-water solution (10 μ l TEMED in 10mL distilled water in the dark. Finally, the gel was washed 3 times in distilled water and imaged on a white light box until the desired contrast was reached.

Electrophysiology

Wandering 3rd instar larvae were fileted and the motor neuron axons cut in a variant of HL3 containing (in mM): 70 NaCl, 5 KCl, .5 CaCl₂, 10 MgCl₂, 10 NaHCO₃, 5 Trehalose, 115 Sucrose, 5 HEPES, pH 7.2. This solution was also used as the bath recording solution. Recordings were made at segment A3 muscle 6 using a 25 \pm 5 M Ω electrode filled with 3M KCl. Muscle health was assessed by measuring resting membrane potential and by passing a 1nA square pulse to measure input resistance. Muscles with a resting membrane potential >-60mV or an input resistance <4M Ω were deemed unhealthy and not used for analysis. Spontaneous mini excitatory post-synaptic potentials (mEPSPs) were recorded for 3 minutes in the absence of stimulation, and later analyzed using a custom written Matlab code. Excitatory post-synaptic potentials (EPSPs) were evoked using a suction electrode and analyzed using Clampfit. Statistics were calculated using a Tukey HSD test.

Leg Muscle Atrophy and Nerve Structure Analyses

For bright field leg images, each leg was removed with tweezers on a silicon (Dow corning, sylgard 184 silicone elastomer kit) plate. The legs were incubated in Vectashield (Fisher NC9532821) overnight at 4°C. The images were taken with Zeiss AX10 Imager M1. *dSod1*^{G85R/G85R} full leg lengths were calculated by tracing along the

midline of the femur on Image J. The nerve integrity of two-week-old *dSod1*^{H71Y/H71Y} legs (and control legs on Figure 2.8.D) was evaluated based on whether they maintained nerve branches or not. For *dSod1*^{G85R/G85R} (Figure 2.9), a blinded undergraduate researcher scored the legs based on different parameters (continuity of nerve bundle, number of kinks, nerve size) on a scale of 1, being the worst, to 5, being the best.

For muscle atrophy imaging, relevant *dSod1* mutants were combined with an *mhc-tau-GFP reporter* (BDSC: 38460): *dSod1*^{WTLoxP/WTLoxP}, *mhc-tau-GFP*; *dSod1*^{G85R/G85R}, *mhc-tau-GFP*; *dSod1*^{H71Y/H71Y} lines were generated. Legs were dissected and fixed as described previously (Soler *et al.*, 2004). Briefly, the full animal was fixed in 4% PFA for 5 hours at room temperature. Then, the legs were dissected and continued to fix more overnight at 4°C. Images were taken at the confocal microscopy as described in the microscopy section.

Tunnel Assay, Immunohistochemistry and Microscopy

Adult or larval brains were dissected in PBTX (Phosphate-buffered saline with 0.1% Tween 20) on a silicon (Dow corning, sylgard 184 silicone elastomer kit) plate. The tissue was fixed with 4% paraformaldehyde for 20 minutes at room temperature on the nuator. After three rounds of quick washes in PBTX, the tissue was blocked in PBTX with 5% normal goat serum. The primary antibodies used in this study were anti-Elav and anti-Repo, (Developmental Studies Hybridoma Bank) both used at 1:200; Alexa-Fluor 488 and 564 secondary antibodies were used at 1:200. DAPI (Invitrogen) was used at 1:1000.

For the TUNEL assay, CF-488 TUNEL kit (Biotium) was used according to manufacturer instructions. After Elav and Repo staining performed as described above. The tissue was re-fixed with 4% paraformaldehyde for 20 minutes at room temperature on the nuator. After three rounds of quick washes in PBTX, the tissue was re-blocked in PBTX with 5% normal goat serum. Each genotype was incubated in 10 μ l TUNEL equilibrium buffer for 5 minutes. Then, the buffer was replaced with the enzyme solution (2 μ l TdT enzyme in 100 μ l TUNEL reaction buffer) and incubated 2 hours at 37°C in a humidifying chamber. Finally, the tissue was washed three times with PBST.

For imaging of 3rd instar neuromuscular junctions (NMJs), wandering 3rd instar larvae of the appropriate genotypes were dissected in 1X PBS on a silicon (Dow corning, sylgard 184 silicone elastomer kit) plate. Larvae positioned dorsal-side-up, pinned anterior and posterior, and cut along the dorsal midline. After the guts were removed, the dorsal edges were pinned to expose the muscles and the filet was fixed for 20 minutes in 1X PBS with 4% formaldehyde. Filets were then blocked in a solution of PBT (1X PBS with 0.3% TritonX) with 1% normal goat serum (NGS, Sigma-Aldrich) for 2 hours. Filets were then incubated overnight at 4°C in a solution of PBT with 1% NGS, 1:300 Rabbit anti-HRP Cy3 (Jackson), 1:200 Mouse anti-Dlg (DSHB), and 1:2500 Phalloidin 488 (Life Technologies). Filets were then washed twice for 5 minutes in PBT and incubated at room temperature for 1hr in PBT with 1% NGS and 1:300 Goat anti-mouse 647 (Life Technologies). After the incubation, filets were washed twice for 5 minutes in PBS and mounted in 70% glycerol with 0.1% N-propyl gallate. Neuromuscular junction 6/7 in segment A2 was imaged using either an LSM510 or LSM710 confocal microscope. Bouton counts and area measurements were done using Image J by a blinded

undergraduate student.

All tissue was mounted in Vectashield (Fisher NC9532821). All confocal Z-series images were obtained by LSM510 confocal microscope. Images were contrast-enhanced in Adobe Illustrator. Each image shown is a representative example of $n \geq 5$ unless otherwise reported.

RESULTS

Generation of SOD1 Mutant *Drosophila* Alleles via Homologous Recombination

In order to develop a model of fALS, we generated *Drosophila* lines carrying the equivalent of human ALS causative pathogenic mutations to interpret whether different SOD1 point mutations cause similar toxic effects when they are expressed from the endogenous locus *in vivo*. We integrated G37R, H48R, H71Y and G85R point mutations into the endogenous *dSod1* locus via HR to model ALS in *Drosophila* (Figure 2.1A and B). These four point mutations have varying significance for the tertiary structure and enzymatic activity of the SOD1 protein in humans, and the patients carrying these mutations have different disease onsets and disease progression (Table 2.1).

The ultimate requirement for HR is that an *in vivo* linear template allele be recognized by the cellular DNA repair machinery. As the first step of HR, we designed a template allele (~5Kb), which includes the *dSod1* in its entirety interrupted by a *mini white* marker (~5Kb) and minimal flanking regions of *dSod1* enough for allele exchange to occur (Figure 1.3). We established nucleotide changes introducing G37R, H48R, H71Y and G85R point mutations by site-directed mutagenesis and ligated the construct into a P[w25.2] vector. P[w25.2] vector that contains all the required sites for later HR

steps such as the P element excision site, FLP recognition sites (FRT) and I-SceI endonuclease cut sites. Injection of the P[w25.2] vector into *Drosophila* embryos led to template allele integration into a random genetic location in the fly genome, generating transgenic animals. Then, through a series of crosses that lead to the excision of the transgene for initiating recombination events at the endogenous site, replacing the endogenous *dSod1* with the construct shown in Figure 1.3. More specifically, we excised the integrated *mini white*⁺ transgene from its original genomic using FLP site-specific recombinase. This produced a circular DNA fragment from the construct and through the use of I-SceI site-specific endonuclease converted the circular fragment into a linear recombinogenic template. Finally, we excised the *mini white* marker via Cre recombinase, which left a single *LoxP* site in the intronic region of *dSod1*. In parallel, to generate proper controls, we targeted a line using the wild type *dSod1*, which generated a wild type control *dSod1*^{WT*LoxP*} with the single 72 bp *LoxP* site in the same exact intronic region. Finally, we have shown that the *LoxP* site does not interfere with alternative splicing of *dSod1* mRNA (Figure 2.1C).

We generated each HR mutant lines from at least 3 independent targeting events. One random *Drosophila* line for each mutation (*dSod1*^{G37R}, *dSod1*^{H48R}, *dSod1*^{H71Y}, *dSod1*^{G85R}) was backcrossed to w¹¹¹⁸ for five generations for removal of any genetic background consequences and we these backcrossed lines for all subsequent studies. In addition, we compared the *dSod1* alleles generated in this study to the previously characterized *dSod1*^{G51S} line that carries a point mutation as a result of EMS mutagenesis (Campbell *et al.*, 1986; Phillips *et al.*, 1995). In order to assess interactions between different alleles, we have generated trans-heterozygote *Drosophila*, which carry multiple

point mutations. Moreover, in order to investigate the dosage effect of these alleles, we combined the point mutations alleles in trans with the *dSod1* deletion alleles (either *dSod1*^{X-39 or X-16}) and intercrossed them to the control *dSod1*^{WTLoxP} allele in order to investigate the heterozygous affects of *dSod1* point mutations.

***dSod1*^{G85R} and *dSod1*^{H71Y} Mutant dSod1 Alleles Severely Affect Viability and Fertility**

All three *dSod1*^{G85R/G85R} lines generated by homologous recombination are homozygous lethal at the end of the pupal stage with a characteristic phenotype: the adults die with their heads exposed from the pupal case (Figure 2.2.A). We observed rare (~1/1000) escaper *dSod1*^{G85R/G85R} homozygous flies that live less than an hour and exhibit severe paraparesis, uncoordinated locomotion, leg muscle twitching, extreme proboscis pulsing and seizures (Supplementary movie 2.1). Homozygous *dSod1*^{H71Y/H71Y} mutant lines exhibit less severe eclosion abnormalities than *dSod1*^{G85R/G85R} homozygous adults (eclosion rate: %33.33+/-6.00) (Figure 2.2.C) and the survivors of *dSod1*^{H71Y/H71Y} are infertile and the majority has an obvious wrinkled wing phenotype (Figure 2.2.B). Interestingly, after two weeks, *dSod1*^{H71Y/H71Y} exhibit a phenotype similar to that of the *dSod1*^{G85R/G85R} escaper flies (Supplementary movie 2.2). The *dSod1*^{G51S} allele that was generated via EMS mutagenesis, was also reported to display eclosion problems (Staveley *et al.*, 1991; Parkes *et al.*, 1998). Here, we confirm that *dSod1*^{G51S/G51S} exhibit lower eclosion rates (%48.48+/-10.00) (Figure 2.2.C). Expectedly, trans-heterozygote *dSod1*^{G85R/H71Y} flies exhibited an eclosion rate in between those of the severe *dSod1*^{G85R/G85R} and *dSod1*^{H71Y/H71Y} alleles (%15.00+/-7.00) (Figure 2.2.C). Moreover, the

severity of the eclosion defect for $dSod1^{H71Y}$ and $dSod1^{G85R}$ flies were dosage dependent (Figure 2.2.D and personal observation for $dSod1^{H71Y}$). Reducing the mutant allele copy number to half partially rescued the eclosion phenotype (%37.14+/-16.01 for $dSod1^{G85R/X-16}$).

The eclosed adults of $dSod1^{H71Y/H71Y}$ exhibited a severely reduced life span (12.37+/-0.27 days) almost identical to that of $dSod1^{G51S/G51S}$ homozygotes (12.70 +/- 0.97) (Figure 2.3.A). The heterozygous alleles ($dSod1^{H71Y/WTLoxP}$ and $dSod1^{G85R/WTLoxP}$) as well as $dSod1^{G37R/G37R}$ and $dSod1^{H48R/H48R}$ alleles did not affect life span (Figure 2.3.A and B).

The primary function of the SOD1 enzyme in the cytoplasm is to convert superoxide adducts to hydrogen peroxide and water (Fridovich, 1986). Treating the heterozygous adults ($dSod1^{H71Y/WTLoxP}$ and $dSod1^{G85R/WTLoxP}$) with a superoxide radical (O_2^-) generator, H_2O_2 , did not alter survival when compared to wild type $dSod1^{WTLoxP/WTLoxP}$ controls (Figure 2.4.A and B). However, homozygote $dSod1^{H71Y/H71Y}$ flies were extremely sensitive to oxidative stress, consistent with previous results regarding the $dSod1^{G51S/G51S}$ homozygous allele (Parkes *et al.*, 1998; Kirby *et al.*, 2008) (Figure 2.4.A and B). Finally, the $dSod1^{G37R/G37R}$ and $dSod1^{H48R/H48R}$ alleles were as insensitive as the wild type control to oxidative stress (Figure 2.4.C and D).

Severe Locomotion Defects of $dSod1^{G85R}$ and $dSod1^{H71Y}$ Mutant Alleles

Motor dysfunction is one of the first apparent symptoms in ALS patients (Pasinelli & Brown, 2006). The easiest way to correlate the molecular consequences of mutated $dSod1$ with behavioral consequences in *Drosophila* is to analyze locomotion

defects by examining crawling behavior in larvae and climbing behavior in adults. In order to investigate the motor ability of mutant Sod1 flies, we measured how far third stage instar larvae were able to crawl by utilizing two different methods. We chose to examine the crawling behavioral assay, because the *dSod1*^{G85R} mutation is homozygous lethal at the pupal stage, but larvae of this genotype are viable and appear to locomote normally. Measuring larval motility reflects whether these homozygous mutants are motor impaired before they die as pupa. To differentiate between homozygous flies in the larval stages, we generated heterozygous G85R lines with TM3-GFP balancer (*dSod1*^{G85R/TM3-GFP}). Therefore, homozygous flies can be easily distinguished due to the absence of GFP. This allows accurate genotyping of animals at the larval stage and comparison of *dSod1*^{G85R/G85R} larvae with their heterozygous siblings.

During late third instar larval stages, *dSod1*^{H71Y}, *dSod1*^{G85R}, and *dSod1*^{G51S} homozygotes crawled at almost half far of the wild type larvae (Figure 2.5.A and C). When we reduced the mutant copy number by half, the crawling defect was completely abolished (Figure 2.5.A). The milder alleles, *dSod1*^{G37R} and *dSod1*^{H48R}, were indistinguishable from wild type as homozygotes (Figure 2.5.C). Surprisingly, heterozygous *dSod1*^{H71Y/WTLoxP} and *dSod1*^{G85R/WTLoxP} larvae also were unable to crawl as well as wild type (Figure 2.5.C). In order to determine the onset of the locomotor defect in larvae, we measured locomotion in the mid third instar larval stage approximately 24 hours before wandering (Figure 2.5.B). We found that *dSod1*^{G85R} and *dSod1*^{H71Y} mutants traveled the same distance as *dSod1*^{WTLoxP} at the mid third instar stage, suggesting that the locomotor defect arises in the late third instar stage.

In adults, we followed the locomotion defect through a negative geotaxis climbing assay. Since the *dSod1*^{G85R} homozygous flies do not survive until adulthood, we did not test them. However, the other severe *dSod1*^{H71Y} and *dSod1*^{G51S} alleles almost completely lose their climbing ability within a week of eclosion (Figure 2.6.A for males and B for females). The heterozygous *dSod1*^{H71Y}, *dSod1*^{G85R}, and *dSod1*^{G51S} flies as well as the homozygous mild alleles, *dSod1*^{G37R} and *dSod1*^{H48R}, were indistinguishable from wild type flies throughout course of the assay (Figure 2.6.C for males and D for females).

Muscle Atrophy and Denervation of *dSod1*^{G85R} and *dSod1*^{H71Y} Mutant Alleles

Denervation of muscles by motor neurons in the limbs of patients is a characteristic symptom of ALS. At the terminal stages, *dSod1*^{G85R/G85R} struggle in the pupa case to eclose. These flies look morphologically wild type except for the fact that their legs are significantly shorter when compared to wild type flies (Figure 2.7.A, B and C). In addition, it was clear from the video of the escaper flies that *dSod1*^{G85R/G85R} flies drag their metathoracic legs (leg 3) while walking (Supplementary video 2.1). Thus, using a scale of 5 being the best and 1 being the worst, overall health scores of legs from *dSod1*^{G85R/G85R} flies overall health scores were determined by a blinded student based on nerve health, lower leg structure and kink severity of the femur were determined by a blinded student (Figure 2.8 A, B, and C and D). Leg 3 was the most severely affected, however leg 2 and leg 1 were not as healthy as a wild type leg. Wild type legs were scored higher than 4.5, whereas *dSod1*^{G85R/G85R} scores were leg 1 (2.87), leg 2 (2.5), and leg 1 (1.40).

Next, we utilized an *mhc-tau-GFP* intrinsic fluorescent muscle reporter to investigate the muscle structure and condition of *dSod1* mutants (Figure 2.7.A, B and C). In *dSod1^{G85R/G85R}* flies, the muscle appeared to be undergoing severe atrophy and the motor neurons surrounding the leg were deformed in the bright field image (Figure 2.7.C). In *dSod1^{H71Y/H71Y}*, the muscle structure and leg length were not affected at eclosion (Figure 2.7.D). However, the motor neurons lost branches by two weeks in 13 out of 15 legs when these flies were at the terminal stage of the disease (Figure 2.7.D).

Electrophysiological and Neuromuscular Junction (NMJ) Analyses of the Wandering Third Instar Larvae Exhibit Mild Defects

Impaired larval locomotion could be partial a result of defects at the neuromuscular junction (NMJ). To explore this possibility, we dissected wandering 3rd instar larvae and examined neuromuscular junction 6/7 in segment A2. We found a significant increase in bouton number in *dSod1^{H71Y/H71Y}*, and a trend toward increased bouton number in *dSod1^{G85R/G85R}*. Presynaptic area between genotypes was not significantly different (Figure 2.9). These surprising results of mild NMJ defects were unlikely to explain larval locomotion defect. The potential role of mutant *dSod1s* in motor neuron impairment was further investigated using electrophysiological analysis.

In a transgenic SOD1-mediated ALS *Drosophila* model, the synaptic transmission along the giant fiber motor pathway, a well defined neuronal circuit in *Drosophila* (Tanouye & Wyman, 1980), is shown to be abnormal and synaptic transmission becomes progressively defective in flies expressing mutant hSOD1 (Watson *et al.*, 2008). Since our *dSod1* mutants develop a movement defect in late 3rd instar and neuromuscular

junction deterioration is a key characteristic of ALS pathology, we measured several electrophysiological properties of the late 3rd instar neuromuscular junctions.

To measure muscle health, we recorded the resting membrane potential of muscle 6, and passed a 1nA square pulse to measure input resistance. The membrane potential of *dSod1*^{H71Y/H71Y} muscles was slightly decreased compared to *dSod1*^{WTLoxP/WTLoxP} and *dSod1*^{G85R/G85R}, but there was no change in input resistance between genotypes (Figure 2.10.A). This suggests that the electrical properties of the muscles are relatively similar between genotypes, with perhaps a slight decrease in driving force in *dSod1*^{H71Y/H71Y} due to the slightly less polarized muscle. When the axon innervating muscle 6 was stimulated with a suction electrode, multiple vesicles are released simultaneously causing a large excitatory post-synaptic potential (EPSP). EPSP amplitude was not different between the three genotypes, although there was a trend toward decreased EPSP amplitude in *dSod1*^{H71Y/H71Y}. This is not necessarily surprising given the decrease in resting muscle potential, and likely does not reflect a presynaptic change.

To analyze vesicle properties, miniature excitatory post-synaptic potentials (mEPSP) were also recorded. This data was analyzed using custom written Matlab code, and the analysis showed a clear increase in *dSod1*^{H71Y/H71Y} mEPSP amplitude. This increased amplitude could reflect an increase in neurotransmitter within presynaptic vesicles or a change in the glutamatergic post-synaptic receptors. The increase in *dSod1*^{H71Y/H71Y} mEPSP amplitude combined with the trending decrease in *dSod1*^{H71Y/H71Y} EPSP amplitude led to a very significant decrease in quantal content (EPSP amplitude/mEPSP amplitude), signifying that although the EPSP amplitudes across

genotypes were similar, *dSod1*^{H71Y/H71Y} uses fewer presynaptic vesicles to achieve the same post-synaptic depolarization.

In addition to mEPSP amplitude, we also analyzed mEPSP frequency and inter-event interval duration. We found that there were strong trends of increased mEPSP frequency in *dSod1*^{G85R/G85R} and *dSod1*^{H71Y/H71Y} (p=.07 and p=.09, Tukey HSD). To examine subtler mEPSP properties, we pooled mEPSP data across samples and plotted them in histograms binned by amplitude (Figure 2.9.B). The histograms suggest a slight increase in mini frequency and a shift in the distribution of both *dSod1*^{G85R/G85R} and *dSod1*^{H71Y/H71Y} mEPSP amplitude. To test if there was a change in frequency, we plotted the cumulative inter-event interval probability and compared the genotypes using a Kolmogorov-Smirnov test. This analysis shows that *dSod1*^{WTLoxP/WTLoxP} has a longer inter-event interval than both *dSod1*^{G85R/G85R} and *dSod1*^{H71Y/H71Y} (p<0.0001). To test if there was a change in mEPSP amplitude, we plotted the cumulative amplitude and compared the genotypes using a Kolmogorov-Smirnov test. We found that all three genotypes have distinct mEPSP amplitude distributions (p<0.0001 between any two genotypes). These changes in mEPSP properties strongly suggest vesicular properties and/or the post-synaptic channels are altered in *dSod1*^{G85R/G85R} and *dSod1*^{H71Y/H71Y} at the time of the movement defect onset.

Although we did not find any electrophysiological changes at the neuromuscular junction, potential vesicular properties and/or the post-synaptic channels could explain the decline in larval motility, and we found several changes suggesting that both the *dSod1*^{G85R/G85R} and *dSod1*^{H71Y/H71Y} neuromuscular junctions are abnormal. In particular, it was interesting that both mutants have a decrease in inter-event interval duration. This

increase in activity mirrors our finding that *dSod1*^{H71Y/H71Y} NMJ bouton number was increased (Figure 2.9). Both the structural and electrophysiological findings suggest increased synaptic activity at the neuromuscular junction. Although this finding is consistent with the lower motor neuron hyperactivity found in ALS patients, it does not explain the decline in larval motility. Further studies will be needed to identify the circuitry defects responsible for the decline in wandering 3rd instar locomotion.

Motor Neuron Cell Bodies of *dSod1* Mutants Did Not Reveal Cell Death and Gliosis

A consensus has not been reached regarding the nature of disrupted cellular pathways in ALS. As one hSOD1^{G85R} transgenic mouse model suggests, in later stages there may be SOD1 protein aggregates in motor neurons and glial cells (Wang, Farr, Zeiss, *et al.*, 2009). Homozygous SOD1 mutant dogs also exhibited misfolded SOD1 species (Awano *et al.*, 2009; Wininger *et al.*, 2011; Crisp *et al.*, 2013; Zeng *et al.*, 2014). On the other hand, in SOD1 mutant patient iPSC models, insoluble SOD1 species were detected only after inhibiting the proteasome (Kiskinis *et al.*, 2014) or using ultra-sensitive methods such as immunogold-staining followed by electron microscopy analysis (Chen *et al.*, 2014). The non-transgenic homozygous mice, on the other hand, did not recapitulate misfolded SOD1 aggregation (Joyce *et al.*, 2015). All of these non-aggregation results from non-transgenic systems suggested that the SOD1 protein aggregation might not be the initial trigger for ALS pathogenesis. Unfortunately, commercial hSOD1 and dSod1 antibodies exhibit non-specific staining and did not work for immunostaining purposes in *Drosophila*. Thus, we could not investigate whether dSod1 mutants form proteinous inclusions via immunostaining (Data not shown). Instead, we examined whether motor neurons died in mutant flies. In order to visualize motor

neurons, we utilized a nuclear GFP protein (*UAS-nlsGFP*) that was expressed under the *ok371* motor neuron specific driver (*ok371-GAL4*) and used DAPI nuclear staining as an experimental control. DAPI staining in motor neurons of *dSod1^{G85R/G85R}* and *dSod1^{H71Y/H71Y}* third instar larval brains and adult ventral nerve cord (specifically T1/T2 region of the thoracic ganglia) did not exhibit gliosis or increased apoptosis (Figure 2.11.A, B, and C). Lack of a change in TUNEL staining in mutants further strengthened the argument for the absence of motor neuron death seen above (Figure 2.11.D, E, and F) in third instar larval brains and adult ventral nerve cord. Another signature of ALS, gliosis in the neuronal samples, was also not seen in larval central nervous system, adult brain or ventral nerve cord as observed by a very uniform Repo staining (glial cell marker) (Figure 2.11.E, and F). Interestingly, we detected density difference in DAPI staining between the mutant *dSod1^{G85R/G85R}* and the wild type *dSod1^{WTLoxP/WTLoxP}*. We hypothesize that this is due to a loss of heterochromatin formation, which will be covered in more detail in Appendix I.

Protein Levels and Dismutase Activity of Mutant dSod1 Alleles Are Altered

In ALS patients, some SOD1 point mutations alter protein folding, protein stability, enzymatic activity, and metal-binding properties, while others maintain wild type SOD1-like properties (Valentine *et al.*, 2005). Next we asked whether the ALS-like phenotypic severity correlates with the possible loss of superoxide scavenging. Superoxide dismutase activity has not yet been characterized from SOD1^{H48R} and SOD1^{H71Y} (Table 2.1). Previously, hSOD1^{G85R} mutation has been shown to retain no enzymatic activity on native gel-based measurement, whereas hSOD1^{G37R} displayed

150% activity of wild type SOD1 protein (Borchelt *et al.*, 1994). Even though the tertiary structure of SOD1 protein was determined from 18 different species, *Drosophila* was not included in this study (Bertini *et al.*, 1998). First, we investigated whether these point mutations affect dSod1 protein stability and function. The H71 residue coordinates zinc binding, while the H48 coordinates copper binding in the human SOD1 protein (Table 2.1). Therefore these mutations might be required for appropriate dSod1 folding and metallation (Saccon *et al.*, 2013). Furthermore, SOD1 G85R and G37R mutations in humans are very unstable with a reduced half life (Borchelt *et al.*, 1994; Farr *et al.*, 2011). First, we measured the state of dSod1 dimerization and enzymatic activity via native gel-based SOD activity assay. According to this assay, activity of dSod1 dimers was visualized by a color change of nitroblue tetrazolium (NBT). In parallel, loaded dSod1 protein amount was quantified via denaturing SDS-polyacrylamide gel. Based on the gel assay, the *dSod1^{H71Y}*, *dSod1^{G85R}*, and *dSod1^{G51S}* homozygous adults did not exhibit any SOD1 activity while *dSod1^{G37R}*, *dSod1^{H48R}*, and the heterozygotes were indistinguishable from wild type Canton-S and *dSod1^{WTLoxP}* (Figure 2.12. A and B). However, surprisingly, the null *dSod1^{H71Y}*, *dSod1^{G85R}*, and *dSod1^{G51S}* homozygotes also did not reveal any monomer protein on the SDS-polyacrylamide denaturing gel. This result is consistent with the reduced protein amount that is observed in the non-transgenic mouse model harboring the mSOD1^{D83G/D83G} mutation (Joyce *et al.*, 2015).

Since the SOD activity assay is based on native gel electrophoresis, we performed a native gel immunoblotting experiment in order to reveal the presence of dSod1 dimers on the native gel for the *dSod1^{H71Y}*, *dSod1^{G85R}*, and *dSod1^{G51S}* homozygous alleles. The native gel revealed that dSod1 dimers are present in all mutants on a non-denaturing gel,

but absent from the denaturing SDS-gel (Figure 2.12.D). Moreover, in the native gel immunoblotting some dSod1-positive protein species at altered motilities were detected not only in homozygote mutants, but also in heterozygotes. These could potentially represent misfolded dSod1 species.

Next we attempted to discern whether the lack of detectable dSod1 on a SDS-PAGE denaturing gel is a general technical artifact, or if it is related to the progression of disease pathology. To assess if the ALS mutations affect dSod1 protein stability in earlier stages as severely as in adults, we measured protein levels of dSod1 during the third instar larval stage from all mutant lines (Figure 2.12.A). As previously observed in endogenously mutant $SOD1^{D83R/D83R}$ mouse, $dSod1^{H71Y}$ and $dSod1^{G85R}$ exhibited a significant reduction in amounts of dSod1 protein. Intriguingly, in the previously named “null or $dSod1^{-/-}$ ” allele $dSod1^{G51S}$ (other names: *n108* or *n1* allele), we observed some protein expression, suggesting that the $dSod1^{G51S}$ point mutation did not result in a protein null expression as previously reported. Next, we asked whether the lack of protein detection on an SDS-PAGE gel is age-specific by performing a developmental denaturing immunoblot analysis of dSod1 mutants. Detection of soluble dSod1 protein from homozygous $dSod1^{H71Y/H71Y}$ and $dSod1^{G85R/G85R}$ appears to decline gradually during development, while in the control line remains constant (Figure 2.13. B, C, and D). More importantly, the loss of dSod1 protein detection on denaturing gels coincides with the onset of locomotor defects that we defined in $dSod1^{H71Y}$ and $dSod1^{G85R}$ (Figure 2.5.B). We then investigated if the undetectable dSod1 on SDS-PAGE gel is in the insoluble protein fraction by extracting protein using six different high-salt or urea protein extraction solutions, however, we did not detect any dSod1 protein in the insoluble

fraction (A representative gel is shown in Figure 2.14). Thus, we conclude that the pathological SOD1 variants in *Drosophila* result in a protein alteration that renders the mutant proteins inaccessible to extraction or penetration into the gel matrix used for denaturing gel electrophoresis. Nevertheless, the native gel results suggest that in all cases, near wild type levels of dSod1 protein are produced in all mutants, are stable, but largely lack enzymatic activity.

The *dSod1*^{G85R} Allele Gain of Toxic Function Is Dosage Dependent

Based on the observation that null dSod1 mutations result in some ALS-like phenotypes, we tested the gain of function nature of the *dSod1* mutations by altering the dosage. In order to clarify whether *dSod1* mutants cause locomotion, eclosion and survival defects through a toxic gain of function related mechanism, we expressed wild type *dSod1* exogenously on the second chromosome in addition to the endogenous locus on the third chromosome. As mentioned above, *dSod1*^{G85R}/*dSod1*^{WTLoxP} display normal longevity, while *dSod1*^{G85R}/*dSod1*^{G85R} homozygotes are lethal. We then introduced one or two copies of the *dSod1* locus on a P-element harboring the entire wild type locus and upstream and downstream sequences, on the second chromosome (see Materials and Methods for details). The expressed wild type *dSod1* loci on the second chromosome in one or two doses ($P[dSod1^{WTLoxP}]/P[dSod1^{WTLoxP}]$; $dSod1^{G85R}/dSod1^{G85R}$ or $P[dSod1^{WTLoxP}]/+;$ $dSod1^{G85R}/dSod1^{G85R}$) fully suppresses the *dSod1*^{G85R}/*dSod1*^{G85R} lethality (Figure 2.15). Contrary to this result, we observed that the eclosion defect is only fully rescued by two doses of wild type dSod1 (Figure 2.16.A). However, in contrast to *dSod1*^{G85R}/*dSod1*^{WTLoxP} flies, the transgenic line carrying two wild type and two mutant

dSod1 alleles ($P[dSod1^{WTLoxP}]/P[dSod1^{WTLoxP}]; dSod1^{G85R}/dSod1^{G85R}$), did not exhibit a wild type life span, they lived 28.98 \pm 0.61 days for males and 39.37 \pm 1.32 days for females, while the wild type line carrying 2 wild type *dSod1* ($dSod1^{WTLoxP}/dSod1^{WTLoxP}$) males lived 52.39 \pm 0.74 days and females lived 61.95 \pm 0.85 days. Furthermore, overexpression of the wild type *dSod1* was also slightly toxic since the transgenic line carrying four wild type copies of *dSod1* ($P[dSod1^{WTLoxP}]/P[dSod1^{WTLoxP}];dSod1^{WTLoxP}/dSod1^{WTLoxP}$) males lived and average of 38.91 \pm 0.55 days and females lived average of 49.80 \pm 1.25 days.

The short lived *dSod1* transgenic lines ($P[dSod1^{WTLoxP}]/P[dSod1^{WTLoxP}]; dSod1^{G85R}/dSod1^{G85R}$, $P[dSod1^{WTLoxP}]/P[dSod1^{WTLoxP}];dSod1^{WTLoxP}/dSod1^{WTLoxP}$) did not exhibit an eclosion defect (Figure 2.16.A) and the eclosed adults did not die with an apparent progressive locomotion defect, unlike *dSod1*^{H71Y/H71Y} and *dSod1*^{G51S/G51S} (Figure 2.16.B for males and C for females). However, right before death, $P[dSod1^{WTLoxP}]/P[dSod1^{WTLoxP}];dSod1^{G85R}/dSod1^{G85R}$ flies exhibited locomotor deficit for a day (Supplementary video 2.3), which is comparable with ALS patients that lose their locomotion ability during the first two years of disease progression just before the need for a diaphragm support (Benditt & Boitano, 2008).

One explanation for the partial suppression of *dSod1*^{G85R}/*dSod1*^{G85R} survival by the transgenic *dSod1*^{WTLoxP} expression is that the wild type *dSod1* might dimerize with the mutant form of *dSod1* and this interaction inhibits its toxicity. However, western blotting analysis did not reveal an increased amount of *dSod1* dimers as an indication of mutant-wild type dimers, when *dSod1*^{WTLoxP} was exogenously expressed on *dSod1*^{G85R} background (Figure 2.17). Thus, we hypothesize that wild type *dSod1* is not necessarily

protecting mutant dSod1, but instead relieves cellular toxicity caused by the mutant dSod1.

Riluzole and Melatonin Are Not Effective Treatments For Eclosion And Life Span

Defects of *dSod1*^{G85R/G85R}

Riluzole, an antagonist for glutamate receptor, is the only approved treatment for ALS. However, it typically prolongs the patient's expected life span by only 2-3 months (Miller, Mitchell, & Moore, 2012). Life span defect and climbing deficit of a glutamate buffering mutant through dEAAT1 glutamate receptor knock down *Drosophila* model is partially suppressed upon administration of Riluzole and a free radical scavenger Melatonin, another chemical that is used in ALS patient trials (Rival *et al.*, 2004). After characterizing *dSod1*^{G85R/G85R} flies, we investigated the effects of Riluzole and Melatonin on their eclosion and life span defect. We fed parental *dSod1*^{G85R/TM3,GFP,Ser,w⁺} flies with various concentrations of Riluzole and/or Melatonin. Riluzole is dissolved into emulsifier 2-hydroxypropyl- β cyclodextrin as described in (Rival *et al.*, 2004). All tested chemical combinations resulted in a moderate effect as seen in ALS patients (Table 2.2). The most effective cocktail included 4mM Riluzole with 8mM emulsifier and resulted in 8.92% eclosion efficiency with a maximum life span of 6 days, compared to 0% of eclosion observed in *dSod1*^{G85R/G85R}. Interestingly, 8mM emulsifier alone had a very similar 7.5% eclosion efficiency and with a maximum life span of 11 days. Thus it was not clear whether the Riluzole really had an effect of the condition of *dSod1*^{G85R/G85R} flies. 1mM Melatonin had a similar effect of 5.66% eclosion rate with a maximum of 4 days life span. Moreover, when 1mM Melatonin was combined with 1mM Riluzole treatment,

the eclosion efficiency decreased to 2.9% with a maximum life span of 4 days (Table 2.2).

DISCUSSION AND FUTURE DIRECTIONS

In this study, in order to model fALS we utilized homologous recombination (HR) to generate at least 3 independent lines each of *dSod1*^{G37R}, *dSod1*^{H48R}, *dSod1*^{H71Y}, *dSod1*^{G85R} and *dSod1*^{WTLoxP} *Drosophila* which are the products of different P element integration events. Generating multiple lines and assessing the same phenotype are very important in HR methodology because Sce endonuclease, FLP and Cre recombinases that are used in the HR process could potentially introduce unintended mutations in the genome that may affect downstream analysis of the targeted alleles (O'Keefe *et al.*, 2007). We also minimized these undesired mutations by backcrossing the post-Cre lines to the white-eyed fly stock *w*¹¹¹⁸. We show that the ALS-related phenotypes described in this study are due to the insertion of *dSod1* point mutations into the endogenous locus. More importantly, the *dSod1* mutations investigated in this study are identical to human fALS mutations (Table 2.1) (Juneja *et al.*, 1997; Rabe *et al.*, 2010; Weis *et al.*, 2011; Özoğuz *et al.*, 2015). Similar to ALS patients, the mutations are within the endogenous *dSod1* gene; hence the mutant *dSod1*s are not overexpressed. Here we show that homozygous *dSod1*^{G85R/G85R} and *dSod1*^{H71Y/H71Y} exhibit an eclosion defect, reduction in survival and locomotion deficits potentially stemming from neuronal retraction from adult muscles and increased synaptic activity at the neuromuscular junction. These ALS-like symptoms are likely due to a toxic gain of function of mutant *dSod1* proteins since transgenic expression of wild type *dSod1* was deleterious within the

context of *dSod1*^{G85R/G85R} phenotype (Figure 2.15). Interestingly, the mutations that cause slow disease progression in ALS patients (Table 2.1), *dSod1*^{G37R} and *dSod1*^{H48R}, did not reveal any gross phenotype in *Drosophila*. Moreover, Riluzole, the only FDA approved drug for ALS and another antioxidant chemical Melatonin that has very moderate effects on patients, also had similar effects in *dSod1* mutant *Drosophila* (Table 2.3). The fALS model *Drosophila* described in this study can be used for future chemical and genetic screening studies with an aim of a better eclosion and life span results obtained by administration of Riluzole.

In humans, 95% of SOD1 mutations are observed in a heterozygote state (Saccon *et al.*, 2013). We found that only homozygous *dSod1*^{G85R/G85R} and *dSod1*^{H71Y/H71Y} displayed an ALS-like phenotype, but heterozygote *dSod1*^{G85R/WTLoxP} and *dSod1*^{H71Y/WTLoxP} did not. This result can be interpreted using several explanations. First, the dosage of mutant dSod1 is insufficient to cause cellular toxicity or because wild type dSod1 has a novel protective effect. This possibility is addressed by lowering *dSod1*^{G85R/G85R} mutant gene copy number by half and generating *dSod1*^{G85R/X-16}. Even though *dSod1*^{G85R/X-16} rescued larval locomotion defect (Figure 2.5.A), it did not rescue the eclosion defect as *dSod1*^{G85R/WTLoxP} did (Figure 2.D). Moreover adult *dSod1*^{G85R/X-16} flies exhibited very uncoordinated behavior (Supplementary video 2.4). Therefore, one copy of *dSod1*^{G85R} is capable of inducing ALS-like phenotypes described in this study, suggesting wild type dSod1 has a novel protective effect when a mutant form of the protein is present. Another interpretation is that lack of significant phenotypes in mutant heterozygotes is due to the fact that flies do not live long enough to exhibit disease pathology. In agreement with this, the non-transgenic and non-human ALS models in a heterozygote state do not reveal

any ALS-like symptoms. For example, mice carrying an endogenous mSOD1^{D83G} point mutation (Joyce *et al.*, 2015) and 73% of reported cases of SOD1 mutant canines developing degenerative myelopathy (Zeng *et al.*, 2014) exhibited ALS-like symptoms only in the homozygote state for the SOD1 mutation. Given the importance of mutant SOD1 protein dosage in accelerating the ALS-like phenotype in transgenic SOD1-mediated ALS models (Acevedo-Arozena *et al.*, 2011), it is possible that heterozygotes may develop symptoms later in life, or would only display symptoms if they lived well beyond their normal life span. Mice, dogs and fruit flies have relatively short life span compared to humans. Since ALS is a late onset disease for humans, we speculate that further ageing of heterozygous fruit flies and non-transgenic SOD1 animal models beyond their life span might be required to cause more dramatic ALS-like phenotypes. Based on our results presented in this study, *dSod1*^{G85R/WTLoxP} and *dSod1*^{H71Y/WTLoxP} heterozygous animals live a wild type-like life span and exhibit no obvious locomotion deficits during adulthood. However, they develop a locomotion defect in the third instar larval stage. This temporary phenotype might stem from the differential gene regulatory events between the larval stage and the adult stage. The molecular mechanisms underlying this discrepancy remain to be determined. It is also quite possible that further experiments with altered environmental conditions such as altered diet, stress levels, or pharmacological interventions, could reveal an ALS-like phenotype for *Drosophila* heterozygous *dSod1* mutant flies. On the other hand, similar to patients developing a late onset ALS as well as exhibiting a short progression quickly followed by death, *P[dSod1*^{WTLoxP}]/*P[dSod1*^{WTLoxP}];*dSod1*^{G85R}/*dSod1*^{G85R} flies exhibited locomotor deficit for a day before they dying 55 days post-eclosion (Supplementary video 2.3), which is

comparable to ALS patients losing their locomotion ability over 1-2 years before the need of a diaphragm support (Benditt & Boitano, 2008).

Here, we have shown that SOD1 mutants that cause fast disease progression in ALS patients, result in ALS-like symptoms in *Drosophila* as a both loss of function and gain of toxic function. Gel-based SOD activity assay revealed no dismutase activity for homozygous dSod1^{G85R/G85R}, dSod1^{H71Y/H71Y}, and dSod1^{G51S/G51S} mutant proteins (Figure 2.11). In addition, rescuing the mutant *dSod1* with one or two copies of exogenously expressed wild type *dSod1* ($P[dSod1^{WTLoxP}]/P[dSod1^{WTLoxP}]$; $dSod1^{G85R}/dSod1^{G85R}$ or $P[dSod1^{WTLoxP}]/+$; $dSod1^{G85R}/dSod1^{G85R}$) did not fully suppress the life span defects observed in $dSod1^{G85R}/dSod1^{G85R}$ mutants (Figure 2.14). Moreover, four copies of *dSod1* ($P[dSod1^{WTLoxP}]/P[dSod1^{WTLoxP}]$; $dSod1^{WTLoxP}/dSod1^{WTLoxP}$) exhibited toxic effects and lead to a shorter life span than wild type $dSod1^{WTLoxP}/dSod1^{WTLoxP}$ flies. Previous studies agree with this finding and underscore the importance of SOD1 protein dosage. Upon overexpression of wild type hSOD1 in mice, wild type SOD1 can acquire an abnormal conformation and lead to ALS-like symptoms such as mitochondrial dysfunction, axon degeneration, premature motor neuron death, and SOD1 aggregation (Jaarsma *et al.*, 2000; Graffmo *et al.*, 2013). The overexpression of hSOD1 also caused locomotion deficit in *Drosophila* (Watson *et al.*, 2008). Alternatively, a copy of wild type *dSod1* might be protective through dimerization with the mutant *dSod1* or through the restoration of cellular damage induced by oxidative stress due to loss of enzymatic activity. However, we showed using an immunoblotting assay that wild type dSod1 did not stabilize the mutant dSod1 protein (Figure 2.17). This is in agreement with current

literature suggesting that hSOD1^{G85R} monomers are unable to form dimers with each other nor with mSOD1 and hSOD1 (Wang, Farr, Zeiss, *et al.*, 2009).

Moreover, we have compared the effects of homologously recombined mutations to another dSod1 mutant line harboring a point mutation *dSod1*^{G51S} that is generated via an EMS screen (Phillips *et al.*, 1989). This allele is referred as “null” or “*dSod1*^{-/-}” allele in the literature despite the fact that it has simply one amino acid change of G49S instead of a full deficiency of the locus. *dSod1*^{G51S} is observed as null in gel-based SOD1 activity assays explaining the “null” description of the allele (Phillips *et al.*, 1989). However, immunoblotting has not been performed on this allele before. In Figure 2.13.A, we demonstrate that this allele exhibits reduced amounts of dSod1 protein on denaturing SDS gel but is certainly not a null allele. Similar to *dSod1*^{G51S}, in *dSod1*^{H71Y} and *dSod1*^{G85R} but not in *dSod1*^{G37R} and *dSod1*^{H48R} homozygotes display significant reduction in dSod1 protein amounts on denaturing SDS-PAGE gels but native gel revealed that this reduction is technique-specific (Figure 2.12.D). In parallel with our findings, for some yet-unexplored reason, SOD1 mutants show reduced protein amounts on denaturing SDS-PAGE gels in mice harboring an endogenous mSOD1^{D83G} point mutation (~10% of wild type in homozygotes) (Joyce *et al.*, 2015) and patient induced pluripotent stem cell-derived motor neurons (Chen *et al.*, 2014; Kiskinis *et al.*, 2014). One explanation for the decreased amounts of SOD1 protein in the mutants is that it may result from the instability of mutant dSod1 and its subsequent degradation (Kabuta, Suzuki, & Wada, 2006). It has been previously reported that mutant SOD1, especially SOD1^{G85R}, has a decreased half-life when compared to wild type SOD1 (Borchelt *et al.*, 1994; Farr *et al.*, 2011). However, we showed that the dSod1 protein amount is constant between all

mutant alleles. Instead, we hypothesize that the reduction in protein amount is related to the disease pathogenesis since it correlates with the onset of the locomotion deficit phenotypes during the late third instar larval stage (Figure 2.12.B, C and D).

Here, our data agrees with the Gal4-UAS system based transgenic *Drosophila* models, in terms of lack of motor neuron loss (Watson *et al.*, 2008), the presence of climbing deficits (Watson *et al.*, 2008; Bahadorani *et al.*, 2013), and sensitivity to oxidative stress (Bahadorani *et al.*, 2013). Our preliminary results suggest that the cell bodies of motor neurons stay intact even at the terminal stages of *dSod1*^{G85R/G85R}. Lack of motor neuron death despite neuromuscular deficits is not surprising because ALS is considered a “dying back” disorder in which muscle denervation precedes the death of the motor neuronal cell body (Dadon-Nachum, Melamed, & Offen, 2011). This phenomenon of NMJ degeneration preceding motor neuron cell body death was observed in transgenic human mutant SOD1 mouse models (Kato, 2008), a non-transgenic mouse model (Joyce *et al.*, 2015) and an early autopsy of an ALS patient who unexpectedly died from other causes (Fischer *et al.*, 2004). In agreement with the dying back phenomena, we observed mild defects in electrophysiological analysis and NMJ boutons of the wandering third instar larvae. The neurodegeneration defects were detectable in the late stages of *dSod1* mutant *Drosophila*. Interestingly, in our model, the distal motor neurons in the leg are more severely affected than the proximal ones (Figure 2.8). The *dSod1*^{G85R/G85R} pharate adults became stuck in the pupal case and all their legs are shorter than wild type legs. However, leg 3 exhibits a distinctively more severe phenotype than leg 2 and leg 1 (Supplementary video 2.1 and 2). In *dSod1*^{H71Y/H71Y}, all the legs look wild type-like until day 14. On day 14, 13 out of 15 legs have completely lost their side

branches diverging from the main nerve. In the future, we will quantify the severity of *dSod1*^{H71Y/H71Y} legs as we did for *dSod1*^{G85R/G85R} in Figure 2.8.

A consensus has not been reached regarding the nature of disrupted cellular pathways in ALS pathogenesis. Although most of the SOD1 transgenic animals exhibit similar cellular responses such as apoptosis and glial response, it is not known whether such responses stem from overexpression of the mutant protein. Our *Drosophila* model provides a rich, fast and efficient system complementary to rodent model organisms for addressing mechanisms associated with human SOD1 mutations causing ALS and for elucidating the dosage sensitive results of SOD1-mediated ALS. *Drosophila* provides a uniquely fast system in which molecular pathways of fundamental neuronal function appear sufficiently conserved to define the foundation for novel therapeutic approaches, and pupal lethality provides an excellent motivation for a genetic suppressor screen, which will be discussed in Chapter 4.

REFERENCES

- ABEL, O., POWELL, J.F., ANDERSEN, P.M. & AL-CHALABI, A. (2012) ALSoD: A user-friendly online bioinformatics tool for amyotrophic lateral sclerosis genetics. *Human mutation* **33**, 1345–1351.
- ACEVEDO-AROZENA, A., KALMAR, B., ESSA, S., RICKETTS, T., JOYCE, P., KENT, R., ROWE, C., PARKER, A., GRAY, A., HAFEZPARAST, M., THORPE, J.R., GREENSMITH, L. & FISHER, E.M.C. (2011) A comprehensive assessment of the SOD1G93A low-copy transgenic mouse, which models human amyotrophic lateral sclerosis. *Disease models & mechanisms* **4**, 686–700.
- ALEXANDER, G.M., ERWIN, K.L., BYERS, N., DEITCH, J.S., AUGELLI, B.J., BLANKENHORN, E.P. & HEIMAN-PATTERSON, T.D. (2004) Effect of transgene copy number on survival in the G93A SOD1 transgenic mouse model of ALS. *Brain research. Molecular brain research* **130**, 7–15.
- AWANO, T., JOHNSON, G.S., WADE, C.M., KATZ, M.L., JOHNSON, G.C., TAYLOR, J.F., PERLOSKI, M., BIAGI, T., BARANOWSKA, I., LONG, S., MARCH, P.A., OLBY, N.J., SHELTON, G.D., KHAN, S., O'BRIEN, D.P., LINDBLAD-TOH, K. & COATES, J.R. (2009) Genome-wide association analysis reveals a SOD1 mutation in canine degenerative myelopathy that resembles amyotrophic lateral sclerosis. *Proceedings of the National Academy of Sciences of the United States of America* **106**, 2794–2799.

- BAHADORANI, S., MUKAI, S.T., RABIE, J., BECKMAN, J.S., PHILLIPS, J.P. & HILLIKER, A.J. (2013) Expression of zinc-deficient human superoxide dismutase in *Drosophila* neurons produces a locomotor defect linked to mitochondrial dysfunction. *Neurobiology of aging* **34**, 2322–2330.
- BATLEVI, Y., MARTIN, D.N., PANDEY, U.B., SIMON, C.R., POWERS, C.M., TAYLOR, J.P. & BAEHRECKE, E.H. (2010) Dynein light chain 1 is required for autophagy, protein clearance, and cell death in *Drosophila*. *Proceedings of the National Academy of Sciences of the United States of America* **107**, 742–747.
- BENDITT, J.O. & BOITANO, L. (2008) Respiratory treatment of amyotrophic lateral sclerosis. *Physical medicine and rehabilitation clinics of North America* **19**, 559–572, x.
- BERTINI, I., MANGANL, S. & VIEZZOLI, M.S. (1998) Structure and Properties of Copper-Zinc Superoxide Dismutases. *Advances in Inorganic Chemistry* **45**, 127–250. Elsevier.
- BILEN, J. & BONINI, N.M. (2005) *Drosophila* as a model for human neurodegenerative disease. *Annual review of genetics* **39**, 153–171.
- BORCHELT, D.R., LEE, M.K., SLUNT, H.S., GUARNIERI, M., XU, Z.S., WONG, P.C., BROWN, R.H., PRICE, D.L., SISODIA, S.S. & CLEVELAND, D.W. (1994) Superoxide dismutase 1 with mutations linked to familial amyotrophic lateral sclerosis possesses significant activity. *Proceedings of the National Academy of Sciences of the United States of America* **91**, 8292–8296.
- BOSCO, D.A., MORFINI, G., KARABACAK, N.M., SONG, Y., GROS-LOUIS, F., PASINELLI, P., GOOLSBY, H., FONTAINE, B.A., LEMAY, N., MCKENNA-YASEK, D., FROSCH, M.P., AGAR, J.N., JULIEN, J.-P., BRADY, S.T. & BROWN, R.H. (2010) Wild-type and mutant SOD1 share an aberrant conformation and a common pathogenic pathway in ALS. *Nature neuroscience* **13**, 1396–1403.
- BUNTON-STASYSHYN, R.K.A., SACCON, R.A., FRATTA, P. & FISHER, E.M.C. (2014) SOD1 Function and Its Implications for Amyotrophic Lateral Sclerosis Pathology: New and Renascent Themes. *The Neuroscientist : a review journal bringing neurobiology, neurology and psychiatry*.
- CAMPBELL, S.D., HILLIKER, A.J. & PHILLIPS, J.P. (1986) Cytogenetic analysis of the cSOD microregion in *Drosophila melanogaster*. *Genetics* **112**, 205–215.
- CASCI, I. & PANDEY, U.B. (2015) A fruitful endeavor: modeling ALS in the fruit fly. *Brain research* **1607**, 47–74.
- CHARCOT, J.M. & JOFFRY, A. (1869) "Deux cas d'atrophie musculaire progressive avec lesions de la substance grise et des faisceaux antero-lateraux de la moelle epiniere. *Arch. Physiol. Neurol. Pathol.* **2**, 744–754.
- CHEN, H., QIAN, K., DU, Z., CAO, J., PETERSEN, A., LIU, H., BLACKBOURN, L.W., HUANG, C.-L., ERRIGO, A., YIN, Y., LU, J., AYALA, M. & ZHANG, S.-C. (2014) Modeling ALS with iPSCs reveals that mutant SOD1 misregulates neurofilament balance in motor neurons. *Cell stem cell* **14**, 796–809.
- CHIA, R., TATTUM, M.H., JONES, S., COLLINGE, J., FISHER, E.M.C. & JACKSON, G.S. (2010) Superoxide dismutase 1 and tgSOD1 mouse spinal cord seed fibrils, suggesting a propagative cell death mechanism in amyotrophic lateral sclerosis. *PloS one* **5**, e10627.
- CRISP, M.J., BECKETT, J., COATES, J.R. & MILLER, T.M. (2013) Canine degenerative myelopathy: biochemical characterization of superoxide dismutase 1 in the first naturally occurring non-human amyotrophic lateral sclerosis model. *Experimental neurology* **248**, 1–9.

- DADON-NACHUM, M., MELAMED, E. & OFFEN, D. (2011) The 'dying-back' phenomenon of motor neurons in ALS. *Journal of molecular neuroscience : MN* **43**, 470–477.
- DEBATTISTI, V. & SCORRANO, L. (2013) D. melanogaster, mitochondria and neurodegeneration: small model organism, big discoveries. *Molecular and cellular neurosciences* **55**, 77–86.
- DEJESUS-HERNANDEZ, M., MACKENZIE, I.R., BOEVE, B.F., BOXER, A.L., BAKER, M., RUTHERFORD, N.J., ET AL. (2011) Expanded GGGGCC hexanucleotide repeat in noncoding region of C9ORF72 causes chromosome 9p-linked FTD and ALS. *Neuron* **72**, 245–256.
- DENG, H.-X., SHI, Y., FURUKAWA, Y., ZHAI, H., FU, R., LIU, E., GORRIE, G.H., KHAN, M.S., HUNG, W.-Y., BIGIO, E.H., LUKAS, T., DAL CANTO, M.C., O'HALLORAN, T. V & SIDDIQUE, T. (2006) Conversion to the amyotrophic lateral sclerosis phenotype is associated with intermolecular linked insoluble aggregates of SOD1 in mitochondria. *Proceedings of the National Academy of Sciences of the United States of America* **103**, 7142–7147.
- DENG, H.X., HENTATI, A., TAINER, J.A., IQBAL, Z., CAYABYAB, A., HUNG, W.Y., GETZOFF, E.D., HU, P., HERZFELDT, B. & ROOS, R.P. (1993) Amyotrophic lateral sclerosis and structural defects in Cu,Zn superoxide dismutase. *Science (New York, N.Y.)* **261**, 1047–1051.
- EZZI, S.A., URUSHITANI, M. & JULIEN, J.-P. (2007) Wild-type superoxide dismutase acquires binding and toxic properties of ALS-linked mutant forms through oxidation. *Journal of neurochemistry* **102**, 170–178.
- FARR, G.W., YING, Z., FENTON, W.A. & HORWICH, A.L. (2011) Hydrogen-deuterium exchange in vivo to measure turnover of an ALS-associated mutant SOD1 protein in spinal cord of mice. *Protein science : a publication of the Protein Society*.
- FISCHER, L.R., CULVER, D.G., TENNANT, P., DAVIS, A.A., WANG, M., CASTELLANO-SANCHEZ, A., KHAN, J., POLAK, M.A. & GLASS, J.D. (2004) Amyotrophic lateral sclerosis is a distal axonopathy: evidence in mice and man. *Experimental Neurology* **185**, 232–240.
- FORSBERG, K., JONSSON, P.A., ANDERSEN, P.M., BERGEMALM, D., GRAFFMO, K.S., HULTDIN, M., JACOBSSON, J., ROSQUIST, R., MARKLUND, S.L. & BRÄNNSTRÖM, T. (2010) Novel antibodies reveal inclusions containing non-native SOD1 in sporadic ALS patients. *PloS one* **5**, e11552.
- FRIDOVICH, I. (1986) Superoxide dismutases. *Advances in enzymology and related areas of molecular biology* **58**, 61–97.
- GELL, S.L. & REENAN, R.A. (2013) Mutations to the piRNA pathway component aubergine enhance meiotic drive of segregation distorter in Drosophila melanogaster. *Genetics* **193**, 771–784.
- GIJSELINCK, I., VAN LANGENHOVE, T., VAN DER ZEE, J., SLEEGERS, K., PHILTJENS, S., KLEINBERGER, G., ET AL. (2012) A C9orf72 promoter repeat expansion in a Flanders-Belgian cohort with disorders of the frontotemporal lobar degeneration-amyotrophic lateral sclerosis spectrum: a gene identification study. *The Lancet. Neurology* **11**, 54–65.
- GRAFFMO, K.S., FORSBERG, K., BERGH, J., BIRVE, A., ZETTERSTRÖM, P., ANDERSEN, P.M., MARKLUND, S.L. & BRÄNNSTRÖM, T. (2013) Expression of wild-type human superoxide dismutase-1 in mice causes amyotrophic lateral sclerosis. *Human molecular genetics* **22**, 51–60.
- GRUZMAN, A., WOOD, W.L., ALPERT, E., PRASAD, M.D., MILLER, R.G., ROTHSTEIN, J.D., BOWSER, R., HAMILTON, R., WOOD, T.D., CLEVELAND, D.W., LINGAPPA, V.R. & LIU, J. (2007) Common

- molecular signature in SOD1 for both sporadic and familial amyotrophic lateral sclerosis. *Proceedings of the National Academy of Sciences of the United States of America* **104**, 12524–12529.
- GURNEY, M.E., PU, H., CHIU, A Y., DAL CANTO, M.C., POLCHOW, C.Y., ALEXANDER, D.D., CALIENDO, J., HENTATI, A, KWON, Y.W. & DENG, H.X. (1994) Motor neuron degeneration in mice that express a human Cu,Zn superoxide dismutase mutation. *Science (New York, N.Y.)* **264**, 1772–1775.
- HO, Y.S., GARGANO, M., CAO, J., BRONSON, R.T., HEIMLER, I. & HUTZ, R.J. (1998) Reduced fertility in female mice lacking copper-zinc superoxide dismutase. *The Journal of biological chemistry* **273**, 7765–7769.
- HUANG, T.T., YASUNAMI, M., CARLSON, E.J., GILLESPIE, A.M., REAUME, A.G., HOFFMAN, E.K., CHAN, P.H., SCOTT, R.W. & EPSTEIN, C.J. (1997) Superoxide-mediated cytotoxicity in superoxide dismutase-deficient fetal fibroblasts. *Archives of biochemistry and biophysics* **344**, 424–432.
- HUDSON, R.R., BAILEY, K., SKARECKY, D., KWIATOWSKI, J. & AYALA, F.J. (1994) Evidence for positive selection in the superoxide dismutase (Sod) region of *Drosophila melanogaster*. *Genetics* **136**, 1329–1340.
- JAARSMA, D., HAASDIJK, E.D., GRASHORN, J. A, HAWKINS, R., VAN DUIJN, W., VERSPAGET, H.W., LONDON, J. & HOLSTEGE, J.C. (2000) Human Cu/Zn superoxide dismutase (SOD1) overexpression in mice causes mitochondrial vacuolization, axonal degeneration, and premature motoneuron death and accelerates motoneuron disease in mice expressing a familial amyotrophic lateral sclerosis mutant SO. *Neurobiology of disease* **7**, 623–643.
- JOYCE, P.I., FRATTA, P., FISHER, E.M.C. & ACEVEDO-AROZENA, A. (2011) SOD1 and TDP-43 animal models of amyotrophic lateral sclerosis: recent advances in understanding disease toward the development of clinical treatments. *Mammalian genome : official journal of the International Mammalian Genome Society* **22**, 420–448.
- JOYCE, P.I., MCGOLDRICK, P., SACCON, R.A., WEBER, W., FRATTA, P., WEST, S.J., ET AL. (2015) A novel SOD1-ALS mutation separates central and peripheral effects of mutant SOD1 toxicity. *Human molecular genetics* **24**, 1883–1897.
- JUNEJA, T., PERICAK-VANCE, M.A., LAING, N.G., DAVE, S. & SIDDIQUE, T. (1997) Prognosis in familial amyotrophic lateral sclerosis: progression and survival in patients with glu100gly and ala4val mutations in Cu,Zn superoxide dismutase. *Neurology* **48**, 55–57.
- KABUTA, T., SUZUKI, Y. & WADA, K. (2006) Degradation of amyotrophic lateral sclerosis-linked mutant Cu,Zn-superoxide dismutase proteins by macroautophagy and the proteasome. *Journal of Biological Chemistry* **281**, 30524–30533.
- KATO, S. (2008) Amyotrophic lateral sclerosis models and human neuropathology: similarities and differences. *Acta neuropathologica* **115**, 97–114.
- KIRBY, K., JENSEN, L.T., BINNINGTON, J., HILLIKER, A.J., ULLOA, J., CULOTTA, V.C. & PHILLIPS, J.P. (2008) Instability of superoxide dismutase 1 of *Drosophila* in mutants deficient for its cognate copper chaperone. *The Journal of biological chemistry* **283**, 35393–35401.
- KISKINIS, E., SANDOE, J., WILLIAMS, L.A., BOULTING, G.L., MOCCIA, R., WAINGER, B.J., ET AL. (2014) Pathways disrupted in human ALS motor neurons identified through genetic correction of mutant SOD1. *Cell stem cell* **14**, 781–795.

- KONSOLAKI, M. (2013) Fruitful research: drug target discovery for neurodegenerative diseases in *Drosophila*. *Expert opinion on drug discovery* **8**, 1503–1513.
- LEBLOND, C.S., KANEB, H.M., DION, P. A & ROULEAU, G. A (2014) Dissection of genetic factors associated with amyotrophic lateral sclerosis. *Experimental Neurology*.
- LEE, Y.M., MISRA, H.P. & AYALA, F.J. (1981) Superoxide dismutase in *Drosophila melanogaster*: biochemical and structural characterization of allozyme variants. *Proceedings of the National Academy of Sciences of the United States of America* **78**, 7052–7055.
- MATZUK, M.M., DIONNE, L., GUO, Q., KUMAR, T.R. & LEBOVITZ, R.M. (1998) Ovarian function in superoxide dismutase 1 and 2 knockout mice. *Endocrinology* **139**, 4008–4011.
- MCGOLDRICK, P., JOYCE, P.I., FISHER, E.M.C. & GREENSMITH, L. (2013) Rodent models of amyotrophic lateral sclerosis. *Biochimica et biophysica acta* **1832**, 1421–1436.
- MILLECAMPS, S., SALACHAS, F., CAZENEUVE, C., GORDON, P., BRICKA, B., CAMUZAT, A., ET AL. (2010) SOD1, ANG, VAPB, TARDBP, and FUS mutations in familial amyotrophic lateral sclerosis: genotype-phenotype correlations. *Journal of medical genetics* **47**, 554–560.
- MILLER, R.G., MITCHELL, J.D. & MOORE, D.H. (2012) Riluzole for amyotrophic lateral sclerosis (ALS)/motor neuron disease (MND). *The Cochrane database of systematic reviews* **3**, CD001447.
- MISHRA, M., SHARMA, A., SHUKLA, A.K., KUMAR, R., DWIVEDI, U.N. & KAR CHOWDHURI, D. (2014) Genotoxicity of dichlorvos in strains of *Drosophila melanogaster* defective in DNA repair. *Mutation research. Genetic toxicology and environmental mutagenesis* **766**, 35–41.
- MISSIRLIS, F., HU, J., KIRBY, K., HILLIKER, A.J., ROUAULT, T.A. & PHILLIPS, J.P. (2003) Compartment-specific protection of iron-sulfur proteins by superoxide dismutase. *The Journal of biological chemistry* **278**, 47365–47369.
- O'KEEFE, L. V, COLELLA, A., DAYAN, S., CHEN, Q., CHOO, A., JACOB, R., PRICE, G., VENTER, D. & RICHARDS, R.I. (2011) *Drosophila* orthologue of WWOX, the chromosomal fragile site FRA16D tumour suppressor gene, functions in aerobic metabolism and regulates reactive oxygen species. *Human molecular genetics* **20**, 497–509.
- O'KEEFE, L. V, SMIBERT, P., COLELLA, A., CHATAWAY, T.K., SAINT, R. & RICHARDS, R.I. (2007) Know thy fly. *Trends in genetics : TIG* **23**, 238–242.
- ÖZOĞUZ, A., UYAN, Ö., BIRDAL, G., ISKENDER, C., KARTAL, E., LAHUT, S., ET AL. (2015) The distinct genetic pattern of ALS in Turkey and novel mutations. *Neurobiology of aging* **36**, 1764.e9–e1764.e18.
- PARDO, C.A., XU, Z., BORCHELT, D.R., PRICE, D.L., SISODIA, S.S. & CLEVELAND, D.W. (1995) Superoxide dismutase is an abundant component in cell bodies, dendrites, and axons of motor neurons and in a subset of other neurons. *Proceedings of the National Academy of Sciences of the United States of America* **92**, 954–958.
- PARKES, T.L., KIRBY, K., PHILLIPS, J.P. & HILLIKER, A.J. (1998) Transgenic analysis of the cSOD-null phenotypic syndrome in *Drosophila*. *Genome / National Research Council Canada = Génome / Conseil national de recherches Canada* **41**, 642–651.

- PASINELLI, P. & BROWN, R.H. (2006) Molecular biology of amyotrophic lateral sclerosis: insights from genetics. *Nature reviews. Neuroscience* **7**, 710–723.
- PETERS, O.M., GHASEMI, M. & BROWN, R.H. (2015) Emerging mechanisms of molecular pathology in ALS. *The Journal of clinical investigation* **125**, 1767–1779.
- PHILLIPS, J.P., CAMPBELL, S.D., MICHAUD, D., CHARBONNEAU, M. & HILLIKER, A.J. (1989) Null mutation of copper/zinc superoxide dismutase in *Drosophila* confers hypersensitivity to paraquat and reduced longevity. *Proceedings of the National Academy of Sciences of the United States of America* **86**, 2761–2765.
- PHILLIPS, J.P., TAINER, J.A., GETZOFF, E.D., BOULIANNE, G.L., KIRBY, K. & HILLIKER, A.J. (1995) Subunit-destabilizing mutations in *Drosophila* copper/zinc superoxide dismutase: neuropathology and a model of dimer dysequilibrium. *Proceedings of the National Academy of Sciences of the United States of America* **92**, 8574–8578.
- RABE, M., FELBECKER, A., WAIBEL, S., STEINBACH, P., WINTER, P., MÜLLER, U. & LUDOLPH, A.C. (2010) The epidemiology of CuZn-SOD mutations in Germany: a study of 217 families. *Journal of neurology* **257**, 1298–1302.
- RAJAN, A. & PERRIMON, N. (2013) Of flies and men: insights on organismal metabolism from fruit flies. *BMC biology* **11**, 38.
- REAUME, A.G., ELLIOTT, J.L., HOFFMAN, E.K., KOWALL, N.W., FERRANTE, R.J., SIWEK, D.F., WILCOX, H.M., FLOOD, D.G., BEAL, M.F., BROWN, R.H., SCOTT, R.W. & SNIDER, W.D. (1996) Motor neurons in Cu/Zn superoxide dismutase-deficient mice develop normally but exhibit enhanced cell death after axonal injury. *Nature genetics* **13**, 43–47.
- RENTON, A.E., MAJOUNIE, E., WAITE, A., SIMÓN-SÁNCHEZ, J., ROLLINSON, S., GIBBS, J.R., ET AL. (2011) A hexanucleotide repeat expansion in C9ORF72 is the cause of chromosome 9p21-linked ALS-FTD. *Neuron* **72**, 257–268.
- RIVAL, T., SOUSTELLE, L., STRAMBI, C., BESSON, M.T., ICHÉ, M. & BIRMAN, S. (2004) Decreasing glutamate buffering capacity triggers oxidative stress and neuropil degeneration in the *Drosophila* brain. *Current Biology* **14**, 599–605.
- ROSEN, D.R., SIDDIQUE, T., PATTERSON, D., FIGLEWICZ, D.A., SAPP, P., HENTATI, A., DONALDSON, D., GOTO, J., O'REGAN, J.P. & DENG, H.X. (1993) Mutations in Cu/Zn superoxide dismutase gene are associated with familial amyotrophic lateral sclerosis. *Nature* **362**, 59–62.
- SACCON, R.A., BUNTON-STASYSHYN, R.K.A., FISHER, E.M.C. & FRATTA, P. (2013) Is SOD1 loss of function involved in amyotrophic lateral sclerosis? *Brain : a journal of neurology* **136**, 2342–2358.
- SCHUTTE, R.J., SCHUTTE, S.S., ALGARA, J., BARRAGAN, E. V, GILLIGAN, J., STABER, C., SAVVA, Y.A., SMITH, M.A., REENAN, R. & O'DOWD, D.K. (2014) Knock-in model of Dravet syndrome reveals a constitutive and conditional reduction in sodium current. *Journal of neurophysiology* **112**, 903–912.
- SOLER, C., DACZEWSKA, M., DA PONTE, J.P., DASTUGUE, B. & JAGLA, K. (2004) Coordinated development of muscles and tendons of the *Drosophila* leg. *Development (Cambridge, England)* **131**, 6041–6051.
- SREEDHARAN, J. & BROWN, R.H. (2013) Amyotrophic lateral sclerosis: Problems and prospects. *Annals of Neurology* **74**, 309–316.

- STABER, C.J., GELL, S., JEPSON, J.E.C. & REENAN, R.A. (2011) Perturbing A-to-I RNA editing using genetics and homologous recombination. *Methods in molecular biology (Clifton, N.J.)* **718**, 41–73.
- STAVELEY, B.E., HILLIKER, A.J. & PHILLIPS, J.P. (1991) Genetic organization of the cSOD microregion of *Drosophila melanogaster*. *Genome / National Research Council Canada = Génome / Conseil national de recherches Canada* **34**, 279–282.
- SUN, L., GILLIGAN, J., STABER, C., SCHUTTE, R.J., NGUYEN, V., O'DOWD, D.K. & REENAN, R. (2012) A knock-in model of human epilepsy in *Drosophila* reveals a novel cellular mechanism associated with heat-induced seizure. *The Journal of neuroscience : the official journal of the Society for Neuroscience* **32**, 14145–14155.
- TANOUE, M.A. & WYMAN, R.J. (1980) Motor outputs of giant nerve fiber in *Drosophila*. *Journal of neurophysiology* **44**, 405–421.
- TROTTI, D., ROLFS, A., DANBOLT, N.C., BROWN, R.H. & HEDIGER, M.A. (1999) SOD1 mutants linked to amyotrophic lateral sclerosis selectively inactivate a glial glutamate transporter. *Nature neuroscience* **2**, 427–433.
- VALENTINE, J.S., DOUCETTE, P. A & ZITTIN POTTER, S. (2005) Copper-zinc superoxide dismutase and amyotrophic lateral sclerosis. *Annual review of biochemistry* **74**, 563–593.
- WANG, J., FARR, G.W., HALL, D.H., LI, F., FURTAK, K., DREIER, L. & HORWICH, A.L. (2009) An ALS-linked mutant SOD1 produces a locomotor defect associated with aggregation and synaptic dysfunction when expressed in neurons of *Caenorhabditis elegans*. *PLoS genetics* **5**, e1000350. Public Library of Science.
- WANG, J., FARR, G.W., ZEISS, C.J., RODRIGUEZ-GIL, D.J., WILSON, J.H., FURTAK, K., RUTKOWSKI, D.T., KAUFMAN, R.J., RUSE, C.I., YATES, J.R., PERRIN, S., FEANY, M.B. & HORWICH, A.L. (2009) Progressive aggregation despite chaperone associations of a mutant SOD1-YFP in transgenic mice that develop ALS. *Proceedings of the National Academy of Sciences of the United States of America* **106**, 1392–1397.
- WATSON, M.R., LAGOW, R.D., XU, K., ZHANG, B. & BONINI, N.M. (2008) A drosophila model for amyotrophic lateral sclerosis reveals motor neuron damage by human SOD1. *The Journal of biological chemistry* **283**, 24972–24981.
- WEIS, J., KATONA, I., MÜLLER-NEUEN, G., SOMMER, C., NECULA, G., HENDRICH, C., LUDOLPH, A.C. & SPERFELD, A.-D. (2011) Small-fiber neuropathy in patients with ALS. *Neurology* **76**, 2024–2029.
- WININGER, F.A., ZENG, R., JOHNSON, G.S., KATZ, M.L., JOHNSON, G.C., BUSH, W.W., JARBOE, J.M. & COATES, J.R. (2011) Degenerative Myelopathy in a Bernese Mountain Dog with a Novel SOD1 Missense Mutation. *Journal of Veterinary Internal Medicine* **25**, 1166–1170.
- YOSHIDA, T., MAULIK, N., ENGELMAN, R.M., HO, Y.S. & DAS, D.K. (2000) Targeted disruption of the mouse Sod I gene makes the hearts vulnerable to ischemic reperfusion injury. *Circulation research* **86**, 264–269.
- ZENG, R., COATES, J.R., JOHNSON, G.C., HANSEN, L., AWANO, T., KOLICHESKI, A., IVANSSON, E., PERLOSKI, M., LINDBLAD-TOH, K., O'BRIEN, D.P., GUO, J., KATZ, M.L. & JOHNSON, G.S. (2014) Breed distribution of SOD1 alleles previously associated with canine degenerative myelopathy. *Journal of Veterinary Internal Medicine* **28**, 515–521.

FIGURES

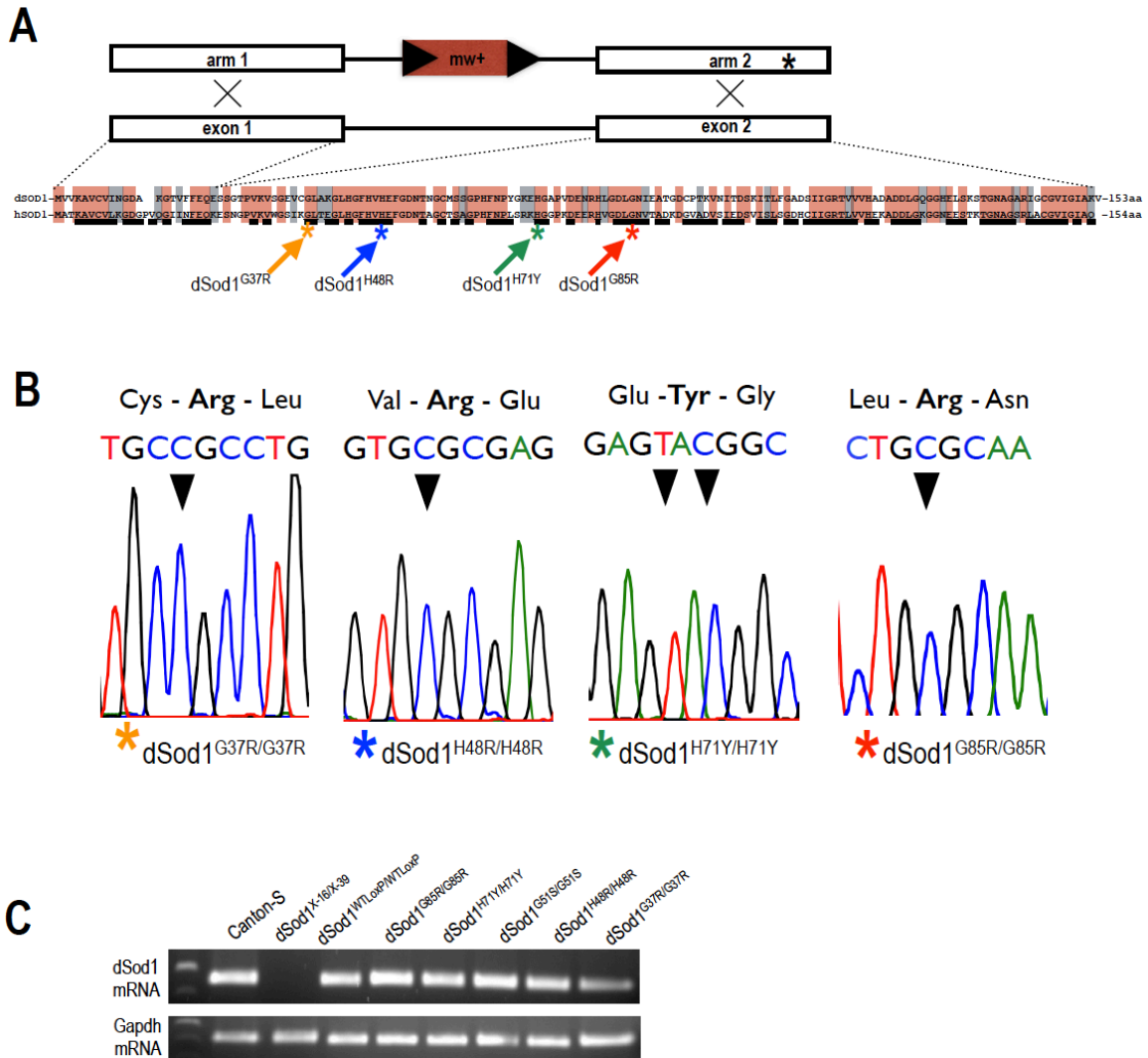


Figure 2.1. Targeted point mutations introduced to the endogenous locus via homologous recombination. **A)** *Drosophila* model of SOD1-mediated ALS employs G37R, H48R, H71Y, and G85R mutant dSod1 proteins as well as wild type (WTLoxP) dSod1 protein. Alignment of human SOD1 (hSOD1) and *Drosophila* SOD1 (dSod1). Key: Black bars are mutations linked to familial ALS; orange residues are conserved between species; grey residues are similarly charged domains between organisms. Stars show the targeted residues. Each mutation is color coded throughout this chapter. **B)** Targeted mutations are depicted in sequencing chromatograms. Orange: G37 (GGC→CGC), blue: H48 (CAC→CGC), green H71 (CAT→TAC), red: G85 (GGC→CGC) **C)** Targeted mutations and the intronic *LoxP* site did not interfere with alternative splicing of dSod1 mRNA. dSod1 full length ~500bp and *Gapdh* gene specific primers were used to amplify the region of interest from total RNA isolates.

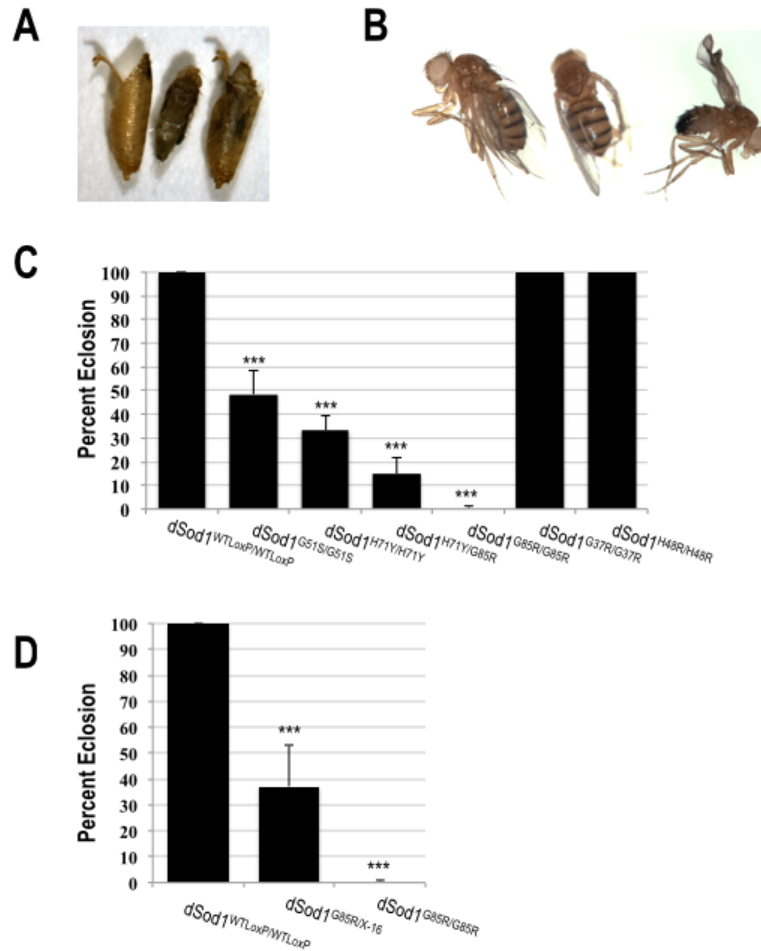


Figure 2.2. Targeted mutations lower organismal fitness and cause eclosion defects.

A) A representative image of *dSod1*^{G85R/G85R} fly died during eclosion. **B)** The wrinkled wing phenotype of eclosed adult *dSod1*^{H71Y/H71Y} flies. **C)** Homozygous *dSod1*^{G51S}, *dSod1*^{H71Y} and *dSod1*^{G85R} flies do not eclose in expected Mendelian ratios. The eclosion rates of heterozygote flies, *dSod1*^{G37R/G37R}, *dSod1*^{H48R/H48R} flies are not affected by the *dSod1* mutant alleles that they carry. *** $p < 0.0001$, One-way Anova followed by Tukey HSD. Error bars are SEM. **D)** *dSod1*^{G85R} eclosion defects are dosage sensitive. The *dSod1* mutant alleles are reduced to half by combining them with the *dSod1*^{X-16} allele that has a deletion of the first exon along with the promoter region. Bars are average eclosion rates from 12 different vials with at least 200 homozygous mutant progeny. *** $p < 0.0001$, Fisher's Exact Test. Error bars are SEM.

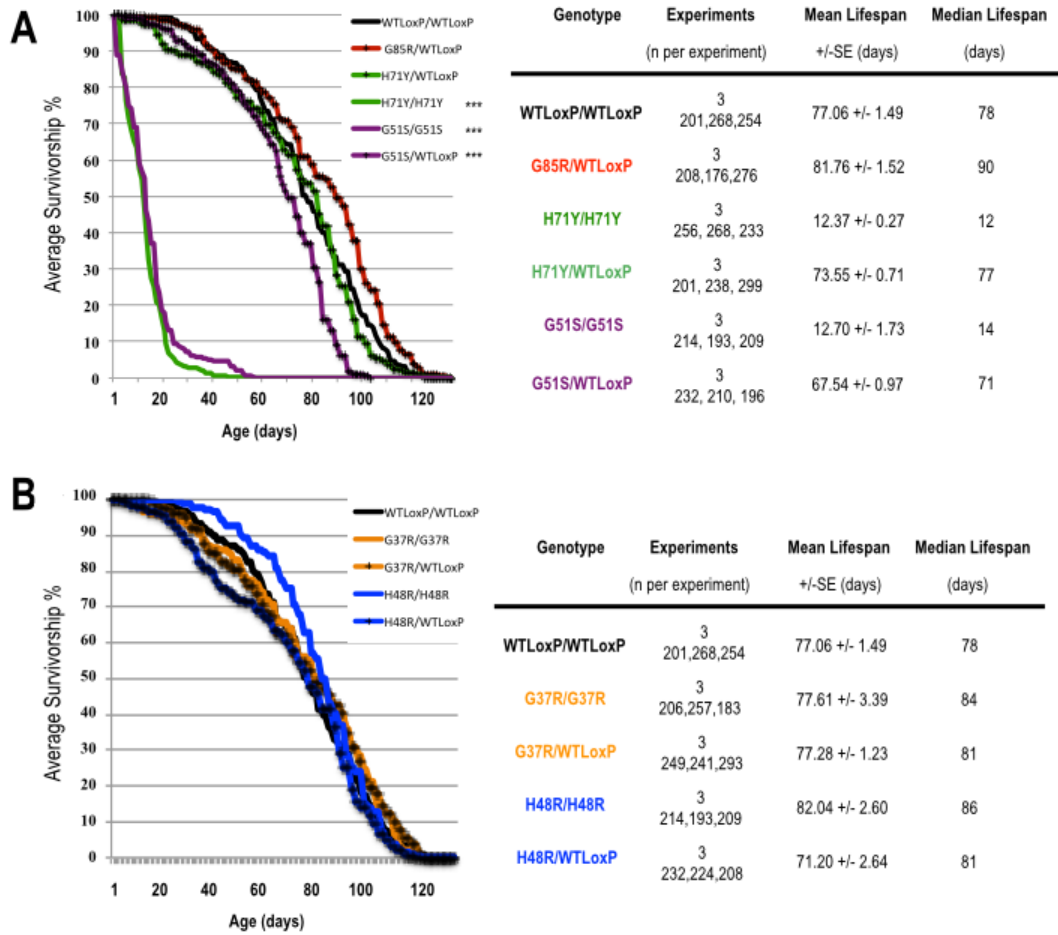


Figure 2.3. Lifespan of flies expressing targeted mutations. Survival curves represent an average of 3 lifespan trials and the adjacent table shows details of lifespan analysis for each genotype of males. **A)** Eclosed *dSod1*^{H71Y/H71Y} flies have a severely shortened life span, similar to the EMS mutagenesis-generated *dSod1*^{G51S/G51S}. *dSod1*^{G85R/G85R} flies do not survive to adulthood, thus are excluded from this experiment. The heterozygous mutants have a normal life span. **B)** *dSod1*^{G37R} and *dSod1*^{H48R} alleles do not have an effect on life span. *** p < 0.0001, log-rank test.

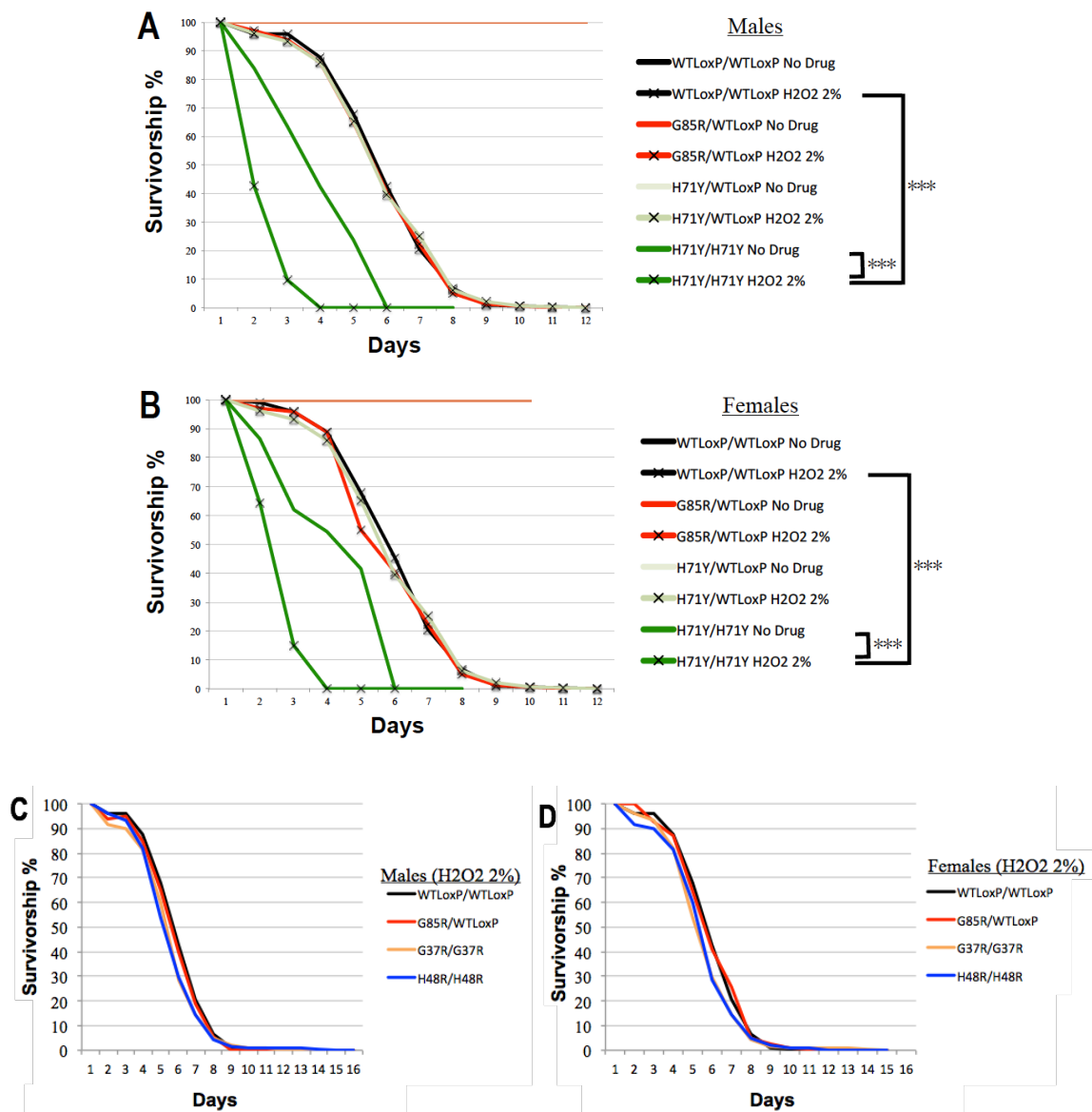


Figure 2.4. Eclosed $dSod1^{H71Y/H71Y}$ flies are sensitive to oxidative stress. Survival curves represent an average of 3 lifespan trials. **A) Male and B) Female $dSod1^{H71Y/H71Y}$ flies are more sensitive to oxidative stress generated by 2% H_2O_2 than wild type $dSod1^{WTLoxP/WTLoxP}$ flies. The C) Male and D) Female $dSod1^{G37R/G37R}$, $dSod1^{H48R/H48R}$ and, $dSod1^{G85R/WTLoxP}$ flies are not sensitive to oxidative stress. *** $p < 0.0001$, log-rank, average of 3 trials.**

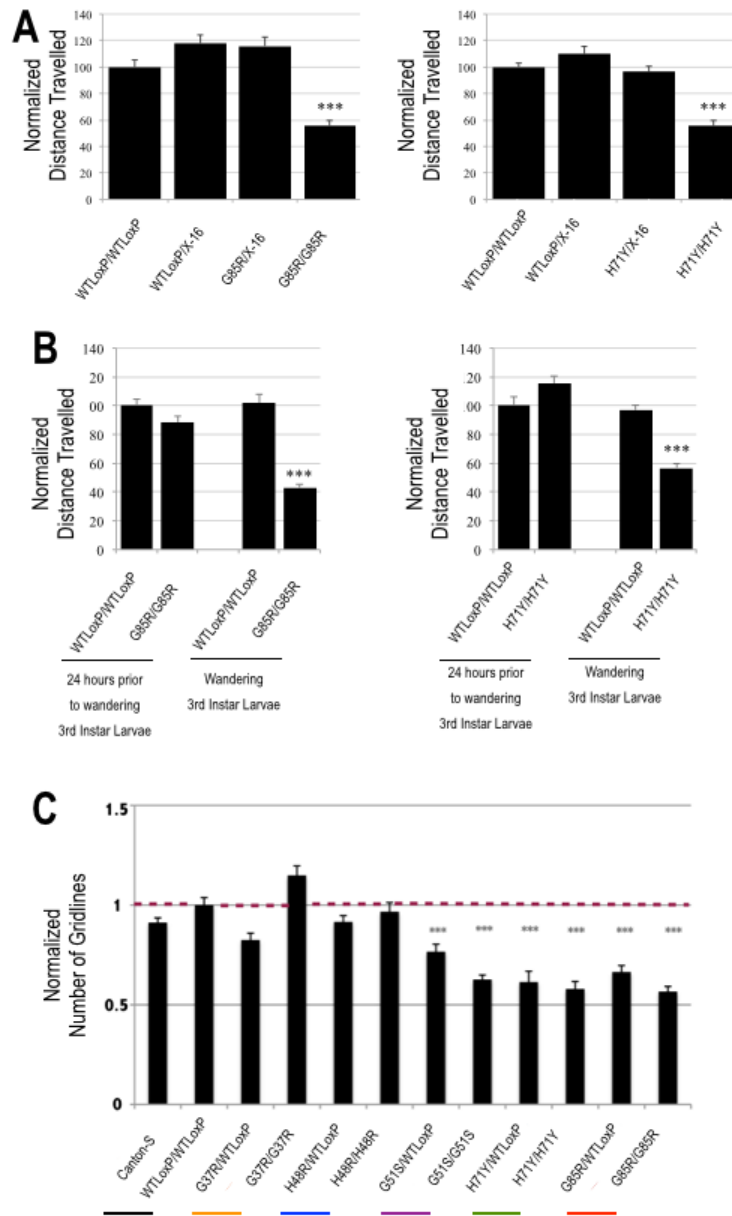


Figure 2.5. *dSod1* mutant larvae display crawling defect in a dosage dependent manner. A) Computational measure of *dSod1*^{G85R} and *dSod1*^{H71Y} larval crawling behavior. Tukey HSD test, ***p< 0.001, N>33 B) *dSod1*^{G85R} and *dSod1*^{H71Y} larval crawling defect begins at late third instar larval stage. Tukey HSD test, ***p< 0.001, N>30 C) Larval crawling speed is measured manually by blinded undergraduate researchers counting the total number of squares each larva traveled in 2 minutes. N>40 Dunnett's test, ***p< 0.001. Error bars are SEM.

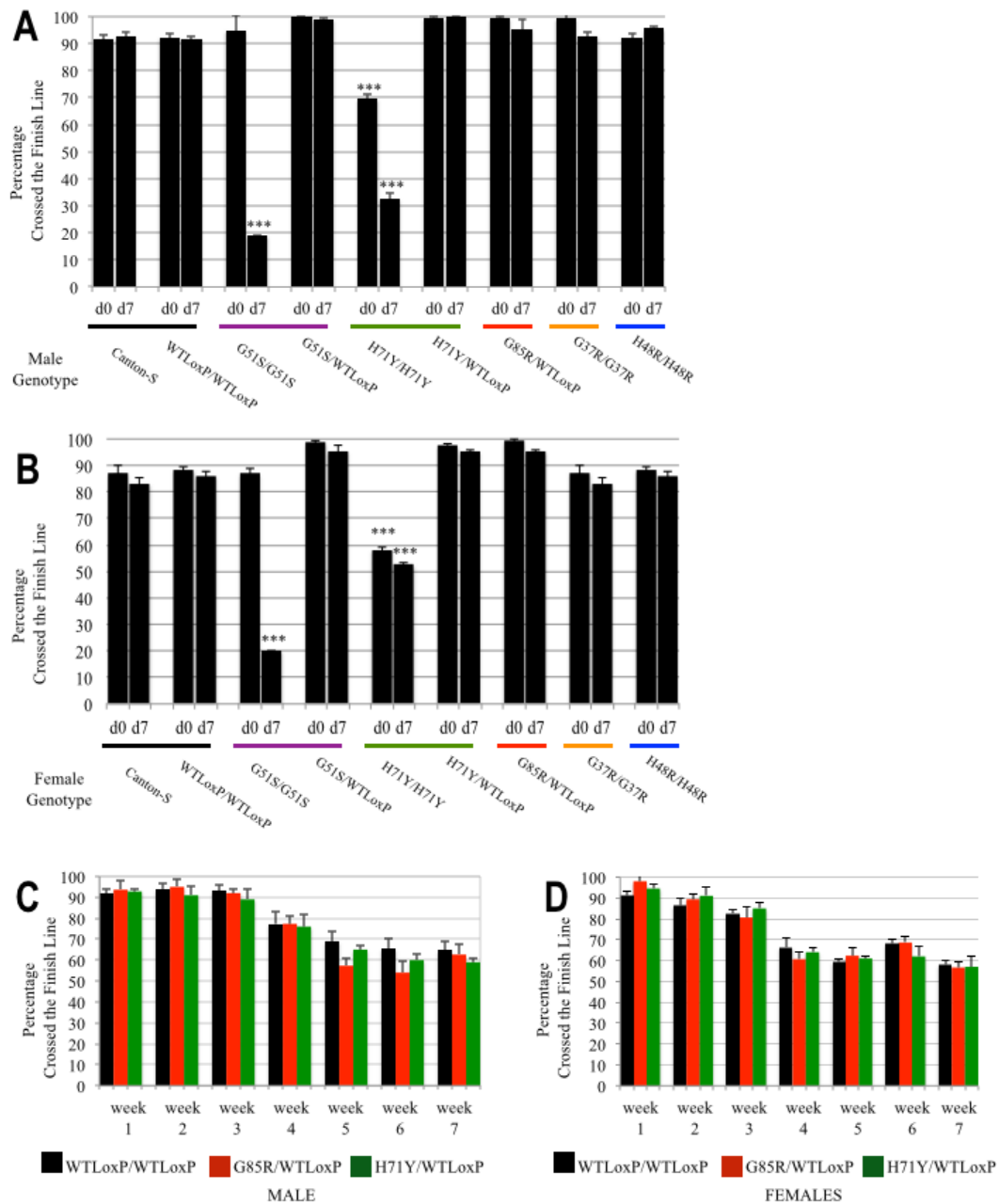


Figure 2.6. *dSod1* mutant adults display climbing defect. **A)** Male and **B)** Female adult climbing ability is significantly reduced in homozygous *dSod1*^{G51S} and *dSod1*^{H71Y} flies within a week of eclosion compared to *dSod1*^{WTLoxP}. In *dSod1*^{WTLoxP/G85R} and *dSod1*^{WTLoxP/H71Y} flies heterozygous for the *dSod1* mutation, the climbing ability is not altered within a 7 weeks period in **C)** males and **D)** females. Error bars S.E.M. *** p < 0.001, One-way Anova followed by Dunnett's post-hoc test.

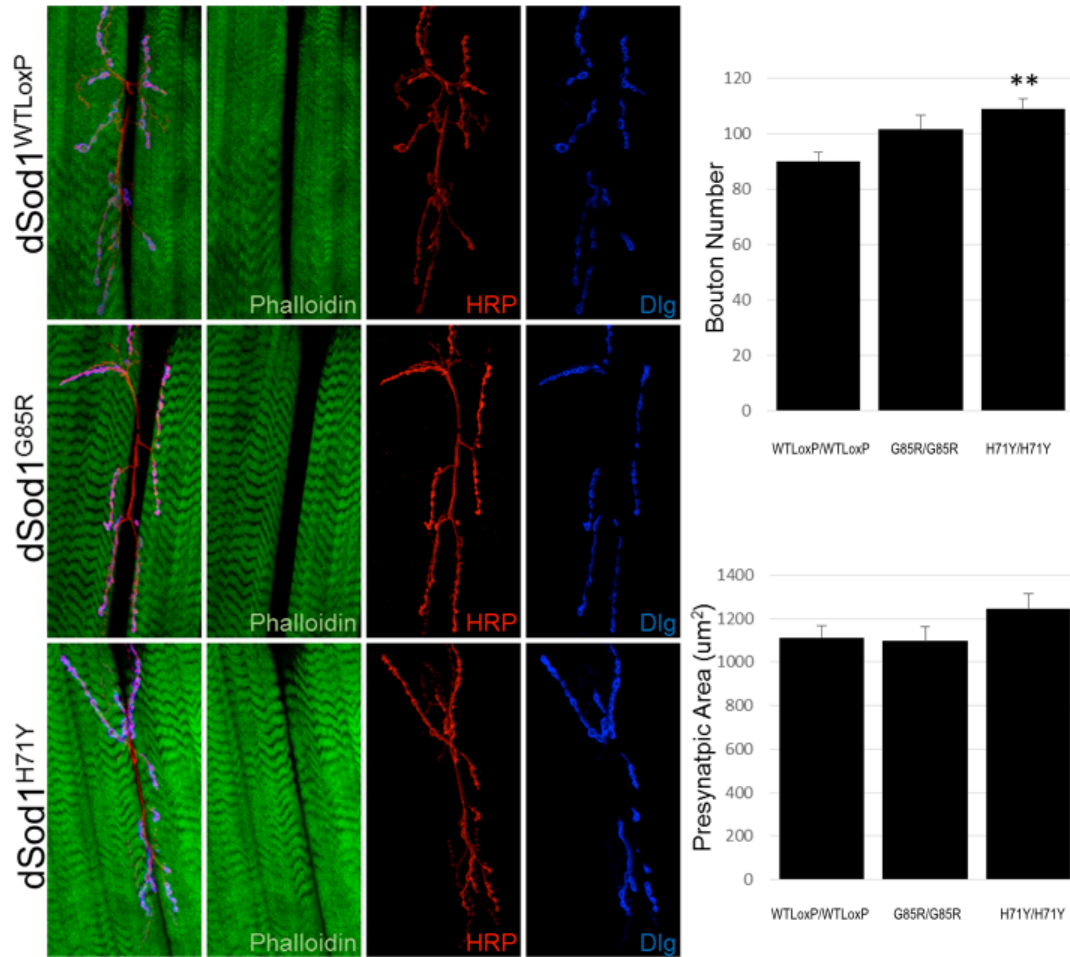


Figure 2.7. *dSod1*^{H71Y} wandering 3rd instar larvae have minor neuromuscular junction structural changes. Neuromuscular junction 6/7 in segment A2 was imaged in *dSod1*^{WTLoxP/WTLoxP}, *dSod1*^{G85R/G85R}, and *dSod1*^{H71Y/H71Y} with phalloidin, HRP (presynaptic), and Discs-large (postsynaptic). There was a significant increase in *dSod1*^{H71Y} bouton number compared to *dSod1*^{WTLoxP}, and *dSod1*^{G85R} showed a trend toward increased bouton number ($p=0.12$, Tukey HSD). Presynaptic area was not statistically different ** $p < 0.01$, $N > 10$.

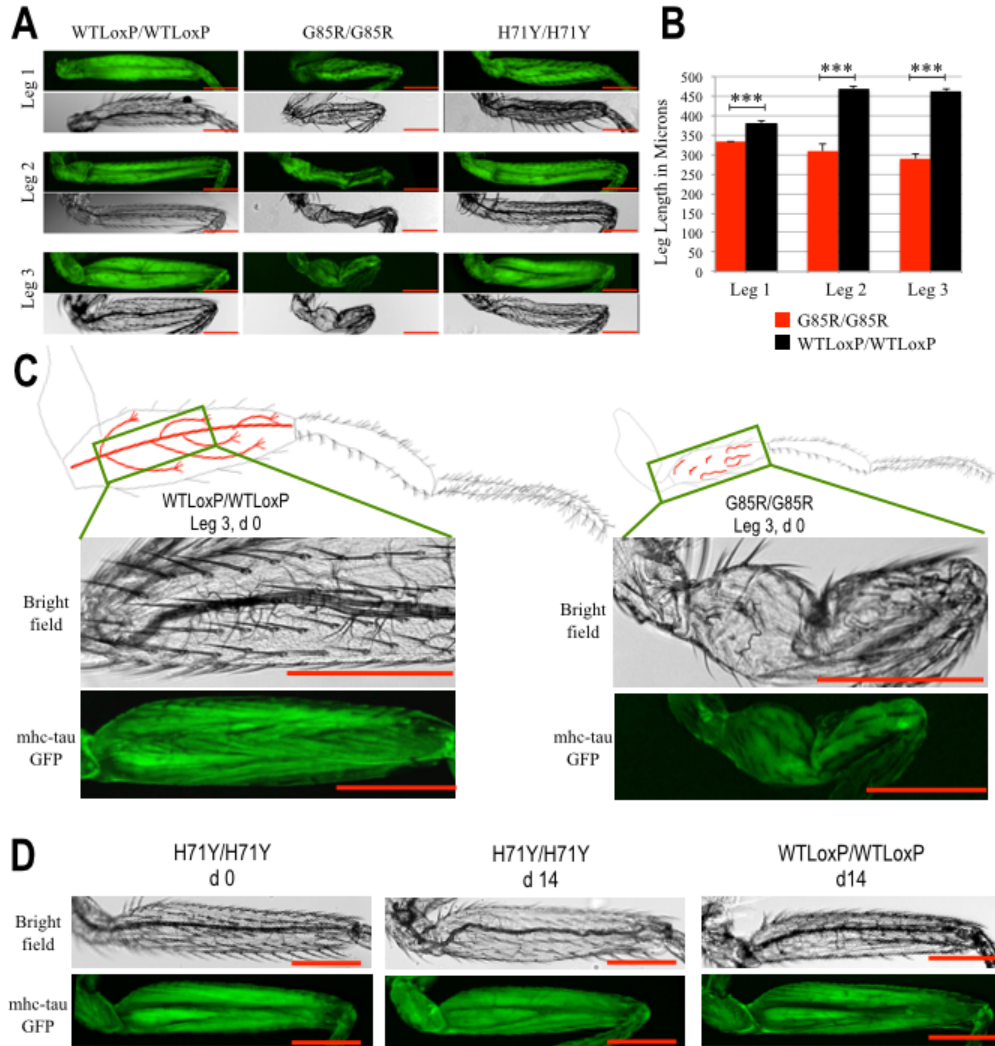


Figure 2.8. *dSod1* mutant adults experience muscle atrophy and progressive denervation. **A)** *dSod1*^{G85R/G85R} flies have shorter legs and malformed muscles. Bright field and fluorescent microscope images of the same leg of 1-day-old adults: *mhc-tau-GFP; dSod1*^{WTLoxP/WTLoxP}, *mhc-tau-GFP; dSod1*^{G85R/G85R}, *mhc-tau-GFP; dSod1*^{H71Y/H71Y}. (N=5) **B)** Average leg length quantification of *dSod1*^{WTLoxP/WTLoxP} and *dSod1*^{G85R/G85R} legs in microns. All *dSod1*^{G85R/G85R} legs are significantly shorter than wild type. (N=10) Error bars S.E.M. ***p< 0.001, One-tailed Student's Test. **C)** Bright field image of the nerve in the femur region of leg 3 exhibit deformation in *dSod1*^{G85R/G85R}. Please see Figure 2.9 for more detailed comparison. Fluorescent microscope image of the femur muscle exhibits muscle atrophy in *dSod1*^{G85R/G85R} (N=5). **D)** Bright field and confocal images show that all *dSod1*^{H71Y/H71Y} flies maintain main femur nerve and branches when they eclose. However, 13 out of 15 leg 3 loses femur nerve branches by 2 weeks. Leg 2 and 1 did not exhibit denervation.

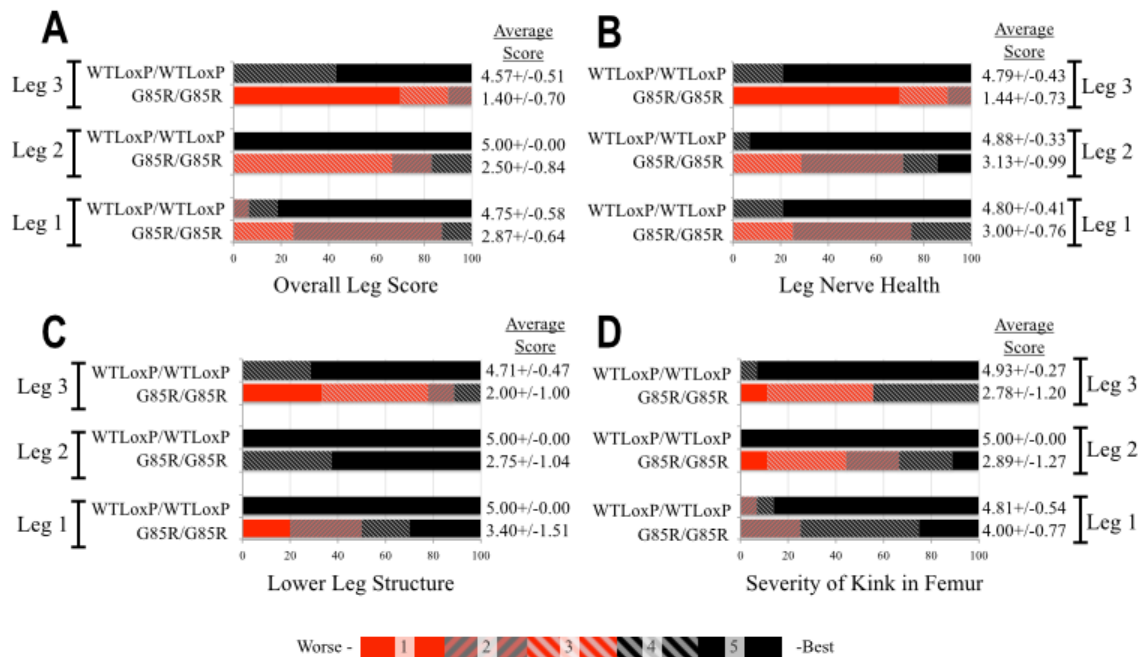


Figure 2.9. *dSod1*^{G85R/G85R} mutant legs exhibit more severe denervation in the distal legs. Scores are determined by a blinded undergraduate researcher. (N=10) **A**) The average of all criteria that we considered in determining the severity of leg phenotype. The score for **B**) Nerve integrity in the femur. **C**) Structure of the lower leg **D**) Severity of kink in the femur.

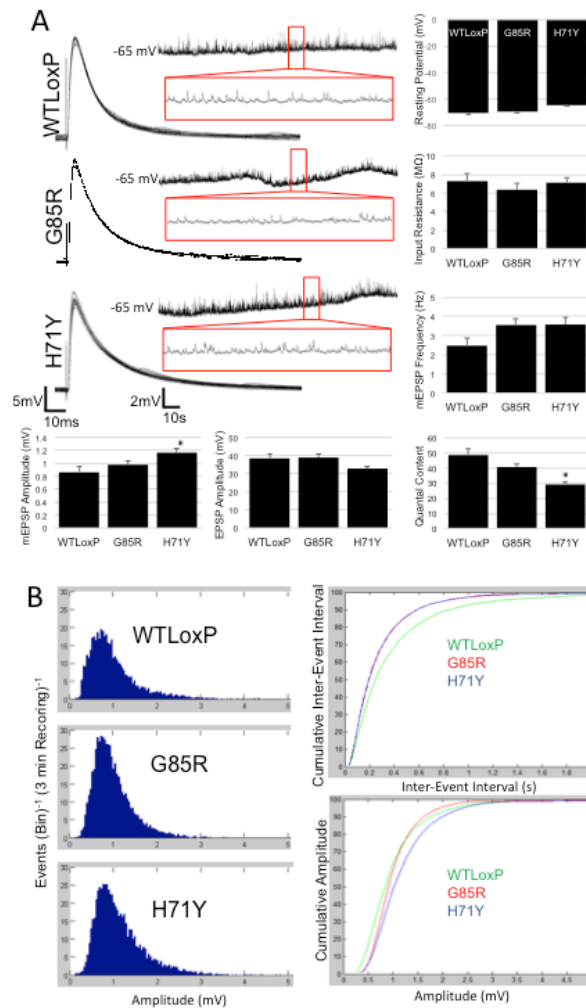


Figure 2.10. *dSod1*^{G85R} and *dSod1*^{H71Y} wandering 3rd instar larvae have minor neuromuscular junction defects. **A)** The majority of parameters measured demonstrate either no change or a relatively minor change in *dSod1*^{H71Y/H71Y}. Both *dSod1*^{G85R/G85R} and *dSod1*^{H71Y/H71Y} had trending increases in mEPSP frequency ($p = .07$ and $p = .09$, respectively), and *dSod1*^{H71Y/H71Y} had an increase in mEPSP amplitude. **B)** When mEPSPs from all recordings are pooled and plotted as histograms, the increased frequency of *dSod1*^{G85R/G85R} and *dSod1*^{H71Y/H71Y} and the shift in *dSod1*^{H71Y/H71Y} mEPSP amplitude become apparent. The cumulative probability plots show that *dSod1*^{WTLoxP/WTLoxP} has a longer inter-event interval than *dSod1*^{G85R/G85R} or *dSod1*^{H71Y/H71Y}, suggesting an increase in activity in these mutants ($p < .0001$, Kolmogorov–Smirnov Test). Additionally, all three genotypes have different mEPSP amplitude distributions ($p < .0001$, Kolmogorov–Smirnov Test).

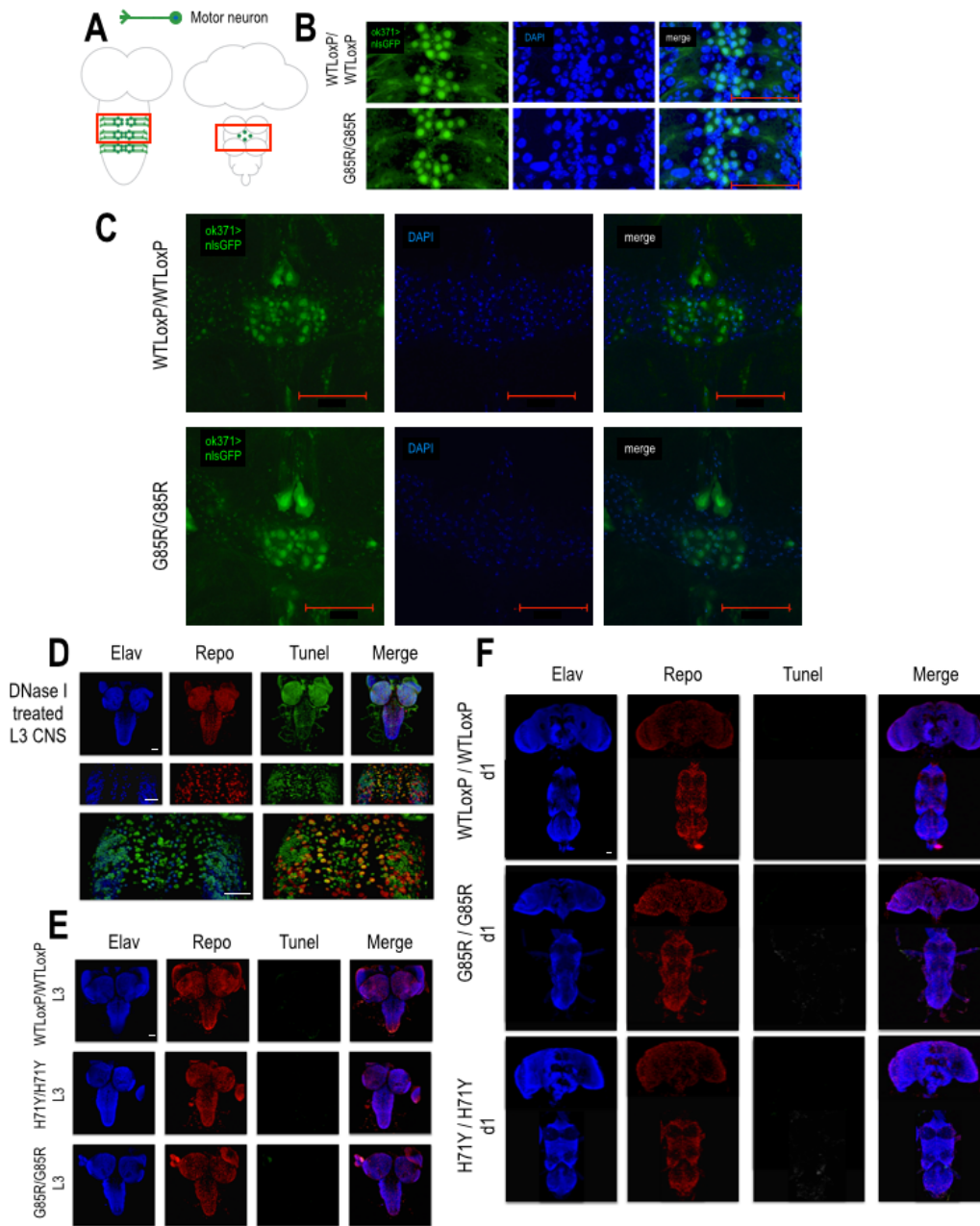


Figure 2.11. Absence of gliosis, apoptosis and motor neuron cell body loss in *dSod1* mutants. **A)** The nuclear GFP protein (*UAS-nlsGFP*) is expressed under the *ok371* motor neuron specific driver (*ok371-GAL4*). The motor neuron regions that are shown in the following pictures are highlighted in red squares. DAPI is used as an experimental control. Motor neurons and DAPI staining in *dSod1*^{G85R/G85R} and *dSod1*^{H71Y/H71Y} **B)** third instar larval brains (N=5) and **C)** adult ventral nerve chord do not exhibit gliosis and apoptosis. (N=1) Please note the difference of DAPI staining between the mutant and the wild type. This will be further covered in Appendix I. **D)** Experimental design control showing that TUNEL assay detects both glial cells (repo-positive) and neuronal cell (elav-positive) upon DNase I treatment of larval wild type brains. *dSod1*^{G85R/G85R} and *dSod1*^{H71Y/H71Y} **E)** third instar larval brains and **F)** adult ventral nerve chord do not exhibit gliosis and apoptosis (N=5). Scale bar 50 μ m.

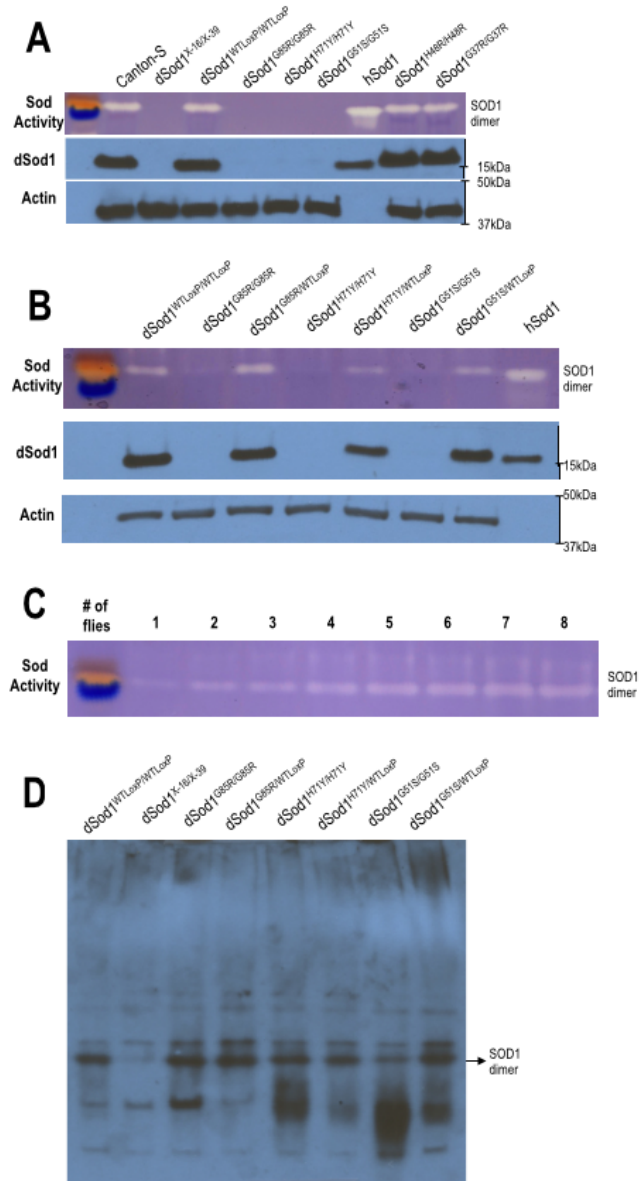


Figure 2.12. Superoxide dismutase activity is diminished in homozygous *dSod1^{G85R}* and *dSod1^{H71Y}* mutants **A)** SOD1 dismutase activity is measured from age-matched adult flies. The samples are run on a native-PAGE gel and SOD1 dismutase activity is assessed using nitroblue treazolium (NBT). Human SOD1 protein is used as a positive control. The same samples are run in SDS-PAGE gel and blotted with antibodies against dSod1 and actin. Superoxide activity is diminished in *dSod1^{G85R}*, *dSod1^{H71Y}* and *dSod1^{G51S}* homozygotes. **B)** The heterozygous dSod1 alleles exhibit superoxide activity comparable to wild type. **C)** The sensitivity of the NBT assay is not sufficient to detect small changes in the superoxide dismutase activity. Each well contains a gradual protein amount and a non-uniform increase is observed. Thus, the superoxide activity is not quantified in sections A and B. The NBT superoxide assay is not sensitive enough to quantify small changes in protein amount. **D)** Native gel showing the dimers of the dSod1 alleles present on the gel. Possibly misfolded dSod1 positive proteinaceous species present in homozygous and heterozygous dSod1 mutants.

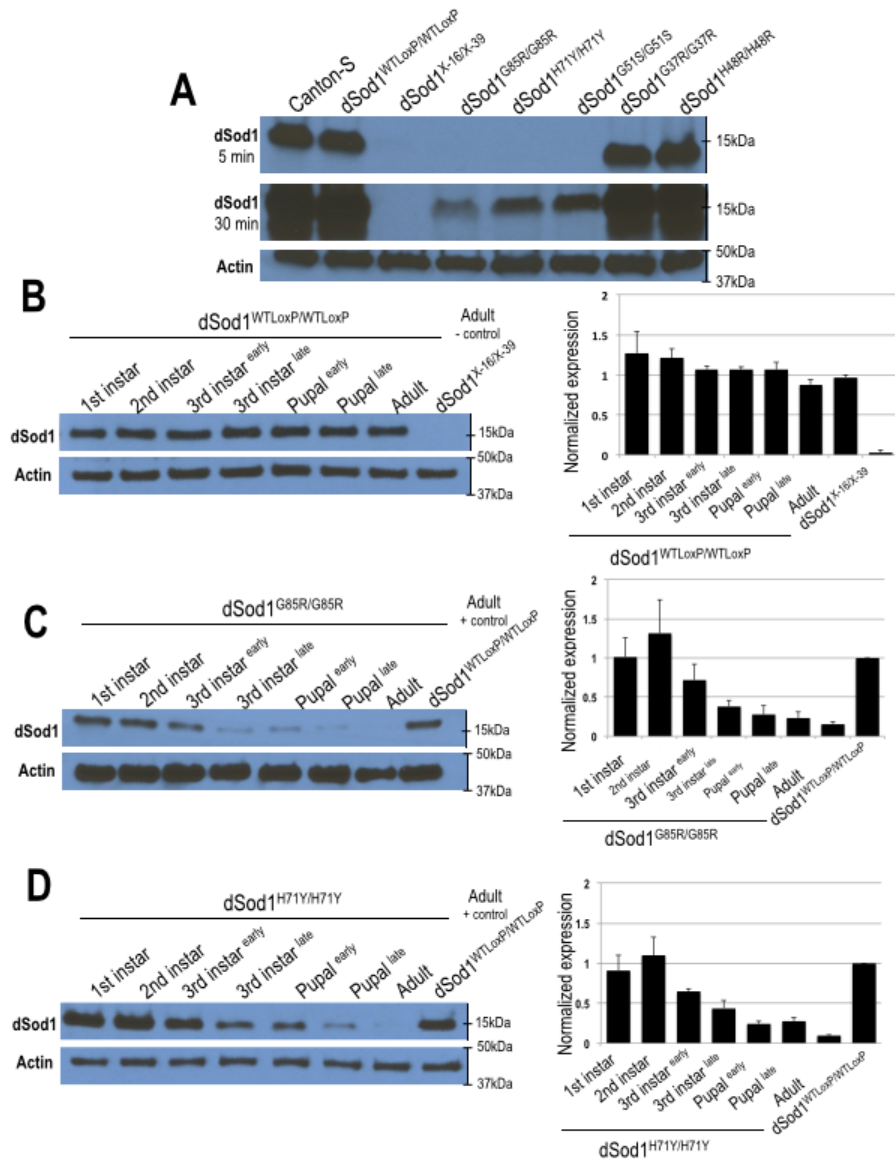


Figure 2.13. Protein expression of mutant SOD1 alleles is altered in *Drosophila* adults. **A)** The dSod1 protein amounts are drastically reduced in *dSod1*^{G85R/G85R}, *dSod1*^{H71Y/H71Y}, and *dSod1*^{G51S/G51S} late third instar larvae. Upon overexposure, a trace amount of protein is visible. 5 male flies are homogenized for this blot. **B)** Constant dSod1 protein amount in wild type line, gradually decreasing dSod1 protein amount throughout development in **C)** *dSod1*^{G85R/G85R} and **D)** *dSod1*^{H71Y/H71Y} flies. The reduction of protein amounts coincides with disease onset as defined in Figure 2.5.B.

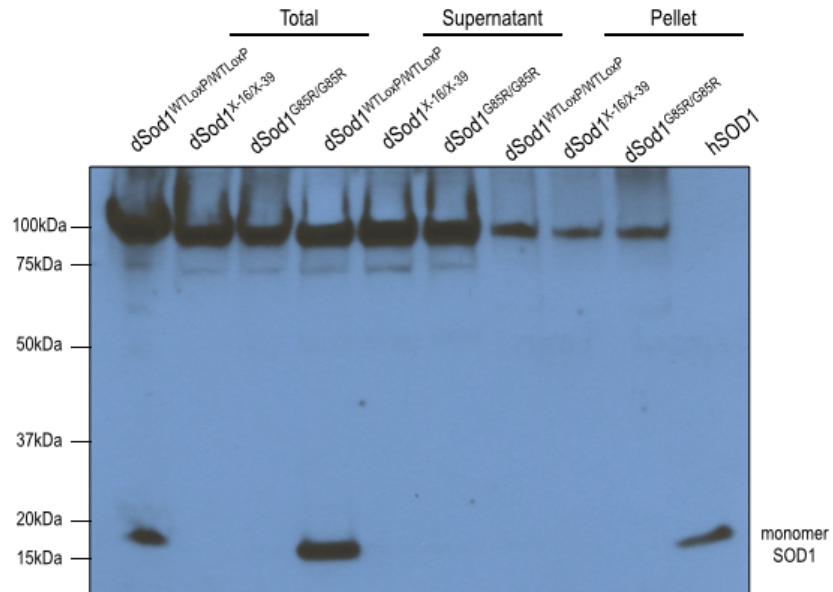


Figure 2.14. Lack of dSod1 in the insoluble protein fraction. A representative image of solubility assay for fractionation SOD1 in homogenates of flies expressing mutant *dSod1^{G85R/G85R}*, wild type *dSod1^{WTLoxP/WTLoxP}*, and deletion *dSod1^{X-39/X-16}* (negative control) Proteins were extracted in high salt buffer (high salt buffer i described in the methods section, 5 adult flies) and then, centrifuged at high speed to isolate soluble and insoluble species. Each fraction is named as: total, supernatant, and pellet.

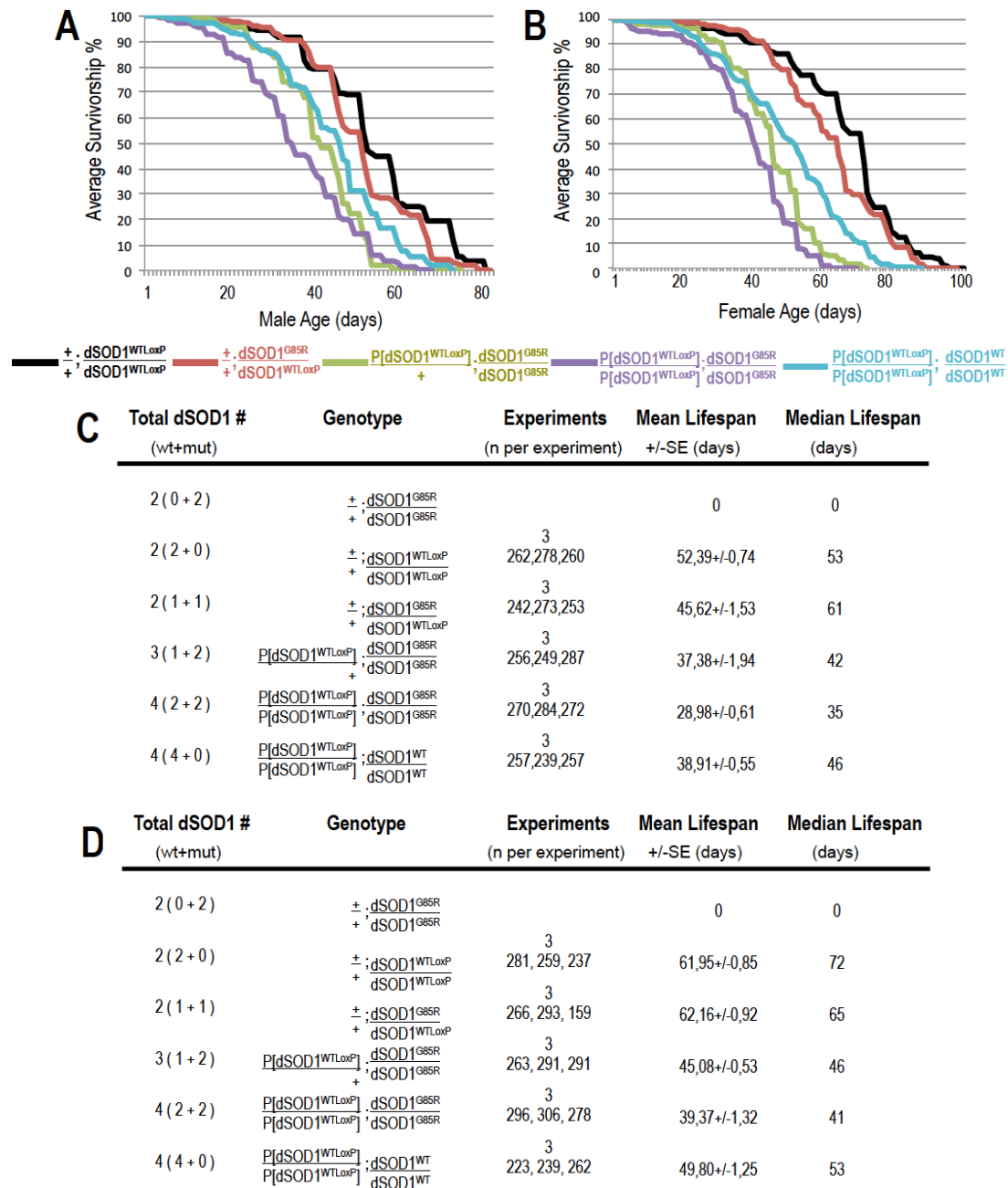


Figure 2.15. *dSod1*^{G85R} allele causes survival defects through gain of toxic function. Average life span of three trials of **A**) males and **B**) females of transgenic lines expressing extra dSod1 on the second chromosome and controls. *dSod1*^{G85R/G85R} flies die in the pupal case and do not survive to adulthood. The details of life span analysis for **C**) males **D**) females. *** p < 0.0001, log-rank test for $P[dSod1^{WTLoxP}]/P[dSod1^{WTLoxP}]$; $dSod1^{G85R}/dSod1^{G85R}$, $P[dSod1^{WTLoxP}]/+$; $dSod1^{G85R}/dSod1^{G85R}$ and $P[dSod1^{WTLoxP}]/P[dSod1^{WTLoxP}]$; $dSod1^{WTLoxP}/dSod1^{WTLoxP}$ life spans compared to wild type ($dSod1^{WTLoxP}/dSod1^{WTLoxP}$) for both sexes. $dSod1^{G85R}/dSod1^{G85R}$ and $dSod1^{WTLoxP}/dSod1^{WTLoxP}$ are not significantly different than each other.

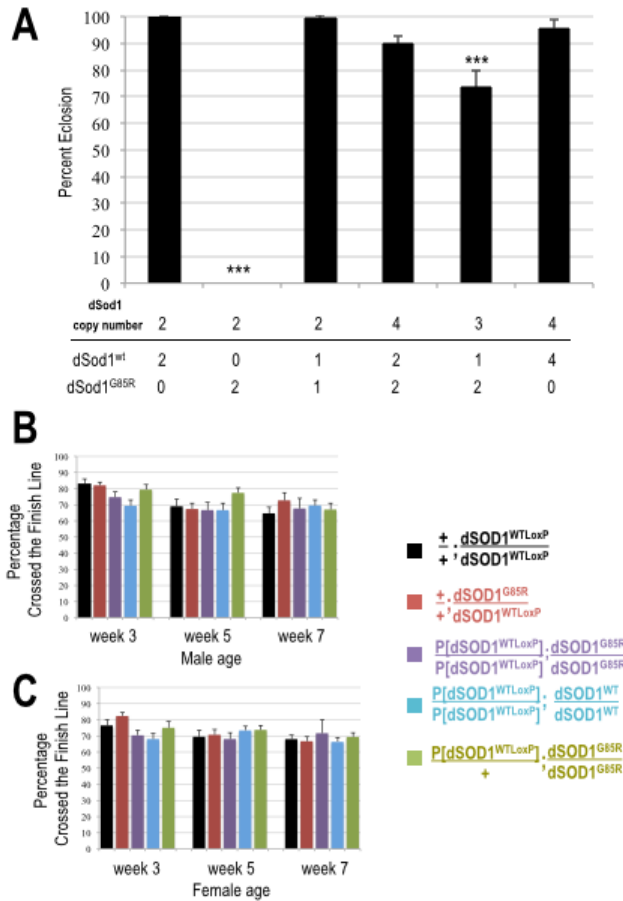


Figure 2.16. Wild type *dSod1* expression suppresses eclosion and locomotion defect. Average life span of three trials of **A)** males and **B)** females of transgenic lines expressing extra *dSod1* on the second chromosome and controls. *dSod1*^{G85R/G85R} flies die in the pupal case and do not survive to adulthood. Addition of two copies of *dSod1*^{WTLoxP} suppresses eclosion defect completely whereas one extra *dSod1*^{WTLoxP} partially suppresses. *** $p < 0.0001$ Fisher's Exact Test. Exogenous wild type *dSod1* expressing **B)** male **C)** female flies do not exhibit any locomotion defect within the 7 week long period.

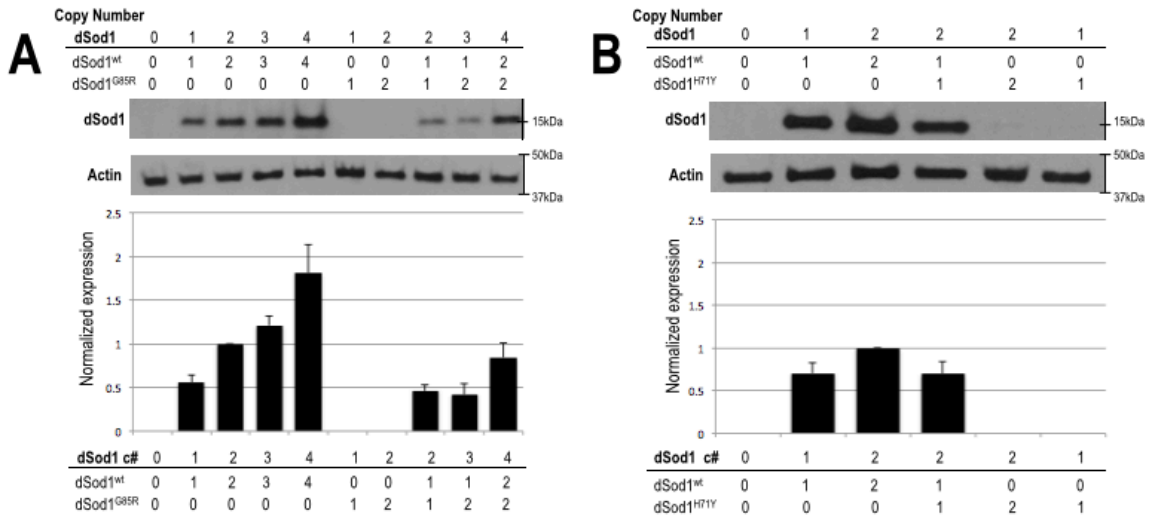


Figure 2.17. Protein expression of mutant *dSod1* alleles is not altered by the presence of extra wild type dSod1. A) Gene copy number is correlated with immunoblotting data for the wild type dSod1 protein. However, addition of wild type dSod1 protein to the *dSod1*^{G85R} background or B) *dSod1*^{H71Y} background does not alter the detectable dSod1 monomer amount.

TABLES

Table 2.1. The SOD1 point mutations investigated in this study G37R, H48R, H71Y, G85R, the most extensively studied G93A SOD1 point mutation in transgenic rodent models, and the D83G SOD1 point mutation expressed in the non-transgenic mouse model of ALS. The table shows the clinical parameters of these mutations on ALS patients. SOD1 enzymatic activity is depicted as a measurement from heterozygous patient tissue samples or total activity on gel-based assays (overall) and total activity on gel-based assays per SOD1 protein amount on denaturing gels (intrinsic).

Mutation	Significance for hSOD1 protein	Patient disease progression, reference	Patient age of onset, reference	SOD1 activity, reference
G37R	none	Slow progression (18 years) (Juneja <i>et al.</i> , 1997)	Early onset (29.3+/-1.2) (Juneja <i>et al.</i> , 1997)	intrinsic: 150% (Borchelt <i>et al.</i> , 1994) in heterozygous patients: 40% (Borchelt <i>et al.</i> , 1994)
H48R	Cu binding site	Slow progression (>12 and >20 years) (Rabe <i>et al.</i> , 2010) (Weis <i>et al.</i> , 2011)	Late onset (52 and 53) (Rabe <i>et al.</i> , 2010) (Weis <i>et al.</i> , 2011)	unknown
H71Y	Zn binding site	Fast progression (8 months) (Özoğuz <i>et al.</i> , 2015)	Variable Onset (N=1 had 57 and N=1 had 19) (Özoğuz <i>et al.</i> , 2015)	unknown
G85R	none	Fast progression (6 years +/-4.5) (Juneja <i>et al.</i> , 1997)	Late onset (55.5+/-12.6) (Juneja <i>et al.</i> , 1997)	intrinsic: 0% (Borchelt <i>et al.</i> , 1994) in heterozygous patients: 39.5% (Deng <i>et al.</i> , 1993)
D83G	Zn binding site	Variable progression (6-151 months) (Millecamps <i>et al.</i> , 2010)	unknown	overall: 0% (Joyce <i>et al.</i> , 2015)
G93A	none	Fast progression (2.4 years +/-1.4) (Juneja <i>et al.</i> , 1997)	Late onset (43.1+/-16.6) (Juneja <i>et al.</i> , 1997)	intrinsic: 102% (Chia <i>et al.</i> , 2010) in heterozygous patients: 35.8% (Deng <i>et al.</i> , 1993)

Table 2.2. Riluzole and Melatonin are not effective therapies for *dSod1^{G85R/G85R}* flies. Since Riluzole is not soluble in water, an emulsifier 2-hydroxypropyl- β cyclodextrin is used to make it soluble as described in (Rival *et al.*, 2004). All the melatonin experiments are performed in dark.

Drug	# of Screened <i>dSod1^{G85R/G85R}</i>	Percent Eclosion	Life Span of eclosed <i>dSod1^{G85R/G85R}</i>
2 mM Emulsifier	100	2.00	<u>1 Day Life Span</u> : 1 male and 1 female
1 mM Riluzole + 2 mM Emulsifier	213	2.82	<u>1 Day Life Span</u> : 1 male <u>2 Days Life Span</u> : 1 male <u>4 Days Life Span</u> : 1 male
1 mM Melatonin (in dark)	106	5.66	<u>1 Day Life Span</u> : 4 males and 1 female <u>4 Days Life Span</u> : 1 male
1mM Riluzole + 2 mM Emulsifier + 1mM Melatonin (in dark)	103	2.91	<u>1 Day Life Span</u> : 1 male <u>2 Days Life Span</u> : 1 male <u>4 Days Life Span</u> : 1 male
2 mM Emulsifier (in dark)	71	2.82	<u>1 Day Life Span</u> : 1 female <u>5 Days Life Span</u> : 1 male
4 mM Emulsifier	100	5.00	<u>1 Day Life Span</u> : 3 males <u>4 Days Life Span</u> : 1 male <u>5 Days Life Span</u> : 1 male
2 mM Riluzole + 4 mM Emulsifier	244	3.69	<u>1 Day Life Span</u> : 2 males and 1 female <u>4 Days Life Span</u> : 1 male <u>5 Days Life Span</u> : 2 males <u>6 Days Life Span</u> : 2 males
2 mM Melatonin (in dark)	93	2.15	<u>3 Days Life Span</u> : 1 male <u>4 Days Life Span</u> : 1 male
8 mM Emulsifier	120	7.50	<u>1 Day Life Span</u> : 1 male and 1 female <u>4 Days Life Span</u> : 3 males <u>5 Days Life Span</u> : 1 female <u>6 Days Life Span</u> : 1 female <u>7 Days Life Span</u> : 1 female <u>11 Days Life Span</u> : 1 male
4 mM Riluzole + 8 mM Emulsifier	157	8.92	<u>1 Day Life Span</u> : 4 males and 1 female <u>4 Days Life Span</u> : 1 male and 1 female <u>5 Days Life Span</u> : 2 males <u>6 Days Life Span</u> : 4 males and 1 female
4 mM Melatonin (in dark)	98	1.02	<u>1 Day Life Span</u> : 1 male
4 mM Riluzole + 8 mM Emulsifier + 4 mM Melatonin (in dark)	74	1.35	<u>1 Day Life Span</u> : 1 female
8 mM Emulsifier (in dark)	73	1.37	<u>7 Days Life Span</u> : 1 female

Table 2.3. Genetic stocks used in this study.

Line	Notes on Genotype	Source	Reference
HR stocks			
FLP-I-SceI		BSC 6930	(Staber et al., 2011)
ey-FLP		BSC 5580	(Staber et al., 2011)
y w Cre; nocSco/CyO		BSC 766	(Staber et al., 2011)
w ¹¹¹⁸		BSC 3605	(Staber et al., 2011)
Balancer Stocks			
w; TM3 sb/ TM6 tb		B. Ganetzky	
w; TM3 sb/ TM6B tb		B. Ganetzky	
w; TM3 GFP ser w+/ sb		BSC 4534	
w; cyo-RFP		BSC 35523	
dSod1 alleles			
dSod1 ^{G51S}		BSC 24492	(Phillips <i>et al.</i> , 1995)
dSod1 ^{X-39}	-homozygous lethal -deletion is found to be 397 bp instead of as reported 395 bp	BSC 24490	(Phillips <i>et al.</i> , 1995)
dSod1 ^{X-16}	-homozygous lethal -11bp deletion confirmed	William C. Orr	(Phillips <i>et al.</i> , 1995)
GAL4-UAS lines			
UAS-nlsGFP		Kristi Wharton	
ok371-GAL4		Kristi Wharton	
Endogenous Fluorescent Lines			
mhc-tau-GFP reporter		BSC 38460	

Table 2.4. Primer sequences used in this study.

Name	Sequence
Cloning Primers for HR	
dSod1 arm1 F	TCGTACGGCACACCAGCAACAGCAG
dSod1 arm1 R	TGGCGCGCCTCGGCACTGAAACATAA
dSod1 arm2 F	TGGTACCGCTGCCTATAAATATTTCC
dSod1 arm2 R	TGCGGCCGCGGAGGAGTCCATCGG
Sequencing Primers for HR	
dSod1 seq1	GGGCAAATAGTGAGGCCCATGGGTG
dSod1 seq2	GTAACAAGCAAGCAAACCACACAAGTAAC
dSod1 seq3	GAATAGTTCCCGCCACTGTCATTGG
dSod1 seq4	GATCTTGGCCAGGGTGGACACGAGCTG
dSod1 seq5	GTAATCAAGATACTCGCCACATGAGTAG
dSod1 seq6	GTGTGAGATAAAGGCATAGGATCAGTGGG
Mutagenic Primers for HR	
dSod1 G37R-F	GTGAAGGTCTCCGGTGAGGTGTGCC
dSod1 G37R-R	CCGTGCAGACCCCTGGCCAGGCGGC
dSod1 H48R-F	GGGTCTGCACGGATTCCACGTGCGC
dSod1 H48R-R	CATTGGTGTGTGTCACCGAACTCGCGC
dSod1 H71Y-F	CTTCAATCCGTATGGCAAGGAGTACG
dSod1 H71Y-R	GATTCTCGTTCGACGGGAGCGCCGTA
dSod1 G85R-F	GAGAATCGTCACCTGGGCGATCTGCGCAACATTGAGGCCACCGGCGGCGAC
dSod1 G85R-R	GAGAATCGTCACCTGGGCGATCTGC
p[W25.2] Specific Validation Primers	
pW-Not1	CACTGTTACGTCGCACTCGAGGGTAC
pW-Not2	GCACTCGAGAGCTCGTTACAGTCCG
pW-Bsi1	CGCACCGGACTGTAACGAGCTAC
pW-Bsi2	GGCGACTCAACGCAGATGCCGTACC
pW-Asc1	GTATGCTATACGAAGTTATCTAGACTAGTCTAGGGCG
pW-Asc2	GCTTGGCTGCAGGTCGACTCTAGAGG
pW-Asc3	CGATCATTCATTATTCGCTGCATGAATTAGC
pW-Acc1	CATTATACGAAGTTATCTAGACTAGTCTAGGGTAC
pW-Acc2	GACGCTCCGTTCGACGAAGCGCCTC
pW-Acc3	GCTCAGCTTGCTTCGCGATGTGTTAC
Figure 2.1C primers	
dSod1 mRNA start	GCATGTATTTCTAAGCTGCTCTGCTA
dSod1 mRNA end	GACCTTGGCAATGCCA
GAPDH F	GACGAAATCAAGGCTAAGGTTCG
GAPDH R	AATGGGTGTCGCTGAAGAAGTC

CHAPTER 3

Transcriptional Profiling of ALS-linked SOD1 Mutations in *Drosophila*

The RNA sequencing experiments described in this chapter were designed by myself along with guidance from Dr. Robert Reenan and Dr. Yiannis Savva. I have carried out all the experiments. Dr. Robert Reenan has analyzed the RNA sequencing results by eye with help from University Summer HHMI undergraduate scholars (Emily Jang, Kirsten Bredvik, Ryan Greene, Godwin Boiful, Joshua Hackney, Karla Navarrete, Natalie Palaychuk, Dina Sabetta, Jimmy Xia, Wendy Gaztanaga). The RNA sequencing results were mapped and measured by Dr. A. Murat Eren and Dr. Tom Delmont. The statistical analysis was run by myself with help from Dr. Ali Bilgin Arslan. Gene set enrichment analysis was performed and methods section was written by Dr. Robert Reenan. The figures and the manuscript were crafted by myself. This research was funded by the ALS Association.

ABSTRACT

Although many distinct mutations in a variety of genes are known to cause Amyotrophic Lateral Sclerosis (ALS), it remains poorly understood how the first discovered ALS-related gene, SOD1, causes neurodegeneration and whether the cellular mechanisms altered through SOD1 converge on common molecular pathways with other ALS-related genes. Recent discoveries that several inherited forms of ALS involve RNA binding proteins such as TDP43 and FUS and hexanucleotide repeat expansion in C9orf72 raise the question of whether RNA metabolism is generally dysregulated in ALS. Here we conducted genome-wide transcriptional profiling of a *Drosophila* model with various knock-in SOD1 mutations. The severe SOD1 mutations that cause fast disease progression in ALS patients resulted in early death, locomotion and eclosion deficit as well as a neurodegeneration phenotype in *Drosophila*. Mutant dSod1 proteins induced a transcriptional signature indicative of metabolic process, defense response and RNA metabolism compared to age-matched wild type flies. Since many ALS-causing genes share misfolded SOD1 signature regardless of SOD1 mutations, we expect these transcriptomic changes that we described in this chapter will be very useful for understanding the overall ALS pathogenesis.

INTRODUCTION

Amyotrophic Lateral Sclerosis (ALS), most commonly known as Lou Gehrig's disease, is a fatal and incurable neurodegenerative disease (Peters, Ghasemi, & Brown, 2015). Classical linkage studies and exome sequencing approaches have demonstrated that ALS can be caused by a variety of mutations in more than 50 genes

acting on diverse cellular functions (Table 1.3). Mutations in the first ALS-associated gene SOD1, thought to gain toxic function by leading to proteinaceous inclusions, was the most common cause of ALS for 18 years (Rosen *et al.*, 1993), until the discovery of C9orf72 G₄C₂ repeat expansions in 2011 (DeJesus-Hernandez *et al.*, 2011; Renton *et al.*, 2011; Gijssels *et al.*, 2012). During this 18 years period, various genes related to RNA metabolism namely TDP-43, FUS, Angiogenin, hnRNPA1 and 2B1, Senataxin, and Matrin 3 mutations as well as C9orf72 expansion repeats were linked to ALS (Table 1.3). Even though the misfolded SOD1 signature is shared by many of these ALS-associated RNA metabolism mutants and sporadic ALS cases (Gruzman *et al.*, 2007; Pokrishevsky *et al.*, 2012), how or if SOD1 contributes to RNA pathology is currently unknown. As next generation sequencing technologies and genome-wide microarray techniques become widely available, it is becoming more and more clear that seemingly unrelated ALS-causing genes bear a common transcriptomic/proteomic profiles when compared with each other. For instance, two independent groups revealed that C9orf72 and SOD1 patient iPSC-derived motor neurons exhibit common aberrant transcriptional profiles (Donnelly *et al.*, 2013; Kiskinis *et al.*, 2014). Even though these transcriptomic/proteomic profiling studies on iPSC-derived motor neurons are profoundly informative for identifying pathogenic processes underlying general mechanisms of ALS, these experiments were performed *in vitro*. On the other hand, *in vivo* transcriptomic/proteomic profiling studies have been performed widely in transgenic ALS mouse and *Drosophila* models (Bandyopadhyay *et al.*, 2013; Vanden Broeck *et al.*, 2013), but whether the alterations described by such studies are due to the mutation itself or secondary responses resulting from superphysiological mutant expression levels is not clear.

In Chapter 2, we described a new *Drosophila* model with specific knock-in SOD1 point mutations. The severe SOD1 mutations that cause fast disease progression in ALS patients resulted in early death, locomotion and eclosion deficit as well as a neurodegeneration phenotype in *Drosophila*. Here, we have taken an unbiased approach to understand the physiological changes that occur in these mutant lines at the transcriptome level. We have combined deep RNA sequencing (RNA-seq) technologies to identify the transcriptional and functional changes induced by the *dSod1*^{G85R} and *dSod1*^{H71Y} homologously recombined alleles, as well as the *dSod1*^{G51S} mutant allele that was previously identified as a result of EMS mutagenesis, and compared them to an age-matched wild type control line that is genomically almost identical (backcrossed to *w*¹¹¹⁸ for 5 generations): *dSod1*^{WTLoxP}. In addition, we have investigated transcriptional changes that occur based on mutant gene dosage by investigating the transcriptomic expression differences in homozygous *dSod1*^{G85R/G85R} and heterozygous *dSod1*^{G85R/WTLoxP} compared them to the wild type control *dSod1*^{WTLoxP/WTLoxP}. Finally, in order to investigate early neuron-specific alterations, we sequenced RNA isolated from the central nervous system of *dSod1*^{G85R/G85R} and *dSod1*^{WTLoxP/WTLoxP} at the start of the locomotion deficit during the third instar wandering larval stage. Thus far, we have analyzed the adult tissue transcriptome changes and notably, we found that mutant SOD1 disrupts the expression of genes that participate in metabolic processes (lipid, glucose and amino acid metabolism), the defense response pathway (innate immunity and inflammation) and the RNA metabolism pathway (mRNA polyadenylation, non-coding RNAs, 3'-UTR expansion).

MATERIALS AND METHODS

Drosophila strains

Drosophila were raised at a constant 25°C, on standard cornmeal molasses food and under 12 h day/night cycles. *dSod1* alleles were balanced over a third chromosome balancer: *TM3,GFP,ser,w⁺* (BDSC 4534). To differentiate between homozygous flies in the larval stages, we used the GFP marker on the balancer. Since the homozygous flies did not carry the balancer chromosome, they did not express GFP. This allowed accurate genotyping of larvae for central nervous system dissection.

Library Generation and Genome Sequencing

Total RNA was derived from 200 heads and thoraces of newly eclosed *dSod1*^{WTLoxP/WTLoxP}, *dSod1*^{H71Y/H71Y}; 20 heads and thoraces of newly eclosed *dSod1*^{WTLoxP/G85R}, *dSod1*^{G51S/G51S} or alive *dSod1*^{G85R/G85R} adults stuck in the pupal case and 60 dissected central nervous systems of third instar wandering larvae of *dSod1*^{G85R/G85R} and *dSod1*^{WTLoxP/WTLoxP}. RNA extractions from *Drosophila* tissues were performed using standard TRIzol (Invitrogen) extraction. The sequencing libraries were made with 50-100 ng of RNA using the NuGEN's Ovation Human Blood RNA-Seq Multiplex System 1-8 (P/N: 0337-32) kit. Ribosomal RNA was removed in the process of library prep as a step for the NuGEN's kit. Deep sequencing was performed using the Illumina HiSeq 2000 or 2500 Platform at the Brown University Genomic Facilities (Multiplexed, 50 bp reads).

Quality Filtering, Mapping and Measurement of Gene Expression

The raw transcriptomic data was analyzed with illumina-utils library version 1.4.1 (accessible at <https://github.com/meren/illumina-utils>) (Eren *et al.*, 2013) (Eren *et al.* 2013). The noisy sequences were removed using “iu-filter-quality-minoche” program with default parameters, which implemented the noise filtering described by Minoche, Dohm, & Himmelbauer, 2011. The *Drosophila melanogaster* reference genome assembly and gene annotations were obtained from the FlyBase Release 6.05 (available at http://ftp.flybase.net/genomes/Drosophila_melanogaster/dmel_r6.05_FB2015_02/fasta/). The short transcripts were mapped to this reference genome with a requirement of 95% sequence identity over 100% of the read length, and results were exported as BAM files for each sample by CLC Genomics Workbench (version 6) (<http://www.clcbio.com>). To quantify the average coverage of each gene across 5 conditions and 3 replicates, and to visualize the mapping results, the anvi'o (available from <http://merenlab.org/projects/anvio/>) version 1.0.0-rc2 software platform was used to visualize and analyze 'omics data. Each sample was profiled using 'anvi-profile' command with default parameters, and then the resulting profiles were merged using 'anvi-merge'. Finally, the coverage information of each gene in each sample from the merged anvi'o database was exported for the analysis of differential gene expression.

Differential expression analysis was performed in three different analyses: (i) Gene expressions between 3 replicates of $dSod1^{WTLoxP/WTLoxP}$ and $dSod1^{H71Y/H71Y}$ were considered differentially expressed when the Benjamini-Hochberg corrected p value was below 0.05, (ii) Gene expressions between 3 replicates of $dSod1^{WTLoxP/WTLoxP}$ and

dSod1^{WTLoxP/G85R}, *dSod1*^{G51S/G51S} or *dSod1*^{G85R/G85R} were considered differentially expressed when the Benjamini-Hochberg corrected p value was below 0.001 or (iii) Gene expressions between 3 replicates of *dSod1*^{WTLoxP/G85R} and *dSod1*^{G51S/G51S} or *dSod1*^{G85R/G85R} were considered differentially expressed when the Benjamini-Hochberg corrected p value was below 0.05. The statistical analyses of one way Anova and Benjamini-Hochberg correction were performed by standard MATLAB (R2015a) functions: ANOVA and BHFDR. The fold changes were calculated by dividing average gene expression of the mutant sample to average gene expression of the control.

Gene Set Enrichment Analysis (GSEA)

Gene set enrichment analyses were performed to compare *dSod1*^{WTLoxP/WTLoxP} and *dSod1*^{H71Y/H71Y} transcriptome using a number of methods utilizing the GORILLA (Gene Ontology enRIchment anaLysis and visualizAtion) tool through its online site: <http://cbl-gorilla.cs.technion.ac.il/> (Eden *et al.*, 2009). This site provides a fast and uncomplicated way to analyze gene expression data based on a single ordered list, or two unordered lists comparing a test set against a background set of genes. In our case, we have used the unordered lists, comparing the list of genes whose expression changes have corrected P-values lower than P=0.05 with the set of all genes whose expression was detected in the data set. GORILLA generates output pathways and processes with P-values and those values corrected for FDR.

RESULTS

Overview of Transcriptional Profiles for *dSod1* Genetically Engineered Alleles

To measure transcriptional differences in *dSod1*^{H71Y/H71Y}, *dSod1*^{WTLoxP/G85R}, *dSod1*^{G51S/G51S}, and *dSod1*^{G85R/G85R} compared to *dSod1*^{WTLoxP/WTLoxP}, we isolated RNA from head and thorax (whole flies after discarding the abdomen) region of adult flies. In addition to the head and thorax region that include the brain and ventral cord, we performed nervous system-specific RNA sequencing from dissected central nervous systems of wandering third instar larvae at the stage where *dSod1*^{G85R/G85R} start exhibiting locomotion defects (2.5.B). Total RNA recovered from relevant tissue was subjected to fragmentation, cDNA synthesis, adaptor ligation, and library amplification according to the standard NuGEN's Ovation Human Blood RNA-Seq Multiplex Protocol (See Materials and Methods). 50 bp single-end multiplex reads were obtained for all the tissues. So far, we have mapped the raw transcriptome data only for the adult tissue samples (*dSod1*^{H71Y/H71Y}, *dSod1*^{WTLoxP/G85R}, *dSod1*^{G51S/G51S}, and *dSod1*^{G85R/G85R} and compared them to *dSod1*^{WTLoxP/WTLoxP}) and performed preliminary analysis only on *dSod1*^{H71Y/H71Y} and *dSod1*^{WTLoxP/WTLoxP}. According to the preliminary analysis based on average reads per gene, a total of 1217 genes were up-regulated and 40 genes were down-regulated at least 2 fold in *dSod1*^{H71Y/H71Y} when compared to *dSod1*^{WTLoxP/WTLoxP} counterparts (Figure 3.1). The names of the top 30 differentially genes based on fold change can be found in Figure 3.1. On the contrary, the expression of a housekeeping gene *Gapdh* did not change between *dSod1*^{H71Y/H71Y} and *dSod1*^{WTLoxP/WTLoxP} samples (Fold difference: 1.38 and p value: 0.23).

Ontology of Transcripts Altered in *dSod1*^{H71Y/H71Y}: Metabolism and Inflammation

To better understand how transcriptomic signatures translate into cellular metabolism, we next performed gene ontology enrichment analysis of *dSod1*^{H71Y/H71Y} expression changes. We did not assign an arbitrary fold change cutoff value and we compiled all the statistically significant genes (FDR 5%) to the GORILLA gene ontology program (Eden *et al.*, 2009). The result summary of gene ontology (GO) terms can be found at Figure 3.2 and Table 3.1 and the full GO terms can be visualized at <http://cbl-gorilla.cs.technion.ac.il/GOrilla/nnvf3v6p/GOResults.html>. Notably, GO terms pointed towards several metabolic processes (lipid, glucose and amino acid metabolism) and the mechanisms of defense response (innate immunity and inflammation).

Alterations in expression of genes involved in metabolic pathways was an unexpected result at first, however considering total RNA was extracted from whole flies, the signal of many potentially interesting nervous system transcripts may have been diluted. Further literature analysis revealed that metabolism is one of the major altered pathways in ALS patients showing early and persistent hypermetabolic signature associated with energy wasting (Desport *et al.*, 2001; Bouteloup *et al.*, 2009) and ALS animal models: The G1 hSOD1^{G93A} transgenic mouse line shows defective energy homeostasis that benefits from a high energy diet (Dupuis *et al.*, 2004) or lowered amounts of leptin, a regulator of whole-animal energy expenditure (Lim *et al.*, 2014). In addition, the hSOD1^{G85R} transgenic mouse model has also been shown to have several metabolic changes consistent with a metabolic switch occurring as an early pathological event (Palamiuc *et al.*, 2015).

Neuroinflammation, on the other hand, is a major hallmark of ALS pathogenesis based on rodent models, fALS and sALS patient samples (Philips & Robberecht, 2011). In very general terms, neuroinflammation can be characterized as extensive astrogliosis, microglial activation, and elevated peripheral immune cells at the sites of neurodegeneration. It is not surprising that inflammation was one of the major GO terms identified in *dSod1^{H71Y/H71Y}* transcriptional profiling. One striking example PGRP-SC2, an innate response transcription factor is up-regulated 45.5 fold (p value 0.029). In *Drosophila*, mutations in an innate immunity modulator protein, *dnr1*, or expression of AMP (anti-microbial peptide) genes trigger progressive, age dependent neuropathology accompanied with shortened life span (Cao *et al.*, 2013).

***dSod1^{H71Y/H71Y}* Exhibit Transcriptional Signatures of Immunity-triggered Cell Death**

One of the few genes that were down regulated in *dSod1^{H71Y/H71Y}* samples was *Dronc* (Figure 3.1, 3.6 fold down-regulated, p value 0.036). Cellular apoptosis is executed by a cascade of caspase activation and *Dronc*, caspase-9 as mammalian ortholog, is one of the initiator caspases of apoptosis (Steller, 2008). Down-regulation of *Dronc* indicates defects in the apoptotic pathway, in agreement with the negative-TUNEL staining performed on age matched *dSod1^{H71Y/H71Y}* central nervous system (Figure 2. 11. E). Furthermore, a recent study suggests defects in the apoptosis pathway can trigger a necrosis-driven systemic immune response through the activation of glycine N-methyltransferase (*Gnmt*) and triacylglyceride lipase (*PNLIP*) leading to an energy wasting phenotype (Obata *et al.*, 2014), similar to an energy wasting state observed in ALS patients (Dupuis *et al.*, 2011). *Gnmt* expression was elevated by 31.5 fold (p value

0.07) and PNLIP, a triacylglyceride lipase, expression was also elevated by 91.3 fold (p value 0.028) in *dSod1*^{H71Y/H71Y} transcriptome analysis. Moreover, Drosocin, an anti-microbial peptide and a hallmark of necrosis (Levy *et al.*, 2004; Obata *et al.*, 2014), was up-regulated 38.9 fold (p value 0.02).

***dSod1* Alleles Exhibit Bunina Body Marker Transferrin**

One of the first defined hallmarks of ALS-FTD pathology in humans was the presence of Bunina Bodies, which are small eosinophilic neuronal inclusions (Bunina, 1962). To date, it is still unclear what are the constituents of Bunina Bodies other than a few identified proteins including Transferrin (Okamoto, Mizuno, & Fujita, 2008). Interestingly, in *dSod1*^{H71Y/H71Y} one-day post eclosion adults, Transferrin was up-regulated by 7.2 fold (p value 0.02), which suggests the presence of Bunina Bodies-like protein inclusions in *dSod1* mutant *Drosophila*.

***dSod1* Alleles Exhibit a Common Signature with TDP-43 *Drosophila* Mutants**

In *Drosophila*, both gain and loss of TDP-43 (dTDP-43) cause pupal lethality and reduced adult viability, impaired larval locomotor activity, axonal loss, and altered synaptic boutons (Feiguin *et al.*, 2009; Li *et al.*, 2010; Lin, Cheng, & Shen, 2011; Wang *et al.*, 2011; Vanden Broeck *et al.*, 2013). Even though it is not clear how other ALS causative genes converge with the SOD1-mediated ALS pathway, it is expected that *dSod1* mutants might share some common transcriptomic signatures with other previously characterized *Drosophila* ALS models. In 2013, a group analyzed the transcriptomic changes that occur due to dTDP-43 knock-out and overexpression from

late pupal heads (Vanden Broeck *et al.*, 2013). Both ubiquitous overexpression and loss of function resulted in similar phenotype that we also observed in $dSod1^{G85R/G85R}$ (Chapter 2), namely late pupal lethality, immature-looking adult escapers and a soft cuticle (Vanden Broeck *et al.*, 2013). Activated innate immunity was a signature observed in both dTDP-43 loss and gain of function transcriptomic analysis, in agreement with our results presented in this chapter. Furthermore, the expression of microtubule-associated protein 205 (Map205) was the most significant change exhibited by both genotypes. It is not clear yet how microtubule structure changes contribute to ALS pathogenesis, however, intriguingly Map205 was also one of the most dramatically altered gene in our expression studies on *dSod1* mutants, not only in homozygotes $dSod1^{H71Y/H71Y}$, $dSod1^{G51S/G51S}$, and $dSod1^{G85R/G85R}$, but also in $dSod1^{WTLoxP/G85R}$ heterozygotes (Figure 3.3). The contribution of Map205 to ALS pathogenesis remains to be determined, however according to Vanden Broeck *et al.*, elevated Map205 expression leads to aberrant cytoplasmic accumulation of Ecdysteroid receptor (EcR) and disrupted EcR signaling, which subsequently leads to apoptosis of bursicon neurons, which play a critical role during the last step of metamorphosis (Vanden Broeck *et al.*, 2013). Bursicon neurons secrete insect neurohormone bursicon, which is required for wing expansion and cuticle hardening in *Drosophila* post-eclosion events (Luan *et al.*, 2006). The death of bursicon neurons might be a possible explanation of late pupal lethality exhibited by $dSod1^{H71Y/H71Y}$, $dSod1^{G51S/G51S}$, and $dSod1^{G85R/G85R}$ flies as well as the wrinkled wing phenotype observed in $dSod1^{H71Y/H71Y}$ and $dSod1^{G51S/G51S}$. The state and contribution of bursicon neurons in *dSod1* mutants remains to be explored.

***dSod1* Alleles Exhibit Signatures of Aberrant RNA Processing**

Altered RNA metabolism with a direct or indirect effect through functional abnormalities of RNA-binding proteins is a recently accepted hallmark of ALS after the discovery of mislocalized key proteins important in RNA metabolism such as TDP-43 and FUS linked to ALS (Droppelmann *et al.*, 2014). However, the extent of SOD1 contribution to RNA pathology and the molecular mechanisms involved in aberrant RNA pathology observed in ALS are currently unknown.

The transcriptional analysis we have performed so far utilizes the average read numbers that are assigned to a particular gene. While this analysis provides an indication on the expression levels of various genes, it does not reveal the read map differences within a particular gene, which is indicative of altered RNA processing events. For instance, an important protein Amyloid Precursor Protein-like (Apl), whose secreted forms can suppress neurodegeneration in *Drosophila* (Wentzell *et al.*, 2012) did not reveal any significant expression changes based on the current analysis (Fold change 1.13X, p value 0.5). However, a normally spliced a long intron within this gene is significantly expressed in *dSod1*^{H71Y/H71Y} (Figure 3.4). The intron skipping coordinate does not seem to be random, since we observed cases argues the intron inclusion. For example, couch potato transcript (Cpo, human ortholog RBPMS), which is involved in RNA granules and synapse formation (Glasscock & Tanouye, 2005), exhibits an unusual extra splicing of a long intron (Figure 3.5). According to current analysis method we utilized, this significant change is also not detectable by fold changes in gene expression alone (Fold change 1.15 and p value 0.44 in *dSod1*^{H71Y/H71Y} samples). Moreover, we observed that the 3' UTR regions are dramatically longer for some transcripts such as the

receptor tyrosine phosphatase *Ptp10D* (Figure 3.6), which interacts with a cell surface ligand to regulate axon guidance and glial-neuronal communication (Lee *et al.*, 2013). According to the current analysis method, Ptp10D expression did not change (fold change 1.44, p value 0.234). It is clear from these examples that, we need to re-analyze our RNA sequencing read maps in order to be able to detect changes in such UTR lengthening as well as splicing abnormalities. The nature of these RNA metabolism defects have the potential to highlight important clues regarding ALS pathogenesis. The other major ALS associated genes TDP-43, FUS and C9orf72 hexanucleotide repeat expansions lead to splicing defects, particularly of long introns in neuronal genes involved in synaptic processes (Da Cruz & Cleveland, 2011; Orozco & Edbauer, 2013; Onodera *et al.*, 2014), however how these abnormalities in RNA metabolism arise and contribute to ALS pathogenesis are currently remain enigmatic.

DISCUSSION AND FUTURE DIRECTIONS

In our era of affordable and accessible sequencing facilities and unprecedented computational power, disease-altered cellular mechanisms can be addressed in a systematic, genome-wide manner. A high throughput RNA sequencing approach promises to be especially useful in a research field like ALS, where the mechanism of disease is a mystery and seemingly unrelated genes are associated with the disease. Transcriptional profiling has been utilized previously in various ALS patient tissue and animal models (reviewed in Heath, Kirby, & Shaw, 2013). The limitation of patient tissue transcriptome analysis is that it can be accessed only at the terminal stage. Conversely, animal models can provide the related tissue homogenates at earlier stages. However, a

basic requirement for experimental accuracy, a precisely controlled *in vivo* system, where mutant gene copy number and wild type gene copy number are equivalent, has been absent in current ALS animal model transcriptional profiling studies. Thus, previous studies mostly compared the transcriptome changes that occur in two different stages of the same transgenic animal line. In one example, Bandyopadhyay *et al.* analyzed the transcriptome profile of laser-dissected spinal cord motor neurons from pre- and post-symptomatic hSOD1^{G85R-YFP} transgenic mice that developed ALS-like symptoms and paralysis during the first 5-6 months of adulthood (Bandyopadhyay *et al.*, 2013). The group reported differentially expressed genes, but such studies bear two major pitfalls: First, it is not clear whether gene profile is affected as a result of the mutation itself, or because of the overexpression nature of the allele. Second, such studies almost always analyze the transcriptomic changes in the cell bodies of neurons, whereas in ALS the disease originates from the neuromuscular junction, and cell bodies are the last sections that are affected (Dadon-Nachum, Melamed, & Offen, 2011). The RNA population of the synapse and neuromuscular junction that potentially plays an essential role in disease pathogenesis is not subject to analysis in these cell body-specific transcriptome profiling studies (Lenzken *et al.*; Chakkalakal & Jasmin, 2003). Furthermore, a SOD1 mutant patient iPSC-derived motor neuron transcriptional profile elaborated these issues and analyzed the transcriptome profile of whole motor neurons with the advantage of a human background (Kiskinis *et al.*, 2014). According to this study, mutant SOD1 protein induced a transcriptional signature indicative of increased oxidative stress, reduced mitochondrial function, altered subcellular transport, and activation of the ER stress and unfolded protein response pathways. Importantly, the control line used in this study was a

wild type allele that was precisely engineered through TALEN-mediated genome editing. One pitfall of the study was the *in vitro* nature of the cell culture system. It is well established that non-motor neuron cells play a major role in ALS (Di Giorgio *et al.*, 2007; Ilieva, Polymenidou, & Cleveland, 2009; Serio *et al.*, 2013).

The ultimate goal of this study is to examine transcriptional changes that occur strictly as a result of expressing ALS-causing mutant genes from its endogenous promoter. We used two distinct homologously recombined mutants (*dSod1*^{G85R} and *dSod1*^{H71Y}), and an EMS introduced point mutation (*dSod1*^{G51S}) allele to eliminate secondary effects of transgenic methods as well as background effects. In addition, we characterized the mutant *dSod1 Drosophila* model described in Chapter 2 for expected ALS-related phenotypes and detected an ALS-like phenotype onset at the wandering third instar larval stage. We extended the initial general transcriptome analysis to the specific central nervous system tissue and to the onset of the disease in *Drosophila* by performing RNA sequencing analysis from the central nervous system from *dSod1*^{G85R/G85R} wandering third instar larvae. We believe the transcriptomic alterations that we discussed in this chapter will be an important step towards understanding altered cellular mechanisms in ALS pathogenesis.

The next goal of this study will be to identify the RNA metabolism changes that occur as a result of SOD1-mediated ALS. With direct linkages of important RNA metabolism genes to ALS, it is becoming clearer that altered RNA metabolism is one of the keystones of ALS pathogenesis. However, the role of SOD1 protein in ALS and its link to the ALS puzzle are not clear. A recent study proposed that cytoplasmic SOD1 is relocated to the nucleus within 20 minutes of intrinsic or extrinsic oxidative stress

induction and acts as a transcription factor in the nucleus by binding to the promoter regions of various genes that associated with oxidative stress (Tsang *et al.*, 2014). Our preliminary results show that various alternative splicing changes and 3'UTR (untranslated region) length alterations occur in *dSod1* mutants. In the near future, we will re-analyze the transcriptome changes in order to be able to detect read mapping differences within the same gene, which will identify potential splicing and UTR lengthening defects. Next, we will compare our transcriptome analysis with previously published SOD1 transcriptome analyses from rodent models with *Sod1* mutations, patient post mortem tissue (Heath *et al.*, 2013), and patient derived iPSCs (Kiskinis *et al.*, 2014), as well as deletion and overexpression of dTDP-43 in *Drosophila* ALS model (Vanden Broeck *et al.*, 2013) and glial and motor neuron specific hSOD1^{G85R} overexpression in *Drosophila* (Kumimoto, Fore, & Zhang, 2013). More importantly, we will perform a complementary RNA sequencing analysis on the Sup(G85R), suppressor of dSod1^{G85R/G85R} that is described in detail in Chapter 4 to pinpoint the indicative cause of lethality.

REFERENCES

- BANDYOPADHYAY, U., COTNEY, J., NAGY, M., OH, S., LENG, J., MAHAJAN, M., MANE, S., FENTON, W.A., NOONAN, J.P. & HORWICH, A.L. (2013) RNA-Seq profiling of spinal cord motor neurons from a presymptomatic SOD1 ALS mouse. *PLoS one* **8**, e53575.
- VANDEN BROECK, L., NAVAL-SÁNCHEZ, M., ADACHI, Y., DIAPER, D., DOURLÉN, P., CHAPUIS, J., KLEINBERGER, G., GISTELINCK, M., VAN BROECKHOVEN, C., LAMBERT, J.-C., HIRTH, F., AERTS, S., CALLAERTS, P. & DERMAUT, B. (2013) TDP-43 loss-of-function causes neuronal loss due to defective steroid receptor-mediated gene program switching in *Drosophila*. *Cell reports* **3**, 160–172.
- BUNINA, T.L. (1962) On intracellular inclusions in familial amyotrophic lateral sclerosis. *Zhurnal nevropatologii i psikiatrii imeni S.S. Korsakova (Moscow, Russia : 1952)* **62**, 1293–1299.
- CAO, Y., CHTARBANOVA, S., PETERSEN, A.J. & GANETZKY, B. (2013) Dnr1 mutations cause neurodegeneration in *Drosophila* by activating the innate immune response in the brain. *Proceedings of the National Academy of Sciences of the United States of America* **110**, E1752–E1760.

- CHAKKALAKAL, J. V & JASMIN, B.J. (2003) Localizing synaptic mRNAs at the neuromuscular junction: it takes more than transcription. *BioEssays : news and reviews in molecular, cellular and developmental biology* **25**, 25–31.
- DA CRUZ, S. & CLEVELAND, D.W. (2011) Understanding the role of TDP-43 and FUS/TLS in ALS and beyond. *Current opinion in neurobiology* **21**, 904–919.
- DADON-NACHUM, M., MELAMED, E. & OFFEN, D. (2011) The ‘dying-back’ phenomenon of motor neurons in ALS. *Journal of molecular neuroscience : MN* **43**, 470–477.
- DEJESUS-HERNANDEZ, M., MACKENZIE, I.R., BOEVE, B.F., BOXER, A.L., BAKER, M., RUTHERFORD, N.J., ET AL. (2011) Expanded GGGGCC hexanucleotide repeat in noncoding region of C9ORF72 causes chromosome 9p-linked FTD and ALS. *Neuron* **72**, 245–256.
- DONNELLY, C.J., ZHANG, P.-W., PHAM, J.T., HAEUSLER, A.R., HEUSLER, A.R., MISTRY, N.A., ET AL. (2013) RNA toxicity from the ALS/FTD C9ORF72 expansion is mitigated by antisense intervention. *Neuron* **80**, 415–428. Elsevier.
- DROPPELMANN, C.A., CAMPOS-MELO, D., ISHTIAQ, M., VOLKENING, K. & STRONG, M.J. (2014) RNA metabolism in ALS: When normal processes become pathological. *Amyotrophic lateral sclerosis & frontotemporal degeneration*, 1–16.
- DUPUIS, L., OUDART, H., RENÉ, F., GONZALEZ DE AGUILAR, J.-L. & LOEFFLER, J.-P. (2004) Evidence for defective energy homeostasis in amyotrophic lateral sclerosis: benefit of a high-energy diet in a transgenic mouse model. *Proceedings of the National Academy of Sciences of the United States of America* **101**, 11159–11164.
- DUPUIS, L., PRADAT, P.-F., LUDOLPH, A.C. & LOEFFLER, J.-P. (2011) Energy metabolism in amyotrophic lateral sclerosis. *Lancet neurology* **10**, 75–82.
- EDEN, E., NAVON, R., STEINFELD, I., LIPSON, D. & YAKHINI, Z. (2009) GOrilla: a tool for discovery and visualization of enriched GO terms in ranked gene lists. *BMC bioinformatics* **10**, 48.
- EREN, A.M., VINEIS, J.H., MORRISON, H.G. & SOGIN, M.L. (2013) A filtering method to generate high quality short reads using illumina paired-end technology. *PloS one* **8**, e66643.
- FEIGUIN, F., GODENA, V.K., ROMANO, G., D’AMBROGIO, A., KLIMA, R. & BARALLE, F.E. (2009) Depletion of TDP-43 affects *Drosophila* motoneurons terminal synapsis and locomotive behavior. *FEBS letters* **583**, 1586–1592.
- GIJSELINCK, I., VAN LANGENHOVE, T., VAN DER ZEE, J., SLEEGERS, K., PHILTJENS, S., KLEINBERGER, G., ET AL. (2012) A C9orf72 promoter repeat expansion in a Flanders-Belgian cohort with disorders of the frontotemporal lobar degeneration-amyotrophic lateral sclerosis spectrum: a gene identification study. *The Lancet. Neurology* **11**, 54–65.
- DI GIORGIO, F.P., CARRASCO, M.A., SIAO, M.C., MANIATIS, T. & EGGAN, K. (2007) Non-cell autonomous effect of glia on motor neurons in an embryonic stem cell-based ALS model. *Nature neuroscience* **10**, 608–614. Nature Publishing Group.
- GLASSCOCK, E. & TANOUYE, M.A. (2005) *Drosophila* couch potato mutants exhibit complex neurological abnormalities including epilepsy phenotypes. *Genetics* **169**, 2137–2149.

- GRUZMAN, A., WOOD, W.L., ALPERT, E., PRASAD, M.D., MILLER, R.G., ROTHSTEIN, J.D., BOWSER, R., HAMILTON, R., WOOD, T.D., CLEVELAND, D.W., LINGAPPA, V.R. & LIU, J. (2007) Common molecular signature in SOD1 for both sporadic and familial amyotrophic lateral sclerosis. *Proceedings of the National Academy of Sciences of the United States of America* **104**, 12524–12529.
- HEATH, P.R., KIRBY, J. & SHAW, P.J. (2013) Investigating cell death mechanisms in amyotrophic lateral sclerosis using transcriptomics. *Frontiers in cellular neuroscience* **7**, 259.
- ILIEVA, H., POLYMERIDOU, M. & CLEVELAND, D.W. (2009) Non-cell autonomous toxicity in neurodegenerative disorders: ALS and beyond. *The Journal of cell biology* **187**, 761–772.
- KISKINIS, E., SANDOE, J., WILLIAMS, L.A., BOULTING, G.L., MOCCIA, R., WAINGER, B.J., ET AL. (2014) Pathways disrupted in human ALS motor neurons identified through genetic correction of mutant SOD1. *Cell stem cell* **14**, 781–795.
- KUMIMOTO, E.L., FORE, T.R. & ZHANG, B. (2013) Transcriptome Profiling Following Neuronal and Glial Expression of ALS-Linked SOD1 in Drosophila. *G3 (Bethesda, Md.)*.
- LEE, H.-K.P., CORDING, A., VIELMETTER, J. & ZINN, K. (2013) Interactions between a receptor tyrosine phosphatase and a cell surface ligand regulate axon guidance and glial-neuronal communication. *Neuron* **78**, 813–826.
- LENZKEN, S.C., ACHSEL, T., CARRI, M.T. & BARABINO, S.M.L. Neuronal RNA-binding proteins in health and disease. *Wiley interdisciplinary reviews. RNA* **5**, 565–576.
- LEVY, F., RABEL, D., CHARLET, M., BULET, P., HOFFMANN, J.A. & EHRET-SABATIER, L. (2004) Peptidomic and proteomic analyses of the systemic immune response of Drosophila. *Biochimie* **86**, 607–616.
- LI, Y., RAY, P., RAO, E.J., SHI, C., GUO, W., CHEN, X., WOODRUFF, E.A., FUSHIMI, K. & WU, J.Y. (2010) A Drosophila model for TDP-43 proteinopathy. *Proceedings of the National Academy of Sciences* **107**, 3169–3174.
- LIM, M. A., BENICE, K.K., SANDESARA, I., ANDREUX, P., AUWERX, J., ISHIBASHI, J., SEALE, P. & KALB, R.G. (2014) Genetically altering organismal metabolism by leptin-deficiency benefits a mouse model of Amyotrophic Lateral Sclerosis. *Human molecular genetics*, 1–14.
- LIN, M.-J., CHENG, C.-W. & SHEN, C.-K.J. (2011) Neuronal function and dysfunction of Drosophila dTDP. *PloS one* **6**, e20371.
- LUAN, H., LEMON, W.C., PEABODY, N.C., POHL, J.B., ZELENSKY, P.K., WANG, D., NITABACH, M.N., HOLMES, T.C. & WHITE, B.H. (2006) Functional dissection of a neuronal network required for cuticle tanning and wing expansion in Drosophila. *The Journal of neuroscience : the official journal of the Society for Neuroscience* **26**, 573–584.
- MINOCHE, A.E., DOHM, J.C. & HIMMELBAUER, H. (2011) Evaluation of genomic high-throughput sequencing data generated on Illumina HiSeq and genome analyzer systems. *Genome biology* **12**, R112.
- OBATA, F., KURANAGA, E., TOMIOKA, K., MING, M., TAKEISHI, A., CHEN, C.-H., SOGA, T. & MIURA, M. (2014) Necrosis-Driven Systemic Immune Response Alters SAM Metabolism through the FOXO-GNMT Axis. *Cell Reports* **7**, 821–833.

- OKAMOTO, K., MIZUNO, Y. & FUJITA, Y. (2008) Bunina bodies in amyotrophic lateral sclerosis. *Neuropathology: official journal of the Japanese Society of Neuropathology* **28**, 109–115.
- ONODERA, O., ISHIHARA, T., SHIGA, A., ARIIZUMI, Y., YOKOSEKI, A. & NISHIZAWA, M. (2014) Minor splicing pathway is not minor any more: implications for the pathogenesis of motor neuron diseases. *Neuropathology: official journal of the Japanese Society of Neuropathology* **34**, 99–107.
- OROZCO, D. & EDBAUER, D. (2013) FUS-mediated alternative splicing in the nervous system: consequences for ALS and FTL. *Journal of molecular medicine (Berlin, Germany)* **91**, 1343–1354.
- PALAMIUC, L., SCHLAGOWSKI, A., NGO, S.T., VERNAY, A., DIRRIG-GROSCH, S., HENRIQUES, A., BOUTILLIER, A.-L., ZOLL, J., ECHANIZ-LAGUNA, A., LOEFFLER, J.-P. & RENÉ, F. (2015) A metabolic switch toward lipid use in glycolytic muscle is an early pathologic event in a mouse model of amyotrophic lateral sclerosis. *EMBO molecular medicine*.
- PETERS, O.M., GHASEMI, M. & BROWN, R.H. (2015) Emerging mechanisms of molecular pathology in ALS. *The Journal of clinical investigation* **125**, 1767–1779.
- PHILIPS, T. & ROBBERECHT, W. (2011) Neuroinflammation in amyotrophic lateral sclerosis: role of glial activation in motor neuron disease. *The Lancet. Neurology* **10**, 253–263.
- POKRISHEVSKY, E., GRAD, L.I., YOUSEFI, M., WANG, J., MACKENZIE, I.R. & CASHMAN, N.R. (2012) Aberrant localization of FUS and TDP43 is associated with misfolding of SOD1 in amyotrophic lateral sclerosis. *PloS one* **7**, e35050.
- RENTON, A.E., MAJOUNIE, E., WAITE, A., SIMÓN-SÁNCHEZ, J., ROLLINSON, S., GIBBS, J.R., ET AL. (2011) A hexanucleotide repeat expansion in C9ORF72 is the cause of chromosome 9p21-linked ALS-FTD. *Neuron* **72**, 257–268.
- ROSEN, D.R., SIDDIQUE, T., PATTERSON, D., FIGLEWICZ, D.A., SAPP, P., HENTATI, A., DONALDSON, D., GOTO, J., O'REGAN, J.P. & DENG, H.X. (1993) Mutations in Cu/Zn superoxide dismutase gene are associated with familial amyotrophic lateral sclerosis. *Nature* **362**, 59–62.
- SERIO, A., BILICAN, B., BARMADA, S.J., ANDO, D.M., ZHAO, C., SILLER, R., BURR, K., HAGHI, G., STORY, D., NISHIMURA, A.L., CARRASCO, M.A., PHATNANI, H.P., SHUM, C., WILMUT, I., MANIATIS, T., SHAW, C.E., FINKBEINER, S. & CHANDRAN, S. (2013) Astrocyte pathology and the absence of non-cell autonomy in an induced pluripotent stem cell model of TDP-43 proteinopathy. *Proceedings of the National Academy of Sciences of the United States of America* **110**, 4697–4702.
- STELLER, H. (2008) Regulation of apoptosis in Drosophila. *Cell death and differentiation* **15**, 1132–1138.
- TSANG, C.K., LIU, Y., THOMAS, J., ZHANG, Y. & ZHENG, X.F.S. (2014) Superoxide dismutase 1 acts as a nuclear transcription factor to regulate oxidative stress resistance. *Nature communications* **5**, 3446. Nature Publishing Group.
- WANG, J.-W., BRENT, J.R., TOMLINSON, A., SHNEIDER, N.A. & MCCABE, B.D. (2011) The ALS-associated proteins FUS and TDP-43 function together to affect Drosophila locomotion and life span. *The Journal of clinical investigation* **121**, 4118–4126. American Society for Clinical Investigation.
- WENTZELL, J.S., BOLKAN, B.J., CARMINE-SIMMEN, K., SWANSON, T.L., MUSASHE, D.T. & KRETZSCHMAR, D. (2012) Amyloid precursor proteins are protective in Drosophila models of progressive neurodegeneration. *Neurobiology of disease* **46**, 78–87.

FIGURES

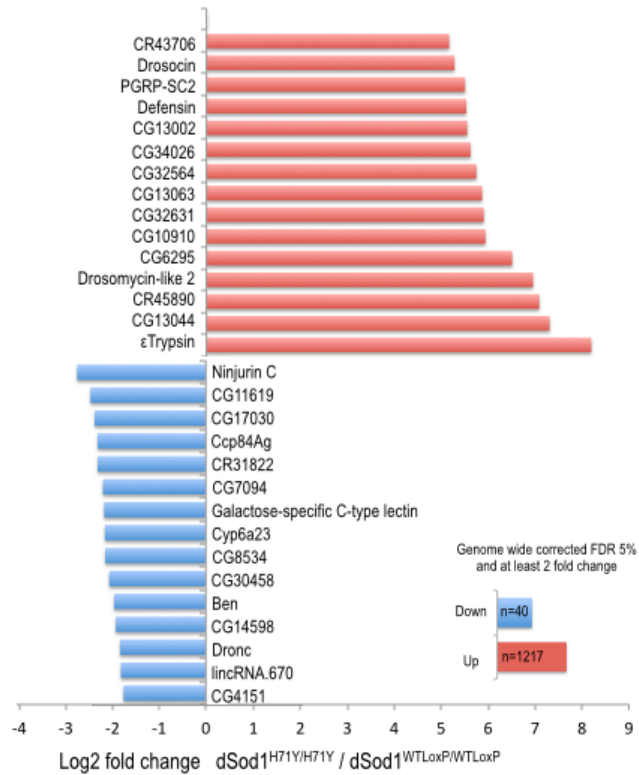


Figure.3.1. Transcriptinal analysis of $dSod1^{H71Y/H71Y}$ compared to $dSod1^{WTLoxP/WTLoxP}$. Top 15 up-regulated and down-regulated genes in $dSod1^{H71Y/H71Y}$ based on average read map per gene. The expression changes represented in log2 scale and a total of 40 genes are up-regulated and 1217 genes are down regulated with a minimum of 2 fold change and 5% FDR in $dSod1^{H71Y/H71Y}$ head and thorax tissue.

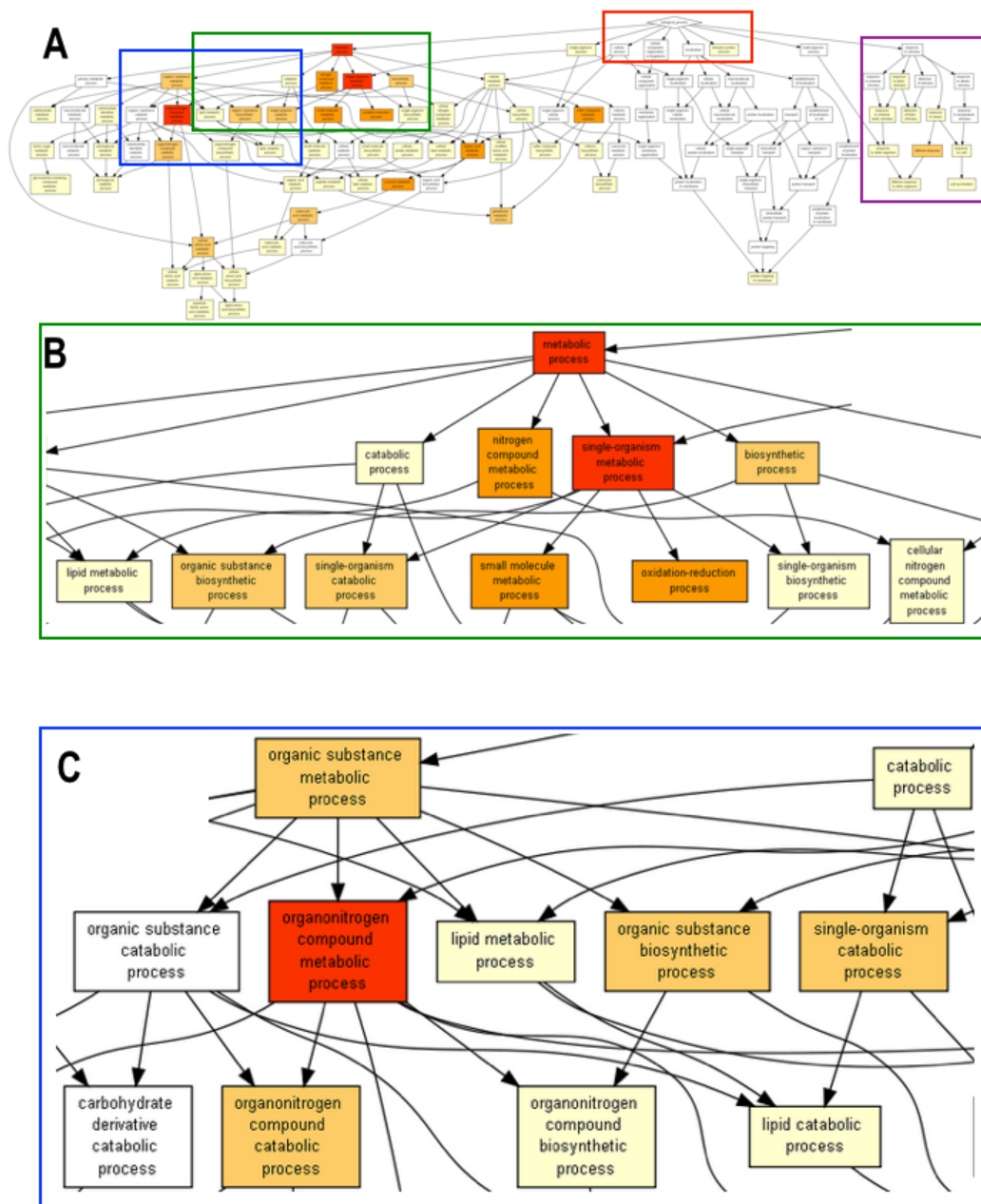


Figure continues in the next page.

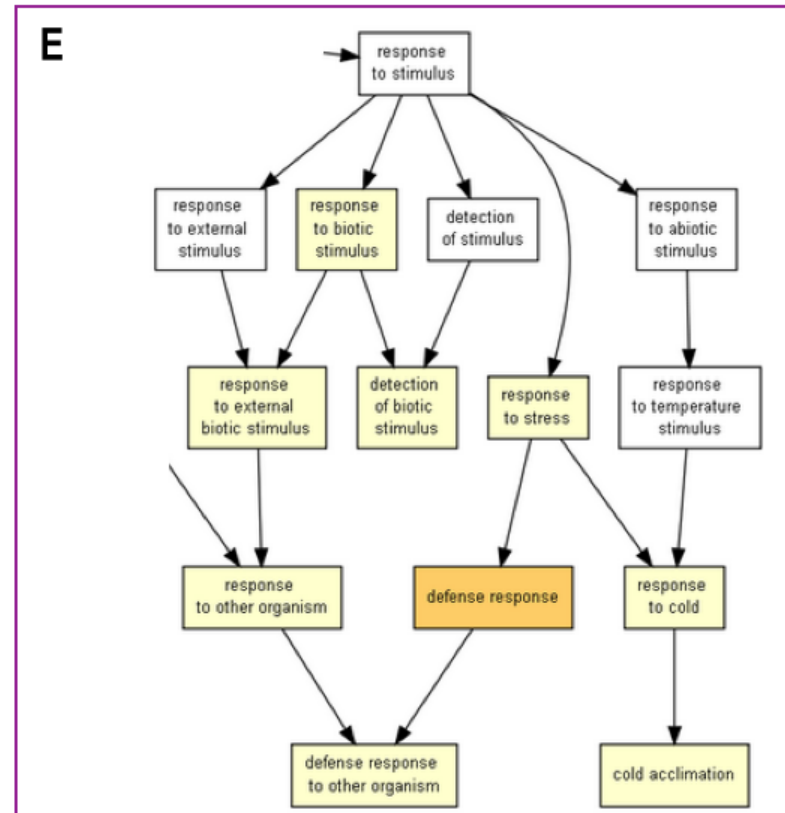
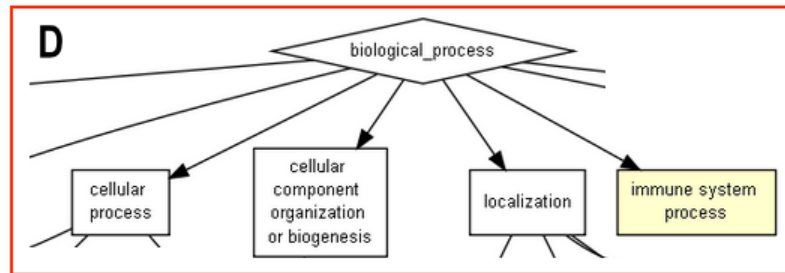


Figure.3.2. Altered pathways in $dSod1^{H71Y/H71Y}$. A summary scheme of gene ontology (GO) terms assigned by the GORILLA software. Metabolic processes (lipid, glucose and amino acid metabolism) and the defense response pathways (innate immunity and inflammation) were significantly altered in $dSod1^{H71Y/H71Y}$ when compared to the control allele, $dSod1^{WTLoxP/WTLoxP}$. The full pathway list can be visualized in Table 3.1 and a comprehensive analysis of the results can be visualized at <http://cbl-gorilla.cs.technion.ac.il/GOrilla/nnvf3v6p/GOResults.html>. A) Full pathway tree B), C), D) and E) highlighted portions from section A.

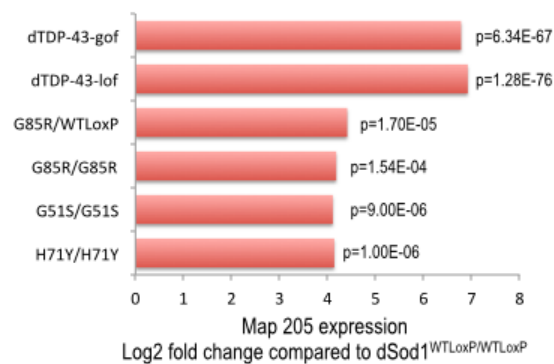


Figure.3.3. Map205 expression changes in *dSod1* mutants and *dTDP-43* mutants. Microtubule-associated protein 205 (Map205) was one of the most dramatic changes observed in not only in homozygotes *dSod1*^{H71Y/H71Y}, *dSod1*^{G51S/G51S}, and *dSod1*^{G85R/G85R}, but also in *dSod1*^{WTLoxP/G85R} heterozygote gene expression analysis. Importantly, Map205 expression changes were most effected upon dTDP-43 ubiquitous over-expression and know-down experiments. dTDP-43 transcriptinal results regarding Map205 are exported from Vanden Broeck *et al.*, 2013. The expression changes are represented in log2 scale.

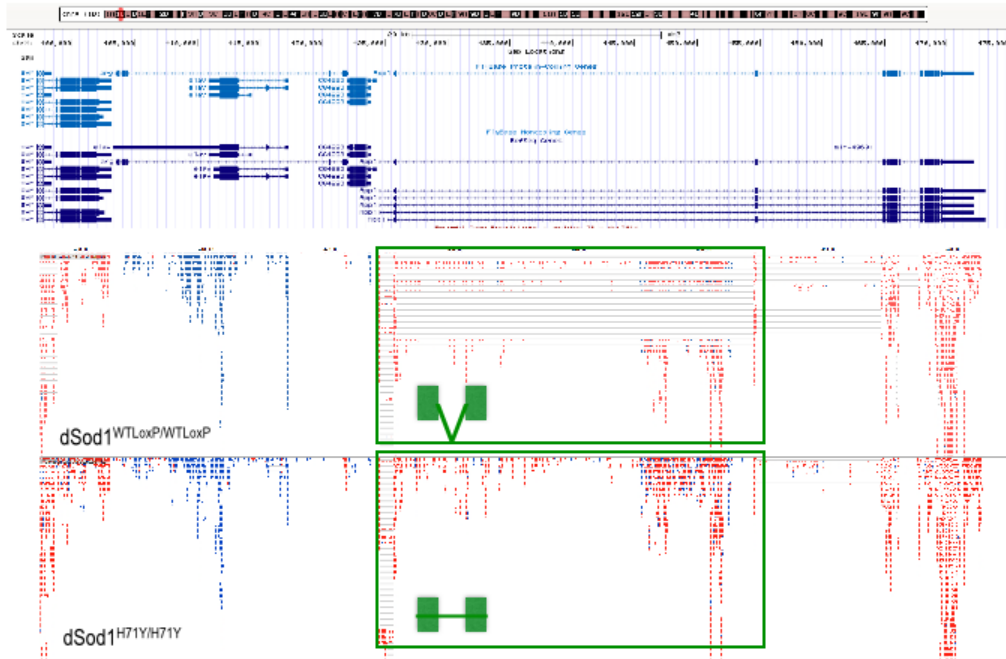


Figure.3.4. Intron skipping in the *Appl* transcript. Aligned read maps for Amyloid Precursor Protein-like (*Appl*) transcript. A long exon is that is normally alternatively spliced skipped specifically in *dSod1*^{H71Y/H71Y}. Changes are highlighted in green squares.

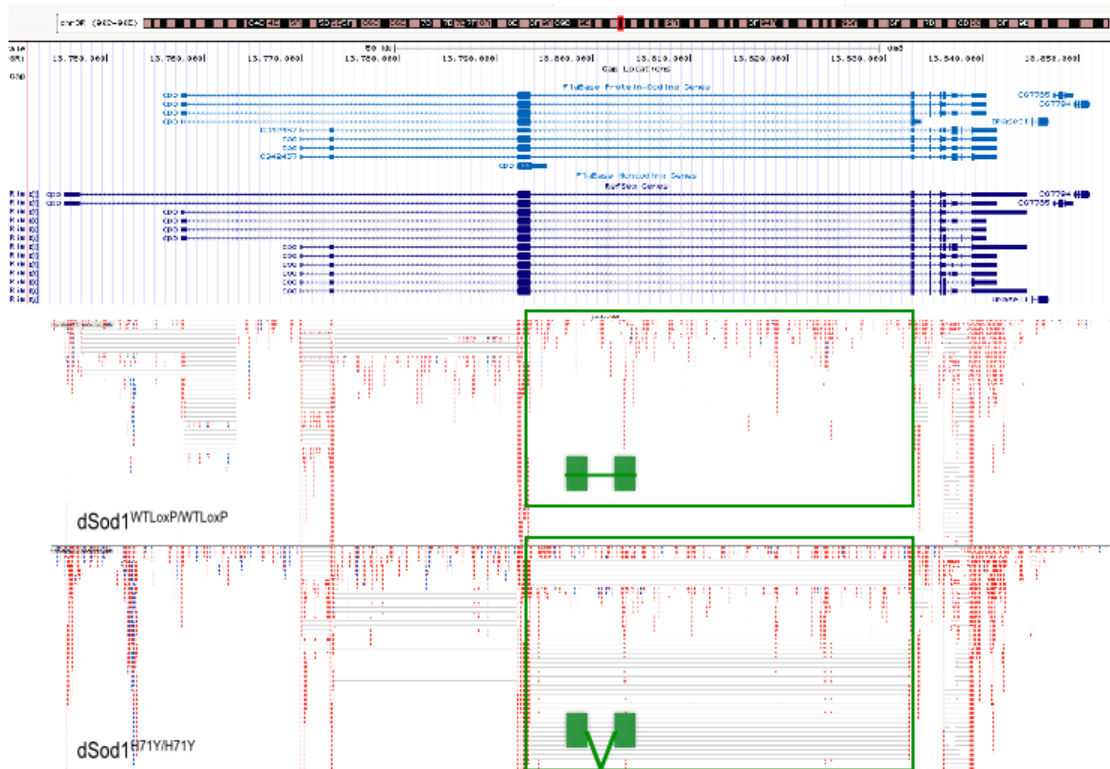


Figure 3.5. Up-regulated Splicing in the *Cpo* transcript. Aligned read maps for couch potato (*Cpo*) transcript. A usually skipped long intron is specifically spliced in *dSod1^{H71Y/H71Y}*. Changes are highlighted in green squares.



Figure 3.6. 3'UTR extension defects in Ptp10D transcript. Aligned read maps for receptor tyrosine phosphatase Ptp10D transcript. The 3' UTR of Ptp10D transcript is dramatically longer in *dSod1*^{H71Y/H71Y}. Changes are highlighted in green squares.

TABLES

Table 3.1. Gene Ontology (GO) analysis of transcription changes in *dSod1*^{H71Y/H71Y} adults, related to Figure 3.2.

GO Accession	GO Term	5% FDR p-value
GO:1901564	organonitrogen compound metabolic process	1.27E-08
GO:0008152	metabolic process	1.83E-08
GO:0044710	single-organism metabolic process	1.03E-07
GO:0044281	small molecule metabolic process	8.83E-06
GO:0006807	nitrogen compound metabolic process	1.02E-05
GO:0055114	oxidation-reduction process	1.22E-05
GO:0006790	sulfur compound metabolic process	1.28E-05
GO:0043436	oxoacid metabolic process	5.90E-05
GO:0006082	organic acid metabolic process	5.25E-05
GO:0044712	single-organism catabolic process	1.06E-04
GO:0019752	carboxylic acid metabolic process	1.51E-04
GO:0006952	defense response	1.58E-04
GO:0071704	organic substance metabolic process	1.05E-03
GO:0009058	biosynthetic process	1.30E-03
GO:0006749	glutathione metabolic process	1.33E-03
GO:1901576	organic substance biosynthetic process	2.90E-03
GO:0006520	cellular amino acid metabolic process	2.81E-03
GO:1901565	organonitrogen compound catabolic process	2.90E-03
GO:0006575	cellular modified amino acid metabolic process	3.77E-03
GO:0044282	small molecule catabolic process	3.58E-03
GO:1901605	alpha-amino acid metabolic process	4.70E-03
GO:0016054	organic acid catabolic process	6.62E-03
GO:0046395	carboxylic acid catabolic process	6.33E-03
GO:0002376	immune system process	7.35E-03
GO:1901607	alpha-amino acid biosynthetic process	9.82E-03
GO:0098542	defense response to other organism	1.02E-02
GO:0006629	lipid metabolic process	1.05E-02
GO:0043207	response to external biotic stimulus	1.07E-02
GO:0005975	carbohydrate metabolic process	1.21E-02
GO:0051188	cofactor biosynthetic process	1.22E-02
GO:0009607	response to biotic stimulus	1.22E-02
GO:0043603	cellular amide metabolic process	1.44E-02
GO:0044237	cellular metabolic process	1.54E-02
GO:0016042	lipid catabolic process	1.80E-02
GO:0051707	response to other organism	2.00E-02

<u>GO:1901566</u>	organonitrogen compound biosynthetic process	1.96E-02
<u>GO:0044249</u>	cellular biosynthetic process	2.20E-02
<u>GO:0008652</u>	cellular amino acid biosynthetic process	2.19E-02
<u>GO:1901135</u>	carbohydrate derivative metabolic process	2.27E-02
<u>GO:0044699</u>	single-organism process	2.34E-02
<u>GO:0044711</u>	single-organism biosynthetic process	2.46E-02
<u>GO:0034641</u>	cellular nitrogen compound metabolic process	2.57E-02
<u>GO:0009066</u>	aspartate family amino acid metabolic process	2.76E-02
<u>GO:0006022</u>	aminoglycan metabolic process	2.88E-02
<u>GO:0009108</u>	coenzyme biosynthetic process	3.79E-02
<u>GO:0009631</u>	cold acclimation	3.71E-02
<u>GO:0044272</u>	sulfur compound biosynthetic process	3.64E-02
<u>GO:0006950</u>	response to stress	4.59E-02
<u>GO:0044283</u>	small molecule biosynthetic process	5.53E-02
<u>GO:0009063</u>	cellular amino acid catabolic process	5.70E-02
<u>GO:0006040</u>	amino sugar metabolic process	5.79E-02
<u>GO:0044255</u>	cellular lipid metabolic process	6.48E-02
<u>GO:0009056</u>	catabolic process	6.47E-02
<u>GO:0006612</u>	protein targeting to membrane	8.19E-02
<u>GO:0009595</u>	detection of biotic stimulus	8.09E-02
<u>GO:0009409</u>	response to cold	8.57E-02
<u>GO:0006518</u>	peptide metabolic process	9.28E-02
<u>GO:1901071</u>	glucosamine-containing compound metabolic process	9.19E-02
<u>GO:0006026</u>	aminoglycan catabolic process	9.48E-02
<u>GO:0044242</u>	cellular lipid catabolic process	9.44E-02

CHAPTER 4

Chemical Mutagenesis Screen for Mutations Suppressing *dSod1*^{G85R} Lethality: Identifying New Avenues to Therapy Through Forward Genetics

The forward genetic screen described in this chapter was designed by myself along with Dr. Robert Reenan and carried out with the help of nine very talented Brown University Summer HHMI undergraduate scholars who competed for positions on the “Disease Hunters” Team (Emily Jang, Kirsten Bredvik, Ryan Greene, Godwin Boaful, Dina Sabetta, Joshua Hackney, Karla Navarrete, Natalie Palaychuk, Jimmy Xia, Wendy Gaztanaga). The suppressor stocks were maintained and mapping crosses were carried out by Dr. Robert Reenan with my assistance. The sequencing analyses to map the suppressor alleles were done by Dr. Yiannis Savva and Ali Rezaei in assistance of Dr. Robert Reenan. The manuscript and the figures were crafted by myself and Dr. Robert Reenan. This research was funded by the ALS Association.

ABSTRACT

A G85R point mutation in the Superoxide Dismutase 1 gene (hSOD1) causes Amyotrophic Lateral Sclerosis (ALS) in humans and is inherited in a dominant fashion. A homologous recombined G85R mutation in *Drosophila melanogaster* results in death in the pupal case during eclosion in a homozygote state. Heterozygous *dSod1*^{G85R/+} animals are phenotypically normal. However, as noted in Chapter 2, small increases in dosage of *dSod1*^{G85R} mutant and *dSod1*^{WTLoxP} and the ratio of *dSod1*^{G85R} to *dSod1*^{WTLoxP} cause increased mortality. We strongly believe that the balance of mutant to wild type SOD1 at the protein level plays a critical role in onset of the disease and severity of phenotypes and that the homozygote lethality observed in *dSod1*^{G85R/G85R} homozygotes is the most extreme phenotypic example. Therefore, genetic suppressors that can potentially attenuate the homozygous lethal phenotype exhibited by *dSod1*^{G85R/G85R} in *Drosophila* may be genes whose human counterparts are potentially involved in the etiology of ALS, SOD1-mediated neurodegeneration, and thus may be potential targets for specific drug therapies. Here we describe an Ethyl methanesulfonate (EMS)-based genetic screen that uncovered 5 independent suppressor lines. Most importantly, all of these suppressor alleles exhibited more than 60 days of survival after eclosion, and exhibited no apparent locomotion defects while carrying the homozygous *dSod1*^{G85R/G85R} mutation.

INTRODUCTION

Amyotrophic lateral sclerosis (ALS) is a lethal disease of motor neuron degeneration that has been known for almost two centuries (Charcot & Joffrey, 1869).

Every year 5000 people are diagnosed with this incurable disease world-wide (Pasinelli & Brown, 2006). Currently, there is one FDA approved palliative drug, the glutamate release inhibitor Riluzole, available for ALS patients. Unfortunately, a possible 2-3 months increase in life expectancy does not outweigh the side effects of the drug for ALS patients (Miller, Mitchell, & Moore, 2012). In recent years, mutations in more than 50 genes have been identified in ALS patients and this has significantly advanced the field (Abel *et al.*, 2012). However, there is an open question relevant to designing an effective treatment for ALS: Are there common cellular mechanisms underlying the motor neuron death that links all ALS-associated genes?

Approximately, 20% of familial ALS (fALS) and 3% of sporadic (sALS) cases result from mutations in the superoxide dismutase 1 (SOD1) gene (Saccon *et al.*, 2013). The G85R point mutation in SOD1 was one of the first mutations identified in ALS patients in 1993 (Rosen *et al.*, 1993). ALS patients heterozygous for the G85R mutation are diagnosed with the disease at a mean age of onset of 55.5 \pm 12.6 and patients normally live a little over six years after diagnosis (Juneja *et al.*, 1997). Since the G85R mutation was identified, more than 100 mutations scattered along the SOD1 gene have been identified in ALS patients (Saccon *et al.*, 2013). Mutant SOD1 is thought to produce a gain of toxic function and generates high molecular-weight cytoplasmic protein aggregates, as observed in pathogenic tissues from ALS patients. SOD1-induced transgenic model organisms including mice, *Drosophila* and *Caenorhabditis elegans*, and cell culture model systems also recapitulate this pathological hallmark (Peters, Ghasemi, & Brown, 2015). More importantly, cytoplasmic SOD1 inclusions have been reported in some sporadic ALS (sALS) post-mortem spinal cord tissues where the presence of a

specific SOD1 mutation is not present (Gruzman *et al.*, 2007; Forsberg *et al.*, 2010; Bosco *et al.*, 2010), indicating that uncovering how mutations in SOD1 ultimately lead to the dysfunction and death of motor neurons may shed light on how ALS pathogenesis develops and progresses in patients with either the sporadic or familial disease.

Over the last decade, genome-wide genetic screens in yeast have led to the identification of important genetic modifiers of TDP-43 and FUS-mediated ALS toxicity (Elden *et al.*, 2010; Ju *et al.*, 2011; Sun *et al.*, 2011; Couthouis *et al.*, 2011). In addition to yeast screens, for decades, genetic screens carried out in *Drosophila* have proven extremely powerful in identifying new genes and/or modifiers (enhancers and suppressors) of genes, especially when it comes to the nervous system (Arrizabalaga & Lehmann, 1999; St Johnston, 2002; Somalinga *et al.*, 2012; Deivasigamani *et al.*, 2014). The sequencing of the *Drosophila* genome using next generation sequencing technologies has revealed the extent of similarity between the *Drosophila* and human nervous system regarding gene context (Adams *et al.*, 2000). *Drosophila* has a very compact genome with ~15,000 genes (Adams *et al.*, 2000) including a vast number of genes (197 of 287) in which mutations are known to cause human disease (St Johnston, 2002). As such, *Drosophila* is an ideal model system for the operation of forward genetic screens to divulge specific genetic mutations that can act as suppressors and modify disease phenotypes.

The most common directed mutagenesis method used in *Drosophila*, EMS, provides a rapid methodology for the introduction of largely unbiased mutations into the entire genome. Though EMS is capable of causing different types of mutations, it is mainly an alkylating agent that induces missense mutations through G-to-A transitions

(Bökel, 2008). Introduction of missense mutations, in contrast to commonly used transposon insertion screens for example, allows for a much greater spectrum of mutations including novel dominant gain of function mutations, contrary to the next generation screening kits in *Drosophila* that mostly introduce loss of function mutations (Wolf & Rockman, 2011).

The SOD1 gene is highly conserved between *Drosophila* and humans. Previously, our group introduced the G85R point mutation into the endogenous locus of *dSod1* via homologous recombination. Among other ALS-like phenotypes such as locomotion defects and muscle denervation, the *dSod1*^{G85R/G85R} homozygotes display a distinct phenotype: flies die in the pupal case during the eclosion period (Chapter 2). After using the power of *Drosophila* genetics to model ALS, we subsequently made use of the unbiased power of *Drosophila* forward genetic screens to identify potential gene products that, when appropriately modified, eliminate the deleterious effect of the *dSod1*^{G85R} allele, namely unconditional late (near adult eclosion) lethality. Genetic suppressors that reverse the homozygous lethal phenotype of *dSod1*^{G85R/G85R} in *Drosophila* may be genes whose human counterparts could potentially be involved in the etiology of ALS and could be potential targets for drugs.

MATERIALS AND METHODS

***Drosophila* strains, EMS mutagenesis and survival screen**

Two independently derived homologous recombinant lines of *dSod1*^{G85R}/*Tm3*, *hs-hid, sb* (Balancer chromosome, Bloomington *Drosophila* Stock Center number: 1558) derived from independent targeting transgene stocks were used: *dSod1*^{G85R}/*Tm3*, *hs-*

hid, sb, line A and line B. Newly eclosed *dSod1^{G85R}/Tm3,hs-hid, sb* (line A) males were aged for 1-7 days and were then mutagenized. The stock of *dSod1^{G85R}/Tm3,hs-hid, sb* (line B) was used for the crosses with the possible suppressor mutation bearing *dSod1^{G85R}/Tm3,hs-hid, sb* (line A) mutagenized males to minimize the possibility of homozygous background mutations. Flies were kept at constant 25°C, on standard molasses food, and under 12-h day/night cycles. 6028 *dSod1^{G85R}/Tm3,hs-hid* (line A) males were starved overnight (12hr) in vials supplied with only water. Surviving males were fed with 25mM EMS (Sigma M-0880) in 5% sucrose solution for 10 hours. The water and sucrose solution containing EMS was administered with Kimwipe wrapped-ceaprene stoppers as described by Christian Bökel (Bökel, 2008). Surviving males were allowed to recover on regular food for 14 hours to allow for the clearance of any excess EMS from the digestive system. Then, the surviving 4800 males were mated with 6400 virgin females *dSod1^{G85R}/Tm3,hs-hid* (line B). The crosses were set up in bottles (Genesee 32-130) with each bottle containing 15 males and 20 virgin females. (Figure 4.1) The parents in the bottle stock were passed after 5 days. The progeny in the bottles were heat shocked on days 5 and 6 for 2 hours at 37°C in order to induce *hs-hid* expression, thus killing any animals containing the Tm3 chromosome. Development was allowed to continue for the remaining cohort of flies, which should be exclusively *dSod1^{G85R/G85R}* homozygotes and were subsequently screened regularly for survivors over the next two weeks. The surviving progeny were named as EMS1 through EMS145. Flies that survived more than 3 days were crossed with 3 flies (*dSod1^{G85R}/Tm3-hsHid*) of the opposite sex. The *dSod1* locus of all the surviving lines were PCR amplified and sequenced with forward primer: 5'-GCATGTATTTCTAAGCTGCTCTGCTACGGTCA

C-3' and, reverse primer: 5' - GTCCACTGCTAAGAGCAGCTGCCCTC-3'.

RESULTS

A Forward Genetic Screen Identifies Five Dominant Suppressor Mutations of *dSod1*^{G85R/G85R} Lethality in *Drosophila*

Drosophila homozygous for *dSod1*^{G85R/G85R} die in the pupal case during eclosion with almost 100% penetrance (Discussed in detail in Chapter 2). Less than 1% of *dSod1*^{G85R/G85R} flies reared under normal food conditions and temperature eclose, and those that eclose die within a few hours and display extreme locomotive uncoordination. In order to attenuate the lethality of the *dSod1*^{G85R} allele, we performed an extensive EMS mutagenesis followed by a comprehensive screen for survivors. The EMS feeding/crossing scheme is designed to allow the exclusive recovery of only *dSod1*^{G85R/G85R} homozygotes (Figure 4.1). More specifically, this is accomplished by using a balancer chromosome (*Tm3*) that is tagged transgenically with a heat shock-inducible “head involution defective” (*hid*) gene. *Hid* expression induces severe cellular apoptosis, therefore any progeny carrying *Tm3,hs-hid* balancer chromosome die during early developmental stages after heat shock. Only *dSod1*^{G85R/G85R} homozygotes that do not carry the balancer chromosome can survive the heat shock, but will die during late pupariation unless they carry a suppressor mutation. Particularly for this genetic screen, males heterozygous for the *dSod1*^{G85R} allele were mutagenized with 25mM EMS. Subsequently, the F1 generation *dSod1*^{G85R/G85R} flies were screened for locomoting adults that survived for at least 3 days (Figure 4.1). Out of ~300,000 screened *dSod1*^{G85R/G85R} flies, 145 adults eclosed from the pupal case and lived at least three days. These potential

suppressor-bearing flies were crossed back to the *dSod1^{G85R}/Tm3,hs-hid* line (line B) to first ensure that the suppression bred true, and simultaneously generated a stock of the suppressor mutation. As expected, not all suppressor mutations restored both viability and fertility. Only 7 of them were healthy enough to mate and establish a viable stock line (Table 4.1). To confirm that these fly lines possibly bearing a suppressor mutation for *dSod1^{G85R}* still genetically carried the G85R point mutation, the *dSod1* locus was sequence-verified via Sanger sequencing. One out of the seven lines was a false positive: In the EMS 140 line, a possible gene conversion event led to a normal *dSod1* locus with *dSod1^{WT}* in addition to *dSod1^{G85R}*. This was additionally confirmed by the fact that a polymorphism in the *dSod1^{G85R}* allele was also not present on the wild type chromosome (See Materials and Methods in Chapter 2). Since EMS mutagenesis can potentially induce random recombination events, we concluded that the gene conversion event occurred through DNA repair of the mutagenized *dSod1^{G85R}* allele using the wild type *dSod1* locus present on the *Tm3* chromosome in the mutagenized males at an early stage of gametogenesis. As this is an anticipated false positive, it was reassuring that it occurred in a minority of the recovered stocks. Moreover, even though the EMS 61 line was fertile, the flies were very uncoordinated in a way similar to *unc* mutants (Kernan, 1994), with a very short life span. As a result, this line was eventually no longer able to be kept as a viable stock and was lost due to robust fecundity of the heterozygous suppressed animals.

The rest of the suppressor lines EMS 35, EMS 81, EMS 94, EMS 102, EMS 130 appear healthy, eclose in expected ratios, are fertile, and live at least 60 days without any obvious locomotor defect. All of these suppressor mutations act in a dominant fashion as

50% of homozygous $dSodI^{G85R/G85R}$ animals (not carrying the suppressor) die in the pupal case. The stocks carrying these unmapped suppressor mutations were backcrossed at least ten generations, as follows: Suppressed females heterozygous for the suppressor and homozygous for $dSodI^{G85R/G85R}$ were crossed to males heterozygous for $dSodI^{G85R}/Tm3,hs-hid$. This procedure was repeated in successive generations to allow recombination (which only occurs in females) to remove secondary irrelevant potentially confounding mutations that were introduced during the mutagenesis process. In each generation of backcross, progeny were assessed for the presence of animals lacking the suppressor by visually checking to see that a significant fraction of progeny die in the pupal case with the characteristics of unsuppressed $dSodI^{G85R/G85R}$ homozygotes (Chapter 2, Figure 2.2.A).

Suppressor Lines EMS 81 and EMS 102 Map to the X chromosome

Observation of progeny ratios in backcrosses quickly revealed that two lines, EMS 81 and EMS 102, gave no surviving $dSodI^{G85R/G85R}$ suppressed males. A closer analysis revealed that $EMS\ 81/Y;;dSodI^{G85R}/dSodI^{G85R}$ males could be observed in the pupal case (presence of sex-combs) but that these animals generally died as pharate adults, or upon eclosion, becoming stuck while exiting the pupal case (as seen in Figure 2.2.A). Rarely, a suppressed EMS 81 male eclosed and could be recovered, but these animals ceased all locomotor activity within one hour. These males appeared to die in a similar fashion to $dSodI^{G85R/G85R}$ homozygotes. Thus, while heterozygous females ($EMS\ 81/+;;dSodI^{G85R}/dSodI^{G85R}$) were completely suppressed, males hemizygous for the suppressor ($EMS\ 81/Y;;dSodI^{G85R}/dSodI^{G85R}$) die at essentially the same point as

dSod1^{G85R}/*dSod1*^{G85R} homozygotes.

The same results were obtained for the EMS 102 suppressor mutation, except that many of the males hemizygous for EMS 102 appear to arrest earlier in metamorphosis, though a few progress to the pharate adult stage. Given that many generations of recombination had occurred during backcrossing of these mutations, the lethality and the suppressor phenotypes must be tightly linked.

Since the EMS 81/102 suppressors cause male lethality in the hemizygous state in the ALS (*dSod1*^{G85R/G85R}) background, we performed crosses to obtain EMS 81 and 102 in a wild type background. Suppressed females (EMS^{X/+}; *dSod1*^{G85R}/*dSod1*^{G85R}) were crossed to Fm7/Y males. EMS^X/Fm7 females were then crossed in single pair matings to Fm7/Y males to establish a stock segregating the lethal phenotype. These crosses were continued over several generations following EMS^X/Fm7 females to introgress the EMS^X alleles into the Fm7 chromosomal background. Both 81 and 102 alleles were found to confer the same phenotypes as described above in hemizygous males in the absence of *dSod1*^{G85R} mutations, namely, late male lethality. In the case of EMS 81, this lethality is at the same stage and appears almost indistinguishable from the final lethal phase of *dSod1*^{G85R/G85R} homozygotes. We were surprised by this outcome, but considered it highly informative, as whatever the genetic alterations are in EMS 81/102, they clearly act in a dominant fashion regarding suppression, but potentially in a recessive fashion regarding lethality.

Genetic and Molecular Mapping of Mutations EMS 81 and EMS 102 Reveal That They are Dominant Gain-of-Function Alleles of a Gene: Su(G85R)

The gene and mutations, which are identified by these studies, are currently being developed for a provisional patent application through Brown University. Therefore, the mapping and sequencing data for the EMS 81/102 suppressor mutations is a generalized description of the identification of the gene.

The EMS 81/102 mutations were first balanced over the Fm7 balancer, as described above, and then heterozygote females were crossed to males of a mapping chromosome stock carrying five recessive visible markers. Non-Fm7 heterozygous females of the F1 (where recombination occurs) were then crossed to wild type males, and phenotypes were scored in the F2. The lethal phenotype of the EMS 81/102 mutations was used to infer the location of these mutations by assessing the lack of particular classes of recombinants. In fact, it was clear that both the EMS 81/102 mutations mapped between two tightly linked (1 cM) visible markers (call them p and q). Thus, recombinants on this interval alone could be used to generate mapping data (Figure 4.2.A). Briefly, the lethal mutation on a wild type background in heterozygous state with a doubly mutant mapping chromosome (p + q, where p, +, and q are the gene order of the p locus, the wild type EMS^X locus, and the q locus respectively) will generate males in the F1 that are either parental non-recombinant (NR) or recombinant (R) chromosomes (Figure 4.2.B). In any case where the resultant chromosome retains the lethal (l) EMS^X allele, no male progeny will be recovered. Recombination can occur on two intervals that result in viable recombinant offspring (I and II, Figure 4.2.B). By measuring the ratios of recombinants on this interval (I/(I+II)), one obtains the distance (after multiplying this

fraction by 1cM) from the p locus. This allowed the mapping of the EMS^X mutations to within a 0.1cM of one another, strongly suggesting that these are mutations in the same gene.

While the genetic mapping was highly informative, the region of the X chromosome is densely populated with genes, and represents a region where the genetic map is contracted compared to other regions of the X chromosome. In fact, the 1cM region that the EMS^X mutations mapped to covers 2 Mb of physical distance on the X chromosome containing hundreds of genes. In order to increase mapping accuracy, we took advantage of an interesting and equally surprising observation. For the EMS 81 allele, it was noticed that when animals were reared in fresh food, complete lethality was always seen with 100% penetrance. However, if the parental animals (and some F1) were carried over in vials to a second generation, and the food was more than two weeks old, and “conditioned” by overcrowding, death, and waste material, EMS 81 hemizygote males could be obtained as viable adults. We will call these males, pseudo-rescued (EMS 81-PR) males.

EMS 81-PR males were found to be fertile and mobile for at least a week. This allowed us to cross these males to molecularly-defined deficiency bearing balanced stocks carrying a series of five deficiencies spanning the 2Mb regions implicated in genetic mapping studies (Cook *et al.*, 2012) (Figure 4.3.A). One of these deficiencies (BSCdf2) failed to complement EMS 81, giving rise to female progeny that died in exactly the same manner as hemizygous EMS 81 males, namely, as pharate adults during eclosion. All other deficiencies tested complemented the lethal phenotype of EMS 81. Thus, we were able to localize the EMS 81 mutation to a ~260kb deficiency, however,

this region still contained around 35 annotated transcription units.

To further refine the mapping, we utilized a series of molecularly defined duplication stocks carrying ~80kb duplications inserted into a common site on the third chromosome, and covering almost completely the entire X chromosome (Venken *et al.*, 2010) (Figure 4.3.B). Females balanced for EMS 81 or 102 (EMS^X/Fm7) were crossed to seven duplication-bearing lines. Duplications could be followed by the presence of eye color, as the EMS stocks were in a white-eyed background. Three duplications (DP2, DP3, DP4) rescued the lethality of EMS 81 and 102. The combination of rescue by these deletions allowed the delimitation of a much smaller genetic interval containing only two genes (here labeled A and B). A lethal mutation (molecularly uncharacterized) happened to have been attributed to the gene B, which we will call Su(G85R) from now on. This mutation (l(1)x) was obtained as a balanced stock and EMS 81-PR males were crossed to this stock, resulting in failure of complementation of the l(1)x mutation.

We then sequenced Su(G85R) for EMS 81, EMS 102 and the l(1)x mutations. In the case of the l(1)x stock, a 13nt deletion was found in the open reading frame of Su(G85R), predicted to truncate the protein at about 2/3 its normal length. Thus, l(1)x is almost certainly a null mutation for Su(G85R). Mutations were also found in the EMS 81 and 102 mutant stocks, G-to-A mutations, which is consistent with EMS as the mutagen. Both mutations cause missense change in different and highly conserved positions within the Su(G85R) protein, which is known to play a role in metabolism.

Mapping suppressor lines EMS 35, EMS 94 and EMS 130

The mutations EMS 35, 94 and 130 were backcrossed in the balanced *dSod1*^{G85R} background through females for >10 generations and it was observed that suppressed males were obtained in the expected ratios. In order to test initial linkage, suppressed *dSod1*^{G85R/G85R} homozygote males were crossed to the balanced G85R stock. In this case, only suppressed G85R homozygous females were obtained. Such females, when crossed to balanced G85R males gave rise to suppressed males and females in the expected ratios. Thus, these suppressor mutations, whose only phenotype appears to be suppression of G85R homozygosity (in contrast to EMS 81 and 102) also appear to map to the X chromosome. Since their only phenotype is suppression, construction of mapping stocks in the balanced G85R background will need to be performed and are underway.

Suppressor Lines Also Suppresses Eclosion Defect and Short Life Span of *dSod1*^{H71Y/H71Y}

EMS 81 and 102 were introgressed into a balanced *dSod1*^{H71Y} genetic background, using alleles of EMS 81 and 102 that had been recombined with the tightly linked *w*⁺ gene, allowing the suppressor alleles to be monitored via eye color. Homozygosity for *dSod1*^{H71Y/H71Y} normally confers a high level of unviability in the pupal stage, and animals only live for about 16 days, with a profound loss of motor function within the first week (Figure 2.3). Females homozygous for *dSod1*^{H71Y/H71Y} but also containing either EMS 81 or EMS 102 appeared in much greater numbers from the doubly balanced stock, and initial experiments showed that they live for at least one month with no apparent loss of locomotor function, compared to controls lacking the

suppressor alleles which behaved as previously described. Further experiments will be necessary to determine the lifespan of these suppressed animals and whether the suppressors continue to prevent locomotor decline during adult life. Nevertheless, these experiments strongly support the notion that EMS 81 and 102, despite being selected for suppression of G85R homozygous lethality, also suppress unviability and locomotor defects in a less severe ALS model.

DISCUSSION AND FUTURE DIRECTIONS

One of the best advantages of establishing ALS models in *Drosophila* was the ability to use the unbiased power of *Drosophila* forward genetics to obtain genetic suppressors of the “disease” phenotype. Using homologous recombination we previously revealed that SOD1 point mutations have serious behavioral and neurological consequences in *Drosophila* (Chapter 2). In this study, we took advantage of the most severe phenotype that we discovered, namely lethality at the terminal stages of eclosion for the *dSod1*^{G85R/G85R} homozygous flies. We have designed an EMS feeding and crossing scheme to allow the recovery of only *dSod1*^{G85R/G85R} homozygous adults (Figure 4.1). As a result, we have identified seven potential suppressor lines, one of which was a false positive and one of which was lost due to the lack of complete recovery from the uncoordinated locomotion defect exhibited by *dSod1*^{G85R/G85R} flies. The rest of the five suppressor lines EMS 35, EMS 81, EMS 94, EMS 102, EMS 130 all mapped to the X chromosome and appear healthy, eclose in expected ratios, are fertile, and live at least 60 days without any obvious locomotor defect. All of these suppressor mutations act in a dominant fashion as 50% of homozygous *dSod1*^{G85R/G85R} flies (not carrying the

suppressor) die in the pupal case.

The suppressor mutations EMS 35, EMS 94, EMS 130 have not been mapped yet. However, EMS 81 and EMS 102 are mapped to the gene Su(G85R). They both confer G-to-A amino acid changes as one expects from an EMS screen. Given the moderate size of the screen, it is likely that we have not covered the whole genome of *Drosophila*. In addition, the rest 138 candidate suppressors isolated as a result of the screen either did not live long enough to mate or could not establish a stock due to fertility defects. Nevertheless, isolation of two different mutations on a very short gene, Su(G85R), conveys the importance of this gene's expression in the ALS pathogenesis in *Drosophila*. In both suppressor cases, it is tempting to speculate that the Su(G85R) gene products act at late in development, and in a way that mimics the ALS-causing *dSod1*^{G85R} mutation itself in terms of viability. Thus, the nature of the suppressor mutations may reveal important mechanistic insight into the etiology of ALS. In fact, a future suppressor screen could be performed to identify suppressors of Su(G85R), which is highly conserved in humans.

The nature of the Su(G85R) will not be discussed in detail here in this section due to a provisional patent application through Brown University. It is surprising that the Su(G85R) protein is involved in the metabolic pathway, considering that motor neuron specific genes were the first candidates expected from an ALS-related suppressor screen. While this discovery was unexpected, perhaps it should not be since it is consistent with human studies indicating that ALS patients show a early and persistent hypermetabolic signature associated with energy wasting (Desport *et al.*, 2001; Bouteloup *et al.*, 2009). Moreover, we observe a strong transcriptomic signature indicating that metabolism is

altered in the ALS flies (Chapter 3). Furthermore, a hSOD1^{G93A} transgenic mouse model of ALS shows defective energy homeostasis that benefits from a high energy diet (Dupuis *et al.*, 2004) or lowered amounts of leptin, a regulator of whole-animal energy expenditure (Lim *et al.*, 2014). In addition, the hSOD1^{G85R} transgenic mouse model has also been shown to have several metabolic changes consistent with a metabolic switch occurring as an early pathological event (Palamiuc *et al.*, 2015). Thus, it is exciting and promising that a suppressor gene of dSod1^{G85R} lethality, which we will call Su(G85R) at this time, is a gene involved in metabolism and may play a role in energy balance in cells at a whole-animal level.

Su(G85R) also suppressed the eclosion defect and short life span of the relatively milder allele *dSod1*^{H71Y}. Further experiments will be performed to determine the extension of eclosion and life span rescue of these suppressed animals and to investigate whether the suppressors also rescues the locomotor decline during adult life. Similar experiments will be performed to determine extensions of the suppression abilities of Su(G85R) by testing it on previously published ALS models involving other ALS related genes such as TDP-43, FUS, C9orf72, Alsin, VAPB, TAF15, EWSR1 and hnRNPA2 (Casci & Pandey, 2015).

In the future, we will map the rest of the mutations. With the given extent of similarity of the *Drosophila* and human genomes, it is likely that some of the suppressor genes will be present in humans. We expect the rest of the suppressors to be proteins that alleviate dSod1 toxic function. Such suppressor proteins will likely overlap with the candidate protein results of previously published transcriptome analyses performed on post mortem ALS tissue and animal models (Heath, Kirby, & Shaw, 2013), and with the

ALS-related pathways that are discussed in detail in the introductory chapter of this thesis.

In addition, in Chapter 3 we started to investigate transcriptome changes that occur due to *dSod1* point mutations in *Drosophila*. We will extend our analysis by re-sequencing the suppressed lines to analyze transcriptional signatures and determine the essential players that operate in the suppression mechanism.

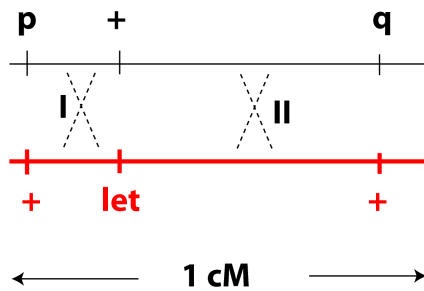
REFERENCES

- ABEL, O., POWELL, J.F., ANDERSEN, P.M. & AL-CHALABI, A. (2012) ALSod: A user-friendly online bioinformatics tool for amyotrophic lateral sclerosis genetics. *Human mutation* **33**, 1345–1351.
- ADAMS, M.D., CELNIKER, S.E., HOLT, R.A., EVANS, C.A., GOCCAYNE, J.D., AMANATIDES, P.G., ET AL. (2000) The genome sequence of *Drosophila melanogaster*. *Science (New York, N.Y.)* **287**, 2185–2195.
- ARRIZABALAGA, G. & LEHMANN, R. (1999) A Selective Screen Reveals Discrete Functional Domains in *Drosophila* Nanos. *Genetics* **153**, 1825–1838.
- BÖKEL, C. (2008) EMS screens : from mutagenesis to screening and mapping. *Methods in molecular biology (Clifton, N.J.)* **420**, 119–138.
- BOSCO, D.A., MORFINI, G., KARABACAK, N.M., SONG, Y., GROS-LOUIS, F., PASINELLI, P., GOOLSBY, H., FONTAINE, B.A., LEMAY, N., MCKENNA-YASEK, D., FROSCH, M.P., AGAR, J.N., JULIEN, J.-P., BRADY, S.T. & BROWN, R.H. (2010) Wild-type and mutant SOD1 share an aberrant conformation and a common pathogenic pathway in ALS. *Nature neuroscience* **13**, 1396–1403.
- BOUTELOUP, C., DESPORT, J.C., CLAVELOU, P., GUY, N., DERUMEAUX-BUREL, H., FERRIER, A. & COURATIER, P. (2009) Hypermetabolism in ALS patients: An early and persistent phenomenon. *Journal of Neurology* **256**, 1236–1242.
- CASCI, I. & PANDEY, U.B. (2015) A fruitful endeavor: modeling ALS in the fruit fly. *Brain research* **1607**, 47–74.
- CHARCOT, J.M. & JOFFRY, A. (1869) "Deux cas d'atrophie musculaire progressive avec lesions de la substance grise et des faisceaux antero-lateraux de la moelle epiniere. *Arch. Physiol. Neurol. Pathol.* **2**, 744–754.
- COOK, R.K., CHRISTENSEN, S.J., DEAL, J.A., COBURN, R.A., DEAL, M.E., GRESENS, J.M., KAUFMAN, T.C. & COOK, K.R. (2012) The generation of chromosomal deletions to provide extensive coverage and subdivision of the *Drosophila melanogaster* genome. *Genome Biology*. .

- COUTHOUIS, J., HART, M.P., SHORTER, J., DEJESUS-HERNANDEZ, M., ERION, R., ORISTANO, R., ET AL. (2011) A yeast functional screen predicts new candidate ALS disease genes. *Proceedings of the National Academy of Sciences of the United States of America* **108**, 20881–20890.
- DEIVASIGAMANI, S., VERMA, H.K., UEDA, R., RATNAPARKHI, A. & RATNAPARKHI, G.S. (2014) A genetic screen identifies Tor as an interactor of VAPB in a *Drosophila* model of amyotrophic lateral sclerosis. *Biology open* **3**, 1127–1138.
- DESPORT, J.C., PREUX, P.M., MAGY, L., BOIRIE, Y., VALLAT, J.M., BEAUFRÈRE, B. & COURATIER, P. (2001) Factors correlated with hypermetabolism in patients with amyotrophic lateral sclerosis. *American Journal of Clinical Nutrition* **74**, 328–334.
- DUPUIS, L., OUDART, H., RENÉ, F., GONZALEZ DE AGUILAR, J.-L. & LOEFFLER, J.-P. (2004) Evidence for defective energy homeostasis in amyotrophic lateral sclerosis: benefit of a high-energy diet in a transgenic mouse model. *Proceedings of the National Academy of Sciences of the United States of America* **101**, 11159–11164.
- ELDEN, A.C., KIM, H.-J., HART, M.P., CHEN-PLOTKIN, A.S., JOHNSON, B.S., FANG, X., ET AL. (2010) Ataxin-2 intermediate-length polyglutamine expansions are associated with increased risk for ALS. *Nature* **466**, 1069–1075. Nature Publishing Group, a division of Macmillan Publishers Limited. All Rights Reserved.
- FORSBERG, K., JONSSON, P.A., ANDERSEN, P.M., BERGEMALM, D., GRAFFMO, K.S., HULTDIN, M., JACOBSSON, J., ROSQUIST, R., MARKLUND, S.L. & BRÄNNSTRÖM, T. (2010) Novel antibodies reveal inclusions containing non-native SOD1 in sporadic ALS patients. *PLoS one* **5**, e11552.
- GRUZMAN, A., WOOD, W.L., ALPERT, E., PRASAD, M.D., MILLER, R.G., ROTHSTEIN, J.D., BOWSER, R., HAMILTON, R., WOOD, T.D., CLEVELAND, D.W., LINGAPPA, V.R. & LIU, J. (2007) Common molecular signature in SOD1 for both sporadic and familial amyotrophic lateral sclerosis. *Proceedings of the National Academy of Sciences of the United States of America* **104**, 12524–12529.
- HEATH, P.R., KIRBY, J. & SHAW, P.J. (2013) Investigating cell death mechanisms in amyotrophic lateral sclerosis using transcriptomics. *Frontiers in cellular neuroscience* **7**, 259.
- JU, S., TARDIFF, D.F., HAN, H., DIVYA, K., ZHONG, Q., MAQUAT, L.E., BOSCO, D.A., HAYWARD, L.J., BROWN, R.H., LINDQUIST, S., RINGE, D. & PETSKO, G.A. (2011) A yeast model of FUS/TLS-dependent cytotoxicity. *PLoS biology* **9**, e1001052. Public Library of Science.
- JUNEJA, T., PERICAK-VANCE, M.A., LAING, N.G., DAVE, S. & SIDDIQUE, T. (1997) Prognosis in familial amyotrophic lateral sclerosis: progression and survival in patients with glu100gly and ala4val mutations in Cu,Zn superoxide dismutase. *Neurology* **48**, 55–57.
- KERNAN, M. (1994) Genetic dissection of mechanosensory transduction: Mechanoreception-defective mutations of *drosophila*. *Neuron* **12**, 1195–1206.
- LIM, M. A., BENICE, K.K., SANDESARA, I., ANDREUX, P., AUWERX, J., ISHIBASHI, J., SEALE, P. & KALB, R.G. (2014) Genetically altering organismal metabolism by leptin-deficiency benefits a mouse model of Amyotrophic Lateral Sclerosis. *Human molecular genetics*, 1–14.
- MILLER, R.G., MITCHELL, J.D. & MOORE, D.H. (2012) Riluzole for amyotrophic lateral sclerosis (ALS)/motor neuron disease (MND). *The Cochrane database of systematic reviews* **3**, CD001447.

- PALAMIUC, L., SCHLAGOWSKI, A., NGO, S.T., VERNAY, A., DIRRIG-GROSCH, S., HENRIQUES, A., BOUTILLIER, A.-L., ZOLL, J., ECHANIZ-LAGUNA, A., LOEFFLER, J.-P. & RENÉ, F. (2015) A metabolic switch toward lipid use in glycolytic muscle is an early pathologic event in a mouse model of amyotrophic lateral sclerosis. *EMBO molecular medicine*.
- PASINELLI, P. & BROWN, R.H. (2006) Molecular biology of amyotrophic lateral sclerosis: insights from genetics. *Nature reviews. Neuroscience* **7**, 710–723.
- PETERS, O.M., GHASEMI, M. & BROWN, R.H. (2015) Emerging mechanisms of molecular pathology in ALS. *The Journal of clinical investigation* **125**, 1767–1779.
- ROSEN, D.R., SIDDIQUE, T., PATTERSON, D., FIGLEWICZ, D.A., SAPP, P., HENTATI, A., DONALDSON, D., GOTO, J., O'REGAN, J.P. & DENG, H.X. (1993) Mutations in Cu/Zn superoxide dismutase gene are associated with familial amyotrophic lateral sclerosis. *Nature* **362**, 59–62.
- SACCON, R.A., BUNTON-STASYSHYN, R.K.A., FISHER, E.M.C. & FRATTA, P. (2013) Is SOD1 loss of function involved in amyotrophic lateral sclerosis? *Brain : a journal of neurology* **136**, 2342–2358.
- SOMALINGA, B.R., DAY, C.E., WEI, S., ROTH, M.G. & THOMAS, P.J. (2012) TDP-43 identified from a genome wide RNAi screen for SOD1 regulators. *PloS one* **7**, e35818.
- ST JOHNSTON, D. (2002) The art and design of genetic screens: *Drosophila melanogaster*. *Nature reviews. Genetics* **3**, 176–188.
- SUN, Z., DIAZ, Z., FANG, X., HART, M.P., CHESI, A., SHORTER, J. & GITLER, A.D. (2011) Molecular determinants and genetic modifiers of aggregation and toxicity for the ALS disease protein FUS/TLS. *PLoS biology* **9**, e1000614. Public Library of Science.
- VENKEN, K.J.T., POPODI, E., HOLTZMAN, S.L., SCHULZE, K.L., PARK, S., CARLSON, J.W., HOSKINS, R.A., BELLEN, H.J. & KAUFMAN, T.C. (2010) A molecularly defined duplication set for the X chromosome of *Drosophila melanogaster*. *Genetics* **186**, 1111–1125.
- WOLF, M.J. & ROCKMAN, H.A. (2011) *Drosophila*, genetic screens, and cardiac function. *Circulation research* **109**, 794–806.

A- Genetic Mapping of Lethality



B- Expected Progeny Classes

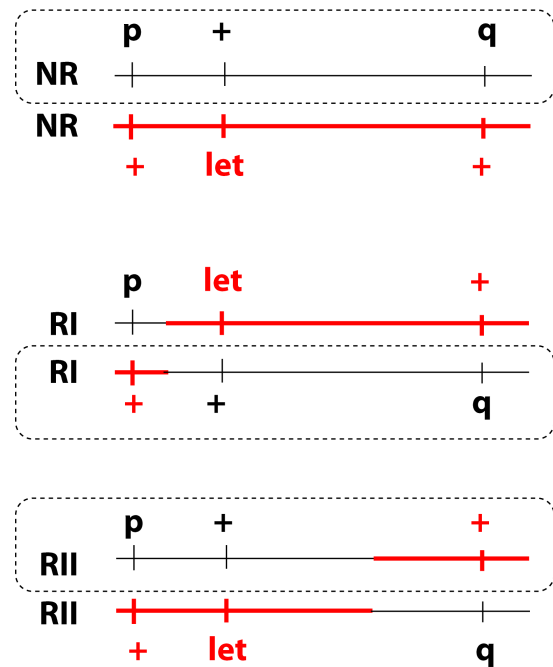


Figure 4.2. Genetic mapping of the lethality of EMS 81 and EMS 102. Genetic crosses were performed to combine the suppressor mutants with a standard mapping chromosome in females. **A)** Since it was clear that the lethal mutants both map to between the p and q loci (where p and q are the recessive alleles, and + indicated wild type), we were able to obtain recombinants on the p-q interval by recombination on either interval I or interval II. The lethal suppressor mutations are indicated by let for mutant, or + for wild type alleles. **B)** Only three classes of viable males (non-let containing) chromosomes could be obtained from this configuration in recombinogenic females, and all are distinguishable by visible markers. The relative distance on the p-q interval was obtained by $[RI/(RI+RII)] \times 1cM$.

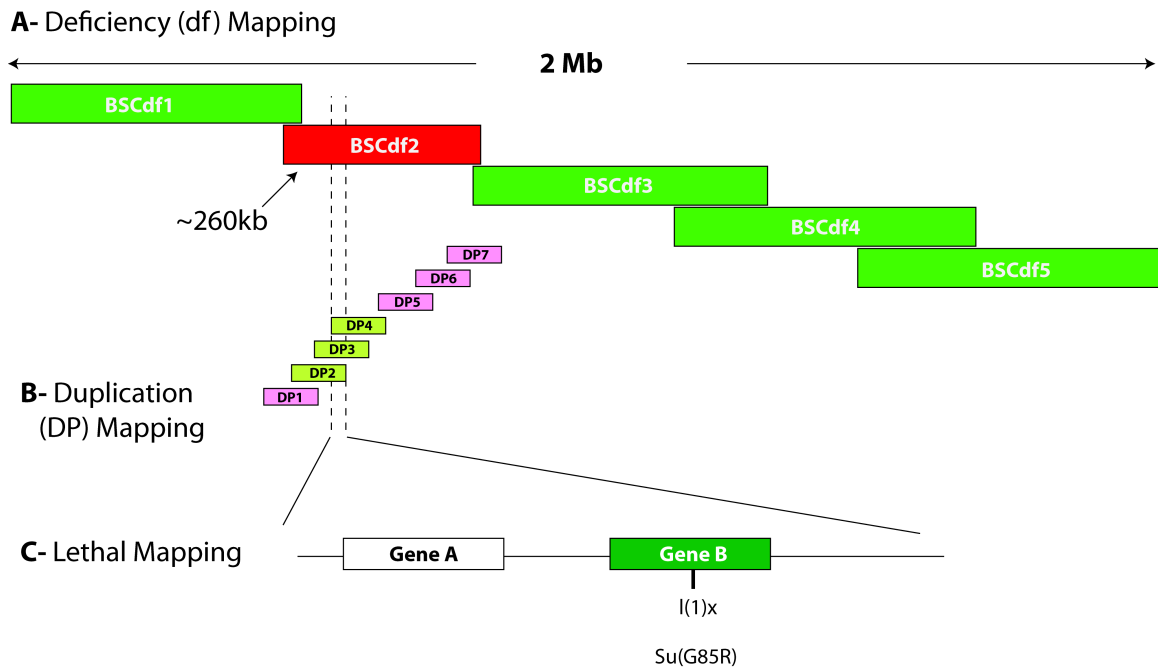


Figure 4.3. Molecular mapping of the lethality of EMS 81 and EMS 102. **A)** EMS 81-PR males were crossed to females of five balanced deficiency stocks for the region determined by genetic mapping (BSCdf1-5). Deficiencies that complement EMS 81 are shown in green. Only BSCdf2 (red) failed to complement EMS 81 lethality, mapping it to a ~260kb region. **B)** Both EMS 81 and EMS 102 balanced females were crossed to males of seven stocks carrying the w^+ -marked duplications on the third chromosome. Duplications that failed to rescue male lethality are shown in pink. Duplications 2-4 rescued male lethality of both EMS 81 and EMS 102, and limit the molecular interval where they are located. **C)** The refined interval contained two genes, A and B. Gene B had a previously molecularly uncharacterized lethal mutation, l(1)x, which was sequence-verified as a 13bp deletion in coding sequence, and EMS 81 failed to complement l(1)x, thus confirming the identity of the gene. Sequence analysis also revealed mutations in both alleles EMS 81 and EMS 102 of the Su(G85R) gene.

TABLES

Table 4.1. Candidate suppressors that are identified from the forward genetic screen. The progeny surviving more than 3 days are named as EMS1 to EMS145. Out of 145 survivor progeny, only 7 of them were able to generate a stock upon mating back to the original balanced stock. In the EMS 140 line, a possible gene inversion led to a false positive. The EMS 61 line was fertile but very uncoordinated. The rest of the suppressor lines EMS 35, EMS 61, EMS 81, EMS 94, EMS 102, EMS 130 look healthy, eclose in expected ratios, are fertile, and live at least 30 days without any obvious locomotion defect. Moreover, only female progeny came out of EMS 81 and EMS 102 crosses, indicating that the suppressor mutations might be on the X chromosome.

Name	<i>dSod1</i> allele	Progeny	Life Span	Locomotion
EMS 35	G85R/G85R	Males & females	>60 days	wt-like
EMS 61	G85R/G85R	Males & females	very short	very uncoordinated
EMS 81	G85R/G85R	Only females	>60 days	wt-like
EMS 94	G85R/G85R	Males & females	>60 days	wt-like
EMS 102	G85R/G85R	Only females	>60 days	wt-like
EMS 130	G85R/G85R	Males & females	>60 days	wt-like
EMS 140	G85R/WT (false positive)	Males & females	>60 days	wt-like

CHAPTER 5

DISCUSSION

Gaps In The Current Knowledge Within The Amyotrophic Lateral Sclerosis Field

Although French neurologist Jean Martin Charcot described Amyotrophic Lateral Sclerosis in great detail in the 19th century as lack (*A-*) of muscle (*myo*) nourishment (*trophic*) leading to stiffening (*sclerosis*) in the sides (*lateral*) of the spinal cord (Charcot, 1874), the etiology and pathogenesis of ALS still remain elusive (Peters, Ghasemi, & Brown, 2015). Two centuries after this definition, there is no current therapy available for the disease except from the only FDA approved palliative ALS drug, Riluzole (Lacomblez *et al.*, 1996). The effectiveness of Riluzole is highly debatable since on average it extends the life expectancy of a patient for 2-3 months with various side effects (Miller *et al.*, 1996). The lack of treatment, despite being in the literature for so long, is not because ALS is an orphan disease. In fact, ALS is the most common adult onset neurodegenerative disease, and it is very likely one of the most devastating ones considering that the cognition of the patients is almost intact during the 3-5 year long disease pathogenesis of muscle wasting and denervation (Peters *et al.*, 2015). The devastating nature of the disease has been very well conveyed to the public, thanks to the ALS ice bucket challenge started in August 2014. Despite the last two decades of intense research on ALS, the field lacks a complete understanding of the molecular mechanisms involved in ALS pathogenesis, which is necessary for the development of effective therapies.

Superoxide Dismutase 1: First ALS-associated Gene

The first ALS associated mutations were mapped to the SOD1 (also called ALS1) gene in 1993 through genetic linkage analysis (Rosen *et al.*, 1993). When SOD1 was

first associated with ALS, it was already one of the most studied human genes in biological science history because of its universal cytoplasmic superoxide scavenging function (Valentine, Doucette, & Zittin Potter, 2005). SOD1 literature dates back to 1930s and SOD1 was originally isolated from blood in 1940 (Keilin & Mann, 1940). When such a devastating disease was linked to such a well-studied enzyme, many groups independently generated transgenic animals overexpressing various SOD1 gene mutations in order to investigate earlier stages of ALS in a laboratory setting (Kato, 2008). Unfortunately, although these models advanced our understanding of ALS tremendously, they fall short in providing a complete understanding of the pathogenesis of ALS for the following reasons.

First, these transgenic models recapitulate ALS-like phenotypes only if the mutant protein is overexpressed in high gene copy numbers. In most cases, the same transgene carrying the same mutation with low mutant gene copy number, in the same animal background, generated by the same laboratory failed to exhibit ALS-like phenotypes, even early death (Gurney *et al.*, 1994). This fact alone was not reason enough to question the validity of the ALS models that exists today, because the expressed protein levels on a denaturing SDS polyacrylamide gel were almost at wild type expression levels regardless of high inserted mutant gene copy numbers. For instance, the difference between protein amounts on a denaturing SDS polyacrylamide gel was only 0.5 times more between G1 hSOD1^{G93A} mouse model harboring 18 mutant gene copy numbers and a wild type mouse carrying only 2 endogenous mSOD1 genes (Gurney *et al.*, 1994). Second, the control line used in these studies harbor a much lower gene copy number. For example, in the same mouse line harboring hSOD1^{G93A}, the control line only contains

7 wild type transgene insertions (Gurney *et al.*, 1994). Thus, the comparative analysis of copy number and protein expression level of control relative to mutant lines is not as accurate. Moreover, the endogenous SOD1 gene is intact in all of these transgene studies, except in one study where the hSOD1^{G85R} transgene is expressed in a null mSOD1 background (Bruijn *et al.*, 1998). Elimination of two copies of the wild type SOD1 protein in the hSOD1^{G85R} overexpression line that harbors 15 transgene insertions did not alter the ALS-like phenotypes such as shorter life span, motor neuron death and aggregation (Bruijn *et al.*, 1998). This result suggested that the extra two copies of wild type SOD1, in other words endogenous SOD1, did not affect the ALS pathogenesis in transgenic animal models. However, it is currently unknown whether the lack of phenotypic change observed in these transgenic mice is due to the extreme overexpression of the mutant protein. The dosage of SOD1 protein finally was considered relevant in light of ALS pathogenesis, when several studies revealed that even wild type SOD1 can acquire toxic properties upon overexpression. The first evidence arose when two groups crossed the hSOD1^{G93A}, hSOD1^{G85R} and hSOD1^{A4V} mice lines with a control line that overexpresses wild type hSOD1 (hSOD1^{wt}). The trans-heterozygote hSOD1^{G85R} and hSOD1^{G93A} mice exhibited an early disease onset upon crossing to hSOD1^{wt}, while hSOD1^{A4V} crossed to hSOD1^{wt} mice developed ALS-like symptoms for the first time (Jaarsma *et al.*, 2000; Deng *et al.*, 2006), unlike mice with hSOD1^{A4V} overexpression alone (Gurney *et al.*, 1994). Furthermore, some ALS symptoms such as mitochondrial dysfunction, axon degeneration, premature motor neuron death and SOD1 aggregation were recapitulated by simply overexpressing hSOD1^{wt} in mice (Graffmo *et al.*, 2013; Jaarsma *et al.*, 2000). One explanation on how wild type SOD1 became toxic is that the

copper chaperone for SOD (CCS), required for the copper (Cu^{2+}) metal binding of the SOD1 monomer, could not compensate for the elevated protein levels (Jonsson *et al.*, 2006). Without Cu^{2+} binding, SOD1 cannot fold properly despite the lack of mutations, exposing sites that are not normally structurally hidden leading to abnormal protein-protein interactions (Son & Elliott, 2014). One example for such an interaction is the ability of Derlin-1 to recognize and bind to misfolded SOD1, which triggers an abnormal ERAD pathway response (Mori *et al.*, 2011). Recently, other studies investigating misfolded SOD1 specific binding partners revealed novel protein functions for SOD1 other than superoxide scavenging, namely stabilizing mRNAs and acting as a transcriptional factor within the nuclear compartment (Lu *et al.*, 2007, 2009; Tsang *et al.*, 2014; Chen *et al.*, 2014). It is apparent from these recent results that there are new arenas of exploration involving non-canonical functions for wild type and mutant SOD1 proteins. Still, the superoxide dismutase enzymatic function of SOD1 is not considered completely independent regarding ALS pathogenesis. Oxidative stress can prompt wild type SOD1 protein to acquire toxic effects (Ezzi, Urushitani, & Julien, 2007), that mediate more severe ALS symptoms or induce an ALS phenotype in those transgenic models initially not exhibiting ALS-like phenotypes upon overexpression of the transgene (Aguirre *et al.*, 1998).

It was known early on that SOD1 gains toxic function in ALS pathogenesis since SOD1 null animals did not recapitulate the disease phenotypes (Reaume *et al.*, 1996; Huang *et al.*, 1997; Ho *et al.*, 1998; Matzuk *et al.*, 1998; Yoshida *et al.*, 2000). However, the oxidative stress-triggered misfolded SOD1 hypothesis brought the focus of the field back to the possible SOD1 loss of function in ALS pathogenesis, in addition to

gain of toxic function. In current SOD1 transgenic models, the endogenous wild type SOD1 gene is functional and an abundance of the SOD1 protein can trigger misfolding of SOD1, independent from the disease pathology.

Given all of these problems with SOD1 transgenic models, it is not surprising that any therapeutic approach previously examined G1 hSOD1^{G93A} mouse line fails to extend life span of these mice even by 10% (Perrin, 2014). The overexpression nature of the ALS model organisms could be a reason for the rate of failure rate regarding the ALS therapeutic studies.

In summary, even though 22 years have passed since SOD1 was linked to ALS, we still do not know how it contributes to ALS pathogenesis. Perhaps, one reason for this is the lack of an accurate, non-transgenic animal model in which the disease phenotypes are independent from the overexpression level of the allele. It is clear from current literature that SOD1-mediated ALS is not a simple gain of toxic function or loss of function disease, because neither the addition of exogenous copy of mutant protein nor the loss of endogenous enzymatic activity necessarily cause full ALS phenotypes alone. The new consensus idea in the field is that the role of oxidative stress is not independent from SOD1 gain of toxic function, because oxidative stress may also induce wild type SOD1 protein to misfold and form toxic aggregates. Therefore, the only way to test this hypothesis, *in vivo*, is the introduction of ALS-causing SOD1 point mutations into the endogenous locus. Recent studies aim to supply the long-awaited need for an accurate non-overexpression based *in vivo* model to study SOD1-mediated ALS mechanisms. An ALS mouse model with an ENU-induced D83G endogenous mutation (Joyce *et al.*, 2015), as well as naturally occurring SOD1-mutant dogs with canine degenerative

myelopathy that resembles human ALS are the only examples of such genetic models (Awano *et al.*, 2009; Wininger *et al.*, 2011; Crisp *et al.*, 2013; Zeng *et al.*, 2014). These current models are new therefore there are not many studies used these non-transgenic animal models other their initial characterization for the known ALS phenotypes.

Mimicking Human Disease Alleles in SOD1 Generates Unique Phenotypes for A Genetic Screen in *Drosophila*

In this thesis work, we have generated a new model of ALS in *Drosophila melanogaster* by precisely introducing four human ALS causing SOD1 mutations (G37R, H48R, H71Y and G85R) into the endogenous locus of *dSod1* through homologous recombination (Chapter 2). First, we have characterized the *dSod1* mutant *Drosophila* based on the ALS pathogenesis phenotypes, namely shortened life span, locomotion deficit, muscle atrophy and denervation, motor neuron death, gliosis, electrophysiological and neuromuscular junction structural alterations (Chapter 2). We have revealed that the mutations that cause fast disease progression in patients (G85R and H71Y) (Table 2.1) lead to a severe eclosion defect, reduction in survival, and locomotion deficits potentially stemming from neuronal retraction from adult muscles and increased synaptic activity at the neuromuscular junction. These ALS-like symptoms are likely due to a combination of both toxic gain of function and loss of function of mutant dSod1 protein. The first indication that pointed to a gain of toxic function was the observation that transgenic expression of wild type *dSod1* did not completely ameliorate the *dSod1*^{G85R/G85R} life span defect (Figure 2.15). Conversely, an observation that pointed to a loss of function was the

fact that homozygous $dSod1^{G85R/G85R}$, $dSod1^{H71Y/H71Y}$, and $dSod1^{G51S/G51S}$ mutant proteins exhibited no dismutase activity as detected via gel-based SOD activity assays (Figure 2.11). Interestingly, the mutations that cause the slow disease progression in ALS patients (Table 2.1), G37R and H48R as well as G85R and H71Y in a heterozygote states did not reveal any observable phenotypes in *Drosophila*.

In humans, 95% of SOD1 mutations are observed in a heterozygote state (Saccon *et al.*, 2013). However, we only observed ALS-like phenotype in the homozygote state for the more severe alleles, G85R and H71Y. We strongly believe that the lack of significant phenotypes in mutant heterozygotes is due to the fact that flies do not live long enough to exhibit disease pathology. In agreement with this, the non-transgenic ALS models of mice and dogs in a heterozygote state do not reveal any ALS-like symptoms (Zeng *et al.*, 2014; Joyce *et al.*, 2015). Given the importance of mutant SOD1 protein dosage in accelerating the ALS-like phenotype in transgenic SOD1-mediated ALS models (Acevedo-Arozena *et al.*, 2011), it is possible that heterozygotes might develop symptoms if they lived well beyond their normal life span. It is also quite possible that further experiments with altered environmental conditions such as altered diet, stress levels, or pharmacological interventions could reveal an ALS-like phenotype for *Drosophila* heterozygous *dSod1* mutant flies.

When we expressed two additional transgenes of wild type *dSod1* on the $dSod1^{G85R/G85R}$ background, we observed a similar phenotype to patients developing late onset ALS with a short progression quickly followed by death. $P[dSod1^{WTLoxP}]/P[dSod1^{WTLoxP}];dSod1^{G85R}/dSod1^{G85R}$ flies exhibited locomotor deficit for a day before they died in day 55 post eclosion (Supplementary video 2.3), which is

comparable to ALS patients losing their locomotion ability over 1-2 years before the need of a diaphragm support (Benditt & Boitano, 2008).

In summary, we present here the initial characterization of a novel *Drosophila* model for ALS carrying *dSod1* mutations (Chapter 2). Our *Drosophila* model provides a rich, fast and efficient system complementary to rodent model organisms for addressing mechanisms associated with human SOD1 mutations causing ALS and for elucidating the dosage sensitive results of SOD1-mediated ALS. Moreover, *Drosophila* provides a uniquely fast genetic system for the usage of an unbiased, powerful forward genetic screen for the identification of novel genetic suppressors of the “disease” phenotype. The pupal lethality of *dSod1*^{G85R/G85R} provides an excellent motivation for such a genetic suppressor screen. In Chapter 4, we described an EMS based forward genetic screen designed to attenuate *dSod1*^{G85R/G85R} lethality. As a result, we have identified five potential suppressor lines, all of which mapped to the X chromosome, appear healthy, eclose in expected ratios, are fertile, and live at least 60 days without any obvious locomotor defects. All of these suppressor mutations act in a dominant fashion as 50% of homozygous *dSod1*^{G85R/G85R} flies (not carrying the suppressor) die in the pupal case. Thus far, we have mapped two of these suppressor mutations to a gene that we refer as Su(G85R). Both suppressor mutations confer a different G-to-A amino acid alteration as one expects from an EMS screen. The nature of the Su(G85R) gene will not be discussed in this thesis work because of a provisional patent application through Brown University. Nevertheless, isolation of two different mutations on a very short gene, Su(G85R), conveys important role for this gene during the ALS pathogenesis in *Drosophila*. Moreover, Su(G85R) mutations also suppressed the eclosion defect and short life span

phenotypes of the relatively milder *dSod1*^{H71Y} allele. In the future, we will investigate whether Su(G85R) mutations will be effective in suppressing ALS phenotype in other *Drosophila* ALS models involving overexpression of other ALS causing genes. Interestingly, EMS isolated suppressor mutations on Su(G85R) lead to lethality in a similar fashion to *dSod1*^{G85R/G85R}. A future suppressor screen could also be performed to identify suppressors of Su(G85R) to further dissect a possible molecular pathway involved in ALS disease.

Riluzole Treatment is not as Effective in *Drosophila* as in Human Patients

In addition to performing a forward screen to alleviate lethality of *dSod1*^{G85R/G85R}, we tested various concentrates of Riluzole, the only FDA approved drug for ALS patients, and another antioxidant chemical, Melatonin, on our *Drosophila* model. In the suppressor screen, our goal was to establish a better improvement of ALS-like phenotype on *dSod1*^{G85R/G85R} since these chemicals have very moderate effects on patients (Miller *et al.*, 1996). Maybe not surprisingly, Riluzole and Melatonin exhibited very moderate effects in *dSod1* mutant *Drosophila* (Table 2.2) as in humans. The most effective cocktail included 4mM Riluzole with 8mM emulsifier (2-hydroxypropyl- β cyclodextrin as described in (Rival *et al.*, 2004) to make Riluzole soluble in water) and resulted in 8.92% eclosion efficiency increase with a maximum life span of 6 days, compared to maximum a few hours life span observed in *dSod1*^{G85R/G85R}. Interestingly, 8mM emulsifier alone had a very similar 7.5% eclosion efficiency and with a maximum life span of 11 days. Thus it was not clear whether the Riluzole really had an effect of the condition of *dSod1*^{G85R/G85R} flies. 1mM Melatonin had a similar effect of 5.66% eclosion rate with a maximum of 4

days life span. Moreover, when 1mM Melatonin was combined with 1mM Riluzole treatment, the eclosion efficiency decreased to 2.9% with a maximum life span of 4 days (Table 2.2).

The Dosage of Sod1 Protein Plays a Critical Role in ALS Pathogenesis

One of the most important reasons for establishing a non-overexpression based ALS model was to investigate the dSod1 protein dosage effects on ALS pathogenesis. In light of this goal, we have decreased the dosage of dSod1 by combining dSod1 mutants with a pre-existing dSod1 deletion allele. *dSod1*^{G85R/X-16} exhibited an ALS-like phenotype that is not as severe as the *dSod1*^{G85R/G85R} allele (Figure 2.5.A, Figure 2.D and Supplementary video 2.4). These results suggest that *dSod1*^{G85R} causes cytotoxicity in a dosage dependent manner.

The dosage dependent cytotoxicity was not specific to the mutant alleles. Four copies of *dSod1* (*P[dSod1*^{WTLoxP}*]/P[dSod1*^{WTLoxP}*]; dSod1*^{WTLoxP}*/dSod1*^{WTLoxP}) exhibited toxic effects and lead to a shorter life span when compared to the wild type *dSod1*^{WTLoxP}*/dSod1*^{WTLoxP} flies. Previous studies are in agreement with this finding, underscoring the importance of SOD1 protein dosage and questioning the validity and accuracy of transgenic models that exclusively depend on protein overexpression. Moreover, upon overexpression of wild type hSOD1 in mice, wild type hSOD1 and mSOD1 can acquire an abnormal conformation and lead to ALS-like phenotypes such as mitochondrial dysfunction, axon degeneration, premature motor neuron death, and SOD1 aggregation (Jaarsma *et al.*, 2000; Graffmo *et al.*, 2013). The overexpression of hSOD1 also caused locomotion deficit in *Drosophila* (Watson *et al.*, 2008). Furthermore, in this

thesis study, we showed that the total gene copy numbers do not directly translate into the protein amounts in the presence of mutant alleles (Figure 2.17), which further calls into question overexpression dependent ALS phenotypes in transgenic models.

An Allele Previously Characterized as Deficient $dSod1^{-/-}$ is not Null

In this thesis study, we have compared the effects of homologously recombined mutations to another $dSod1$ mutant line harboring a point mutation $dSod1^{G51S}$ that was generated via an EMS screen (Phillips *et al.*, 1989). This allele is referred to as “null” or “ $dSod1^{-/-}$ ” allele in the literature by many groups despite the fact that it has simply one amino acid change of G49S instead of a full deficiency at the locus. $dSod1^{G51S}$ is observed as null in gel-based SOD1 activity assays explaining the “null” description of the allele (Phillips *et al.*, 1989). However, immunoblotting has not been performed on this allele before. In Figure 2.13.A, we demonstrate that this allele exhibits reduced amounts of $dSod1$ protein on denaturing SDS gel but is certainly not a null allele.

Other ALS causing genes and SOD1: where does SOD1 stand in ALS pathogenesis?

Even though how SOD1, the first ALS causative gene, mediates ALS pathology still remains a mystery, ALS researchers have made plausible progress in discovering new ALS causative genes. The second ALS associated gene, ALS2 (Alsin) was identified in juvenile ALS cases 8 years after the discovery of SOD1 (Yang *et al.*, 2001). However, in recent years, with the advancement of exome/next generation sequencing, mutations were found in a total of 61 genes (plus 2 loci with unknown genes) in ALS patients versus matched controls (Abel *et al.*, 2012; Peters *et al.*, 2015). In addition, many

susceptibility genes have been identified through genome wide association studies (GWAS) (Abel *et al.*, 2012; Peters *et al.*, 2015). Currently, the most common ALS causative gene is the hexanucleotide repeat expansions within the C9orf72 locus, which was identified 18 years after the discovery of SOD1 (DeJesus-Hernandez *et al.*, 2011; Renton *et al.*, 2011; Gijselinck *et al.*, 2012). However, how these mutations merge into a common cellular pathway that promotes ALS pathogenesis is still unknown.

In order to investigate the altered pathways in ALS pathogenesis, we analyzed the transcriptomic changes occurring in adult flies for two kinds of precise genetically engineered mutants (*dSod1*^{G85R} and *dSod1*^{H71Y}) and an EMS introduced point mutation (*dSod1*^{G51S}). We extended the initial general transcriptome analysis specifically to the central nervous system tissue and to the disease onset in *Drosophila* by performing RNA sequencing analysis from the central nervous system of *dSod1*^{G85R/G85R} wandering third instar larvae. We have completed a very preliminary analysis on *dSod1*^{H71Y/H71Y} adults so far (Chapter 3). We believe that the transcriptomic alterations observed in these flies will reveal important clues towards understanding the altered cellular pathways during ALS pathogenesis.

Concluding Remarks

The fALS model established in this study has started a new venue to study SOD1-mediated ALS pathogenesis in an accurate and highly controlled experimental setting. The initial characterization of four *Drosophila* lines harboring human ALS-causing mutations is described in this thesis work. Targeting of the *dSod1* locus by homologous recombination presents an opportunity to investigate the use of gene targeting for the

generation of human disease models in the fly. Such models would allow for current and future experiments aimed at understanding the cellular mechanisms of pathogenesis that would be technically difficult and time-consuming in higher organisms. For example, disease models in flies may serve as a starting point for forward genetic screens by providing a sensitized genetic background that can aid in the identification of novel genes involved in either suppression or enhancement of the disease phenotype. Additionally, disease models can be used to test various pharmacological agents that may affect disease specific processes.

Drosophila has a very compact genome with ~5% of the size of a human genome (Wolf & Rockman, 2011). Despite this fact, out of 287 known human disease genes, 197 of them have a homolog in *Drosophila* (St Johnston, 2002). *Drosophila*, with its conserved nervous system genes and 100,000 neurons, each synapsing about 1000 times, provides a simple but elegant model organism to study human neurodegenerative diseases (Wade, 2010). Homologous recombination has not widely been used to specifically model human disease in *Drosophila* other than epilepsy (Sun *et al.*, 2012; Schutte *et al.*, 2014) and now ALS, but with recent advances in CRISPR/Cas9 technology, this is expected to change. In this thesis work, we demonstrate that *Drosophila* is a useful genetic system to model neurodegenerative diseases without relying on overexpression.

REFERENCES

- ABEL, O., POWELL, J.F., ANDERSEN, P.M. & AL-CHALABI, A. (2012) ALSod: A user-friendly online bioinformatics tool for amyotrophic lateral sclerosis genetics. *Human mutation* **33**, 1345–1351.
- ACEVEDO-AROZENA, A., KALMAR, B., ESSA, S., RICKETTS, T., JOYCE, P., KENT, R., ROWE, C., PARKER, A., GRAY, A., HAFEZPARAST, M., THORPE, J.R., GREENSMITH, L. & FISHER, E.M.C. (2011) A comprehensive assessment of the SOD1G93A low-copy transgenic mouse, which models human amyotrophic lateral sclerosis. *Disease models & mechanisms* **4**, 686–700.
- AGUIRRE, T., VAN DEN BOSCH, L., GOETSCHALCKX, K., TILKIN, P., MATHIJS, G., CASSIMAN, J.J. & ROBBERECHT, W. (1998) Increased sensitivity of fibroblasts from amyotrophic lateral sclerosis patients to oxidative stress. *Annals of Neurology* **43**, 452–457.
- AWANO, T., JOHNSON, G.S., WADE, C.M., KATZ, M.L., JOHNSON, G.C., TAYLOR, J.F., PERLOSKI, M., BIAGI, T., BARANOWSKA, I., LONG, S., MARCH, P.A., OLBY, N.J., SHELTON, G.D., KHAN, S., O'BRIEN, D.P., LINDBLAD-TOH, K. & COATES, J.R. (2009) Genome-wide association analysis reveals a SOD1 mutation in canine degenerative myelopathy that resembles amyotrophic lateral sclerosis. *Proceedings of the National Academy of Sciences of the United States of America* **106**, 2794–2799.
- BENDITT, J.O. & BOITANO, L. (2008) Respiratory treatment of amyotrophic lateral sclerosis. *Physical medicine and rehabilitation clinics of North America* **19**, 559–572, x.
- BRUIJN, L.I., HOUSEWEART, M.K., KATO, S., ANDERSON, K.L., ANDERSON, S.D., OHAMA, E., REAUME, A.G., SCOTT, R.W. & CLEVELAND, D.W. (1998) Aggregation and motor neuron toxicity of an ALS-linked SOD1 mutant independent from wild-type SOD1. *Science (New York, N.Y.)* **281**, 1851–1854.
- CHARCOT, J.M. (1874) De la sclérose latérale amyotrophique. *Le Progrès Médical* **2**, 325–455.
- CHEN, H., QIAN, K., DU, Z., CAO, J., PETERSEN, A., LIU, H., BLACKBOURN, L.W., HUANG, C.-L., ERRIGO, A., YIN, Y., LU, J., AYALA, M. & ZHANG, S.-C. (2014) Modeling ALS with iPSCs reveals that mutant SOD1 misregulates neurofilament balance in motor neurons. *Cell stem cell* **14**, 796–809.
- CRISP, M.J., BECKETT, J., COATES, J.R. & MILLER, T.M. (2013) Canine degenerative myelopathy: biochemical characterization of superoxide dismutase 1 in the first naturally occurring non-human amyotrophic lateral sclerosis model. *Experimental neurology* **248**, 1–9.
- DEJESUS-HERNANDEZ, M., MACKENZIE, I.R., BOEVE, B.F., BOXER, A.L., BAKER, M., RUTHERFORD, N.J., ET AL. (2011) Expanded GGGGCC hexanucleotide repeat in noncoding region of C9ORF72 causes chromosome 9p-linked FTD and ALS. *Neuron* **72**, 245–256.
- DENG, H.-X., SHI, Y., FURUKAWA, Y., ZHAI, H., FU, R., LIU, E., GORRIE, G.H., KHAN, M.S., HUNG, W.-Y., BIGIO, E.H., LUKAS, T., DAL CANTO, M.C., O'HALLORAN, T. V & SIDDIQUE, T. (2006) Conversion to the amyotrophic lateral sclerosis phenotype is associated with intermolecular linked insoluble aggregates of SOD1 in mitochondria. *Proceedings of the National Academy of Sciences of the United States of America* **103**, 7142–7147.
- EZZI, S.A., URUSHITANI, M. & JULIEN, J.-P. (2007) Wild-type superoxide dismutase acquires binding and toxic properties of ALS-linked mutant forms through oxidation. *Journal of neurochemistry* **102**, 170–178.

- GIJSELINCK, I., VAN LANGENHOVE, T., VAN DER ZEE, J., SLEEGERS, K., PHILTJENS, S., KLEINBERGER, G., ET AL. (2012) A C9orf72 promoter repeat expansion in a Flanders-Belgian cohort with disorders of the frontotemporal lobar degeneration-amyotrophic lateral sclerosis spectrum: a gene identification study. *The Lancet. Neurology* **11**, 54–65.
- GRAFFMO, K.S., FORSBERG, K., BERGH, J., BIRVE, A., ZETTERSTRÖM, P., ANDERSEN, P.M., MARKLUND, S.L. & BRÄNNSTRÖM, T. (2013) Expression of wild-type human superoxide dismutase-1 in mice causes amyotrophic lateral sclerosis. *Human molecular genetics* **22**, 51–60.
- GURNEY, M.E., PU, H., CHIU, A.Y., DAL CANTO, M.C., POLCHOW, C.Y., ALEXANDER, D.D., CALIENDO, J., HENTATI, A., KWON, Y.W. & DENG, H.X. (1994) Motor neuron degeneration in mice that express a human Cu,Zn superoxide dismutase mutation. *Science (New York, N.Y.)* **264**, 1772–1775.
- HO, Y.S., GARGANO, M., CAO, J., BRONSON, R.T., HEIMLER, I. & HUTZ, R.J. (1998) Reduced fertility in female mice lacking copper-zinc superoxide dismutase. *The Journal of biological chemistry* **273**, 7765–7769.
- HUANG, T.T., YASUNAMI, M., CARLSON, E.J., GILLESPIE, A.M., REAUME, A.G., HOFFMAN, E.K., CHAN, P.H., SCOTT, R.W. & EPSTEIN, C.J. (1997) Superoxide-mediated cytotoxicity in superoxide dismutase-deficient fetal fibroblasts. *Archives of biochemistry and biophysics* **344**, 424–432.
- JAARMA, D., HAASDIJK, E.D., GRASHORN, J. A., HAWKINS, R., VAN DUIJN, W., VERSPAGET, H.W., LONDON, J. & HOLSTEGE, J.C. (2000) Human Cu/Zn superoxide dismutase (SOD1) overexpression in mice causes mitochondrial vacuolization, axonal degeneration, and premature motoneuron death and accelerates motoneuron disease in mice expressing a familial amyotrophic lateral sclerosis mutant SO. *Neurobiology of disease* **7**, 623–643.
- JONSSON, P.A., GRAFFMO, K.S., ANDERSEN, P.M., BRÄNNSTRÖM, T., LINDBERG, M., OLIVEBERG, M. & MARKLUND, S.L. (2006) Disulphide-reduced superoxide dismutase-1 in CNS of transgenic amyotrophic lateral sclerosis models. *Brain : a journal of neurology* **129**, 451–464.
- JOYCE, P.I., MCGOLDRICK, P., SACCON, R.A., WEBER, W., FRATTA, P., WEST, S.J., ET AL. (2015) A novel SOD1-ALS mutation separates central and peripheral effects of mutant SOD1 toxicity. *Human molecular genetics* **24**, 1883–1897.
- KATO, S. (2008) Amyotrophic lateral sclerosis models and human neuropathology: similarities and differences. *Acta neuropathologica* **115**, 97–114.
- KEILIN, D. & MANN, T. (1940) Carbonic anhydrase. Purification and nature of the enzyme. *The Biochemical journal* **34**, 1163–1176.
- LACOMBLEZ, L., BENSIMON, G., LEIGH, P.N., GUILLET, P. & MEININGER, V. (1996) Dose-ranging study of riluzole in amyotrophic lateral sclerosis. Amyotrophic Lateral Sclerosis/Riluzole Study Group II. *Lancet* **347**, 1425–1431.
- LU, L., WANG, S., ZHENG, L., LI, X., SUSWAM, E.A., ZHANG, X., WHEELER, C.G., NABORS, L.B., FILIPPOVA, N. & KING, P.H. (2009) Amyotrophic lateral sclerosis-linked mutant SOD1 sequesters Hu antigen R (HuR) and TIA-1-related protein (TIAR): implications for impaired post-transcriptional regulation of vascular endothelial growth factor. *The Journal of biological chemistry* **284**, 33989–33998.
- LU, L., ZHENG, L., VIERA, L., SUSWAM, E., LI, Y., LI, X., ESTÉVEZ, A.G. & KING, P.H. (2007) Mutant Cu/Zn-superoxide dismutase associated with amyotrophic lateral sclerosis destabilizes vascular

- endothelial growth factor mRNA and downregulates its expression. *The Journal of neuroscience : the official journal of the Society for Neuroscience* **27**, 7929–7938.
- MATZUK, M.M., DIONNE, L., GUO, Q., KUMAR, T.R. & LEBOVITZ, R.M. (1998) Ovarian function in superoxide dismutase 1 and 2 knockout mice. *Endocrinology* **139**, 4008–4011.
- MILLER, R.G., BOUCHARD, J.P., DUQUETTE, P., EISEN, A., GELINAS, D., HARATI, Y., MUNSAT, T.L., POWE, L., ROTHSTEIN, J., SALZMAN, P. & SUFIT, R.L. (1996) Clinical trials of riluzole in patients with ALS. ALS/Riluzole Study Group-II. *Neurology* **47**, S86–S90; discussion S90–S92.
- MORI, A., YAMASHITA, S., UCHINO, K., SUGA, T., IKEDA, T., TAKAMATSU, K., ISHIZAKI, M., KOIDE, T., KIMURA, E., MITA, S., MAEDA, Y., HIRANO, T. & UCHINO, M. (2011) Derlin-1 overexpression ameliorates mutant SOD1-induced endoplasmic reticulum stress by reducing mutant SOD1 accumulation. *Neurochemistry international* **58**, 344–353.
- PERRIN, S. (2014) Preclinical research: Make mouse studies work. *Nature* **507**, 423–425.
- PETERS, O.M., GHASEMI, M. & BROWN, R.H. (2015) Emerging mechanisms of molecular pathology in ALS. *The Journal of clinical investigation* **125**, 1767–1779.
- PHILLIPS, J.P., CAMPBELL, S.D., MICHAUD, D., CHARBONNEAU, M. & HILLIKER, A.J. (1989) Null mutation of copper/zinc superoxide dismutase in *Drosophila* confers hypersensitivity to paraquat and reduced longevity. *Proceedings of the National Academy of Sciences of the United States of America* **86**, 2761–2765.
- REAUME, A.G., ELLIOTT, J.L., HOFFMAN, E.K., KOWALL, N.W., FERRANTE, R.J., SIWEK, D.F., WILCOX, H.M., FLOOD, D.G., BEAL, M.F., BROWN, R.H., SCOTT, R.W. & SNIDER, W.D. (1996) Motor neurons in Cu/Zn superoxide dismutase-deficient mice develop normally but exhibit enhanced cell death after axonal injury. *Nature genetics* **13**, 43–47.
- RENTON, A.E., MAJOUNIE, E., WAITE, A., SIMÓN-SÁNCHEZ, J., ROLLINSON, S., GIBBS, J.R., ET AL. (2011) A hexanucleotide repeat expansion in C9ORF72 is the cause of chromosome 9p21-linked ALS-FTD. *Neuron* **72**, 257–268.
- RIVAL, T., SOUSTELLE, L., STRAMBI, C., BESSON, M.T., ICHÉ, M. & BIRMAN, S. (2004) Decreasing glutamate buffering capacity triggers oxidative stress and neuropil degeneration in the *Drosophila* brain. *Current Biology* **14**, 599–605.
- ROSEN, D.R., SIDDIQUE, T., PATTERSON, D., FIGLEWICZ, D.A., SAPP, P., HENTATI, A., DONALDSON, D., GOTO, J., O'REGAN, J.P. & DENG, H.X. (1993) Mutations in Cu/Zn superoxide dismutase gene are associated with familial amyotrophic lateral sclerosis. *Nature* **362**, 59–62.
- SACCON, R.A., BUNTON-STASYSHYN, R.K.A., FISHER, E.M.C. & FRATTA, P. (2013) Is SOD1 loss of function involved in amyotrophic lateral sclerosis? *Brain : a journal of neurology* **136**, 2342–2358.
- SCHUTTE, R.J., SCHUTTE, S.S., ALGARA, J., BARRAGAN, E. V, GILLIGAN, J., STABER, C., SAVVA, Y.A., SMITH, M.A., REENAN, R. & O'DOWD, D.K. (2014) Knock-in model of Dravet syndrome reveals a constitutive and conditional reduction in sodium current. *Journal of neurophysiology* **112**, 903–912.
- SON, M. & ELLIOTT, J.L. (2014) Mitochondrial defects in transgenic mice expressing Cu,Zn Superoxide Dismutase mutations, the role of Copper Chaperone for SOD1. *Journal of the Neurological Sciences*.

- ST JOHNSTON, D. (2002) The art and design of genetic screens: *Drosophila melanogaster*. *Nature reviews. Genetics* **3**, 176–188.
- SUN, L., GILLIGAN, J., STABER, C., SCHUTTE, R.J., NGUYEN, V., O'DOWD, D.K. & REENAN, R. (2012) A knock-in model of human epilepsy in *Drosophila* reveals a novel cellular mechanism associated with heat-induced seizure. *The Journal of neuroscience : the official journal of the Society for Neuroscience* **32**, 14145–14155.
- TSANG, C.K., LIU, Y., THOMAS, J., ZHANG, Y. & ZHENG, X.F.S. (2014) Superoxide dismutase 1 acts as a nuclear transcription factor to regulate oxidative stress resistance. *Nature communications* **5**, 3446. Nature Publishing Group.
- VALENTINE, J.S., DOUCETTE, P. A & ZITTIN POTTER, S. (2005) Copper-zinc superoxide dismutase and amyotrophic lateral sclerosis. *Annual review of biochemistry* **74**, 563–593.
- WADE, N. (2010) Decoding the Human Brain, With Help From a Fly. *The New York Times*, D4.
- WATSON, M.R., LAGOW, R.D., XU, K., ZHANG, B. & BONINI, N.M. (2008) A drosophila model for amyotrophic lateral sclerosis reveals motor neuron damage by human SOD1. *The Journal of biological chemistry* **283**, 24972–24981.
- WININGER, F.A., ZENG, R., JOHNSON, G.S., KATZ, M.L., JOHNSON, G.C., BUSH, W.W., JARBOE, J.M. & COATES, J.R. (2011) Degenerative Myelopathy in a Bernese Mountain Dog with a Novel SOD1 Missense Mutation. *Journal of Veterinary Internal Medicine* **25**, 1166–1170.
- WOLF, M.J. & ROCKMAN, H.A. (2011) *Drosophila*, genetic screens, and cardiac function. *Circulation research* **109**, 794–806.
- YANG, Y., HENTATI, A., DENG, H.X., DABBAGH, O., SASAKI, T., HIRANO, M., HUNG, W.Y., OUAHCHI, K., YAN, J., AZIM, A.C., COLE, N., GASCON, G., YAGMOUR, A., BEN-HAMIDA, M., PERICAK-VANCE, M., HENTATI, F. & SIDDIQUE, T. (2001) The gene encoding alsin, a protein with three guanine-nucleotide exchange factor domains, is mutated in a form of recessive amyotrophic lateral sclerosis. *Nature genetics* **29**, 160–165.
- YOSHIDA, T., MAULIK, N., ENGELMAN, R.M., HO, Y.S. & DAS, D.K. (2000) Targeted disruption of the mouse Sod I gene makes the hearts vulnerable to ischemic reperfusion injury. *Circulation research* **86**, 264–269.
- ZENG, R., COATES, J.R., JOHNSON, G.C., HANSEN, L., AWANO, T., KOLICHESKI, A., IVANSSON, E., PERLOSKI, M., LINDBLAD-TOH, K., O'BRIEN, D.P., GUO, J., KATZ, M.L. & JOHNSON, G.S. (2014) Breed distribution of SOD1 alleles previously associated with canine degenerative myelopathy. *Journal of Veterinary Internal Medicine* **28**, 515–521.

APPENDIX I

Loss of Heterochromatic Gene Silencing in *Drosophila* ALS Model with *dSOD1*^{G85R} Mutation

This section investigates the heterochromatic gene silencing in *Drosophila* expressing G85R mutation on *dSOD1*. Dr. Yiannis Savva helped with the experimental design. Undergraduate student Ronak Jani collected virgins to combine *dSOD1* mutants with PEV reporters. I have done the rest of the experimental work, analyzed results and crafted figures.

INTRODUCTION

DNA within a given nuclei is wrapped around histone proteins and the complex together forms the chromatin architecture. The obvious function of chromatin is to package DNA into a smaller volume to fit in the nucleus and to act as a mechanism for the regulation of gene expression (Girton & Johansen, 2008). The density of the chromatin can alter gene expression. For example, the dense form, heterochromatin, protects cells from DNA damage and silences DNA, and the loose form, euchromatin, allows gene expression (Elgin & Reuter, 2013). Heterochromatin and euchromatin states are interchangeable with each other depending on environmental and cellular cues. Heterochromatin formation depends critically on methylation of histone H3 at lysine 9 (H3K9me2/3) and its association with other proteins such as heterochromatin protein 1 (HP1) (Grewal & Elgin, 2007).

Position-effect variegation (PEV) occurs when a gene normally expressed is silenced due to a change in chromatin state from euchromatin to heterochromatin or the opposite (Elgin & Reuter, 2013). When heterochromatin packaging spreads across the heterochromatin/euchromatin borders, it causes transcriptional silencing in a stochastic pattern. PEV is intensely studied in *Drosophila* using the *mini white* gene reporter that visually reports gene silencing via eye color mosaicism (Schulze & Wallrath, 2007).

To my knowledge, the state of heterochromatin has not yet been investigated in any current ALS models. During immunofluorescence staining studies, while characterizing *dSOD1* mutants in *Drosophila*, we made an intriguing observation that the nuclear DAPI stain is diffused in G85R homozygous flies. DAPI (4',6-diamidino-2-phenylindole) is a fluorescent DNA stain that strongly binds to the heterochromatic

chromocenter compared to euchromatin regions. In order to investigate the possible alterations in heterochromatic structure and thus silencing of specific regions in the *Drosophila* ALS model, we made use of HP1 nuclear staining and a PEV reporter, *Hok^{mw}*, that expresses the *mini white* gene from the 4th chromosome (Savva *et al.*, 2013). Interestingly, not only homozygous G85R flies that are at the terminal stage of ALS, but also the seemingly wild type-looking heterozygous G85R flies showed reduced heterochromatic gene silencing.

RESULTS and DISCUSSION

First, in order to verify our preliminary observations with DNA density, we immunostained the brains of near-death *dSOD1^{G85R}* homozygous flies that are pharate in the pupal case for DAPI and HP1. The *dSOD1^{G85R}* homozygous flies showed diffused DAPI and HP1 staining (Figure A1). In controls, HP1 staining appears as a single strong puncta, which denotes the chromocenter. In *dSOD1^{G85R/G85R}* flies, the spot becomes less concentrated. According to RNA sequencing analysis described in Chapter 3, the HP1 mRNA levels are not affected by the dSOD1 ALS alleles (Figure A2). This result has not yet been verified with Western blot analysis. It is also not yet clear if near death (10-14 days old) *dSOD1^{H71Y/H71Y}* flies exhibit similar defects in heterochromatin density that potentially lead to increased gene expression. In the future, we will expand this staining for other adult and larval stages of ALS mutants, namely *dSOD1^{G85R/WTLoxP}*, *dSOD1^{H71Y/WTLoxP}*, *dSOD1^{H71Y/H71Y}*. In addition, we will investigate other heterochromatin markers such as histone H3 at lysine 9 as described previously (Savva *et al.*, 2013).

Furthermore, in order to investigate transcriptional gene silencing via heterochromatinization in the severe ALS alleles *dSOD1*^{G85R} and *dSOD1*^{H71Y}, we made use of *Hok*^{mw}, a PEV reporter on the fourth chromosome. Previous studies suggest that chromosome 4 is under intense heterochromatinization and can be used to assess the status of heterochromatin *in vivo* (Riddle, Shaffer, & Elgin, 2009). By crossing *dSOD1* mutants with the *Hok*^{mw} heterochromatic gene silencing reporter allele, we generated fly strains that visually reported differences in heterochromatic gene silencing via eye color when compared to controls. If gene silencing is globally unaffected, variegation (red-white mosaic) equal to that of controls is observed. An enhanced degree of gene silencing yields increased mosaicism (mostly white) or no variegation (only white). Diminished gene silencing yields reduced mosaicism (mostly red) or no variegation (only red) (Similar spectrum of eye color depicted in the PEV scale in AB3.A)

It should be noted that ALS-causing *SOD1* mutations in humans are dominantly inherited; affected patients are heterozygous for the *SOD1* mutation. During the generation of ALS model flies by homologous recombination, we observed that heterozygous flies are outwardly indistinguishable from *dSOD1*^{WTLoxP/WTLoxP} homologous recombination controls for any ALS-related phenotype (Chapter 2). G85R and H71Y heterozygotes exhibit wild type phenotype for adult locomotion and survival analyses. However, they do have reduced larval crawling speed as compared to the wild types (Chapter 2). We examined gene silencing only in G85R and H71Y heterozygotes. It was not possible to combine the G85R and H71Y homozygotes, that result in the ALS phenotype discussed in details in Chapter 2, with *Hok*^{mw} reporter that is on the 4th

chromosome due to lack of balancers on the 4th chromosome and the lethality and infertility of G85R and H71Y homozygotes.

Interestingly, qualitative (mosaicism rating) and quantitative (spectrophotometric absorbance readings from head homogenates) measures revealed marked abnormalities in *dSOD1*^{G85R/+} but not in *dSOD1*^{H71Y/+} (Figure A3). *dSOD1*^{G85R/+} flies had dramatically increased red eye pigmentation relative to *dSOD1*^{LoxP/+} controls, reflected in significantly higher 480 nm absorbance readings. *dSOD1*^{G85R/+} flies appeared to exhibit drastically lower levels of gene silencing, while *dSOD1*^{H71Y/+} flies seemed to display a small to negligible increase in silencing.

Here we show that G85R heterozygous and homozygous *Drosophila* exhibit deregulated heterochromatic gene silencing. One hypothesis is that repressive heterochromatin is established through the RNA interference pathway (Castel & Martienssen, 2013). Thus, it would be interesting to investigate RNA interference involvement in ALS in the near future.

MATERIALS and METHODS

Microscopy and immunohistochemistry

All confocal images were obtained on a Zeiss LSM 510 meta confocal microscope and analyzed with ZEN Software version 2009. 63X oil lens was used. Adult brains were dissected from newly eclosed *dSOD1*^{WTLoxP/WTLoxP} flies or alive *dSOD1*^{G85R/G85R} pharate adults stuck in the pupal case. Brains were fixed in 4% paraformaldehyde (PFA) and blocked in 5% normal goat serum before antibody

incubation. Primary antibodies, secondary antibodies, and stains were used at the following concentrations: 1:200 anti-HP1 antibody (Developmental Studies Hybridoma Bank (DSHB), overnight incubation at 4°C; 1:200 goat anti-mouse 488 Alexa Fluor (Invitrogen Molecular Probes), 2-3 hours incubation at room temperature, and 10mg/mL DAPI (Invitrogen). Images were contrast-enhanced in Adobe Illustrator.

PEV and Eye-pigmentation Assays

Drosophila were raised and aged at a constant 25°C, on standard molasses food and under 12 h day/night cycles. PEV and eye-pigmentation assays were performed as previously described in (Savva *et al.*, 2013).

dSOD1 mutant (H71Y or G85R) females were crossed with males carrying PEV reporter carrying *mini white* on the 4th chromosome: *Hok^{mw1/mw1}* males:

(♀) [*dSOD1*^{H71Y or WTLoxP or G85R} /TM3,GFP, Ser ; +/+] × (♂) [+/+ ; *Hok^{mw1} / Hok^{mw1}*]

Resulting progeny *dSOD1*^{H71Y or WTLoxP or G85R} /+ ; *Hok^{mw1} /+* were used to quantify eye color mosaicism due to PEV reporter expression.

For eye pigmentation assays, heads of 5 male or female flies (7 days old) from each genotype were placed in methanol and acidified with 0.1% HCl at 4°C overnight for pigment extraction. Heads were homogenized and eye pigmentation was represented as the absorbance of the supernatant at 480 nm. For quantification purposes, this assay was repeated for 5 rounds.

Transcriptome Analysis

Please see chapter 3.

REFERENCES

- CASTEL, S.E. & MARTIENSSEN, R.A. (2013) RNA interference in the nucleus: roles for small RNAs in transcription, epigenetics and beyond. *Nature reviews. Genetics* **14**, 100–112. Nature Publishing Group, a division of Macmillan Publishers Limited. All Rights Reserved.
- ELGIN, S.C.R. & REUTER, G. (2013) Position-effect variegation, heterochromatin formation, and gene silencing in *Drosophila*. *Cold Spring Harbor perspectives in biology* **5**, a017780.
- GIRTON, J.R. & JOHANSEN, K.M. (2008) Chromatin structure and the regulation of gene expression: the lessons of PEV in *Drosophila*. *Advances in genetics* **61**, 1–43.
- GREWAL, S.I.S. & ELGIN, S.C.R. (2007) Transcription and RNA interference in the formation of heterochromatin. *Nature* **447**, 399–406.
- RIDDLE, N.C., SHAFFER, C.D. & ELGIN, S.C.R. (2009) A lot about a little dot - lessons learned from *Drosophila melanogaster* chromosome 4. *Biochemistry and cell biology = Biochimie et biologie cellulaire* **87**, 229–241.
- SAVVA, Y.A., JEPSON, J.E.C., CHANG, Y.-J., WHITAKER, R., JONES, B.C., ST LAURENT, G., TACKETT, M.R., KAPRANOV, P., JIANG, N., DU, G., HELFAND, S.L. & REENAN, R.A. (2013) RNA editing regulates transposon-mediated heterochromatic gene silencing. *Nature communications* **4**, 2745. Nature Publishing Group.
- SCHULZE, S.R. & WALLRATH, L.L. (2007) Gene regulation by chromatin structure: paradigms established in *Drosophila melanogaster*. *Annual review of entomology* **52**, 171–192.

FIGURES and TABLES

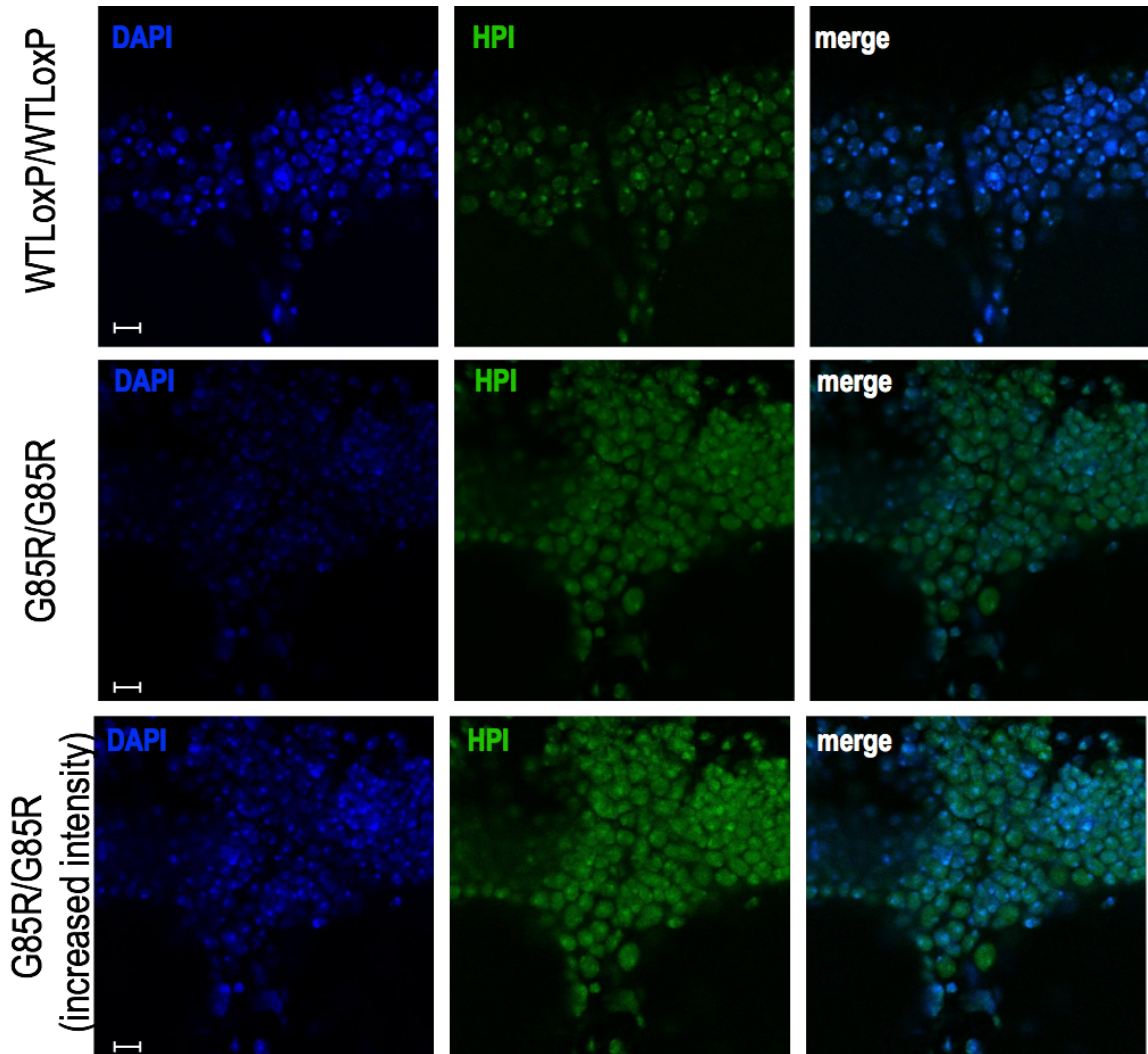


Figure A1. Abnormal chromatin structure in $dSOD1^{G85R/G85R}$ adult brains. Representative confocal stacks showing Heterochromatin Protein 1 (HP1) expression in the ellipsoid body neuronal nuclei from control $dSOD1^{WTLoxP/WTLoxP}$ and experimental $dSOD1^{G85R/G85R}$ adult male brains. N=5, Scale bar, 5 μ m.

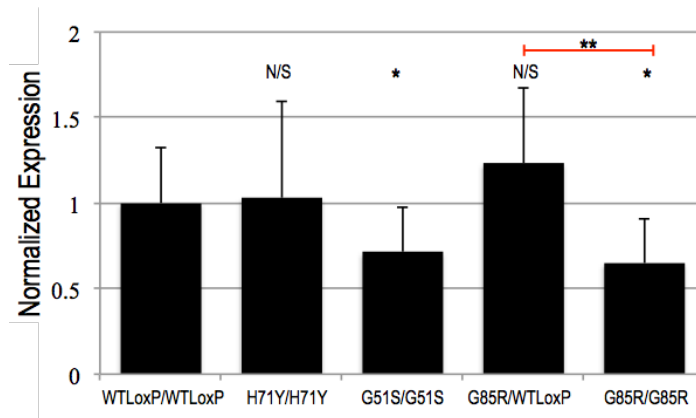


Figure A2. HP1 mRNA expression is altered in other *dSOD1* alleles. HP1 expression based on the RNA sequencing analysis described in chapter 3, in head and thorax tissue together. The expression of each mutant line is normalized to the homologous recombination control WTLoxP. Error bars: SEM. (N = 3 trials). One-way anova test p values ** <0.01 and * <0.05.

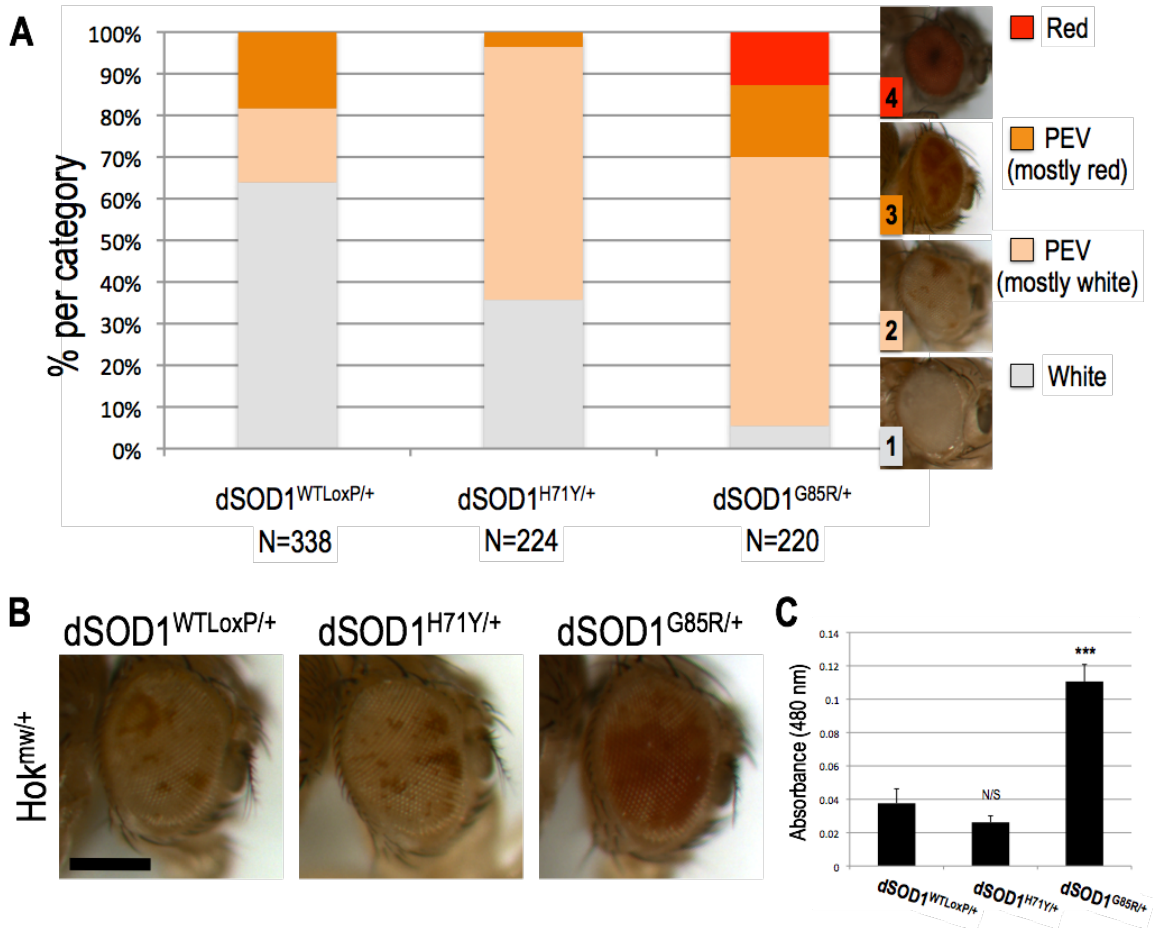


Figure A3. Heterochromatic gene silencing of PEV reporter (Hok^{mw}) is reduced in *Drosophila* ALS model carrying heterozygous $dSOD1^{G85R}$ mutation. A) Position effect variegation qualitative scale and eye color distribution resulting from PEV reporter silencing in $dSOD1^{WTLoxP/+}$, $dSOD1^{G85R/+}$, $dSOD1^{H71Y/+}$. $N > 200$ for each genotype. B) Representative images of Hok^{mw} expression in 7 days old $dSOD1^{WTLoxP/+}$, $dSOD1^{G85R/+}$, $dSOD1^{H71Y/+}$. $dSOD1^{G85R/+}$ eye color is more red due to less silencing of the Hok^{mw} . Scale bar, 150 μm . C) PEV-mediated eye color mosaicism is qualitatively abnormal in $dSOD1^{G85R/+}$. Spectrophotometric absorbance of head homogenates at 480 nm was higher in $dSOD1^{G85R/+}$, indicating decreased silencing of *mini white* ($N = 5$ independent trials of 5 heads each). ($p = 0.0009$, t-test.) Absorbance in $dSOD1^{H71Y/+}$ was not significantly different than controls (N/S). ($p = 0.30$, t-test.) * $p < 0.001$. Error bars: SEM**

APPENDIX II

Specific RNA Editing is not Affected in *dSOD1*^{G85R} *Drosophila* ALS Model

This section investigates the status of RNA editing in *Drosophila* harboring the G85R mutation in *dSOD1*. All the work was done by myself except the sequence chromatograms, which were either analyzed with the help from Dr. Arthur Sugden or with the help of Brown University Summer HHMI undergraduate scholars: Disease Hunters Team (Emily Jang, Kirsten Bredvik, Godwin Boafu, Joshua Hackney, Karla Navarrete, Natalie Palaychuk, Dina Sabetta, Jimmy Xia, Ryan Greene, Ronak Jani). Ronak Jani also helped with RNA isolation and PCR.

INTRODUCTION

One hallmark of ALS in almost all postmortem tissue analyses and animal models is excessive glutamate-induced excitotoxicity of motor neurons eventually leading to degeneration and cell death (Bogaert, d'Ydewalle, & Van Den Bosch, 2010). Excitotoxic motor neuron death is mediated via the influx of calcium ions (Ca^{2+}) through L- α -amino-3-hydroxy-5-methyl-4-isoxazolepropionic acid (AMPA) receptors (Hideyama & Kwak, 2011). AMPA receptors have homo- or hetero-tetrameric structure composed of the GluA1-4 subunits (Previously called GluR1-4 or GluR-A-to-D). The presence of the GluA2 subunit in the tetrameric structure makes the channel impermeable. The mechanism in which the GluA2 subunit diverges from the other subunits and becomes impermeable is through a specific post-transcriptional modification known as A-to-I RNA editing.

A-to-I RNA editing is a site-specific deamination of adenosine bases on double stranded RNA substrates by Adenosine deaminase acting on RNA (ADAR) family enzymes. In mammals three separate loci encode the expression of the editing enzymes: ADAR1, ADAR2 and ADAR3. These enzymes are highly expressed within the nervous system of metazoans. Adenosines are deaminated to inosines, which are recognized by the translational machinery as guanosines. Consequently, A-to-I RNA editing may alter the literal genomic sequence. In this way, ADARs allow neurons powerful fine-tuning abilities through the expansion of genomic capacity and production of extra-genomic proteins (Savva, Rieder, & Reenan, 2012). For example, in the Q/R site of GluA2 subunit mRNA, CAG (coding for glutamine at position 586) edited to CIG, hence translated as CGG (coding for arginine). The edited form results in Ca^{2+} impermeability

(Higuchi *et al.*, 2000). In mammalian motor neurons almost all GluA2 pre-mRNA is edited (>95%), hence AMPA channels are relatively impermeable and resistant to hyperexcitability (Higuchi *et al.*, 1993).

Kwak and colleagues provided the first evidence that A-to-I nucleotide conversion is decreased in sporadic ALS patients (Takuma *et al.*, 1999). In fact, in some patients the editing was completely abolished in a motor neuron specific manner, but not in dying neurons with other neurodegenerative diseases such as degenerating Purkinje cells of patients with spinocerebellar degeneration (Kawahara *et al.*, 2004). In 2012, the same group narrowed down the reason for GluA2 hypo-editing to downregulation of the RNA editing enzyme ADAR2. The levels of the other editing enzymes, ADAR1 and ADAR3, did not change (Hideyama, Yamashita, *et al.*, 2012). The significance of RNA editing in motor neurons became more apparent when motor neuron specific ADAR2-deficient (AR2) mice exhibited decline in motor neuron function later in adulthood and underwent slow death, similar to transgenic rodent models of ALS (Hideyama *et al.*, 2010). Moreover, this slow and progressive motor dysfunction phenotype can be reversed through the expression of the edited version of the GluR2 subunit, highlighting an important role for RNA editing in motor neuron function. Further studies showed that AR2 mice recapitulated the astrogliosis phenotype (Sasaki *et al.*, 2014) and TDP-43 mislocalization, both of which are hallmarks of ALS (Hideyama, Teramoto, *et al.*, 2012). TDP-43 is a nuclear protein involved in the regulation of RNA processing. In ALS patients, TDP-43 is cleaved and mislocalized to the cytoplasm where it forms inclusions (Janssens & Van Broeckhoven, 2013; Ling, Polymenidou, & Cleveland, 2013). Cell culture studies further suggest that TDP-43 mislocalization is a downstream event of

inefficient RNA editing of the GluA2 Q/R site in motor neurons (Yamashita *et al.*, 2012).

Another proposed mechanism of excitotoxicity in ALS is the lack of glutamate removal from the synapses of motor neurons due to reduced expression of the glutamate transporter, EAAT2, in astrocytes (Lin *et al.*, 1998) which is also linked to ALS. A specific adenosine that is a target for ADAR1 within the EAAT2 pre-mRNA is highly edited in affected areas of ALS postmortem tissue and cerebrospinal fluid (CSF) of living ALS patients. The edited version of the EAAT2 protein has reduced glutamate uptake abilities due to creation of an alternative polyadenylation site that leads to intron 7 retention (Flomen & Makoff, 2011).

In addition to direct evidence of the consequences of altered RNA editing on important targets in sporadic ALS patients, a diverse array of other molecular data coming from fALS patients implicates the RNA editing process in ALS. First, hnRNPA2/B1, an enhancer of RNA editing (Garncarz *et al.*, 2013), was recently linked to ALS (Kim *et al.*, 2013). Second, RNA foci from iPSC-derived motor neurons from ALS patients with C9orf72 expansion of hexanucleotide repeats contain ADAR2 and/or ADAR3 proteins (Donnelly *et al.*, 2013).

All of these findings on specific adenosine modifications in primary sequence of mRNA and downregulation of RNA editing enzymes in ALS suggest that RNA processing/RNA editing may represent a common pathogenic mechanism involved in the development of ALS pathogenesis. RNA editing deficiencies in *Drosophila* result in striking neurological phenotypes similar to ALS as discussed in chapter 2, including extreme uncoordination and neurodegeneration (Palladino *et al.*, 2000). To provide new

avenues for exploration into the disease's connection to RNA processing/metabolism, we sought to examine ADAR activity in a *Drosophila* model of SOD1-caused ALS. A fly model was chosen due to the wealth of genetic manipulations available, speed and quantity of reproduction, and high degree of conservation of *SOD1* and *dAdar* sequence. Most importantly, *Drosophila* has single RNA editing enzyme, dAdar, while mammals have three (Savva *et al.*, 2012).

RESULTS and DISCUSSION

Since ADAR protein levels are reduced in sALS patients, we first investigated whether dAdar protein levels are reduced in our *Drosophila* model of ALS expressing G85R point mutation. There is no commercially available ADAR antibody. However, our laboratory previously generated an HA tagged dAdar via homologous recombination (Jepson *et al.*, 2011). Western blot assays revealed no difference in ADAR protein in both homozygous and heterozygous ALS mutant flies (Figure B1).

In order to investigate whether there is a specific RNA editing reduction on certain dADAR targets as in GluR2 editing reduction in ALS patients, next we calculated RNA editing efficiency at some of the neurologically relevant dAdar targets in *Drosophila dSOD1^{G85R/G85R}* from head and thorax of male and female flies. No major differences in RNA editing or expression levels of dAdar were noted in G85R homozygotes relative to genetic controls (Table B1, B2, B3, B4). It is important to note here that all dAdar targets were not able to be amplified via generic PCR primers described in Supplementary Table D2, which suggests possible RNA metabolism

differences, such as expression differences or alternative splicing differences in *dSOD1*^{G85R/G85R} flies.

dAdar is highly expressed in the adult nervous system (Jepson & Reenan, 2009). It is possible that *dSOD1*^{G85R/G85R} flies dying during eclosion are not affected by possible dAdar RNA editing consequences. Despite these discouraging results, we recommend further studies to clarify potential involvement of dAdar on *dSOD1*^{H71Y/H71Y} flies which can live an average of two weeks adult life (Chapter 2). Transcriptome analysis, widely discussed in chapter 3, suggest a modest reduction in dADAR mRNA levels in the other ALS mutant alleles: *dSOD1*^{H71Y/H71Y} and *dSOD1*^{G51S/G51S} (Figure B.2).

MATERIALS and METHODS

RNA Editing Analysis

Drosophila were raised at a constant 25°C, on standard molasses food and under 12 h day/night cycles. For analysis of RNA editing targets, RNA was derived from 20 heads or thoraces of newly eclosed *dSOD1*^{WTLoxP/WTLoxP} flies or alive *dSOD1*^{G85R/G85R} adults stuck in pupal case. RNA extractions from *Drosophila* tissues were performed using standard TRIzol (Invitrogen) extraction. cDNAs were synthesized using random primers (Life Technologies 48190-011). Editing target cDNAs were amplified via PCR using target specific primers and Sanger sequenced via target specific primers listed in Supplementary Table D2.

The editing ratios are calculated by two methods: computational calculation described in Appendix IV (Savva, Jepson, et al., 2012) or ImageJ calculation. In sequencing electropherograms, editing sites were located using published editing atlas

Supplementary Figure D1. ImageJ was used to calculate area under the curve of editing site adenosine (A) and guanosine (G) peaks in individual electropherogram traces. Percent editing is expressed at $100*[G/(A+G)]$. A minimum of three independent PCR amplicons were used to measure RNA editing levels for each gene analyzed.

Western Blotting

dSOD1^{WTLoxP} and *dSOD1^{G85R}* alleles were combined with *dAdar^{HA}* allele. *dSOD1* alleles are described in Chapter 2 and the *dAdar^{HA}* allele is described in Supplementary figure C1. In *dAdar^{Hypomorph}*, the endogenous locus is interrupted via mini white gene leading to hypomorph allele of dAdar (Jepson et al., 2011).

Protein samples were prepared in buffer containing SDS and β -mercaptoethanol, and run out on a 10% gel (Amresco). 10 adult heads or thoraces/50 μ L of buffer were used per sample. 20 μ L of sample was loaded to each lane. Anti-HA antibody (Covance) was used at 1:500, and anti-actin (Millipore) was used at 1:50000, goat anti-mouse polyclonal HRP secondary antibody (ab5930) was used at 1:5000. Band intensities were quantified on ImageJ.

Transcriptome Analysis

Please see chapter 3.

REFERENCES

- BOGAERT, E., D'YDEWALLE, C. & VAN DEN BOSCH, L. (2010) Amyotrophic lateral sclerosis and excitotoxicity: from pathological mechanism to therapeutic target. *CNS & neurological disorders drug targets* **9**, 297–304.
- DONNELLY, C.J., ZHANG, P.-W., PHAM, J.T., HAEUSLER, A.R., HEUSLER, A.R., MISTRY, N.A., ET AL. (2013) RNA toxicity from the ALS/FTD C9ORF72 expansion is mitigated by antisense intervention. *Neuron* **80**, 415–428. Elsevier.

- FLOMEN, R. & MAKOFF, A. (2011) Increased RNA editing in EAAT2 pre-mRNA from amyotrophic lateral sclerosis patients: Involvement of a cryptic polyadenylation site. *Neuroscience Letters* **497**, 139–143.
- GARNCARZ, W., TARIQ, A., HANDL, C., PUSCH, O. & JANTSCH, M.F. (2013) A high-throughput screen to identify enhancers of ADAR-mediated RNA-editing. *RNA biology* **10**, 192–204.
- HIDEYAMA, T. & KWAK, S. (2011) When Does ALS Start? ADAR2?GluA2 Hypothesis for the Etiology of Sporadic ALS. *Frontiers in Molecular Neuroscience*. .
- HIDEYAMA, T., TERAMOTO, S., HACHIGA, K., YAMASHITA, T. & KWAK, S. (2012) Co-occurrence of TDP-43 mislocalization with reduced activity of an RNA editing enzyme, ADAR2, in aged mouse motor neurons. *PLoS one* **7**, e43469.
- HIDEYAMA, T., YAMASHITA, T., AIZAWA, H., TSUJI, S., KAKITA, A., TAKAHASHI, H. & KWAK, S. (2012) Profound downregulation of the RNA editing enzyme ADAR2 in ALS spinal motor neurons. *Neurobiology of disease* **45**, 1121–1128.
- HIDEYAMA, T., YAMASHITA, T., SUZUKI, T., TSUJI, S., HIGUCHI, M., SEEBURG, P.H., TAKAHASHI, R., MISAWA, H. & KWAK, S. (2010) Induced loss of ADAR2 engenders slow death of motor neurons from Q/R site-unedited GluR2. *The Journal of neuroscience : the official journal of the Society for Neuroscience* **30**, 11917–11925.
- HIGUCHI, M., MAAS, S., SINGLE, F.N., HARTNER, J., ROZOV, A., BURNASHEV, N., FELDMEYER, D., SPRENGEL, R. & SEEBURG, P.H. (2000) Point mutation in an AMPA receptor gene rescues lethality in mice deficient in the RNA-editing enzyme ADAR2. *Nature* **406**, 78–81.
- HIGUCHI, M., SINGLE, F.N., KÖHLER, M., SOMMER, B., SPRENGEL, R. & SEEBURG, P.H. (1993) RNA editing of AMPA receptor subunit GluR-B: a base-paired intron-exon structure determines position and efficiency. *Cell* **75**, 1361–1370.
- JANSSENS, J. & VAN BROECKHOVEN, C. (2013) Pathological mechanisms underlying TDP-43 driven neurodegeneration in FTLD-ALS spectrum disorders. *Human Molecular Genetics* **22**.
- JEPSON, J.E.C. & REENAN, R.A. (2009) Adenosine-to-inosine genetic recoding is required in the adult stage nervous system for coordinated behavior in Drosophila. *The Journal of biological chemistry* **284**, 31391–31400.
- JEPSON, J.E.C., SAVVA, Y.A., YOKOSE, C., SUGDEN, A.U., SAHIN, A. & REENAN, R.A. (2011) Engineered alterations in RNA editing modulate complex behavior in Drosophila: regulatory diversity of adenosine deaminase acting on RNA (ADAR) targets. *The Journal of biological chemistry* **286**, 8325–8337.
- KAWAHARA, Y., ITO, K., SUN, H., AIZAWA, H., KANAZAWA, I. & KWAK, S. (2004) Glutamate receptors: RNA editing and death of motor neurons. *Nature* **427**, 801.
- KIM, H.J., KIM, N.C., WANG, Y.-D., SCARBOROUGH, E.A., MOORE, J., DIAZ, Z., ET AL. (2013) Mutations in prion-like domains in hnRNPA2B1 and hnRNPA1 cause multisystem proteinopathy and ALS. *Nature* **495**, 467–473.
- LIN, C.L., BRISTOL, L.A., JIN, L., DYKES-HOBERG, M., CRAWFORD, T., CLAWSON, L. & ROTHSTEIN, J.D. (1998) Aberrant RNA processing in a neurodegenerative disease: the cause for absent EAAT2, a glutamate transporter, in amyotrophic lateral sclerosis. *Neuron* **20**, 589–602.

- LING, S.C., POLYMERIDOU, M. & CLEVELAND, D.W. (2013) Converging mechanisms in ALS and FTD: Disrupted RNA and protein homeostasis. *Neuron* .
- PALLADINO, M.J., KEEGAN, L.P., O'CONNELL, M.A. & REENAN, R. A (2000) A-to-I pre-mRNA editing in *Drosophila* is primarily involved in adult nervous system function and integrity. *Cell* **102**, 437–449.
- SASAKI, S., YAMASHITA, T., HIDEYAMA, T. & KWAK, S. (2014) Unique nuclear vacuoles in the motor neurons of conditional ADAR2-knockout mice. *Brain Research* **1550**, 36–46.
- SAVVA, Y.A., RIEDER, L.E. & REENAN, R.A. (2012) The ADAR protein family. *Genome biology* **13**, 252.
- TAKUMA, H., KWAK, S., YOSHIKAWA, T. & KANAZAWA, I. (1999) Reduction of GluR2 RNA editing, a molecular change that increases calcium influx through AMPA receptors, selective in the spinal ventral gray of patients with amyotrophic lateral sclerosis. *Annals of neurology* **46**, 806–815.
- YAMASHITA, T., HIDEYAMA, T., TERAMOTO, S. & KWAK, S. (2012) The abnormal processing of TDP-43 is not an upstream event of reduced ADAR2 activity in ALS motor neurons. *Neuroscience research* **73**, 153–160.

FIGURES and TABLES

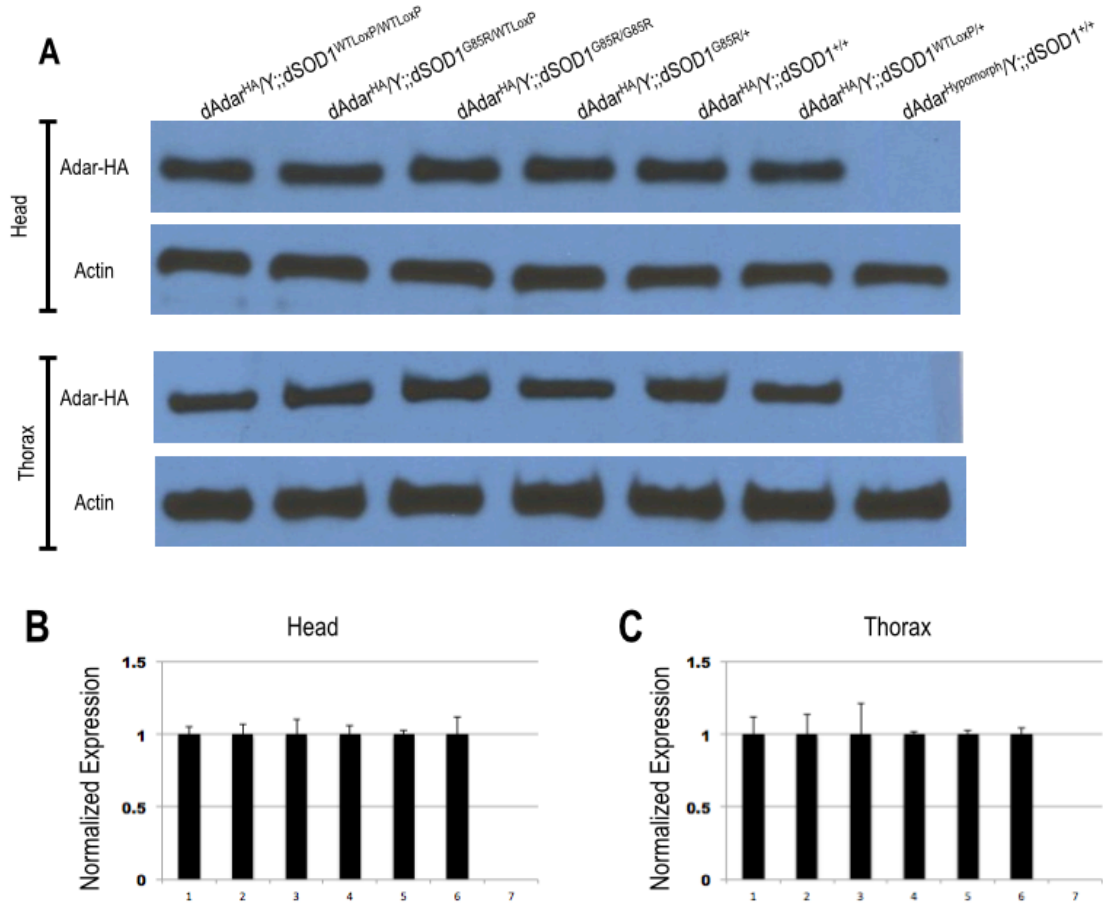


Figure B1. dAdar protein levels have not changed in response to the presence of *dSOD1^{G85R}* allele. **A)** Representative Western blots showing expression of dAdar in *Drosophila* mutants for *dSOD1^{G85R}* (N = 3 gels). In head and thorax tissue separately, dAdar was probed via HA (human influenza hemagglutinin) tag and normalized to an internal reference actin. *dAdar^{hypomorph}* allele is used as a negative control. *dAdar^{hypomorph}* expresses trace amount of dAdar (Jepson *et al.*, 2011). **B)** Head; **C)** Thorax western blot quantification. Equal amounts of dAdar protein were detected in all lines tested except engineered dAdar hypomorph. Data were expressed as a relative ratio of immunoblot reactivity of the antibody staining for HA to actin. Error bars: SEM.

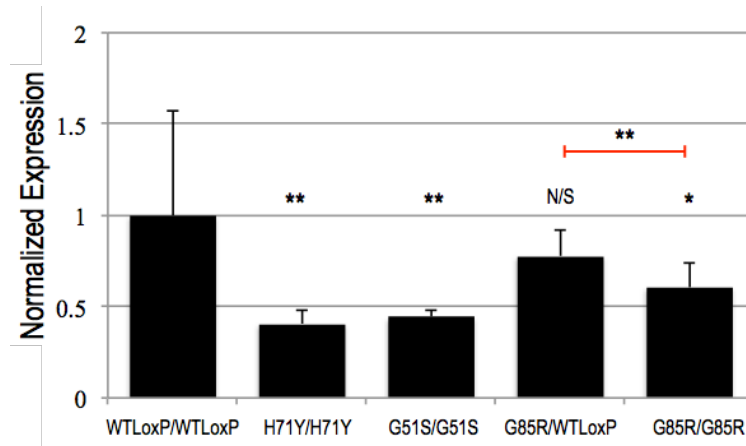


Figure B2. dAdar mRNA expression is altered in other *dSOD1* alleles. dAdar expression based on the average of three trials of RNA sequencing analysis described in chapter 3, in head and thorax tissue together. The expression of each mutant line is normalized to the homologous recombination control WTLoxP. Error bars: SEM. (N = 3 trials). One-way anova test p values ** <0.01 and * <0.05.

Table B1. Measurement of A-to-I editing percentage in male *Drosophila* thorax. The average editing percentage is obtained from at least 3 experimental replicates. No major editing level change is observed. Full names of the RNA Editing targets and their functions can be found in Supplementary Table D1.

RNA Editing Target Name	G85R Average	G85R std dev	WTLoxP Average	WTLoxP std dev	% Change G85R ^{Ave} -WTLoxP ^{Ave}
syt1	9.33	0.79	21.00	3.55	-11.68
syt2	51.77	1.91	58.08	3.01	-6.31
syt3	70.67	2.07	72.36	2.27	-1.69
syt4	91.83	1.36	92.72	1.17	-0.89
syt5	4.48	3.66	11.22	2.31	-6.74
syt6	3.84	1.79	13.07	2.53	-9.23
cpx1	92.92	1.89	91.87	1.51	1.05
cpx2	39.21	1.02	35.98	2.30	3.23
cpx3	74.75	0.85	73.67	1.05	1.09
unc1	50.93	1.84	67.44	0.71	-16.50
stn1	84.86	2.86	84.66	1.82	0.20
dsc1	34.67	3.48	37.79	3.00	-3.12
stj1	89.90	1.54	91.56	2.09	-1.66
stj2	34.63	3.03	36.40	2.04	-1.77
stj3	44.94	4.50	50.92	4.70	-5.98
cat1	58.36	4.49	71.76	1.29	-13.40
eag1	100.00	100.00	93.61	2.50	6.39
eag2	96.39	1.60	94.64	2.62	1.75
eag3	19.80	4.26	20.84	2.70	-1.04

RNA Editing Target Name	G85R Average	G85R std dev	WTLoxP Average	WTLoxP std dev	% Change G85R ^{Ave} -WTLoxP ^{Ave}
eag4	96.16	1.90	92.04	3.66	4.12
eag5	7.90	2.91	11.56	4.33	-3.65
eag6	51.38	1.35	52.32	3.95	-0.94
eag7	2.33	2.04	3.24	2.87	-0.91
slo1	91.90	1.12	94.73	0.75	-2.83
slo2	97.68	0.86	97.74	0.37	-0.06
rdl1	55.16	1.84	48.98	0.99	6.18
rdl2	90.55	0.78	88.24	0.98	2.31
rdl3	86.57	8.51	90.16	2.89	-3.59
rdl4	21.12	7.38	22.38	3.19	-1.26
rdl5	19.52	5.27	12.16	2.35	7.36
rdl6	45.19	5.89	43.96	0.98	1.22
daf1	84.21	0.98	88.43	0.47	-4.22
daf2	75.65	5.44	83.48	2.26	-7.83
daf3	97.89	2.53	99.54	0.70	-1.65
daf4	40.13	2.25	51.05	4.06	-10.92
daf5	34.08	6.02	46.68	2.93	-12.60
daf6	77.00	2.18	82.56	2.37	-5.56
daf7	20.10	2.37	19.98	1.17	0.12
daf8	86.14	1.74	87.41	1.51	-1.27
daf9	30.39	3.23	33.22	3.55	-2.83
das1	21.33	2.51	19.12	3.48	2.21
das2	26.85	1.24	30.66	3.30	-3.81
das3	74.74	2.21	78.79	1.13	-4.05
das4	71.03	2.55	73.61	1.79	-2.58
das5	81.56	1.42	77.94	1.33	3.62
das6	61.38	1.08	66.12	3.18	-4.74
ard1	70.80	3.22	72.09	2.11	-1.29
ard2	91.70	7.20	89.03	5.53	2.67
ard3	59.24	1.20	60.46	0.87	-1.21
ard4	100.00	0.00	100.00	0.00	0.00
adr1	53.90	9.13	51.18	6.39	2.72
glu1	28.36	4.15	24.75	1.76	3.61
glu2	46.84	10.34	70.42	0.66	-23.58
glu3	20.96	2.24	5.25	0.76	15.72
dop1	21.46	1.12	22.12	5.36	-0.66
dop2	10.75	2.81	15.92	1.89	-5.17
dop3	21.35	1.53	19.54	2.76	1.80
dop4	42.88	3.63	48.45	7.89	-5.57
dop5	19.44	0.79	22.16	1.04	-2.72
dop6	19.29	3.89	14.95	1.21	4.34
dop7	53.35	0.64	58.65	5.43	-5.30
dop8	79.65	5.41	77.31	0.40	2.33
dop9	86.11	0.78	92.06	4.25	-5.96
dop10	4.98	3.57	3.45	0.72	1.53

Table B2. Measurement of A-to-I editing percentage in female *Drosophila* thorax. The average editing percentage is obtained from at least 3 experimental replicates. No major editing level change is observed. Full names of the RNA Editing targets and their functions can be found in Supplementary Table D1.

RNA Editing Target Name	G85R Average	G85R std dev	WTLoxP Average	WTLoxP std dev	% Change G85R ^{Ave} -WTLoxP ^{Ave}
syt1	4.91	2.59	16.56	4.48	-11.64
syt2	48.60	3.61	51.83	2.62	-3.22
syt3	75.80	3.35	70.58	0.49	5.22
syt4	90.52	0.94	91.06	0.88	-0.54
syt5	20.68	5.85	12.65	5.07	8.03
syt6	3.32	5.66	9.88	1.43	-6.56
cpx1	90.32	3.12	92.67	0.27	-2.35
cpx2	37.32	2.10	34.64	3.21	2.68
cpx3	75.33	1.75	73.74	1.82	1.59
unc1	53.13	0.95	62.76	1.27	-9.63
stn1	80.44	0.54	83.03	4.01	-2.60
stj1	83.29	1.02	91.77	0.87	-8.48
stj2	32.57	3.66	34.57	1.43	-2.00
stj3	43.21	4.26	47.20	2.02	-3.99
cat1	62.94	4.27	65.81	1.22	-2.87
eag1	89.15	1.73	85.19	6.47	3.96
eag2	93.85	3.90	95.41	1.96	-1.56
eag3	18.88	4.85	18.25	1.70	0.63
eag4	95.91	4.11	95.39	2.47	0.51
eag5	11.12	0.04	15.61	4.43	-4.49
eag6	58.30	4.95	56.21	5.90	2.10
eag7	1.21	0.28	3.06	2.66	-1.86
slo1	92.39	1.80	91.25	2.71	1.13
slo2	96.33	0.86	95.70	0.66	0.62
rdl1	40.59	9.51	47.27	3.59	-6.68
rdl2	69.05	6.19	75.84	9.34	-6.80
rdl3	92.23	3.12	92.24	4.25	-0.01
rdl4	26.09	4.83	20.97	0.92	5.12
rdl5	11.72	5.66	16.34	1.03	-4.62
rdl6	26.17	3.18	32.91	2.04	-6.74
daf1	83.85	3.38	87.88	1.44	-4.02
daf2	77.50	3.64	84.55	2.06	-7.05
daf3	92.30	6.13	97.82	2.07	-5.52
daf4	51.67	4.10	50.23	4.81	1.44
daf5	41.28	4.65	46.44	4.03	-5.16
daf6	78.43	3.25	81.43	2.95	-3.00
daf7	25.78	13.69	17.93	0.91	7.85
daf8	78.62	6.67	84.82	1.67	-6.19
daf9	22.49	4.68	36.90	3.14	-14.41
das1	12.41	4.43	16.79	0.91	-4.38

RNA Editing Target Name	G85R Average	G85R std dev	WTLoxP Average	WTLoxP std dev	% Change G85R ^{Ave} -WTLoxP ^{Ave}
das2	29.85	3.59	28.25	1.57	1.60
das3	67.36	2.15	74.30	2.77	-6.94
das4	67.98	3.40	74.29	2.20	-6.31
das5	72.48	2.79	73.71	3.64	-1.24
das6	65.28	6.99	63.16	4.78	2.11
ard1	66.01	2.56	65.74	5.31	0.27
ard2	87.14	5.23	80.20	7.34	6.94
ard3	51.20	3.12	55.83	2.67	-4.62
ard4	97.02	4.54	100.00	0.00	-2.98
adr1	56.15	5.65	52.45	4.18	3.71

Table B3. Measurement of A-to-I editing percentage in male *Drosophila* head. The average editing percentage is obtained from at least 3 experimental replicates. No major editing level change is observed. Full names of the RNA Editing targets and their functions can be found in Supplementary Table D1.

RNA Editing Target Name	G85R Average	G85R std dev	WTLoxP Average	WTLoxP std dev	% Change G85R ^{Ave} -WTLoxP ^{Ave}
syt1	0.20	0.28	0.25	0.43	-0.05
syt2	32.82	0.17	24.88	3.37	7.94
syt3	51.55	2.32	53.49	2.91	-1.94
syt4	81.49	1.46	84.11	0.63	-2.62
syt5	0.50	0.91	0.00	0.00	0.50
syt6	0.00	0.00	0.00	0.00	0.00
cpx1	70.00	3.71	70.15	2.68	-0.15
cpx2	22.84	2.65	22.37	4.15	0.47
cpx3	47.16	1.56	45.11	3.35	2.05
unc1	62.67	0.74	69.71	0.38	-7.04
stn1	77.95	1.16	76.58	0.66	1.37
stj1	92.18	3.11	84.19	3.55	7.99
stj2	32.91	2.66	27.78	5.66	5.13
stj3	40.10	1.68	32.94	3.57	7.17
cat1	91.02	1.17	88.14	1.74	2.88
eag1	61.72	1.61	70.47	2.23	-8.75
eag2	87.32	0.68	90.58	2.00	-3.26
eag3	12.57	1.20	12.31	3.30	0.26
eag4	83.65	0.80	86.34	1.86	-2.69
eag5	10.46	1.06	7.90	2.26	2.56
eag6	58.60	1.41	55.69	0.72	2.91
eag7	3.53	0.64	0.00	0.00	3.53
slo1	90.07	1.94	81.15	1.70	8.93
slo2	99.21	1.36	94.46	1.79	4.76
rdl1	24.21	4.14	25.08	2.99	-0.86
rdl2	63.46	1.58	65.83	0.06	-2.37
rdl3	95.36	2.75	94.15	3.38	1.22
rdl4	19.22	2.04	20.01	1.88	-0.78

RNA Editing Target Name	G85R Average	G85R std dev	WTLoxP Average	WTLoxP std dev	% Change G85R ^{Ave} -WTLoxP ^{Ave}
rdl5	6.35	1.51	8.85	4.58	-2.51
rdl6	14.76	1.08	13.15	1.17	1.61
daf1	84.11	0.76	87.17	1.95	-3.06
daf2	70.45	8.58	75.83	1.74	-5.38
daf3	99.94	0.13	98.28	0.66	1.66
daf4	48.98	4.21	34.30	5.17	14.68
daf5	36.75	3.68	30.96	3.38	5.79
daf6	69.57	3.22	66.99	4.40	2.58
daf7	17.91	4.19	15.60	2.86	2.30
daf8	80.86	1.35	73.16	4.02	7.70
daf9	17.59	1.68	12.08	4.10	5.51
das1	16.25	2.68	13.26	2.90	2.99
das2	28.02	3.20	23.93	2.22	4.09
das3	78.73	2.49	81.00	1.93	-2.27
das4	77.30	3.16	77.49	2.77	-0.19
das5	84.93	1.49	79.59	1.63	5.34
das6	64.86	1.96	66.87	3.97	-2.02
ard1	60.03	1.88	64.31	1.65	-4.28
ard2	67.43	0.56	78.26	3.90	-10.82
ard3	19.32	0.88	26.74	1.79	-7.42
ard4	92.38	3.37	93.81	2.38	-1.43
adr1	53.17	8.20	56.25	11.03	-3.08

Table B4. Measurement of A-to-I editing percentage in female *Drosophila* head. The average editing percentage is obtained from at least 3 experimental replicates. No major editing level change is observed. Full names of the RNA Editing targets and their functions can be found in Supplementary Table D1.

RNA Editing Target Name	G85R Average	G85R std dev	WTLoxP Average	WTLoxP std dev	% Change G85R ^{Ave} -WTLoxP ^{Ave}
syt1	0.34	0.77	0.52	1.04	-0.18
syt2	30.85	3.13	22.33	3.09	8.52
syt3	57.19	2.88	52.53	1.77	4.66
syt4	81.99	1.22	81.30	0.76	0.69
syt5	15.74	2.92	11.69	2.76	4.05
syt6	0.00	0.00	0.59	0.72	-0.59
cpx1	67.69	2.47	68.93	1.72	-1.24
cpx2	18.68	2.27	17.61	1.03	1.07
cpx3	42.10	4.44	39.34	3.30	2.76
unc1	60.71	1.06	66.30	0.95	-5.58
stn1	78.93	1.73	73.01	5.45	5.92
stj1	88.93	1.65	82.10	6.34	6.84
stj2	29.91	5.92	26.79	4.52	3.12
stj3	34.27	4.49	34.30	2.09	-0.03
cat1	86.17	1.28	91.72	2.85	-5.55
eag1	54.25	0.37	63.26	7.54	-9.02

RNA Editing Target Name	G85R Average	G85R std dev	WTLoxP Average	WTLoxP std dev	% Change G85R^{Ave}-WTLoxP^{Ave}
eag2	89.49	0.28	86.30	2.21	3.20
eag3	17.26	0.68	18.03	15.89	-0.77
eag4	86.02	0.50	79.41	4.17	6.61
eag5	12.31	0.32	13.31	7.37	-1.00
eag6	51.29	2.88	50.00	0.00	1.29
eag7	2.92	2.58	0.00	0.00	2.92
slo1	90.01	1.59	90.29	2.39	-0.28
slo2	97.54	0.35	97.60	1.01	-0.06
rdl1	25.36	5.96	26.24	2.33	-0.88
rdl2	63.13	0.88	65.88	4.01	-2.75
rdl3	94.09	1.26	94.24	1.86	-0.15
rdl4	21.68	0.50	22.36	2.15	-0.67
rdl5	6.77	2.38	5.75	0.82	1.02
rdl6	15.20	1.81	13.57	1.76	1.63
daf1	86.25	1.66	83.12	1.91	3.13
daf2	82.38	3.69	75.34	3.24	7.03
daf3	97.92	2.57	97.74	1.91	0.18
daf4	42.00	4.71	34.78	4.09	7.22
daf5	34.65	3.31	29.81	1.97	4.84
daf6	71.29	3.57	63.70	3.20	7.59
daf7	16.12	0.87	16.02	1.40	0.10
daf8	79.40	1.06	76.05	0.90	3.35
daf9	14.97	1.09	14.49	3.06	0.48
das1	10.39	1.22	12.29	0.34	-1.90
das2	18.92	1.06	20.85	0.36	-1.93
das3	73.21	0.75	73.14	1.25	0.07
das4	71.80	3.05	72.32	1.08	-0.52
das5	82.12	1.47	78.58	1.58	3.53
das6	54.94	4.93	67.13	1.39	-12.19
ard1	60.19	0.26	61.16	3.58	-0.97
ard2	76.55	1.02	75.97	11.53	0.58
ard3	21.82	5.80	30.97	2.06	-9.15
ard4	93.68	0.37	91.30	5.41	2.38
adr1	51.26	10.31	51.14	4.37	0.12

APPENDIX III

Engineered Alterations in RNA Editing Modulate Complex Behavior in *Drosophila*: Regulatory diversity of Adenosine Deaminase Acting on RNA (ADAR) Targets

This section consists of previous published data. “Engineered Alterations in RNA Editing Modulate Complex Behavior in *Drosophila*. Jepson JE, Savva YA, Yokose C, Sugden AU, Sahin A and Reenan RA. Journal of Biological Chemistry 286 (10): 8325-8337, 2011. I performed the behavioral analysis of ADAR hypomorphs along with Jepson JE.

ABSTRACT

Select proteins involved in electrical and chemical neurotransmission are re-coded at the RNA level via the deamination of particular adenosines to inosine by adenosine deaminases acting on RNA (ADARs). It has been hypothesized that this process, termed RNA editing, acts to “fine-tune” neurophysiological properties in animals and potentially downstream behavioral outputs. However, the extreme phenotypes resulting from deletions of *adar* loci have precluded investigations into the relationship between ADAR levels, target transcripts, and complex behaviors. Here, we engineer *Drosophila* hypomorphic for ADAR expression using homologous recombination. A substantial reduction in ADAR activity (>80%) leads to altered circadian motor patterns and abnormal male courtship, although surprisingly, general locomotor coordination is spared. The altered phenotypic landscape in our *adar* hypomorph is paralleled by an unexpected dichotomous response of ADAR target transcripts, *i.e.* certain adenosines are minimally affected by dramatic ADAR reduction, whereas editing of others is severely curtailed. Furthermore, we use a novel reporter to map RNA editing activity across the nervous system, and we demonstrate that knockdown of editing in *fruitless*-expressing neurons is sufficient to modify the male courtship song. Our data demonstrate that network-wide temporal and spatial regulation of ADAR activity can tune the complex system of RNA-editing sites and modulate multiple ethologically relevant behavioral modalities.

INTRODUCTION

Informational recoding of RNA by the catalytic deamination of adenosine to inosine proceeds through the action of ADARs (Nishikura, 2010). Long double strand RNA duplexes exhibiting perfect complementarity can be modified extensively by promiscuous ADAR activity. However, mRNAs may also serve as site-specific substrates for ADARs via base pairing interactions that generate short imperfect duplexes that generally include the exon destined for editing and a *cis*-acting complementary sequence, usually found in a neighboring intron (Higuchi et al., 1993; Reenan, 2005). Because inosine is recognized by the translation machinery as guanosine (Basillo et al., 1962), A-to-I editing in mRNAs can lead to the incorporation of amino acids differing from those specified by the literal genome.

In *Drosophila*, the spectrum of ADAR substrates is peculiarly specific, consisting primarily of mRNAs encoding an array of voltage- and ligand-gated ion channels, as well as numerous pre-synaptic proteins involved in exo- and endocytosis of synaptic vesicles (Grauso et al., 2002; Hoopengardner et al., 2003; Semenov and Pak, 1999; Smith et al., 1998). Similarly, several mammalian ion channels and G-protein-coupled receptors are also subject to RNA editing (Bhalla et al., 2004; Burns et al., 1997; Higuchi et al., 1993; Hoopengardner et al., 2003; Ohlson et al., 2007). In light of the ontological class and high sequence conservation of ADAR target genes, RNA editing has been invoked as an essential function in controlling synaptic transmission and neurophysiology. Correspondingly, deletion of the single *Drosophila adar* locus (*dAdar*) results in severe adult-stage behavioral abnormalities, including extreme uncoordination, seizures and a complete lack of courtship in *dAdar* null (*dAdar*^{sg1}) males (Palladino et al., 2000a),

whereas mice lacking ADAR2 suffer from seizures and early mortality (Higuchi et al., 2000).

Due to the presence of a single X-linked *adar* locus and more than 100 mRNA sites of dADAR modification, *Drosophila* provides an ideal system to study the correlation between deaminase levels and recoding output. We have previously shown that restoration of editing in the adult nervous system partially rescues the locomotor defect of *dAdar*-deficient males, an effect that appears to be independent of any interactions between *dAdar* and the RNAi pathway (Jepson and Reenan, 2009). However, the pattern of dADAR expression and activity within the fly nervous system is currently unknown. Furthermore, although previous studies have focused on the relationship between dADAR activity and motor control, it is unclear whether complex behaviors require regulated editing and, if so, whether subpopulations of edited proteins contribute to distinct behavioral outputs.

Here, we investigate these issues using homologous recombination and a molecular reporter for RNA editing activity. Although dADAR expression can be detected in almost all neuronal nuclei, significant variation in dADAR activity exists between genetically distinct neurons. Finally, through the generation of a novel hypomorphic *dAdar* allele, we demonstrate an unexpectedly complex relationship between *in vivo* dADAR levels and deamination of specific RNA editing targets. These data, combined with neuron-specific dADAR knockdown, demonstrate that correct regulation of editing activity at both cell-autonomous and network levels is required for behavioral outputs in *Drosophila* and provide mechanistic insight into the complex landscape of proteomic diversity generated by RNA editing.

MATERIALS AND METHODS

***Drosophila* Strains and Genetics**

For a full list of *Drosophila* strains used, see supplemental Tables S2.1 and S2.2. Flies were raised at a constant 25 °C, on standard molasses food, and under 12-h day/night cycles. Both *dAdar* RNAi transgenes were obtained from the Vienna *Drosophila* RNAi Stock Center. Generation of the double RNAi line was described previously (Jepson and Reenan, 2009). Tissue-specific Gal4 lines were obtained from the Bloomington stock center.

Ends-out Homologous Recombination of the dAdar Locus

We performed ends out homologous recombination using a similar methodology to that reported previously (Maggert et al., 2008). Briefly, we utilized the ends-out targeting vector p [w25.2] that contains the *white+* selectable eye color mini-gene flanked by LoxP sites for subsequent removal by Cre-recombinase. Homology arms were cloned and sequenced in pTOPO (Invitrogen) and then shuttled into the multiple cloning sites of the vector to generate p [w25-dADAR-HA], which was then introduced into the *Drosophila* genome by standard transgenic methods (Genetic Services Inc.).

The cloning strategy is as follows, where all genomic coordinates are given by the *Drosophila melanogaster* draft, BDGP Release 5, with release 5.12 annotation provided by FlyBase at the UCSC Genome Browser. Arm 1 is the 5' arm of p [w25-dADAR-HA] (see Fig. 2.1) and was generated by PCR amplification to incorporate cloning sites as follows: Arm 1, *BsiWI*-1,673,865–1,676,526-*AscI*. Arm 2 is the 3' arm of P[w25-

dADAR-HA] and was generated in two parts by PCR amplification to incorporate cloning sites and an HA epitope tag; Arm2, *Acc65I*-1,676,602–1677784-HA/*NheI*-1,677,788–1,679,400-*NotI*. The HA tag sequence was inserted after the terminal glutamate codon of *dAdar* (GAA) ending in an opal (TGA) stop codon and an *NheI* (gctagc) cutting site as follows: GAAtacccttacgatgttctctgattacgccagcctgTGAgctagc.

Targeting was performed to generate multiple independent targeting events in which the HA tag was incorporated or excluded from the recombination events. Targeted alleles were validated by amplification using primers outside the region of targeting. All targeted alleles were sequenced to verify only the presence of indicated sequences. Subsequent removal of the *white+* mini-gene selectable marker was achieved by performing crosses to animals expressing Cre-recombinase and re-isolation of targeted chromosomes containing a single LoxP site. The recombinant alleles were subsequently backcrossed to Canton-S for five generations.

Behavioral Analysis

Locomotor patterns were recorded using horizontal, single fly activity monitors (TriKinetics). Flies were left to acclimatize for ~12 h before recording was initiated. An average daily pattern was calculated for each fly by averaging data from 3 consecutive days. These values were then further averaged across the experimental population. Mating assays and song recording were performed in a custom-made chamber. For each assay, 5–7-day-old males and 3–5-day-old virgin females were used, and the time taken for male initiation of courtship (latency) and the courtship index (time spent courting/total time) was recorded over 10 min. All mating assays were performed in an

arrow window (7–10 a.m.) to minimize circadian influences on experimental outcome, blind to experimental genotype where possible. Mating songs were recorded using a MicroTrack mobile digital recorder (M-Audio) and were analyzed in Audacity. Because *dAdar^{hyp}* males expressed a *white+* mini-gene and *dAdar^{WTLoxP}* did not, we crossed a *white+* mini-gene-containing p [w25.2] vector inserted in the 3rd chromosome into the *dAdar^{WTLoxP}* background to restore eye pigment expression.

RNA Editing Analysis

RNA extractions from *Drosophila* heads (15–20 per sample) were performed using TRIzol reagent (Invitrogen). Edited cDNAs were amplified via RT-PCR using target-specific primers (Jepson and Reenan, 2009). Levels of editing were determined by measuring the area under A- and G-peaks in individual electropherogram traces using ImageJ. The percent editing is expressed as $G/(A + G) * 100$.

Western Blotting

Protein samples were prepared in buffer containing SDS and β -mercaptoethanol and electrophoresed on a 10% gel (Amresco). Anti-HA antibody (Covance) was used at 1:500; anti-actin (Millipore) was used at 1:20,000–80,000. Band intensities were quantified on a Kodak Image Station following background subtraction. For adult heads, 20-heads/100 ml of buffer were used per sample. For developmental analysis, we used 250 1st instar larvae, 10 3rd instar larvae, and 10 whole adult males per 100 ml of buffer.

Confocal Microscopy and Immunohistochemistry

A Zeiss LSM 510 meta-confocal microscope was used to obtain all images. Samples for immunohistochemistry were prepared as described previously (Wu and Luo, 2006). Primary antibodies were used at the following concentrations: mouse anti-Lamin, anti-Elav, anti-Repo, and anti-Dachshund (Developmental Studies Hybridoma Bank) were all used at 1:50; mouse anti-HA and rabbit anti-HA (Santa Cruz Biotechnology) were used at 1:50. Alexa-Fluor secondary antibodies (goat anti-mouse Cy3 and goat anti-mouse and anti-rabbit FITC (Invitrogen) were used at 1:200. DAPI (Invitrogen) was used at 1:1000. Confocal images were obtained at subsaturation levels of fluorescent intensity. Images were contrast-enhanced in Adobe Photoshop. Each image shown is a representative example of $n \geq 5$.

RESULTS

dADAR Is Localized to the Neuronal Nucleus in the *Drosophila* Brain

The endogenous dADAR protein expression pattern within the adult *Drosophila* nervous system has not been determined. To remedy this, we used ends-out homologous recombination (Rong et al., 2002) to generate three independent recombinant lines, two with HA epitope-tagged sequences at the 3' end of the *dAdar* locus (Fig.C.1A and B) and one without. Editing levels did not significantly differ between both *dAdar*^{HA} lines and *w*¹¹¹⁸ controls (supplementary Fig.C.1).

During homologous recombination, screening for recombinant flies is facilitated by the insertion of an ~5-kb *white*⁺ mini-gene eye color selection cassette within an intron

of the *dAdar* locus, subsequently removed via a Cre-recombinase step (Rong and Golic, 2000; Rong et al., 2002). Western blotting using an anti-HA antibody revealed robust expression of an HA-immunoreactive protein at the predicted size of dADAR in both recombinant lines lacking the *white*⁺ mini-gene (Fig.C.1C). We used these lines to detail the expression pattern of dADAR. Because dADAR-HA levels and endogenous editing were indistinguishable between the two independent lines, we use them interchangeably throughout all subsequent experiments. Confocal microscopy revealed broad expression of dADAR in the brain and thoracic ganglion (supplementary Fig. SC.1). Co-immunostaining for HA and the nuclear envelope protein Lamin showed that dADAR expression was prominent only within nuclei (Fig.C.1D). No significant dADAR localization to the cytoplasmic, axonal, or dendritic compartments was observed. In addition, dADAR co-localized with Elav (a marker for neuronal nuclei) but not Repo (a glial nuclear marker), indicating that nuclear dADAR expression is widespread and enriched in the neuronal nucleus (Fig.C.1E).

Editing Activity Varies Widely between Neuronal Subpopulations

Our initial analysis of dADAR localization revealed clear differences in dADAR protein expression even between neighboring neurons (Fig.C.1D and E), suggesting that dADAR expression is under spatial control in the *Drosophila* brain, as is the case in mammals (Jacobs et al., 2009). To investigate how dADAR activity varies in genetically defined neurons, we used a molecular reporter of editing activity based on *syt-1*, which contains four editing sites in exon 9, of which sites 3 and 4 are edited most robustly (Fig.C.2A) (Hoopengardner et al., 2003; Reenan, 2005). The reporter (termed *syt-T*)

consists of the edited exon flanked by the upstream and downstream introns and exons cloned into a pUAS vector (Jepson and Reenan, 2009), allowing targeted expression using the UAS-Gal4 binary expression system (Brand and Perrimon, 1993).

We used 21 neuronal Gal4 lines to drive two independent insertions of *syt-T* (see supplemental Table SC.2) and observed production of full-length transcripts with all Gal4 drivers. Sequence analysis confirmed that all full-length transcripts were the result of accurate splicing. In certain cases, a minor band corresponding to exon 9 skipping was observed. However, alterations in editing of the reporter did not correlate with alternative splicing of the edited exon (supplementary Fig. SC.2). Editing at site 4 was detected in all neurons defined by the library of Gal4 lines but varied widely from 27 to 82% (Fig.C.2B–D). In contrast, editing at site 3 was either undetectable or <10% in 16/21 driver lines tested, and it was only observed at robust levels (>20%) in the five subpopulations that yielded the highest editing at site 4, suggesting that although low dADAR levels are sufficient for robust editing of site 4, editing at site 3 only occurs once a certain threshold of dADAR expression has been exceeded.

To test whether dADAR expression correlated with editing of the *syt-T* reporter, we examined dADAR expression in two neuronal subtypes representing high and low levels of dADAR activity indicated by the *syt-T* reporter, glutamatergic (*ok371*) and mushroom body neurons, respectively (see supplemental Table SC.2). Robust dADAR levels were detected in many glutamate-releasing neurons labeled with a nuclear red fluorescent protein (Fig.C.2E) (Barolo et al., 2004). In contrast, mushroom body cells labeled with the nuclear marker Dachshund showed strikingly lower dADAR expression levels relative to surrounding neurons (Fig.C.2F). These data suggest that cell-

autonomous regulation of dADAR expression contributes to neuron-to neuron variation in editing of the molecular reporter.

Stringent Reduction of dADAR Expression Reveals Differential Affinities of Edited Substrates

Initially, the two pre-Cre recombinant lines generated contain a *white*⁺ mini-gene inserted in an inverse orientation relative to *dAdar* transcription. Western blots revealed that prior to removal of this *white*⁺ mini-gene insertion, dADAR-HA staining was reduced by $80 \pm 5\%$ and $87 \pm 7\%$ relative to post-Cre counterparts (Fig.C.1C and D). Thus, insertion of *white*⁺ serendipitously generated independent hypomorphic alleles of *dAdar* (which we refer to as *dAdar*^{hyp}; control flies harboring a single LoxP site in intron 7 of *dAdar* are referred to as *dAdar*^{WTLoxP}).

The substantial reduction in dADAR expression also led to a tissue-specific decrease in auto-editing of the *dAdar* transcript, a developmentally regulated event that acts to down-regulate dADAR activity by re-coding a conserved serine residue to glycine near the active site (Keegan et al., 2005). Amplification of the *dAdar* transcript revealed that auto-editing was slightly but significantly reduced in *dAdar*^{hyp} heads relative to *dAdar*^{WTLoxP} (*WTLoxP*, 53.8%; *hyp*, 49.1%, $n = 8$ RT-PCRs, $p \leq 0.005$, Mann-Whitney *U* test). In contrast, auto-editing in thorax tissue dropped from 38.1% in *dAdar*^{WTLoxP} controls to 23.1% in *dAdar*^{hyp} thoraxes ($n = 5-8$, $p \leq 0.005$). The decrease in ADAR protein production by the *dAdar*^{hyp} allele results in comparable or only slightly reduced levels of the less active (edited) form of *Drosophila* ADAR protein. Thus, any system-wide changes in target deamination should be largely due to changes in ADAR levels

rather than effects due to misregulated auto-editing.

Complete loss of A-to-I RNA editing in *Drosophila* results in multifaceted adult-stage behavioral abnormalities (Palladino et al., 2000a), consistent with the functional pleiotropy of dADAR. However, the extreme uncoordination exhibited by *dAdar*^{5g1} null flies has made investigations into the relation between A-to-I editing activity and complex behavior impossible. Surprisingly, despite the severe reduction in dADAR expression in *dAdar*^{hyp} males, locomotor activity appeared relatively robust under casual observation (supplemental movie), and no obvious uncoordination was apparent. These observations suggested that editing might perdure in a behaviorally relevant subpopulation of adenosines in *dAdar* hypomorphs, despite the severe reduction in dADAR protein expression. We tested this hypothesis by comparing editing in 68 target adenosines in the hypomorph and control backgrounds. Like editing in the *dAdar*^{HA} genetic background (supplemental Fig. SC.1), *dAdar*^{WTLoxP} males did not significantly differ from wild-type Canton-S (data not shown). In *dAdar*^{hyp} heads and thoraxes, however, editing was reduced by an average of $68 \pm 4\%$ and $56 \pm 4\%$, respectively, relative to the post-Cre control (Fig.C.3A). We observed a similar reduction in editing in *dAdar*^{HA} males in which the *white*⁺ mini-gene was not removed (data not shown).

Intriguingly, the reduction in specific editing of targets was highly nonuniform (Fig.C.3A and supplemental Fig. SC.3A and B). Editing at a substantial fraction of sites was reduced by 70–100% in hypomorph heads and thoraxes. In contrast, despite the extreme curtailing of wild-type dADAR levels, a subpopulation of adenosines was modified at nearly wild-type levels (Fig.C.3A and supplemental Table SC.3). For example, in the male thorax, *syt-1* site 4 and site 2 of the *ard* acetylcholine receptor (also

known as Db1) are edited at similar levels ($95 \pm 1\%$ and $94 \pm 2\%$, respectively) (supplemental Table SC.3). However, in *dAdar^{hyp}* thoraxes, editing at *syt-1* site 4 was reduced by 12% relative to *dAdar^{WTLoxP}*, while *ard* site 2 was reduced by 71%. A further striking example is site 4 of *eag* and the single site in *Caa1T*. Site 4 of *eag* is slightly reduced from $84 \pm 0.6\%$ to $79 \pm 0.4\%$ in *dAdar^{hyp}* heads, while editing in *Caa1T* is completely abolished in *dAdar^{hyp}* heads, despite its high level of editing in *dAdar^{WTLoxP}* heads ($87 \pm 0.7\%$).

Based upon these data, we classified dADAR substrates into two groups according to their sensitivity to dADAR protein levels, which we term “high and low efficiency” (HE and LE) sites. We defined HE sites as those reduced by $<30\%$ in *dAdar^{hyp}* thoraxes, while LE sites are reduced by $>70\%$. Importantly, HE and LE sites also exhibited similar responses to dADAR reduction in male *dAdar^{hyp}* head samples, although these were shifted toward slightly lower reductions in HE sites and greater reductions in LE sites (supplemental Fig. SC.3). Many dADAR targets are edited at higher levels in the thorax relative to head tissue (average increase, $16 \pm 6\%$ for all sites edited $>10\%$; Fig. 2.3A), although notable exceptions such as *shab* site 5 and *Caa1T* were apparent. This trend may reflect increased dADAR activity in the thoracic ganglion relative to the head, perhaps due to lower levels of auto-editing in *dAdar^{hyp}* thoraxes.

We took advantage of the *dAdar^{5g1}* null and hypomorphic *dAdar^{hyp}* alleles to generate females with a graded range of dADAR expression, and we examined editing at 10 HE and 8 LE sites in head samples from four genetic backgrounds: *hyp/hyp*, *5g1/FM7* (where *FM7* is a balancer chromosome with a wild-type copy of *dAdar⁺*), *hyp/FM7*, and *WTLoxP/WTLoxP*. These genotypes have predicted relative dADAR expression levels of

~ 20, 50, 60, and 100%, respectively. As expected, all LE sites exhibited very low levels of editing in *hyp/hyp* heads (0–23%), in contrast to HE sites (30–84%) (Fig.C.3B and C). Every HE site tested showed wild-type levels of editing in *5g1/FM7* heads, and the mean reduction in *hyp/hyp* heads relative to wild-type controls was only $26 \pm 4\%$. Thus, only a minimal concentration of dADAR is sufficient to yield robust editing of HE sites.

In contrast, the mean reduction in LE sites in *hyp/hyp* heads relative to wild-type controls was $80 \pm 4\%$. However, within the LE sites we examined, we could delineate two subpopulations. Five of the eight sites tested (*ard* sites 1–3, *DSCI* and *Caa1T*) showed wild-type editing levels in *5g1/FM7* heads, despite severely reduced editing in the *dAdarhyp* background. The remaining three sites (*unc-13*, *Caa1D* site 1, and site 6 of the Da6 acetylcholine receptor) showed sequentially increased editing in proportion to higher dADAR levels and did not reach wild-type levels of editing in either *5g1/FM7* or *hyp/FM7* heads. We also examined five HE and LE sites in *hyp/hyp*, *5g1/FM7*, *hyp/FM7*, and *WTLoxP/WTLoxP* thoraxes, with similar results (supplemental Fig. SC.3C and D). Finally, Western blotting indicated that there was no significant up-regulation of expression from a wild-type *dAdar* locus in *dAdarHA/5g1* trans-heterozygote females (supplemental Fig. SC.3E), indicating that there does not appear to be a compensatory mechanism counteracting decreased ADAR production.

The unexpectedly complex relationship between dADAR concentration and editing levels appears to vary on a site-by-site basis. One possible explanation for the variation in the sensitivity of edited adenosines to dADAR concentration is a differential ratio of substrate mRNA to dADAR enzyme, *i.e.* LE sites are present in mRNAs with high steady-state expression levels, although the converse is true for HE sites. However,

this explanation is not consistent with the close proximity of HE and LE sites within transcripts from a single gene, which was observed for several mRNAs, including *Caa1D* and *Da6* (Fig.C.3B and C), as well as *shaker*, *shab*, and *eag* (supplemental Table SC.3). For example, sites 5 and 6 of *shaker* are separated by just six nucleotides yet exhibit strikingly different reductions in editing in *dAdar^{hyp}* heads, with site 5 reduced by 22% and site 6 by 76% (supplemental Table SC.3). In addition, proteins re-coded by dADAR that function in the same sub-cellular compartment also exhibited drastically divergent responses in *dAdar^{hyp}*. *Synaptotagmin-1 (syt-1)* and *unc-13* both act to promote vesicle release at pre-synaptic nerve terminals. Nonetheless, site 4 of *syt-1* is robustly edited in *dAdar^{hyp}*, although editing of *unc-13* is almost abolished in both *dAdar^{hyp}* heads and thoraxes (Fig.C.3). Therefore, our data strongly suggest that the sensitivity of editing sites to changes in dADAR levels is a function of inherent primary sequence and/or structural properties specific to the double strand RNA structural intermediates required for ADAR-mediated deamination.

High and Low Efficiency Editing Sites Exhibit Distinct Patterns of Developmental Regulation

Editing at many, but not all, dADAR substrates is under strong temporal control, appearing predominantly at the pupal and adult stages of *Drosophila* development. Edited adenosines exhibiting differential developmental regulation may even be found within the same transcript (Ingleby et al., 2009; Jones et al., 2009), yet how this is achieved remains unknown. Previous data has shown that *dAdar* transcription is low during the larval stages and rapidly peaks at the late pupal and adult stages (Palladino et al., 2000b). We

hypothesized that adenosines showing high levels of editing throughout development represent HE sites and require low levels of dADAR expression for robust editing. Conversely, pupae/adult-specific sites would require higher concentrations of dADAR for efficient modification and populate the LE class.

We assessed whether temporal changes in *dAdar* transcription result in similar alterations in dADAR protein levels by comparing dADAR expression in the adult thoracic ganglion and the ventral nerve cord of 3rd instar larvae (L3) (Fig.C.4A). Although strong dADAR expression was observed in neuronal nuclei in the adult thoracic ganglion, dADAR was largely undetectable by immunohistochemistry in the larval ventral nerve cord. Furthermore, Western blotting revealed robust bands corresponding to dADAR-HA isoforms in adult male tissue, which were undetectable in samples prepared from the 1st instar (L1) and L3 larval stages (Fig.C.4B, *inset*). Thus, the increase in *dAdar* mRNA between the larval and adult stages is mirrored by a similar change in detectable dADAR protein expression.

We next investigated whether HE and LE sites show distinct patterns of developmental regulation, in keeping with the above hypothesis. We measured editing at the same HE and LE sites examined above (Fig.C.3B and C), amplified from Canton-S L1, L3, and adult-stage cDNAs. Editing sites representing HE and LE classes showed strikingly different developmental regulation (Fig.C.4B and C). As predicted, all LE sites tested showed clear increases in editing between the L3 and adult stages (Fig.C.4B). Across the eight sites studied, editing levels at the L3 stage averaged only $8 \pm 3\%$ of the corresponding adult values. In contrast, HE sites were enriched for adenosines that were robustly edited in the early and late larval stages (Fig.C.4C), with the mean values at L3

averaging $53 \pm 10\%$ of adult levels. Three of the four HE adenosines that did show developmental regulation mapped to the same transcript, encoding the *Ca α 1D* voltage-gated calcium channel. Thus, although deamination of particular transcripts may be developmentally modulated by factors distinct from dADAR itself, editing site-specific responses to dADAR protein levels explains a significant proportion of the temporal variation in editing and correlates well with our functional definition of HE and LE classes.

Reduction of dADAR Expression Affects Complex Behavior

The lack of severe uncoordination in *dAdar*^{hyp} males allowed us to examine, for the first time, whether complex adult-stage behaviors are altered in a genetic background with an engineered alteration in editing levels. Under light-dark (12:12 h) conditions, wild-type *Drosophila* exhibit diurnal peaks of activity centered on the lights-on (dawn) and lights-off (dusk) transitions. Importantly, spikes in activity are preceded by anticipatory increases in locomotion that are driven by an endogenous circadian clock (Allada and Chung, 2010). We examined rhythmic locomotor patterns using automated, single-fly activity monitors. *dAdar*^{WTLoxP} males displayed peaks of activity at subjective morning and evening, as well as anticipation of both dark-light and light-dark transitions (Fig.C.5A and supplemental Fig. SC.4). Under constant dark conditions, *dAdar*^{WTLoxP} males displayed anticipation of subjective morning and night (data not shown), illustrating that the circadian clock remains intact in our control genotype. In *dAdar*^{hyp} males, peaks of morning and evening activity were present but reduced in amplitude relative to *dAdar*^{WTLoxP} (Fig.C.5B), and anticipation of morning, but not night, was

completely abolished. Importantly, this pattern of locomotor activity was distinct from *dAdar*^{5g1} males, which lack coordinated locomotor patterns (Fig.C.5C and supplemental Fig. SC.4) (Palladino et al., 2000a). We quantified the degree of morning anticipation in the above three genotypes (defined as the number of beam breaks in the 3 h before lights-on normalized to the 6 h before lights-on). *dAdar*^{WTLoxP} males exhibited a 60 and 45% increase respectively in the degree of morning anticipation relative to *dAdar*^{hyp} and *dAdar*^{5g1} males, respectively (Fig.C.5D). Thus, although limited expression of dADAR (~20%) is sufficient to restore a degree of locomotor coordination and activity, including startle responses to changes in light stimuli, more robust dADAR expression is required for the manifestation of circadian anticipation of morning, a complex behavior. Analysis of total locomotor activity revealed that locomotion in a (n=26, Fig.C.6D) (Peixoto and Hall, 1998; Zehring et al., 1984). In contrast, pulse songs from *dAdar*^{hyp} males often exhibited abnormal waveforms characterized by polycyclic pulses and additional peaks (Fig.C.6E). Of the 44 songs analyzed from *dAdar*^{hyp} males, only 7 were similar to the *dAdar*^{WTLoxP} pulse pattern. The change in waveform was accompanied by alterations in several other song parameters, including a reduced number of pulses per song train, an increased pulse frequency, and a small but highly significant increase in the inter-pulse interval (*dAdar*^{WTLoxP}, 38.6 ms ± 0.4, n = 312; *dAdar*^{hyp}, 40.8 ms ± 0.4, n = 281; p <0.0001, Mann-Whitney U test) (Fig.C.6F–H). In addition, we observed striking variability in the *dAdar*^{hyp} pulse waveforms, even between distinct song trains from the same male (Fig.C.6E). The coefficient of variation (defined as the S.D divided by the mean) of the pulse frequency increased from 0.121 in *dAdar*^{WTLoxP} to 0.265 in *dAdar*^{hyp}, but it was similar when comparing the inter-pulse intervals of the two genotypes

(*dAdar*^{WTLoxP}, 0.175; *dAdar*^{hyp}, 0.155). Thus, in addition to influencing multiple song parameters, robust editing also appears to be required for maintaining aspects of male song pulse stereotypy.

Inhibition of RNA Editing in a Small Subset of Neurons Is Sufficient to Alter Complex Behavior

In *Drosophila*, the male-specific isoform of the transcription factor *Fruitless* (FruM) is a key mediator of male-specific behaviors, and the output of *fruitless* (*fru*) neurons is known to be essential for correct courtship behavior and generation of the mating song (Clyne and Miesenbock, 2008; Manoli et al., 2005; Stockinger et al., 2005). Because both of these behavioral parameters were altered in *dAdar*^{hyp} males, we examined the pattern and function of A-to-I editing in this behaviorally important subset of neurons.

Fru neurons are present in both the male and female central brain and thoracic ganglion, composing ~2% of the total neuronal population. Although the distribution and projection patterns of *fru* neurons are broadly similar between male and female *Drosophila* (Demir and Dickson, 2005; Manoli et al., 2005; Stockinger et al., 2005), subpopulations of *fru* neurons have been shown to exhibit sexual dimorphism in both number and wiring (Datta et al., 2008; Kimura et al., 2008; Kimura et al., 2005). We initially tested whether editing activity in *fru* neurons also showed sexual dimorphism by driving the two independent insertions of the *syt-T* reporter (Fig.C.2) using *fru*-Gal4 and analyzing editing at *syt-T* sites 3 and 4 following RT-PCR amplification from male and female head and thorax cDNA. Interestingly, editing at site 4, which is more robustly

edited than site 3, indeed showed subtle but significant sexual dimorphism. Site 4 exhibited a relative increase of ~20% in male *versus* female head cDNA ($p = 0.004$, Mann-Whitney U test). This trend was reversed in thorax cDNA, where site 4 editing in *fru* neurons was reduced by ~10% in males relative to females ($p = 0.03$; Fig.C.7A and B.). Editing at site 3 showed a similar trend, albeit at lower levels (Fig.C.7B). Furthermore, site 4 editing was statistically unchanged between *fru* neurons in male heads and thoraxes ($p = 0.94$) but increased by 30.5% between female head and thorax samples ($p = 0.003$; Fig.C.7B). No sex-specific alternative splicing of the *syt-T* reporter was observed in either head or thorax tissues (supplemental Fig. SC.5).

Because *dAdar* is X-linked, our results could potentially reflect sex-specific differences in dADAR expression throughout the nervous system. Thus, we examined editing of the endogenous *syt-I* transcript in male and female whole head and thorax cDNA and found no significant sexual dimorphism at either site (supplemental Fig. SC.6). We next measured editing at a further five LE and eight HE sites (Fig.C.3) in the same tissues. In this combined data set of 15 editing sites, we found a small but significant reduction in overall editing in female relative to male heads (mean reduction, 9%, $p = 0.0013$, paired t test). However, in contrast to editing of the *syt-T* reporter, there was no significant alteration in editing of endogenous mRNAs when comparing male and female thoraxes ($p = 0.198$) nor a significant difference in editing of the 15 sites between female head and thorax samples ($p = 0.68$) (supplemental Fig. SC.6). Thus, the female tissue-specific differences in editing of *syt-T* cannot be explained in terms of a global alteration in editing activity. Collectively, these data suggest that dADAR activity is differentially controlled in male and female *fru* neurons.

The existence of sexually dimorphic editing activity suggested a functional role in dADAR activity in *fru* neurons. Robust dADAR expression was detected in many *fru* neurons in both the male brain and the thoracic ganglion (Fig.C.7C). Importantly, dADAR is expressed in *fru* neurons in the mesothoracic segment of the ventral nerve cord, which are thought to be a key component of the song pattern generator (Fig.C.7C) (Hall, 1979; von Schilcher and Hall, 1979). We made use of a previously validated double-RNAi line (*adr-IR1 + 2*) directed against the 3' region of the *dAdar* transcript and under the control of the upstream activation sequence promoter (Jepson and Reenan, 2009) to selectively reduce dADAR expression in *fru* neurons. Knockdown of dADAR solely in *fru* neurons did not significantly alter male locomotor activity, latency to court, or total time spent courting (supplemental Fig. SC.7). Male-male courting, a hallmark of *fruitless* mutants, was not observed in *fru-Gal4 > adr-IR1 + 2* males (data not shown). This, as well as the robust courtship of females, indicates that the development and wiring of *fru* neurons are unlikely to be adversely affected by dADAR knockdown.

We next examined the mating song in the experimental and both control genotypes. Song waveforms from control males containing driver or transgenes alone were indistinguishable from *dAdar*^{W^TLoxP} (Fig.C.7D and E). In contrast, 12/27 song trains from males with dADAR expression inhibited in *fru* neurons exhibited polycyclic waveforms and/or additional peaks that were not observed in either genetic control (Fig.C.7F), as was also observed in *dAdar*^{hyp} males (albeit in a higher proportion of songs). This was accompanied by an increase in the average number of pulses per song train (*fru-Gal4 > adr-IR1 + 2*, 12.9 ± 1.7 ; *fru-Gal4/+*, 6.6 ± 1 ; *adr-IR1 + 2/+*, 8 ± 1.3 ; $p \leq 0.005$, Mann-Whitney *U* test) but no significant alteration in either pulse frequency or

inter-pulse interval relative to both control genotypes. Thus, knockdown of dADAR in *fru* neurons can partially phenocopy a discrete subset of the multifaceted alterations in courtship behavior observed in *dAdar^{hyp}* males, namely the generation of mating songs with abnormal, often polycyclic, waveforms.

DISCUSSION

Using a novel hypomorphic allele of *dAdar* generated through homologous recombination coupled with cell-specific dADAR knockdown, we have demonstrated that RNA editing serves a modulatory role in multiple adaptive behaviors in *Drosophila*. In short, we provide linkage between the loss of conserved and taxa-specific amino acid re-coding sites and alterations in wild-type ethological outputs that directly impinge on organismal fitness. Importantly, the behavioral defects observed in *dAdar^{hyp}* males correlate with the severe loss of a particular subset of edited adenosines, namely those that are preferentially edited at the adult stage (Fig.C.4B).

Our molecular analysis of *dAdar* hypomorphs revealed a striking diversity in the response of edited adenosines to changes in endogenous dADAR levels (Fig.C.3). Both the local sequence surrounding edited adenosines and their predicted secondary structures vary widely between dADAR substrates, providing a potential mechanism to generate differential affinities for dADAR binding and deamination (Bhalla et al., 2004; Hall, 1979; Reenan, 2005). This finding has important implications as follows. First, it provides an explanatory basis for the developmental regulation of a select population of editing sites (Fig.C.4), a phenomenon common to both *Drosophila* and mammals (Hanrahan et al., 2000; Ingleby et al., 2009; Jones et al., 2009; Rula et al., 2008). Second,

cell-specific variation in dADAR expression (Fig.C.2) may allow spatial control of LE sites while simultaneously maintaining robust network-wide editing of HE sites, thus providing a means to fine-tune neuronal physiology through the diversification of a constrained population of proteins (see Fig.C.8, for model).

We have previously shown that pan-neuronal expression of the two hairpin RNAi constructs used in this study reduces locomotor activity by ~90% (Jepson and Reenan, 2009), and this effect could not be phenocopied by dADAR knockdown in any particular neuronal subset tested. Furthermore, dADAR knockdown under these conditions was robust enough to strongly reduce editing even at HE sites such as *syt-1* site 4. Although knockdown is subject to the level of hairpin expression and efficiency of RNAi in particular neurons, the abrogation of ADAR expression by transgenic knockdown was clearly effective. In contrast, editing at HE sites is still maintained in our purely genetic model using *dAdar^{hyp}* mutant males and females (Fig.C.3), as is coordinated locomotion (albeit at lower levels; Fig.C.5). Indeed, even *dAdar^{hyp}/dAdar^{sg1}* trans-heterozygote females, predicted to express dADAR at ~10% of wild-type levels, do not appear uncoordinated. Collectively, these data imply that network-wide editing of HE sites is sufficient to provide motor tone and prevent the extreme uncoordination observed in *dAdar* null flies.

Conversely, it is tempting to speculate that developmentally regulated LE sites modulate adult-specific behaviors. Indeed, we examined two ethologically relevant behaviors in *dAdar^{hyp}* males, which show a severe disruption of developmentally regulated editing (Fig.C.4), and we found both to be defective (Figs. E.5 and E.6). *dAdar^{hyp}* males did not show the circadian anticipation of lights-on seen in wild-type

Drosophila (Fig.C.5), and multiple aspects of courtship behavior were abnormal in *dAdar^{hyp}* males, including the time required to initiate courtship and the waveform of the mating song (Fig.C.6). It should be stressed that defects in both of the above parameters are likely to be severely detrimental to reproductive fitness under competitive conditions in the wild.

Although our data lead us to hypothesize that loss of adult stage LE sites may underlie the locomotor and courtship defects exhibited by *dAdar* hypomorphs, we cannot currently link the loss of particular editing sites to the behavioral defects seen in *dAdar^{hyp}* males due to the large number of characterized dADAR substrates. Over 100 editing sites in 24 mRNAs have been identified either serendipitously or through comparative genomics approaches (Hoopengardner et al., 2003), although a recent bioinformatic screen identified a further potential 27 mRNAs subject to re-coding (Stapleton et al., 2006). The existence of functionally epistatic interactions between editing sites also makes it unlikely that any particular phenotype observed in *dAdar^{hyp}* males can be fully mapped to the loss of a single editing site (Ingleby et al., 2009; Jones et al., 2009). Rather, the relationship between re-coding and behavior can instead be viewed through the prism of the pleiotropic actions of dADAR on a wide range of RNA substrates, with many edited proteins simultaneously contributing to the total phenotype of interest.

We mapped the cellular foci for behavioral abnormalities associated with stringent loss of dADAR expression using transgenic RNAi (Dietzl et al., 2007). Knockdown of dADAR specifically in *fruitless*-expressing neurons partially recapitulated the polycyclic songs observed in *dAdar^{hyp}* males (Fig.C.7) but did not phenocopy alterations in other song properties or mating behavior, suggesting that these highly

specific phenotypic components are influenced by editing in other *fru*-negative neurons and/or muscle tissue. Surprisingly, targeted expression of a molecular reporter for editing activity suggests that male and female *fru* neurons within both the brain and thoracic ganglion may differ in terms of dADAR activity (Fig.C.7). Because only small subpopulations of *fru* neurons exhibit morphological sexual dimorphism, it has been hypothesized that expression of the male-specific isoform of Fruitless (FruM) may modify the physiological properties of *fru* neurons (Clyne and Miesenbock, 2008; Demir and Dickson, 2005; Manoli et al., 2005; Stockinger et al., 2005). Given the large number of transcripts re-coded by A-to-I editing (Hoopengardner et al., 2003), an alteration of dADAR expression or activity by FruM could hypothetically provide a means of enabling functional modulation of a wide range of ion channels and synaptic release proteins. Further experiments will be required to test whether the alterations in editing observed between male and female *fru* neurons represent large differences in a subset of *fru* neurons, subtle alterations across the *fru* neuron network, or are due to numerical sexual dimorphism in the *fru* neuron population.

That RNA editing can modulate song properties is particularly intriguing, because editing sites are not static throughout insect evolution (Grauso et al., 2002; Jin et al., 2007; Reenan, 2005). Indeed, even within the *Drosophila* lineage, we have observed species-specific changes in the magnitude of editing at orthologous adenosines in several ion channels (Hanrahan et al., 2000; Hoopengardner et al., 2003). Therefore, our data open the possibility that alterations in RNA editing may contribute to species-specific song waveforms, a key mechanism implicated in the reproductive isolation between *Drosophilids*. More broadly, our data suggest that, in principle, evolutionary divergences

in RNA editing may contribute to the generation of adult-stage species-specific behavioural patterns.

REFERENCES

- Allada, R., and Chung, B.Y. (2010). Circadian organization of behavior and physiology in *Drosophila*. *Annual review of physiology* 72, 605-624.
- Barolo, S., Castro, B., and Posakony, J.W. (2004). New *Drosophila* transgenic reporters: insulated P-element vectors expressing fast-maturing RFP. *BioTechniques* 36, 436-440, 442.
- Basillo, C., Wahba, A., Lengyel, P., Speyer, J., and Ochoa, S. (1962). Synthetic polynucleotides and the amino acid code. V. Proceedings of the National Academy of Sciences of the United States of America 48, 613-616.
- Bhalla, T., Rosenthal, J.J., Holmgren, M., and Reenan, R. (2004). Control of human potassium channel inactivation by editing of a small mRNA hairpin. *Nature structural & molecular biology* 11, 950-956.
- Brand, A.H., and Perrimon, N. (1993). Targeted gene expression as a means of altering cell fates and generating dominant phenotypes. *Development (Cambridge, England)* 118, 401-415.
- Burns, C.M., Chu, H., Rueter, S.M., Hutchinson, L.K., Canton, H., Sanders-Bush, E., and Emeson, R.B. (1997). Regulation of serotonin-2C receptor G-protein coupling by RNA editing. *Nature* 387, 303-308.
- Clyne, J.D., and Miesenbock, G. (2008). Sex-specific control and tuning of the pattern generator for courtship song in *Drosophila*. *Cell* 133, 354-363.
- Datta, S.R., Vasconcelos, M.L., Ruta, V., Luo, S., Wong, A., Demir, E., Flores, J., Balonze, K., Dickson, B.J., and Axel, R. (2008). The *Drosophila* pheromone cVA activates a sexually dimorphic neural circuit. *Nature* 452, 473-477.
- Demir, E., and Dickson, B.J. (2005). Fruitless splicing specifies male courtship behavior in *Drosophila*. *Cell* 121, 785-794.
- Dietzl, G., Chen, D., Schnorrer, F., Su, K.C., Barinova, Y., Fellner, M., Gasser, B., Kinsey, K., Oppel, S., Scheiblauer, S., *et al.* (2007). A genome-wide transgenic RNAi library for conditional gene inactivation in *Drosophila*. *Nature* 448, 151-156.
- Grauso, M., Reenan, R.A., Culetto, E., and Sattelle, D.B. (2002). Novel putative nicotinic acetylcholine receptor subunit genes, *Dalpha5*, *Dalpha6* and *Dalpha7*, in *Drosophila melanogaster* identify a new and highly conserved target of adenosine deaminase acting on RNA-mediated A-to-I pre-mRNA editing. *Genetics* 160, 1519-1533.
- Hall, J.C. (1979). Control of *Drosophila*: dissection of a courtship pathway by genetic mosaics. *Genetics* 92, 437-457.
- Hanrahan, C.J., Palladino, M.J., Ganetzky, B., and Reenan, R.A. (2000). RNA editing of the *Drosophila* para Na⁽⁺⁾ channel transcript. Evolutionary conservation and developmental regulation. *Genetics* 155, 1149-1160.
- Higuchi, M., Maas, S., Single, F.N., Hartner, J., Rozov, A., Burnashev, N., Feldmeyer, D., Sprengel, R.,

- and Seeburg, P.H. (2000). Point mutation in an AMPA receptor gene rescues lethality in mice deficient in the RNA-editing enzyme ADAR2. *Nature* 406, 78-81.
- Higuchi, M., Single, F.N., Kohler, M., Sommer, B., Sprengel, R., and Seeburg, P.H. (1993). RNA editing of AMPA receptor subunit GluR-B: a base-paired intron-exon structure determines position and efficiency. *Cell* 75, 1361-1370.
- Hoopengardner, B., Bhalla, T., Staber, C., and Reenan, R. (2003). Nervous system targets of RNA editing identified by comparative genomics. *Science (New York, NY)* 301, 832-836.
- Ingleby, L., Maloney, R., Jepson, J., Horn, R., and Reenan, R. (2009). Regulated RNA editing and functional epistasis in Shaker potassium channels. *The Journal of general physiology* 133, 17-27.
- Jacobs, M.M., Fogg, R.L., Emeson, R.B., and Stanwood, G.D. (2009). ADAR1 and ADAR2 expression and editing activity during forebrain development. *Developmental neuroscience* 31, 223-237.
- Jepson, J.E., and Reenan, R.A. (2009). Adenosine-to-inosine genetic recoding is required in the adult stage nervous system for coordinated behavior in *Drosophila*. *The Journal of biological chemistry* 284, 31391-31400.
- Jin, Y., Tian, N., Cao, J., Liang, J., Yang, Z., and Lv, J. (2007). RNA editing and alternative splicing of the insect nAChR subunit alpha6 transcript: evolutionary conservation, divergence and regulation. *BMC evolutionary biology* 7, 98.
- Jones, A.K., Buckingham, S.D., Papadaki, M., Yokota, M., Sattelle, B.M., Matsuda, K., and Sattelle, D.B. (2009). Splice-Variant- and Stage-Specific RNA Editing of the *Drosophila* GABA Receptor Modulates Agonist Potency. *J Neurosci* 29, 4287-4292.
- Keegan, L.P., Brindle, J., Gallo, A., Leroy, A., Reenan, R.A., and O'Connell, M.A. (2005). Tuning of RNA editing by ADAR is required in *Drosophila*. *The EMBO journal* 24, 2183-2193.
- Kimura, K., Hachiya, T., Koganezawa, M., Tazawa, T., and Yamamoto, D. (2008). Fruitless and doublesex coordinate to generate male-specific neurons that can initiate courtship. *Neuron* 59, 759-769.
- Kimura, K., Ote, M., Tazawa, T., and Yamamoto, D. (2005). Fruitless specifies sexually dimorphic neural circuitry in the *Drosophila* brain. *Nature* 438, 229-233.
- Maggert, K.A., Gong, W.J., and Golic, K.G. (2008). Methods for homologous recombination in *Drosophila*. *Methods in molecular biology Clifton, NJ* 420, 155-174.
- Manoli, D.S., Foss, M., Villella, A., Taylor, B.J., Hall, J.C., and Baker, B.S. (2005). Male-specific fruitless specifies the neural substrates of *Drosophila* courtship behaviour. *Nature* 436, 395-400.
- Nishikura, K. (2010). Functions and regulation of RNA editing by ADAR deaminases. *Annual review of biochemistry* 79, 321-349.
- Ohlson, J., Pedersen, J.S., Haussler, D., and Ohman, M. (2007). Editing modifies the GABA(A) receptor subunit alpha3. *RNA (New York, NY)* 13, 698-703.
- Palladino, M.J., Keegan, L.P., O'Connell, M.A., and Reenan, R.A. (2000a). A-to-I pre-mRNA editing in *Drosophila* is primarily involved in adult nervous system function and integrity. *Cell* 102, 437-449.
- Palladino, M.J., Keegan, L.P., O'Connell, M.A., and Reenan, R.A. (2000b). dADAR, a *Drosophila* double-stranded RNA-specific adenosine deaminase is highly developmentally regulated and is itself a target for RNA editing. *RNA New York, NY* 6, 1004-1018.

- Peixoto, A.A., and Hall, J.C. (1998). Analysis of temperature-sensitive mutants reveals new genes involved in the courtship song of *Drosophila*. *Genetics* *148*, 827-838.
- Reenan, R.A. (2005). Molecular determinants and guided evolution of species-specific RNA editing. *Nature* *434*, 409-413.
- Rong, Y.S., and Golic, K.G. (2000). Gene targeting by homologous recombination in *Drosophila*. *Science* (New York, NY *288*, 2013-2018.
- Rong, Y.S., Titen, S.W., Xie, H.B., Golic, M.M., Bastiani, M., Bandyopadhyay, P., Olivera, B.M., Brodsky, M., Rubin, G.M., and Golic, K.G. (2002). Targeted mutagenesis by homologous recombination in *D. melanogaster*. *Genes & development* *16*, 1568-1581.
- Rula, E.Y., Lagrange, A.H., Jacobs, M.M., Hu, N., Macdonald, R.L., and Emeson, R.B. (2008). Developmental modulation of GABA(A) receptor function by RNA editing. *J Neurosci* *28*, 6196-6201. 91
- Semenov, E.P., and Pak, W.L. (1999). Diversification of *Drosophila* chloride channel gene by multiple posttranscriptional mRNA modifications. *Journal of neurochemistry* *72*, 66-72.
- Smith, L.A., Peixoto, A.A., and Hall, J.C. (1998). RNA editing in the *Drosophila* DMCA1A calcium-channel alpha 1 subunit transcript. *Journal of neurogenetics* *12*, 227-240.
- Stapleton, M., Carlson, J.W., and Celniker, S.E. (2006). RNA editing in *Drosophila melanogaster*: New targets and functional consequences. *RNA* (New York, NY *12*, 1922-1932.
- Stockinger, P., Kvitsiani, D., Rotkopf, S., Tirian, L., and Dickson, B.J. (2005). Neural circuitry that governs *Drosophila* male courtship behavior. *Cell* *121*, 795-807.
- von Schilcher, F., and Hall, J.C. (1979). Neural topography of courtship song in sex mosaics of *Drosophila melanogaster*. *Journal of Comparative Physiology [A]*, 85-95.
- Wu, J.S., and Luo, L. (2006). A protocol for dissecting *Drosophila melanogaster* brains for live imaging or immunostaining. *Nature protocols* *1*, 2110-2115.
- Zehring, W.A., Wheeler, D.A., Reddy, P., Konopka, R.J., Kyriacou, C.P., Rosbash, M., and Hall, J.C. (1984). P-element transformation with period locus DNA restores rhythmicity to mutant, arrhythmic *Drosophila melanogaster*. *Cell* *39*, 369-376

FIGURES

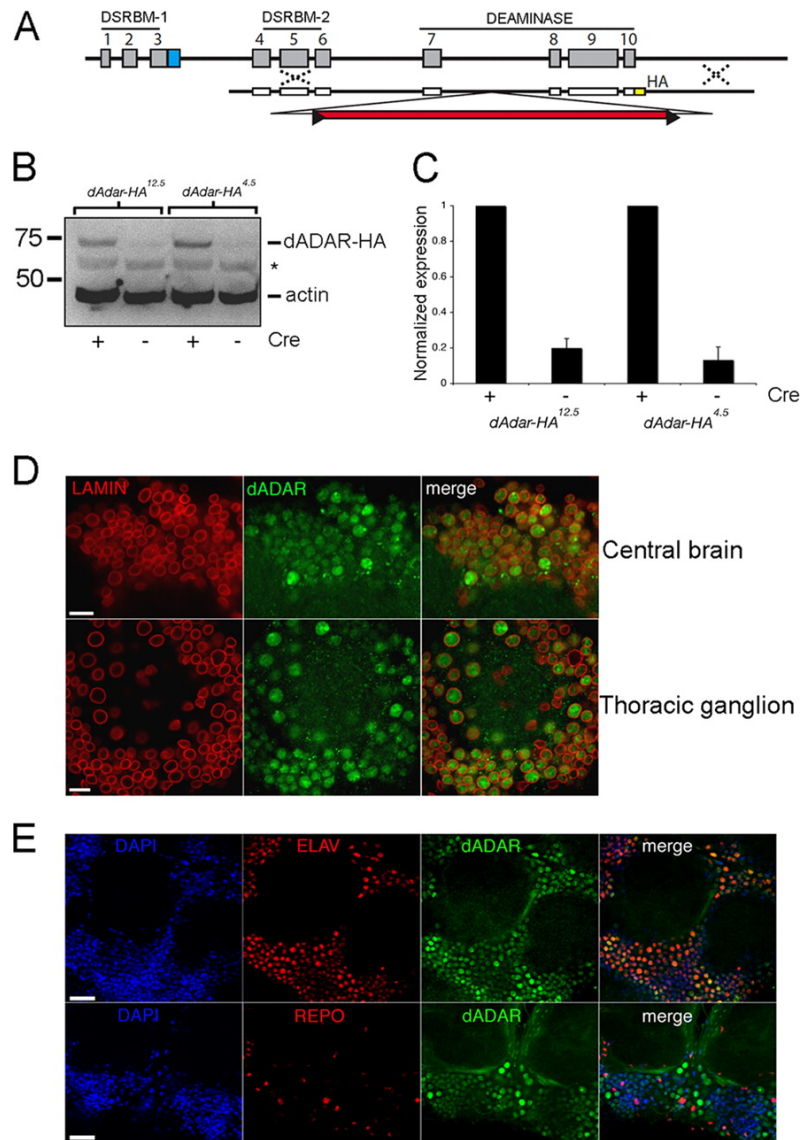


Figure C1. Visualization of dADAR expression using ends-out homologous recombination. **A)** schematic representation of the targeting construct used to insert an HA epitope tag at the 3' of the *dAdar* locus. **B)** representative Western blot showing HA-positive bands in two independent lines lacking the *white+* mini-gene. Actin was used as a loading control. *, nonspecific labeling. This is likely to be a head/brain-specific cross-reaction because it is not observed when using whole fly tissue (see Fig. E4B). **C)** quantification of relative dADAR-HA levels (normalized to actin) before and after Cre expression. Values are expressed relative to the mean of each post-Cre *dAdar*^{HA} line (n = 6 Western blots, three independent samples). Error bars, S.E. values. **D)** lamin and dADAR-HA staining in the male brain and thoracic ganglion. Scale bar, 10 μ m. **E,** dADAR-HA co-localizes with DAPI-stained nuclei and *Elav*, but not *Repo*, in the male brain. Scale bar, 20 μ m.

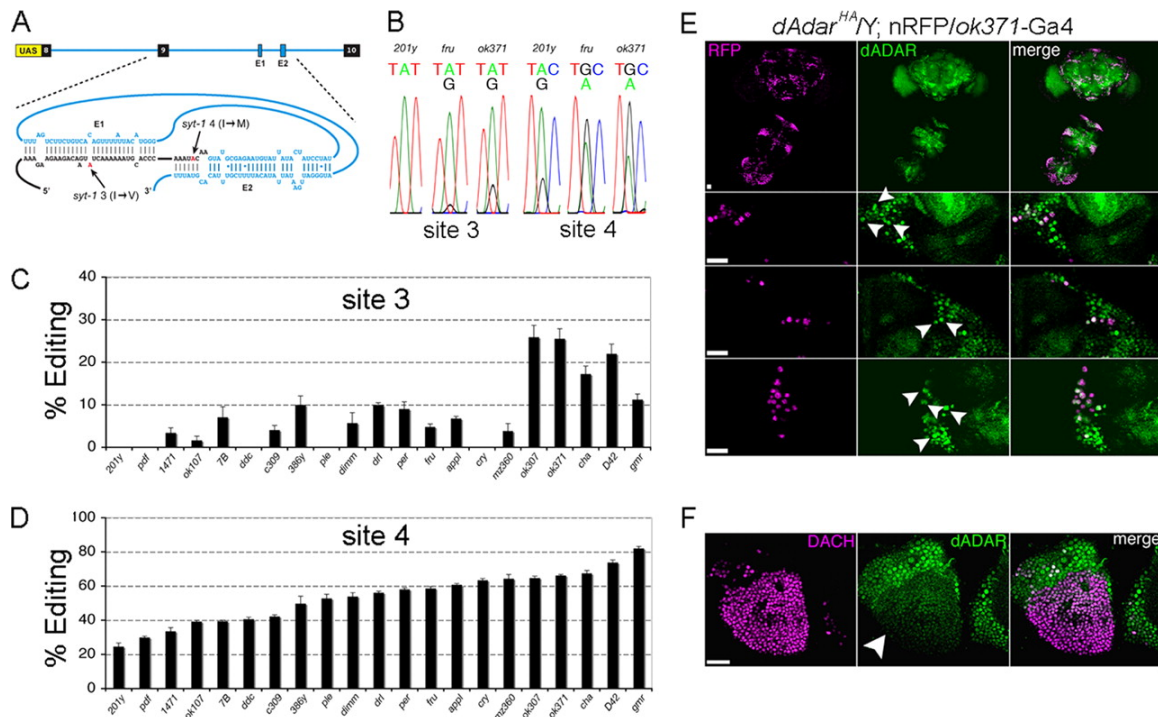


Figure C2. Molecular reporter of RNA editing reveals neuron-specific patterns of dADAR activity. **A)** design of the reporter, termed syt-T. Exons 8–10 of syt-1, along with the intervening introns, were cloned into the pUAS expression vector. Upon transcription, the E1 and E2 elements form a pseudo-knot structure by base pairing with coding sequences in exon 9 (3), leading to formation of a dADAR substrate and editing of sites 3 and 4. **B)** example electropherograms showing editing of sites 3 and 4 in three genetically distinct cell types as follows: mushroom body γ neurons (201y), fruitless-positive (*fru*), and glutamatergic (*ok371*) neurons. Average editing of site 3 and 4 in 21 classes of neurons, defined by distinct Gal4 drivers, is shown in **C** and **D**. Each value is the mean of 4–6 RT-PCRs derived from males carrying each Gal4 driver and one of two independent insertions of syt-T. Error bars, S.E. values. **E)** dADAR expression in glutamatergic neurons. dADAR-HA and the nuclear red fluorescent protein red-stinger (21) driven by *ok371*-Gal4 are shown in the male brain and thoracic ganglion (upper panel), and at higher magnification in the central brain (middle) and thoracic ganglion (lower panel). **F)** dADAR-HA expression in Dachshund-positive Kenyon cells is clearly reduced relative to the surrounding nuclei. Scale bars, 20 μ m.

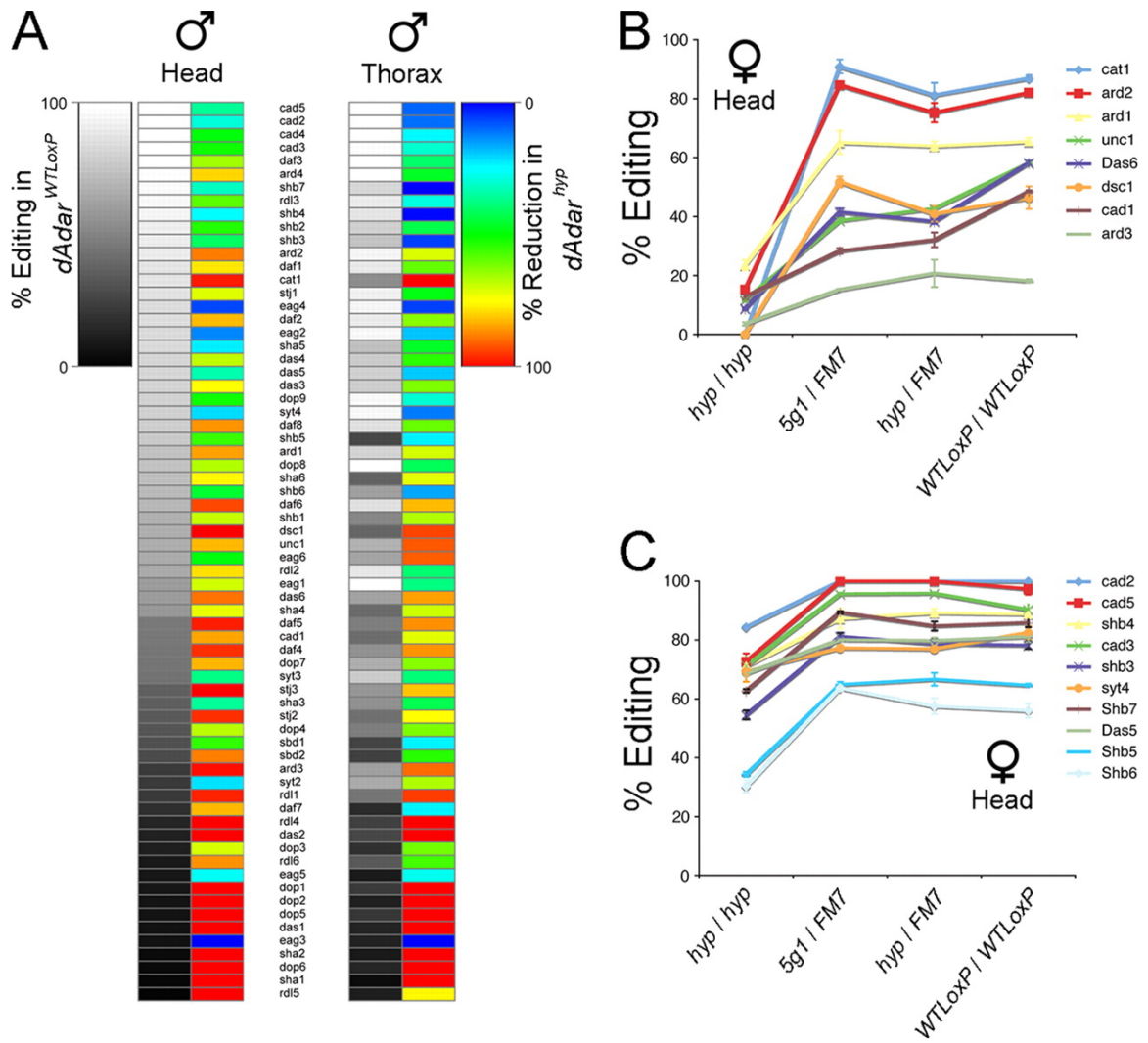


Figure C3. Varied impacts on mRNA re-coding following reduction of dADAR expression. **A**) Heat map representation of editing levels at 68 sites in $dAdar^{WTLoxP}$ heads and thoraxes, and the corresponding reduction of editing in the same tissue from $dAdar^{hyp}$ males. Each editing site is represented by a four-symbol code (see supplemental Table C3 for details). **B and C**, editing levels in female heads for 8 LE sites (B) and 10 HE sites (C). The homozygotic and heterozygotic backgrounds containing various $dAdar$ alleles are noted below each graph. Each value is the mean of ≥ 3 RT-PCRs. Error bars, S.E. values.

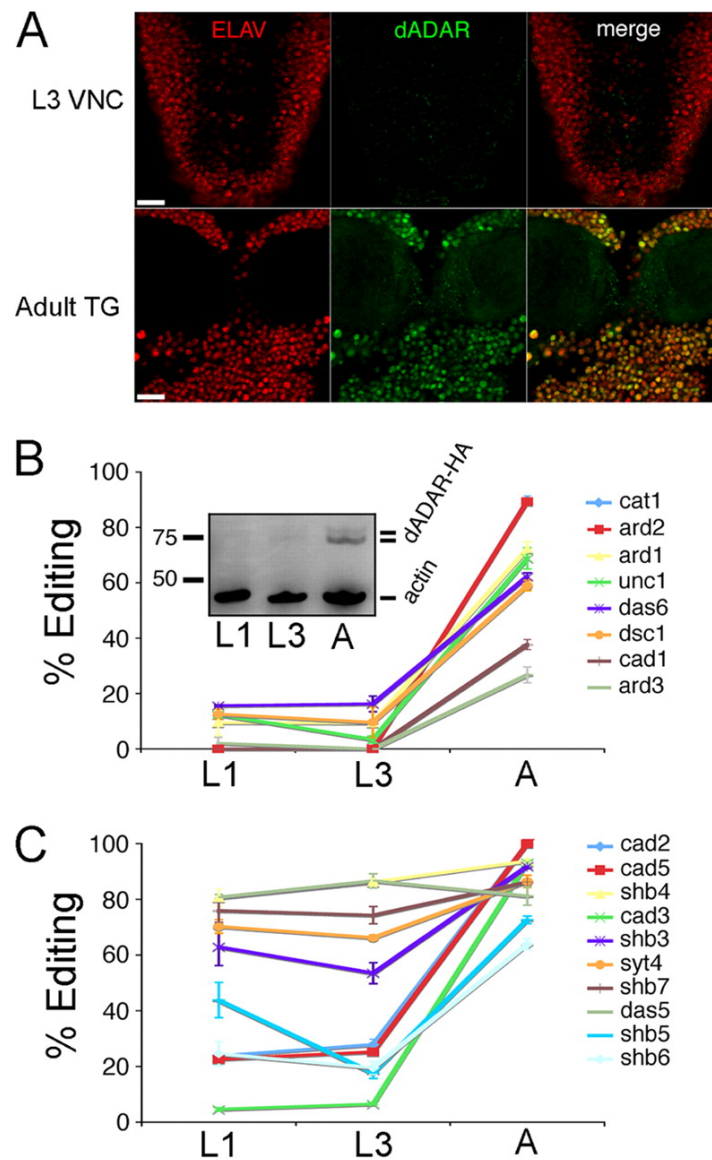


Figure C4. Dynamic control of dADAR expression underlies developmental patterns of editing at low efficiency sites. **A)** dADAR and Elav expression in the L3 ventral nerve chord (VNC) and the adult thoracic ganglion (TG). Scale bar, 20 μ m. **B)** LE sites are subject to strong developmental regulation. Editing at eight LE sites was examined at two larval stages (L1 and L3) and in adult males (A). Inset, representative example of $n = 4$ Western blots showing a strong increase in dADAR expression at the male adult-stage relative to L1 and L3. The two dADAR-HA bands likely represent dADAR proteins containing or lacking the alternatively spliced 3a exon, which is included at a higher level in the abdomen relative to the head and thorax (43). **C)** developmental profiles of 10 HE sites in L1, L3, and adult (A) males. Error bars, S.E. values.

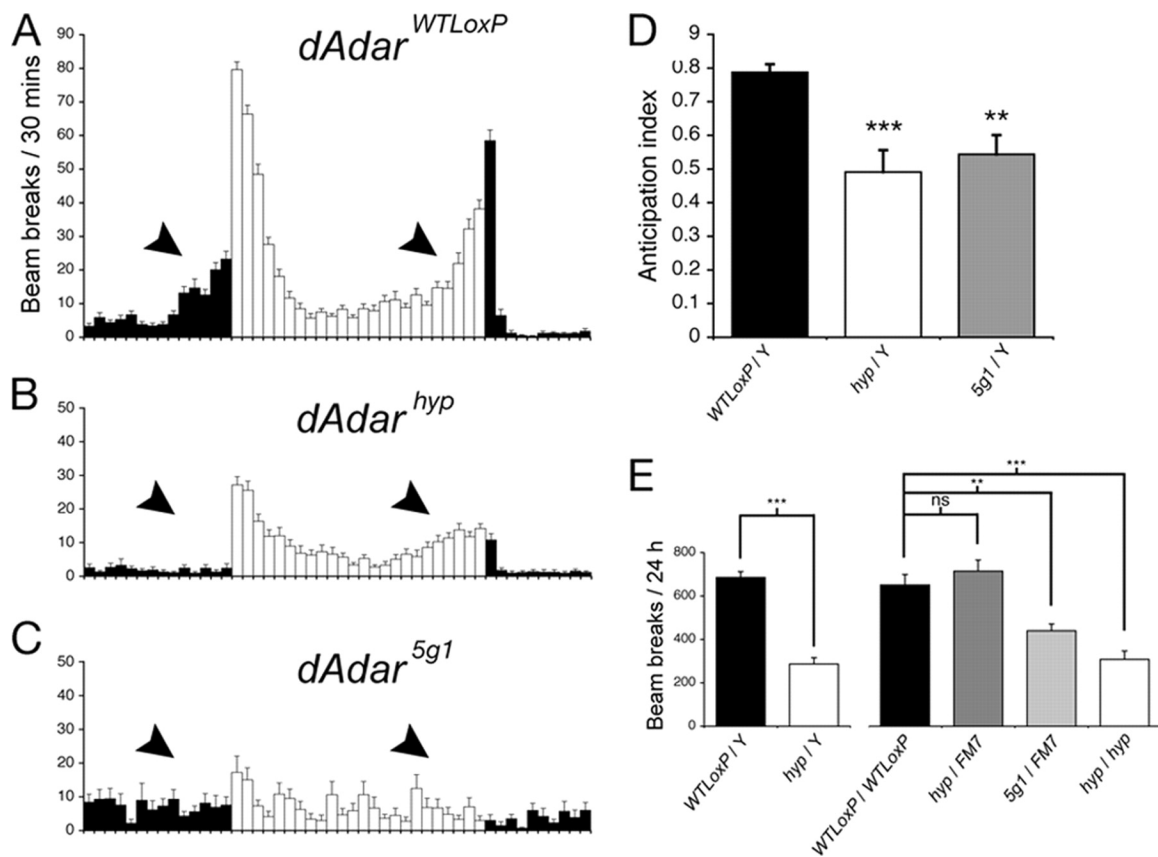


Figure C5. Global reduction in dADAR activity leads to altered patterns of locomotor activity. **A–C)** mean activity profile of *dAdar*^{WTLoxP} (**A**, $n = 30$), *dAdar*^{hyp} (**B**, $n = 30$), and *dAdar*^{5g1} males (**C**, $n = 16$) under 12-h light-dark cycles (white and black bars). Each bar is an average value of time points from three consecutive days. In *dAdar*^{WTLoxP}, but not *dAdar*^{hyp} or *dAdar*^{5g1} males, anticipation of morning and evening can be observed under both environmental conditions (arrowheads). **D)** quantification of morning anticipation in the three experimental genotypes. **E)** mean locomotor activity in male and female *dAdar* allelic backgrounds. Error bars, S.E. values. **, $p < 0.005$; ***, $p < 0.0005$; not significant (ns): $p > 0.05$ (Mann-Whitney U test).

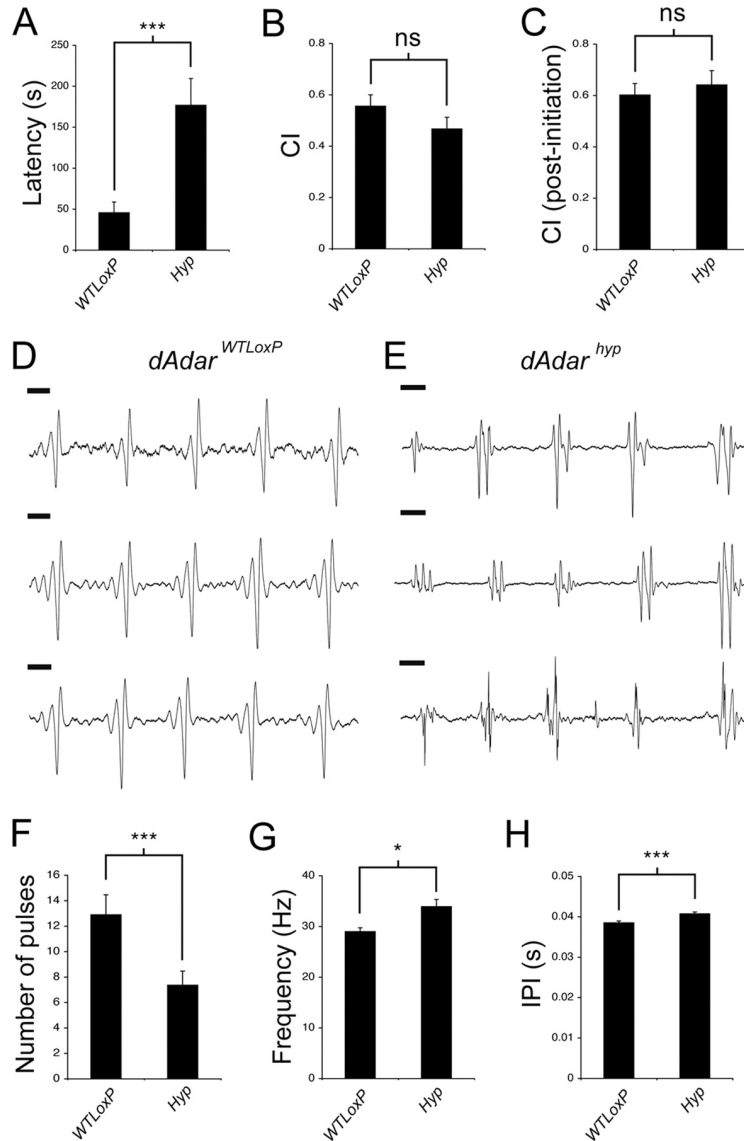


Figure C6. RNA editing is required for appropriate male courtship. **A)** time taken to initiate courtship (latency) is significantly higher in *dAdar*^{hyp} males (n = 20) relative to *dAdar*^{WTLoxP} controls (n = 15), yet the total time spent courting virgin females over a 10-min period (courtship index, CI) is not significantly different between either genotype (**B** and **C**). Courtship index was either calculated over the whole 10 min (**B**) or following initiation of courtship (**C**). Examples of three separate song trains are shown from a single *dAdar*^{WTLoxP} (**D**) or *dAdar*^{hyp} male (**E**). Note that although the trains from the *dAdar*^{WTLoxP} male are highly stereotyped, trains from even a single *dAdar*^{hyp} male show striking variability in waveform pattern. Scale bar, 10 ms. **F–H**) song parameters in *dAdar*^{WTLoxP} (n = 26 songs, 5 males) and *dAdar*^{hyp} (n = 44 songs, 9 males). Error bars, S.E. values. *, p < 0.05; ***, p < 0.0005; not significant (ns): p > 0.05 (Mann-Whitney U test).

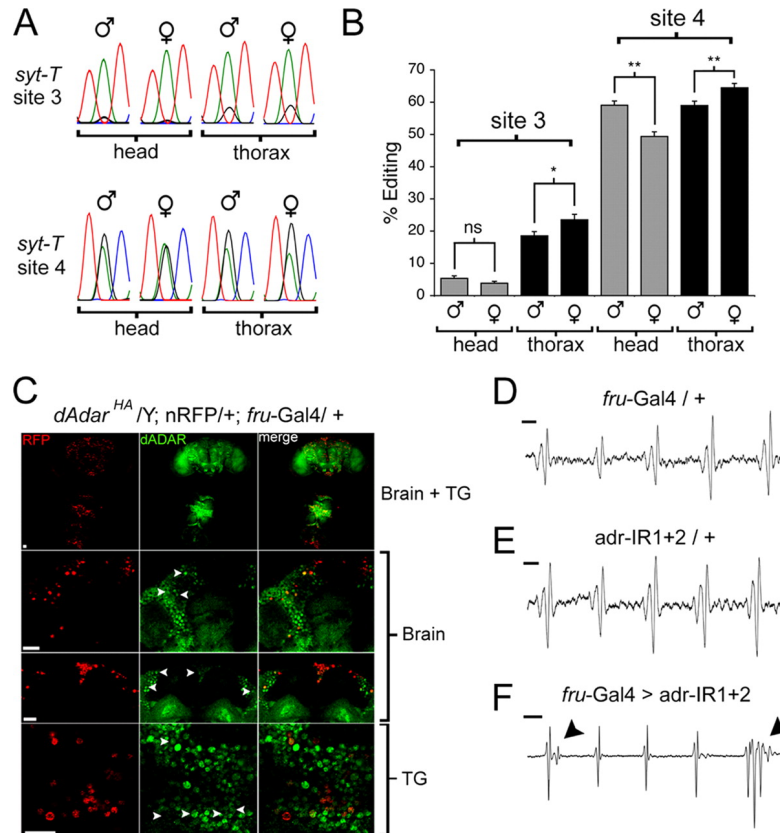


Figure C7. Knockdown of dADAR in fruitless-expressing neurons alters the male courtship song. **A)** example of electropherograms showing editing of syt-T site 3 and 4 expressed in fruitless-positive (*fru*) neurons within the male and female head or thorax. **B)** quantification of editing of two independent insertions of syt-T ($n = 6-7$ RT-PCRs for each value). **C)** dADAR expression was examined specifically in *fru* neurons by expressing a nuclear red fluorescent protein (23) using the *fru-Gal4* driver line, in a *dAdar^{HA}* background. Nuclei of *fru* neurons can be detected throughout the brain and thoracic ganglion (upper panel). Examples of dADAR expression in *fru* neurons in the dorsal anterior segment and pars intercerebralis (middle panels) and meso-thoracic ganglion (lower panel) are shown at higher magnification below. **D and E)** example of song trains from control males heterozygous for driver ($w^+; +; fru-Gal4/+$, $n = 26$ song trains, 10 males) or RNAi transgenes ($w^+; adr-IR1/+; adr-IR2/+$, $n = 30$ song trains, 10 males). Note the similarity in waveform between song trains shown in D and E compared with those from *dAdar^{WTLoxP}* males (Fig. E6D). **F)** example of song trains from males with reduced dADAR expression in *fru* neurons ($w^+; adr-IR1/+; fru-Gal4/adr-IR2$) ($n = 27$ song trains, 11 males). Note the extra spike in the first pulse and the polycyclic waveform in the last pulse. Scale bar, 10 ms. Error bars, S.E. values. *, $p < 0.05$; **, $p < 0.005$; not significant (ns): $p > 0.05$ (Mann-Whitney U test).

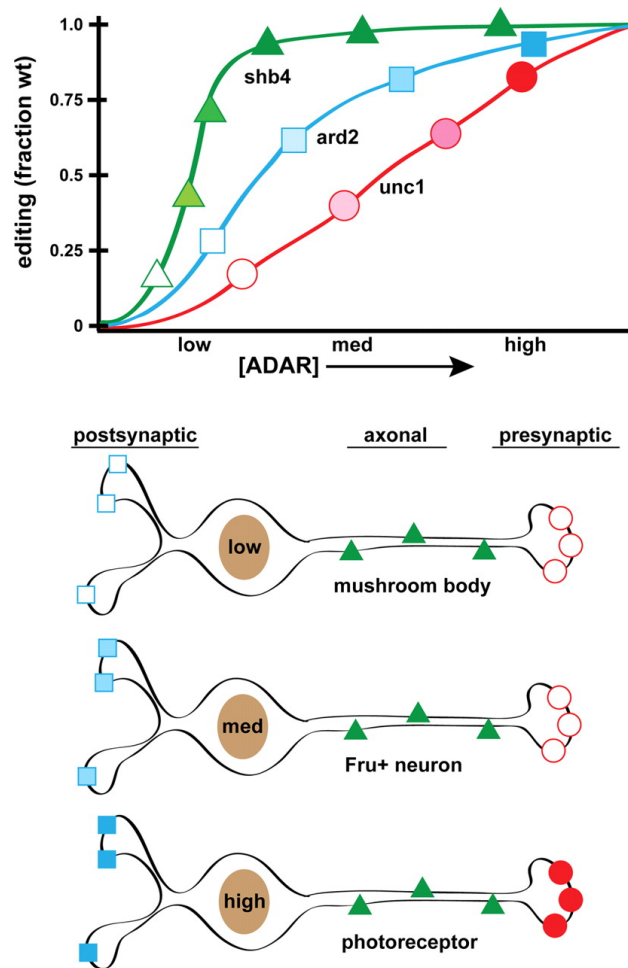
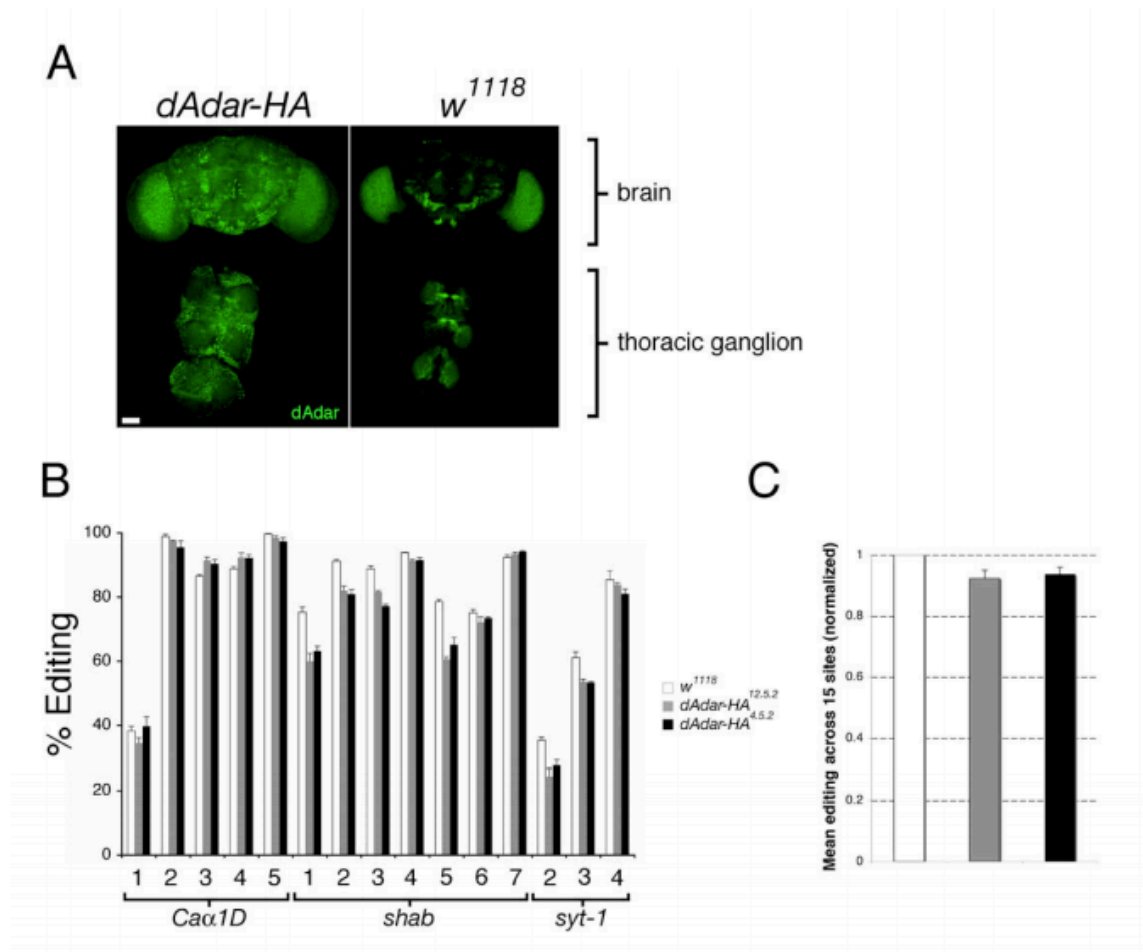
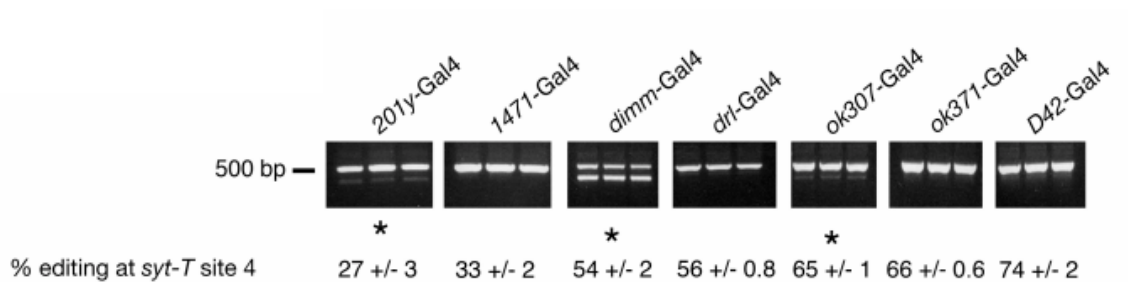


Figure C8. Model for neuron to neuron variation in editing levels within the *Drosophila* nervous system. Top panel shows a graphical representation of the change in editing of one HE site (shab site 4; shb4) and two LE sites (ard site 2; ard2, and unc-13; unc1). Shab site 4 is edited at almost wild-type levels even in genotypes with very low dADAR expression, as is the case for all HE sites (Fig. E3). Thus, editing at this, and similar sites, is unlikely to vary widely from neuron to neuron, even though dADAR activity is highly variable in different neuronal populations (Fig. E2). In contrast, editing at LE sites is likely to vary substantially in neurons with differing levels of dADAR expression. Certain LE sites only required 50% of wild-type dADAR expression for achieving wild-type editing levels, while others required more robust dADAR expression (Fig. E3). The bottom panel shows a diagrammatic representation of three distinct neuronal subtypes (derived from Fig. E2), with low, medium (med), and high relative expression of dADAR. In neurons with low dADAR activity (such as mushroom body neurons), only HE sites such as shab site 4 are likely to be strongly edited. At slightly higher levels (for example, fru neurons), both shab site 4 and ard site 2 (i.e. the “higher efficiency” LE sites) will show editing but not weak LE sites such as unc-13. Finally, in neurons with high dADAR expression (such as photo-receptors; supplemental Table C2), all subclasses may be open to robust editing.

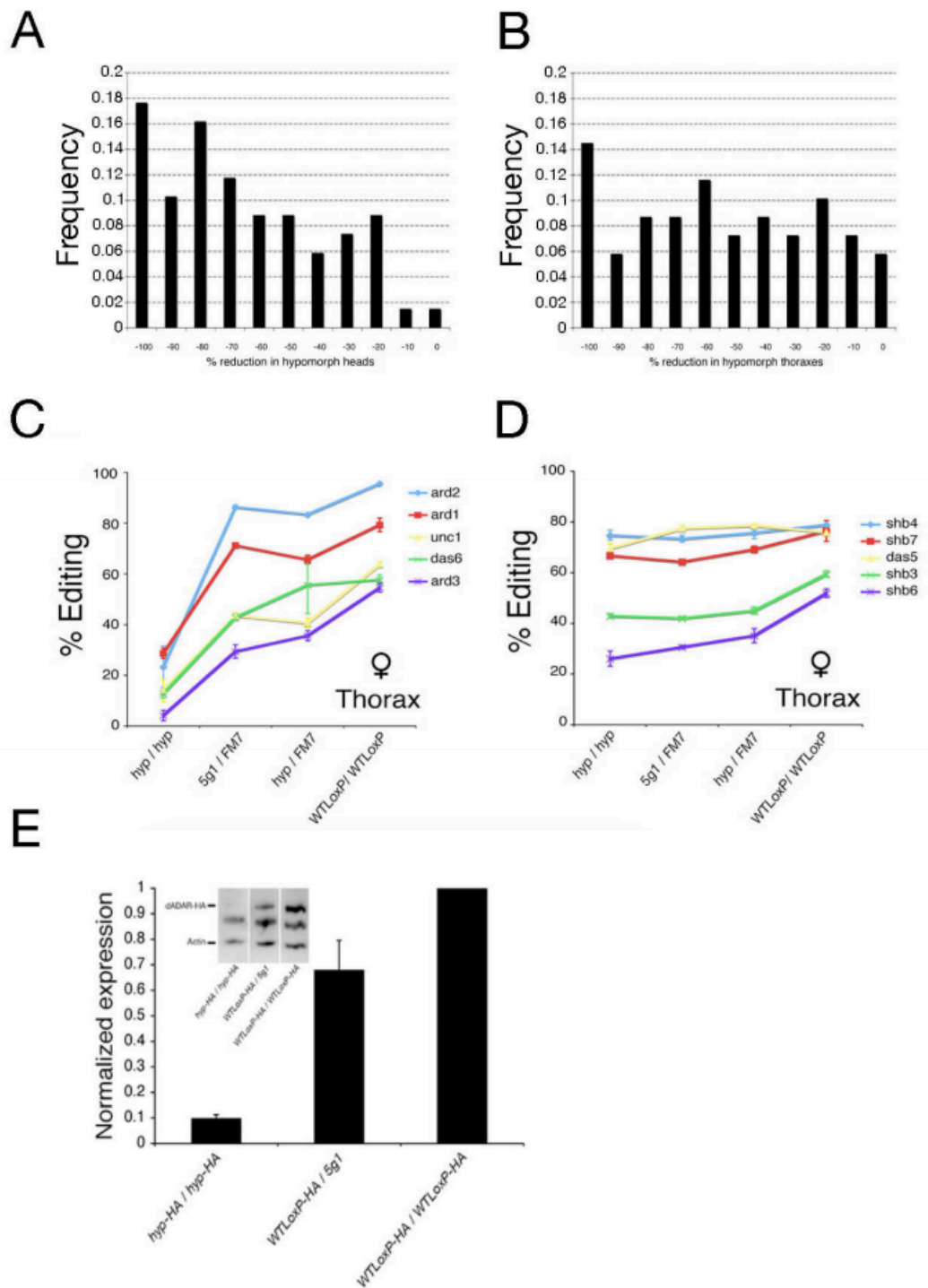
SUPPLEMENTARY MATERIAL



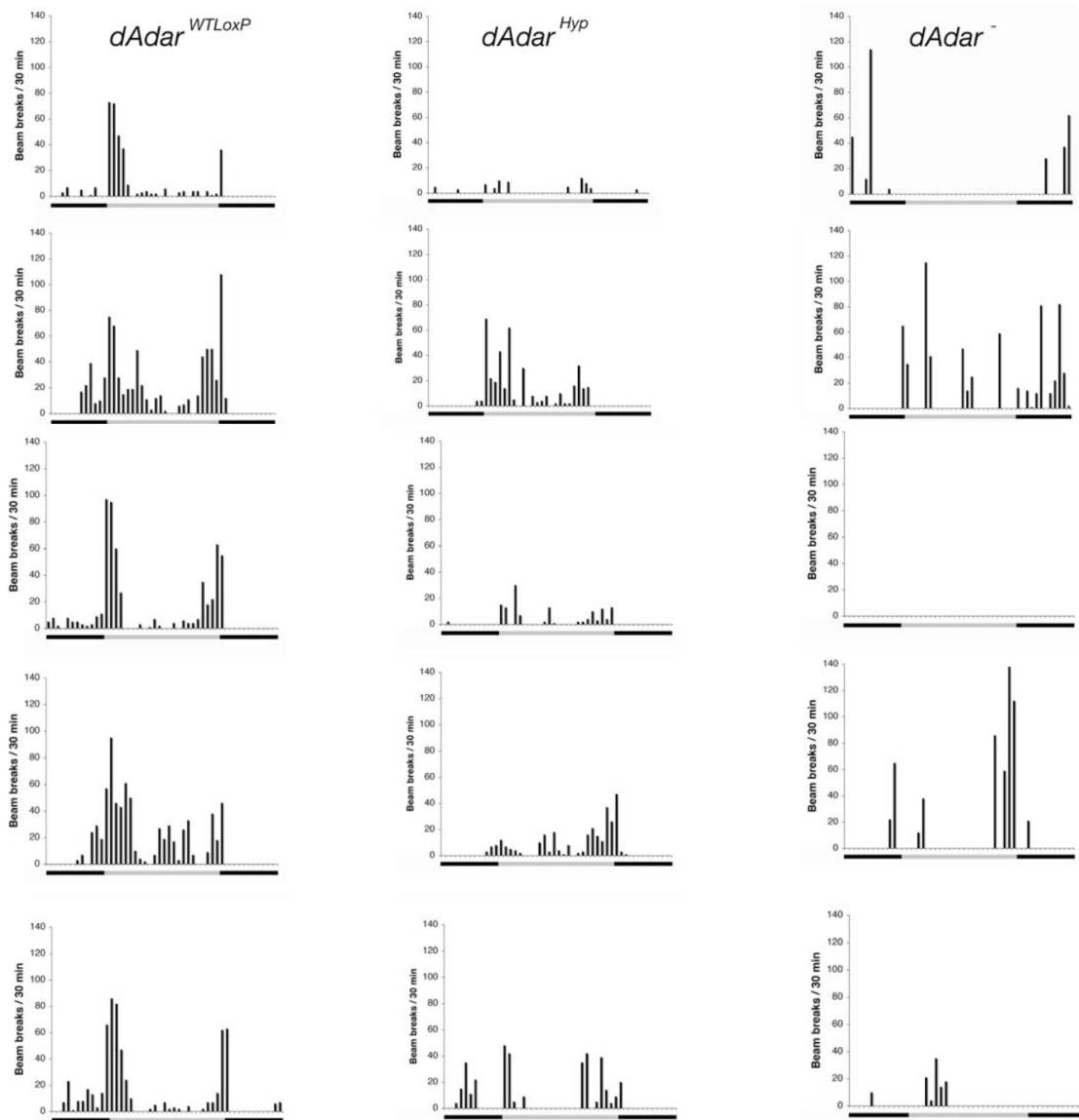
Supplementary Figure C1. A) Expression of dADAR-HA in the male brain and thoracic ganglion (TG). Punctate HA-positive staining was observed in nuclear regions throughout both the brain and thoracic ganglion (TG) in dAdar HA males but not *w*¹¹¹⁸ negative controls. Scale bar = 50 μ m. **B)** Editing levels at 15 adenosines in three different transcripts were not affected by addition of the HA-tag to the dAdar locus. Two independent dAdar^{HA} alleles (12.5.2 and 4.5.2) were compared to *w*¹¹¹⁸ males. Mean values for the population of editing sites are shown in **C)** after normalization to *w*¹¹¹⁸. Error bars, S.E values.



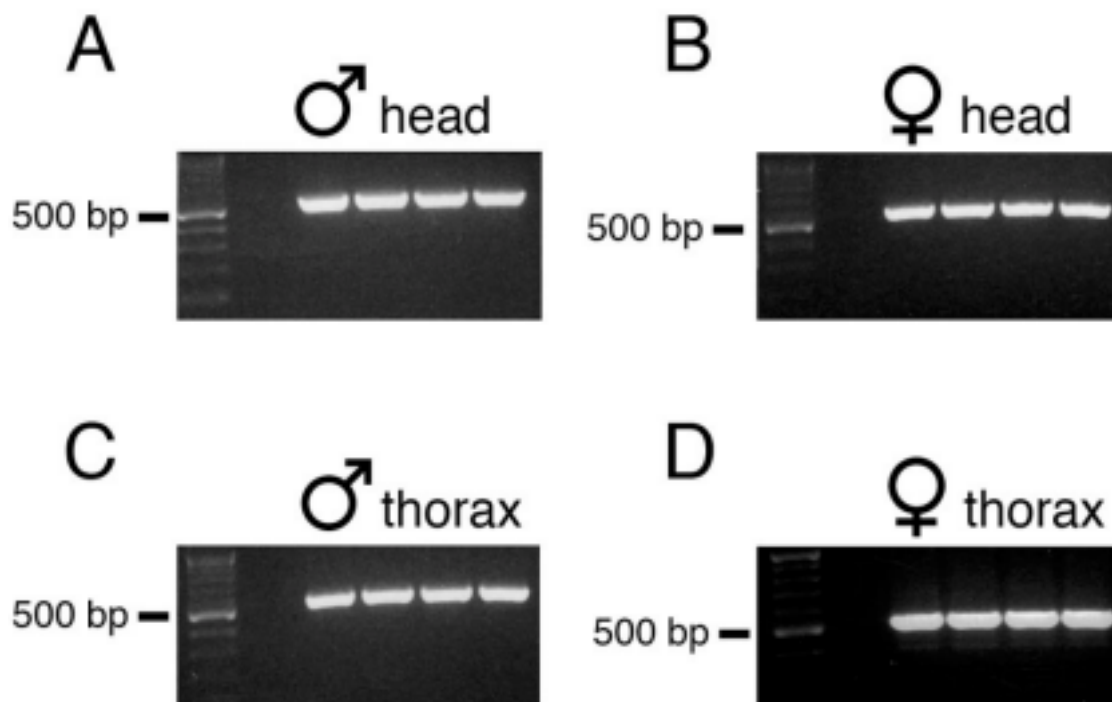
Supplementary Figure C2. Exon skipping of the *syt-T* reporter does not account for neuron-specific differences in editing. Only in a minority of the 21 neuronal sub-types in which the reporter was expressed (supplemental Table C2), did we observe skipping of the edited exon (exon 9, Figure C2) in RT-PCR products (three independent PCR reactions are shown for each Gal4 line). However, the degree of skipping did not correlate with the level of editing at either editing site in the *syt-T* construct. For example, when *syt-T* was driven using both 201y- and ok307-Gal4, we observed a small degree of skipping, yet these two neurons exhibit contrasting levels of editing at *syt-T* site 4. In adult heads, robust skipping only occurred when *syt-T* was driven in one neuronal subtype (peptidergic neurons) by *dimm*-Gal4. In this neuronal subtype, editing at site 4 is not significantly different from that seen when *syt-T* is driven by *drl*-Gal4 (MB and CC expression, Supp. Table C2), yet we observed no alternative splicing using this driver.



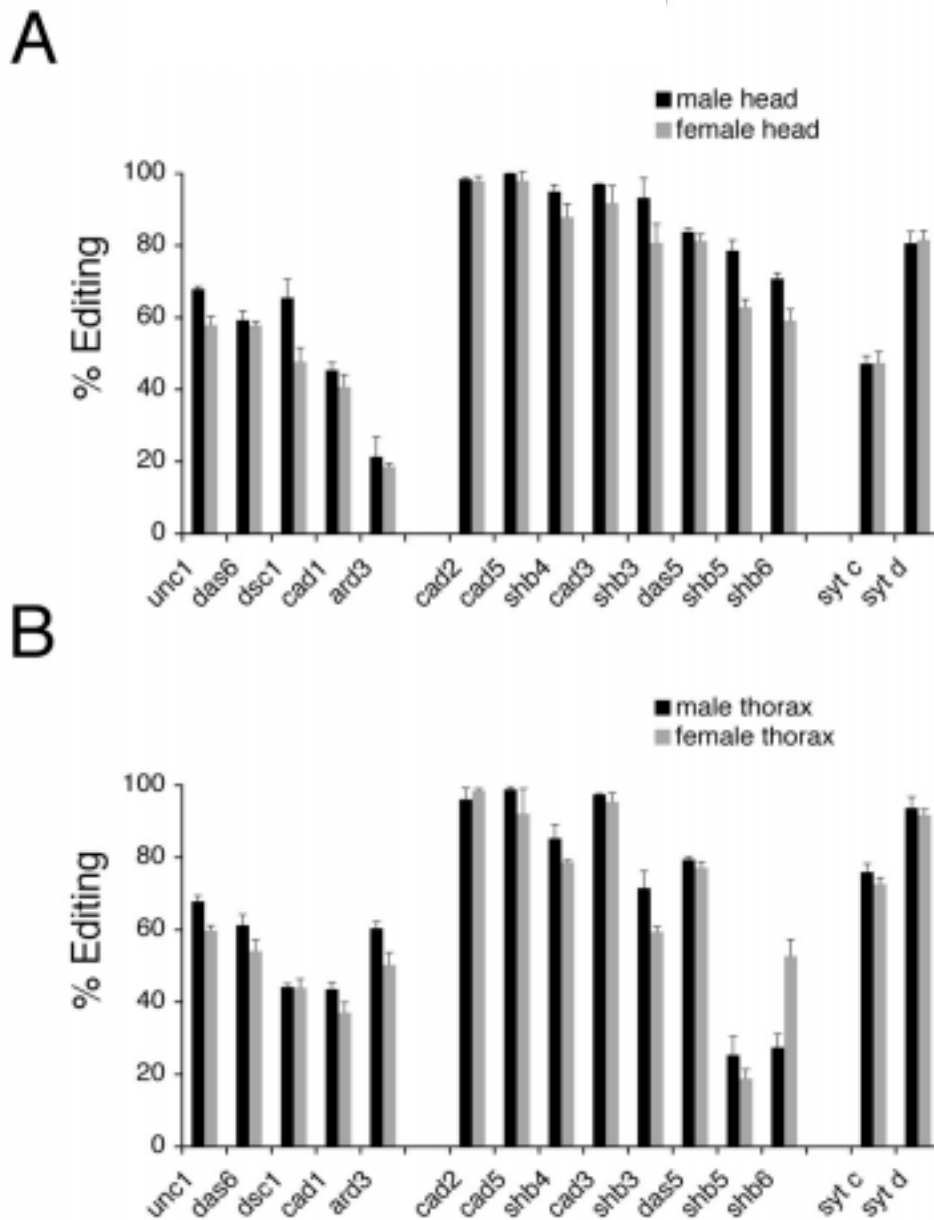
Supplementary Figure C3. Frequency distribution of the reduction in editing levels observed at 68 dADAR target adenosines amplified from dAdar^{hyp} heads (A) and thoraxes (B), compared to the same tissue in dAdar WTLoxP males. (C-D) Editing levels in female thoraxes for five ‘low efficiency’ (LE) sites (C) and high-efficiency (HE) sites (D). The female genetic backgrounds are noted below each graph. Each mean was calculated from ≥ 3 RT-PCRs. E) dADAR-HA expression levels in hyp, HA, WTLoxPHA /5g1 and WTLoxPHA females. Inset shows example western blot from the above genotypes. We did not observe signs of any substantial feedback loop indicating increased expression from the single wild-type dAdar locus in WTLoxPHA /5g1 female (n = 3 western blots). Error bars, S.E values



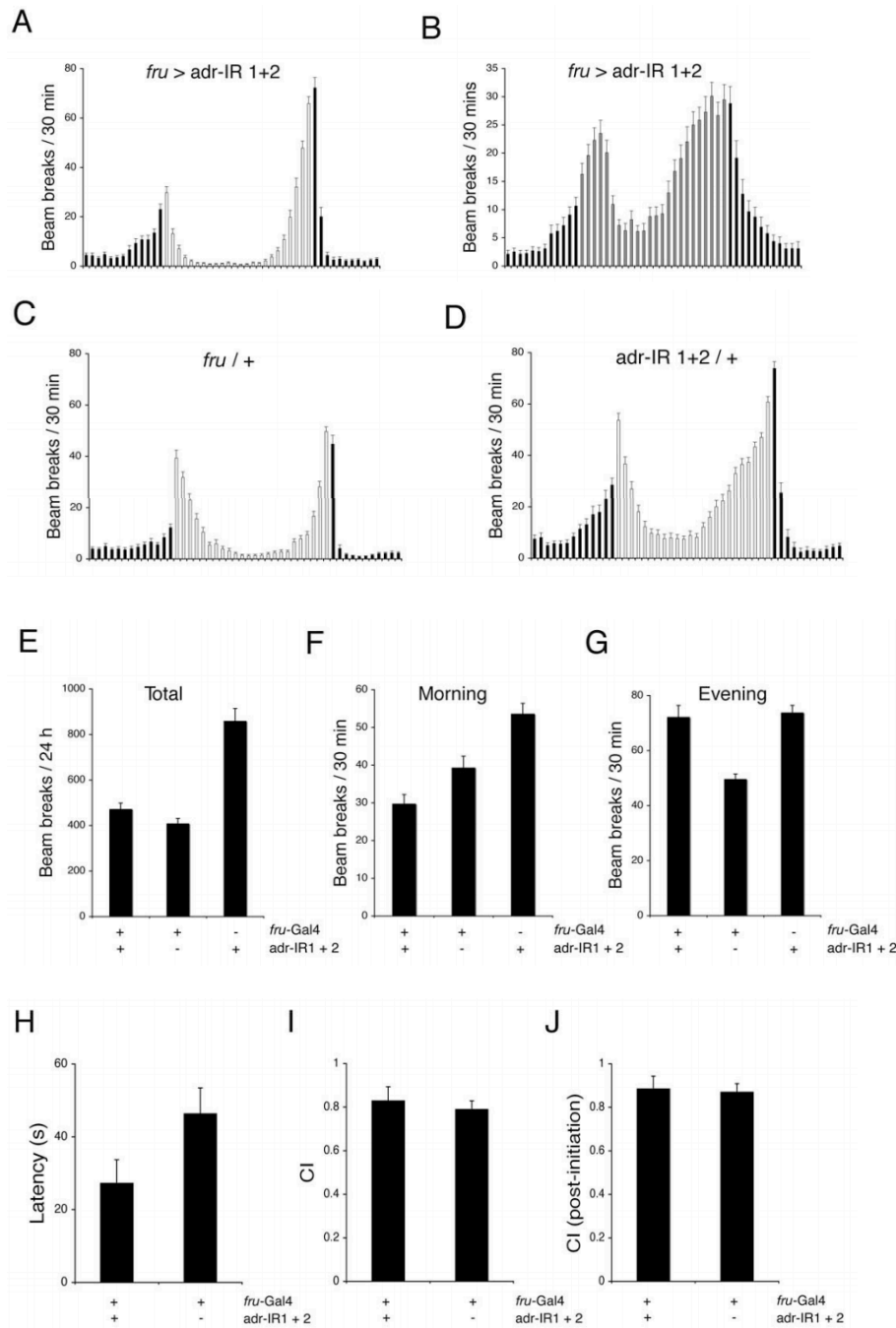
Supplementary Figure C4. Examples of single-fly profiles of locomotor activity. For each genotype, five individual traces are shown across a single 24 h period. Dark bars represent lights-off and grey bars lights-on. Locomotion in $dAdar^{WTLoxP}$ males is highly stereotyped, with peak levels of activity occurring at lights-on and lights-off in all cases, and very little activity observed under dark conditions. $dAdar$ hypomorphs also show peaks at lights-on and lights-off, but the peaks are reduced in magnitude relative to $dAdar^{WTLoxP}$. In addition, the increase in activity preceding lights-on, which can be observed in $dAdar^{WTLoxP}$ males, is not generally present in $dAdar$ hypomorphs. In contrast to $dAdar$ hypomorphs, $dAdar$ null ($dAdar^{5g1}$) males exhibit an essentially random pattern of activity, with brief increases in beam breaks even observed in dark conditions. In some cases, no activity is observed over a 24 h period (third example). In the example given, locomotor activity was detected in the next 24 h period, indicating that the fly was not simply dead, but inactive.



Supplementary Figure C5. No sex-specific exon skipping of the syt-T reporter when driven by fru-Gal4. Four independent PCR products of syt-T amplified from male (A, C) or female (B, D) head and thorax are shown. No difference syt-T splicing in male head vs. thorax or male vs. female head tissue was observed. We noticed a slight degree of skipping in female thoraxes (D), but this was insignificant relative to the full length PCR product which was subjected to sequence analysis.



Supplementary Figure C6. Lack of sexual dimorphism between endogenous transcripts in male and female heads (**A**) and thoraxes (**B**). Five LE sites and eight HE sites were examined (see Figures E3B and E3C), as well as the *syt-1* transcript that is the basis for the *syt-T* reporter. Importantly, there was no significant difference between editing at either site in *syt-1* amplified from either male or female tissue. Small reductions in female heads and thoraxes were observed relative to the corresponding male transcripts at several other sites. Notably, at only one site (*shab* site 6) was there an increase in females relative to males, but only in the female thorax. $n > 3$ RTPCRs for each data point. Error bars, S.E values.



Supplementary Figure C7. Inhibiting dADAR activity in fruitless neurons does not alter circadian rhythms. **(A-C)** Average locomotor activity profiles for the three genotypes used in Figure 7. All genotypes showed anticipation of both lights on (morning) and lights of (evening) ($n = 32$ for each genotype). Black bars represent lights-off, white bars represent lights-on. **(D)** Under constant-dark conditions, males with reduced dADAR expression in *fru*-positive neurons still exhibit anticipation of lights-on and lights-off, illustrating that the circadian clock is intact under these conditions. **(E-F)** Average locomotion over 24 h (E), and for morning (F) and evening (G) peaks of activity. Error bars, S.E values.

Supplementary Table C1. Description of *Drosophila* strains used in this study

<i>Drosophila</i> strain	Homologous recombinant, mutant allele or transgene?	Description
<i>dAdar</i> ^{5g1}	Null allele of <i>dAdar</i>	P-element derived deletion of the <i>dAdar</i> locus
<i>dAdar</i> ^{WTLoxP}	Recombinant <i>dAdar</i> allele	Control allele of <i>dAdar</i> containing a single loxP site in intron 7 of the <i>dAdar</i> locus
<i>dAdar</i> ^{hyp}	Recombinant <i>dAdar</i> allele	Wild-type <i>dAdar</i> locus with the addition of a ~ 5 kb white ⁺ mini-gene cassette in intron 7, leading to a stringent loss of dADAR expression
<i>dAdar</i> ^{HA}	Recombinant <i>dAdar</i> allele	In addition to the loxP site in intron 7, contains a HA epitope-tag sequence at the 3' of the <i>dAdar</i> locus
<i>Syt-T</i>	Transgene under control of UAS promoter	Vector contains exons 8-10 of the <i>syt-1</i> locus and the intervening intronic regions containing cis-elements directing RNA editing at site 3 and 4 of <i>syt-1</i>
<i>w</i> ¹ ; <i>adr-IR1</i> ; <i>adr-IR2</i> (<i>adr-IR1+2</i>)	Double transgene RNAi line	Contains two independent insertions (one chromosomes II and III) of inverted repeat sequences directed to the 3' of the <i>dAdar</i> locus
<i>w</i> ¹ ; <i>red-stinger</i> /CyO	Transgene insertion	Drives a modified RFP fluorophore localized to the nuclear compartment
Canton-S		Control stock
<i>w</i> ¹¹¹⁸		Control stock

Supplementary Table C2. Expression of a molecular reporter for RNA editing in discrete neuronal sub-populations. Mean values from two independent lines expressed using each driver are shown for both site 3 and 4 of the ectopically expressed region of *syt-1* (termed *syt-T*).

Driver	Predominant cell-type	Site 3 (mean \pm s.e.m)	Site 4 (mean \pm s.e.m)
<i>201y</i>	mushroom bodies	7 \pm 3	27 \pm 3
<i>pdf</i>	circadian neurons	0	30 \pm 0.8
<i>1471</i>	mushroom bodies	3 \pm 1	33 \pm 2
<i>Ok107</i>	mushroom bodies	1.6 \pm 1	39 \pm 0.8
<i>7B</i>	mushroom bodies	7 \pm 2	39 \pm 0.8
<i>ddc</i>	dopaminergic neurons	0	41 \pm 1
<i>c309</i>	mushroom bodies	4 \pm 1	42 \pm 1
<i>386y</i>	peptidergic neurons	10 \pm 2	50 \pm 4
<i>ple</i>	dopaminergic neurons	0	53 \pm 2
<i>dimm</i>	peptidergic neurons	6 \pm 2	54 \pm 2
<i>drl</i>	mushroom bodies and central complex	10 \pm 0.6	56 \pm 0.8
<i>per</i>	circadian neurons	9 \pm 2	58 \pm 0.8
<i>fru</i>	<i>fruitless</i> neurons	5 \pm 0.7	59 \pm 1
<i>appl</i>	pan-neuronal	7 \pm 0.5	61 \pm 0.7
<i>cry</i>	circadian neurons	0	63 \pm 1
<i>mz360</i>	serotonergic neurons	4 \pm 2	64 \pm 2
<i>ok307</i>	giant descending neuron	26 \pm 2	65 \pm 1
<i>ok371</i>	glutamatergic neurons	26 \pm 2	66 \pm 0.6
<i>cha</i>	cholinergic neurons	17 \pm 2	67 \pm 2
<i>D42</i>	motor neurons	22 \pm 2	74 \pm 2
<i>gmr</i>	eye	11 \pm 1	82 \pm 0.1

Supplementary Table C3. Editing levels at 68 target adenosines in *dAdar*^{WTLoxP} and *dAdar*^{hyp} male head and thorax.

CG number	Gene	Chromosome	Coordinate	Editing site	name	<i>dAdar</i> ^{WTLoxP} head % editing (mean ± s.e.m)	<i>dAdar</i> ^{hyp} head % editing	<i>dAdar</i> ^{WTLoxP} thorax % editing	<i>dAdar</i> ^{hyp} thorax % editing
10537	<i>rdl</i>	3L	9144936	site 5	rdl5	1 ± 0.7	0	11 ± 0.7	0.3 ± 0.02
12348	<i>shaker</i>	X	17846750	site 1	sha1	2 ± 0.7	0	4 ± 1	0
18314	<i>DopEcR</i>	3L	4369207	site 7	dop7	3 ± 0.9	0	14 ± 1	0
12348	<i>shaker</i>	X	17846749	site 2	sha2	4 ± 0.1	0	10 ± 0.9	0
10952	<i>eag</i>	X	14893953	site 3	eag3	7 ± 0.7	9 ± 0.7	13 ± 0.6	14 ± 0.3
4128	<i>Dca6</i>	2L	9809367	site 1	das1	7 ± 0.5	0	14 ± 0.9	0
18314	<i>DopEcR</i>	3L	4369208	site 6	dop6	7 ± 0.4	0	21 ± 1	0
18314	<i>DopEcR</i>	3L	4369455	site 2	dop2	8 ± 0.7	0	12 ± 0.1	0
18314	<i>DopEcR</i>	3L	4369459	site 1	dop1	8 ± 0.6	0	22 ± 0.9	0
10952	<i>eag</i>	X	14893971	site 5	eag5	8 ± 0.9	6 ± 2	10 ± .5	7 ± 0.6
10537	<i>rdl</i>	3L	9144935	site 6	rdl6	9 ± 0.6	1.3 ± 1.3	34 ± 1	15 ± 0.5
18314	<i>DopEcR</i>	3L	4369445	site 3	dop3	12 ± 1	3 ± 0.9	18 ± 1	7 ± 0.8
4128	<i>Dca6</i>	2L	9809365	site 2	das2	13 ± 0.6	0	27 ± 0.7	0
10537	<i>rdl</i>	3L	9148285	site 4	rdl4	14 ± 0.4	0	25 ± 4	0
32975	<i>Dca5</i>	2L	14089233	site 7	daf7	18 ± 1	3 ± 0.3	16 ± 0.2	13 ± 0.6
10537	<i>rdl</i>	3L	9156024	site 1	rdl1	22 ± 1	0.7 ± 0.7	45 ± 0.5	3 ± 0.1
3139	<i>syt-1</i>	2L	2785621	site 2	syt2	22 ± 1	17 ± 1	65 ± 1	22 ± 1
11348	<i>ard</i>	3L	4433319	site 3	ard3	22 ± 1	0.3 ± 0.3	61 ± 0.7	6 ± 0.2
6798	<i>sbd</i>	3R	20337373	site 2	sbd2	29 ± 1	4 ± 0.4	25 ± 0.1	12 ± 0.4
6798	<i>sbd</i>	3R	20337378	site 1	sbd1	30 ± 0.6	14 ± 0.6	26 ± 0.8	20 ± 0.8
18314	<i>DopEcR</i>	3L	4369313	site 4	dop4	32 ± 0.9	10 ± 1	48 ± 2	18 ± 0.6
12295	<i>stj</i>	2R	9697112	site 2	stj2	34 ± 0.6	2 ± 0.3	43 ± 1	11 ± 0.1
12348	<i>shaker</i>	X	17844090	site 3	sha3	36 ± 0.6	23 ± 1	55 ± 1	32 ± 0.3
12295	<i>stj</i>	2R	9697467	site 3	stj3	37 ± 2	0	57 ± 0.3	11 ± 2
3139	<i>syt-1</i>	2L	2785610	site 3	syt3	44 ± 4	16 ± 0.2	78 ± 1	48 ± 1
18314	<i>DopEcR</i>	3L	4369185	site 8	dop8	45 ± 1	8 ± 1	66 ± 0.5	25 ± 2
32975	<i>Dca5</i>	2L	14089207	site 4	daf4	45 ± 2	2 ± 0.4	56 ± 2	8 ± 0.5
4894	<i>Cac1D</i>	2L	16174116	site 1	cad1	46 ± 0.4	7 ± 0.2	41 ± 1	12 ± .06
32975	<i>Dca5</i>	2L	14089212	site 5	daf5	46 ± 8	1 ± 0.3	48 ± 0.2	7 ± 0.2
12348	<i>shaker</i>	X	17824766	site 4	sha4	58 ± 16	16 ± 0.3	41 ± 1	12.5 ± 1
4128	<i>Dca6</i>	2L	9807941	site 6	das6	60 ± 2	7 ± 0.2	62 ± 0.2	10 ± .6
10952	<i>eag</i>	X	14890707	site 1	eag1	60 ± 0.9	18 ± 2	1	62 ± 2
10537	<i>rdl</i>	3L	9156017	site 2	rdl2	65 ± 0.9	14 ± 0.5	88 ± 0.5	54 ± 2
10952	<i>eag</i>	X	14894656	site 6	eag6	65 ± 2	33 ± 2	63 ± 1	6 ± 0.1
2999	<i>unc-13</i>	4	895009	site 1	unc1	66 ± 1	12 ± 1	68 ± 0.5	6 ± 0.4
34405	<i>DSC1</i>	2R	20800371	site 1	dsc1	67 ± 2	0	39 ± 2	3 ± 2
1066	<i>shab</i>	3L	2941131	site 1	shb1	67 ± 3	21 ± 2	52 ± 1	17 ± 0.4
32975	<i>Dca5</i>	2L	14089221	site 6	daf6	70 ± 0.6	5 ± 0.3	85 ± 0.3	15 ± 1
1066	<i>shab</i>	3L	2941425	site 6	shb6	71 ± 1	39 ± 1	61 ± 1	51 ± 0.1
12348	<i>shaker</i>	X	17824684	site 6	sha6	72 ± 1	17 ± 0.7	37 ± 0.3	11 ± 1
18314	<i>DopEcR</i>	3L	4369184	site 9	dop9	74 ± 0.2	25 ± 2	99 ± 0.1	58 ± 0.5

11348	<i>ard</i>	3L	4432486	site 1	ard1	74 ± 0.2	11 ± 0.4	81 ± 0.7	24 ± 3
1066	<i>shab</i>	3L	2941396	site 5	shb5	77 ± 0.8	34 ± 0.1	27 ± 2	21 ± 1
32975	<i>Dα5</i>	2L	14089236	site 8	daf8	79 ± 0.8	11 ± 0.2	86 ± 0.3	34 ± 1
3139	<i>syt-1</i>	2L	2785542	site 4	syt4	79 ± 4	64 ± 0.3	95 ± 1	84 ± 1
18314	<i>DopEcR</i>	3L	4369162	site 10	dop10	80 ± 1	39 ± 2	95 ± 0.5	67 ± 2
4128	<i>Dα6</i>	2L	9809350	site 3	das3	81 ± 0.8	21 ± 0.7	79 ± 1	30 ± 2
4128	<i>Dα6</i>	2L	9809297	site 5	das5	82 ± 1	54 ± 0.9	79 ± 1	64 ± 1
4128	<i>Dα6</i>	2L	9809349	site 4	das4	82 ± 0.3	26 ± 0.7	78 ± 1	36 ± 1
12348	<i>shaker</i>	X	17824691	site 5	sha5	83 ± 6	64 ± 0.3	73 ± 0.6	39 ± 1
10952	<i>eag</i>	X	14893901	site 2	eag2	84 ± 0.3	73 ± 0.4	95 ± 0.2	77 ± 2
32975	<i>Dα5</i>	2L	14083517	site 2	daf2	84 ± 0.3	15 ± 1	89 ± 1	33 ± 1
10952	<i>eag</i>	X	14893957	site 4	eag4	84 ± 1	79 ± 0.4	94 ± 0.6	88 ± 0.6
12295	<i>stj</i>	2R	9697052	site 1	stj1	86 ± 0.4	25 ± 2	92 ± 0.4	47 ± 4
15899	<i>Cα1T</i>	X	6009458	site 1	cat1	87 ± 0.7	2 ± 1	54 ± 3	0
32975	<i>Dα5</i>	2L	14083516	site 1	daf1	87 ± 0.4	19.2 ± 0.1	89 ± 0.9	36 ± 1
11348	<i>ard</i>	3L	4432487	site 2	ard2	90 ± 0.6	11 ± 3	94 ± 2	27 ± 2
1066	<i>shab</i>	3L	2941312	site 3	shb3	90 ± 3	54 ± 1	75 ± 2	70 ± 0.6
1066	<i>shab</i>	3L	2941132	site 2	shb2	91 ± 0.5	42 ± 0.8	79 ± 3	45 ± 0.8
1066	<i>shab</i>	3L	2941364	site 4	shb4	94 ± 0.9	70 ± 2	88 ± 0.4	87 ± 0.9
10537	<i>rdl</i>	3L	9148318	site 3	rdl3	95 ± 0.2	39 ± 2	90 ± 2	64 ± 0.9
1066	<i>shab</i>	3L	2941426	site 7	shb7	96 ± 1	66 ± 0.7	82 ± 2	84 ± 1
11348	<i>ard</i>	3L	4433320	site 4	ard4	97 ± 0.1	20 ± 0.1	1	54 ± 2
32975	<i>Dα5</i>	2L	14089204	site 3	daf3	98 ± 0.8	34 ± 2	99 ± 0.5	60 ± 0.2
4894	<i>Cα1D</i>	2L	16174152	site 3	cad3	99 ± 1	48 ± 1	97 ± 0.1	68 ± 2
4894	<i>Cα1D</i>	2L	16174153	site 4	cad4	99 ± 0.5	51 ± 1	99 ± 0.1	75 ± 0.9
4894	<i>Cα1D</i>	2L	16174138	site 2	cad2	100	71 ± .9	100	89 ± 3
4894	<i>Cα1D</i>	2L	16174194	site 5	cad5	100	64 ± 0.5	100	90 ± 0.6

APPENDIX IV

Auto-Regulatory RNA Editing Fine-Tunes mRNA Re-Coding and Complex Behaviour in *Drosophila*

This section consists of data that was published in a manuscript: “Auto-Regulatory RNA Editing Fine-Tunes mRNA Re-Coding and Complex Behaviour in *Drosophila* Savva YA, Jepson JE, Sahin A, Sugden AU, Dorsky JS, Alpert L, Lawrence C, Reenan RA. Nature Communications 2012 Apr 24;3:790.” I assessed RNA editing in the recombinant lines along with Savva YA, made initial observation on altered climbing behavior in mutant *Drosophila* lines, and performed behavioral analyses along with Jepson JE.

ABSTRACT

Auto-regulatory feedback loops are a common molecular strategy used to optimize protein function. In *Drosophila* many mRNAs involved in neuro-transmission are re-coded at the RNA level by the RNA editing enzyme dADAR, leading to the incorporation of amino acids that are not directly encoded by the genome. dADAR also re-codes its own transcript, but the consequences of this auto-regulation *in vivo* are unclear. Here we show that hard wiring or abolishing endogenous dADAR auto-regulation dramatically remodels the landscape of re-coding events in a site-specific manner. These molecular phenotypes correlate with altered localization of dADAR within the nuclear compartment. Furthermore, auto-editing exhibits sexually dimorphic patterns of spatial regulation and can be modified by abiotic environmental factors. Finally, we demonstrate that modifying *dAdar* auto-editing affects adaptive complex behaviors. Our results reveal the *in vivo* relevance of auto-regulatory control over post-transcriptional mRNA re-coding events in fine-tuning brain function and organismal behavior.

INTRODUCTION

ADARs (adenosine deaminases that act on RNA) mediate RNA editing through the deamination of adenosine (A) to inosine (I) in dsRNA templates (Nishikura et al., 2010). Intriguingly, in mammals and insects, mRNAs that encode proteins involved in electrical and chemical neuro-transmission are highly over-represented in the population of transcripts known to undergo editing (Hoopengardner et al., 2003; Seeburg et al., 2003). Importantly, since inosine is interpreted as guanosine by the ribosome, RNA

editing in exonic regions often leads to amino acid re-coding, and thus translation into proteins that are not literally encoded by genomic DNA templates (Basilio et al., 1962).

Analysis of mutations in *adar* alleles in several diverse model organisms has demonstrated that RNA editing is crucial to neuronal function and integrity across a broad range of phyla (Higuchi et al., 2000; Palladino et al., 2000a; Tonkin et al., 2002). Loss of mouse ADAR2 expression leads to early mortality associated with severe seizures (Higuchi et al., 2000). Null mutations in the single *Drosophila adar* (*dAdar*), while not lethal, result in extreme adult-stage behavioral defects, including uncoordinated locomotion, temperature-sensitive paralysis, seizures, and a lack of the male courtship display (Palladino et al., 2000a).

In the majority of dADAR target mRNAs, between one and several adenosines are deaminated, often at low to moderate levels (Hoopengardner et al., 2003; Jepson et al., 2009) and studies have thus far demonstrated relatively subtle modifications of ion channel function through dADAR-mediated amino acid re-coding (Ingleby et al., 2009; Jones et al., 2009) suggesting that RNA editing generally acts to ‘fine-tune’ protein activity (Bass et al., 2002). The extreme phenotype observed in *dAdar* null flies may therefore reflect the cumulative action of dADAR’s functional pleiotropy. Comparative genomics approaches and serendipitous observations have identified a host of edited adenosines in mRNAs encoding ion channels and regulators of exo- and endocytosis (Hoopengardner et al., 2003; Grauso et al., 2002; Hanrahan et al., 2000; Smith et al., 1998; Smith et al., 1996). Similarly, mammalian ADAR substrates include several G-protein coupled receptors and ion channels (Seeburg et al., 2002). Recent bioinformatic analysis and deep sequencing experiments have identified hundreds of additional

potential ADAR targets in both the *Drosophila* and human transcriptomes (Graveley et al., 2011; Li et al., 2009; Stapleton et al., 2006).

Interestingly, hyper-activity of ADARs has also been shown to cause physiological and behavioral abnormalities. Over-expression of ADAR2 in mice leads to both adult-onset obesity and increased anxiety-related behaviors (Singh et al., 2007; Singh et al., 2009) while global over-expression of a dADAR isoform in *Drosophila* results in larval lethality (Keegan et al., 2005). These observations imply that precise control of mRNA re-coding is essential for development and adaptive behavior. Intriguingly, both mammalian and *Drosophila* ADARs have evolved distinct auto-regulatory feedback loops as a mechanism to alter enzymatic activity through deamination of adenosines within their own transcripts (Palladino et al., 2000b; Rueter et al., 1999). Rodent ADAR2 auto-editing acts as a negative feedback mechanism by generating a novel splicing acceptor site (AA→AI), leading to an N-terminal frame-shift and translation of a truncated ADAR2 isoform at reduced levels (Rueter et al., 1999). Correspondingly, abolition of ADAR2 auto-editing *in vivo* increases ADAR2 expression and editing at several target adenosines (Feng et al., 2006). In contrast, *dAdar* auto-editing results in a serine to glycine (S→G) coding change in the C-terminal catalytic domain (Palladino et al., 2000b). Auto-editing of *dAdar* mRNA is developmentally regulated, occurring predominantly at the pupal and adult stages, and is mediated by a complementary sequence within the edited exon (Keegan et al., 2005; Palladino et al., 2000b). *In vitro* experiments using two dADAR substrates, supported by *in vivo* data gained from expression of differentially edited dADAR transgenes, indicate that auto-editing acts to reduce dADAR activity, suggesting an evolutionary convergence in

function of dADAR and ADAR2 auto-regulation (Keegan et al., 2005). However, it is unknown whether *dAdar* auto-editing acts globally to reduce editing at all target adenosines *in vivo* or, rather, to modify particular target adenosines in a substrate-specific manner.

To understand how *dAdar* auto-regulation shapes RNA editing patterns *in vivo*, we genetically engineered *Drosophila* with either fully edited or un-edited *dAdar* alleles, and assessed editing levels across 100 adenosines in various dADAR mRNA targets in multiple male and female tissues, revealing a non-uniform modification of complex spatially regulated patterns of mRNA re-coding. Furthermore, we show that both preventing and constitutive hard-wiring of *dAdar* auto-regulation adversely affects adult-stage behaviors. Our results shed light on the adaptive importance of fine-tuning the ‘fine-tuner’ in *Drosophila*.

MATERIALS and METHODS

***Drosophila* stocks and homologous recombination**

Drosophila were raised at a constant 25°C, on standard molasses food and under 12 h day/night cycles. For analysis of RNA editing, RNA was derived from 3–5 day old flies. For experiments involving *dAdar* null males, we used the *dAdar*^{5g1} allele, previously shown to lack all detectable RNA editing activity (Palladino et al., 2000a). Stocks of *D. simulans*, *D. sechellia*, *D. yakuba* and *D. erecta* were obtained from the *Drosophila* species stock center (University of California, San Diego).

Extensive details of the constructs used to manipulate the *dAdar* locus using homologous recombination have been published previously (Jepson et al., 2011a). Briefly, we cloned two arms encompassing exons 4–7 (arm 1) and 8–10 (arm 2) of the *dAdar* genomic sequence into the p[w25.2] vector. We used mutagenic primers to convert the endogenous AGT serine codon to a synonymous TCT codon or a GGT glycine codon. An arm 1 with an AGT codon served as a control. Arm 2 contains a HA epitope-tag immediately after the last coding amino acid of dADAR, and prior to an opal (TGA) stop codon. Following recombination, the *white*⁺ mini-gene selection cassette was removed via cre-recombinase and each recombinant strain was back-crossed into a Canton-S control stock for at least five generations.

PCR and computational calculation of editing levels

RNA extractions from *Drosophila* tissues were performed using TRIzol (Invitrogen). Edited cDNAs were amplified via RT-PCR using target-specific primers (Supplementary Table D2). To computationally calculate editing ratios of the chosen 100 editing sites, edited adenosines were initially selected from RT-PCR electropherograms via an automated search for the local sequence surrounding the edited adenosine. All sequential peaks were then fit with a Gaussian mixture model (GMM; Supplementary Fig. D.8A). This prevents errors in which neighboring peaks of the same nucleotide artificially inflate the area under the curve. A grid search determines the relative positions of the peaks and a Markov Chain Monte Carlo process is used to find the best values for height (h), width (w), and standard deviation (c), as determined by the minimum chi-square of the sum of the areas of the predicted peaks and the chromatogram data (Supplementary Fig. D.8B). A minimum of three independent PCR amplicons were used

to derive the editing levels for each adenosine. To determine the degree of auto-editing in male hemizygotes and females heterozygous for various engineered *dAdar* alleles, we used the following methodology: *dAdar*^S and *dAdar*^G males and females were assumed to have auto-editing levels of 0% and 100% respectively. For the remaining genotypes, auto-editing was calculated using bulk RT-PCR electropherograms of the *dAdar* mRNA from male and female heads, with the % auto-editing calculated as $G/(A+G) \times 100$. For *dAdar*^S/*dAdar*^{WTLoxP} females, harboring both TCT and AGT serine alleles, the total level of un-edited *dAdar* was calculated by summing the A and T peaks. The auto-editing level was then derived as $G/(A+T+G) \times 100$.

Confocal microscopy and western blotting

All confocal images were obtained on a Zeiss LSM 510 meta confocal microscope. Adult brain and 3rd instar larval salivary glands were fixed in 4% PFA and blocked in 5% normal goat serum prior to antibody incubation. Primary antibodies were used at the following concentrations: rabbit anti-HA (Santa Cruz Biotech) - 1:50; goat anti-human fibrillarlin (kind gift of K. M. Pollard, TSRI, San Diego, CA) – 1: 200; mouse anti-Lamin (Developmental Studies Hybridoma Bank) – 1:40; DAPI (Invitrogen) was used at 1:1000. Images were contrast-enhanced in Adobe Photoshop. Protein samples were prepared in buffer containing SDS and β -mercaptoethanol, and run out on a 10% gel (Amresco). Anti-HA antibody (Covance) was used at 1:500, and anti-actin (Millipore) was used at 1:20000. Band intensities were quantified on a Kodak Image Station following background subtraction. 20 adult heads/100 μ L of buffer were used per sample.

To quantify the degree of extranucleolar punctal dADAR, images were split by hand into individual cells, using DAPI as a marker for nuclear location (blue). For each cell, the nucleolus, N, is defined as the contiguous region surrounding the brightest pixel of fibrillarin staining (red), F, where the intensity of every pixel is greater than 1/4 of F. The region of dADAR staining (green), P, was similarly identified. P is defined as the contiguous region surrounding the brightest pixel of dADAR staining, A, where the intensity of every pixel is greater than 1/2 of A. For the measures P/D and # P > 0 which examine extra-nucleolar punctate dADAR staining, P is considered 0 unless it is punctate (the area of P is less than the area of N) and extranucleolar (the position of A lies outside the area of N) (Supplementary Fig. D.4).

Behavioural analysis

Locomotor patterns were recorded using horizontal single fly or vertical population activity monitors (TriKinetics). For single-fly monitors, mean locomotor patterns were calculated for each fly by averaging data from three consecutive days, which were then further averaged across the experimental population. To quantify climbing ability using vertical population monitors, we took advantage of the presence of three concentric infra-red beams at the bottom, middle and top portions of the vial. We calculated the total number of beam breaks for all levels, and solely for the top level (close to the top of the vial). Relative climbing ability was calculated by dividing the number of beams breaks in the top ring by the total for all three rings, for each vial. Analysis of circadian parameters (period, % rhythmicity and power) was performed using FaasX (M. Boudinot and F. Rouyer).

To analyze courtship behavior, we measured two parameters: the time taken to initiate courtship (defined as the first orientation of the male to the female), and the total time spent courting. Males were aged for 5–7 days, and female virgins 3–5 days, prior to single-fly pairing. We used a custom-made chamber to observe behavior. Courtship occurs in circular chamber with a diameter of ~ 1 cm and height ~ 0.5 cm. To recapitulate ethologically relevant conditions, live, rather than decapitated, females were used. To control for circadian influences on behavior, experiments were performed in a relatively narrow time window (8–11 am). Attempted mating was observed over a 10 min time-span, or until the male successfully copulated.

RESULTS

Modifying the Edited Residue in the *dAdar* Locus

The auto-edited serine residue of dADAR is conserved throughout metazoan dADAR and ADAR2 homologs and structurally maps to a loop near the active site in the human ADAR2 crystal structure (Macbeth et al., 2005) (Fig. D.1A-B). In order to determine the *in vivo* significance of auto-editing, we performed ends-out homologous recombination (Rong et al., 2002) on the endogenous X-linked *dAdar* locus to generate *Drosophila* with either constitutive serine (S) or glycine (G) residues (Fig. D.1C). An allele producing only auto-edited dADAR protein (*dAdar*^G) was engineered by mutating the edited adenosine of the serine codon (AGT) to guanosine (GGT), converting it to an obligate glycine codon. Conversely, a *dAdar*^S allele, producing only un-edited dADAR, was generated by altering the same serine codon to its degenerate counterpart

(TCT), rendering A-to-I modification impossible. A *dAdar* allele containing a single intronic loxP site but with no alteration at the edited serine residue (*dAdar*^{WTLloxP}) served as a wild-type control. In addition, we generated identical targeted recombinant flies with the above alleles and also containing an HA-epitope tag at the 3' terminus of the *dAdar* coding sequence (Fig. D.1C). We have previously shown that the HA-tag has no effect on dADAR activity on several known targets (Jepson et al., 2011a), and western blot analyses revealed that modifying auto-editing has no significant effect on levels of dADAR protein expression (Fig. D.1D). We therefore used the above lines to investigate the functional consequences of auto-editing in a genetic background where the remaining endogenous control of dADAR expression is intact.

***dAdar* Editing Reduces RNA Editing at Certain Target mRNAs**

A-to-I signatures have been detected in a wide range of mRNAs encoding ion channels and regulators of endo- and exocytosis (Hoopengardner et al., 2003). To comprehensively determine the influence of *dAdar* auto-editing on mRNA re-coding, we examined editing levels at 100 adenosines in 23 mRNAs amplified from *dAdar*^{WTLloxP}, *dAdar*^S and *dAdar*^G male head cDNA (Fig. D.1E-G, Fig. D.2A, Supplementary Fig. D.1 and Supplementary Table D1, Supplementary Data 1–6). Although recent deep sequencing data has suggested the existence of potentially hundreds of previously unidentified editing targets (Graveley et. al., 2011), we limited our analysis to neuronally expressed mRNAs in which mixed A/G peaks have been shown to be abolished in a *dAdar* null background, and whose orthologous mRNAs exhibit signatures of editing in other *Drosophilid* species. The 100 adenosines analyzed

represent > 80% of the ~120 known editing sites that fit the above criteria. We were able to delineate three categories of editing sites from our initial dataset: adenosines that were completely insensitive to the edited state of dADAR (Fig. D.1E); adenosines where elimination of auto-editing was inconsequential, yet exhibited a significant reduction in editing level upon hard-wiring of *dAdar* auto-editing (Fig. D.1F); and finally, adenosines which exhibited a bi-directional response to elimination or hard-wiring of auto-editing (Fig. D.1G). Examples of each class could even be found in the same mRNA (Supplementary Fig. D.2A,B). Thus, it is unlikely that the responsiveness of a given site to auto-regulatory state is due to transcript abundance. Importantly, the above classes were not biased towards adenosines with particular levels of editing and comprise diverse mRNAs (Supplementary Fig. D.2C,D). Thus, *dAdar* auto-editing acts as a negative auto-regulatory feedback mechanism to selectively modulate dADAR activity on particular target adenosines in the male *Drosophila* head.

To test whether the selective negative-feedback effect of *dAdar* auto-editing observed in male heads was tissue- and/or sex-specific, we analyzed the same set of 100 adenosines using RNA derived from male antennal, eye and thorax cDNA (Supplementary Data 1–3), and head and thorax cDNA from all possible female allelic combinations (Fig. D.2B and Supplementary Data 1–6), and found a similar reduction in editing levels across many dADAR targets in all *dAdar*^G hemi- and homozygotic tissues. Furthermore, in both male and female head and thorax tissues, inhibiting the intrinsic regulation of *dAdar* auto-editing resulted in global alterations in the relative quantitative dynamics of RNA editing of the 100 adenosines studied (Fig. D.3A–D).

In addition, we observed novel editing sites that were only apparent in bulk RT-PCR from *dAdar*^S backgrounds (Fig. D.3E–H). One of these, a K → E substitution in the cyclic nucleotide binding domain of *eag*, is 100 nucleotides from the closest known editing site (Hoopengardner et al., 2003), suggesting the presence of a novel dADAR substrate that is only deaminated in neurons where *dAdar* auto-editing is very low or absent. This data raises the possibility of the existence of an undefined number of adenosines where editing occurs only when high levels of the dADAR^S isoform are present.

Spatial Control of *dAdar* Editing

Previous *in vitro* experiments have suggested that *dAdar* mRNA is efficiently deaminated by unedited dADAR protein, but the edited version is far less effective (Keegan et al., 2005). This observation provided a clear prediction that the presence of either of our modified *dAdar* alleles should shift the auto-editing of a wild-type allelic counterpart in the opposite direction i.e total auto-editing levels in *dAdar*^{WTLoxP}/*dAdar*^S and *dAdar*^{WTLoxP}/*dAdar*^G heterozygotes should tend towards a similar equilibrium value, presumably close to wild-type levels (~50%; Fig. D.4A). In contrast, however, we found a linear increase in auto-editing levels when comparing *dAdar*^{WTLoxP}/*dAdar*^S, *dAdar*^{WTLoxP}/*dAdar*^{WTLoxP} and *dAdar*^{WTLoxP}/*dAdar*^G female heads (Fig. D.4A), indicating that auto-editing of *dAdar* mRNA is insensitive to the edited status of co-expressed dADAR proteins and that there is no compensation at the level of auto-editing.

Furthermore, we observed strong sexual dimorphism of auto-editing levels in the thorax, but only a small difference between male and female heads (Fig. D.4B), illustrating that *dAdar* auto-regulation can be spatially controlled in a sex-specific manner. To test whether this spatial variation was conserved amongst other *Drosophilids*, we examined auto-editing in four other members of the *D. melanogaster* subgroup: *D. simulans*, *D. sechellia*, *D. yakuba* and *D. erecta* (Fig. D.5A). We found that robust sexual dimorphism in thoracic auto-editing was conserved in *D. simulans* and *D. sechellia*, the closest species to *D. melanogaster*, whereas in the more divergent species *D. yakuba* and *D. erecta*, only subtle differences were observed (Fig. D.5B). Furthermore, each species within the *D. melanogaster* subgroup possessed a distinct level of auto-editing in male and female head and thorax tissue (Fig. D.5C–F), indicating that spatial control over dADAR auto-editing is fine-tuned in a species-specific manner, potentially resulting in distinct landscapes of RNA editing levels of target transcripts across even recently diverged *Drosophilid* species.

***dAdar* Editing Alters its Nuclear Localization**

What is the mechanism by which auto-editing selectively reduces dADAR function? We recently engineered a novel hypomorphic allele of *dAdar* (*dAdar*^{hyp}), in which dADAR expression is reduced by ~ 80% (Jepson et al., 2011a). In this background, editing at many sites, but not all, is significantly reduced. Similarly to *dAdar*^{hyp}, males and females hemi- or homozygous for the *dAdar*^G allele also show reduced editing at a subset of adenosines (Fig. D.2). Interestingly, for the editing sites that showed a significant reduction in *dAdar*^G males, we found a significant correlation between the degree of reduction in both *dAdar*^G and *dAdar*^{hyp} heads ($r = 0.57$, $P = 0.008$,

permutation test; Fig. D.4c). Thus, in essence, auto-editing appears to post-transcriptionally phenocopy a known hypomorphic allele of *dAdar*.

To explore this further, we examined the localization of dADAR in our various genetic backgrounds using HA-tagged versions of each allele (Fig. D.1A), with the underlying hypothesis that auto-editing might in some way be lowering the effective concentration of dADAR within the nuclear compartment. Mammalian ADARs have been shown to localize to the nucleolus and alter their localization in response to substrate abundance (Sansam et al., 2003). dADAR transgenes comparable to the *dAdar*^{WTLoxP} and *dAdar*^S alleles also localized to the nucleolus when ectopically expressed in 3rd instar larval salivary gland nuclei (Supplementary Fig. D.3A).

We next examined the endogenous localization of dADAR isoforms in neuronal nuclei of the adult brain. Both ectopically expressed dADAR transgenes and endogenous dADAR protein derived from all HA-tagged *dAdar* alleles localized to within the nuclear envelope (Supplementary Fig. D.3B,C). Within the nucleus, we observed two patterns of expression that were common to all engineered dADAR isoforms (Fig. D.6A–C). Firstly, concordant with the localization of dADAR expressed from transgenes in larval salivary glands, we observed a strong co-localization with the nucleolar marker fibrillarin. dADAR levels in all genetic backgrounds studied were often strongly elevated in the nucleolus relative to the expression in the remainder of the nucleus. Secondly, diffuse expression was detected throughout the non-nucleolar region of the nucleus. However, we also observed an intriguing mode of localization that was robustly observed in neurons expressing the dADAR^{G-HA} isoform, but not the dADAR^{S-HA} isoform, characterized by the presence of intense punctae of nuclear dADAR expression outside

the nucleolus, smaller in size relative to the nucleolus, and distinct from the general diffuse staining observed within the nucleus (depicted in Fig. D.6D; see also Fig. D.6A–C and Supplementary Fig. D.3C).

We computationally analyzed the relative co-localization of dADAR with the nucleolus and the abundance of extra-nucleolar punctae in the HA-tagged dADAR backgrounds (Supplementary Fig. D.4). All endogenous HA-tagged dADARs co-localized with the nucleolus to a degree that was independent of auto-editing status (Fig. D.6E). In contrast, the number of nuclei exhibiting extra-nucleolar punctae, and the intensity of the dADAR signal within such punctae, exhibited striking variation depending on the auto-edited status of dADAR (Fig. D.6F-G; Supplementary Fig. D.5). In dADAR^{S-HA} neurons, dADAR-positive extra-nucleolar punctae were detected in only ~ 10% of nuclei, whereas this value rose to > 50% in dADAR^{G-HA} neurons (Fig. D.6F). Furthermore, the intensity of the dADAR signal in extra-nucleolar punctae was significantly higher in dADAR^{G-HA} neurons relative to either unedited or wild-type HA-tagged dADARs (Fig. D.6G). We observed a similar pattern of localization using a different anti-HA antibody (Supplementary Fig. D.6), indicating that this effect is not antibody-specific.

These results suggest that auto-editing leads to the sequestration of dADAR^G isoform to a distinct nuclear compartment, perhaps reflecting binding to a form of dsRNA that is not bound by dADAR^{S-HA} stably enough to be detectable by confocal microscopy. We hypothesize that this localized depot of dADAR^G effectively lowers the concentration of total dADAR at active sites of target transcription, generating a

molecular phenocopy of a *dAdar* hypomorph to which only specific dADAR targets are sensitive.

***dAdar* Editing Modulates Adult Behavior**

A common theme of ADAR mutations in several higher metazoan model genetic systems is the disruption of normal nervous system function (Higuchi et al., 2000; Palladino et al., 2000a; Tonkin et al., 2002; Jepson et al., 2011a). We therefore asked whether the relatively subtle changes in editing observed in the *dAdar*^S and *dAdar*^G backgrounds could also confer abnormal adult-stage behaviors. We assessed adult locomotor patterns using both automated horizontal single-fly and vertical population monitors. In constant dark conditions, all genotypes exhibited rhythmic locomotor patterns (Supplementary Fig. D.7), indicating that the circadian clock is intact in the recombinant lines. However, in 12 h light: 12 h dark conditions, we observed a reduction in morning anticipation in *dAdar*^G compared to *dAdar*^{WTLoxP} and *dAdar*^S males (Fig. D.7A,B). The anticipation of morning is an output of a subset of the circadian neuronal network, and interestingly is also absent in *dAdar* hypomorphs (Jepson et al., 2011a; Allada et al., 2010). To quantify the degree of increase in locomotor activity in the hours preceding the onset of morning, we calculated the total number of beam breaks occurring in the three hours before lights-on divided by the total in the six hours before lights-on (i.e a value of 0.5 indicates no anticipation). Although *dAdar*^G males did show a detectable degree of anticipation (0.72 ± 0.02), the level was significantly reduced relative to both to *dAdar*^{WTLoxP} (0.82 ± 0.02 ; $P = 0.0059$, ANOVA with Dunnett post-hoc test) and *dAdar*^S (0.81 ± 0.02 ; $P = 0.022$) males. In both single-fly and population settings (Fig. D.7C,D), altering auto-editing did not change

locomotor activity relative to $dAdar^{WTLoxP}$, although $dAdar^S$ males were significantly more active than $dAdar^G$ under horizontal conditions (Fig. D.7C). In addition, in the vertical assay, the proportion of time $dAdar^S$ males spent towards the top of the vial was significantly lower compared to $dAdar^{WTLoxP}$ and $dAdar^G$ males, suggesting that loss of auto-editing impairs normal climbing ability while sparing general horizontal locomotor activity (Fig. D.7E).

Since both null and hypomorphic mutations in $dAdar$ result in abnormal mating behaviors (Palladino et al., 2000a; Jepson et al., 2011a), we also investigated courtship in recombinant males with hard-wired or abolished dADAR auto-editing. While the total time spent courting females was equivalent to wild-type, $dAdar^G$ males initiated courtship significantly slower than $dAdar^{WTLoxP}$ controls or $dAdar^S$ males (Fig. D.7F-G). Thus, homeostatic control of dADAR function through auto-regulation modulates behaviors that are subject to natural selection and would be expected to affect fitness.

Abiotic Modulation of $dAdar$ Editing

dADAR auto-regulation is subject to both temporal (Palladino et al., 2000b) and spatial control (Fig. D.4B and Fig. D.5B). We were interested in examining whether external abiotic factors were also able to modulate dADAR auto-editing. To do so, we raised wild-type *Drosophila* at 25°C and then exposed newly eclosed males to one of three test temperatures for 72 h: 15°C, 25°C or 35°C. We subsequently examined the magnitude of editing in the $dAdar$ transcript. Interestingly, we observed a bidirectional alteration in the levels of dADAR auto-editing: lowering the ambient temperature by 10°C resulted in a 20% increase in auto-editing. In contrast, an increase of 10°C led to a

30% reduction in auto-editing levels (Fig. D.8A,B). These results point to an intriguing interaction between changing environmental conditions and post-transcriptional mRNA re-coding events that possess the capacity to modulate adult-stage behaviors.

DISCUSSION

Drosophila ADAR and mouse ADAR2 primarily contribute to nervous system function through their ability to diversify the neuronal proteome via mRNA re-coding (Higuchi et al., 2000; Jepson et al., 2009). Intriguingly, both of these ADAR homologues have evolved auto-regulatory feedback loops as a mechanism to optimize enzyme function (Keegan et al., 2005; Palladino et al., 2000b; Rueter et al., 1999). Here we have used ends-out homologous recombination to define the role of *dAdar* auto-editing at the molecular, cellular and behavioral levels.

While *in vitro* data have suggested that auto-editing might broadly reduce enzymatic function on all substrates (Keegan et al., 2005), our data demonstrates that, *in vivo*, only a fraction of *Drosophila* RNA editing sites are modulated by *dAdar* auto-regulation. Furthermore, this modulation is distinctly non-uniform, with adenosines showing either mono- or bi-directional alterations in the degree of editing upon hard-wiring or abolishing *dAdar* auto-editing. Thus, post-transcriptional auto-regulation of dADAR activity induces a complex alteration in the magnitude of deamination across the spectrum of edited adenosines, adding a further multi-faceted regulatory layer to control mRNA re-coding, in addition to spatio-temporal regulation of dADAR expression and alternative splicing (Pallidino et al., 2000).

How does such a non-uniform response arise? A comparison of reductions in editing in *dAdar*^G hemizygotes and those in a recently engineered hypomorphic allele of *dAdar* (*dAdar*^{hyp}) indicates that auto-editing effectively acts to generate a weakly hypomorphic allele of *dAdar* rather than to modify substrate-specificity. Importantly, we provide a mechanistic basis for such an effect: the sequestration of auto-edited dADAR proteins to an as yet unidentified nuclear sub-compartment, thus potentially lowering the active concentration of dADAR at sites of transcription.

In mammalian cells, transcripts with high inosine content are often retained within the nucleus in paraspeckle-associated complexes (Chen et al., 2009; Prasanth et al., 2005; Zhang et al., 2001). We speculate that auto-edited dADAR specifically binds to a similar dsRNA source within paraspeckle-like domains in *Drosophila* neurons. It should also be noted, however, that auto-editing still affects catalytic function even in an *in vitro* system (Keegan et al., 2005). Thus, we cannot rule out the possibility that alterations in dADAR catalysis through auto-editing also contributes to the results observed *in vivo*. Both sequestration of dADAR and a reduction in the efficiency of substrate deamination may act synergistically to define the net effect of auto-editing.

Our findings suggest an intriguing convergent function of dADAR and mammalian ADAR2 auto-editing. *De novo* generation of an AI splicing acceptor site by ADAR2 in its own transcript results in a frame-shift that forces the translational machinery to initiate from an internal methionine at lower efficiency, thus reducing ADAR2 protein levels (Rueter et al., 1999). Our data indicates that *Drosophila* deploys a distinct molecular strategy to achieve a similar regulatory outcome: *dAdar* auto-editing

does not reduce the total levels of dADAR, but instead acts to alter catalysis and limit the concentration of dADAR at active sites of transcription.

One surprising discrepancy between our *in vivo* data and previous *in vitro* experiments is the effect of auto-editing on deamination of dADAR's own transcript. *In vitro*, *dAdar* mRNA is robustly edited by the genomically encoded dADAR, but only weakly by its auto-edited counterpart (Keegan et al., 2005). This differential feedback would be expected to result in total auto-editing levels within a given neuron reaching an equilibrium value that would exhibit minimal variability between different neurons. Regional differences in dADAR expression would be unlikely to result in substantial deviation from this equilibrium, since large reductions in dADAR levels do not strongly affect auto-editing levels (Jepson et al., 2011a). However, we found no evidence for such feedback *in vivo*, suggesting that *dAdar* auto-editing could be controlled in a cell-specific manner. Supporting this concept, we found sex-specific regulation of auto-editing in the adult thorax and species-specific divergences in spatial patterns of auto-editing.

Using a novel *in vivo* fluorescent reporter of dADAR activity, we have recently shown that auto-editing is also differentially regulated within distinct neuronal subpopulations in the *Drosophila* brain (Jepson et al., 2011b). In concert with the findings presented in this paper detailing the molecular consequences of dADAR auto-editing, our data suggests that auto-editing levels are set on a neuron-to-neuron basis and may contribute to the optimization of cellular physiology by generating cell-specific repertoires of differentially modified ion channels and synaptic release proteins (Fig. D.8c,d). In concordance with this hypothesis, we observed alterations in adult behavior in

males containing *dAdar* alleles either abolishing or hard-wiring auto-editing. Interestingly, the behavioral defects observed in *dAdar*^G males (such as reduced locomotor activity and an increase in the latency to court females) are also observed to a greater degree in *dAdar* hypomorphs (Jepson et al., 2011a), in agreement with the concept that the effect of auto-editing phenocopies a weak hypomorphic variant of dADAR. The mechanistic basis for spatial regulation of auto-editing is unknown. One attractive hypothesis is that the degree of auto-editing is controlled by *trans*-acting factors whose expression varies between tissues (and potentially between neurons), thus explaining the discrepancy between our *in vivo* data and dADAR's actions *in vitro* (Palladino et al., 2000b).

Our data has also uncovered an unexpected abiotic regulation of dADAR auto-editing. Reducing or increasing the external temperature for a relatively short period (72 h) induced significant shifts in the magnitude of dADAR auto-editing, presumably as a combinatorial consequence of altered dADAR catalysis and temperature-induced changes in the structural stability of the substrate within the *dAdar* transcript. It will be intriguing to examine the effect of temperature-changes on the remainder of the *Drosophila* editing sites, and whether the temperature-induced modifications in dADAR auto-editing act to buffer or enhance any alterations in other dADAR targets. If this phenomenon is broadly applicable, environmental fluctuations in temperature have the capacity to substantially and specifically modify the proteomic content of the nervous systems of insect and other poikilothermic species via altered RNA editing.

In summary, our results greatly expand on previous methods used to investigate *dAdar* auto-regulation and yield distinct paradigms in relation to the

functional consequences of *dAdar* auto-editing in an *in vivo* setting. These findings further elaborate the complex nature of A-to-I RNA editing in the *Drosophila* nervous system and the multi-layered regulatory mechanisms that control mRNA re-coding, neuronal physiology and behavior.

REFERENCES

- Allada R, Chung BY. Circadian organization of behavior and physiology in *Drosophila*. *Annu Rev Physiol*. 2010;72:605–624.
- Bass BL. RNA editing by adenosine deaminases that act on RNA. *Annu Rev Biochem*. 2002;71:817–846.
- Basilio C, Wahba AJ, Lengyel P, Speyer JF, Ochoa S. Synthetic polynucleotides and the amino acid code. *V. Proc Natl Acad Sci U S A*. 1962;48:613–616.
- Chen LL, Carmichael GG. Altered nuclear retention of mRNAs containing inverted repeats in human embryonic stem cells: functional role of a nuclear noncoding RNA. *Mol Cell*. 2009;35:467–478.
- Feng Y, Sansam CL, Singh M, Emeson RB. Altered RNA editing in mice lacking ADAR2 autoregulation. *Mol Cell Biol*. 2006;26:480–488.
- Grauso M, Reenan RA, Culetto E, Sattelle DB. Novel putative nicotinic acetylcholine receptor subunit genes, *Dalpha5*, *Dalpha6* and *Dalpha7*, in *Drosophila melanogaster* identify a new and highly conserved target of adenosine deaminase acting on RNA-mediated A-to-I pre-mRNA editing. *Genetics*. 2002;160:1519–1533.
- Graveley BR, et al. The developmental transcriptome of *Drosophila melanogaster*. *Nature*. 2011;471:473–479.
- Hanrahan CJ, Palladino MJ, Ganetzky B, Reenan RA. RNA editing of the *Drosophila* para Na(+) channel transcript. Evolutionary conservation and developmental regulation. *Genetics*. 2000;155:1149–1160.
- Higuchi M, et al. Point mutation in an AMPA receptor gene rescues lethality in mice deficient in the RNA-editing enzyme ADAR2. *Nature*. 2000;406:78–81.
- Hoopengardner B, Bhalla T, Staber C, Reenan R. Nervous system targets of RNA editing identified by comparative genomics. *Science*. 2003;301:832–836.
- Keegan LP, et al. Tuning of RNA editing by ADAR is required in *Drosophila*. *EMBO J*. 2005;24:2183–2193.
- Li JB, et al. Genome-wide identification of human RNA editing sites by parallel DNA capturing and sequencing. *Science*. 2009;324:1210–1213.
- Ingleby L, Maloney R, Jepson J, Horn R, Reenan R. Regulated RNA editing and functional epistasis in Shaker potassium channels. *J Gen Physiol*. 2009;133:17–27.

- Jepson JE, Reenan RA. Adenosine-to-inosine genetic recoding is required in the adult stage nervous system for coordinated behavior in *Drosophila*. *J Biol Chem*. 2009;284:31391–31400.
- Jepson JE, et al. Engineered alterations in RNA editing modulate complex behavior in *Drosophila*: regulatory diversity of adenosine deaminase acting on RNA (ADAR) targets. *J Biol Chem*. 2011a;286:8325–8337.
- Jepson JE, Savva YA, Jay KA, Reenan RA. Visualizing adenosine-to-inosine RNA editing in the *Drosophila* nervous system. *Nat Methods*. 2011b;9:189–194.
- Jones AK, et al. Splice-variant- and stage-specific RNA editing of the *Drosophila* GABA receptor modulates agonist potency. *J Neurosci*. 2009;29:4287–4292.
- Macbeth MR, et al. Inositol hexakisphosphate is bound in the ADAR2 core and required for RNA editing. *Science*. 2005;309:1534–1539.
- Nishikura K. Functions and regulation of RNA editing by ADAR deaminases. *Annu Rev Biochem*. 2010;79:321–349.
- Palladino MJ, Keegan LP, O'Connell MA, Reenan RA. A-to-I pre-mRNA editing in *Drosophila* is primarily involved in adult nervous system function and integrity. *Cell*. 2000a;102:437–449.
- Palladino MJ, Keegan LP, O'Connell MA, Reenan RA. dADAR, a *Drosophila* double-stranded RNA-specific adenosine deaminase is highly developmentally regulated and is itself a target for RNA editing. *RNA*. 2000b;6:1004–1018.
- Prasanth KV, et al. Regulating gene expression through RNA nuclear retention. *Cell*. 2005;123:249–263.
- Rong YS, et al. Targeted mutagenesis by homologous recombination in *D. melanogaster*. *Genes Dev*. 2002;16:1568–1581.
- Rueter SM, Dawson TR, Emeson RB. Regulation of alternative splicing by RNA editing. *Nature*. 1999;399:75–80.
- Sansam CL, Wells KS, Emeson RB. Modulation of RNA editing by functional nucleolar sequestration of ADAR2. *Proc Natl Acad Sci U S A*. 2003;100:14018–14023.
- Seeburg PH, Hartner J. Regulation of ion channel/neurotransmitter receptor function by RNA editing. *Curr Opin Neurobiol*. 2003;13:279–283.
- Seeburg PH. A-to-I editing: new and old sites, functions and speculations. *Neuron*. 2002;35:17–20.
- Singh M, et al. Hyperphagia-mediated obesity in transgenic mice misexpressing the RNA-editing enzyme ADAR2. *J Biol Chem*. 2007;282:22448–22459.
- Singh M, Zimmerman MB, Beltz TG, Johnson AK. Affect-related behaviors in mice misexpressing the RNA editing enzyme ADAR2. *Physiol Behav*. 2009;97:446–454.
- Smith LA, Peixoto AA, Hall JC. RNA editing in the *Drosophila* DMCA1A calcium-channel alpha 1 subunit transcript. *J Neurogenet*. 1998;12:227–240.
- Smith LA, et al. A *Drosophila* calcium channel alpha1 subunit gene maps to a genetic locus associated with behavioral and visual defects. *J Neurosci*. 1996;16:7868–7879.
- Stapleton M, Carlson JW, Celniker SE. RNA editing in *Drosophila melanogaster*: New targets and functional consequences. *RNA*. 2006;12:1922–1932.

Tonkin LA, et al. RNA editing by ADARs is important for normal behavior in *Caenorhabditis elegans*. EMBO J. 2002;21:6025–6035.

Zhang Z, Carmichael GG. The fate of dsRNA in the nucleus: a p54(nrb)-containing complex mediates the nuclear retention of promiscuously A-to-I edited RNAs. Cell. 2001;106:465–475.

FIGURES

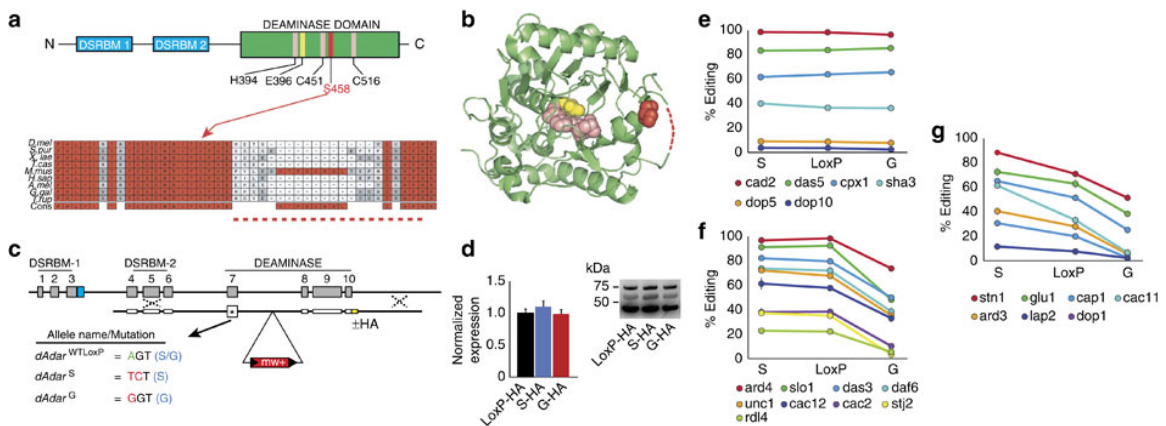


Figure D1. *dAdar* auto-editing selectively modulates mRNA re-coding. **A)** The auto-edited residue resides within the C-terminal catalytic deaminase domain, which is downstream of the two double-strand RNA-binding motifs (DSRBMs). Zinc-ion coordinating residues (H394, C541 and C516) are shown in pink, and the proton-shuttling residue (E396) is shown in yellow. Auto-editing results in an amino-acid substitution (S458G), at a residue highly conserved in ADAR2 homologues. **B)** The orthologous position in the human ADAR2 crystal structure (PDB-1ZY7) is close to the active site of the deaminase domain²⁶. Dotted lines indicate unstructured region. **C)** Schematic of the *dAdar* locus and nomenclature for the three engineered *dAdar* alleles. **D)** Modifying *dAdar* auto-editing does not affect dADAR expression ($n=5-6$ western blots from 3 separate head-protein samples; $P>0.63$, one-way ANOVA with Tukey's HSD *post-hoc* test). Values are presented as dADAR (top band)/actin (lower band). Middle band: nonspecific signal. **E-G)** Examples of edited adenosines that show no alteration (**e**), a mono- (**f**) or bi-directional (**g**) shift in editing levels in *dAdar*^S and *dAdar*^G male heads when compared with *dAdar*^{WTLoxP}. Mean values for each site were defined as significantly different ($P<0.05$) from *dAdar*^{WTLoxP} using one-way ANOVA with Dunnett *post-hoc* test ($n=3-14$ PCRs per site). Error bars, s.e.m.

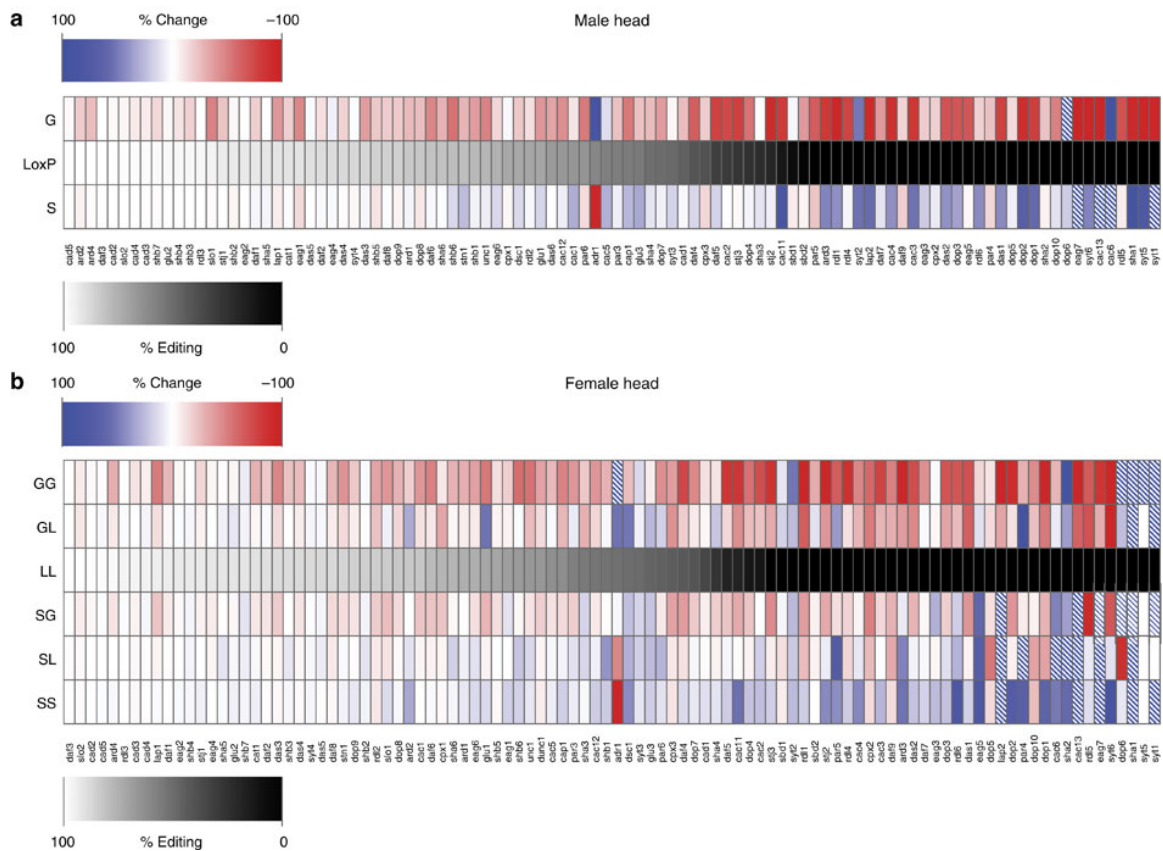


Figure D2. Inhibiting or hard-wiring *dAdar* auto-regulation results in widespread alterations in RNA editing of target adenosines. **A)** Heat-map representation of alterations in editing at 100 adenosines in *dAdar^S* and *dAdar^G* males relative to *dAdar^{WTLoxP}* controls. All PCRs were performed using male head cDNA. Data are derived from $n \geq 3$ RT-PCRs for each adenosine, and are presented in rank order relative to the endogenous editing levels in *dAdar^{WTLoxP}*. Dashed boxes indicate a >100% increase. **(b)** Heat map showing levels of editing at 100 adenosines in mRNAs amplified from *dAdar^{S/S}*, *dAdar^{S/L}*, *dAdar^{S/G}*, *dAdar^{L/L}*, *dAdar^{G/L}* and *dAdar^{G/G}* female heads, presented in rank order relative to the endogenous editing levels in *dAdar^{L/L}*. L indicates the *dAdar^{WTLoxP}* allele.

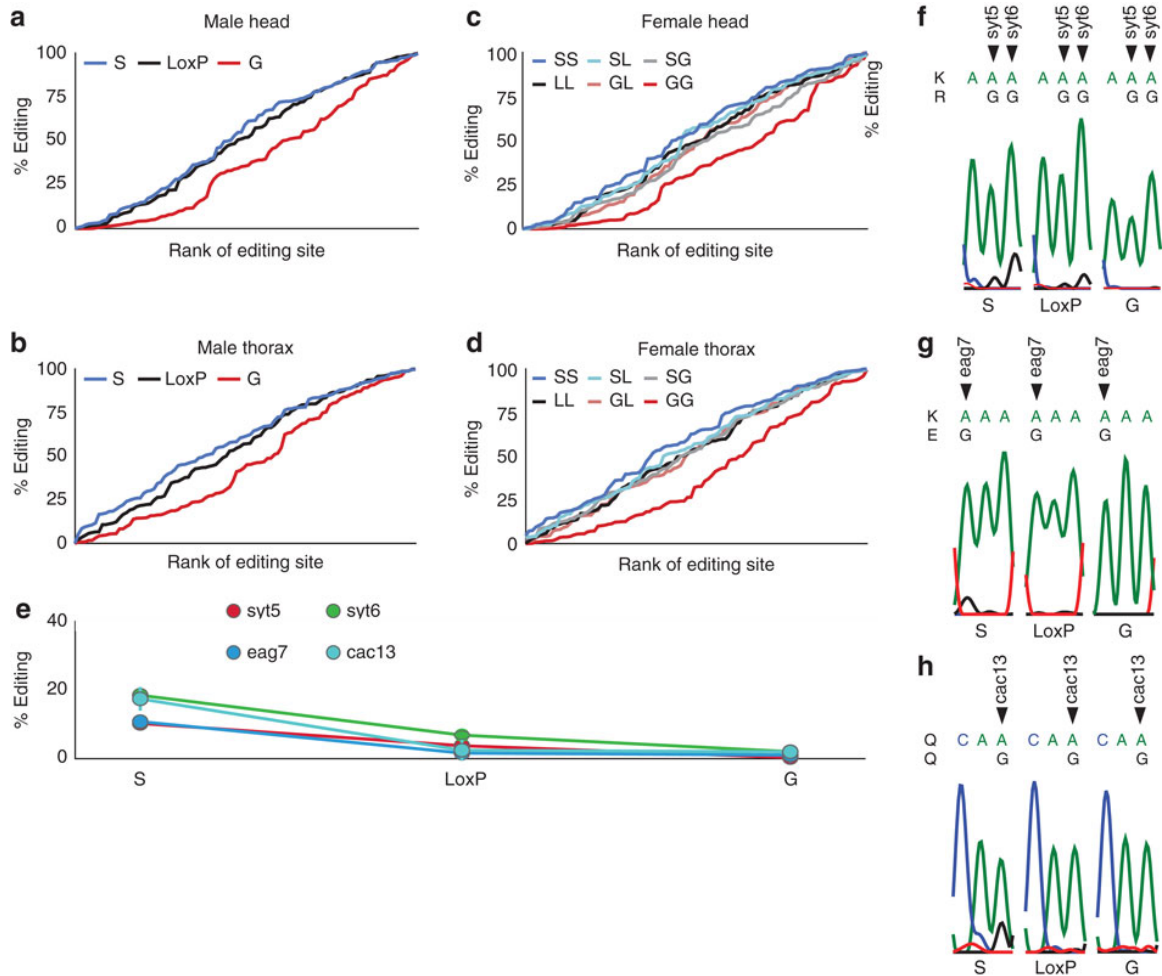


Figure D3. Hard-wiring of *dAdar* auto-editing modifies the quantitative pattern of RNA editing. **A-B)** Rank-ordered editing levels at 100 adenosines amplified from *dAdar*^S, *dAdar*^{WTLoxP} and *dAdar*^G male head (a) and thorax tissues (b). Each population is rank-ordered independently to assess the relative abundance of adenosines edited at low, medium and high levels. Note the substantial downward shift in the rank ordering of editing sites amplified from *dAdar*^G tissues compared with both *dAdar*^{WTLoxP} and *dAdar*^S. **C-D)** Rank-ordered editing levels at 100 adenosines amplified from head (c) and thorax (d) tissue of the six female allelic *dAdar* combinations. Note the substantial downward shift in the rank ordering of editing sites amplified from *dAdar*^{G/G} tissues compared with all other allelic combinations. **E-H)** Editing levels at novel editing sites that were solely or predominantly detected in *dAdar*^S hemi- and homo-zygotic backgrounds. All of the novel sites were detected at relatively low levels (e). Editing at *Synaptotagmin-1* site 5 (*syt5*) (f) and *eag* site 7 (*eag7*) (g) lead to the amino-acid substitutions K→R and K→E, respectively. RNA editing at *synaptotagmin-1* site 6 (*syt6*) (f) and *cacophony* site 13 (*cac13*) (h) result in synonymous changes. Data are derived from $n \geq 3$ RT-PCRs for each adenosine. Error bars, s.e.m.

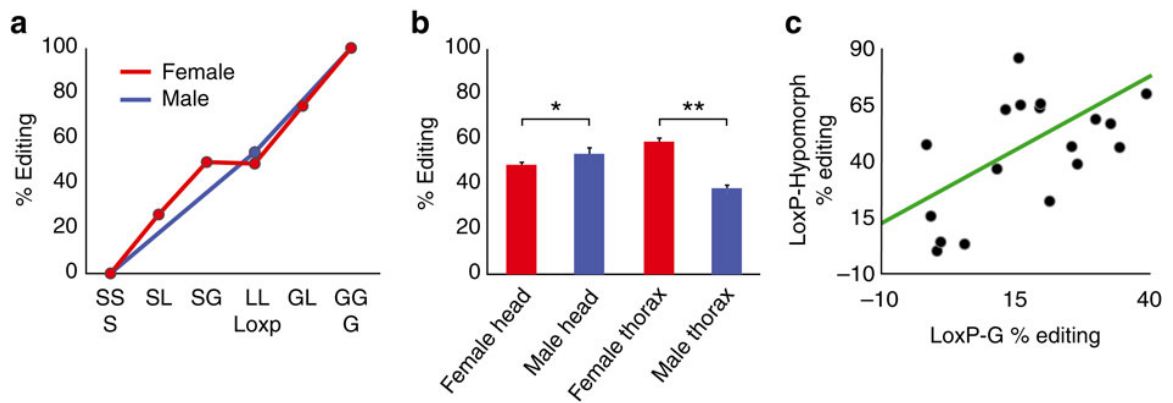


Figure D4. Spatial regulation of dADAR auto-editing. **A)** Total auto-editing levels at a wild-type *dAdar* locus in combination with engineered mutations in *dAdar* auto-editing. *dAdar*^S hemi- and homo-zygotes are defined as having 0% auto-editing, whereas *dAdar*^G is 100%. Auto-editing levels in the remaining allelic combinations were determined experimentally (Methods). L, wild-type LoxP allele. **B)** Auto-editing levels in *dAdar*^{WTLoxP} male and female head and thoracic tissues. *n*=5–8 PCRs. *: *P*<0.05, **: *P*<0.005, Mann–Whitney *U*-test. **C)** Correlation between the reduction in editing at 18 adenosines in *dAdar*^G and *dAdar*^{hyp} male heads. Error bars, s.e.m.

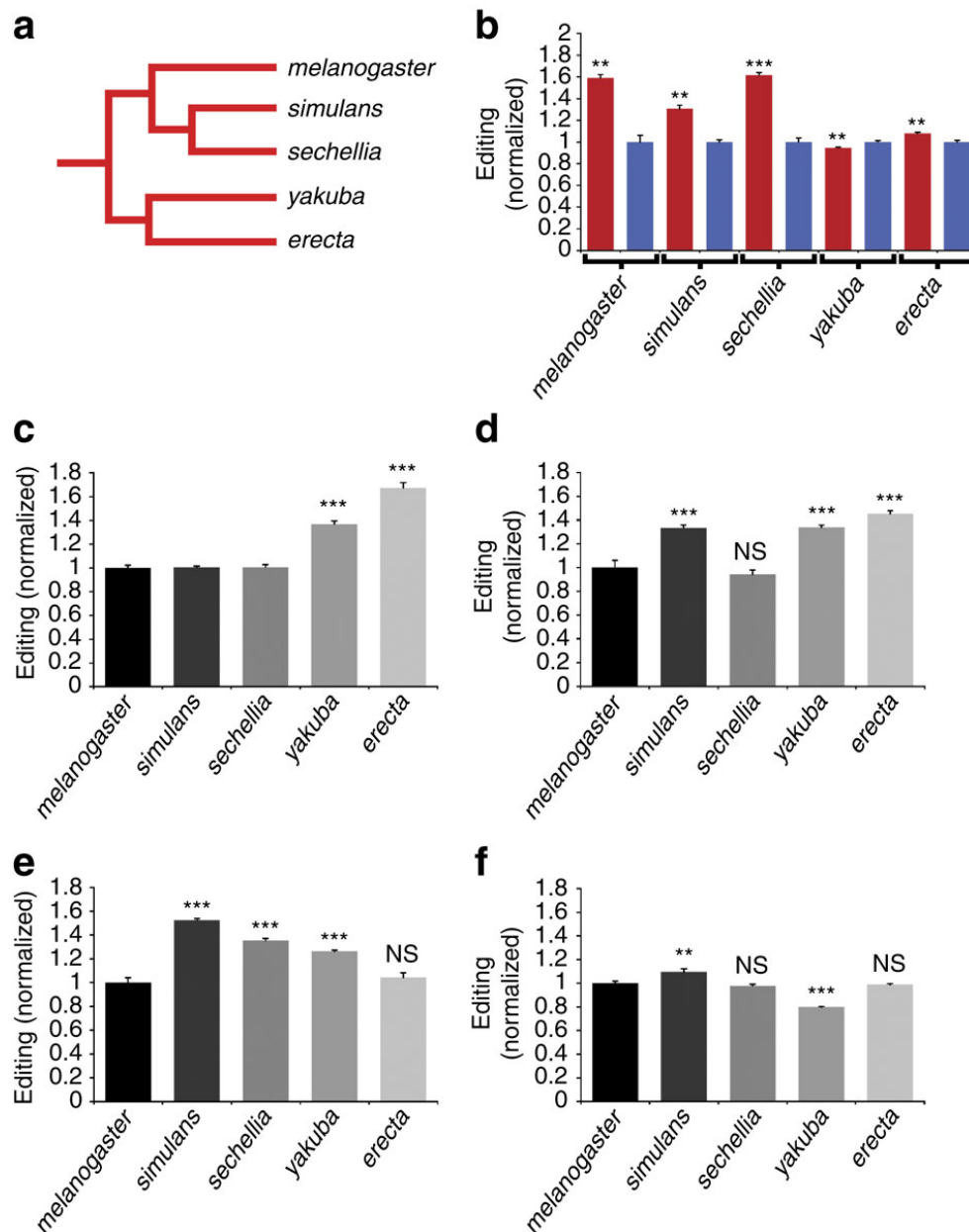


Figure D5. dADAR auto-editing in *Drosophilid* species of the *D. melanogaster* subgroup.

A) Schematic phylogenetic tree indicating evolutionary relationships between each species within the *D. melanogaster* subgroup. **B)** dADAR auto-editing in male (blue) and female (red) thoraxes in the five species of the *D. melanogaster* subgroup. Values are normalized to the mean auto-editing level in male thoraxes for each species. **: $P < 0.005$, ***: $P < 0.0005$, Mann–Whitney *U*-test; $n = 5–8$ PCRs per tissue. **(c–f)** dADAR auto-editing levels in male heads **C)**, male thoraxes **D)**, female heads **E)** and female thoraxes **F)** in the five species of the *D. melanogaster* subgroup. dADAR auto-editing levels in *D. sechellia*, *D. simulans*, *D. yakuba* and *D. erecta* were normalized to *D. melanogaster* auto-editing levels for each tissue-type. **: $P < 0.005$, ***: $P < 0.0005$, NS: $P > 0.05$, one-way ANOVA with Dunnett *post-hoc* test; $n = 5–8$ PCRs per tissue. Error bars, s.e.m.

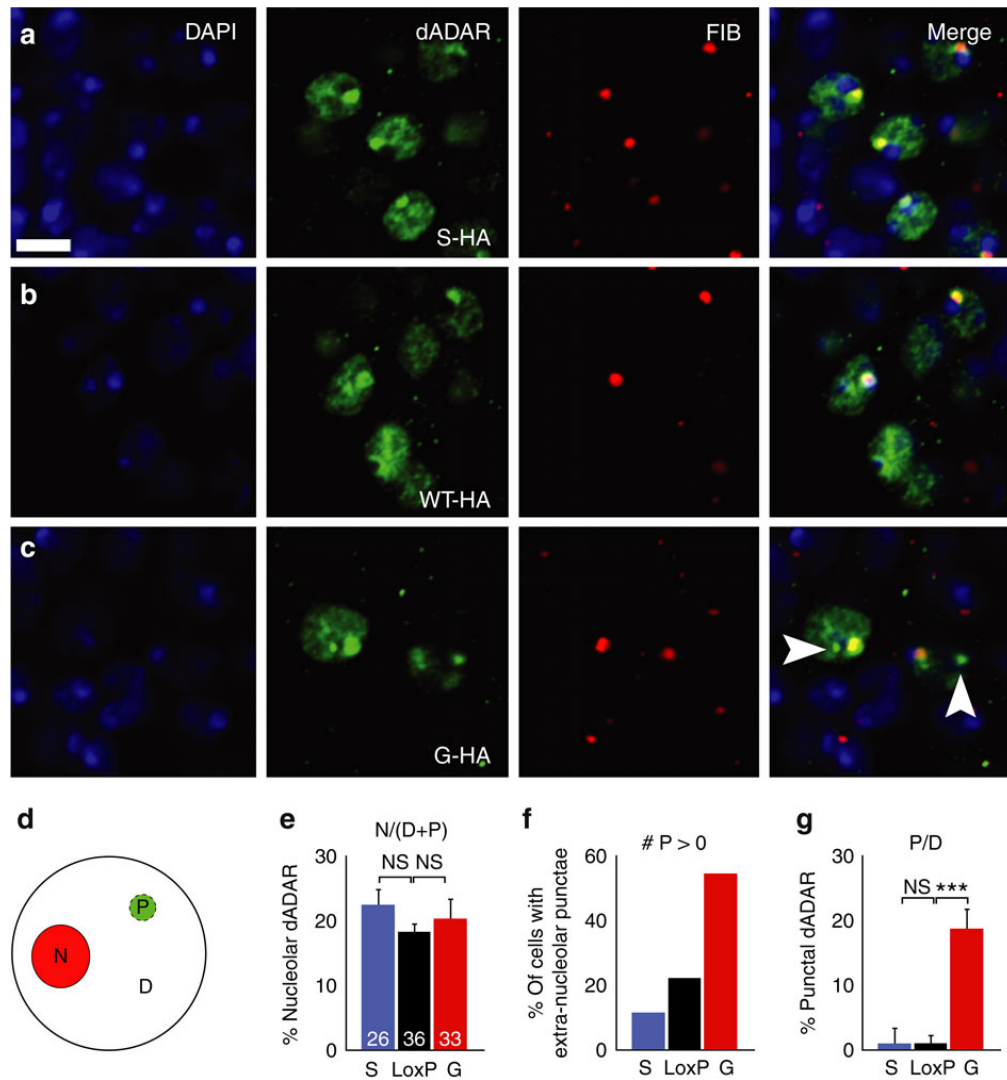


Figure D6. Auto-editing modifies the sub-nuclear localization of dADAR. A-C) Confocal slices illustrating the nuclear localization of HA-tagged dADAR^S (a), dADAR^{WTLoxP} (b) and dADAR^G (c) alleles in the adult male nervous system. To control for spatial differences in dADAR localization, slices were obtained from nuclei surrounding the antennal lobes. All dADAR alleles co-localized with DAPI-stained DNA (blue) and the nucleolus (stained with fibrillarin, red). D) Schematic diagram illustrating quantification of the regional dADAR signal intensity in the nucleolus (N) compared with dispersed (D) or punctate (P, arrowheads) extra-nucleolar staining between WTLoxP-HA, S-HA and G-HA dADARs. E) Altering auto-editing does not alter the proportion of total dADAR signal co-localizing with fibrillarin. F) Proportion of neurons exhibiting ≥ 0 extra-nucleolar puncta in the three experimental genotypes. Number of cells used for computational analysis: dADAR^{WTLoxP-HA}—36; dADAR^{S-HA}—26; dADAR^{G-HA}—33. G) Proportion of dADAR signal that is both non-nucleolar and punctate in the three experimental genotypes. ***: $P < 0.0005$, one-way ANOVA with Dunnett *post-hoc* test. Error bars, s.e.m. Images were derived from $n \geq 5$ brains for each genotype. Scale bars, 5 μm .

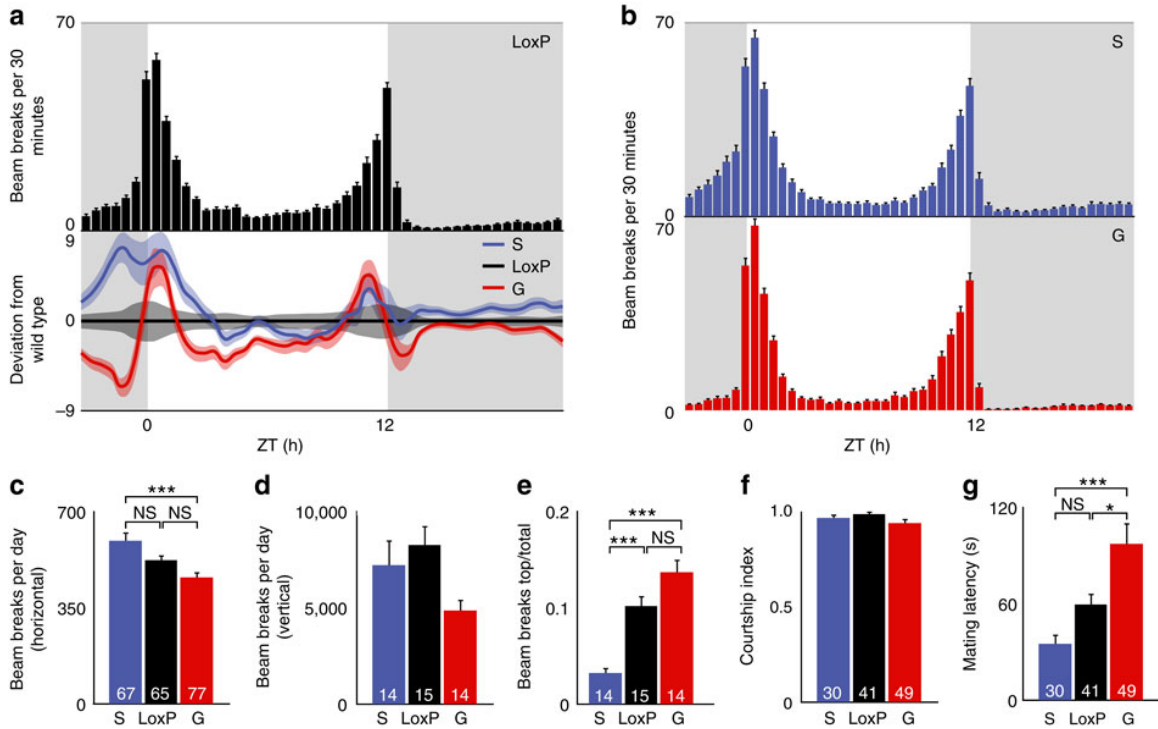


Figure D7. Dysregulation of *dAdar* auto-editing alters complex behaviours. **A)** Locomotor profile of *dAdar*^{WTLoxP} control males under 12-h light: 12-h dark (LD) conditions. Top panel, bar graph showing mean LD activity in *dAdar*^{WTLoxP} males ($n=65$). Grey background indicates lights-off; white background indicates lights-on. Lower panel, mean locomotion in *dAdar*^S ($n=67$) and *dAdar*^G ($n=77$) males, normalized to *dAdar*^{WTLoxP}. Light bars indicate s.e.m. **B)** Locomotor profiles of *dAdar*^S and *dAdar*^G males. **C)** Total locomotor levels derived from single-fly activity data. **D-E)** Total locomotor levels (**d**) and relative climbing ability (**e**) derived from vertical population activity monitors. Climbing was quantified by normalizing the beam breaks in the top third of the vertical vial to the total number of beam breaks. *dAdar*^{WTLoxP}: $n=15$ vials each containing 5 male flies; *dAdar*^S: $n=14$; *dAdar*^G: $n=14$. **F-E)** Courtship in *dAdar*^{WTLoxP}, *dAdar*^S and *dAdar*^G males. Although the fraction of time spent courting females was not significantly different between experimental and control genotypes (**f**), *dAdar*^G males ($n=49$) took significantly longer to initiate courtship relative to *dAdar*^{WTLoxP} ($n=41$) or *dAdar*^S ($n=30$) males (**g**). *: $P<0.05$, ***: $P<0.0005$, one-way ANOVA with Tukey's HSD *post-hoc* test. Error bars, s.e.m.

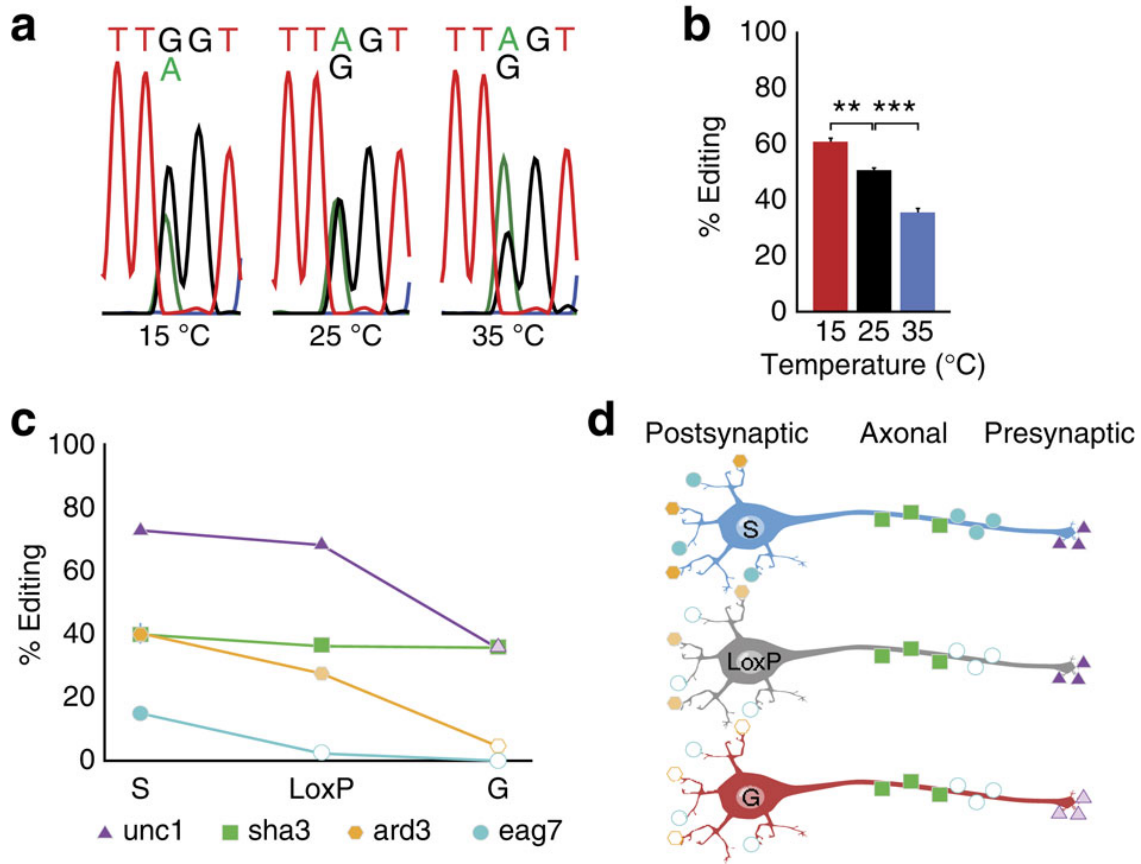


Figure D8. Environmental modulation of dADAR auto-editing. **A-B)** Auto-editing level in adult males kept at differing temperatures for 72 h. Representative electropherograms are shown in **(a)**, and averaged data in **(b)**. Experimental temperatures are indicated. $n=3$ RT-PCRs per population. **: $P<0.005$, ***: $P<0.0005$, one-way ANOVA with Dunnett *post-hoc* test. Error bars, s.e.m. **C)** Model depicting the functional consequences of neuron-to-neuron variation in auto-editing. The graph depicts the change in editing of four substrate adenosines in the $dAdar^{WT/LoxP}$, $dAdar^S$, and $dAdar^G$ genetic backgrounds. *Shaker* site 3 (*sha3*) belongs to the category of editing sites that was insensitive to the edited status of *dAdar*. *Unc-13* site 1 (*unc1*) belongs to the class of editing sites that displayed no effect on elimination of auto-editing, but exhibited a significant reduction on hard-wiring of *dAdar* auto-editing, whereas *ard* site 3 (*ard3*) belongs to the group of editing sites that displayed a bi-directional change on elimination or hard-wiring of auto-editing. Finally, *eag* site 7 (*eag7*) is a novel RNA editing site that only appears on elimination of auto-editing. **D)** Diagrammatic representation of three distinct neuronal subtypes: a neuron in which *dAdar* auto-editing is lacking (S), a neuron in which edited and unedited states of *dAdar* are present at wild-type levels (LoxP), and a neuron in which *dAdar* auto-editing is at maximum (G). *dAdar* auto-editing regulates the editing levels of the four adenosines in a site-specific manner. While the levels of editing of *shaker* site 3 are the same between the three different neuronal subtypes, *ard* site 3 and *unc-13* site 1 exhibit differential editing levels depending on the degree of *dAdar* auto-editing. Finally, *eag* site 7 is only edited in neurons where auto-editing is absent, or possibly very low.

SUPPLEMENTARY MATERIAL

Supplementary Data including 6 excel tables can be found online:

<http://www.nature.com/ncomms/journal/v3/n4/full/ncomms1789.html#supplementary-information>. This printed section consists of supplementary tables and figures.

Supplementary Figure D1. Conserved RNA editing sites. Shown below are the editing sites in the 23 mRNAs analyzed in this study, alongside the surrounding local sequence. Sensitivity to dADAR auto-editing was defined based on data from male heads.

*= intron location

A= editing site

A= non-sensitive site

A= G-sensitive site

A= S- and G-sensitive site

syt (CG3139)

TTGAAGAAGATGGACGTGGGCGGATTGTCTG*ATCCATATGTGAAAA¹TTGCAATCA
TGCAAAATGGCAAACGTTTGAAAAAGAA²GAAGACAAGTA³TCAA⁴A⁵AAATGCACCC
TCAACCCTTACTATAATGAGTCGTTCTCATTGGAAGTACCATTGAA⁶CAA*⁷CAA*⁸
AAAATCTGTCTCGTTGTGACCGTCGTGGACTACGATCGTATTGGCACCTCCGAACCC
ATCGGCCGCTG

cap (CG33653)

GACACAAGGTCTAAGCGGTAAACTTA¹TGTCTGTGCTAGAGTCGACTTTGTC

cpx (CG32490)

AACTGAAAAATCAAAT¹GAAACGCAAGTAA²A³TGAGCTAAAACTCAAATAGAGG
GAAAATGTGTCATGCAGTGA

unc (CG2999)

ACGCAATTGACGCAGTGTTTCGATGTTGTT¹GCAAACCTCGAGTGTCTGATCCAGA
AATTTGGA

stn (CG40306)

GTTTACTATGCCCCGCCACGCAGGTCTCCCAT^{A1}CCACCGTGCGCTCGGTGAGTGTCCA
GGATTCCGATGGCGATGAACCGC

lap (CG2520)

ACTAGCAGCGGTGCTGCTGGCGCTAGCGCTGCACTAA^{A1}CAAATCCATTTCTATCGTC
GCCGCCAGCCGCGCAGGCTGGCCAGCCGATA^{A2}GTTGATCTGTTCCGGTGCCGCGTCGG

dsc (CG34405)

TATGAAGGAGGAGTGTGGAA^{A1}TGTTTCTCACCGAATCTCAAAAACACTA

sbd (CG6798)

GCCCAGCGATTCCGGGCGAAAAG^{A1}GTTA^{A2}CGTT^{A3}TGTATTTGATACTCGTGTC

stj (CG12295)

TTCAATGTTGGGACAGAGGCTAGATA^{A1}TCGCAAAGCATGTTGTCAATACGATATTAG
GTACAAATGACTTTGTGAACA^{A2}TCTTCACCTTTGATAAGGAAGTGAG

ACTGAAAGAAGGGATTGAACTGTTA^{A3}GACCCAAATCGATCGCCAATTATAC

cat (CG15899)

GGTGGCCATTTTGGTTGAGGGATTCA^{A1}GTTCAGAG^{A2}CGAAATGAACGTCGCGA

cad (CG4894)

CAGCGGAATGTGTTATGAAAATTTT^{A1}GCATATGGTTTTGTGTTACATA^{A2}ATGGTGCA
TATCT^{A3}A^{A4}GAAATGGATGGAATTTATTAGATTTTATTAGATTTTACAATTGTAGTTAT
A^{A5}GG^{A6}GGCGATAAGTACTGCACTCTCCC

shb (CG1066)

GGTGGTGCAGGTCTTTTCGCATCATGCGCATCCTGCGA^{A1}A^{A2}TCCTTAAGCTGG
CCCGTCACTCAACGGGCCTG

TCGTTTCAATACCGGAA^{A3}CATTTTGGTGGGCGGGTATTACAATGACAACT
GTTGGCTACGGGACATCT^{A4}TCCCACAACGCACTGGGAAAGGTTATTGGTA^{A5}C

CTGIGTGTTGCATATGCGGTGTTCTGGT^{A6}A^{A7}TCGCTTTGCCTATTCCCA
TCATCGTTAACAATTTTGCTGAATTTTATAAGAATCAG

eag (CG10952)

TCGCCGCGGAGACAGACAACGAGA¹GGTGTTCACCATCTGCATGATGATC
CTGGATACCGAGAAG²GTA³CTAAACTA⁴TTGTCGAAAGATATGAAGGCTGAC
TATGTGTTTCATCTAAATCGCAAAGTA⁵TTTA⁶ACGAGCATCCGGCA⁷TTTCGTCTGGCC
TCGGATGGTTGTC
CTCAGACATCGACTGATTTTTTCGCA⁸GGTGGCCGATGTGAAGCGCGAAAAA
GTGATTTGCATGCCATCAAACGTGATA⁹AATTGCTCGAAGTCCTCGATTCT

slo (CG10693)

GA¹ACTCTGGCGATCCGCTGGATTTT²ATAATGCTCATCGTTTATCGTATTG
CATGATAACAG³AACTGGTCAATGATA⁴GTAACGTGCAGTTTCTCGATCAAGA

rdl (CG10537)

GTCAATTTTGGACCGATCCTCGTTT¹GCGTATA²GAAAACGACCTGGTGTAGAAACA
CT
CTACATACCCTCTGGACTGATCGTTA³TTATATCATGGGTATCATT⁴TTGGCTATGGGT
ATCATT⁵TTGGCTCAATCGCA⁶ATGCAACGCCGGCGCGTGTGGCGCT
GTCGGCTACATGGCAAAACGAATTCAA⁷A⁸TGCGAAAACAAAGATTTATGGCGAT

daf (CG32975)

CTACTTCCGATGCGGTGCCATTGCTGG¹GTA²CATATTTCAATTGCATAATGTTTATG
GTAGCTTCATCCGTTGTGTCAACGATTTT³A⁴A⁵TATTAAATTATCATCATCGAAATGC
TGACAGACTGTGCCTTATCATATTCACAATGTTCA⁶CAA⁷TATT⁸A⁹GCCACAATA¹⁰GCT
GTACTACTA¹¹TCA¹²GCACCACATATTATTGTCTCGT

das (CG4128)

GGATTTCGATGGCACGTATCACACCAA¹CA²TTGTGGTCAAACATA³A⁴CGGCAG
TTGTCTGTACGTGCCCCCT

GTATCTTCAAGAGCACATGCAAGATA⁵GACATCACGTGGTTC⁵CCATTGATG
GGAAATCAG*TTGGATTTGGTTTTGAA⁶TTCCGAAGATGGAGGGGATCTTTC

ard (CG11348)

AGAATATGACACAAAAAGTTGGAGT¹A¹A²GATTTGGTTTGGCGTTCGTACAGCT
TAATCAATGTC*²AATGAGAAAAATCA³A⁴TTATGAAATCAAACGTTTGGTTACG

sha (CG12348)

ATGTCCTTTAGACGTATTTAGTGAAGAAATA¹A²ATTTTATGAATTAGGTGATCAA
GCA
CGAATCAGGCTATGTCCTTGGCAAT³TTACGAGTGATACGATTAGTTCGAG
AAAATTGTCGGCTCTTTGTGCGTGA⁴TCGCTGGTGTGCTGACAATCGCACT
TTTCAATTACTTCTATCACCGCGAAA⁵CGGATCA⁶GGAGGAGATGCAGAGCCA

adr (CG12598)

CAGCACCTTGTGGGGATGCACGGATATTT¹A¹GTCCTCACGAAAACGACACTGGTGT
GATAAAC

cac (CG1522)

TTCAACCGATTTGATTGCGTTGTCATT¹A¹GTGGTTCGATATTCGAAGTGATCTGGTCC
G
ATGCCCAAGAATAACAGCAGCCGAAGAGGA²ACA¹³GTCGAA³GAGGATAAAGAG
AAACAAC⁴TGCAGGAGC
ACCCTGGCAGCTATTTAAGAGAATTCTGGAA⁴TATTATGGATGCTGTGGTTCGTTATAT
GCGC
GCGTCGTGAACTCATTGAAAAATGTTGTTAA⁵CATTCTAATCGTGTACATATTGTTTC
AATT
AATGGAAAATTTTTTATTGTACGGACGAAA⁶GTAACATACTTCCGCAGAGTGCCA*
GGCT

CATGATATCGGGTCTCCGATACCGTATCTA¹¹ATGTTGTAGAGATGGTCAAGGAGAC
TCGTC

AGGCATGGCAACAGTCATCCGCGGTATCCA¹²GAG^{*}GTTTCATGGTCAGCATCGACA
AGTCCGG

par (CG9907)

CAATTTACGACTGAAAACCTTTTC³A⁴TTAATTGA⁵A⁶ATAAATATTTTGAAACAGCT
GTTATCACTATG

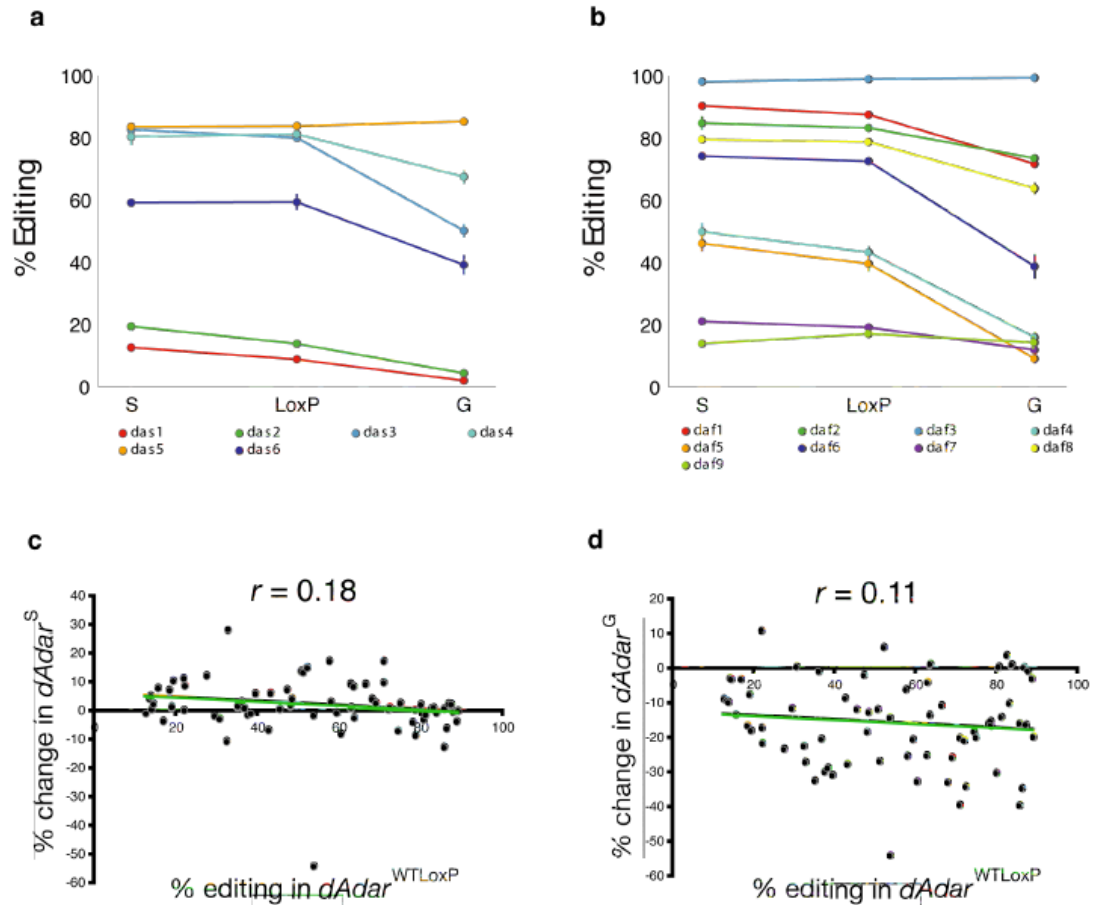
glu (CG7535)

CACTAGCAAATAATGCCAA¹A²TAAATTTCCGAGAAAAGGAGAAAAAAGTC
GCCTCAAAGTCGATCTACTATTCA³GCGAGAATTCTCATATTACTTAATACAAATT

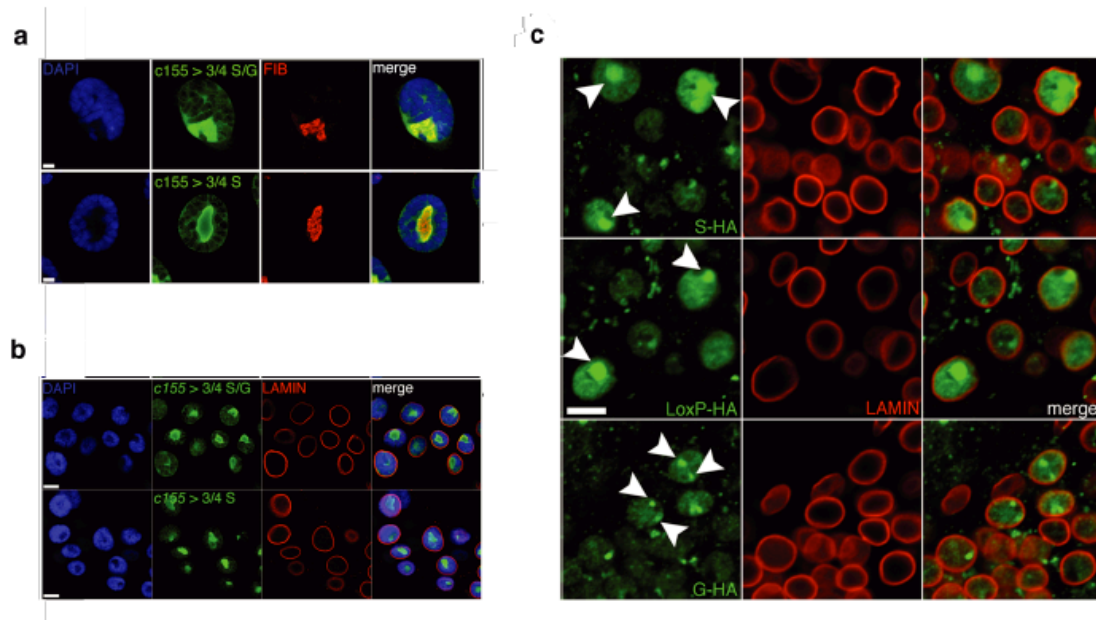
dop (CG18314)

AACTGCTCTGGCTGAAA¹TTT²TCGAACCCT³GTCAT⁴TGATGTCATTTCGCATT⁵
⁴GTCTTTGCATTCTGGGTGTCCTGGCTGCCATGGATTCTG

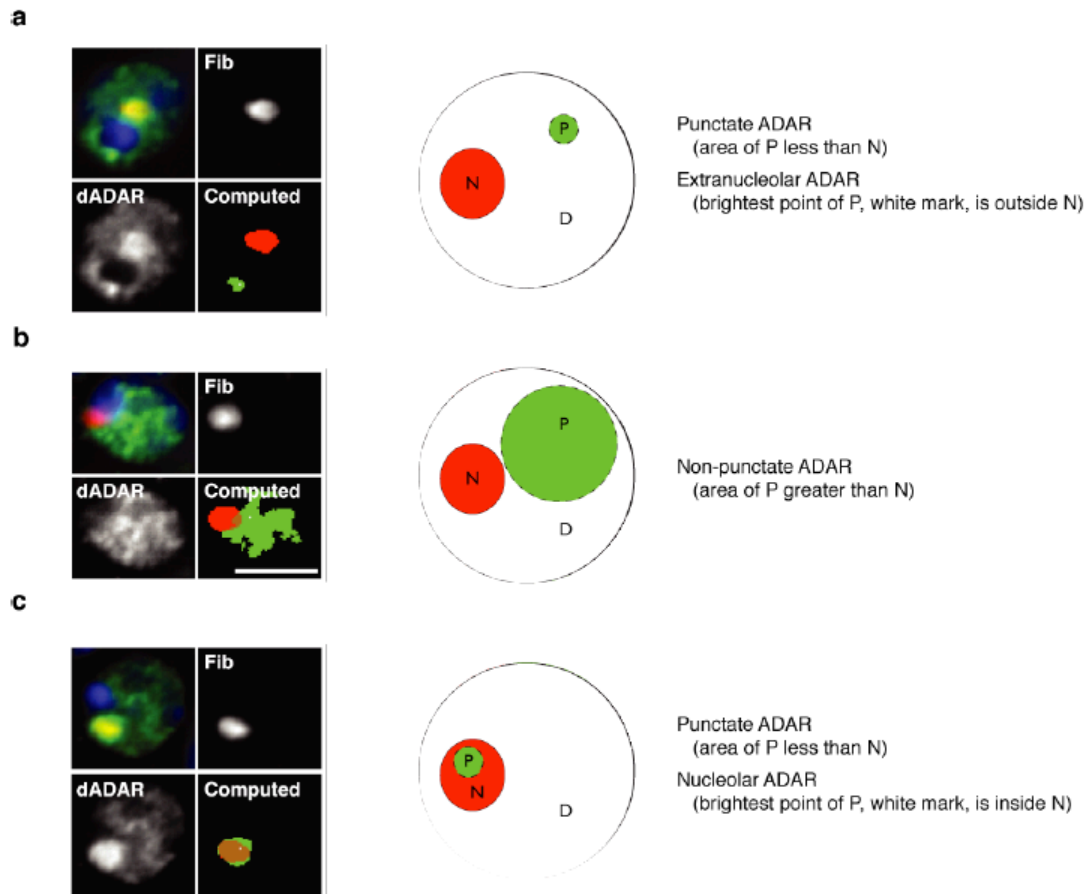
TGCTTAACCATTTGTTGTAAGACT¹A²GGGCCGTTTGCAAGCAGAGCT³A⁴TCGGGT
TGGACCCAGATGACT⁵GAGTTAGATTTAGATTTTCATTCTCC



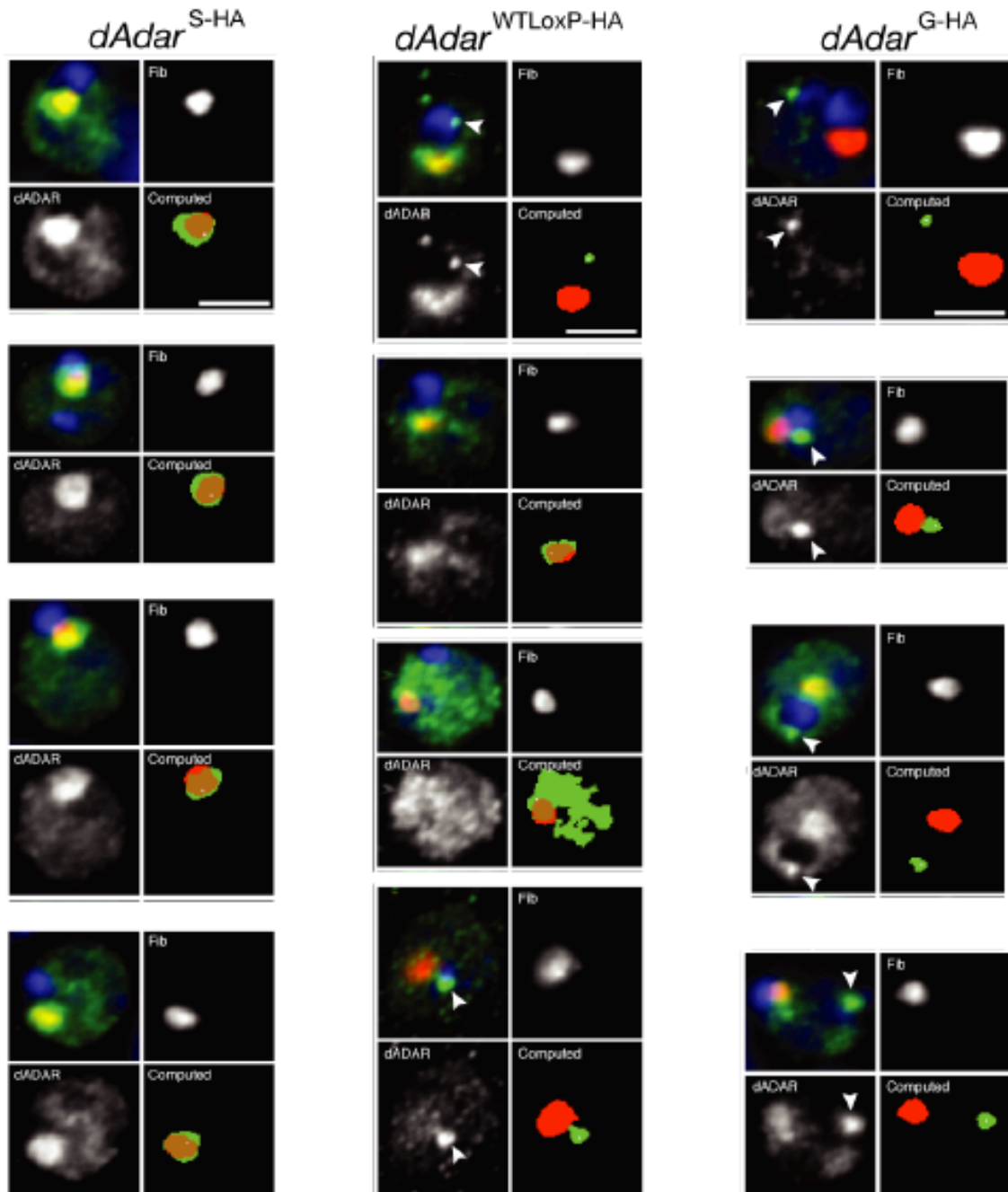
Supplementary Figure D2. Effects of altering dADAR auto-editing are not biased to sites with high or low editing levels. **A)** Six editing sites in the $D\alpha 6$ acetylcholine receptor transcript show differential regulation in dAdar^S and dAdar^G when compared to dAdar^{WTLoxP}. One site in $D\alpha 6$ shows no alteration, three sites show a mono-directional alteration, and two sites show a bidirectional alteration in response to abolishing or hardwiring dAdar auto-editing. **B)** Nine editing sites in the $D\alpha 5$ acetylcholine receptor transcript show differential regulation in dAdar^S and dAdar^G when compared to dAdar^{WTLoxP}. Two sites in $D\alpha 5$ show no alteration, five sites show a mono-directional, and two sites a bi-directional alteration upon changes in dAdar auto-editing. mRNAs were amplified from male head cDNA. Mean values for each site were defined as significantly different ($P < 0.05$) from dAdar^{WTLoxP} using one-way ANOVA with Dunnett post-hoc test ($n = 3-8$ PCRs per site). Error bars, s.e.m. (c-d) For all sites analyzed with editing levels between 10-90%, increased editing in dAdar^S male heads **C)** and reduced editing in dAdar^G male heads **D)** are not correlated with the endogenous level of editing for each site in dAdar^{WTLoxP} male heads.



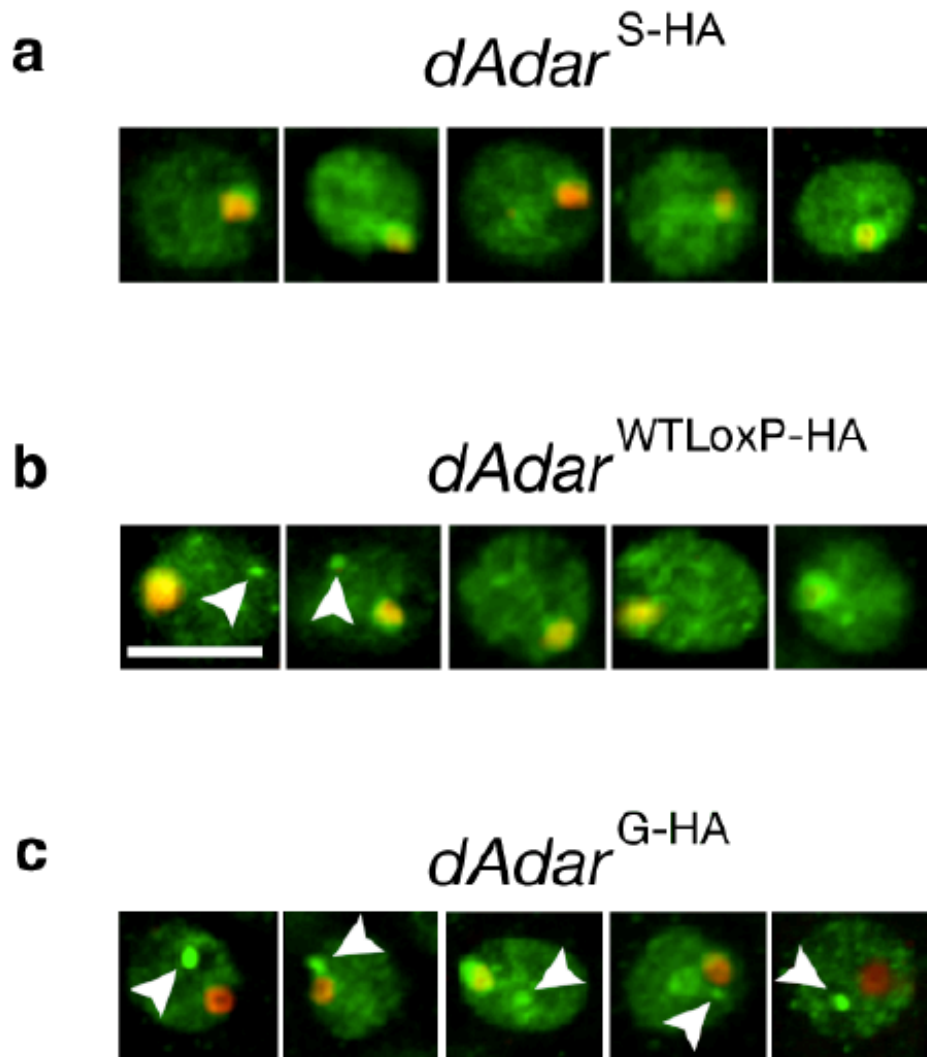
Supplementary Figure D3. dADAR localization in 3rd instar larval salivary glands and adult neurons. **A)** Two separate transgenes representing the predominant adult-stage isoforms of dADAR, which lacks the alternatively spliced 3a exon23 (termed ‘3/4’) were expressed in larval salivary glands using the *elavc155-Gal4* driver. At the auto-editing site, the serine codon was either wild-type (AGT) (‘S/G’) and is capable of being edited by the dADAR transgene, or was mutated to an un-editable synonymous TCT codon (‘S’). When expressed in the dAdar null adult nervous system, the wild-type dADAR transgene is robustly auto-edited²³. Both the 3/4 S/G (upper panels) and the 3/4 S transgene (lower panels) primarily co-localized with the nucleolus, labeled with an anti-fibrillarlin (FIB) antibody. Scale bar, 5 μ m. **B)** Both the 3/4 S/G (upper panel) and the 3/4 S (lower panel) transgenes localize internally to the nuclear envelope (labeled with an anti-Lamin antibody) in 3rd instar larval salivary glands. Scale bars, 20 μ m. **C)** In adult neuronal nuclei, WTLoxP-HA, S-HA and G-HA dADARs also localize to within the nuclear envelope. Arrows indicate the primary concentrations of nuclear dADAR. Note the presence of multiple punctae within the nucleus in neurons expressing G-HA dADAR, but not S-HA dADAR. Scale bar, 5 μ m.



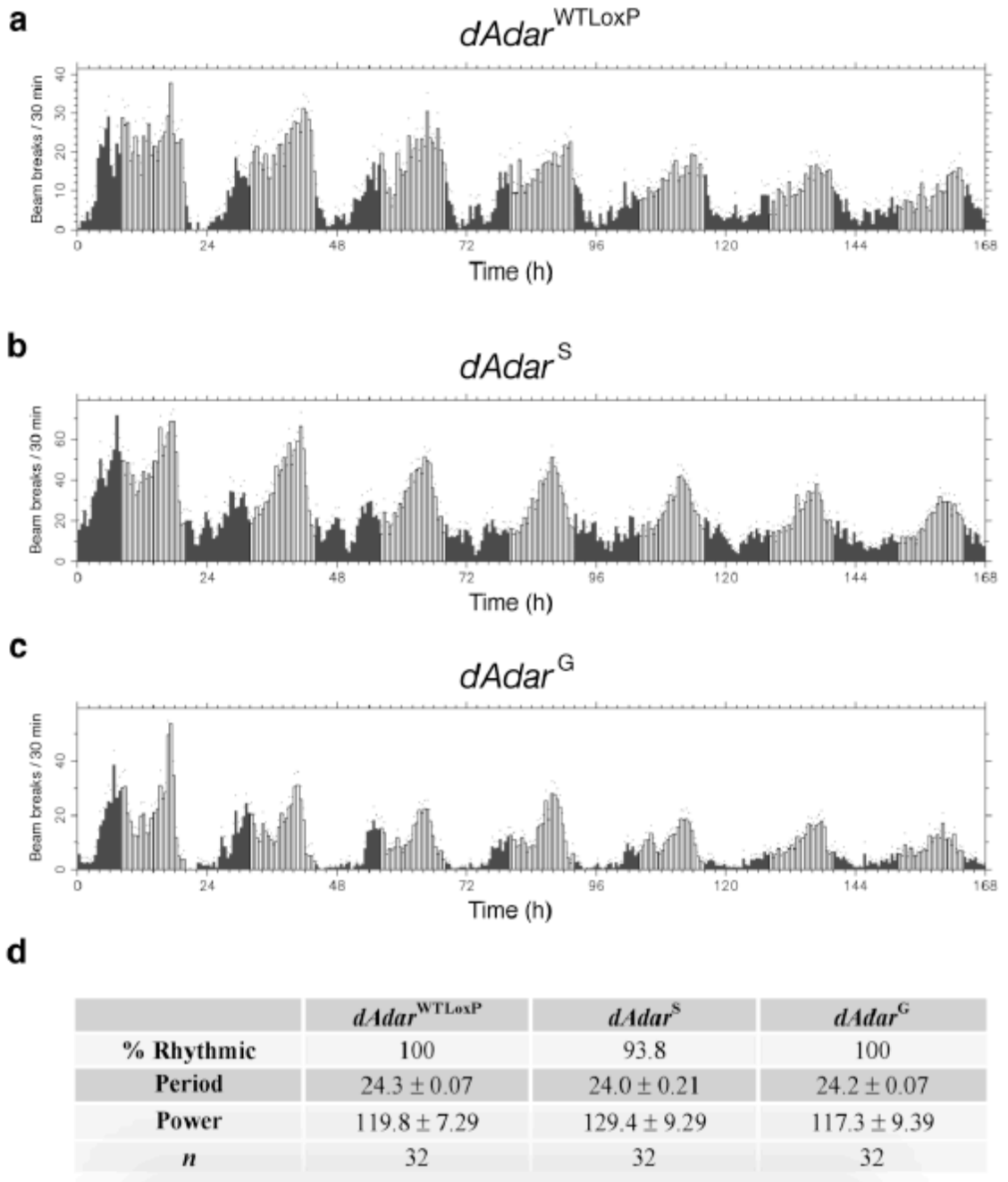
Supplementary Figure D4. Computational analysis of dADAR localization in adult neurons. Automated categorization of extranucleolar punctate dADAR staining. Each category contains an example image, a model of its category, and the definition of the category. The tetrad of images show a merged image with DAPI (blue), dADAR (green), and fibrillar (red), the individual dADAR and fibrillar channels, and the computer's identification of the nucleolus and puncta. The computer's identification shows measures A (white), P (green), and N (red) as described in the methods. Next is a model of the computer's categorization of the cell followed by the definitions of that category. **A)** Extranucleolar punctate dADAR staining. **B)** Nonpunctate dADAR staining. **C)** Punctate non-extranucleolar dADAR staining. Scale bar, 5 μm .



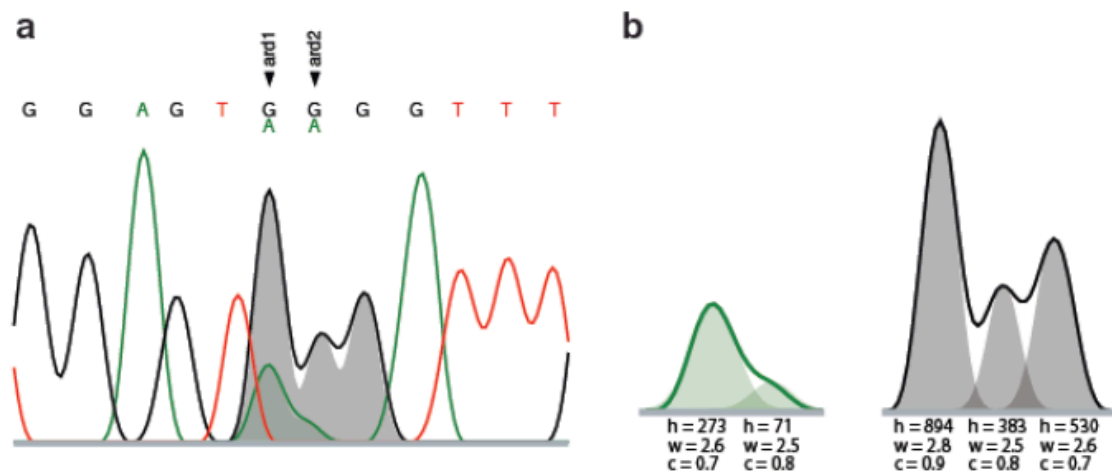
Supplementary Figure D5. Examples of dADAR localization in $dAdar^{S-HA}$, $dAdar^{WTLoxP-HA}$ and $dAdar^{G-HA}$ adult neurons. For each example, confocal slices showing individual dADAR (green) and Fibrillarin (red) signals, alongside merged image with DAPI (blue), are shown, as well as the computed signals for dADAR and Fibrillarin. dADAR in $dAdar^{S-HA}$ neurons is predominantly localized to the nucleolus and extranucleolar puncta are rarely observed, while in $dAdar^{G-HA}$ neurons, strong extranucleolar puncta are frequently observed (arrowheads). Wildtype $dAdar^{WTLoxP-HA}$ controls exhibit an intermediate phenotype, although dADAR is mainly nonpunctal. Scale bars, 5 μm .



Supplementary Figure D6. Additional images of differences in dADAR localization following manipulation of dADAR auto-editing. In each case, 5 representative adult neuronal nuclei are shown. dADAR (green) was visualized using a mouse anti-HA antibody, rather than the rabbit anti-HA antibody used for all other confocal experiments in the adult brain. **A)** Consistent with the data obtained using the rabbit anti-HA antibody, $dADAR^{S-HA}$ stained with mouse anti-HA shows a generally diffuse pattern of expression within the nucleus, and colocalizes with fibrillar (red). **B)** This pattern was also predominantly observed in $dADAR^{WTLoxP-HA}$ neurons, although small puncta were sometimes observed. **C)** In $dADAR^{G-HA}$ neurons, we additionally observed strong extranucleolar puncta (arrowheads), as was similarly seen using the rabbit anti-HA antibody. Scale bar, 5 μ m.



Supplementary Figure D7. Altering *dAdar* auto-editing does not result in arrhythmic behavior in constant-dark (DD) conditions. **A-C)** For each genotype indicated, activity plots were averaged over seven days in DD. Males bearing all *dAdar* alleles exhibited rhythmic locomotor patterns. Light bars - subjective day, dark bars – subjective night. Dots represent s.e.m. **D)** Table indicating % rhythmicity, period and the power of rhythmicity for all genotypes. Values are presented as mean ± s.e.m. n-values are also indicated.



Supplementary Figure D8. Computational methods to determine editing levels. **A)** Example electropherogram showing the edited adenosines ard1 and ard2 (sites 1 and 2 of the ard acetylcholine receptor), in which the best fit Gaussian curves for the A and G residues are shown as filled green and black, respectively. **B)** A and G chromatograms on the left and right in which each best fit Gaussian curve and its parameters are shown.

Supplementary Table D1. Nomenclature for the 23 transcripts analyzed in various dAdar allelic backgrounds. Sites (1, 2...) are labeled in a 5' to 3' order within the transcript.

Abbreviation	Locus	Synonyms/ full name	Molecular function
adr	<i>dAdar</i>	<i>Drosophila adenosine deaminase acting on RNA</i>	RNA editing enzyme
ard	<i>Ard</i>	nAcR β -64B	Nicotinic acetylcholine receptor α -subunit
cac	<i>cacophony</i>	Dm α 1A	Voltage-gated calcium channel α -subunit
cad	<i>Ca-alpha1D</i>	Dm α 1D	Voltage-gated calcium channel α -subunit
cap	<i>caps</i>	Calcium activated protein for secretion	Regulator of exocytosis
cat	<i>Ca-alpha1T</i>	Dm α 1T	Voltage-gated calcium channel α -subunit
cpx	<i>complexin</i>		Regulator of exocytosis
daf	<i>Dα5</i>	nAcR α -34E	Nicotinic acetylcholine receptor α -subunit
das	<i>Dα6</i>	nAcR α -30D	Nicotinic acetylcholine receptor α -subunit
dop	<i>DopEcR</i>		Dopamine/Ecdysteroid receptor
dsc	<i>dsc1</i>	NaCP60E	Voltage-gated sodium channel
eag	<i>Eag</i>	<i>Ether-a-go-go</i>	Voltage-gated potassium channel α -subunit
glu	<i>GluClα</i>		Glutamate-gated chloride channel
lap	<i>Lap</i>	like-API80	Regulator of endocytosis
par	<i>para</i>	<i>paralytic</i>	Voltage-gated sodium channel α -subunit
rdl	<i>Rdl</i>	<i>resistance to dieldrin</i>	GABA receptor α -subunit
sbd	<i>Sbd</i>	nAcR β -96A	Nicotinic acetylcholine receptor β -subunit
sha	<i>shaker</i>		Voltage-gated potassium channel α -subunit
shb	<i>shab</i>		Voltage-gated potassium channel α -subunit
slo	<i>slowpoke</i>		Ca ²⁺ -activated potassium channel
stj	<i>straightjacket</i>	α 2 δ	Voltage-gated calcium channel
stn	<i>stoned-B</i>		Regulator of endocytosis
syt	<i>synaptotagmin-1</i>		Regulator of exocytosis
unc	<i>unc-13</i>		Regulator of exocytosis

Supplementary Table D2. Primers used in this study

Gene	CG Number	Sites	Primer Type	Sequence (5' - 3')
syt	CG3139	1 to 6	Forward	GCTGCGCTACGTGCCGACCGCCGG
			Reverse	GTAGTCCACGACGGTCACAACGAG
			Sequencing	GCTGCGCTACGTGCCGACCGCCGG
cap	CG33653	1	Forward	GATTTGAAAAAGAACGATGGGAAAG
			Reverse	CAGCATATTAATCTGCTGCGAATACC
			Sequencing	CGGGTGTGCCACTTCTGAAGATTTAT
cpx	CG32490	1 to 3	Forward	AGCTAAGCAGATGGTTGGAAA
			Reverse	TGCATGACACATTTTCCCTCT
			Sequencing	CCCAAGAAGAGCCCAAT
unc	CG1501	1	Forward	TGGACAGTTATCAGCATCTTCAA
			Reverse	ATTCGTGGCTCCAAACTGAT
			Sequencing	GCTGTGGACATGAAGTACGC
stn	CG40306	1	Forward	TCAAGGGTATCGAGCGAATC
			Reverse	GGCCAAGATGCCTTTGATAA
			Sequencing	TGCATACACCACACATCAGC
lap	CG2520	1 and 2	Forward	CGATGCGTTGGATCTTTACA
			Reverse	GGACAGCCAAGTATGATGGG
			Sequencing	TTGTTAGATGCCTTGGAGCA
dsc	CG34405	1	Forward	GCAAGGAATGCGGATTGTAG
			Reverse	GCGTTGCTCACTTCCAGAAT
			Sequencing	CGGATCGTTCTTCACACTGA
sbd	CG6798	1 and 2	Forward	GACCTACAATGGTGCCCAAG
			Reverse	CACATCGATCTCGTTGGTGT
			Sequencing	CCCAAGTGGATCTGAAGCAT
stj	CG12295	1 to 3	Forward	CGTCCGGAATTCACAATAC
			Reverse	CCTCCTTGCCAATCAGGTAG
			Sequencing	CGACGAGTCCGAAGGATATT
cat	CG15899	1	Forward	GTTGCTGCGAATCCTCAAAT
			Reverse	GTTGGTGGTCGAGGAGTCTG
			Sequencing	TGTGGCACTAATGACGTTTCG
cad	CG4894	1 to 5	Forward	GCATCGATTCTATGGGCATT
			Reverse	CAGTGGACGTAGCACTCGAA
			Sequencing	TTGCCAACTGTATTGCCTTG
shb	CG1066	1 to 7	Forward	GAAGGTAAATGCGCCGAGTA
			Reverse	GTCCGTTTGCGAGAGATTGT
			Sequencing	GGAAACGAATAAGAATGCAACG
eag	CG10952	1 to 5	Forward	CAATACAGCTGGCTGTGGAA
			Reverse	TCACCCTTCTCGACATCACTT

			Sequencing	GACGGCCCTATATTTACCA
		6 to 7	Forward	CAATACAGCTGGCTGTGGAA
			Reverse	TCACCCTTCTCGACATCACTT
			Sequencing	GCGACGAAATTTGGAGAAGA
slo	CG10693	1	Forward	CAGCATTGCATCCCTCATTA
			Reverse	TGGTTCCTTGGGAAGAACTCC
			Sequencing	CGGTCTTCGATTTCTTCGAG
		2	Forward	CTACCACGAGCTGAAACACG
			Reverse	CGGGTGGGTTGGTTATTACA
			Sequencing	GATGACCTTTGACGACACGA
rdl	CG10537	1 and 2	Forward	CATGCTGGGTGACGTAAACA
			Reverse	CATACCGACGCCACATT
			Sequencing	CGGAGTCACCATGTATGTGC
		3 to 6	Forward	CATGCTGGGTGACGTAAACA
			Reverse	CATACCGACGCCACATT
			Sequencing	TGCCCAATTTAAGGTCTTG
daf	CG32975	1, 2 and 9	Forward	CACTGGGTGTTACCATCTTGC
			Reverse	CTACGAGACAATAATATGTGGTG
			Sequencing	ACTGGGTGTTACCATCTTGC
		3 to 8	Forward	CACTGGGTGTTACCATCTTGC
			Reverse	CTACGAGACAATAATATGTGGTG
			Sequencing	CGTGCATCAAATCATCAACT
das	CG4128	1 to 6	Forward	AATCTGCGCTGGAATGAAAC
			Reverse	CAATGTGAAGCCCAGTAGGG
			Sequencing	TGGAATGAAACGGAATACGG
ard	CG11348	1 to 4	Forward	GACCTACAATGGTGCCCAAG
			Reverse	CACATCGATCTCGTTGGTGT
			Sequencing	CCCAAGTGGATCTGAAGCAT
sha	CG12348	1 and 2	Forward	CTGGTCATGGCTTTGGTGGCGGACC
			Reverse	CCGTGTGATCAGTCAGACCTGGCG
			Sequencing	GGATCTGTGATGTCAGGCACCTCG
		3 to 6	Forward	CTGGTCATGGCTTTGGTGGCGGACC
			Reverse	CCGTGTGATCAGTCAGACCTGGCG
			Sequencing	CGAGGTGCCTGACATCACAGATCC
adr	CG12598	1	Forward	CCACAGCATATCAGTCGATTT
			Reverse	TGGAATCGTCCCCTACCCGGAC
			Sequencing	CCACAGCATATCAGTCGATTT
cac	CG1522	1	Forward	GCGGAGAAAAGGTTTCGTTT
			Reverse	GAGTGTGCAAGACCTGTGG
			Sequencing	TCAACAGTGCTATCGGGAAA
		2 to 5	Forward	CCACAGCATATCAGTCGATTT

			Reverse	TGGAATCGTCCCCTCACCGGAC
			Sequencing	ATGCATTTACCGGCGTATTC
		6	Forward	GTACGAGGAGGAGGACGAACTGC
			Reverse	CTGAAGTCTAGCGGGACTCG
			Sequencing	GTACGAGGAGGAGGACGAACTGC
		11	Forward	GTACGAGGAGGAGGACGAACTGC
			Reverse	CTGAAGTCTAGCGGGACTCG
			Sequencing	CACTGGCCTACGCCTACTTC
		12	Forward	GTACGAGGAGGAGGACGAACTGC
			Reverse	CTGAAGTCTAGCGGGACTCG
			Sequencing	CTCCAGTGGCCAGATCTCC
par	CG9907	1 to 4	Forward	CATTGGTGCAAATCGAACAA
			Reverse	GCTCCGAATGGACATCTTCT
			Sequencing	CATTATTCATGCACACGACGA
glu	CG7535	1 to 2	Forward	GGCAGCGGACACTATTTCTG
			Reverse	GCATCTAAACTGGCCTGCTC
			Sequencing	CTGACTATGGCGGGACCA
		3	Forward	GGCAGCGGACACTATTTCTG
			Reverse	GCATCTAAACTGGCCTGCTC
			Sequencing	CCTACCTCGCTTCACACTGG
dop	CG18314	1 to 9	Forward	GGTGCCCTTCTCCGTGTAT
			Reverse	TTGAGGAGAATGAAAATCTAAATCT AA
			Sequencing	GACCGGAGAATGGATGTACG